Advances in Delivery Science and Technology

Juergen Siepmann
Ronald A. Siegel
Michael J. Rathbone *Editors*

# Fundamentals and Applications of Controlled Release Drug Delivery

CRS Delivering Bioactives

Springer

# Advances in Delivery Science and Technology

**Series Editor:**
Michael J. Rathbone

For further volumes:
http://www.springer.com/series/8875

Juergen Siepmann • Ronald A. Siegel
Michael J. Rathbone
Editors

# Fundamentals and Applications of Controlled Release Drug Delivery

Springer

*Editors*
Juergen Siepmann
College of Pharmacy
University Lille Nord de France
Lille, France
juergen.siepmann@univ-lille2.fr

Michael J. Rathbone
School of Pharmacy
Griffith University
Southport, QLD, Australia
m.rathbone@griffith.edu.au

Ronald A. Siegel
Departments of Pharmaceutics
and Biomedical Engineering
University of Minnesota
Minneapolis, MN, USA
siege017@umn.edu

ISSN 2192-6204 e-ISSN 2192-6212
ISBN 978-1-4614-0880-2 e-ISBN 978-1-4614-0881-9
DOI 10.1007/978-1-4614-0881-9
Springer New York Dordrecht Heidelberg London

Library of Congress Control Number: 2011939206

# Forward

Controlled Release Systems impact the health and well being of tens of millions of people every year. And yet, it is a relatively new field built both on solid fundamentals of chemistry and mass transport, as well as new discoveries in materials science and biology. It is also an interdisciplinary field and involves the convergence of a broad range of engineering, scientific, and medical disciplines. Ron Siegel, Juergen Siepmann, and Mike Rathbone have put together a book that explains and discusses the fundamentals of this field.

*Fundamentals and Applications of Controlled Release Drug Delivery* examines various aspects of fundamentals of drug delivery from why and when controlled release is needed to the different mechanisms and processes involved, including aspects of mathematically modeling these systems. This work also covers biodegradable polymers, hydrogels, hydrophobic polymers, and other materials of significance. A significant portion of this volume is devoted to delivering drugs over both the right time period and to the right place in the body. Mechanisms of release for achieving appropriately timed drug release such as diffusion, swelling, osmosis, and polymer degradation are discussed. For accomplishing targeting to the right place in the body, approaches such as nanosystems, liposomes, and receptor targeted release are examined. Finally, various selected applications of drug delivery are evaluated. These include cancer, heart disease, vaccines, and tissue repair. The need for sophisticated drug delivery systems which take into account circadian and other physiological rhythms is also explored.

As the twenty-first century emerges, there is little question that drug delivery will play a major role in health care. This book will clearly help those who want to design and utilize these important systems.

Cambridge, MA, USA — Robert Langer, Sc.D.

# Preface

This volume provides an overview of fundamental principles relating to the science and technology of drug delivery. It approaches the subject from a mechanistic perspective using language that is understandable to those entering the field and who are not familiar with its common phrases or complex terms. It provides a simple encapsulation of concepts and then expands on them as the reader progresses through the book. Once the concepts are laid out, applications to various disease states are described in detail.

Drug delivery is an interdisciplinary field concerned with the proper administration of bioactive compounds to achieve a desired clinical response in humans or animals. Drug delivery is beneficial to billions of people (and animals) worldwide and is achieved by designing and developing technologies that modify the temporal and spatial drug release profile, resulting in enhanced product safety and improved patient convenience and compliance. Rational design of a drug delivery technology requires the convergence of many fields of science and engineering.

Technologies have been developed for delivery of bioactives via many routes of administration including the oral, topical (e.g., skin), transmucosal (nasal, buccal/sublingual, vaginal, ocular, and rectal), and inhalation routes. A broad range of bioactive compounds are incorporated into delivery technologies, from simple molecules to peptides and proteins, antibodies, vaccines, and gene-based drugs. A well-designed drug delivery technology offers the advantages of reduction in dose frequency, a more uniform effect of the drug over time, reduction of drug side effects, reduced unwanted fluctuations in circulating drug levels, and extension of the commercial value of a drug or formulation. Disadvantages of drug delivery systems include their high cost, and sometimes a decreased ability by the clinician or patient to adjust dosages.

The outcomes of recent efforts in the field of drug delivery are rapidly emerging, as is expansion of knowledge of the underlying science. Recent advances include the development of targeted delivery systems in which the drug is only active in a specific area of the body such as cancer tissues, microscopic novel long acting

formulations such as microparticles and nanoparticles in which the drug is released over a period of time in a controlled manner, liposomes, in situ forming implants, and drug polymer conjugates.

This book is divided into six parts. The first part covers the *value of drug delivery*, starting with a chapter written by Wilson on the advantages that drug delivery brings and why drug delivery is needed to treat a specific condition. Terms used in the drug delivery area are defined and controlled release resources are identified. An overview of mechanisms of drug delivery is then provided in a chapter by Siegel and Rathbone. The second part of the book covers *polymeric delivery materials* and includes a description of the synthesis, manufacture, and characterization of polymeric materials used to deliver drugs. Chapters emphasize the need for materials characterization and the need to fully characterize manufacturing processes to avoid process and product failures. Hydrophobic polymers are discussed by Jones et al., hydrogels are reviewed by Omidian and Park, and Burgess and Tsung co-author a chapter on biodegradable polymers The third part of the book deals with *temporal delivery systems and mechanisms*. Siepmann et al. author two chapters on diffusion and swelling controlled systems, Schwendeman and Wischke provide a summary of degradable polymeric carrier systems, and Siegel presents an overview of porous systems. In the fourth part concerning *spatial delivery systems and mechanisms*, Minko provides a chapter on receptor targeted release, Torchilin reviews liposomes for targeted drug delivery, and Fattal discusses targeted delivery using biodegradable polymeric nanoparticles. The fifth part deals with present and potential future clinical *applications* of controlled drug delivery. This part begins with an extensive review of chronotherapeutics and drug delivery by Smolensky et al., which is followed by chapters on approaches to treatment of cardiovascular disease (Fishbein et al.), cancer (Bardhwaj and Ravi Kumar), and infectious disease (Senel). A final chapter in the fifth part covers controlled release in tissue engineering (Suggs). The sixth, final part is a *future outlook* consisting of a chapter written by Dr. Stephen Perrett surveying the present and future regulatory and commercial landscape for advanced drug delivery systems.

The Editors are indebted to the willingness and expertise of the authoritative contributors who have donated their valuable time to write chapters for this volume. Without them this book would not have become a reality.

Lille, France — Juergen Siepmann
Minneapolis, MN, USA — Ronald A. Siegel
Southport, QLD, Australia — Michael J. Rathbone

# Contents

# Contributors

**Osama A. Abu-Diak** School of Pharmacy, Queen's University of Belfast, Belfast, UK

**Ivan S. Alferiev** Abramson Research Center, The Children's Hospital of Philadelphia, Philadelphia, PA, USA

**Gavin P. Andrews** School of Pharmacy, Queen's University of Belfast, Belfast, UK

**Vivekanand Bhardwaj** Strathclyde Institute of Pharmacy and Biomedical Science, University of Strathclyde, Glasgow, UK

**Diane J. Burgess** Department of Pharmaceutical Sciences, University of Connecticut, Storrs, CT, USA

**Michael Chorny** Abramson Research Center, The Children's Hospital of Philadelphia, Philadelphia, PA, USA

**Charles T. Drinnan** Department of Biomedical Engineering, University of Texas at Austin, Austin, TX, USA

**Elias Fattal** Laboratoire de Physico-Chimie, Pharmacotechnie et Biopharmacie, Faculté de Pharmacie, Université Paris-Sud, Châtenay-Malabry, France

**Ilia Fishbein** Abramson Research Center, The Children's Hospital of Philadelphia, Philadelphia, PA, USA

**Laura R. Geuss** Department of Cellular and Molecular Biology, University of Texas at Austin, Austin, TX, USA

**Erhard Haus** Department of Laboratory Medicine and Pathology, University of Minnesota, Minneapolis, MN, USA

Health Partners Medical Group, Regions Hospital, St. Paul, MN, USA

**Ramon Hermida** Bioengineering & Chronobiology Laboratories, University of Vigo, Vigo, Spain

**Hervé Hillaireau** Laboratoire de Physico-Chimie, Pharmacotechnie et Biopharmacie, Faculté de Pharmacie, Université Paris-Sud, Châtenay-Malabry, France

**David S. Jones** School of Pharmacy, Queen's University of Belfast, Belfast, UK

**Robert Langer** Department of Chemical Engineering, Massachusetts Institute of Technology, Cambridge, MA, USA

**Robert J. Levy** Abramson Research Center, The Children's Hospital of Philadelphia, Philadelphia, PA, USA

**Tamara Minko** Department of Pharmaceutics, Ernest Mario School of Pharmacy, Rutgers, The State University of New Jersey, Piscataway, NJ, USA

**Simona Mura** Laboratoire de Physico-Chimie, Pharmacotechnie et Biopharmacie Faculté de Pharmacie, Université Paris-Sud, Châtenay-Malabry, France

**Julien Nicolas** Laboratoire de Physico-Chimie, Pharmacotechnie et Biopharmacie Faculté de Pharmacie, Université Paris-Sud, Châtenay-Malabry, France

**Hossein Omidian** Health Professions Division, College of Pharmacy, Nova Southeastern University, Fort Lauderdale, FL, USA

**Kinam Park** Departments of Biomedical Engineering and Pharmaceutics, Purdue University, West Lafayette, IN, USA

**Stephen Perrett** Portfolio Development, Eurand, Yardley, PA, USA

**Francesco Portaluppi** Department of Clinical and Experimental Medicine, Hypertension Center, University Hospital S. Anna, University of Ferrara, Ferrara, Italy

**Michael J. Rathbone** School of Pharmacy, Griffith University, Southport, QLD, Australia

**M.N.V. Ravi Kumar** Strathclyde Institute of Pharmacy and Biomedical Science, University of Strathclyde, Glasgow, UK

**S.P. Schwendeman** Department of Pharmaceutical Sciences, University of Michigan, Ann Arbor, MI, USA

**Sevda Şenel** Department of Pharmaceutical Technology, Faculty of Pharmacy, Hacettepe University, Ankara, Turkey

**Ronald A. Siegel** Departments of Pharmaceutics and Biomedical Engineering, University of Minnesota, Minneapolis, MN, USA

**Florence Siepmann** College of Pharmacy, University Lille Nord de France, Lille, France

**Juergen Siepmann** College of Pharmacy, University Lille Nord de France, Lille, France

**Michael H. Smolensky** Department of Biomedical Engineering, University of Texas at Austin, Austin, TX, USA

**Laura J. Suggs** Department of Biomedical Engineering, University of Texas at Austin, Austin, TX, USA

**Vladimir Torchilin** Center for Pharmaceutical Biotechnology and Nanomedicine, Northeastern University, Boston, MA, USA

**Nicolas Tsapis** Laboratoire de Physico-Chimie, Pharmacotechnie et Biopharmacie Faculté de Pharmacie, Université Paris-Sud, Châtenay-Malabry, France

**Jamie Tsung** Shire HGT, Cambridge, MA, USA

**Clive G. Wilson** Strathclyde Institute of Pharmacy and Biomedical Sciences, Glasgow, Scotland, UK

**C. Wischke** Department of Pharmaceutical Sciences, University of Michigan, MI, USA

Center for Biomaterial Development, Berlin-Brandenburg Center for Regenerative Therapies, Institute of Polymer Research, Helmholtz Center Geesthacht, Teltow, Germany

**Ge Zhang** Department of Biomedical Engineering, University of Akron, Akron, OH, USA

# Part I
# The Value of Drug Delivery

# Chapter 1
# The Need for Drugs and Drug Delivery Systems

**Clive G. Wilson**

**Abstract** Disease processes and ageing require therapeutic intervention to ameliorate or eliminate, when possible, the effects of pathologies on everyday living. Ageing is associated with a gradual degeneration and subsequent alteration of the balance of the body's control systems. Drugs are useful therapeutic agents that interact with cellular targets to produce an effect that amplifies or more usually blocks cellular processes selectively, provided that dose and access are sufficient. This redresses the balance in ageing and pathology to increase patient comfort. The relationship between presentation of the drug and effect can be defined mathematically and is used to calculate the target window for administration; however, both pathological processes and ageing can alter exposure as changes occur in structure and function of the body, leading to decreased control of drug effectiveness.

## 1.1 Introduction

Although health and well-being are best managed by appropriate diet and lifestyle, human beings undergo a continuous progression toward old age, beset by infection and incapacity. Disease is the general description of a health condition not caused by the direct result of a physical injury and there are many approaches to categorization of disease, as illustrated in Table 1.1. Diseases vary in severity, impact, and individual susceptibility, and can be traced to a mixture of circumstance, exposure, age, and predisposing factors. Disease processes have consequences or *sequelae* – pathological processes or complications resulting from an adaptive change as the body attempts to repair the damage caused by the disease process. For example, a wound scars and there may be subsequent limitation in function, i.e., both structural

C.G. Wilson (✉)
Strathclyde Institute of Pharmacy and Biomedical Sciences, Glasgow, Scotland, UK
e-mail: c.g.wilson@strath.ac.uk

J. Siepmann et al. (eds.), *Fundamentals and Applications of Controlled Release Drug Delivery*, Advances in Delivery Science and Technology,
DOI 10.1007/978-1-4614-0881-9_1, 

**Table 1.1** Alternative approaches for classifying diseases

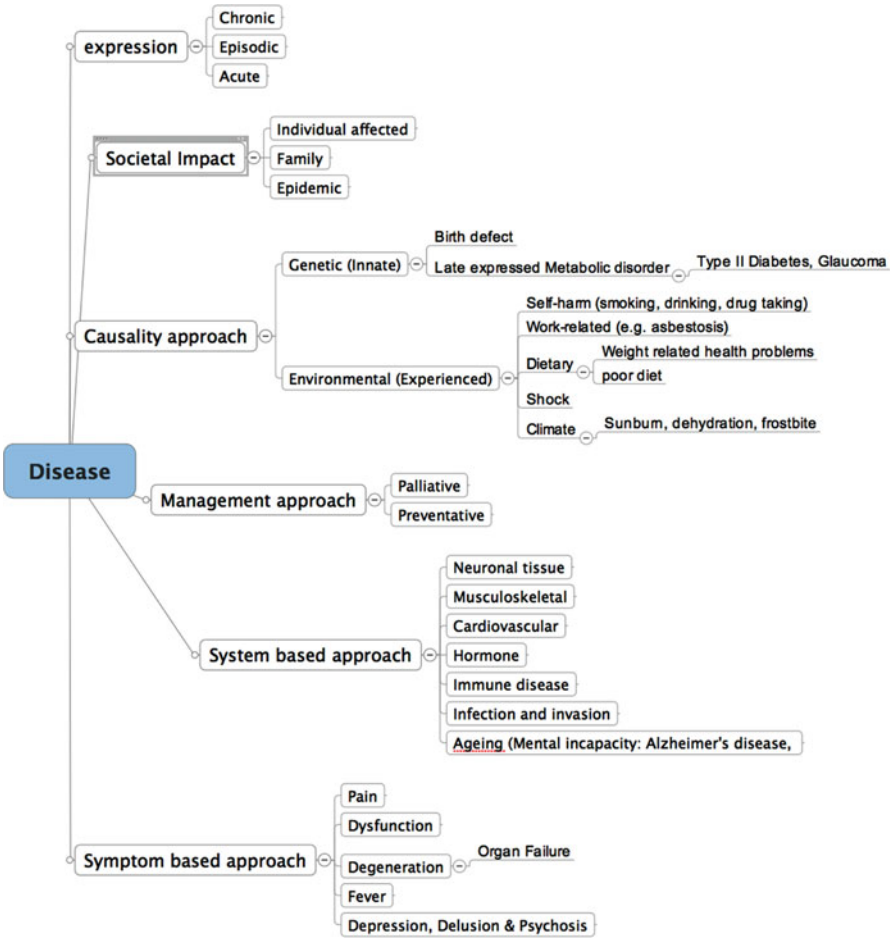


and functional manifestations. Pathologies are generally identified by a characteristic set of symptoms, which may together be described as a *syndrome*: the sum of the signs of a morbid state whose characteristics were well-described initially but whose underlying causality was not appreciated. Examples include Cushing's syndrome, Down's syndrome, and Alzheimer's disease.

The important characteristics of a disease are that functionality is disturbed and that it may be associated with pain, deprivation of sleep, mood changes, and loss of appetite which are distressing to the individual and to the caregiver.

Appropriate treatment of the body's disorders by medicine and surgery is one of the cornerstones of an advanced civilization. Achievement of valuable, high-quality life experience is dependent on health and unfortunately, the human machine has a limited span before disease and irreversible ageing processes limit function.

A major goal of medical and drug therapy is to slow down, and sometimes reverse the effects of infection, inflammation, injury, and overindulgence, and to counter genetic predisposition to certain illnesses.

## 1.2 Why We Need Drugs

Drugs are needed to correct imbalances caused by genetic predispositions, ageing, injury, and foreign invasion. They are sometimes needed as *replacements*, such as in hormone therapy. Sometimes, drug therapy is directed to counter the growth and development of injurious populations of cells by direct antagonism of their metabolism. In such a system, the specificity of the toxic assault is very important. More commonly, we use drugs to subtly adjust the changes that occur due to inadequate endogenous compensation to physiological challenges. As an example, ageing involves the loss of function and most drug therapy is accessed by ageing individuals in order to counteract the effects associated with old age, as summarized in Table 1.2. The inability to deal with these diseases produces frustration, a decrease in the quality of life, pain, and depression.

The power of drugs was appreciated by the ancients and was associated with religion and superstition. Systematic study of anatomy and physiology and reevaluation of old remedies drove mankind toward a systematized approach to research and the birth of allopathic medicine, wherein the actions of compounds on tissue receptors could be studied, transmitters and humoral agents could be identified, and the dose–activity relationship could be quantified. Thus, the actions of drugs discovered in the past, especially the plant-based medicines including salicylin, digitalis, atropine, ergotamine, and opium, became better understood. Successful treatment of illnesses with drugs was largely based on better purification and analytical methods, robust hypotheses, and physiological and biochemical measurements. At the turn of the nineteenth century, the age of chemistry led to the synthesis of active small molecules, such as acetylsalicylic acid and acetamidophen, the first concepts of targeting, Ehrlich's "magic bullet," and the discovery of biopharmaceuticals beginning with molecules, such as penicillin. Modern drug discovery and development now draw from the astounding advances in the physical, chemical, and biological sciences that have occurred in the past century and parallel innovations in engineering and manufacturing.

## 1.3 Drug Substances

A compound is classified as a drug if it has a reproducible effect on the body which can be observed and, better still, measured. This is achieved by ligand binding of the molecule to a receptor. However, not all ligands are useful drugs. This is partly

**Table 1.2** Changes associated with ageing

| System | Consequence |
|---|---|
| Central neurons | Loss of fine muscular control, cognition and memory. Loss of senses. Depression. |
| Peripheral neuro-muscular function | Loss of strength, muscle co-ordination, sensory feedback. |
| Muscular Body mass | Changes in blood concentrations. Replacement of muscle by fat. Weakness. Loss of plasma protein, loss of water. Changes in nutritional status |
| Organ function accumulation of toxins | Changes in clearance, |
| Immune function | Failure to control pro-inflammatory events |
| Skeletal function | Loss of bone mass including dentition, fractures, loss of mobility |
| Uncontrolled stem cell activation | Cancer |

because of hindered ability to access and sustain sufficient concentration at the intended site of action, poor discrimination of subtypes, or issues of stability. Drugs cause their effects generally by mimicking natural transmitters or more commonly by blocking receptors. Since drugs are usually released into the circulation, their actions are analogous to hormones, whose action is distal to the point of release. Drugs with high specificity act at low concentration on a particular receptor subtype, whereas global pharmacons act on a variety of receptor types simultaneously. To understand the implications of this, the process of physiological balance or homeostasis must be considered.

## 1.4 The Importance of Accelerators and Brakes in Homeostasis

The human system attempts to produce a consistent homeostasis, with tissue activities held in balance by the influence of opposing drives. Standing, walking, and digestion all involve sequences of different muscles operating in a programmed order. Thus, each organ system has an effector and antagonist component. In the case of muscles which must contract to exert an action, the opposing muscle relaxes/contracts while the effector contacts/relaxes, adjusting the movement of a joint or caliber of a sphincter to a target configuration. If both muscle sets contract appropriately but to different degrees, tension is generated and the position of a limb can be controlled. In addition, the extent of muscle movement is "sensed" to control action and prevent spasm – this represents a feedback mechanism. For this, the body needs separate motor nerve supplies and afferent and efferent sensory nerve fibers. In addition, the system provides an overall adjustment of tone, generally produced by secretion of hormones, such as adrenaline. In this way, the body is ready, like an idling engine, to react quickly to a stimulus.

Thus, adrenaline acts on the sympathetic system to increase a parameter, such as heart rate, and thus blood flow while parasympathetic, cholinergically mediated stimuli slow the heart down. The two arms of the autonomic nervous system can each be controlled by pharmacologic stimulation or repression, leading to alterations in cardiovascular function. For example, to reduce the actions of adrenaline, it can be either blocked, e.g., using a beta blocker, or opposed by a parasympathetic agonist, mimicking and supplementing natural opposition (Fig. 1.1).

In this way, therapy is able to alter the balance by addition to one side, i.e., agonism, or antagonism of the opposing system. The second reason for therapy is the reduction of inflammation associated with aggressive remodeling of tissues caused

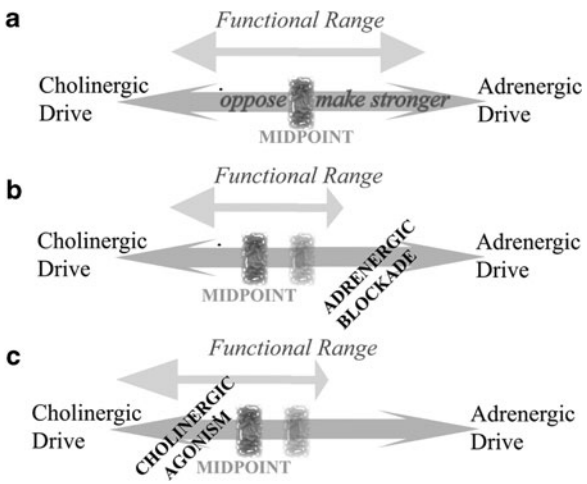


**Fig. 1.1** The opposition of adrenergic and cholinergic drive. The adrenergic system can be antagonized by blockade (*middle panel*) or cholinergic drive increased with an agonist

by the immune cascade. This is also an element of the third rationale for using drugs, the supplementation of the body's natural response to infection or uncontrolled growth of tissues, as in cancer. Finally, the body may fail to produce or absorb sufficient quantities of hormones, vitamins, or nutrients, requiring supplementation.

## 1.5 Access

With few exceptions, all internal and external surfaces of the body are covered by an epithelial layer. Epithelial layers differ in morphology: on an outside surface which is subject to abrasion, such as skin, cells are set into a multilayered, striated, squamous epithelium and may be keratinized, whereas internal tissue-covering membranes and absorptive membranes, such as intestinal villi, are thinner, columnar epithelial layer systems. Permeability is governed both by physicochemical factors, according to Fick's Law (Chap. 6), and by physiological factors, as illustrated in Fig. 1.2. Flux through transport systems is sensitive to affinity, contact time, area, and substrate concentration.

Most drug absorption is mediated by passive diffusion through external surfaces and by a combination of passive, facilitated, and active transport (sometimes, against a concentration gradient) internally. Passive diffusion is a function of the drug's mobility and solubility in the membrane, and is influenced by the drug's polarity, ionization state, and size. These factors can be accounted for physicochemical mechanisms and may be predicted in silico with relative certainty. Using both facilitated and active transporters, the body selectively extracts nutrients from the digestive tract contents or from assimilated materials in the systemic circulation, and attempts to reject the uptake of toxic substances. The most familiar transporters are those for polar key nutrients, including glucose, essential amino acids, and

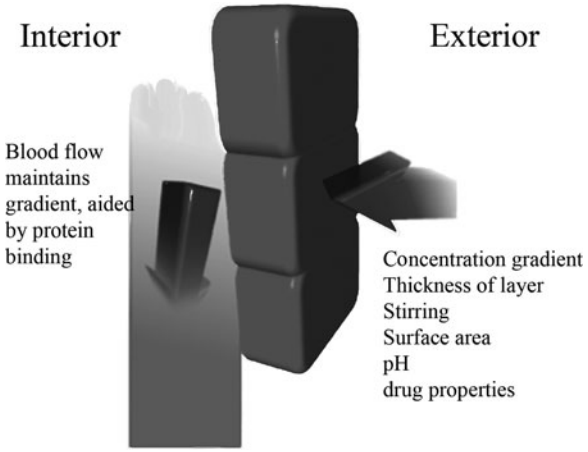


**Fig. 1.2** Role of physiological processes maintaining concentration gradient

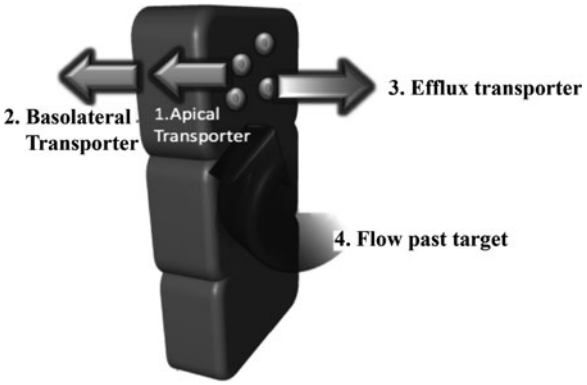


**Fig. 1.3** Net active transport flux is the resultant of uptake and efflux processes

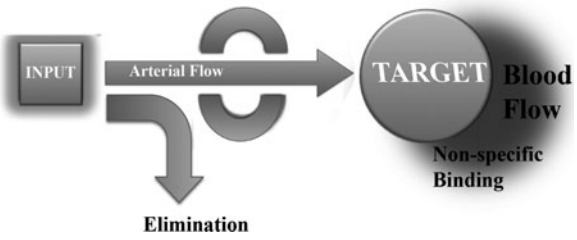


**Fig. 1.4** Target organ perfusion is an important variable, especially as the target is distal to the input process

nucleotides. Of special importance for drug delivery, however, are efflux systems that expel materials through transporters located on the apical membranes of transporting epithelia.

Transporting epithelial cell layers are anatomically polarized with differential expression of apical and basolateral transporter systems as illustrated in Fig. 1.3. For the gut, it was appreciated early on that oligopeptide transporters, including human intestinal peptide transporter 1 (hPEPT1), have wide substrate specificities and can transport a chemically diverse selection of substrates, provided that the key motifs are conserved. The efflux proteins, which attenuate drug flux across epithelial membranes, contain ATP-binding regions which are critical to their transport activity. Active transport results from binding of ATP and the substrate to the transporter, followed by hydrolysis of bound ATP to ADP with accompanying translocation of substrate across the membrane, and then release of ADP to regenerate the transporter's native state [1].

Once access to the systemic circulation is achieved, the physiological factors impinging on target tissue concentration are principally total body volume of distribution, since the drug concentration is diluted and taken up by other tissues, protein binding, clearance by metabolism, renal and biliary secretion, and persistence of the vehicle or drug in the circulation. Around the target site, other tissues compete for ligand binding as illustrated in Fig. 1.4. Therefore, a key parameter is the vascularity of the target.

## 1.6 Blood Flow

Tissues can be divided into three groups with respect to blood flow. The heart, brain, and lung are well-perfused, as are the liver and kidneys. Skeletal muscle is less well-perfused and skin and adipose tissue have poor perfusion. Microcirculation is affected by blood pressure, and in the elderly it has been suggested that tissue perfusion is adversely affected by too low diastolic pressure [2].

Blood supply to the tissue affects the time over which drug equilibrium is established in a tissue, as illustrated in Fig. 1.5, which illustrates the case for a single dose. In well-perfused tissues, concentration in tissue roughly follows that in plasma, with a relatively brief delay, while in poorly perfused tissues the peak in concentration is attenuated but drug may remain in tissue much longer than in plasma.

## 1.7 Potency, Affinity, and Efficacy

In tissue preparations with pure drugs applied in buffer or saline, clearance mechanisms do not influence outcome and the response of a tissue to local drug concentration shows a curve similar to that portrayed in Fig. 1.6a. This curve shows three zones as concentration increases: first, nonspecific binding producing no response, followed by a graded response according to concentration, and finally saturation.

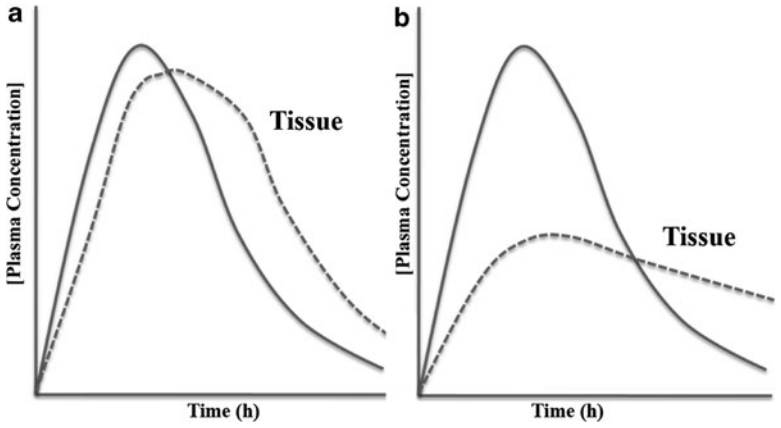


**Fig. 1.5** The relationship between central systemic (*solid curve*) and tissue (*dashed curve*) concentrations in (**a**) well- and (**b**) poorly perfused tissue

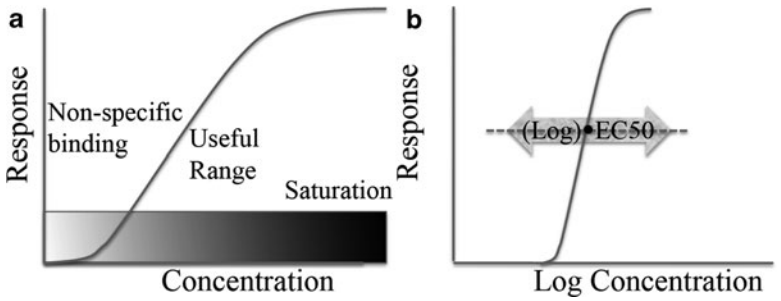


**Fig. 1.6** Plot of response against concentration (**a**) and the log-dose versus response curve (**b**)

The curve in Fig. 1.6a is not so convenient for comparing molecular target affinity between drugs as these concentrations may span several decades in concentration. Response is, therefore, plotted against the $\log_{10}$ molar concentration of drug as shown in Fig. 1.6b. The sigmoidal log-dose/response relationship is very familiar in pharmacology.

Potency of a drug is described in common parlance as the amount of drug needed to produce an effect of given intensity. Potency is a reflection of *affinity*, i.e., the concentration of drug needed to bind to a receptor, and *efficacy*, the relationship between binding and drug effect. Potency of a drug is usually expressed as EC50, the concentration required to produce 50% of the maximum response. The dose required to elicit a measurable effect varies substantially. For example, in pain control, a small dose of an opiate produces a large effect. Acetaminophen or ibuprofen at equivalent doses would be almost without measurable effect, and in any case they do not act on the same receptors. In clinical practice, potency varies considerably, depending on receptor distribution and the modes and sites of delivery and elimination processes.

## 1.8 Specificity

To achieve high levels of control of an integrated process, the body needs many transmitters, each directed against particular tissue subtargets. Thus, the gut uses many different chemical transmitters and nerve networks to control motility, including dopaminergic, adrenergic, gabaminergic, and parasympathetic neurons. In other tissues, exemplified by the heart, the sympathetic and vagal (parasympathetic) supply opposes each other. The vagus nerve is important in many sensory physiological functions communicating the state of organs to the brain, and it affects central, respiratory, gastric, inflammatory, and central nervous system functions. Sympathetic nerves activate the key physiological functions involved in mental or physical stress, whereas the parasympathetic system lowers activity,

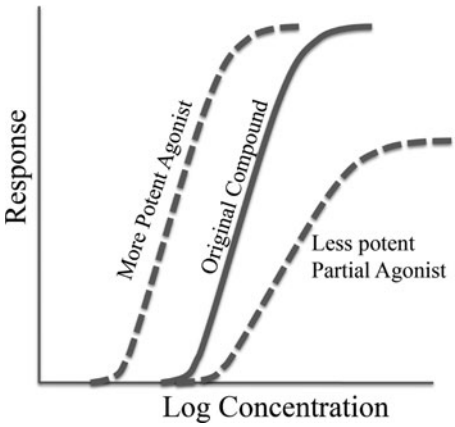


**Fig. 1.7** Illustrating log-dose response curves for three chemically related compounds on receptor action

operates during periods of quiet physical activity, supports muscle activity during digestion, and is involved in anabolic metabolism (conservation of energy).

An example of this accelerator/brake balance is seen classically in cardiac tissue. Stimulation of the heart by the sympathetic system increases heart rate and contraction force, whereas stimulation of the vagus slows the heart down and decreases atrial contraction force. Action is mediated by neurotransmitters between the motor neuron and muscle. These compounds are quickly broken down or reabsorbed after action to allow the tissue to prepare for restimulation. If one pathway shuts down or is amplified, then there may be a gradual change in physiological function in the region of focal impairment. This provides a chance for an imbalance to gradually manifest itself leading to illness. Some drugs mimic the action of transmitters and are able to cause full or partial agonist action, as shown in Fig. 1.7. Other drugs, e.g., hormones, act on control systems and their action is more subtle and prolonged as compensatory processes need to be readjusted.

Another important feature is the range of actions that a drug may have, according to the distribution of receptors in the tissues. The local environment causes modifications in receptor subtypes allowing specificity. Pure specificity is rare in that once the dose is raised other receptor subtypes come into play, although a full effect may not be seen if the drug is not a complete agonist (see Fig. 1.7). For example, increasing the dose of a bronchodilator $\beta_2$-agonist produces increased heart rate and tremor as $\beta_1$-adrenoreceptors are partially stimulated. Partial agonists are widely used in medicine, and they can be regarded as having both antagonistic and agonist effects. Thus, they stimulate to give a submaximal response but compete when a full agonist is present and decrease the action. The beta blockers acebutalol, oxprenolol, and pindolol, are said to have an intrinsic sympathomimetic effect because they are partial agonists.

Physically targeted systems are important in maximizing the local concentration, which is one of the principal benefits of close arterial injection. This reduces bystander effects or collateral damage to nontarget tissues.

## 1.9 The Relationship Between Presentation and Effect

The pharmacodynamic profile reflects the sum of the affinity, absorption, and excretion processes, as well as blood flow to the target site. A certain amount of nonspecific binding occurs which does not elicit a response, and therefore the effect profile lags behind tissue accumulation which in turn may be time shifted relative to the peak plasma concentration time profile. Such time shifted relationships are illustrated in Fig. 1.8. If the tissue is well-perfused, for example the brain, the effect is not noticeable, but for poorly perfused tissues, such as bone and adipose tissue, peak concentrations build slowly, according to the dosing interval. The relationship between derived pharmacokinetic parameters, such as Tmax and Cmax, and effect is more difficult to describe in these tissues.

## 1.10 Drug Absorption: The Balance Between Solubility and Permeability

To be effective, a drug must reach the target site of action in sufficient quantity. Thus, the compound must dissolve, be absorbed through the gut, and possess sufficient metabolic stability to generate adequate drug concentrations at the pharmacologically relevant site so that the desired action is obtained in a reproducible manner.

Drug absorption is influenced by three main groups of factors broadly classified into physicochemical and physiological parameters, with additional influences of diet, race, and genetic influences. Physicochemical processes dominate the first part of this scheme (disintegration and dissolution), and therefore in vitro simulations of the solubilization process have validity, at least for gastrointestinal (GI) delivery. Table 1.3 illustrates some common terms encountered in the description of drugs.

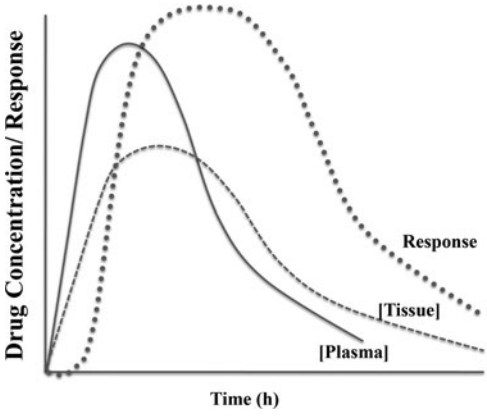


**Fig. 1.8** The relationship between plasma and tissue concentrations and the response profile

**Table 1.3** Drug and formulation attributes

| DRUG ATTRIBUTES & CONSEQUENCES | |
|---|---|
| ACTIVE PRINCIPLE INGREDIENT | The drug in the formulation. Commonly referred to as API. |
| PARTICLE SIZE (of API). | Influences rate of dissolution |
| DOSE | Scaled to body weight, age and disease severity. |
| HIGHLY SOLUBLE | Dissolves in 250 mL at all pH's |
| EXCIPIENTS | Other components of the dose form added to aid manufacture, stability and release properties of the API. |
| DISSOLUTION RATE | The process of release of ingredient into solution, often measured in vitro in a compendial apparatus. |
| DISSOLUTION PROFILE | The characteristic rate of release in vitro. The shape of the release profile is controlled by the physicochemical properties of the drug, supplemented by the release mechanism, which subsequently affects absorption into the systemic circulation. |
| HIGHLY VARIABLE DRUGS | Drugs which show greater than 30% variation in bioavailability, leading to difficulties in assessing bioequivalence. Probably show extensive first pass extraction. In spite of this, they tend to be very safe because of the large therapeutic index associated with these drugs. |

*Solubility*. The increase in molecular size of modern drugs starts to limit aqueous solubility, and the average solubility of current drugs on the market is around 3 mM. Thus, solubility is a limiting variable, and solubility issues are addressed by various means, including selection of an amorphous form where appropriate, reduction in particle size, and the use of cosolvents. Some tissues present different environments. For example, the GI tract shows a marked gradient in pH among stomach, intestine, and colon, and there are variations even within the stomach [3, 4]. Thus, solubility of drug may change as it passes through various stages of the GI tract, which may impinge on bioavailability.

*Permeability*. The other term relating to biological properties is permeability. Experts argue about the use of this term and some prefer to describe the net process as absorption. When permeability problems are encountered, a mechanism to increase flux by alteration of membrane/microenvironment conditions or even a simple increase in concentration gradient might achieve the goal.

## 1.11 A Place for Formultion

Oral drug formulations remain the mainstay of therapy, being cheapest for the manufacturer to produce, simplest to dispense, and most convenient for the patient. Drug in a solid form provides good stability over the intended lifetime of the product, and many innovations have appeared to overcome the shortcomings of the active compound.

Although modern drugs are proving to be harder to bring to market due to poor bioavailability problems, early drug treatments were hit or miss affairs. A few plant-derived toxins were well known to the Greeks and the Romans but as the intended outcome was death, titration might have been unnecessary! It was important that the poison was disguised and no doubt Lucretia Borgia was an exemplary teacher of taste masking. The drugs known to the ancients were galenicals: simple pharmaceutical preparations originally produced by extraction of the sought-for active from plant material. The pharmaceutical tablet was derived from compressing medicinal agents with a suitable liquid adhesive into pills: Burroughs and Wellcome coined the term "tablet" to describe their invention of a compressed pill in 1878. Remington described the process of making tablets at the pharmacy shop using an upper and lower die and a compression cylinder. The material was placed into the cylinder with the lower die in place and the upper die struck with a mallet.

The age of synthetic and analytical chemistry brought into control the proportion of active pharmaceutical ingredient in a formulation. The need to deliver a set amount of a therapeutic agent brought with it new concepts in pharmaceutical sciences, embodied in pharmacopeia, including identity, purity, product robustness, and control of drug release. The extension into extended release was enthusiastically embraced as a method of sustaining drug concentrations and improving patient compliance. Furthermore, physicians became aware of another key improvement due to extended release: reducing peaks and troughs associated with treatment with immediate release dosage forms, as illustrated in Fig. 1.9.

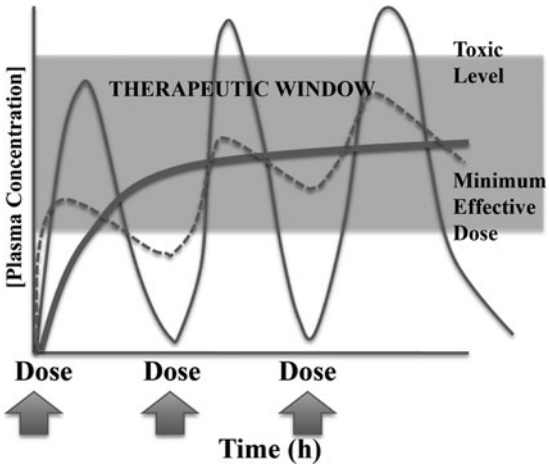


**Fig. 1.9** How peaks and troughs move in an out of the therapeutic window? Tissue concentrations (*dotted line*) may, however, be more smoothed, depending on tissue perfusion

## 1.12 The Concept of the Therapeutic Window

In Fig. 1.9, attention is drawn to the fact that at high concentrations of the drug there is a problem with unwanted effects being triggered by binding to low affinity receptors. This gives rise to the concept of the therapeutic window: a minimum concentration is required to produce a wanted effect but as levels are elevated, a toxic threshold is crossed. Sometimes, this concept is expressed as a ratio of toxic level to minimum effective concentration, the therapeutic index.

When a drug is administered and is absorbed into the systemic circulation, it is diluted into the fluids in the compartments available to it, is bound to plasma protein, and starts to associate with body tissues. On repeated dosing, concentrations rise and fall according to the dose size, volume of distribution, clearance, and dosing interval. This is illustrated in Fig. 1.10. The sawtooth pattern associated with the immediate-release dosage form can be compared to the I.V. dose and the controlled-release dosage form. Thus, controlled-release systems have both advantages of patient compliance, namely, fewer doses and less fluctuation in plasma concentration.

## 1.13 How Old Age and Disease Interfere with Drug Exposure

In general, we attempt to treat the sick and rarely intervene preventatively in the healthy. The consequence of illness is that the safety and exposure of medicines may be altered. For example, gastroenterologists report a higher probability of slowed gastrointestinal transit in the hospitalized patient, in addition to malabsorption. Fat malabsorption is of special interest, since most drugs are lipophiles.

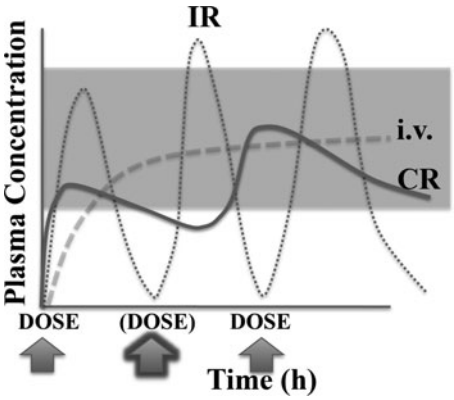


**Fig. 1.10** Comparison of immediate release (IR), controlled release (CR), and intravenous dose. Note how the CR dose form allows therapy to move from three to two times per day

**Table 1.4** Physiological changes associated with ageing which impact on treatment

| DISEASE & TREATMENT FACTORS | |
|---|---|
| ALTERED ACCESS | ***Altered blood flow,*** for example following remodelling of vessels which occurs in some cancers. |
| | ***Mucosal accessibility,*** for example in cystic fibrosis. A thickerlayer of more viscous mucus is secreted. |
| PERMEABILITY | ***Iatrogenic development of increased intestinal permeability***, for example following long term treatment with NSAIDS. |
| | ***Changes in intestinal tissue fluid*** (edema associated with disease) lead to decreased permeability and |
| | ***Alteration in mucosal micro-climate*** (secretion of lactic acid into the lumen due to intestinal oedema) |
| ALTERED SOLUBILITY | ***Decreased secretion of gastric acid*** described clinically as hypochlorhydria, leading to decreased solubility of basic drugs. |
| ALTERED TRANSIT | ***Changes in intestinal transit*** associated with drugs or altered neuro-muscular connections. Slowed transit associated with coma, ageing, constipation, |
| ALTERED METABOLISM AND CLEARANCE | ***Iatrogenic induction of hepatic metabolism*** transporter effects of ureic toxins on Class III drugs. |
| ALTERED BODY MASS | ***General poor nutrition*** leading to changes in distribution and Cmax in uncorrected therapy; obesity and or edema leading to altered Volumes of distribution |

Milovic and Stein recently reviewed gastrointestinal disease and dosage form performance and identified functional changes in the lumenal and mucosal phases of digestion and transport defects, which would be expected to alter fat handling and thus present an altered milieu for drug absorption. Drug flux is also reduced by diseases involving structural modification. For example, Crohn's disease is associated with bleeding, atrophy, and necrosis of the absorptive epithelia of the intestinal tract leading to decreased absorption and changes in gastrointestinal function [5].

The impact of failure of vascular systems on gut absorption is seen in the frail elderly, where malnutrition resulting from cardiovascular disease (cachexia associated with chronic congestive heart failure) is common, although the ageing process per se does not appear to be associated directly with malnutrition.

Old age often results in decrease in colonic motility and aggressive self-treatment with laxatives, which could markedly interfere with the effectiveness of controlled-release dosage forms. Thus, the influence of agents or conditions that modify motility must always be considered in the selection of the most appropriate oral dosage form (Table 1.4).

## 1.14 Conclusions

In this chapter, we review some fundamental principles of drug therapy from a organismic systems point of view. The concept of homeostasis is introduced, as is the notion of drugs as agonists or antagonists used to reestablish desired body states that are perturbed as a result of disease, injury, and ageing. Control of a drug's effect in space and time requires proper consideration of the rate that drug is introduced into plasma following administration using a chosen dosage form, the rates of distribution of drug into target and nontarget tissues, the latter sometimes being associated with toxic side effects, and the relationships between tissue concentrations and drug effects. Understanding of a drug's physicochemical properties, such as its solubility, permeability through membranes, and its specific interactions with receptors and transporter systems, is required in order to determine its suitability for treatment of specific disorders and to choose a proper means for drug delivery.

**Acknowledgments** My thanks to Professor Ron Siegel for helpful suggestions with regard to this manuscript.

## References and Further Reading

1. Rosenberg M, Velarde G, Ford R, Martin C, Berridge G, Kerr I, Callaghan R, Schmidlin A, Wooding C, Linton K, Higgins C (2001) Repacking of the transmembrane domains of P glycoprotein during the transport ATPase cycle. EMBO J 20(20):5615–5625
2. Hulin I, Kinova S, Paulis L, Slavkoksky P, Duris I, Mravec B (2010) Diastolic blood pressure as a major determinant of tissue perfusion: potential clinical consequences. Bratisl Lek Listy 111 (1):54–56
3. Wilson CG, Weitschies W (2009a) Modern drug delivery: physiological considerations for orally administered medications. In: van de Waterbeemd (ed) Drug bioavailability, estimation of solubility, permeability, absorption and bioavailability. Wiley-VCH Verlag, Weinheim, Germany pp. 571–595.
4. Wilson CG, Weischies W, Butler JM (2010) Gastrointestinal transit and drug absorption. In: Dressman JD, Lennernas H (eds) Oral drug absorption, 2nd edn. Marcel Dekker, New York
5. Milovic V, Stein J (2010) Gastrointestinal disease and dosage form performance. In: Dressman JD, Lennernas H (eds) Oral drug absorption, 2nd edn. Marcel Dekker, New York
6. Physiological Pharmaceutics : Biological barriers to drug absorption (2001) N Washington, C Washington & C G Wilson pub Taylor & Francis (London) ISBN 0-748-40610-7 (hardback) & ISBN 0-748-40562-3 (paperback)
7. Wilson CG, Weitschies W (2009) Modern drug delivery: physiological considerations for orally administered medications. In: van de Waterbeemd (ed) Drug bioavailability, estimation of solubility, permeability, absorption and bioavailability. Wiley-VCH Verlag, Weinheim, Germany pp. 571–595
8. Wilson CG, Weischies W, Butler JM (2009) Gastrointestinal transit and drug absorption. In: Dressman JD, Lennernas H (ed) Oral drug absorption, 2nd edn, Marcel Dekker, New York

# Chapter 2
# Overview of Controlled Release Mechanisms

**Ronald A. Siegel and Michael J. Rathbone**

**Abstract** Controlled release systems have been developed to improve the temporal and spatial presentation of drug in the body, to protect drug from physiological degradation or elimination, to improve patient compliance, and to enhance quality control in manufacturing of drug products. When designing controlled-release systems, it is important to identify and understand particular mechanisms involved in the release process. Often, more than one mechanism is involved at a given time or different mechanisms may dominate at different stages of the drug delivery process. This chapter begins with several vignettes, each highlighting a mode of controlled drug delivery and identifying associated mechanisms. An introductory description of several of the mechanisms follows. Details regarding these mechanisms are provided in subsequent chapters.

## 2.1 Introduction

Controlled-release systems are designed to enhance drug therapy. There are several motivations for developing controlled-release systems, which may depend on the drug of interest. Controlled release systems have been devised to enable superior control of drug exposure over time, to assist drug in crossing physiological barriers, to shield drug from premature elimination, and to shepherd drug to the desired site of action while minimizing drug exposure elsewhere in the body. Controlled release systems

R.A. Siegel (✉)
Departments of Pharmaceutics and Biomedical Engineering, University of Minnesota, Minneapolis, MN 55419, USA

Department of Pharmaceutics WDH 9-177, University of Minnesota, 308 Harvard St. S.E., Minneapolis, MN 55455, USA
e-mail: siege017@umn.edu

M.J. Rathbone
School of Pharmacy, Griffith University, Southport, QLD 4222, Australia

J. Siepmann et al. (eds.), *Fundamentals and Applications of Controlled Release Drug Delivery*, Advances in Delivery Science and Technology,
DOI 10.1007/978-1-4614-0881-9_2, 

may also increase patient compliance by reducing frequency of administration, and may add commercial value to marketed drugs by extending patent protection. Finally, use of controlled release technology may reduce variability of performance of drug products. The latter aspect is increasingly important given the current emphasis on "quality by design" by regulatory agencies such as FDA.

The mechanisms used to achieve these goals are diverse and complex, and depend on the particular application. In fact, several mechanisms may operate simultaneously or at different stages of a delivery process. An understanding of these mechanisms is important when designing and manufacturing controlled-release systems, and in identifying potential failure modes. Delineation of mechanism is also important in intellectual property prosecution and quality assurance/quality control.

This chapter starts with a series of vignettes illustrating mechanisms and their interplay in particular controlled release systems. Essentials of individual mechanisms are then outlined. More elaborate descriptions are deferred to later chapters.

## 2.2 Vignettes

### *2.2.1 Zero Order Oral Delivery*

Zero order, or constant rate release of drug is desirable in order to minimize swings in drug concentration in the blood. Such excursions, which may lead to periods of underexposure or overexposure, are particularly likely to occur for drugs that are rapidly absorbed and rapidly eliminated. Figure 2.1 illustrates the plasma concentration profile over time for such drugs when administered from rapid-release dosage forms. A rapid increase in concentration is followed by a rapid decrease, and little time is spent inside the so-called therapeutic range, which is bounded below by a minimum effective concentration (MEC) and above by a minimum toxic concentration (MTC) (see also Figs. 1.9 and 1.10). Frequent repetitive dosing is required to maintain concentration within these limits, and compliance and control are difficult.

Dosage forms that prolong release can maintain drug concentration within the therapeutic range for extended periods and minimize episodes of underexposure or toxicity. A well designed system displays a narrow, predictable residence time distribution in the gastrointestinal (GI) tract, and releases drug by a controlled mechanism. As shown in Fig. 2.1, zero order release leads, in principle, to the best control of plasma concentration. Such control leads to constant drug effect, provided the drug's pharmacokinetic and pharmacodynamic properties, including absorption, distribution, metabolism, and excretion (ADME), and its pharmacodynamic properties relating plasma concentration to drug effect, are stationary. While this proviso is believed to apply to most drugs, there are notable exceptions, as detailed in Chap. 13.

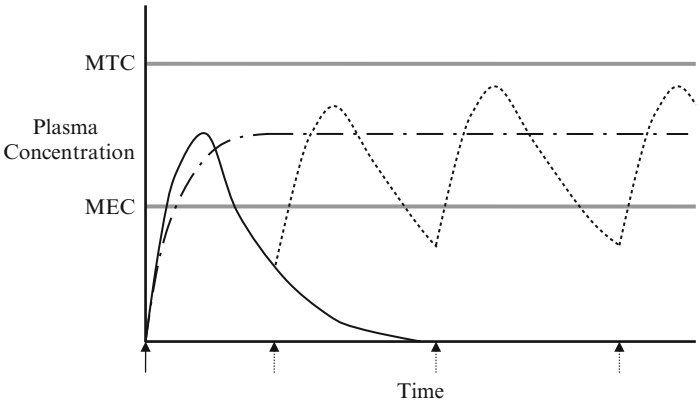


**Fig. 2.1** Efficacious, nontoxic therapy requires that drug concentration in plasma lies within the therapeutic range, which is bounded below by the minimum effective concentration (MEC) and above by the minimum toxic concentration (MTC). For rapidly absorbed, rapidly eliminated drugs, a single dose (*solid arrow*) leads to a rapid rise and fall in drug concentration (*solid curve*). Multiple dosing at regular intervals (*solid arrow* followed by *dotted arrows*) leads to oscillating drug concentrations (*solid curve* followed by *dotted curve*), which may fall outside the therapeutic range for significant time periods. Zero order release (*dot–dash curve*) leads, after an initial rise, to a constant concentration in plasma which, with proper dosing, lies between MEC and MTC

Zero order oral drug release can be achieved, in principle, by surrounding a core tablet with a membrane that is permeable to both drug and water, as illustrated in Fig. 2.2a. After swallowing, the core becomes hydrated, and drug dissolves until it reaches its saturation concentration or solubility. The core serves as a saturated reservoir of drug. Drug release proceeds by partitioning from the reservoir into the membrane, followed by diffusion across the membrane into the gastrointestinal fluid. So long as saturation is maintained in the core, there will be a stationary concentration gradient across the membrane, and release will proceed at constant rate. Eventually, the dissolved drug's concentration in the core falls below saturation, reducing the concentration gradient and hence the release rate, which decays to zero.

If the membrane consists of a water-soluble polymer of high molecular weight, then it will initially swell into a gel, through which drug diffuses. The thickness of the gel layer initially increases with time due to swelling, but ultimately it decreases due to disentanglement and dissolution of polymer chains. At intermediate times, the gel layer may be of approximately constant thickness, and release occurs at a relatively constant rate.

As an alternative to dissolution/partition/diffusion based devices, osmotic pumps have been developed to provide zero order release. An elementary osmotic pump, illustrated in Fig. 2.2b, is a tablet or capsule consisting of a core of drug surrounded by a membrane that is permeable to water but not to the drug. A small hole is drilled into the membrane. Upon ingestion, water is osmotically imbibed into the core through the semipermeable membrane, dissolving the drug. A constant osmotic pressure gradient is established between core and the external medium,

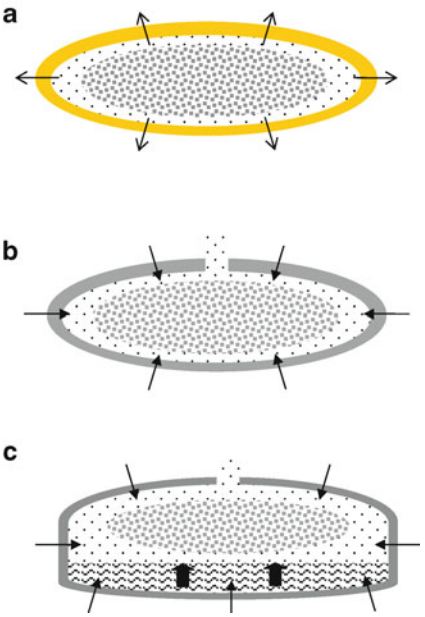


**Fig. 2.2** Schematics of devices designed for zero-order drug release. (**a**) Membrane diffusion-controlled release. Drug in core (*granulated pattern*) dissolves to form saturated solution (*dilute dots*). Drug then diffuses across membrane (*thin tipped arrows*). Zero order release persists as long as there is sufficient drug in core to form saturated solution. (**b**) Elementary osmotic pump. Core is surrounded by a semipermeable membrane, with a small, drilled orifice. Osmotic water flow (*full tipped arrows*) through membrane dissolves drug and displaces it through the orifice. Zero-order release persists so long as a constant osmotic pressure gradient between core and external medium is maintained. (**c**) Push–pull osmotic pump. Similar to elementary pump, except a soluble polymer excipient layer (*curlies*) is added "below" the drug. Osmotic flow into drug layer primarily dissolves drug while osmotic flow into polymer pushes dissolved drug through the orifice (*fat arrows*)

setting the stage for water influx, which displaces drug through the hole at a constant rate. Eventually, drug concentration falls below its solubility, and the rate of osmotic pumping decays.

The efficiency of osmotic devices can be improved by enriching the core with excipients such as water soluble polymers. For example, in push-pull osmotic systems, depicted in Fig. 2.2c, the drug formulation is layered between the water-soluble polymer and the exit orifice. As water crosses the semipermeable membrane, drug is dissolved. Meanwhile, swelling of the polymer excipient, which is also caused by osmosis, pushes drug through the orifice.

### *2.2.2 Oral Delivery Directed to the Gut and Colon*

Numerous drugs are susceptible to hydrolysis in the acidic environment of the stomach. Enteric coatings, which are pH-sensitive polymers that are insoluble in acid but dissolve in the neutral or slightly alkaline environment of the gut,

are designed to protect drug as it passes through the stomach. If the molecular weight of the coating polymer is relatively low, then it will dissolve and drug will be released rapidly. If the molecular weight of the polymer is high enough, however, it will swell into a gel layer that controls drug release as above. Passage of the dosage form through the stomach to the small intestine affects the time required following ingestion to activate swelling and diffusion.

Certain drugs are more efficacious when released in the colon. The colon is rich in bacterial azoreductases, which cleave polymers with azoaromatic crosslinks. By encapsulating drug in such polymers, colon-specific drug delivery can be achieved. Further encapsulation by a rapidly dissolving enteric coating would permit colon-specific delivery of acid-labile drugs. The enteric coating is first stripped off upon entering the gut, but drug is released only when the internal polymer is degraded by the azoreductases in the colon.

### *2.2.3 Oral Delivery of Polypeptides*

Polypeptides, including proteins, are extremely challenging to deliver orally. Problems include acid lability, susceptibility to peptidases and proteases in the stomach and gut, and limited absorption due to high molecular weight and charge. Most protein bioavailabilities, measured as fraction absorbed into the systemic circulation, hover around or below 1%. Reliable, efficient delivery of polypeptides, if possible, will have enormous payoffs.

Let us assume that acid lability can be handled by an enteric coating layer and that the polypeptide is incorporated into micro- or nanoparticles that are designed to adhere to the gut wall. The particles release their payload into the wall or are taken up by endocytosis into enterocytes. While encapsulated in the particles, the polypeptide molecules are protected from attack by enzymes. By these means, it is postulated that bioavailability will be improved.

### *2.2.4 Delivery of Drugs Through the Skin*

Numerous drugs are problematic for oral delivery due to their low solubility and susceptibility to first pass metabolism in the liver. For such drugs, alternative ports of entry are of interest, and practically every available body surface and orifice has been considered. Since the skin is readily accessible and has a large surface area, transdermal drug delivery has been the subject of much research and product development.

The primary barrier layer of skin is the stratum corneum, a thin layer of dead squamous cells that are packed in a kind of brick and mortar configuration, as depicted in Fig. 2.3, with specialized lipids serving as the mortar. Lipophilic drugs can readily dissolve in this layer and diffuse through it at a rate that depends primarily on molecular size and lipophilicity. Very little drug enters the dead

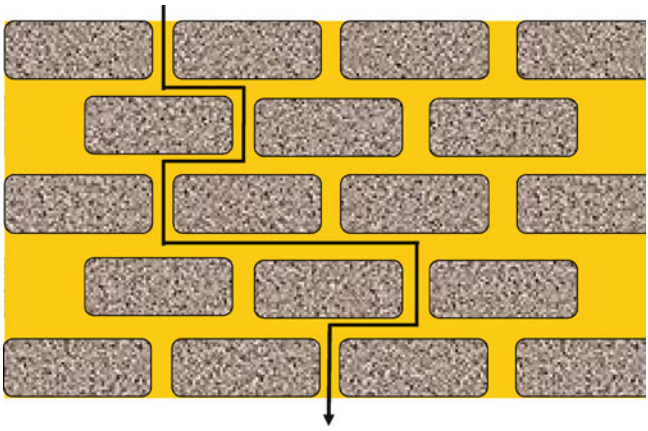

**Fig. 2.3** Simplified representation of the mortar and brick configuration of the stratum corneum (s.c.) showing the paracellular pathways taken by lipophilic drugs around dead proteinaceous cells. The *zig-zagging arrow* is one possible path taken by a drug molecule through s.c.

cells, and the lipid pathways for diffusion are marked by numerous detours. After passing through the stratum corneum, drug encounters the more hydrophilic, viable epidermis and dermis, before being absorbed in capillaries perfusing the dermis. Drug that is absorbed through the skin is not susceptible to first pass metabolism by gut and liver, although some metabolism may occur in the skin itself.

While ointments and creams are usually used for topical delivery to the skin, patches have been developed for controlled systemic delivery. The simplest patch consists of an adhesive layer containing drug in the dissolved or in a finely divided solid form, and an impermeable backing layer, as illustrated in Fig. 2.4a. For such patches, delivery rate is controlled primarily by the permeability of the stratum corneum, which depends on the drug's partition coefficient between the patch material and the stratum corneum, the drug's diffusivity in the stratum corneum, and the thickness of the stratum corneum. Provided these parameters remain constant during application of the patch, and if drug activity in the patch remains constant by dissolution of solid drug into the adhesive, then zero order, constant rate delivery can be achieved.

The simple adhesive patch design is best for drugs with a large therapeutic range, since skin permeabilities may vary across patients and between sites of application in an individual patient. When more precise control of drug concentration in blood is desired, it is useful to insert a rate controlling membrane between the drug reservoir and the adhesive layer, as shown in Fig. 2.4b. The membrane's permeability must be less than that of the skin in order to provide effective rate control.

Since the skin naturally functions as an environmental barrier, only a few drugs can penetrate it at an adequate rate by partitioning and diffusion. Generally, a drug molecule should be sufficiently lipophilic that it partitions into the stratum corneum, but sufficiently hydrophilic that it can also cross the viable layers. Its molecular weight should be low to ensure adequate mobility in the stratum corneum.

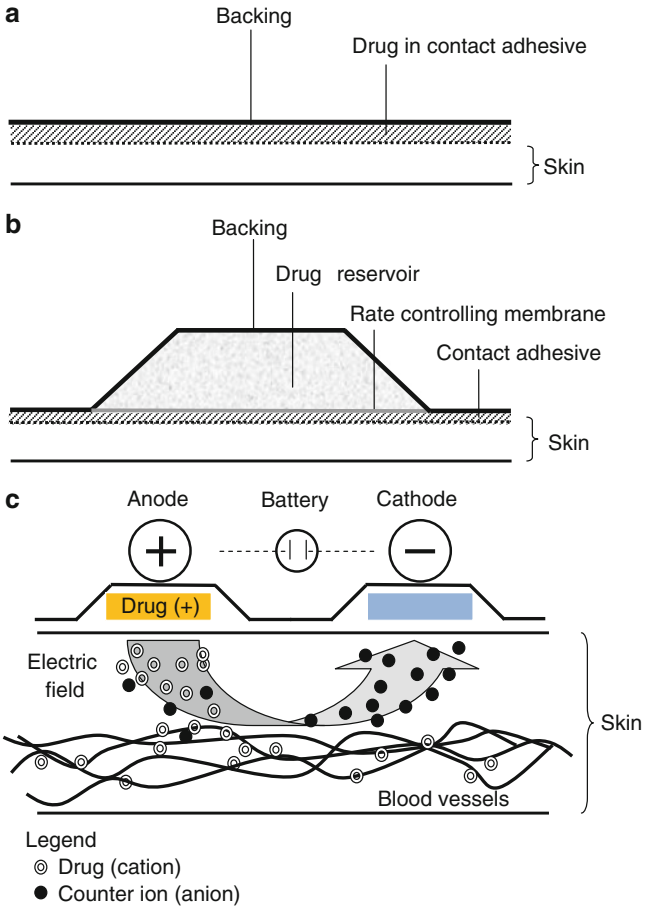


**Fig. 2.4** Various transdermal patch designs (**a**) skin permeability control, (**b**) membrane control, (**c**) iontophoretic patch design for a cationic drug

Finally, the drug's potency and pharmacokinetic properties should be such that delivery through the skin places drug concentration in plasma within the therapeutic range. While the rate of delivery can be increased by using larger patches, there are practical size limitations.

Because the skin is so accessible, much effort has been devoted to expanding the spectrum of transdermally deliverable drugs using more complex delivery systems. For example, the skin's barrier function can be disrupted temporarily by applying chemical permeation enhancers, microneedles, ultrasound, heat, or short, high voltage bursts of electricity (electroporation). During or immediately following disruption, drug can be administered. Alternatively, drugs can be delivered by iontophoresis, in which a steady electrical current is applied through the skin, as illustrated in Fig. 2.4c. This process relies on aqueous channels in hair follicles and

sweat glands, or new channels formed by the current. Charged drug molecules are driven through these channels by a like-charged electrode while uncharged drug molecules are delivered through the channels by electroosmotic convection.

Ideas discussed in this vignette may apply to drug delivery across other well perfused epithelia, including the rectum, vagina, scrotum, cornea and sclera, and the buccal and nasal mucosae.

### 2.2.5 *Depot Delivery of Reproductive Hormones*

While the introduction of daily oral steroid contraceptives in the mid-twentieth century was a breakthrough with historic medical and social consequences, it is recognized that there is substantial room for improvement. Daily oral dosing can lead to incomplete compliance and effectiveness, so other routes have been studied. For example, a transdermal, patch-based contraceptive system that delivers its payload over 1 week has appeared on the market (ORTHO EVRA®), as has an insertable vaginal ring that releases drug over three weeks (NuvaRing®).

The Norplant® system was introduced in the 1980s to provide five years continuous release of levonorgestrel. Drug is incorporated into silicone capsules that are placed under the skin in a routine clinical procedure. Release is mediated by slow diffusion through the silicone matrix. Because the silicone capsules do not degrade, they must be retrieved after they are spent. An alternative biodegradable implant called Capronor was investigated but was not marketed.

Besides steroid hormones, analogs of luteinizing hormone-releasing hormone (LHRH) have been developed. LHRH is the master hormone that is secreted rhythmically in the hypothalamus, and activates numerous hormones on the reproductive axis. Both LHRH agonists and antagonists have been developed as contraceptives, and they also have been used to treat disorders, such as endometriosis, vaginal bleeding due to fibroids, precocious puberty, and prostate cancer. When these analogs are delivered continuously, they interfere with the rhythmic signaling by endogenous LHRH. Because they are extremely potent, they can be injected as a slow-release depot. In one system, Leupron Depot®, leuprolide acetate is formulated into biodegradable polymer microspheres, which degrade and release drug over three months. In this system, drug release is controlled by diffusion through a pore network whose structure evolves as the polymer degrades.

Osmotic pumping provides another potential approach to long-term contraceptive delivery. One example is a narrow metal cylinder containing two compartments that are separated by a movable piston, as shown in Fig. 2.5. The drug formulation is introduced into one compartment, which is capped on the end, except for a small exit orifice. The other compartment contains an osmotically active agent, and is capped by a membrane that is permeable to water but not to that agent. Osmotic water flow across the membrane displaces the piston, and drug is pushed out through the exit orifice. By proper selection of the semipermeable membrane, the pumping rate and hence duration of release can be precisely controlled.

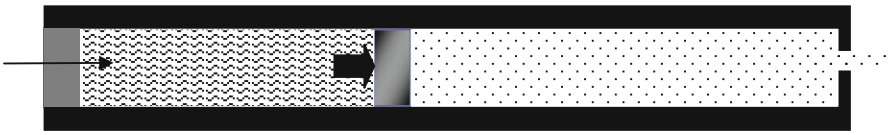

**Fig. 2.5** Implantable cylindrical osmotic pump with piston. Water flows through semipermeable membrane at *left* into a chamber containing osmotic excipient (*curlies*), displacing piston, which in turn pushes drug formulation (*dots*) out through the orifice at *right*

Complementary to contraception is fertility therapy. Patients with lesions that suppress LHRH secretion can be treated with rhythmic intravenous injections of LHRH, delivered from an externally worn, programmed pump through a catheter. This mode is best for short term needs, such as induction of fertility, but it is less desirable when the need is long term, as in the treatment of arrested puberty. Since LHRH is exceptionally potent, each dose is very small, so the possibility of an implantable rhythmic dosing device is intriguing. Such devices may ameliorate the inconvenience associated with intravenous delivery. One approach under consideration is a controlled-release microchip, into which thousands of microwells are machined. Each well is filled with a single dose of LHRH and sealed by a thin gold membrane that is addressably connected to a current source. Under the control of a microprocessor, individual membranes are ruptured with a current pulse and their encapsulated doses are released. By proper programming, any sequence of release pulses can be programmed into the system.

### *2.2.6 Regional Drug Delivery*

Thus far, we have discussed scenarios in which drug enters the systemic circulation after release. Drug then distributes according to its relative affinities to all tissues, and only a small fraction is present at or near the target site. Drug toxicity and side effects are often associated with accumulation in tissues not associated with the target. In regional (sometimes called local or topical) delivery, drug is administered directly to the target tissues. Under proper conditions, regional delivery should permit substantially reduced drug dosing to reach the desired effect, with reduced exposure of other tissues to the drug.

Regional delivery is potentially most effective when drug is not transferred substantially from the target tissue to the systemic circulation due to anatomic or physiological barriers, or when systemic drug is rapidly eliminated. Traditional examples include topical drugs, inhalation based asthma therapies, and chemotherapies directed by drug pumps to tumors. The release of chemotherapeutic agents from polymer disks implanted next to brain tumors provides another example, as does insulin delivery to the peritoneal cavity, which drains through the hepatic portal vein into the liver, a primary target for insulin.

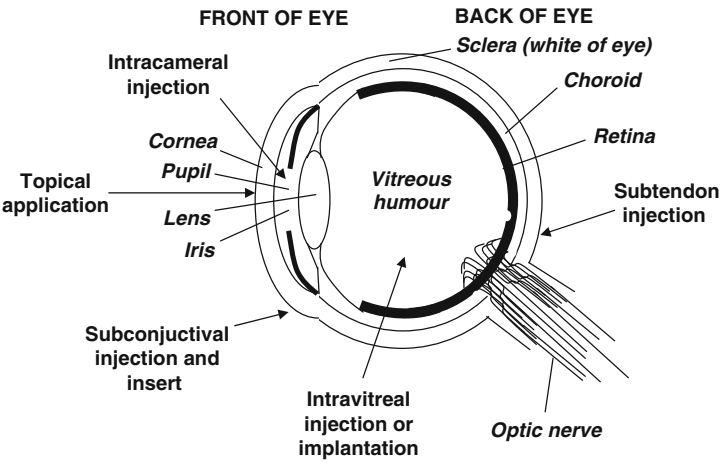


**Fig. 2.6** A schematic representation of various ocular routes of administration. Topical application may involve eye drops, gels or ointments, or drug-soaked contact lenses. Intracameral injections are used in cataract surgery with injection volumes of approximately 100 μL. Ocusert®, an early controlled-release system based on a saturated pilocarpine reservoir, was administered to the subconjunctival sac. Patches have been designed for application to the sclera for transscleral delivery. Polymeric delivery systems, such as micelles, gels, nanoparticles, microparticles, and solid implants, may be formulated and act as depots for long-term, controlled delivery of drugs to the various parts of the eye

In this vignette, we first consider local delivery to the eye, noting different strategies that must be applied to delivery into the aqueous humor and the retina. We then discuss drug-eluting stents, which provide local delivery of drugs to arteries following injury.

Anatomical features and routes for drug delivery to the eye are shown in Fig. 2.6. The eye cavity is a useful port of entry for antibiotics and drugs meant to treat disorders in tissues perfused by tears and aqueous humor. To reach the aqueous humor, which lies under the cornea and houses the lens and iris, drug must cross the cornea, which contains both lipophilic and hydrophilic layers. Conventional eye drops are notoriously inefficient, since much of the drop is lost by overflow and drainage into the nasolacrimal duct. To increase drug retention in the eye cavity and hence bioavailability, drug can be formulated in gels that spread over and adhere to the ocular surface. Alternatively, drug-soaked contact lenses have been considered for topical delivery. In addition to increasing bioavailability, these formulations may prolong the release process, reducing the required frequency of administration. An early drug delivery product was Ocusert®, in which a saturated pilocarpine reservoir was placed between two membranes which could control release, by the partition/diffusion mechanism, of the drug for up to 1 week. This product was placed under the lower eyelid and released drug at constant rate into the tear fluid, with subsequent absorption through the cornea.

Drug administered into the eye cavity is generally not available to the retina. To reach the retina, drug can be delivered to the vitreous humor, which lies behind

the lens. The vitreous is a viscous gel that slowly circulates, providing convective transport of drug to the retinal surface. Several schemes have been investigated. The ocular sclera (white) provides a large surface area, and patches have been devised for transscleral delivery into the vitreous. A problem arises because the sclera is heavily perfused by choroidal blood vessels, which remove drug before it reaches the vitreous by diffusion. Alternatively, solid implants that slowly release the drug can be injected or placed surgically into the vitreous. Presentation of drug to the retina, then, depends both on the rate of release by diffusion and rate of convection to the retinal surface.

Drug eluting stents, discussed in Chap. 14, have recently been developed to prevent restenosis or reclosing of coronary arteries following angioplasty and stenting procedures in response to heart attacks. Restenosis is an inflammatory response to these procedures, and involves the growth of arterial smooth muscle cells over the stents. To arrest such growth, small amounts of anti-inflammatory and antiproliferative drugs are coated onto the stents and are released directly into the adjacent arterial tissue by dissolution, partitioning, and diffusion. Because the dose is so small and targeting is so precise, it is possible to prevent restenosis without releasing detectable amounts of drug into the systemic circulation and other tissues.

### *2.2.7 Nanoparticulate Targeting of Drugs to Specific Tissues*

Besides improving systemic bioavailability and the temporal and regional patterns of drug release and absorption, controlled release systems have been developed to alter the residence time of circulating drug. In these systems, drug is incorporated in nanocarriers that have access to the whole systemic circulation, but are cleared less rapidly than free drug. The nanocarriers can be regarded as circulating drug depots. Nanocarriers may also have favorable distribution properties into target tissues and away from tissues associated with toxic side effects. Examples of nanocarriers include microemulsions, liposomes, dendrimers, block polymer micelles, solid lipid and polymer nanoparticles, and soluble polymers with drug attached on side chains by biodegradable linkages.

At the nano level, it is also possible to incorporate targeting ligands that permit particles to bind preferentially to specific cell types and promote the uptake and drug release into those cells. It has been suggested that cellular processes that rely on multivalent attachment, including particle uptake, can be modulated by drug/nanoparticle composites by suitable placement of multiple-targeting ligands on particle surfaces.

Design of nanoparticulate drug delivery systems must take into account normal physiological scavenging processes that remove small foreign objects from the blood. Special coatings, such as poly(ethylene oxide)s, are used for this purpose. Suitably coated nanoparticulates exhibit reduced opsonization and clearance by the reticuloendothelial system. Renal clearance is avoided when nanoparticulates are larger than glomerular pores. Hence, circulating half-lives of nanoparticulates and

their associated drugs are prolonged. Furthermore, coated nanoparticles and their associated drug are largely restricted to the vascular space, in contrast to free drug which may have much a larger volume of distribution. It should be noted, however, that if drug is released from the nanoparticle into systemic circulation, as opposed to a specific target site, it will possess the same pharmacokinetic properties as otherwise administered free drug.

It is believed that nanoparticulate delivery systems may be very useful in treating some cancers due to the enhanced permeation and retention (EPR) effect. Compared to normal tissues, tumors have leaky capillaries with large fenestrations in the capillary walls that permit the passage of nanoparticulates. Drug loaded into the nanoparticulates is, therefore, relatively more accessible to tumor tissues compared to tissues associated with toxic side effects.

## 2.3 Survey of Mechanisms

The previous vignettes highlighted several controlled-release mechanisms, including dissolution, partitioning, diffusion, osmosis, swelling, erosion, and targeting. Basic principles associated with these mechanisms are presented in this section.

### *2.3.1 Dissolution*

Most drug molecules form crystals at room temperature. In fact, they may take on various crystal forms (polymorphs) or form crystal hydrates, depending on their processing conditions. In some cases drug particles can be processed into an amorphous, glassy form. These forms have differing thermodynamic stabilities, and interconversion between solid forms can occur during storage and after administration. Dissolution involves transfer of drug from its solid phase to the surrounding medium, which may be water, polymer, or tissue. The solubility of drug in a medium, $C_{S,medium}$, is defined as the concentration of drug in the medium at saturation, i.e., in equilibrium with the solid form. Higher concentrations of drug are thermodynamically unstable, and with time drug crystallizes out of solution until its concentration equals $C_{S,medium}$. Useful rules of thumb are that $C_{S,medium}$ decreases with increasing melting point of the drug and increases with increasing chemical compatibility of drug with the surrounding medium.

While solubility is a thermodynamic property of a drug and a medium, the dissolution rate is a kinetic property. Dissolution rate increases with solubility and decreases with drug particle size. As discussed below, dissolution rate is commonly controlled by diffusion.

### 2.3.2 Partitioning

During drug delivery, drug molecules often encounter an interface between two materials or phases. The partition coefficient is a measure of the relative affinity for drug between the two phases, and is roughly given by the ratio of drug solubilities in the two phases. At the interface, the partition coefficient prescribes the relative frequency that a molecule moves into one medium compared to the other.

As an example, recall that drugs of high lipid solubility are suitable for entry into the stratum corneum. However, if the drug is not sufficiently water soluble, i.e., its lipid/water partition coefficient is too high, it will not partition efficiently into the viable epidermis, and drug will be detained in the stratum corneum. Absorption into capillaries might then occur at an unacceptably low rate.

As a second example, block copolymer micelles are formulated with hydrophobic cores and hydrophilic coronas, hence they are soluble in blood. Hydrophobic drugs preferentially partition into the core, where they are retained for extended periods of time. Pharmacokinetic characteristics of such drugs, i.e., clearance and volume of distribution, reflect those of the micelles, leading to longer retention in the circulation and preferred distribution into tumors due to the EPR effect.

### 2.3.3 Diffusion

Diffusion is a very important component of many controlled-release systems, hence we devote considerable space in this chapter to it. More details about diffusion-controlled drug delivery systems are provided in Chaps. 6 and 9.

#### 2.3.3.1 Molecular Basis

All molecules constantly undergo random collisions with other molecules. As a result, molecules execute thermal or Brownian motion. At any step, the direction of motion of a molecule is random, and it repeatedly changes due to collisions with other molecules. Over time, the displacement of the molecule from its point of origin is the result of a multitude of such random steps. Macroscopically, the independent random walks taken by large number of drug molecules lead them from regions of higher concentration to regions of lower concentration. Thus diffusion of a substance occurs down its concentration gradient.

The theory of random walks shows that the average (actually, root mean squared) distance that molecules travel by diffusion is proportional to the *square root* of time, i.e., average distance traveled $\sim \sqrt{Dt}$, where $D$ ($cm^2/s$) is the diffusion coefficient, or diffusivity, and $t$ is time (s). The diffusion coefficient is a measure of the molecule's mobility in the medium. Conversely, the typical time required to diffuse over a particular distance is proportional to the *square* of that distance and

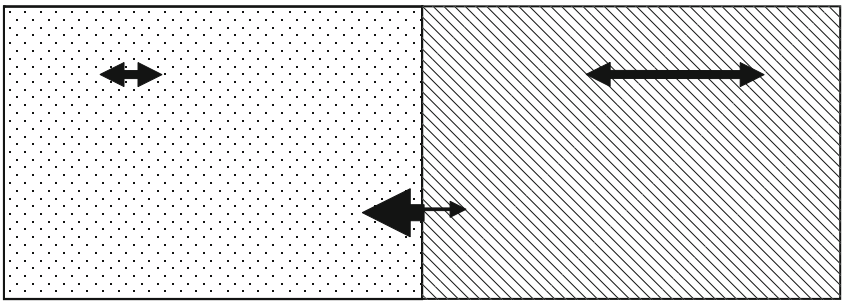

**Fig. 2.7** Partitioning and diffusion. Two host media are placed in contact. Diffusion coefficient of drug in each medium away from interface is indicated by length of corresponding *double arrow*. At the interface, drug chooses to partition into one of the media. Relative frequencies of entry into the two media from the interface are depicted by the breadths of *arrows* pointing into the media. The ratio of *arrow* widths is the partition coefficient. Upon entering either medium, drug diffuses according to the medium's diffusion coefficient, as illustrated by differing *arrow* lengths at interface. In the present example, drug partitions preferentially into the *left* medium (⁘), but diffuses more rapidly in the *right* medium (▨)

inversely proportional to the diffusion coefficient. Thus, while diffusion is an efficient means of mass transport over short distances, its effectiveness decreases over longer distances.

Figure 2.7 illustrates and contrasts partitioning and diffusion. Two media are placed next to each other. Within each medium, symmetric arrows depict the magnitude of the diffusion coefficient, which characterizes the motion of the molecule exclusively inside that medium. A molecule moves in either direction with equal probability. At the interface between the media, however, the molecule must make a choice. The partition coefficient determines the relative frequencies that this molecule "jumps" into either medium. The two different frequencies are depicted by arrows of different thicknesses. The lengths of the arrows correspond to the respective diffusion coefficients.

#### 2.3.3.2 Reservoir Versus Monolithic Systems

We have already introduced systems in which a membrane mediates diffusion from a reservoir. In reservoir systems, drug first partitions into the membrane from the reservoir and then diffuses to the other side of the membrane, where it is taken up by the receiving medium. While the reservoir is saturated, a constant concentration gradient of drug is maintained in the membrane, the rate of drug flux is constant, and zero order release is achieved. Eventually, drug concentration in the reservoir falls below saturation, and the gradient across the membrane and release rate both decay.

In reservoir systems, the purpose of the membrane is to mediate diffusion of drug. Because of their simplicity of mechanism and their ability to produce zero order

release, reservoir systems would seem to be highly advantageous. However, reservoir systems can be difficult to fabricate reliably. Pinhole defects and cracks in the membrane can lead to dose dumping. These problems are avoided in monolithic systems, in which drug is loaded directly into a polymer, which now acts as both a storage medium and a mediator of diffusion.

Drug is typically loaded uniformly into monolithic devices, and release is controlled by diffusion through the monolith's matrix material or through aqueous pores. Monolithic devices typically exhibit an initial burst of release from the surface. With passing time, release rate decreases as drug that is deeper inside the monolith must diffuse to the surface, since it has farther to travel, and the quadratic relation between distance and time becomes important. This effect occurs in planar monoliths, but it is even more prominent with cylinders or spheres, as the amount of drug available decreases with distance from the surface. This geometric factor can be substantially reversed using specially coated wedge, cone, or hemisphere monoliths to provide near-zero-order release, but such devices are not easy to fabricate.

#### 2.3.3.3 Factors Affecting Diffusivity

The diffusivity, $D$, depends on the molecule and the medium. For a hard spherical molecule in a liquid solvent, the Stokes-Einstein equation prescribes $D = k_B T/6\pi a\eta$, where $a$ is the molecule's radius, $\eta$ is the solvent's viscosity, $k_B$ is Boltzmann's constant, and $T$ is absolute (Kelvin) temperature. This relation confirms the intuition that large molecules should diffuse more slowly than small ones and that diffusion should be slowed in viscous liquids. The factor $k_B T$ accounts for the intensity of thermal agitation, which drives Brownian motion.

In typical polymeric controlled release systems, the polymer matrix does not flow like a liquid, and bulk viscosity is not the correct parameter to use in predicting mobility of drug. The matrix may possess, however, a "microviscosity" that is related to molecular mobility. Free volume theory provides a useful picture that accounts for both bulk and microviscosity. While it may be natural to think of a polymer matrix as a static solid, it is actually a dynamic fluctuating structure, and $D$ may be thought of as a measure of the degree that these fluctuations accommodate random motion of the diffusing molecule. In free volume theory, each drug, solvent, and polymer molecule contains an impenetrable core that is surrounded by nanovoids, called free volume. Thermal motions cause the size of voids to fluctuate. Occasionally, a void becomes large enough for a diffusing molecule to move into or through it. Clearly, if this mechanism is operative, then the diffusion coefficient will decrease sharply with increasing molecular radius and when the matrix's density increases upon cooling. At a critical density, often associated with the medium's glass transition temperature, $T_g$, free volume becomes so sparse that the diffusion coefficient drops by several orders of magnitude.

In addition to temperature, the free volume of a polymer matrix depends on its composition. For homogeneous materials, free volume increases as the difference

between ambient temperature and $T_g$ increases. Copolymerization and blending can lead to matrices with suitably averaged free volumes and mobility properties. Free volume can also be increased substantially by sorption of small molecules, such as water. Thus, a glassy dry polymer can be converted to the rubbery state by sorption of a small amount of water, substantially increasing the mobility of drug molecules in the polymer.

Besides the glass transition, polymers can form crystalline domains which exclude drug molecules and obstruct diffusion. The propensity to crystallize depends on the polymer's melting point and its stereoregularity. Random copolymers generally do not form crystalline domains. Crystallization can be mediated by the polymer backbone or by the side chains, especially when the latter are long.

For a molecule diffusing through a water-swollen hydrogel, diffusivity of drug is affected by the viscosity of the water space and also by obstructions placed in the drug molecule's path by the hydrogel chains. Many models of diffusion in hydrogels, therefore, combine elements of Stokes–Einstein and free volume theories. In this case, the size of water-filled spaces between hydrogel chains is assumed to fluctuate, making room for movement of the diffusing drug molecule. The characteristic distance between points of chain crossings in the hydrogel is called the correlation length, and the ratio of molecular radius of drug to the correlation length is considered to be the primary structural parameter governing the drug's diffusion coefficient in the hydrogel.

#### 2.3.3.4 Heterogeneous Systems

Thus far, we have discussed diffusion mediated systems in which the medium is a uniform polymer matrix or hydrogel. Local matrix fluctuations were assumed to control the rate of diffusion. In more heterogeneous media, other factors also become important.

We have already noted that the presence of dead cell bodies in the stratum corneum increases the effective path length for drugs diffusing through skin lipids. We have also seen that crystalline domains in a polymer can obstruct and retard diffusion. More generally, diffusion of drug through a heterogeneous medium depends on the solubility and diffusivity of drug in the different material domains of the medium, and the geometric manner in which the domains are dispersed.

For example, consider a polymer blend or block structure, where one component has a much higher drug solubility than the other. If the "drug-philic" domains comprise a discrete phase dispersed in a "drug-phobic" continuous phase, then the disconnected phases will retain drug and retard its release, by analogy to affinity chromatography. If on the other hand the drug-philic domain is continuous, then release will be controlled by diffusion through the continuous phase, but will be retarded by detours around the drug-phobic domains.

Porous systems are often encountered in controlled release. Empty pores can be introduced into a matrix during fabrication to serve as pathways for drug diffusion through water that enters the pores. Alternatively, solid drug or excipient particles can be introduced into a polymer, and pores form around the particles. Also drug and excipient may precipitate from a polymer solution during solvent removal, again resulting in a porous amalgam of drug and polymer. The pores then act as both depots for drug storage and as conduits for diffusion. Pore structure and connectivity may have a profound effect on release by diffusion, as is discussed in Chap. 9.

#### 2.3.3.5 Diffusion Affects Dissolution

We conclude this section with a discussion of dissolution and diffusion in drug delivery. Dissolution occurs when the solvating medium surrounding a solid drug particle is not saturated. This process involves two steps. First, drug must dissociate from the surface of the particle and surround itself with solvent. Second, the newly solvated drug must diffuse away from the surface. The first process is usually more rapid than the second, unless the drug is extremely insoluble. Thus, the drug is very close to its saturation concentration in the immediate vicinity of the particle. A concentration gradient is, therefore, established between the particle/medium interface and the "bulk" of the medium, and diffusion controls the rate that drug flows down this gradient. In drug delivery systems containing solid drug particles, both $C_{S,medium}$ and $D$ are therefore important determinants of release rate.

In an important class of drug delivery systems discussed in Chap. 6, solid drug particles are incorporated into a monolithic matrix. Release of drug occurs by dissolution followed by diffusion through the matrix. Particles at the surface dissolve quickly, leading to a burst. Particles further inside dissolve more slowly, since dissolution rate is controlled by diffusion through the matrix. At intermediate times, a moving front is observed, separating a central core containing solid drug from a periphery containing completely dissolved drug. Because the diffusion distance from the front to the monolith's surface increases with time, the march of this front slows down as the release process proceeds, and the rate of release decreases with time.

### *2.3.4 Osmosis*

Osmosis is a dramatic phenomenon that occurs when a membrane that is permeable to water but not to particular solutes, called osmolytes, separates aqueous solutions of the osmolytes. Water flows through the semipermeable membrane in an effort to equalize concentrations of the impermeable solutes on both sides of the membrane. In most cases of interest, water flow occurs by diffusion through the semipermeable membrane. However, the nature of water transport may differ from that discussed

above for drugs. First, it should be emphasized that there tends to be a lot of water on both sides of the membrane, and flux of water through the membrane is determined by the difference in chemical potentials of water on the two sides, not simply the concentration gradient of water. These chemical potentials may depend on both concentrations of the osmolytes and the thermodynamic compatibility of water with the osmolytes. When the osmolytes are small molecules, such as salts, osmotic pressure is reasonably accounted for osmolyte concentrations according to van't Hoff's law, but when the osmolytes are polymers, osmotic pressure is determined jointly by polymer concentration and polymer/water compatibility. Second, when the membrane is adequately hydrated, water molecules are in contact with each other and neighboring molecules' motions are correlated. The Brownian mode of diffusion discussed for drug molecules is then replaced by the so-called collective mode.

The rate of osmotic flow across a unit area of the membrane is determined by the concentration and nature of osmolytes on both sides of the membrane, temperature, and the hydraulic permeability of the membrane, which can be determined by measuring water flow when a hydrostatic pressure is applied across the membrane. Osmotic flow is reduced when the membrane is partially permeable to the osmolytes. As water flows into a device containing osmolytes, it dilutes the osmolytes, lowering the osmotic pressure, unless new osmolytes are introduced, for example, by dissolution.

We have already described osmotic pumps in which water invasion across a membrane displaces drug through an orifice. Another way to use osmosis is to coat individual drug particles with semipermeable polymers. After release from a capsule, these particles are exposed to gastric fluid. Water crosses the polymer coatings and dissolves the drug, leading to a gradient in solute concentration that drives even more water inside. To accommodate, the coating must expand, and wall stresses are developed. With sufficient osmotic driving force, the coating ruptures, releasing the drug. Using different coating thicknesses, particles can be programmed to burst at different times. The original time release capsules were based on this principle.

A variation of the elementary osmotic pump theme involves particles or tablets that are coated with a semipermeable polymer membrane which includes sparsely but well-distributed aqueous pores. These pores can be created by excipients blended into the membrane, which dissolve upon exposure to water. Here, water flows across the semipermeable parts of the membrane and displaces dissolved drug inside through the aqueous pores into the release medium.

### *2.3.5 Swelling*

Swelling refers to the uptake of water by a polymer system, with increase in volume. Swelling is often a prelude to polymer dissolution. However, swelling may occur without dissolution if water and the polymer are insufficiently compatible, if polymer chain length is sufficiently large, or if crosslinks are introduced to form

a polymer network. Swollen polymer networks or hydrogels reviewed in Chap. 4 may imbibe many times their weight in water.

The swelling process is analogous to osmosis, since water enters the polymer relatively rapidly, while dissolution of polymer into water, if it occurs, is comparatively slow because of the need for polymer chains to disentangle. The extent of swelling depends on the compatibility of water with the polymer material, i.e. the polymer's hydrophilicity, and on the density of crosslinks between polymer chains, if present. Hydrophobic polymers, reviewed in Chap. 3, imbibe very little water and hence do not swell significantly.

Swelling is a mechanism by which release of otherwise confined drug is activated. If swelling is rapid, then drug diffusion through the swollen polymer is the controlling process for drug release. If swelling is relatively slow, then it can be the process controlling the rate of drug release. A more detailed description of swelling controlled systems is given in Chap. 7.

Swelling controlled release systems are typically glassy polymers at room and body temperatures. Water uptake is initially resisted by the glass, but eventually it makes its way into the free volume at the surface. The glassy polymer at the surface relaxes to a configuration that is more compatible with water, and swells. This permits water to intrude even further, and a moving front is often observed separating a swollen outer layer from a dry inner core. Usually, swelling is accompanied by a glass-to-rubber transition. If drug is trapped inside the glass, it will be liberated when the polymer swells, and if it can diffuse through the softened matrix faster than water can invade, then the release process is swelling controlled. Swelling dynamics are often complex, and a variety of temporal release patterns are observed under swelling control. Under proper conditions, swelling, dissolution of polymer chains, and drug release may occur simultaneously, further contributing to complexity.

Swelling in a polymer may be induced or accelerated by drugs or other additives, which act as effective osmolytes, drawing water into the polymer. By proper selection of polymer, it is also possible to induce swelling by changes in external parameters, such as temperature and pH, which may occur, for example, upon ingestion. Reversible swelling and shrinking of hydrogels can also be induced by alternating these parameters with concomitant on/off patterns of drug release.

### *2.3.6 Erosion and Degradation*

Erodible and degradable drug delivery systems are popular, particularly for implantable or injectable therapies, since they do not require retrieval after drug is fully released. Presently, the most common erodible systems are based on poly(lactic acid) or poly (lactic acid-*co*-glycolic acid), although systems based on poly(ε-vinyl caprolactone), poly(ortho esters), polyanhydrides, polyphosphates, poly(phosphazenes), and pseudo-poly(amino acids) have also been utilized or studied. Important characteristics of erodible systems are their mechanism and kinetics of erosion. Erosion products must be nontoxic and excretable or resorbable. Principles and applications of erodible

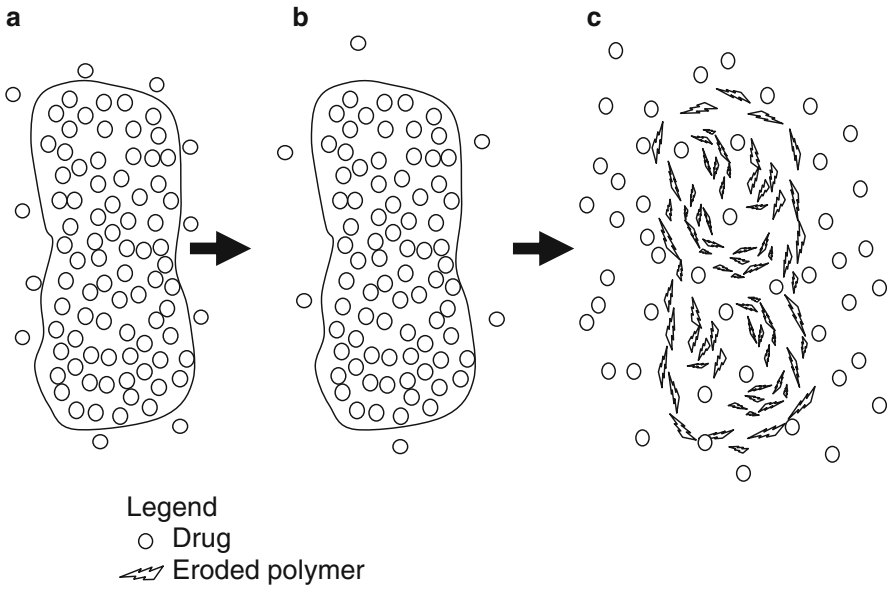


**Fig. 2.8** Diagrammatic representation of the three stages of release of drug from bulk eroding polymers. The first stage (**a**) corresponds to drug that is released from the device surface or from pores that are connected to the surface. A second, latent stage follows, during which there is little degradation of polymer and the remaining drug is trapped (**b**). In the third stage, the trapped drug is released rapidly when the polymer autocatalytically disintegrates (**c**)

systems are elaborated in Chaps. 5, 8, and 10. In this section, we call attention to two limits of behavior in erodible systems, namely, bulk erosion and surface erosion.

Erosion of polymer monoliths occurs when components of the release medium, especially water, attack covalent bonds in the polymer matrix. For hydrolytically labile bonds, availability of water is an important determinant of local erosion rate. Hydrolysis of bonds may also be acid or base catalyzed, and if so depends on local concentration of proton donors and acceptors. For PLA and PLGA and other polyesters or polyamides, acidic protons are provided by chain ends; hence, concentration of acid protons is inversely proportional to chain length.

Bulk erosion, depicted in Fig. 2.8, occurs when water invades the polymer more rapidly than hydrolysis can occur. In this case, water establishes its presence throughout the matrix, and chain scission processes are initiated everywhere. Hydrolysis may initially be very slow, however, especially if the polymer chains are long. Moreover, initial scissions may endow chains with sufficient mobility that they migrate and form crystallites, which are less susceptible to hydrolysis. However, once a certain degree of hydrolysis has occurred, the process may accelerate. For example, formation of short chains may lead to overall loss of polymer and increase in water concentration by diffusion and/or osmosis. If chain scission results in the formation of acidic end groups and the scission process is acid

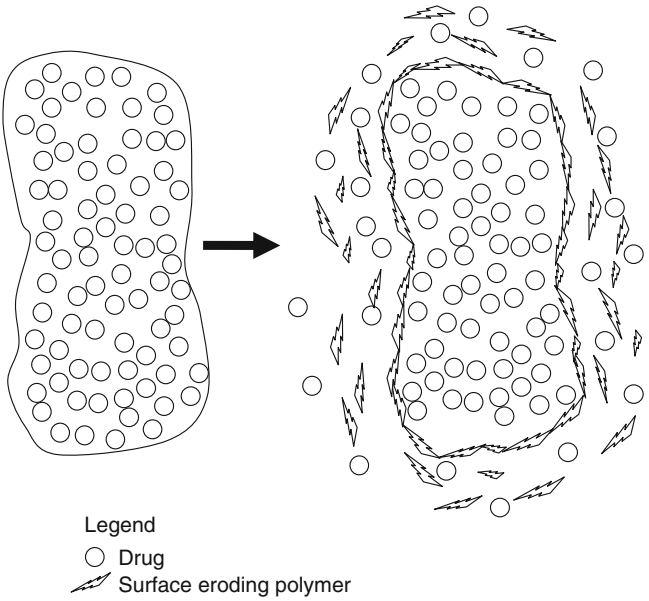


**Fig. 2.9** Diagrammatic representation of surface erosion. Drug trapped in the outer layers of the delivery system is released into the surrounding media following erosion of the surface of the polymer. Remaining drug is trapped in the delivery system; however, as time progresses, the polymeric devise erodes from the surface inward and reduces in size, eventually resulting in all drug being released

catalyzed, then erosion will be autocatalytic. Thus, bulk erosion may exhibit a sustained quiescent phase, followed by rapid disintegration of the matrix. Prior to disintegration, the dimensions of the device remain relatively constant.

Release of drug from bulk eroding polymers typically exhibits three stages. The first stage corresponds to drug that is released from the device surface or from pores that are connected to the surface. A second, latent stage follows, during which there is little degradation of polymer, and the remaining drug is trapped. In the third stage, the trapped drug is released rapidly when the polymer disintegrates.

Surface erosion, illustrated in Fig. 2.9, occurs either when water invasion is slow or hydrolysis is rapid. For example, polyanhydrides are exceptionally hydrophobic, and the hydrolytically labile anhydride bonds are protected from exposure to water in the interior of the polymer matrix. Thus, hydrolysis with accompanying drug release only occurs at or close to the surface.

A hallmark of surface erosion is that device dimensions decrease with time. If the device is formulated as a slab, then release will be approximately zero order, since each time interval will correspond to the erosion of a layer of polymer and release of drug incorporated in that layer. Erosion rate of cylinders and spheres decreases with time, however, due to reduction in exposed surface area. In principle, drug release correlates with erosion.

While the idealized mechanisms underlying bulk and surface erosion-controlled release are simple, practical systems exhibit extra complexity. Pure surface erosion is almost impossible to achieve, and diffusion of drug out of a matrix may occur ahead of erosion. The drug itself may draw in water, and osmotic stresses (due also to small chain fragments) in the polymer can lead to fracture and uneven penetration. In bulk eroding systems, degradation may even occur more rapidly in the interior of the device due to accumulation of autocatalytic erosion products while leaching of these products leads to slower erosion at the surface. When this is true, thicker matrices may erode more rapidly than thinner matrices.

This section has focused on erosion as a means for controlling drug release. However, it is also possible to program polymer degradation to occur after drug release is more or less complete. For example, hydrogels with degradable crosslinks have been prepared for release of proteins. As these crosslinks degrade, the hydrogel first swells, and then it eventually disintegrates when too few crosslinks are left to maintain the polymer network. Eventually, only primary polymer chains remain, and these are either excreted or resorbed. If degradation is slow, then release is controlled by protein diffusion through the swollen hydrogel network. If degradation of crosslinks is relatively rapid, then the swelling state of the network may change during the release process, and a complex interplay between swelling and diffusion will determine release kinetics.

Finally, we note that water need not be the only agent causing polymer degradation. Incorporating enzyme-labile chains or crosslinkers into a polymer network renders it susceptible to enzymatic degradation. For example, collagen and fibrin gels are specifically degraded in the presence of collagenase and plasmin, respectively. Enzyme-labile peptide fragments of collagen and fibrin can be incorporated into other hydrogels, yielding similar, enzyme specific degradation patterns. Enzyme-mediated degradation exhibits either surface- or bulk mediated erosion features, depending on the ability of enzyme to diffuse into the network and the reactivity of enzyme with the labile components of the network. Such enzyme-degradable systems may be useful in tissue engineering applications, reviewed in Chap. 17, as degradation of a hydrogel may be desirable with growth of tissue, which is signaled by local release of enzyme by cells.

Besides enzymes, small molecules can trigger erosion by cleaving polymer chains or crosslinks. For example, reducing agents can degrade polymers that include disulfide bonds. Since small molecules readily diffuse in even moderately swollen networks, bulk erosion is expected to predominate.

### *2.3.7 Regional Delivery and Targeting*

The benefit of a drug can be greatly enhanced if it can be targeted to its preferred site of action and kept away from sites associated with toxicity. Localization can occur at the organ, tissue, cellular, and subcellular compartment or organelle level. Direct administration at or near the site of action has already been discussed, with

examples provided by systems designed for drug delivery to the eye and coronary arteries. Direct injection of drug carriers into solid tumors or wound sites provides another example. As a third example, the growth, integration, and vascularization of surgically implanted tissue engineered constructs (Chap. 17) may require the localized and well-timed release of growth and angiogenesis factors.

We have also discussed nanocarriers that distribute preferentially in tumors by the EPR effect. To further specify delivery at the cellular level, it is necessary to coat the carrier surface with ligands that bind to specific cell surface features, such as polysaccharides or receptor proteins. Antibodies raised against antigens expressed at the cell surface are the most obvious targeting ligands, but in recent years peptide ligands have been designed based on other known interactions between cell surface receptors and both soluble and extracellular matrix proteins.

Since tumor cells express multiple drug resistance transporters, release of drug from the carrier at the cell surface may not result in increased drug uptake in target cells. The drug/nanocarrier combination is likely to be more effective if it can be brought into the cell by active processes, such as coated pit-mediated endocytosis. Once in the cell, the drug needs to dissociate from the carrier and exit the endosome, in either order. Further targeting of drug to an organelle may require that an organelle-specific "address label" be conjugated to the drug. For example, gene and protein delivery to the nucleus may require that a nuclear localization sequence be conjugated to the active biomolecule in order for the latter to be able to penetrate through nuclear pores.

Targeting systems are the subject of Chaps. 10–12 and further examples are provided in Chaps. 14–16.

## 2.4 Concluding Remarks

This chapter has illustrated a variety of controlled release strategies and underlying mechanisms. We emphasize that several mechanisms may be at play in a particular controlled release system, especially when more than one stage is involved. We also have reviewed methods to achieve the various goals of controlled release, including improved temporal presentation, drug protection, and localization of drug at the preferred site of action.

This chapter and this book are written from the perspective that controlled release adds substantial value to a drug. However, it should be recognized that development of a controlled-release product can be expensive. For many drugs, the extra expense may not be warranted on purely therapeutic grounds, although developers may pursue controlled release formulations for marketing, quality control, and regulatory reasons. Drugs with a relatively narrow therapeutic range, drugs that are eliminated rapidly from the body, drugs whose efficacy would be enhanced by targeting, and drugs that are susceptible to physiological degradation before absorption are probably the best candidates for controlled release.

Paradoxically, molecular entities that possess these attributes are often screened out early in the discovery and development stages. With improved understanding of controlled-release mechanisms and improved development of technologies, it may be possible to increase the number of bioactive molecules that can be developed fully into drug products [1–35].

## References

1. Amidon GL, Lee PI, Topp EM (eds) (2000) Transport processes in pharmaceutical systems. Marcel Dekker, New York
2. Amiji M (ed) (2005) Polymeric gene delivery. CRC, Boca Raton, FL
3. Arshady R (ed) (2003) Biodegradable polymers. Citus Ltd, London
4. Baker RW (1987) Controlled release of biologically active agents. Wiley, New York
5. Chasin M, Langer R (eds) (1990) Biodegradable polymers as drug delivery systems. Marcel Dekker, New York
6. Fang J, Nakamura H, Maeda H (2011) The EPR effect: unique features of tumor blood vessels for drug delivery, factors involved, and limitations and augmentation of the effect. Adv Drug Deliv Rev 63(3):136–151
7. Flynn GL, Yalkowski SH, Roseman TJ (1974) Mass transfer phenomena and models: theoretical concepts. J Pharm Sci 63:479–510
8. Friend DR (ed) (1992) Oral colon specific drug delivery. CRC, Boca Raton, FL
9. Grassi M, Grassi G, Lapasin R, Colombo I (eds) (2007) Understanding drug release and absorption mechanisms. CRC, Boca Raton, FL
10. Guy RH, Hadgraft J (eds) (2003) Transdermal drug delivery systems: second edition, revised and expanded. Marcel Dekker, New York
11. Hillery AM, Lloyd AW, Swarbrick J (2001) Drug delivery and targeting for pharmacists and pharmaceutical scientists. Taylor & Francis, Oxford
12. Kim C-J (1999) Controlled release dosage form design. Technomic, Lancaster, PA
13. Kydonieus A (ed) (1993) Treatise on controlled release. Marcel Dekker, New York
14. Langer R (1990) New methods in drug delivery. Science 249:1527–1533
15. Langer R (1998) Drug delivery and targeting. Nature 392:5–10
16. Langer R, Peppas NA (1981) Present and future applications of biomaterials in controlled drug delivery systems. Biomaterials 2:201–214
17. Langer R, Peppas NA (2003) Advances in biomaterials, drug delivery, and bionanotechnology. AIChE J 49:2990–3006
18. Lee VHL (ed) (1991) Peptide and protein drug delivery. CRC, Boca Raton, FL
19. Mahato R (ed) (2005) Biomaterials for delivery and targeting of proteins and nucleic acids. CRC, Boca Raton, FL
20. Mathiowitz E (ed) (1999) Encyclopedia of controlled drug delivery. Wiley, New York
21. Mathiowitz E, Chickering DE, Lehr C-M (eds) (1999) Bioadhesive drug delivery systems. Marcel Dekker, New York
22. Mitra AK (ed) (2003) Ophthalmic drug delivery systems. Marcel Dekker, New York
23. Ottenbrite R, Kim SW (eds) (2001) Polymeric drugs and drug delivery systems. CRC, Boca Raton, FL
24. Park K (ed) (1997) Controlled drug delivery. Challenges and strategies. American Chemical Society, Washington, DC
25. Park K, Shalaby WSW, Park K (1993) Biodegradable hydrogels for drug delivery. Technomic, Lancaster, PA
26. Peppas NA (ed) (1987) Hydrogels in medicine and pharmacy. CRC, Boca Raton, PA

27. Peppas NA, Hilt JZ, Khademhosseini A, Langer R (2006) Hydrogels in biology and medicine: from molecular principles to bionanotechnology. Adv Mater 18:1345–1380
28. Ranade VV, Hollinger MA (eds) (2003) Drug delivery systems. CRC, Boca Raton, FL
29. Rathbone MJ, Hadgraft J, Roberts MS (eds) (2003) Modified-release drug delivery technology. Marcel Dekker, New York
30. Saltzman WM (2001) Drug delivery: engineering principles for drug therapy. Oxford University Press, New York
31. Santini JT, Cima MJ, Langer R (1999) A controlled release microchip. Nature 397:335–338
32. Santus G, Baker RW (1995) Osmotic drug delivery: a review of the patent literature. J Contr Rel 35:1–21
33. Tanquary AC, Lacey RE (eds) (1974) Controlled release of biologically active agents. Plenum, New York
34. Uchegbu IF, Schatzlein AG (eds) (2008) Polymers in drug delivery. Taylor and Francis, Boca Raton, FL
35. Wise DL (ed) (2000) Handbook of pharmaceutical controlled release technology. Marcel Dekker, New York

# Part II
# Delivery Materials

# Chapter 3
# Hydrophobic Polymers of Pharmaceutical Significance

**Osama A. Abu-Diak, Gavin P. Andrews, and David S. Jones**

**Abstract** Over the recent years, the use of hydrophobic polymers for drug delivery applications has dramatically increased. These materials offer particular promise for controlled/sustained-drug release, thereby enhancing the pharmacological effects of the drug. These controlled/sustained release drug delivery systems can result in considerable clinical and economic advantages. The physicochemical properties of the hydrophobic polymers and the design of the drug delivery system both affect the mechanism by which a drug diffuses from the polymeric system. This chapter provides an overview of the different types of pharmaceutical hydrophobic polymers, drug delivery applications of these polymers.

## 3.1 Introduction

The use of hydrophobic polymers in the pharmaceutical industry has received great attention within the last few decades (8), due principally to the clinical and economic benefits that can be achieved from the use of these polymers. Hydrophobic polymers can be used to produce drug delivery systems that can sustain or control drug release for longer periods in the gastrointestinal tract (GI tract) and hence result in more reproducible and uniform drug blood levels (88, 100). As a result of extending the pharmacological effects of the drug, both drug dose and frequency of administration can be reduced, thereby resulting in a lower incidence of side effects. These effects can enhance the cost effectiveness and safety profiles of drugs and thus improve patient compliance (8).

Sustained release dosage forms based on hydrophobic polymers can be fabricated either as matrix systems (19, 72), in which the drug is dispersed homogeneously

O.A. Abu-Diak • G.P. Andrews • D.S. Jones (✉)
School of Pharmacy, Queen's University of Belfast, 97, Lisburn Road, Belfast BT9 7BL, UK
e-mail: D.Jones@qub.ac.uk

J. Siepmann et al. (eds.), *Fundamentals and Applications of Controlled Release Drug Delivery*, Advances in Delivery Science and Technology,
DOI 10.1007/978-1-4614-0881-9_3, 

in the polymeric matrix, or as reservoir systems, in which the polymer surrounds the drug core, release being controlled by the nature of membrane (40, 86). The hydrophobic properties of these polymers reduce/minimize water penetration into and through the system, resulting in retarded drug diffusion and hence lowered drug release rate (41, 53).

Moreover, hydrophobic polymers can be used efficiently in drug colon targeting applications with combination to the pH-dependent hydrophilic polymers to provide more controlled drug release behavior in colonic fluid medium (3). Additionally, hydrophobic polymers have been used efficiently to target the highly water soluble polysaccharides such as pectin and chitosan to colon, where enzymatic degradation can take place (35, 80).

Hydrophobic polymers may be broadly categorized as biodegradable or nonbiodegradable. Biodegradable polymers have advantages over the nonbiodegradable polymers when employed as controlled release implants as there is no need to remove the implants physically after completion of therapy (98).

Within the pharmaceutical literature, different manufacturing technologies have been utilized to prepare hydrophobic polymer based drug delivery systems. These include wet granulation (38, 63), direct compression (53, 72), hot melt extrusion (HME) (79, 104), injection molding (69, 70), wet mass extrusion–spheronization (1, 2, 15), and film coating (21, 40). Under certain circumstances, drug release from hydrophobic polymeric platforms may be insufficient to ensure that the required mass of drug is released over the normal residence time of the drug delivery system within the GI tract. Therefore, the inclusion of hydrophilic polymer(s) within such formulations may be used to enhance the drug release rate, thereby ensuring complete drug release within 12–24 h (81, 91). Conversely, the inclusion of hydrophobic polymers within hydrophilic polymer platforms containing highly water soluble drugs can be a useful strategy to ensure successful controlled drug delivery (8, 53).

Examples of pharmaceutically approved hydrophobic polymers that are currently being investigated for drug delivery applications include: ammoniomethacrylate copolymers (Eudragit® RL/RS), poly(ethylacrylate–methylmethacrylate) (Eudragit® NE30D), ethylcellulose, polyvinylacetate, polyethylenevinylacetate, and poly(ε-caprolactone). This chapter provides an overview of hydrophobic polymers that are approved for pharmaceutical use, and describes examples of their applications as drug delivery systems.

## 3.2 Examples of Hydrophobic Polymers and Their Drug Delivery Applications

There are several examples of hydrophobic polymers that have been/are currently being used for pharmaceutical applications. This section seeks to describe the key properties of these polymers and to provide examples of their pharmaceutical uses. In the interest of brevity, only the most common polymer and uses have been described.

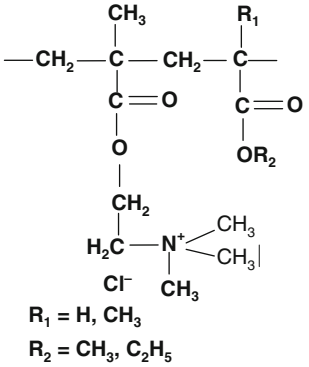


**Fig. 3.1** Chemical structure of ammoniomethacrylate copolymers

## *3.2.1 Ammoniomethacrylate Copolymers*

Eudragit® RL100/RLPO and RS100/RSPO are referred to as ammoniomethacrylate copolymers (Types A and B, respectively) in the USP/NF 23 monograph. RL100 and RS100 are colorless clear to cloudy granules, whereas RLPO and RSPO are white fine powders. RL100/RLPO and RS100/RSPO have a slight amine-like odor and are freely soluble in acetone and alcohols (73). They are copolymers of ethyl acrylate, methyl methacrylate, and a low content of a methacrylic acid ester with quaternary ammonium groups (trimethyl ammonioethyl methacrylate chloride) (Fig. 3.1) of average molecular weight about 150,000 $gmol^{-1}$. Eudragit® RL100/RLPO and RS100/RSPO are chemically defined as poly (ethyl acrylate, methyl methacrylate, trimethyl ammonio ethyl methacrylate chloride) in the ratio of monomers, viz., 1:2:0.2 and 1:2:0.1, respectively. Eudragit® RL100/RLPO contains a higher percentage of ammoniomethacrylate units (8.85–11.96% on dry substance) compared to Eudragit® RS100/RSPO (4.48–6.77% on dry substance) (USP/NF). The ammonium groups are present as salts, making these polymers water permeable and physiologically pH-independent (45, 83). As a result of the difference in the content of ammonium groups, RL100/RLPO and RS100/RSPO differ in their water permeation rate, which is considerably higher in case of RL100/RLPO (72). It was reported that films prepared from RL are freely permeable to water, whereas films prepared from RS are only slightly permeable to water (88).

### 3.2.1.1 Hydrophobic Matrices Based on Ammoniomethacrylate Copolymers

The hydrophobic and the pH-independent properties of RL/RLPO and RS100/RSPO polymers make them suitable for producing oral controlled/sustained release drug delivery systems. Different approaches can be used for producing controlled/sustained release dosage forms. Among these different approaches, matrix tablets are still considered to be one of the most efficient and interesting from both the economic and the process development aspects (51). It was reported that RLPO has

better compaction properties than RSPO (72), and hence matrix tablets of excellent flow and physical properties can be produced using RLPO by direct compression even in absence of other excipients (10).

Due to the differences in their permeability, RLPO and RSPO can be used in combination to produce matrix tablets of desired sustained release drug profiles. RLPO and RSPO have been combined to modulate the release kinetics of theophylline from matrix tablets prepared by direct compression (72). The release rate of theophylline from RLPO matrix tablets was observed to be too high; however, this was effectively modified by the addition of RSPO to the matrix. The use of an RLPO–RSPO ratio of 1:9 resulted in formulations that offered a similar release profile of theophylline to that observed with commercial formulations.

As previously described, the release of a water soluble drug from a water soluble polymeric platform is often rapid, and therefore, hydrophobic polymers may be included within the matrix formulation to offer greater control of drug release. In this scenario, hydrophobic polymers reduce the rapid diffusion of the dissolved drug through the hydrophilic gel network (8). For this purpose, Eudragit® RSPO was combined with a hydrophilic polymer, Methocel K100M, to reduce water penetration and retard the drug release of venlafaxine from matrix tablets prepared by direct compression (53). The desired 16 h sustained release profile was achieved using drug/polymer/ ratio of 1:2.2:2.2 and followed Higuchi kinetics, with cumulative release proportional to the square root of time (see Chap 6).

In an alternative strategy, matrix tablets have been developed by direct compression based on combination of hydrophobic polymers (RSPO and RLPO) and a gelling hydrophilic polymer, hydroxypropylmethylcellulose (HPMC 60SH) to achieve a (20 h) sustained release formulation of diltiazem hydrochloride (8). Film coating of the matrix tablets using Eudargit® NE30D produced a delivery system in which the release of diltiazem hydrochloride was pH-independent (from 1.2 to 7.4). Eudragit® RSPO was employed to delay the penetration of dissolution medium into the matrix, thereby decreasing the drug release rate.

Inclusion of RLPO/RSPO as hydrophobic polymers in matrix tablets containing gelling hydrophilic polymers such as HPMC can be used efficiently to further sustain the release of water soluble drugs. The hydrophobicity of these polymers reduces water penetration into the matrix tablets, which results in further retardation of drug release rate.

#### 3.2.1.2 Solid Dispersions Based on Ammoniomethacrylate Copolymers

It has been demonstrated that the use of hydrophobic matrices containing solid drug dispersions, i.e., systems in which a drug is molecularly dispersed within a polymeric platform, is a valuable strategy in the production of sustained release products. For example, solid dispersions of verapamil hydrochloride with Eudragit® RLPO or Kollidon® SR, a directly compressible polymeric blend composed primarily of polyvinylacetate (PVAc) and povidone (PVP), were prepared using solvent evaporation method and then compressed into tablets (75). Drug release from RLPO tablets at

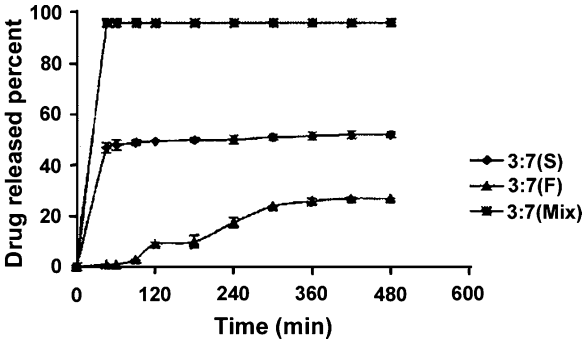


**Fig. 3.2** Drug release profiles from solid dispersions (3:7 Eudragit RLPO–RSPO containing 7% metoprol tartrate, particle size of 200 μm) prepared with fusion method (F) or solvent method (S) compared with physical mixture of drug with the same ratios of polymers in phosphate buffer solution (pH 6.8) ($n = 3$) (88)

drug–polymer ratio (1:3) were able to sustain the drug release up to 12 h, whereas Kollidon® SR tablets at similar drug–polymer ratio only sustained drug release up to 8 h. In a similar fashion, Dahiya et al. prepared solid dispersions of promethazine hydrochloride and Eudragit® RLPO and RS100 at different drug–polymer ratios (1:1 and 1:5) by solvent evaporation. The authors reported that drug release from the solid dispersions was highly dependent on the type and amount of the polymer used. Dissolution of the drug from RLPO matrices was greater than from systems containing RS100, due principally to the higher swelling and permeation characteristics of RLPO over a range of pH values (1.2–7.4). Tablets prepared by direct compression from RLPO solid dispersions (ratio of 1:5) displayed extended release of drug for 12 h (19).

In a similar fashion solid dispersions of metoprolol tartrate (7, 15, or 25% w/w) were prepared by melting and solvent methods using different ratios of RLPO–RSPO (0:10, 3:7, 5:5, 7:3, and 10:0) (88). At high drug contents (15 and 25% w/w), a significant initial burst effect was observed as a result of a nonhomogeneous dispersion of the drug in the polymer and the unincorporated metoprolol around the matrix, which immediately dissolves in the medium. Solid dispersions containing higher ratios of RSPO showed slower release rates than those containing higher ratios of RLPO due to its lower permeability. Drug release from dispersions was slower than from the physical mixtures (Fig. 3.2). Furthermore, at similar drug–polymer ratios, drug release from systems prepared using the fusion method was significantly slower than that from systems prepared using the solvent method. Figure 3.3a and b show the effect of particle size on the drug release profiles from platforms containing 7% drug loading and composed of two different ratios of RLPO and RSPO (3:7 prepared using the fusion method and 5:5 prepared using the solvent method). Solid dispersions with a particle size of 100 μm containing (7% w/w) of metoprolol and 5:5 ratio of RLPO–RSPO prepared by solvent method or 3:7 ratio of RLPO–RSPO with fusion method had similar release pattern to Lopressor® sustained-release tablets up to 8 h.

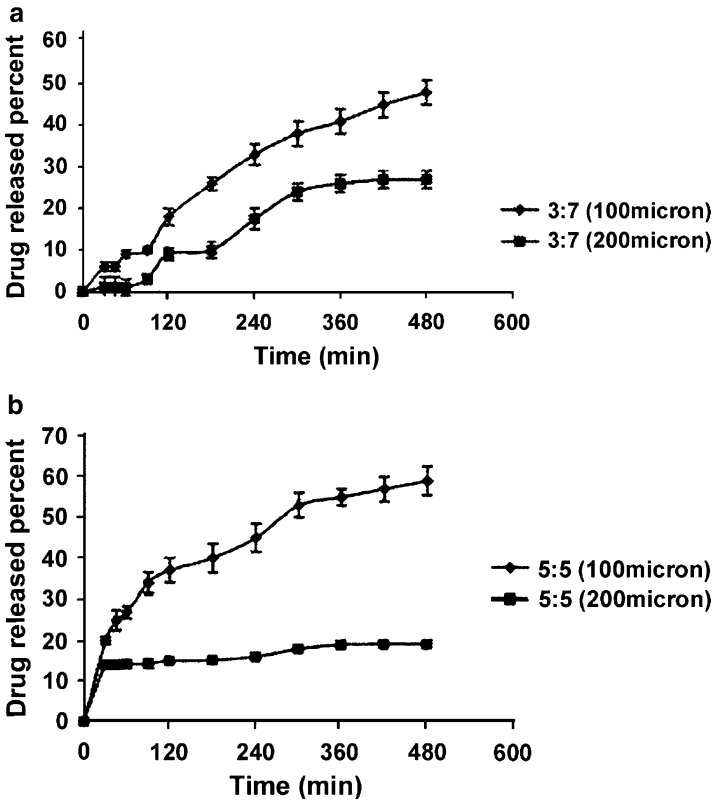


**Fig. 3.3** Drug release profiles from solid dispersions of (**a**) 3:7 (by fusion method), (**b**) 5:5 (by solvent method) Eudragit RLPO–RSPO with different particle sizes containing 7% metoprolol tartrate in phosphate buffer solution (pH 6.8) ($n = 3$). (88)

RLPO and RSPO can be used alone or in combination as efficient carriers in solid dispersions to produce sustained drug release profiles. Matrix tablets prepared from RLPO/RSPO solid dispersions usually have slower drug release profiles than matrix tablets prepared from the corresponding physical mixtures. The intimate contact between the drug and the polymers within the solid dispersions plays an important role in such further retardation effects. Preparation method, drug loading, RLPO–RSPO ratio, and particle size of the solid dispersions are important factors that can affect the drug release profile, which need to be considered in optimizing the final formulation to achieve the desired drug release profile.

#### 3.2.1.3 Hot Melt Extrusion Based on Ammoniomethacrylate Copolymers

Hot melt extrusion (HME) technology has received great interest in the pharmaceutical industry over the last decade as an alternative manufacturing process to produce

different dosage forms such as tablets, pellets, and granules (9, 16). This process has been employed to prepare controlled release hydrophobic matrix tablets using Eudragit® RSPO (79, 104). For efficient hot melt extrusion, a plasticizer may be required to facilitate polymer flow and to lower processing temperatures, thereby reducing drug degradation during the process and increasing the stability of the drug and the polymer. In addition to the state of the drug and the composition of the formulation, plasticizers may affect drug release from hydrophobic polymeric matrices prepared by HME. For example, citric acid monohydrate (a solid state plasticizer) has been shown to enhance the release of diltiazem hydrochloride from melt extruded RSPO tablets, due principally to enhanced pore formation, improved drug dispersion in the plasticized polymer and the increase in the polymer aqueous permeability (79). The influence of the level of triethylcitrate (TEC), a water soluble plasticizer, on drug release from hot melt extrudates containing RSPO and highly water soluble drugs, chlorpheniramine maleate and diltiazem hydrochloride has been described by Zhu et al., (103, 104). In these studies, chlorpheniramine maleate, but not diltiazem hydrochloride, was observed to offer solid state plasticization of Eudragit® RSPO on RSPO (103, 104). The release of chlorpheniramine maleate from the melt extrudates was increased with increasing TEC concentration. The authors attributed these observations to the leaching out of triethyl citrate from the melt extrudates, thereby creating channels within the melt extruded matrix tablet (11, 104). Therefore, it is important to consider the effects of the plasticizer type and amount used on the drug release profiles during formulation of hot melt extruded dosage forms. Additionally, these formulations must be monitored in terms of drug release properties during stability as liquid plasticizers may leach out of the formulations during storage as a result of their volatility. Additionally, the change in the amount of plasticizer during storage may affect the mechanical properties of hot-melt extruded matrix tablets, which significantly may affect the drug release profiles and drug bioavailability.

#### 3.2.1.4 Drug Coatings Based on Ammoniomethacrylate Copolymers

Eudragit® RL and RS are commonly used in film coating of solid dosage forms to produce controlled release reservoir systems. Typically, the coating is applied as an organic polymer solution or as an aqueous colloidal polymer dispersion (64). Aqueous colloidal dispersions of Eudragit® RL30D and RS30D (30% w/w dry substance) form water-insoluble pH independent swellable films across which drug release may be effectively controlled (93). Film coatings that have been deposited from aqueous polymeric dispersions are frequently associated with physical aging during storage (39). The mechanism by which films are formed from aqueous polymeric dispersions is more complex than those encountered with organic polymer solutions (24). In aqueous systems, the coalescence of individual colloidal particles and the interdiffusion of polymeric particles must occur to form a continuous film (28). Since the coalescence of the colloidal polymer particles into a homogeneous film is often incomplete after coating with aqueous polymeric dispersions, further coalescence of the colloidal particles occurs during storage as the polymer relaxes toward an

equilibrium state (termed physical aging) (99). These effects result in a decreased void volume (porosity), an increase in polymer tortuosity, and a resultant decrease in the rate of drug release (102). Therefore, with aqueous colloidal polymer dispersions, a thermal after-treatment (curing) at elevated temperatures (above the Tg of the polymer) is often recommended to complete film formation and to avoid changes in the release profiles during storage (4, 97). Various strategies have been proposed to overcome aging of hydrophobic coatings of pharmaceutical dosage forms.

For example,

1. Storage of the dosage form at high humidity may increase the physical aging of polymeric films and therefore this factor must be controlled (96, 99).
2. The degree of coalescence of the colloidal polymeric particles increases as the mass of plasticizer in the coating increases, producing less pronounced aging effects (4).
3. Thermal treatment along with high concentrations of micronized talc stabilizes drug release from pellets coated by Eudragit® RS/RL30D plasticized with TEC (54).
4. Curing of Eudragit® RS30D film coated pellets at an elevated temperature (above the glass transition temperature), Tg of the polymeric film, after coating is efficient in reducing the aging effects and hence in stabilizing drug release rate (99).
5. Inclusion of the enteric polymer of high Tg, e.g., Eudragit® L100-55, to RS30D, results in a more stabilized drug release rate from theophylline coated pellets during storage compared with the pellets coated with RS30D alone without Eudragit® L100-55. These results are mostly attributed to the network change in the RS polymeric films as a result of the formation of miscible system between Eudragit® L100-55 and RS30D, which has a single higher Tg than the Tg of RS polymeric films without L100-55. This increase in the Tg of RS30D polymeric films with the inclusion of L100-55 results in a greater restriction of the mobility of RS30D polymeric films. Hence, the aging effects during storage under accelerated conditions are minimized (99).
6. Addition of a hydrophilic polymer, hydroxyethylcellulose (HEC) to Eudragit® RS30D dispersions stabilizes the drug release rates during storage. This stabilization effect of HEC is related to the formation of an immiscible secondary phase surrounding the colloidal particles, which interferes with further coalescence of the colloidal RS particles (102).
7. The ionic electrostatic interactions between lactic acid (LA) and aqueous dispersions of RL and RS minimize the physical aging effects, resulting in stabilized paracetamol release from the coated tablets during storage at different accelerated storage conditions (59).

To reduce the physical aging problems associated with the incomplete coalescence of polymer particles after coating from aqueous colloidal dispersions, it is important to consider the coating formulations in terms of adding optimum type and amount of plasticizer that can aid in coalescence of polymer particles during coating process. Consequently, more reproducible drug release properties can be

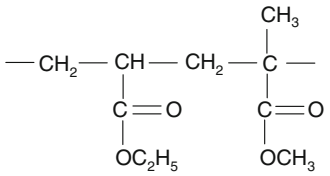


**Fig. 3.4** Chemical structure of ethylacrylate and methylacrylate copolymer

achieved following storage. Additionally, as described in the aforementioned examples, additives can play important roles in such stabilization based on their miscibility and interactions with the coating polymer. Regarding the process, it is better to leave the batch after the coating process for a certain period of time for drying at a specific temperature above the glass transition temperature of the coating polymer to improve the coalescence of polymer particles.

### *3.2.2 Poly(ethylacrylate–methylmethacrylate)*

Eudragit® NE 30D and Eudragit® NE 40D (30% and 40% w/w dry substance, respectively) are aqueous colloidal dispersions based on neutral (nonionic) poly (ethylacrylate–methylmethacrylate) (2:1) copolymers (Fig. 3.4) that are prepared by emulsion polymerization. Highly flexible film coatings may be produced by poly (ethylacrylate–methylmethacrylate) aqueous dispersions without using any plasticizers, as the polymer has low minimum film-forming temperature (5°C) (6, 85). This film flexibility is related to strong interchain interactions (6). The nonionic hydrophobic properties of poly(ethylacrylate–methylmethacrylate) make this polymer suitable to be used as a sustained release coating material for solid dosage forms forming pH-independent drug release profiles over entire pH range of the GI tract (95). There have been several examples of the use of this polymer, as a coating, for the development of controlled drug release formulations. For example, Tian et al (86) reported the formulation of a controlled release pellet formulation containing venlafaxine hydrochloride that was coated with Eudragit® NE30D. Using this approach, a once daily sustained release formulation was possible. Similarly, improved release profiles of ofloxacin were obtained from pellets that had been coated with Eudragit® NE30D and Eudragit® L30D55, at a ratio of 1:8 (w/w) and containing the plasticizer diethyl phthalate (DEP) (18). Finally, using a combination of Eudragit NE 30D and Eudragit L30D-55 as coatings, El-Malah and Nassal (25) successfully reported the delayed release of verapamil hydrochloride.

Poly(ethylacrylate–methylmethacrylate) has additionally been successfully been employed for colonic delivery of therapeutic agents. For example, in one study theophylline pellets were coated with Eudragit® NE30D aqueous dispersions, containing various pectin HM:Eudragit® RL30D ionic complexes (80). It was shown that without pectinolytic enzymes, the release of theophylline from the coated pellets, after an initial latency phase, occurs linearly as a function of time and was dependent on the pectin HM content. The lowest theophylline release from the coated pellets was

obtained whenever the pectin HM content was 20.0% w/w (related to Eudragit® RL), i.e., when the complexation between pectin HM and Eudragit® RL is optimal. Consequently, the coating permeability and the release of theophylline from the coated pellets was also minimal resulting in the slowest drug release rate. The degradation and leaching of pectin from the coatings in presence of the pectinolytic enzymes resulted in the solvation, swelling of Eudragit® RL. This, in turn, induced stresses in the film coatings, thereby facilitating (increasing) the release of theophylline (80).

Film coatings based on poly(ethylacrylate–methylmethacrylate) are efficient in sustaining release profiles of different drugs. The composition of the cores can determine the permeability of the surrounding film-coatings and consequently the drug release profiles through these films.

### *3.2.3 Ethylcellulose*

Ethylcellulose (EC) is a semisynthetic cellulose derivative that widely used in the pharmaceutical industry as a pharmaceutical coating due to its excellent film forming properties, good mechanical strength, and relatively low cost (42). This polymer has been widely used to control drug release from solid dosage forms (63).

#### 3.2.3.1 Hydrophobic Matrices Based on Ethylcellulose

Owing to its hydrophobic properties, ethylcellulose reduces the penetration of water into the solid polymeric matrix, hence reducing drug release. Combination of this polymer with hydroxypropylmethylcellulose (HPMC K100M) in matrix tablets prepared by direct compression was reported to sustain the release of venlafaxine hydrochloride up to 16 h at drug–ethylcellulose–HPMC ratio of 1:2.2:2.7 with the release following Higuchi kinetics (53). Similarly, inclusion of ethylcellulose, at a concentration of 14% w/w of the matrix of tablets composed of RLPO and RSPO prepared by wet granulation resulted in an extended release profile of zidovudine for up to 12 h, whereas only a maximum of 6 h sustained release profile was achieved from the matrix tablets formulated without ethylcellulose (41). The authors accredited these observations to the effects of ethylcellulose on the hydrophobicity of the tablet matrix and the concomitant reduction in the rate of penetration of dissolution fluid into the matrix. Moreover, the addition of ethylcellulose to the RLPO and RSPO formulations reduced the initial burst release of zidovudine in the acidic medium, hence decreasing the chances of dose dumping. The drug release kinetics the indicated a combined effect of diffusion and erosion release mechanisms from the matrix tablets. In a further example, ibuprofen mini tablets containing HPMC or ethylcellulose were produced by direct compression. At similar drug/polymer ratio, tablets based on ethylcellulose provided a greater sustained release of drug than the HPMC counterpart (50). A final example of the use of ethylcellulose involves the formulation of sustained-release bilayer matrix tablets of propranolol hydrochloride, reported by Patra et al. (63). In these, one

layer was formulated (using superdisintegrants) to offer rapid release to provide the loading dose of the drug. The second layer was composed of Eudragit® RLPO, Eudragit® RSPO and ethylcellulose and was designed to provide controlled release. The hydrophobic polymers were added at three different drug/polymer ratios (1:0.5, 1:1, and 1:1.5). The increase in the proportion of ethylcellulose resulted in a decrease in drug release. Using drug/ethylcellulose ratios of 1:1 and 1:1.5 resulted in the desired release profile over the test period of 12 h, whereas only the drug/polymer ratio of 1:1.5 for RLPO and RSPO polymers resulted in the 12-h sustained release profiles.

The previously mentioned examples suggest a high efficiency of ethylcellulose to act as a drug release retardant from matrix tablets when it is used alone or in combination with other hydrophobic or hydrophilic retardant polymers to further sustain the drug release profiles. This sustained drug release effect by ethylcellulose is highly dependent on the concentration of polymer used and is mostly related to its hydrophobicity.

Sustained-release hot-melt extruded matrices of ibuprofen (89) and metoprolol tartrate (90) have been produced using ethylcellulose. No plasticizer was required to process ibuprofen containing formulations due to the solid state plasticization effect of ibuprofen. Conversely, dibutyl sebacate was added as a plasticizer at 50% (w/w) of the ethylcellulose concentration to metoprolol tartrate formulations. Controlled drug release was achieved from these formulations. Furthermore, the authors illustrated that the release of each drug may be enhanced by the addition of xanthan gum due to the higher liquid uptake into these formulations.

The effect of the concentration and molecular weight of a hydrophilic polymer (polyethylene glycol or polyethylene oxide) on metoprolol tartrate release kinetics from ethylcellulose minimatrices were described by Verhoeven et al. (91, 92). The authors found that increasing the concentration of either hydrophilic polymer increased the rate of drug release, whereas the influence of molecular weight of the hydrophilic polymers was dependent on its concentration. The mechanisms of drug release from these formulations were strongly dependent on the composition of the formulations. At high concentrations of polyethylene glycol or polyethylene oxide (20%) and/or intermediate concentrations (2.5–10%) of low molecular weight variants of these hydrophilic polymers ($\leq$100,000 Da), drug diffusion was the predominant release mechanism. Conversely, at low concentrations of these hydrophilic polymers contents and intermediate concentrations of high molecular weight (1,000,000 and 7,000,000 Da.) variants of these polymers, changes in matrix porosities significantly affected the diffusion of the drug from the ethylcellulose-based minimatrices.

A hot melt extruded ethylcellulose pipe surrounding a drug-containing hydroxypropyl methylcellulose (HPMC)–Gelucire® 44/14 core was developed (55). The developed drug delivery system was successful in producing a sustained zero-order, erosion controlled, release profile that was independent of drug solubility. Shortening the length of the ethylcellulose cylinder accelerated drug release, while modifying the diameter did not affect the drug release rate. These unexpected results were justified by the authors based on calculating the relative surface area of the matrix core of the matrix-in-cylinder system, where the drug release rate was

independent of the diameter of the matrix-in-cylinder and it was only a function of the length of ethylcellulose cylinder. A randomized cross over in vivo study in dogs revealed that the matrix-in-cylinder system containing propranolol hydrochloride has an ideal sustained release profile with constant plasma levels maintained over 24 h (56). Moreover, administration of the matrix-in-cylinder system resulted in a fourfold increase in propranolol bioavailability when compared with a commercial sustained release formulation (Inderal®).

Sustained release injection molded matrix tablets of metoprolol tartrate were developed based on ethylcellulose (69). Formulations containing ethylcellulose, plasticized with dibutyl sebacate, and low substituted hydroxypropylcellulose (L-HPC) were first melt extruded and subsequently injection molded into tablets at different temperatures. Incomplete drug release (<50%) within 24 h was observed from tablets containing only ethylcellulose (4 cps). Increasing the mass of L-HPC in the formulation resulted in significantly higher drug release rates due to its hydrophilic swelling properties, achieving complete drug release after 16 h. Based on the Ritger–Peppas classification, the release mechanism shifted from diffusion controlled, in formulations without L-HPC, toward anomalous transport at higher L-HPC concentration. In the later case, the drug release occurred via drug diffusion through the micro capillary network formed after dissolution of metoprolol clusters in the tablet and by disruption of the matrix structure due to the swelling properties of L-HPC. Similarly, the effect of hydroxypropylmethylcellulose (HPMC) on the release of metoprolol tartrate from ethylcellulose matrix tablets prepared by combination of HME and injection molding was studied. Tablets containing 30% metoprolol and 70% ethylcellulose showed an incomplete drug release within 24 h (<50%). Substituting part of the ethylcellulose fraction with HPMC (HPMC–ethylcellulose ratios of 2:5 and 1:1) resulted in faster and constant drug release rates. Formulations containing 50% HPMC had a complete and first order drug release profile with drug release controlled via the combination of diffusion and swelling/erosion (70).

These examples suggest the efficiency of ethylcellulose to act as a controlled release platform in hot melt extrusion using either liquid plasticizers or the solid state plasticizing effects of the drug. HME based on ethylcellulose was efficient in producing sustained release dosage forms such as tablet matrices, minimatrices, matrix-in-cylinder, injection molded tablets. Incorporation of hydrophilic additives such as xanthan gum, polyethylene glycol/polyethylene oxide, L-HPC, and HPMC can enhance the diffusion of drug from ethylcellulose matrix due to the hydrophilicity of these additives that result in increasing water penetration through the matrix and hence increasing drug diffusion.

#### 3.2.3.2 Coatings Based on Ethylcellulose

Ethylcellulose is widely used to coat solid dosage forms, being applied either as organic polymeric solutions or aqueous colloidal polymeric dispersions (65). Two aqueous colloidal polymeric dispersions are available for use in controlled release

applications (Aquacoat® ECD and Surelease®). These are highly concentrated (30% and 25% w/w ethylcellulose, respectively) with relatively low viscosities (71).

It has been reported that theophylline release rates from pellets coated with aqueous ethylcellulose dispersions (Aquacoat®) were too slow due to the poor permeability of ethylcellulose films to drug diffusion (81). This problem was overcome by the inclusion of a low percentage of a water soluble poly (vinyl alcohol)-poly (ethylene glycol) (PVA-PEG) graft copolymer. Even at low loadings, this hydrophilic copolymer significantly increased the rate and extent of water uptake and hence the permeability of the films to drug diffusion. It was demonstrated that a broad spectrum of pH independent drug release rates were obtained from drug loaded pellets by simply varying the PVA–PEG graft copolymer content. In addition to its contribution in enhancing theophylline release rate from EC coated pellets, it has been shown by Siepmann et al. (82) that the addition of small amounts of PVA-PEG graft-copolymer to aqueous EC dispersions provides long term stable drug release patterns even upon open storage under stress conditions. The presence of this hydrophilic compound can be expected to trap water within the film coatings during coating and curing, thus facilitating polymer particle coalescence.

Drug release from ethylcellulose-coated pellets (coated using Surelease®) has been reported to be highly dependent on drug type and coating level (74). As the coating load of Surelease® increased the rate of drug release decreases. It was shown that at similar coating load metoclopramide hydrochloride (a water-soluble cationic drug) release from the ethylcellulose coated pellets was slower than from diclofenac sodium (a sparingly soluble anionic drug) coated pellets. The slower release of metoclopramide hydrochloride may be due to an in situ formation of a poorly soluble complex of the cationic drug and the anionic ammonium oleate present in Surelease® as a surfactant. This complex, because of its large molecular size, may diffuse more slowly through the film, causing a reduction in the release rate of metoclopramide hydrochloride.

A dry powder coating technology using micronized ethylcellulose has been developed for application in a fluidized bed coater (Glatt® GPCG-1, Wurster insert), and this technology has been applied as a pellet coating to produce a sustained-release propranolol hydrochloride dosage form (65). The dry coating process (batch size = 1.2 kg) was performed using a powder feed rate of 10–14 g $min^{-1}$ at a product temperature 45–47°C. It was shown that despite its high Tg (133.4°C), micronized ethylcellulose powder can be used for dry powder coating (with the aid of a plasticizer). Although the coated pellets had an uneven surface, an extended drug release profile was produced using a coating level of 15% w/w after curing the pellets at 80°C for 24 h. This curing step was required for complete coalescence of the polymer particles. Both the cured and uncured ethylcellulose coated pellets showed unchanged drug release profiles upon storage at room temperature for 3 years mostly because of its high Tg (Fig. 3.5). In a subsequent study, it was shown that EC coated pellets prepared using the dry powder coating required a higher coating level than pellets coated with the aqueous dispersions, Aquacoat® ECD, to achieve a similar extended release profile (66). In addition, a higher amount of plasticizer was used with the dry powder coating. Pellets coated with the ethanolic ethylcellulose solution had the slowest release.

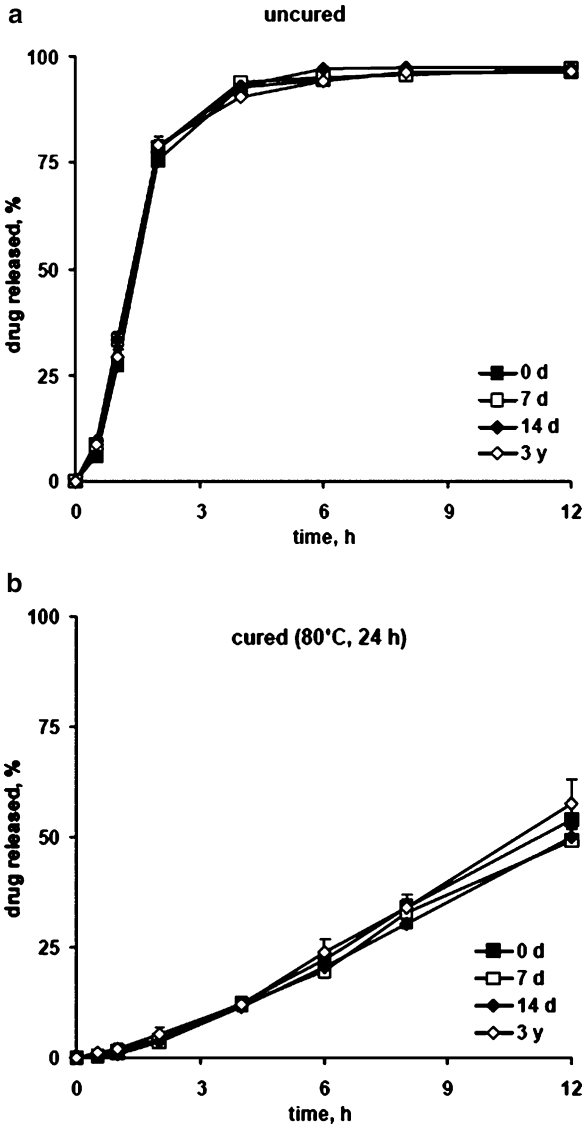


**Fig. 3.5** Effect of storage at room temperature on propranolol hydrochloride release from ethylcellulose powder coated pellets: (**a**) uncured pellets; and (**b**) cured pellets at 80°C for 24 h (coating level, 30.3%; 40% acetylated monoglyceride) (65)

The use of ethylcellulose as a coating polymer is highly efficient in producing sustained drug release profiles. Drug release from ethylcellulose based film-coatings depends on the coating level, drug solubility, and the form in which the polymer is applied in the coating process, i.e. as powder, aqueous colloidal dispersion, or organic solution. Addition of hydrophilic additives such as PVA-PEG graft copolymer may increase the drug release rate and the stability of ethylcellulose-based coated dosage forms.

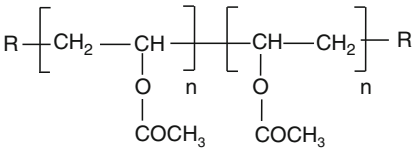


**Fig. 3.6** Chemical structure of polyvinylacetate (PVAc)

## *3.2.4 Polyvinylacetate*

Polyvinylacetate (PVAc) is a thermoplastic synthetic amorphous homopolymer (Fig. 3.6) with a relatively low glass transition temperature (Tg = 32.7 and 35.9°C for PVAc of molecular weight 12,000 and 45,000, respectively). It is a predominantly water insoluble polymer that is used to produce controlled release drug delivery systems.

### 3.2.4.1 Hydrophobic Matrices Based on Polyvinylacetate

The thermoplastic properties of PVAc and its relatively low glass transition temperature make this polymer particularly suitable for HME. Sustained-release theophylline matrix tablets based on PVAc have been prepared by HME at a temperature of 70°C (101). The cylindrical extrudates were either cut into tablets or ground into granules and compressed with other excipients into tablets. Theophylline was present in the extrudate in its crystalline form and was released from the tablets by diffusion. Increasing the granule size resulted in a significant decrease in drug release rate as a result of the longer diffusion pathway. Higher drug loading levels resulted in faster drug release due to presence of drug clusters on the surface of the matrix. Inclusion of water soluble polymers such as hydroxypropylcellulose and polyethylene oxide in the matrix resulted in significant increase in drug release rates due to the formation of highly porous structure as a result of the dissolution of these hydrophilic polymers, and hence more drug diffusion through the matrix system.

Kollidon® SR is an extended release excipient based on polyvinylacetate and polyvinylpyrrolidone (8:2) and is used in preparation of sustained-release matrix tablets. Extended-release matrix tablets containing ZK 811 752, a weakly basic drug, were successfully prepared based on Kollidon® SR (38). Addition of the (highly swellable) maize starch and (the water-soluble) lactose accelerated the drug release in a more pronounced manner compared to the water insoluble calcium phosphate. Drug release rate from the matrix tablets prepared by wet granulation was faster than the tablets prepared by direct compression. Stability studies conducted at 25°C/60% RH, 30°C/70% RH and 40°C/75% RH showed no drug degradation upon storage at 25°C/60% RH, 30°C/70% RH and 40°C/75% RH for up to 6 months. Reproducible drug release patterns were obtained for matrix tablets stored at 25°C/60% RH, 30°C/70% RH for up to 6 months that remained almost unchanged compared to the initial release profiles. On the contrary, drug release

from matrix tablets stored at 40°C/75% RH decreased slightly. After 6 h initially 53% drug has been released versus only 47 and 43% drug release after storage for 3 and 6 months, respectively. These changes in the in vitro drug release for tablets stored at 40°C/75% RH may be related to the increase in the hardness of the tablets as a result of storing the matrix tablets at 40°C above the glass transition (Tg) of the polymer (PVA/PVP) (Tg = 35°C) and then storing them at room temperature before dissolution testing.

In another study, hot-melt extruded extended-release minimatrices were developed based on Kollidon® SR using ibuprofen and theophylline as model drugs (60). It was shown that ibuprofen had solid-state plasticization effects on Kollidon® SR, whereas no such effects were observed on the polymer by theophylline. Increasing ibuprofen concentrations resulted in a significant decrease in the Tg of Kollidon® SR and the torque generated during the HME process. According to the differential scanning calorimetry (DSC) and X-ray diffraction (XRD) analyses, ibuprofen (<35% w/w) remained in an amorphous or dissolved state within the extrudates, whereas theophylline was dispersed in the polymer matrix. This can be related to the higher miscibility of ibuprofen with Kollidon® SR than theophylline especially that ibuprofen showed solid state plasticization effects on Kollidon® SR, whereas theophylline did not show such effects. The drug release rates were increased with increasing amounts of ibuprofen or theophylline in the hot-melt extrudates. A higher processing temperature resulted in decreasing theophylline release rate, which was most probably due to the formation of extrudates that have more dense structure and lower porosity as a result of decreasing the melt viscosity during HME with increasing the processing temperature. Conversely, ibuprofen release rate increased with increasing extrusion temperature, which was mostly due to the increase in the water uptake by the extrudates as a result of the plasticizing effects of ibuprofen on Kollidon® SR. Inclusion of a plasticizer (Triethyl citrate) at 5% w/w in theophylline/Kollidone® SR formulations was sufficient to improve their processibility. Theophylline release rate from hot melt extrudates decreased with increasing TEC level due to formation of a denser matrix. Inclusion of Klucel® LF as a hydrophilic additive to the melt extrudates resulted in increasing ibuprofen and theophylline release rates as a result of its leaching out from the extrudates, creating a more porous matrix.

The low glass transition temperature of PVAc makes Kollidon® SR suitable for HME. Sustained-release hot melt extruded matrix tablets and minimatrices can be produced efficiently based on Kollidon® SR. The drug release from Kollidon® SR formulations depends on the drug loading, type and amount of hydrophilic additives added to the formulations. Attention must be taken upon storage of PVAc based matrices at temperatures above its glass transition temperature. The effect of extrusion temperature on the drug release profiles from Kollidon® SR matrices depends on the type of drug used and its miscibility and interactions with Kollidon® SR, which as well may affect the solid state properties of the drug within the matrix tablets.

### 3.2.4.2 Coatings Based on Polyvinylacetate

In addition to its use as a tablet matrix, polyvinylacetate and its copolymers have been used as a coating for solid dosage forms. For example, Dashevsky et al. (21) investigated the properties of Kollicoat® SR, an aqueous colloidal dispersions based on polyvinylacetate (27%, w/v) and polyvinylpyrrolidone (2.5%, w/v), that can be used for sustained release coatings. The release of propranolol HCl from Kollicoat® SR 30D coated pellets was reported to decrease with increasing coating level. Using this approach, a 12-h controlled release profile was obtained for propranolol hydrochloride, in which the mass of the coating was from 10 to 15% w/w.

Based on their mechanical and dissolution properties, coatings based on chitosan/Kollicoat® SR 30D films have been proposed for use as colon targeted systems. The extent of film digestion in simulated colonic fluid (SCF) by rat cecal bacterial enzymes or β-glucosidase was directly proportional to the amount of chitosan present within the film (94). The release rate of theophylline from tablets coated by different chitosan/Kollicoat® RS 30D blends was influenced by the amount of chitosan present in the film and the coating levels. Increasing the coating levels resulted in a decrease in the release rate due to the increased diffusion pathway. The drug release was faster in simulated gastric fluid (SCF) than that in simulated intestinal fluid (SIF) since chitosan dissolved and leached from the coating in acidic medium as a result of the protonation of its amine groups. Faster drug release in SCF than in simulated gastric fluid (SGF) or SIF demonstrated the susceptibility of chitosan to degradation by the bacterial enzymes in SCF. Drug release was controlled by polymer relaxation. The in vivo pharmacokinetic studies of the coated tablets in rats showed delayed Tmax, decreased Cmax, and prolonged mean residence time (MRT), indicating the efficiency of Chitosan/Kollicoat® SR30D coating system to target drug delivery to the colon (46).

SAG/ZK, a potent drug candidate for the oral treatment of inflammatory diseases, has a short biological half life and it exhibits a pH-dependent solubility because of its weakly basic nature. Drug release from conventional pellet formulations decreased with increasing pH values of the dissolution medium. Extended drug release pellets were prepared by extrusion/spheronization followed by film coating with Kollidon® SR (28). To achieve pH-independent drug release, different organic acids were incorporated into the core pellets. The addition of fumaric acid was found to lower the pH values within the core pellets during the release of SAG/ZK in phosphate buffer pH 6.8. Therefore, increased release rates at higher pH values were observed leading to pH-independent drug release. Conversely, drug release remained pH-dependent for pellets containing tartaric and adipic acid as a result of their lower acidic strength and higher aqueous solubility of these acids.

These aforementioned examples indicate that Kollicoat® SR can produce efficient sustained release film-coatings. Drug release rate from these film-coatings depends on the coating level and the composition of the cores and the films.

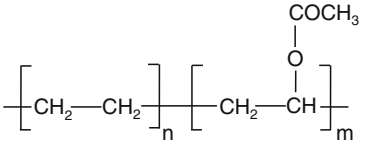


**Fig. 3.7** Chemical structure of polyethylenevinylacetate copolymer (EVA)

## *3.2.5 Polyethylenevinylacetate*

Polyethylenevinylacetate (EVA) copolymer is composed of long chains of ethylene and vinyl acetate groups randomly distributed throughout the chains (Fig. 3.7). The weight percent of vinyl acetate usually varies from 10 to 40%, with the remainder being ethylene. EVA is inexpensive, nonbiodegradable, biocompatible polymer that has been approved for human use by Food and Drug Administration (43, 77, 78).

### 3.2.5.1 Hydrophobic Matrices Based on Polyethylenevinylacetate

EVA copolymer has been widely used as a polymeric matrix to produce controlled-release polymeric implant devices of high (macromolecules) or small molecular weight compounds (30). HME is a highly viable method of producing implants of EVA as it is thermoplastic, heat processable and flexible (58, 87). The vast majority of papers that have employed EVA have been designed as biomedical implants, some of which are described in this section.

Implanon® is a controlled-release implants based on EVA copolymer developed by Organon using HME technology. Implanon® is designed to release progestagen for a period of 3 years (87). The properties of the polymer can be adapted by varying the amount of vinyl acetate (12, 76). By increasing the amount of vinyl acetate, the crystallization process of the polyethylene segments is disturbed. As a consequence, the copolymer becomes less crystalline and thus more permeable (32, 44).

Haik-Creguer et al. (30) developed very small uniformly sized implants based on microextrusion technology. Using microextrusion it was possible to incorporate small masses of drugs into EVA polymer and consequently this technology was successfully used to produce controlled release implant devices (based on EVA polymer) of several compounds such as alpha-methyl-*p*-tyrosine, diazepam, quinolinic acid, and phencyclidine. Each substance was slowly released from the polymer for up to 120 days at daily rates varying from 18.4 μg for phencyclidine to 97.6 μg/day for diazepam. Release was dependent on the hydrophilic properties of the drug. Drug release resulted in the formation of pores formation within the EVA matrix thereby facilitating further release.

An implantable stent containing 5-fluorouracil (5-FU) was fabricated by coating a film, composed of one 5-FU-containing EVA copolymer layer and one drug free EVA protective layer, around a commercial self-expandable nitinol stent with the drug free EVA layer facing the lumen of the stent (27). The stents with various drug loadings were implanted into rabbit esophagus. Quantitative analysis of 5-FU

showed that the 5-FU concentration adjacent to the esophageal tissue was overwhelmingly higher than that in serum or liver at all the investigation time points until 45 days. The authors concluded that the 5-FU-loaded esophageal stent offered long term, effective local drug delivery.

A biocompatible sustained-release subretinal implant was developed successfully based on coating nitinol, poly(methyl methacrylate), or chromic gut core filament with a drug eluting polymer matrix composed of a mixture of poly(butyl methacrylate) and poly(ethylene-co-vinyl acetate) (5). Triamcinolone acetonide and sirolimus were used as model drugs. The implant had the ability to elute triamcinolone acetonide for a period of at least 4 weeks without eliciting an inflammatory response or complications, suggesting good biocompatibility and efficacy.

Controlled DNA delivery systems based on EVA implantable polymer matrices were developed and characterized (52). Herring sperm DNA and bacteria phage lambda DNA were encapsulated as a model system. Released DNA concentration was determined by fluoroassays. Agarose electrophoresis was used to determine the dependence of release rate on DNA size. Both small and large DNA molecules (herring sperm DNA, 0.1–0.6 kb; GFP, 1.9 kb; lambda DNA, 48.5 kb) were successfully encapsulated and released from EVAc matrices. Release from the DNA-EVAc systems was diffusion controlled. When coencapsulated in the same matrix, the larger lambda DNA was released more slowly than herring sperm; the rate of release scaled with the DNA diffusion coefficient in water. The chemical and biological integrity of released DNA was not changed. These low cost and adjustable controlled DNA delivery systems, using the FDA approved implantable/injectable material, EVAc could be useful for in vivo gene delivery, such as DNA vaccination and gene therapy.

The sublingual formulation of buprenorphine has been associated with variable drug blood levels and requires frequent dosing that limits patient compliance. Sustained release buprenorphine implants based on EVA (26 mm in length and 2.4 mm in diameter) were developed to improve patient compliance (37). In vitro studies showed a steady-state drug release (0.5 mg/implant/day). In vivo pharmacokinetic studies conducted in beagle dogs showed that peak buprenorphine concentrations were generally reached within 24 h after implantation. Steady state plasma levels were attained between 3 and 8 weeks, and were maintained for study duration (52 weeks), with a calculated mean release rate of $0.14 \pm 0.04$ mg/implant/day. There were no serious adverse effects reported. These results suggest that this delivery system can provide long term stable systemic buprenorphine levels that may improve patient compliance, thereby improving outcome for opioid dependent patients.

Pharmacotherapy treatment for alcoholism is limited by poor compliance, adverse effects, and fluctuating drug levels after bolus administration. To overcome compliance issues, a sustained release implant based on EVA and containing nalmefene, an opioid antagonist used for treatment of alcoholism was developed by melt extrusion and characterized (17). The extrudates of 2.8 mm $\times$ 27 mm rods were further coated with EVA to optimize release. In vitro release after subcutaneous implantation into rats was high from the uncoated rods, and they were depleted

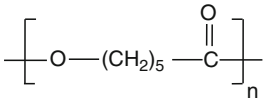


**Fig. 3.8** Chemical structure of poly(ε-caprolactone) (PCL)

of drug fairly quickly; however, EVA coatings maintained release over longer periods. The 25 wt% coated rods provided in vitro release of 0.36 mg/day/rod and in vivo release of 0.29 mg/day/rod over 6 months, and showed dose dependent nalmefene plasma concentrations. After explanation, nalmefene plasma concentrations were undetectable by 6 h. A sustained release nalmefene rod provided 6 months of drug with no adverse effects.

A nonbiodegradable polymeric episcleral implant based on EVA was developed as a controlled intraocular delivery system of betamethasone (BM) to the posterior pole of the eye (34). For in vivo studies, the implants were placed on the sclera of the eyes of rabbits so that the drug releasing surface could attach to the sclera at the posterior pole. The implant released BM in a zero-order fashion for 4 weeks, thereby maintaining drug concentrations in the retina-choroid above the concentrations effective for suppressing inflammatory reactions, suggesting that the episcleral implant can be a useful drug carrier for the intraocular delivery of BM to the posterior part of the eye.

These examples indicate the efficiency of EVA copolymer as a sustained release carrier in implantable devices. Its ability to produce long term drug release profiles make EVA based implants applicable in wide range of drug delivery systems such as ocular, subcutaneous, sublingual, gene delivery, esophageal for local or systemic effects.

### *3.2.6 Poly(ε-caprolactone)*

Poly(ε-caprolactone) (PCL) is an aliphatic, biodegradable, semicrystalline polyester (Fig. 3.8) (31, 49, 61) that has found several applications as a biodegradable drug delivery system. PCL is highly permeable to small drug molecules of molecular weight less than 400 Da (67). This high permeability of PCL coupled with the long controllable induction period prior to polymer weight loss enables the development of delivery devices that offer diffusion-controlled drug delivery (67). Increasing PCL crystallinity reduces the permeability of the polymer, thereby lowering the drug release rate. In particular, the slow rate of degradation of PCL renders it suitable for long-term delivery of therapeutic agents, for periods greater than 1 year (62, 84). Conversely, for many drug delivery applications, the degradation rate of PCL is too slow to directly influence drug release. Therefore, to increase the rate of degradation, PCL has been copolymerized with other more hydrophilic cyclic esters, including L-LA and γ-butyrolactone (23, 31). Additionally, it has been demonstrated that copolymerization of ε-caprolactone with hydrophilic segments

such as poly (ethylene glycol) (PEG), methoxy poly (ethylene glycol) (MPEG) or poly(ethylene oxide)-poly(propylene oxide)-poly(ethylene oxide) (PEOPPO-PEO) can effectively change the hydrophobicity and improve the biodegradability of PCL (20, 29, 36). The properties of these copolymers can be controlled to exhibit various degradation rates and permeability behaviors. Moreover, the degradation rate of PCL may also be manipulated by addition of acidic and basic additives, which can facilitate polymer degradation (68). For example, the incorporation of oleic acid caused an increase in the rate of degradation that was proportional to the amount of acid added. An increased rate of degradation was also obtained with the addition of decylamine, as the amine functional group can launch a nucleophilic attack on the ester bond. Lin et al. (47) incorporated primary, secondary and tertiary alkylamines into PCL. Primary alkylamines caused the most rapid degradation, whereas the effect of the tertiary alkylamines was not significant. Inclusion of a polar phospholipid, phosphorylcholine (PC), into PCL (PC–PCL) effectively improved the hydrophilicity and biodegradability of PCL (57). It was shown that ibuprofen release rate was faster from PC–PCL matrix systems than that from PCL systems with drug release mechanism governed mainly by diffusion kinetics (48).

PCL has been employed for drug delivery to the eye. For example, a drug delivery system based on combinations of different molecular weights of PCL was developed (7). Increasing the proportion of high-MW PCL to low-MW PCL decreased the rate of degradation of PCL and consequently resulted in slowing down 5-FU release. These devices showed promising in vivo results for the treatment of proliferative retinopathy. Similarly, implants composed of PLGA-co-PCL were investigated in vivo and were found to inhibit inflammation in experimental uveitis by controlling cyclosporine A release, with no systemic or local toxicity (22).

A sustained release monolithic implant based on gabapentin (GBP)-loaded PCL matrices that produces constant plasma levels over a 1-week period was designed by melt-molding/compression procedure to overcome the clinical problems associated with the chronic treatment with gabapentin (GBP) (13). In vitro release studies showed that the uncoated implants displayed release profiles according to a pseudo-first order model. In order to further regulate the release, two sided coated implants where drug free layers would perform as membranes controlling the delivery rate were prepared. A more moderated burst effect and a relatively linear (zero-order) release between days 1 and 7 were apparent. Implants were investigated in vivo by inserting them subcutaneously in mice and the plasma levels monitored during 10 days. Findings indicated that after a more pronounced release during day 1 and the achievement of the levels in blood comparable to a twice a day intraperitoneal management, relatively constant levels were attained until day 7. Overall results support the usefulness of this manufacturing method for the production of implants to attain more prolonged GBP release profiles.

Combination of twin-screw extruder and injection molding technologies were efficient in producing a long term sustained release PCL implants containing praziquantel (PZQ), a broad-spectrum antiparasite drug (14). Uniform dispersion of the drug within the polymeric matrices were achieved whatever the drug

loadings (6.25–50%). X-ray diffraction analyses showed that PZQ exists primarily in its crystalline state in the fabricated implants. In vitro release studies showed that all implants, regardless of drug loading, exhibit similar release patterns and about 70% of PZQ was released after 365 days from PCL implants. It has been demonstrated that the release of PZQ was based on a gradual diffusion of the drug from the exterior to interior of the implants.

Poly(ε-caprolactone) can be used to fabricate implantable devices that can sustain drug release profiles for moderate and long terms. The drug release from poly(ε-caprolactone) based implants is diffusion controlled and depends on the molecular weight, crystallinity, and chemical modification of the polymer. Additionally, inclusion of additives to poly(ε-caprolactone) based implantable devices can modify the degradation rate of the polymer making these devices more flexible to be used in many drug delivery applications.

## 3.3 Conclusions

This chapter provides an overview of examples of hydrophobic polymers that are used in pharmaceutical industry and focuses on the applications of these polymers in the drug delivery systems. The diversity in the physicochemical properties of these hydrophobic polymers provides potential opportunities to develop drug delivery systems with tailored drug release profiles that can meet different clinical conditions and can improve the patient compliance, the cost effectiveness, and the safety profile of the drug. Based on the valuable clinical and economic benefits that the hydrophobic polymers can provide, it is expected that the significance of hydrophobic polymers as drug delivery systems will continue to evolve in the near future.

## References

1. Abbaspour M, Sadeghi R, Garekani HA (2005) Preparation and characterization of ibuprofen pellets based on Eudragit RSPO and RLPO or their combination. Int J Pharm 303:88–94
2. Abbaspour M, Sadeghi R, Garekani HA (2007) Thermal treating as a tool to produce plastic pellets based on Eudragit RSPO and RLPO aimed for tableting. Eur J Pharm Biopharm 67:260–267
3. Akhgari A, Sadeghi F, Garekani HA (2006) Combination of time-dependent and pH-dependent polymethacrylates as a single coating formulation for colonic delivery of indomethacin pellets. Int J Pharm 320:137–142
4. Amighi K, Moës AJ (1996) Influence of plasticizer concentration and storage conditions on the drug release rate from Eudragit® RS 30 D film-coated sustained-release theophylline pellets. Eur J Pharm Biopharm 42(1):29–35
5. Beeley NR, Stewart JM, Tano R, Lawin LR, Chappa RA, Qiu G, Anderson AB, de Juan E, Varner SE (2005) Development, implantation, in vivo elution, and retrieval of a biocompatible, sustained release subretinal drug delivery system. J Biomed Mater Res 76A(4):690–698

6. Bodmeier R, Paeratakul O (1994) Mechanical properties of dry and wet cellulosic and acrylic films prepared from aqueous colloidal polymer dispersions used in the coating of solid dosage forms. Pharm Res 11(6):882–888
7. Borhani H, Rahimy MH, Peymann GA (1993) Sustained release of 5-FU from biodegradable-matrix delivery for intraocular application: in vitro and in vivo evaluation. Invest Ophthalmol Vis Sci 34:1488 (Suppl.)
8. Boyapally H, Nukala RK, Douroumis D (2009) Development and release mechanism of diltiazem HCl prolonged release matrix tablets. Drug Deliv 16(2):67–74
9. Breitenbach J (2002) Melt extrusion: from process to drug delivery technology. Eur J Pharm Biopharm 54:107–117
10. Buckton G, Ganderton D, Shah R (1988) In vitro dissolution of some commercially available sustained-release theophylline preparations. Int J Pharm 42:35–39
11. Bruce LD, Shah NH, Malick AW, Infeld MH, McGinity JW (2005) Properties of hot-melt extruded tablet formulations for the colonic delivery of 5-aminosalicylic acid. Eur J Pharm Biopharm 59:85–97
12. Brinker KC (1977). EVA Copolymers: raw materials for hot melt pressure-sensitive adhesives. Adhes Age 20(8):38–40
13. Carcaboso AM, Chiappetta DA, Höcht C, Blake MG, Boccia MM, Baratti CM, Sosnik A (2008) In vitro/in vivo characterization of melt-molded gabapentin-loaded poly(epsilon-caprolactone) implants for sustained release in animal studies. Eur J Pharm Biopharm 70:666–673
14. Chenga L, Guo S, Wub W (2009) Characterization and in vitro release of praziquantel from poly(ε-caprolactone) implants. Int J Pharm 377:112–119
15. Chivate AA, Poddar SS (2008) Designing, optimization and characterization of sustained release matrix pellets prepared by extrusion spheronization containing mixtures of proteolyrtic enzymes. Curr Drug Deliv 5:265–274
16. Crowley MM, Zhang F, Repka MA, Thumma S, Upadhye SB, Battu SK (2007) Pharmaceutical applications of hot-melt extrusion: Part I. Drug Dev Ind Pharm 33:909–926
17. Costantini LC, Kleppner SR, McDonough J, Azar MR, Patel R (2004) Implantable technology for long-term delivery of nalmefene for treatment of alcoholism. Int J Pharm 283:35–44
18. Cui Y, Zhang Y, Tang X (2008) In vitro and in vivo evaluation of ofloxacin sustained release pellets. Int J Pharm 360:47–52
19. Dahiya S, Pathak K, Sharma R (2008) Development of extended release coevaporates and coprecipitates of promethazine HCl with acrylic polymers: formulation considerations. Chem Pharm Bull 56(4):504–508
20. Das GS, Rao GHR, Wilson RF, Chandy T (2000) Colchicine encapsulation within poly (ethylene glycol)-coated poly (lactic acid)/poly (epsiloncaprolactone) microspheres-controlled release studies. Drug Deliv 7:129–138
21. Dashevsky A, Wagner K, Kolterb K, Bodmeier R (2005) Physicochemical and release properties of pellets coated with Kollicoat® SR 30 D, a new aqueous polyvinyl acetate dispersion for extended release. Int J Pharm 290:15–23
22. Dong X, Shi W, Yuan G, Xie L, Wang S, Lin P (2006) Intravitreal implantation of the biodegradable cyclosporine: a drug delivery system for chronic uveitis. Graefes Arch Clin Exp Ophthalmol 244:492–497
23. Duda A, Biela T, Libiszowski J, Penscek S, Dubois P, Mecerreyes D, Jerome R (1997) Block and random copolymers of ε-caprolactone. Polym Degrad Stab 59:215–222
24. El-Malah Y, Nazzal S (2008) Effect of Eudragit® RS 30D and talc powder on verapamil hydrochloride release from beads coated with drug layered matrices. AAPS PharmSciTech 9 (1):75–83
25. El-Malah Y, Nazzal S (2008) Novel use of Eudragit® NE 30D/Eudragit® L 30D-55 blends as functional coating materials in time-delayed drug release applications. Int J Pharm 357:219–227
26. Fukumori Y (1994) Coating of multiparticulates using polymeric dispersion. In: Ghebre-Sellassie I (ed) Multiparticulate oral drug delivery-drugs and pharmaceutical science, vol 65. Marcel Dekker, New York, NY, pp 79–117

27. Guo S, Wang Z, Zhang Y, Lei L, Shi J, Chen K, Yu Z (2010) In vivo evaluation of 5-Fluorouracil containing self-expandable nitinol stent in rabbits: efficiency in long-term local drug delivery. J Pharm Sci 99:3009–3018, (www.interscience.wiley.com). DOI 10.1002/jps.22066
28. Guthmann C, Lipp R, Wagner T, Kranz H (2007) Development of a multiple unit pellet formulation for a weakly basic drug. Drug Dev Ind Pharm 33:341–349
29. Ha JC, Kim SY, Lee YM (1999) Poly (ethylene oxide)-poly (propylene oxide)-poly (ethylene oxide) (Pluronic)/Poly (ε-caprolactone) (PCL) amphiphilic block copolymeric nanospheres. I. Preparation and characterization. J Control Release 62:381–392
30. Haik-Creguer KL, Dunbar GL, Sabel BA, Schroeder U (1998) Small drug sample fabrication of controlled release polymers using the microextrusion method. J Neurosci 80:37–40
31. Jiang G, Jones IA, Rudd CD, Walker GS (2003) Modelling the post treatment of model implants prepared by in situ polymerized poly (ε-caprolactone) using a BF3-glycerol catalyst. Polymer 44:1809–1818
32. Kagayama A, Mustafa R, Akaho E, Khawam N, Truelove J, Hussain A (1984) Mechanism of diffusion of compounds through ethylene vinyl acetate copolymers. I. Kinetics of diffusion of 1-chloro-4-nitrobenzene, 3,4-dimethylphenol and 4-hexylresorcinol. Int J Pharm 18:247–258
33. Karasulu HY, Ertan G, Köse T (2000) Modelling of theophylline release from different geometrically erodible tablets. Eur J Pharm Biopharm 49:177–182
34. Kato A, Kimura H, Okabe K, Okabe J, Kunou N, Ogura Y (2004) Feasibility of drug delivery to the posterior pole of the rabbit eye with an episcleral implant. Invest Ophthalmol Vis Sci 45 (1):238–244
35. Kaur K, Kim K (2009) Studies of chitosan/organic acid/Eud RS/RL-coated system for colonic delivery. Int J Pharm 366:140–148
36. Kim MS, Seo KS, Hyun H, Khang G, Cho SH (2006) Controlled release of bovine serum albumin using MPEG-PCL diblock copolymers as implantable protein carriers. J Appl Polym Sci 102:1561–1567
37. Kleppner SR, Patel R, McDonough J, Costantini LC (2006) In-vitro and in-vivo characterization of a buprenorphine delivery system. J Pharm Pharmacol 58:295–302
38. Kranz H, Wagner T (2006) Effects of formulation and process variables on the release of a weakly basic drug from single unit extended release formulation. Eur J Pharm Biopharm 62:70–76
39. Kucera SA, McGinity JW (2007) Use of proteins to minimize the physical aging of Eudragit® sustained release films. Drug Dev Ind Pharm 33:717–726
40. Kucera SA, Stimpel D, Shah NH, Mallick W, Infeld MH, McGinity JW (2008) Influence of fumed silicon dioxide on the stabilization of Eudragit® RS/RL 30D film-coated theophylline pellets. Pharm Dev Technol 13:245–253
41. Kuksal A, Tiwary AK, Jain NK, Jain S (2006) Formulation and in vitro, in vivo evaluation of extended-release matrix tablet of zidovudine: influence of combination of hydrophilic and hydrophobic matrix formers. AAPS PharmSciTech 7(1):E1 (http://aapspharmscitech.org)
42. Lai HL, Pitt K, Craig DQM (2010) Characterization of the thermal properties of ethylcellulose using differential scanning and quasi-isothermal calorimetric approaches. Int J Pharm 386:178–184
43. Langer R, Brem H, Tapper D (1981) Biocompatibility of polymeric delivery systems for macromolecules. J Biomed Mater Res 15:167–277
44. Lee EK, Londsdale HK, Baker RW (1985) Transport of steroids in poly(etherurethane) and poly(ethylene vinyl acetate) membranes. J Memb Sci 24:125–143
45. Lehmann K (1997) O., R. Chemistry and application properties of polymethacrylate coating systems. In: McGinity JW (ed) Aqueous polymeric coatings for pharmaceutical dosage forms. Marcel Dekker, New York, pp 101–176
46. Li-Fang F, Wei H, Yong-Zhen C, Bai X, Qing D, Feng W, Min Q, De-Ying C (2009) Studies of chitosan/Kollicoat SR 30D film-coated tablets for colonic drug delivery. Int J Pharm 375:8–15

47. Lin W, Flanagan D, Linhardt RJ (1994) Accelerated degradation of polycaprolactone by orgainic amines. Pharm Res 11:1030–1034
48. Lin M, Meng S, Zhong W, Li Z, Du Q, Tomasik P (2008) Novel biodegradable blend matrices for controlled drug release. J Pharm Sci 97(10):4240–4248
49. Liu L, Li Y, Liu H, Fang Y (2004) Synthesis and characterization of chitosan-graft-polycaprolactone copolymers. Eur Polym J 40:2739–2744
50. Lopes CM, Manuel J, Lobo S, Costa P, Pinto JF (2006) Directly compressed mini matrix tablets containing ibuprofen: preparation and evaluation of sustained release. Drug Dev Ind Pharm 32:95–106
51. Lordi N (1986) Sustained release dosage forms. In: Lachman L, Lierberman HA, Kanig JL (eds) The theory and practice of industrial pharmacy. Lea and Febiger, Pheladelphia, pp 430–478
52. Luo D, Woodrow-Mumford K, Belcheva N, Saltzman WM (1999) Controlled DNA delivery systems. Pharm Res 16(8):1300–1308
53. Makhija SN, Vavia PR (2002) Once daily sustained release tablets of venlafaxine, a novel antidepressant. Eur J Pharm Biopharm 54:9–15
54. Maejima T, McGinity JW (2001) Influence of additives on stabilizing drug release rates from pellets coated with acrylic polymers. Pharm Dev Technol 6(2):211–221
55. Mehuys E, Vervaet C, Remon JP (2004) Hot-melt extruded ethylcellulose cylinders containing a HPMC-Gelucire® core for sustained drug delivery. J Control Release 94:273–280
56. Mehuys E, Vervaet C, Gielen I, Van Bree H, Remon JP (2004) In vitro and in vivo evaluation of a matrix-in-cylinder system for sustained drug delivery. J Control Release 96:261–271
57. Meng S, Zhong W, Chou LL, Wang Q, Liu ZJ, Du QG (2007) Phosphorylcholine end-capped poly ε-caprolactone: a novel biodegradable material with improved antiadsorption property. J Appl Polym Sci 103:989–997
58. Miyazaki S, Ishi K, Sugibayashi K, Morimoto Y, Takada M (1982) Antitumor effect of ethylene–vinyl acetate copolymer matrices containing 5-fluorouracil on ehrlich ascites carcinoma in mice. Chem Pharm Bull 30:3770–3775
59. Omari DM, Sallam A, Abd-Elbary A, El-Samaligy M (2004) Lactic acid-induced modifications in films of Eudragit® RS and RL aqueous dispersions. Int J Pharm 274:85–96
60. Özgüney I, Shuwisitkul D, Bodmeier R (2009) Development and characterization of extended release Kollidon® SR mini-matrices prepared by hot-melt extrusion. Eur J Pharm Biopharm 73:140–145
61. Park H, Park K, Shalaby WSW (1993) Types of biodegradable hydrogels. In: Biodegradable hydrogels for drug delivery. Technomic, Lancaster, PA, pp 35–67
62. Park JH, Ye M, Park K (2005) Biodegradable polymers for microencapsulation of drugs. Molecules 10:146–161
63. Patra CN, Kumar AB, Pandit HK, Singh SP, Devi MV (2007) Design and evaluation of sustained release bilayer tablets of propranolol hydrochloride. Acta Pharm 57:479–489
64. Pearnchob N, Bodmeier R (2003) Dry powder coating of pellets with micronized Eudragit® RS for extended drug release. Pharm Res 20(12):1970–1976
65. Pearnchob N, Bodmeier R (2003) Coating of pellets with micronized EC particles by a dry powder coating technique. Int J Pharm 268:1–11
66. Pearnchob N, Bodmeier R (2003) Dry polymer powder coating and comparison with conventional liquid-based coatings for Eudragit® RS, ethylcellulose and shellac. Eur J Pharm Biopharm 56:363–369
67. Pitt CG, Jeffcoat AR, Zweidinger RA, Schindler A (1979) Sustained drug delivery systems. I. The permeability of poly(ε-caprolactone), poly(DL-lactic acid) and their copolymers. J Biomed Mater Res 13:497–507
68. Pitt CG, Gu Z (1987) Modification of the rates of the chain cleavage of polycaprolactone and related polyesters. J Control Release 19:283–292
69. Quinten T, Gonnissen Y, Adriaens E, De Beer T, Cnudde V, Masschaele B, Van Hoorebeke L, Siepmann J, Remon JP, Vervaet C (2009) Development of injection moulded matrix

tablets based on mixtures of ethylcellulose and low-substituted hydroxypropylcellulose. Eur J Pharm Sci 37:207–216
70. Quinten T, De Beer T, Vervaet C, Remon JP (2009) Evaluation of injection moulding as a pharmaceutical technology to produce matrix tablets. Eur J Pharm Biopharm 71:145–154
71. Rekhi SR, Jambhekar SS (1995) Ethylcellulose – a polymer review. Drug Dev Ind Pharm 21 (1):61–77
72. Rodreiguez L, Caputo O, Cini M, Cavallari C, Grecchi R (1993) In vitro release of theophylline from directly-compressed matrices containing methacrylic acid copolymers and/or dicalcium phosphate dihydrate. Farmaco 48(11):1597–1604
73. Rowe R, Sheskey P, Owen S (2006) Handbook of pharmaceutical excepients, 5th edn. Pharmaceutical Press/The American Pharmaceutical Association, London, UK/Washington, DC, pp 462–468
74. Sadeghi F, Ford JL, Rajabi-Siahboomi A (2003) The influence of drug type on the release profiles from Surelease-coated pellets. Int J Pharm 254:123–135
75. Sahoo J, Murthy PN, Biswal S, Manik (2009) Formulation of sustained release dosage form of verapamil hydrochloride by solid dispersion technique using Eudragit® RLPO or Kollidon® SR. AAPS PharmSciTech 10(1):27–33
76. Salyer IO, Kenyon AS (1971) Structure and property relationships in ethylene-vinyl acetate copolymers. J Polym Sci 9:3083–3103
77. Sam AP (1992) Controlled release contraceptive devices: a status report. J Control Release 22:35–46
78. Shastri PV (2002) Toxicology of polymers for implant contraceptives for women. Contraception 65:9–13
79. Schilling SU, Bruce CD, Shah NH, Malick AW, McGinity JW (2008) Citric acid monohydrate as a release-modifying agent in melt extruded matrix tablets. Int J Pharm 361:158–168
80. Semdé R, Amighi K, Devleeschouwer MJ, Moës AJ (2000) Studies of pectin HM:Eudragit® RL:Eudragit® NE film-coating formulations intended for colonic drug delivery. Int J Pharm 197:181–192
81. Siepmann F, Hoffmann A, Leclercp B, Carlin B, Siepmann J (2007) How to adjust desired drug release patterns from ethylcellulose-coated dosage forms. J Control Release 119:182–189
82. Siepmann F, Muschert S, Leclercq B, Carlin B, Siepmann J (2008) How to improve the storage stability of aqueous polymeric film coatings. J Control Release 126:26–33
83. Sun YM, Hsu SC, Lai JY (2001) Transport properties of ionic drugs in the ammonio methacrylate copolymer membranes. Pharm Res 18:304–310
84. Sun H, Mei L, Song C, Cui X, Wang P (2006) Biodegradable implantable fluconazole delivery rods designed for the treatment of fungal osteomyelitis: Influence of gamma sterilizataion. J Biomed Mater Res A 77:632–638
85. Sungthongjeen S, Sriamornsak P, Puttipipatkhachorn S (2008) Design and evaluation of floating multi-layer coated tablets based on gas formation. Eur J Pharm Biopharm 69:255–263
86. Tian L, Zhang Y, Tang X (2008) Sustained-release pellets prepared by combination of wax matrices and double-layer coatings for extremely water-soluble drugs. Drug Dev Ind Pharm 34:569–576
87. van Laarhoven JAH, Kruft MAB, Vromans H (2002) Effect of supersaturation and crystallization phenomena on the release properties of a controlled release device based on EVA copolymer. J Control Release 82:309–317
88. Varshosaz J, Faghihian H, Rastgoo K (2006) Preparation and characterization of metoprolol controlled-release solid dispersions. Drug Deliv 13:295–302
89. Verhoeven E, Vervaet C, Remon JP (2006) Xanthan gum to tailor drug release of sustained-release ethylcellulkose mini-matrices prepared via hot-melt extrusion: in vitro and in vivo evaluation. Eur J Pharm Biopharm 63:320–330

90. Verhoeven E, De Beer TRM, Van den Mooter G, Remon JP, Vervaet C (2008) Influence of formulation and process parameters on the release characteristics of ethylcellulose sustained-release mini-matrices produced by hot-melt extrusion. Eur J Pharm Biopharm 69:312–319
91. Verhoeven E, De Beer TRM, Schacht E, Van den Mooter G, Remon JP, Vervaet C (2009) Influence of polyethylene glycol/polyethylene oxide on the release characteristics of sustained-release ethylcellulose mini-matrices produced by hot-melt extrusion: in vitro and in vivo evaluations. Eur J Pharm Biopharm 72:463–470
92. Verhoeven E, Siepmann F, De Beer TRM, Van Loo D, Van den Mooter G, Remon JP, Vervaet C, Seipmann J, Vervaet C (2009) Modeling drug release from hot-melt extruded mini-matrices with constant and non-constant diffusivities. Eur J Pharm Biopharm 73:292–301
93. Wagner KG, McGinity JW (2002) Influence of chloride ion exchange on the permeability and drug release of Eudragit® RS30D films. J Control Release 82:385–397
94. Wei H, Li-Fang F, Bai X, Chun-Lei L, Qing D, Yong-Zhen C, De-Ying C (2009) An investigation into the characteristics of chitosan/Kollicoat SR30D free films for colonic drug delivery. Eur J Pharm Biopharm 72:266–274
95. Wouessidjewe D (1997) Aqueous polymethacrylate dispersions as coating materials for sustained and enteric release systems. STP Pharm Sci 7(6):469–475
96. Wu C, McGinity JW (2000) Influence of relative humidity on the mechanical and drug release properties of theophylline pellets coated with an acrylic polymer containing methylparaben as a non-traditional plasticizer. Eur J Pharm Biopharm 50(2):277–284
97. Wu C, McGinity JW (2001) Influence of ibuprofen as a solid-state plasticizer in Eudragit® RS 30 D on the physicochemical properties of coated beads. AAPS PharmSciTech 2:1–9
98. Jones DS, McLaughlin DMJ, McCoy CP, Gorman SP (2005) Physicochemical characterisation and biological characterisation of hydrogel-poly(epilson caprolactone) interpenetrating polymer networks as novel urinary biomaterials. Biomaterials 26(14): 1761–1770
99. Wu C, McGinity JW (2003) Influence of an enteric polymer on drug release rates of theophylline pellets coated with Eudragit® RS 30 D. Pharm Dev Technol 8(1):103–110
100. Young CR, Koleng JJ, McGinity JW (2002) Production of spherical pellets by a hot-melt extrusion and spheronization process. Int J Pharm 242:87–92
101. Zhang F, McGinity JW (2000) Properties of hot-melt extruded theophylline tablets containing poly(vinyl acetate). Drug Dev Ind Pharm 26(9):931–942
102. Zheng W, Sauer D, McGinity JW (2005) Influence of hydroxyethylcellulose on the drug release properties of theophylline pellets coated with Eudragit® RS 30 D. Eur J Pharm Biopharm 59(1):147–154
103. Zhu Y, Shah NH, Mallick AW, Infeld MI, McGinity JW (2002) Influence of thermal processing on the properties of chlorpheniramine maleate tablets containing an acrylic polymer. Pharm Dev Technol 7(4):481–489
104. Zhu Y, Mehta KA, McGinity JW (2006) Influence of plasticizer level on the drug release from sustained release film coated and hot melt extruded dosage forms. Pharm Dev Technol 11:285–294

# Chapter 4
# Hydrogels

**Hossein Omidian and Kinam Park**

**Abstract** Hydrogels are crosslinked polymers with the ability to swell in an aqueous medium. Crosslinking in hydrogels occurs by chemical or physical means depending on the polymer properties and experimental conditions. Owing to a large variety in chemical structure and crosslinking methods, various hydrogels have been prepared for various applications in pharmaceutical and biomedical fields. This chapter begins with hydrogel classification, properties, and their methods of preparation. The chapter continues with intelligent hydrogels, which are able to respond to environmental changes such as temperature, pH, and solvent composition, by changing their dimensions. Hydrogel based on polysaccharides, hydrocolloids, and synthetic polymers are discussed accordingly. Finally, the chapter concludes with known hydrogel applications in the pharmaceutical area. These include superdisintegrants, ion exchanging resins, superporous hydrogels, hydrogel implants, hydrogel inserts, osmotic products (devices, implants, and tablets), as well as tissue expanding hydrogels and contact lenses.

## 4.1 Introduction

### *4.1.1 Hydrosol and Hydrogel*

In a simple binary system of a polymer and a liquid, a sol is formed when the polymer–liquid interaction are more favored than both polymer–polymer and liquid–liquid interactions. If the polymer is hydrophilic and the liquid is water, the

H. Omidian (✉)
Health Professions Division, College of Pharmacy, Nova Southeastern University,
3200 S. University Drive, Fort Lauderdale, FL, USA
e-mail: omidian@nova.edu

K. Park
Departments of Biomedical Engineering and Pharmaceutics
Purdue University, West Lafayette, IN, USA

J. Siepmann et al. (eds.), *Fundamentals and Applications of Controlled Release Drug Delivery*, Advances in Delivery Science and Technology,
DOI 10.1007/978-1-4614-0881-9_4, © Controlled Release Society 2012

product of the polymer–liquid interaction is called a hydrosol. The extent of this reaction is generally dependent on the polymer structure, functional groups, type, and amounts of ions in the polymer structure as well as in the solution, pH, and temperature. The dissolution of a hydrophilic polymer in water can be prevented by adding crosslinks via either a physical or a chemical process. A crosslinked hydrosol is called a hydrogel and can only swell in the surrounding liquid to a certain swelling ratio, depending on the number of crosslinks, i.e., the crosslinking density.

### *4.1.2 Physical and Chemical Gels*

In physical gels, the nature of the crosslinking process is physical. This is normally achieved via utilizing physical processes such as association, aggregation, crystallization, complexation, and hydrogen bonding. On the contrary, a chemical process, i.e., chemical covalent crosslinking is utilized to prepare a chemical hydrogel. Figures 4.1 and 4.2 show different approaches to make physical and chemical hydrogels, respectively. While physical hydrogels are reversible due to the conformational changes, chemical hydrogels are permanent and irreversible as a result of configurational changes. More details about the hydrogels are found in Table 4.1.

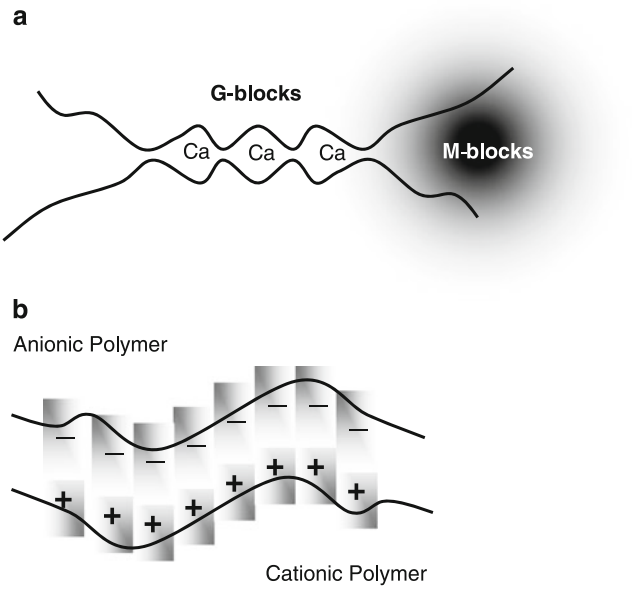


**Fig. 4.1** Examples of physical hydrogels crosslinked by ion–polymer complexation (**a**), polymer–polymer complexation (**b**), hydrophobic association (**c**), chain aggregation (**d**), and hydrogen bonding (**e**)

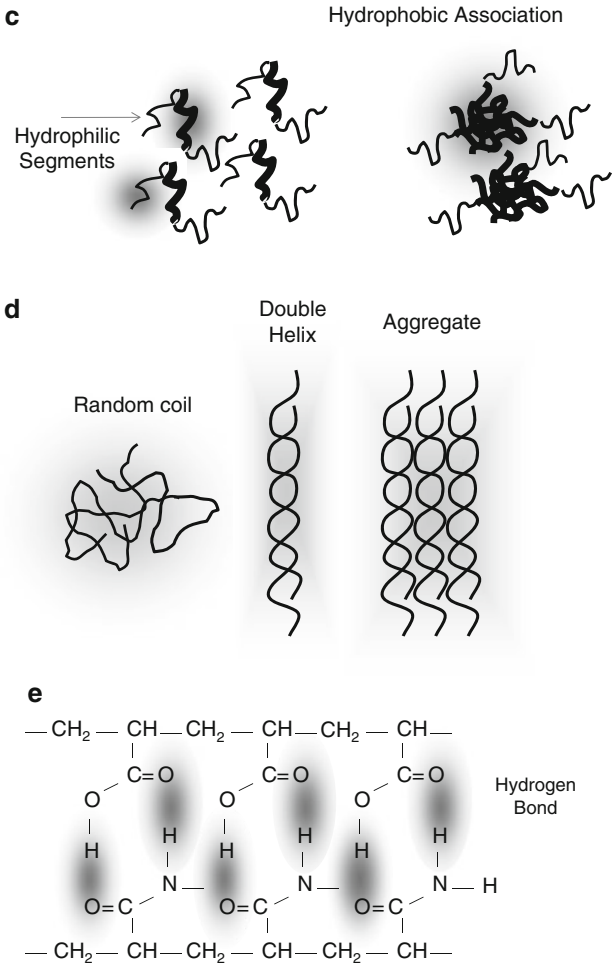


**Fig. 4.1** (continued)

### *4.1.3 Responsive Hydrogels*

Hydrogels are also classified as shown in Table 4.2 in terms of their interaction with the surrounding environment, i.e., responses to the changes in pH, temperature, and the composition of the surrounding liquid. Depending on its structure, hydrogel can respond to environmental changes by changing its size or shape. Most important factors that trigger a hydrogel response are pH, temperature, and swelling medium. While nonionic hydrogels are almost insensitive to pH changes, ionic hydrogels display a dramatic change in size with the pH change. As far as the temperature is

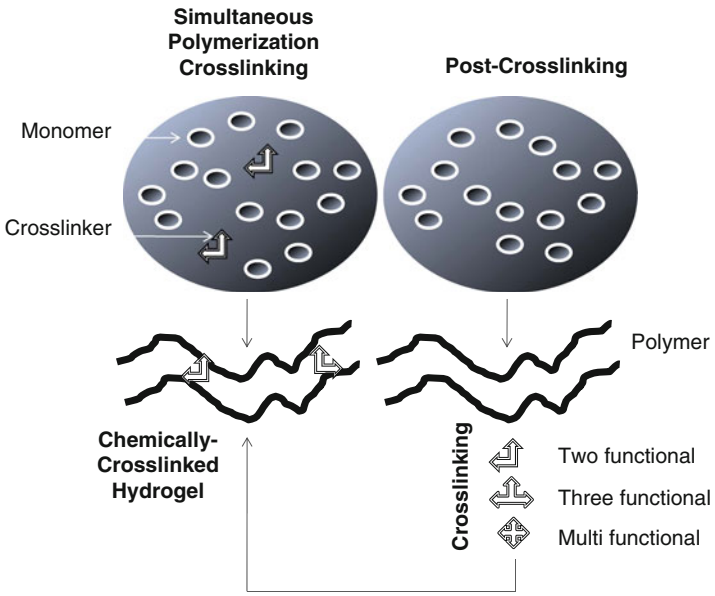


**Fig. 4.2** Methods to prepare chemical hydrogels

**Table 4.1** Sol–gel (hydrosol–hydrogel) transition in physical and chemical hydrogels

| Physical hydrogels | Chemical hydrogels |
|---|---|
| *Hydrophobic association*: isopropyl groups in poly(*N*-isopropyl acrylamide); methyl groups in methyl cellulose; propylene oxide blocks in (ethylene oxide)–(propylene oxide)–(ethylene oxide) terpolymers | Covalent crosslinking using olefinic crosslinkers containing unsaturated bonds or reactive functional groups |
| *Ion–polymer complexation*: acrylic-based hydrogels treated with calcium, aluminum, iron; sodium alginate treated with calcium and aluminum; poly(vinyl alcohol) treated with borax | *Simultaneous polymerization and crosslinking*: Acrylic acid or acrylamide, crosslinked with methylene bisacrylamide, ethylene glycol diacrylate, ethylene glycol dimethacrylate, poly(ethylene glycol dimethacrylate) |
| *Polymer–polymer complexation*: alginate and chitosan; gum Arabic and gelatin | *Post-polymerization chemical crosslinking*: Acrylic-based hydrogel, crosslinked with glycerin; gelatin cross-linked with glutaraldehyde; poly(vinyl alcohol) crosslinked with an aldehyde |
| *Chain aggregation*: heat treatment of hydrocolloids in water | |
| *Hydrogen bonding*: poly(vinyl alcohol)/poly (vinyl alcohol) chains; poly(acrylic acid)/ polyacrylamide chains | |

**Table 4.2** Examples of hydrogels responsive to changes in environmental factors

| Hydrogels responsive to: | | |
|---|---|---|
| pH | Temperature | Liquid composition |
| (If the hydrogel is ionic) | (If the hydrogel can form hydrophobic association and chain aggregation) | (If the surrounding environment of the hydrogel contain nonsolvents and salts) |
| *With increase in pH* | *With increase in temperature* | *With changes in swelling medium* |
| *Swelling increases in* anionic hydrogels containing carboxyl group such as poly (sodium acrylate) and sodium alginate | *Solubility decreases in* cellulose derivatives such as cellulose-based polymers containing methyl or hydroxypropyl groups and poly(*N*-isopropyl acrylamide) | *Swelling decreases sharply in* ionic hydrogels such as poly(potassium acrylate) and sodium alginate with increase in concentration of nonsolvent, salts, as well as salt valence |
| *Swelling decreases in* cationic hydrogels containing amino groups such as poly (dimethyl aminoethyl) acrylate and chitosan | *Solubility increases in* hydrocolloids such as gelatin and agar agar | *Swelling decreases moderately in* nonionic hydrogels such as polyacrylamide and poly(vinyl alcohol) with increase in concentration of nonsolvent, salts as well as salt valence |

concerned, hydrogels containing hydrophobic groups or those susceptible to chain aggregation respond to the temperature change to a great extent. Given the fact that solubility and swellability are driven by same forces, the response of the hydrogel to temperature change can be either direct or inverse. With the former, the solubility and swellability of the hydrogel can increase with increase in temperature, while an opposite trend is observed with inverse thermoresponsive hydrogels. Hydrogels can also change their size with the change in the composition of the swelling medium. Apparently the hydrogel response would be dramatic if the swelling medium contains salt and a nonsolvent. These facts are shown in Fig. 4.3.

### *4.1.4 Hydrogel Properties*

Hydrogels are generally characterized by their ultimate capacity to absorb liquids (swelling thermodynamics), the rate at which the liquid is absorbed into their structure (swelling kinetics), as well as their mechanical property in wet or hydrated state (wet strength). Table 4.3 shows factors affecting the hydrogel properties among which, the crosslink density and the structural integrity (porosity, pore size and its distribution) have the most significant effect. Hydrogels

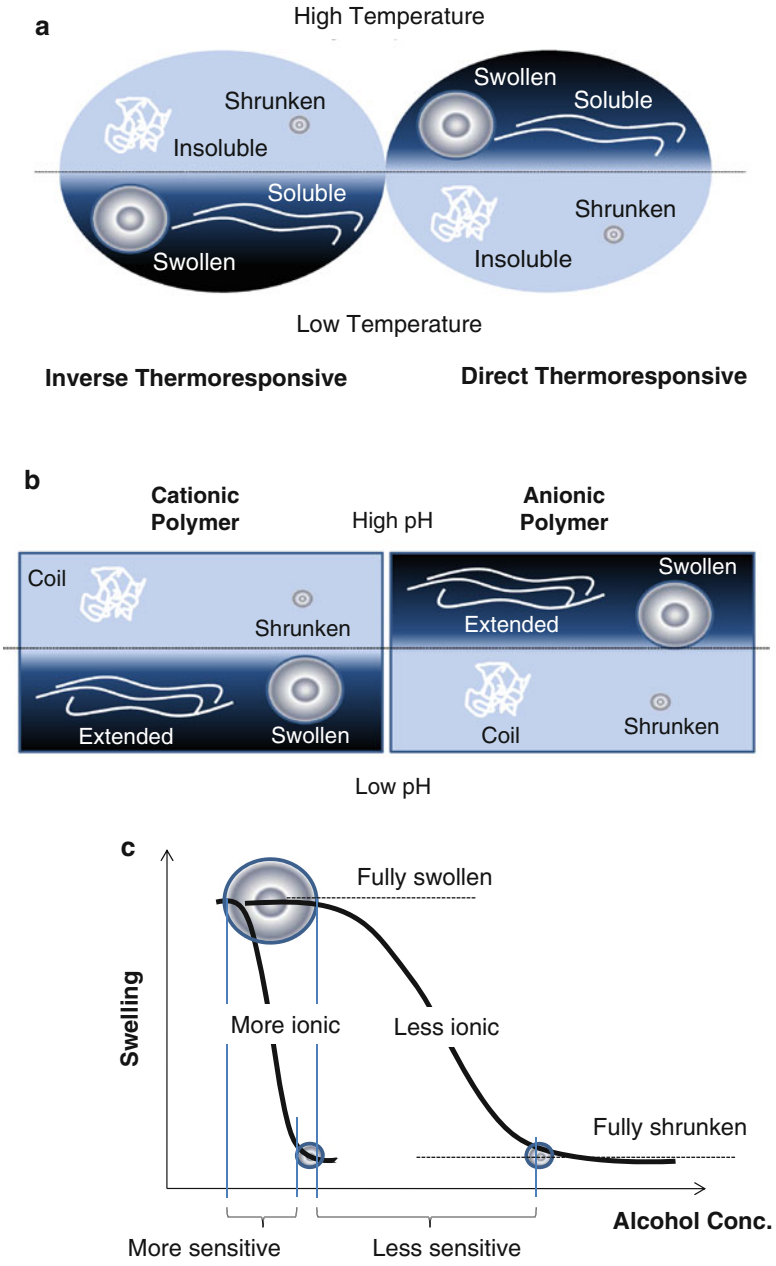


**Fig. 4.3** Hydrogel swelling and hydrosol solubility dependence on (**a**) temperature, (**b**) pH, and (**c**) nonsolvent concentration

**Table 4.3** Changes in hydrogel properties due to the hydrogel structure and liquid composition

| Swelling capacity ↑ | Swelling rate ↑ | Wet strength ↑ |
|---|---|---|
| *Hydrogel structure*: very hydrophilic polymers, ionic polymers containing monovalent ions, lower crosslink density, hydrophilic crosslinkers | *Hydrogel structure*: more hydrophilic, higher crosslink density, more porosity, open pores, interconnected pores | *Hydrogel structure*: high crosslink density (there is an optimum crosslink density at which, the mode of hydrogel failure changes from ductile to brittle), low porosity, more hydrophobicity |
| *Liquid composition*: more solvent, less salts, low ionic strength, less numbers of di and trivalent cations | *Liquid composition*: Presence of permeation enhancers for more hydrophobic hydrogels, more solvent | *Liquid composition*: more nonsolvent, more salts |

have been attractive to the pharmaceutical industry for several reasons including the controlled release of an active pharmaceutical ingredient, disintegration of dosage forms, protecting an active and to increase the product life cycle management.

The general concepts and applications of hydrogels within the pharmaceutical area are outlined below with focuses on the most recent research activities in the field.

## 4.2 Hydrogels in Pharmaceutical Applications

### *4.2.1 Inverse Thermoresponsive Hydrogels*

The solubility and swellability of the hydrogels containing hydrophobic groups and segments is dependent on the temperature of the swelling medium. Polyacrylamide derivatives containing hydrophobic pendant groups display reverse temperature sensitivity. These are soluble in water at low temperature and become insoluble when temperature rises. This behavior is a result of a delicate balance between the hydrogen bonding and hydrophobic interactions, which depends on temperature. The transition temperature at which a water soluble polymer becomes insoluble is called the lower critical solution temperature (LCST), below which, the hydrogen bonding and above which, hydrophobic association prevails. Below and above the LCST, the hydrogel displays a sharp transition in size from a sol to a gel (a so-called sol–gel transition point). Hydrogels based on poly(*N*-isopropyl acrylamide) (polyNIPAM), cellulose derivatives, and ethylene oxide–propylene oxide–ethylene oxide terpolymers display this behavior. In subcutaneous or parenteral drug delivery, a solution dosage form containing a drug and a thermosensitive

polymer are injected into the patient's body at room temperature. The polymer part of the dosage form then starts to gel at a higher body temperature, depending on its sol-gel transition temperature. Macromed, a US-based drug delivery company, has a delivery technology, ReGel®, based on ABA triblock copolymers in which the A and B blocks are poly(lactide-*co*-glycolide) and poly(ethylene glycol), respectively. ReGel® is a temperature sensitive and bioerodible hydrogel, which is intended for parenteral delivery [1].

#### 4.2.1.1 Hydrogels Based on Acrylamide Derivatives

PolyNIPAM and its copolymer nanoparticles with acrylic acid have been prepared. The thermosensitive property of these hydrogels was shown to be manipulated by changing the molar ratio of the two monomers. The anticancer drug 5-fluorouracil (5-FU) was first loaded into both hydrogel nanoparticles with a loading efficiency as high as 4%. The release of the drug was found to be clearly dependent on temperature and pH [2]. A magnetic thermosensitive hydrogel has been prepared by incorporating superparamagnetic $Fe_3O_4$ particles into polyNIPAM hydrogels. A pulsatile drug release was remotely triggered and controlled by a high frequency alternating magnetic field [3]. Nanoparticles of poly(NIPAM-*co*-allylamine) and poly(NIPAM-*co*-acrylic acid) have been synthesized and crosslinked with glutaric dialdehyde and adipic acid dihydrazide, respectively. Dextrans of different molecular weights were used as a macromolecular drug for the release study. While dextran was not released from a highly crosslinked polyNIPAM gel, its release from NIPAM–allylamine copolymer gel was found to be temperature dependent. Low molecular weight dextrans were released from the NIPAM–acrylic acid copolymer gel almost independent of temperature [4]. An optically responsive hydrogel for drug delivery has been developed based on gold nanoparticles (60 nm) coated with a thermally responsive biocompatible hydrogel (20–90 nm). The hydrogel is based on NIPAM and acrylic acid and its properties can be tailored to exhibit a LCST slightly above the body temperature. Drug loaded hydrogel could be photothermally activated by an exposure to light, which can be absorbed by the plasmon resonance of the gold nanoparticle cores [5]. Thermosensitive copolymer hydrogels of NIPAM and butyl methacrylate have been prepared and examined for indomethacin delivery. A zero order kinetic at 20°C indicates that swelling and chain relaxation are rate determining steps (Case II diffusion). The release kinetic was found to be sigmoidal at 10°C, where a faster drug release is attributed to a faster swelling and disappearing the glassy core of the hydrogel [6]. Hydroxyethyl, hydroxybutyl and hydroxyhexyl derivatives of methacrylate polymer, and their copolymers with NIPAM and acrylic acid have been prepared. The surface, mechanical, and swelling properties of these hydrogels were measured using a dynamic contact angle analysis, tensile analysis, and thermogravimetry, respectively. The thermal transition points including the $T_g$ and LCST were determined using modulated DSC and oscillatory rheometry, respectively. The drug chlorhexidine

diacetate was loaded into the hydrogels by immersing the hydrogel into the drug solution at a temperature below the LCST of the polymer [7].

#### 4.2.1.2 PEG-Based Hydrogels

An aqueous solution of PEG–PLGA–PEG triblock copolymers at low molecular weight and specific composition has been shown to become gel at the body temperature. Drug release from these thermosensitive hydrogels has been examined in vitro by injecting the drug loaded polymer solution into a 37°C aqueous environment. Ketoprofen as a hydrophilic drug model was released over a 2 week period with a first order kinetic, while spironolactone, a hydrophobic model drug, was released over a two month period following a sigmoidal kinetic [8]. Gel paving hydrogels are locally applied or polymerized on vascular endoluminal surfaces and function as a physical barrier limiting deposition of cells and proteins, and hence reducing thrombogenicity. A thermoreversible and photopolymerizable gel paving system based on PEG-lactide hydrogels has been outlined [9]. A thermoreversible gel with gelling temperature close to the body temperature has been designed based on hyaluronic acid and poloxamer polymers. With an optimum hydrogel formulation, acyclovir could be released over a 6 h period [10].

A pH-sensitive and thermoresponsive hydrogel with higher swelling at higher pH and temperatures has been prepared based on hydroxyethyl chitin and polyacrylic acid. The hydrogel was claimed as an enteric delivery system for potassium diclofenac [11].

### *4.2.2 pH-Responsive Hydrogels*

Polymers containing carboxyl groups or amino groups respond to the pH changes by changing their size in the swollen state. At low pH values, the carboxyl-containing anionic polymers display minimum ionization and hence reduced hydration. Once the pH of the swelling medium rises above the p$K_a$ of the polymer, the carboxyl groups start to ionize and hydrate, which results in polymer expansion and hence higher swelling. On the contrary, cationic polymers containing amino groups (quaternary ammonium salts) display a stronger ionization and hence higher swelling at low pH. Current commercial products and ongoing research activities are overwhelmingly focused on acrylic or methacrylic acid functional groups to make a pH-sensitive carrier. Commercial polymers such as Eudragit® L100-55, L30D-55, L100, or S100 are anionic polymers with methacrylic acid as functional group. These are dissolved at pH above 5.5, which provide drug protection at low pH and drug release at high pH environment, which makes them suitable for drug delivery in duodenum, jejunum, ileum, and colon area. Eudragit® E100 is, on the contrary, a cationic polymer based on butyl and methyl methacrylate containing

dimethylaminoethyl methacrylate to provide a pH-sensitive functionality. The polymer is soluble in gastric juice and used for the taste or odor masking applications.

#### 4.2.2.1 Acrylic Based Hydrogels

Silicone discs containing a pH-sensitive hydrogel have been used to release drugs with different water solubility and partitioning. The hydrogel granules were made of poly(acrylic acid), poly(ethylene oxide) interpenetrating networks; and salicylamide, nicotinamide, clonidine HCl, and prednisolone were used as the model drug. Owing to the anionic nature of the hydrogel blend, a bimodal release behavior was observed, a burst release at low pH and a high release later on at a higher pH medium. At high drug loading and at high pH medium, the release rate of clonidine HCl was reduced due to an ionic interaction with the carboxyl group of the IPN structure [12]. Hydrogels of glycidyl methacrylate dextran and poly(acrylic acid) have been prepared by UV irradiation for colon-specific drug delivery. The hydrogels displayed a pH-dependent swelling with the swelling capacity of 20 at the body temperature. The hydrogel displayed an enhanced swelling up to 45 fold in the presence of dextranase at pH 7.4, and is claimed as a dual sensitive drug carrier for sequential release in the gastrointestinal tract [13]. A pH-sensitive hydrogel has been prepared based on polyethylene glycol (PEG) and acrylic acid (AAc) in an aqueous solution utilizing gamma radiation. Swelling capacity of the hydrogel and the diffusion coefficient was found critically dependent on the pH and the ionic strength, respectively. Ketoprofen was used as a model drug to evaluate the hydrogel carrier for colon delivery at different pH [14]. An amphiphilic hydrogel has been prepared based on hydrophilic polyacrylic acid/hydrophobic polybutyl acrylate and tested for delivery of melatonin. The drug release was found pH dependent, and the burst effect associated with the hydrophilic networks was diminished due to the hydrophobic contribution of butyl acrylate [15]. Starch poly(acrylic acid-*co*-acrylamide) hydrogels have been prepared by physical mixing of the starch and polyacrylonitrile, followed by hydrolysis in the presence of sodium hydroxide. The hydrogel showed a swelling/shrinking cycle at pH 2 and 8, respectively. Poorly water soluble ibuprofen was released from the hydrogel much faster at the intestinal pH than at the gastric pH [16].

#### 4.2.2.2 Methacrylic Based Hydrogels

An IPN network of poly(methacrylic acid) and poly(vinyl alcohol) crosslinked with glutaraldehyde has been prepared utilizing a water-in-oil emulsion system. The hydrogel displayed a pulsatile swelling behavior with the change in pH, and ibuprofen release was found dependent on the pH, crosslink density, and drug loading [17]. Two monomers of methacrylic acid and methacrylamide have been used to prepare hydrogels utilizing a free radical solution polymerization. The hydrogel was intended

for oral delivery of an antimalarial drug under physiological conditions. With high loading efficiency of about 98%, the amount of release in simulated gastric (pH 1.2) and colonic environment (pH 7.4) was extensively varied from 29 to 75% respectively [18]. A pH-sensitive hydrogel of hydroxyethyl methacrylate, methacrylic acid and ethylene glycol dimethacrylate was prepared, and its release behavior was examined utilizing a water-soluble drug (ephedrine HCl) and a water insoluble drug (indomethacin) [19].

#### 4.2.2.3 Chitosan-Based Hydrogels

Enteric coated multiparticulate chitosan hydrogel beads with pH-sensitive property have been reported as potential orally administrable drug carriers for site specific colon delivery [20]. Satranidazole has been examined with this delivery system [21]. A water-soluble derivative of chitosan (2-carboxybenzyl chitosan) has been synthesized and characterized using FTIR, HNMR, and UV. The degree of carboxybenzyl substitution was determined using a colloid titration method. The hydrogel swelling was decreased with an increase in glutaraldehyde concentration, and was higher in basic medium than in acidic environment. The release of fluorouracil (5-FU), a poorly water soluble drug was found to be much faster at pH 7.4 than pH 1.0, which justifies the use of this hydrogel as a potential pH-sensitive carrier for the colon specific drug delivery [22]. A glutaraldehyde-crosslinked carboxymethyl chitosan hydrogel was prepared and its release behavior was tested using salicylic acid as the model drug. The hydrogel showed a significantly higher swelling capacity in alkaline than in acidic media [23]. A pH-sensitive semi-IPN hydrogel of *N*-carboxyethyl chitosan and 2-hydroxyethyl methacrylate was prepared via photopolymerization. The hydrogel showed a good mechanical strength in its hydrated wet state, claimed to be nontoxic and offered a prolonged release with 5-flurouracil as a model drug [24]. A hydrogel system composed of carboxymethyl chitosan (a water soluble derivative of chitosan) and alginate blended with genipin (naturally occurring crosslinker) has been developed for controlled delivery of bovine serum albumin. The protein was released up to 20 and 80% respectively at simulated gastric and intestine conditions, which suggests its application as a potential drug carrier for site-specific intestinal delivery [25].

#### 4.2.2.4 Miscellaneous Hydrogels

Methacrylic anhydride and succinic anhydride derivatives of inulin have been synthesized via UV irradiation to produce a pH-sensitive hydrogel. Diflunisal at different concentrations was used as a model drug [26]. A pH-sensitive hydrogel of methyl methacrylate and dimethylaminoethyl methacrylate crosslinked with divinyl benzene was prepared and its release behavior was tested using a water soluble drug, aminopyrine [27]. Acrylamide has been grafted onto xanthan gum to prepare a pH-sensitive hydrogel network. Drug release from the hydrogels was

studied using ketoprofen. FTIR, DSC/X-ray, and SEM were respectively used to confirm grafting/hydrolysis, to determine the crystal nature of the loaded drug, and to monitor the porosity of the hydrogel structure. Different release behavior was observed at low and high pH conditions [28].

### *4.2.3 Natural Polymer Based Hydrogels*

Drug release from a controlled release platform is practically controlled by a delicate balance of solubility and swellability (gelling properties) of the drug carrier. Depending on their source and structure, hydrocolloids offer a vast range of solubility and gelling properties in aqueous media. Moreover, rheological properties of the drug solutions, dispersions, or emulsions can also be modified using hydrocolloids or hydrocolloid hybrids. They are also well established as food ingredients in nutraceutical industries.

#### 4.2.3.1 Cellulose Derivatives

As an important class of excipients, polysaccharides such as methyl cellulose (MC), carboxymethyl cellulose (CMC), and different grades of hydroxypropyl methylcellulose (HPMC) have found numerous applications as binder, disintegrant, and most importantly as a controlled release platform. HPMC polymers offer different solubility and gelling properties, which are critically dependent on the degree of substitution, hydroxypropyl content, molecular weight, and temperature. Currently, there are about 130 drugs in the US market, which contain HPMC (hypromellose) as a matrix of controlled delivery. These include simvastatin niacin extended release (Simcor®), carbamazepine extended release (Carbatrol®), fluvastatin sodium (Lescol®), alprazolam (Zanax XR®), niacin, and lovastatin (Advicor®) [29]. Different grades of HPMC with different viscosities were used to study the release of buflomedil pyridoxal phosphate. Study of HPMC hydrogels coated with an impermeable membrane shows that the drug release is not affected by the polymer viscosity, but it is very dependent on the contact area with the dissolution medium [30].

#### 4.2.3.2 Hydrocolloids

Owing to their attractive solution properties, molecular weight, structure, and availability, various hydrocolloids such as alginate, xanthan, guar gum, and a few others have been added to the list of pharmaceutical excipients. They are used in designing new dosage forms and formulations, novel drug delivery systems, in

microparticle and microcapsule preparation, and to control the rheology of liquid (solution, suspension, and emulsion), semisolid (wax based), and solid dosage forms (powders).

Konjac, a plant extract gum, can be used as a thickener and gelling agent and is intended for colon specific drug delivery if blended with xanthan gum at a particular concentration [31]. Gellan, a microbial gum has been suggested as a swelling agent (in disintegration of ibuprofen tablets) [32], tablet binder [33], and a rheology modifier [34]. Gellan gum can be found in Timoptic-XE® 0.25% and 0.5% (timolol maleate) ophthalmic gel forming solution [29]. Carrageenan, a seaweed extract, has been claimed for capillary electrophoresis as a chiral selector [35] as well as for topical delivery systems (examined as a viscosity modifier in sodium fluorescein delivery) [36]. Carrageenan can be found in Vantin® (cefpodoxime proxetil) oral suspension [29]. Chitosan, an animal extract gum, has been tested as a taste masker [37], dietary fiber [38], drug delivery matrix [39, 40], protein and peptide delivery platform [41], disintegrant [42], absorption enhancer of macromolecular drugs [43], and used in emulsion-like solutions and creams [44], mucoadhesive delivery [45], microparticle formation [46], local or systemic delivery of drugs and vaccines [47], and for biomedical and cosmetic applications [48, 49]. Other polysaccharides have also been mentioned as a drug delivery carrier for different applications. These include alginate (for microencapsulation) [50, 51], scleroglucan (for theophylline release) [52], guar gum (as a tablet binder for paracetamol [53] and for colon specific delivery [54]), heparin (as an anticoagulant) [55], schizophyllan (in cancer therapy as immunostimulant) [56, 57] and xanthan (as rheology modifier [58], tablet binder [59], and swelling agent [60]). Xanthan gum can be found in many dosage forms in the US market including Tricor® (fenofibrate) 145 mg tablets, Pepcid for oral suspension, Pepcid® PRD orally disintegrating tablets (famotidine), and Renova® (tretinoin) cream 0.02% [29]. Sodium alginate is used in a variety of commercially available dosage forms such as Prolixin® (fluphenazine), Tolinase® (tolazamide) tablets, and Axid® (nizatidine) oral solution [29].

### Hydrogels Based on Alginic Acid

Composite hydrogel of collagen and alginate has been used for ocular protein delivery. The hydrogel provides 11 days sustained release for bovine serum albumin in neutral buffer and supports corneal epithelial cell growth with good mechanical strength and transparency [61]. Sodium alginate/carboxymethyl guar gum hydrogels have been prepared via an ion complexation with barium ions. This anionic hydrogel has displayed swelling capacity of about 15 and 310% in simulated gastric (pH 1.2) and intestinal fluids (pH 7.4), respectively. The hydrogel was able to release 20 and 70% of its loaded vitamin B12 in gastric and intestinal medium respectively. Hydrogels crosslinked with 5 or 6 w/v% barium chloride solution displayed 50% loading efficiency [62].

### Hydrogels Based on Guar Gum

Poly(vinyl alcohol) guar gum IPN hydrogels have been prepared utilizing glutaraldehyde as a crosslinker. It was shown that an increased crosslink density changes the release of nifedipine from Fickian to non-Fickian. The drug release was found to be dependent on the crosslink density, drug loading, and loading method [63]. A graft copolymer hydrogel of acrylamide and guar gum has been prepared utilizing glutaraldehyde as a crosslinker. It was loaded with two water soluble (verapamil hydrochloride) and water insoluble (nifedipine) antihypertensive drugs. The drugs were added into the hydrogel after crosslinking or incorporated during the hydrogel preparation [64].

### Hydrogels Based on Chitosan

A transparent, water soluble and water miscible gel has been developed as an ointment base by dissolving 93% deacetylated chitosan F in a solution of lactic acid. Using rheological tests, the gel was proved to be stable when loaded with drugs such as clotrimazole, piroxicam, estradiol, progesterone, lidocaine HCl, or a sodium salt of heparin but loses its stability with metronidazole or suspending hydrocortisone [65]. The swelling behavior and in vitro release of nifedipine from alginate–chitosan hydrogel beads has been investigated. The hydrogels were prepared via ionotropic gelation and characterized by FTIR (structure) and SEM (morphology) [66]. Microcrystalline chitosan hydrogel alone and in combination with methylcellulose or Carbopol has been studied for the release of diclofenac-free acid and its salt. Drug release and rheological properties of the drug carrier were studied in the presence of hydrophilizing agents such as 1,2-propylene glycol and glycerol [67]. $NaBO_3$-treated chitosan with different molecular weights has been used to coat theophylline tablets to evaluate their sustained release properties. The release rate of theophylline was decreased with increasing the amount of coated chitosan and increased with decreasing the chitosan molecular weight [68]. Carboxymethyl–hexanoyl chitosan has been synthesized with desirable swelling properties and used as a drug carrier for amphiphatic agents. The hydrogel has both hydrophilic (carboxymethyl) and hydrophobic (hexanoyl) moieties, but the hydrophobic part retards the deswelling process, causing better water-retention properties. It was shown that partially hydrophobic drugs such as ibuprofen has better encapsulation efficiency in this hydrogel than in chitosan or carboxymethyl chitosan, which are more hydrophilic [69]. Chitosan-coated polyphosphazene-$Ca^{2+}$ hydrogel have been prepared by dropping polyphosphazene into calcium chloride/chitosan gelling solution. With myoglobin as a model drug, an encapsulation efficiency of 93% has been obtained [70]. Chitosan grafted with acrylic acid and acrylamide have been prepared utilizing gamma irradiation. The hydrogels showed ampholytic and reversible pH responsive properties and claimed for controlled release of antibiotics (amoxicillin trihydrate) into the gastric medium.

The release is driven by the ratio of hydrogel swelling to erosion capacity [71]. Chitosan/tripolyphosphate and chitosan/tripolyphosphate/chondroitin sulfate core–shell biocompatible hydrogels have been prepared and used for the delivery of ofloxacin. It was shown that chondroitin sulfate as a second polyanion contributed to an increased mechanical strength of the hydrogel [72]. Release behavior of cimetidine from glutaraldehyde-crosslinked chitosan has also been studied [73]. An aqueous solution of photo-crosslinkable chitosan containing azide groups and lactose moieties containing paclitaxel has been reported to form an insoluble hydrogel following an ultraviolet irradiation for 30 s. The hydrogels effectively inhibited tumor growth and angiogenesis in mice. The study shows that chitosan hydrogel may be a promising site specific carrier for drugs such as FGF-2 and paclitaxel to control vascularization [74].

### Hydrogels Based on Carrageenan

Betamethasone acetate, a water soluble model drug, has been loaded into a hydrogel blend of carrageenan and sodium alginate. Maximum loading was found to be dependent on temperature and pH as it appeared to be 71% at pH 4.8 and 55°C. The hydrogel was compared with two other similar systems of Ca-alginate and K-Carrageenan at different pH [75]. To enhance its therapeutic effectiveness, the hydrophobic anticancer drug, camptothecin, was solubilized in a cationic surfactant (dodecyltrimethylammonium bromide) and loaded into an anionic kappa-carrageenan hydrogel [76]. A repetitive pulsatile drug release was displayed when dibucaine hydrochloride as a model drug loaded into an erodible hydrogel system based on kappa-carrageenan. This behavior was attributed to the carrageenan oscillatory loss during the drug release process [77].

### Scleroglucan-Based Hydrogels

In the presence of borax, scleroglucan can form a gel. The hydrogel has been used as a matrix for tablets loaded with three different model molecules, theophylline, vitamin B12, and myoglobin. The release pattern of the drug theophylline was also studied in gastric and intestinal conditions. Results showed that the scleroglucan hydrogel has the potential to be used in sustained release formulations, in which the drug release is dependent on the size of the drug molecule [78–80]. Borax treated scleroglucan polymer for delivery of theophylline has also been tested and proposed for delivery of vitamin B12 and myoglobin [81]. The efficacy of bFGF (basic fibroblast growth factor)–gelatin hydrogel complex for bone regeneration around implants has been studied for the development of a new drug delivery system [82].

### Hydrogels Based on Hyaluronic Acid

Hyaluronan (HA) has the ability to control cell migration, differentiation, proliferation, and contribute to the invasiveness of human cancers. A study shows that a crosslinked hyaluronan can be used to investigate the sensitivity of cancer cells to antimitotic agents [83]. New hyaluronic acid (HA) based hydrogels has been developed by converting the HA to adipic dihydrazide derivative, followed by crosslinking with poly(ethylene glycol)-propiondialdehyde. Dried film of this hydrogel could swell sevenfold in volume in buffer in less than 2 min. Morphology and enzymatic degradation of hydrogel by hyaluronidase were examined using SEM and a spectrophotometric assay. This novel biomaterial has been claimed for controlled release of therapeutic agents at wound sites [84].

### Pectin Based Hydrogels

Drug release from high methoxy pectin has been studied in terms of tablet compression force, amount, and type of pectin. The drug release was found to be unaffected by compression force [85]. Acrylamide grafted pectin was characterized by FTIR, DSC and X-ray diffraction. The polymer was crosslinked with glutaraldehyde and tested for salicylic acid release using a Franz diffusion cell. A grafted hydrogel displayed better film-forming properties than pectin [86]. Hydrogel membrane based on pectin and polyvinylpyrrolidone have been prepared by physical blending and conventional solution casting methods. The release of salicylic acid was monitored at different aqueous media using a UV–Vis spectrophotometer at 294 nm wavelength. The presence of secondary amide, decrease in crystallinity at higher PVP ratio, increased $T_g$ of pectin-PVP blend and hydrogel cytocompatibility was shown by FTIR, XRD, DSC and B16 melanoma cells respectively [87]. Amidated pectin complexes with calcium were used in preparation of a multiparticulate system with the potential for site-specific colon delivery. Indomethacin and sulphamethoxazole release was found to be dependent on the pH and drug loading. Although drug release in both low and high pH media was higher for a more water-soluble drug, it was significantly reduced when particles were coated with chitosan [88].

### Miscellaneous Hydrocolloid-Based Hydrogels

IPN hydrogels of acrylamide and gelatin were prepared and their swelling in water and citric acid phosphate buffer at various pH studied. More specifically, the hydrogel swelling behavior at physiological pH was studied in the temperature range of 25–60°C [89]. Agarose hydrogel nanoparticles prepared in an emulsifier-free dispersion system have been claimed for protein and peptide delivery. A study with ovalbumin protein has shown a temperature dependent, diffusion controlled release [90]. Dextran based hydrogels for controlled drug release and tissue

engineering have also been reviewed [91]. Inulin hydrogel has been prepared by derivitizing a vinyl containing inulin (methacrylated inulin) followed by free radical polymerization with redox initiating systems. It was characterized using linear oscillatory shear measurement (for gelation), dynamic mechanical analysis, and solution viscosity [92, 93].

### *4.2.4 Nonionic Synthetic Hydrogels*

Hydrogels of this class do not carry functional groups, and hence they are not sensitive to the pH of the swelling medium. As a result, their swelling will be solely governed by the polymer–liquid interaction forces, which determine the polymer solubility in the liquid medium. These hydrogels are generally based on hydroxyethyl methacrylate, acrylamide, ethylene oxide, ethylene glycol, and vinyl pyrrolidone. Owing to the lack of electrostatic forces that operate in the pH sensitive hydrogels, these hydrogels swell to a limited extent.

#### 4.2.4.1 Hydrogels Based on Hydroxyethyl Methacrylate

Poly (2-hydroxyethyl methacrylate) (polyHEMA) is known as a biocompatible polymer, which resists biodegradation and microbial attack. Copolymers of this polymer have been used as a subcutaneous reservoir hydrogel implant, capable of long term delivery of predetermined doses of various active compounds [94]. Hydrogel sponges were prepared based on HEMA and ethylene glycol dimethacrylate (EGDMA), and characterized for iontophoretic drug delivery. The effect of different sterilization techniques, gamma irradiation, ethylene oxide, and autoclave on hydrogel properties has been examined [95]. A biomedical membrane based on HEMA and *p*-vinylbenzyl-poly (ethylene oxide) (V-PEO) macromonomer has been synthesized utilizing photoinitiation polymerization. Infrared, thermal, and SEM analysis was used for the hydrogel characterization. The study showed that the V-PEO content could affect the thermal stability and hydrophobicity of the HEMA hydrogel. The hydrogel containing the highest PEO content was used to study the release of an antibiotic as a potential transdermal antibiotic carrier [96]. A hydrogel based on HEMA and *N*,*N*′-dimethyl-*N*-methacryloyloxyethyl-*N*-(3-sulfopropyl) ammonium betaine has been studied with sodium salicylate as a model drug [97]. Thin films of a novel polyacrylate-based hydrogel were claimed to be a good drug carrier in orthopedic field. HEMA, poly(ethylene glycol) diacrylate, and acrylic acid were used to prepare hydrogels utilizing an electrochemical polymerization. X-ray photoelectron spectroscopy and water content measurement were used to characterize the structure and swelling behavior of the hydrogels [98]. Feasibility of using solid hydrogels of EGDMA-crosslinked HEMA and crosslinked dextran has been studied for injecting drugs in to the eye upon application of low current iontophoresis. The hydrogels were examined for their mechanical suitability,

absorption of drug solution, and in vitro release properties into a solid-agar surface [99]. The HEMA hydrogels have been tested for the release of dexamethasone phosphate [100] and gentamicin sulfate [101] into healthy rabbit eyes. The drug loss and side effects associated with eye drops could potentially be alleviated by using disposable soft contact lenses based on HEMA. The contact lens is loaded with the drug in a microemulsion system stabilized with silica, and releases the drug for 8 days at the therapeutic level. The delivery rates could be tailored by controlling the particle size and the drug loading [102].

#### 4.2.4.2 Poly (Ethylene Glycol) Hydrogels

Bovine serum albumin and poly(ethylene glycol) were polymerized and used as a controlled release system for soluble, hydrophobic, even protein drugs. The study shows that the hydrogel has a very high water content (>96%) and releases the drug by a diffusion-controlled mechanism. Drugs such as theophylline, lysozyme, and hydrocortisone have been tested [103]. In order to modulate the release properties, the hydrogel thickness and its composition was also changed [104]. A poly(ethylene glycol) based copolymer hydrogel containing multiple thiol (−SH) groups has been claimed as a suitable carrier for protein delivery, offering sustained release feature of 2–4 weeks and prolonged biological activity [105]. An acrylated poly (ethylene glycol)-poly(propylene glycol) amphiphilic hydrogel polymer has been developed utilizing inverse emulsion photopolymerization. The matrix contains hydrophobic propylene glycol domains, which can incorporate hydrophobic drugs. Doxorubicin has been incorporated to a 9.8w/w% level [106]. Poly(ethylene oxide) gels crosslinked by urethane bonds have been studied for the release of acetaminophen and caffeine. The study showed an inverse correlation between the release and the hydrogel crystallinity, which is perturbed even at low drug concentrations. With acetaminophen, this behavior has been attributed to drug hydrogel complexation. Hydrogel crystallinity and structural transition were studied using small and wide angle X-ray scattering [107, 108]. PLGA-PEG-PLGA polymers with molecular weight of 3 K–7 K have been synthesized from L-lactide and glycolide as well as PEG with molecular weight of 1 K–4.6 K. A dynamic viscoanalyzer and fluorescence spectroscopy were used to investigate the sol–gel transition of the hydrogel system and to understand the gelling mechanism of the hydrogel respectively. Ceftazidime was used for the controlled release study [109].

#### 4.2.4.3 Hydrogels Based on Poly (Vinyl Alcohol)

Glutaraldehyde-crosslinked poly(vinyl alcohol) hydrogel films have been optimized for controlled delivery of theophylline in terms of crosslinker concentration, drug loading, and release mechanism [110]. Composite hydrogels of poly (vinyl alcohol) and PLGA have been prepared and suggested for long term protein delivery. Bovine serum albumin was encapsulated into PVA nanoparticles, and the

nanoparticles were then loaded into the PLGA microspheres. The composite hydrogel provided a two month delivery of BSA [111]. IPN hydrogels of polyacrylamide and poly(vinyl alcohol) have been prepared and tested for controlled delivery of crystal violet and bromothymol blue as model drugs [112]. In order to alleviate the associated problems with low encapsulation efficiency and high burst effect in biodegradable microcapsules, pentamidine/poly(vinyl alcohol) hydrogels were prepared via freeze-thawing, then microencapsulated in PLGA using a solvent evaporation technique [113].

#### 4.2.4.4 Acrylamide Based Hydrogels

Drug binding ability of albumin has been utilized in preparing hydrogels of acrylamide crosslinked with bovine serum albumin and claimed to be the cause of sustained release of salicylic acid from the BSA-crosslinked hydrogel [114]. Copolymer hydrogel of acrylamide and itaconic acid was prepared and studied for the controlled release of paracetamol in aqueous media of varying pH [115]. Polymer blends made by electrochemical polymerization of polypyrrole onto polyacrylamide were intended as a controlled release device for the delivery of safranin. Drug release from this device was expected to be controlled by an electrochemical potential. Voltametry and Raman spectroscopy were used for hydrogel characterization [116]. Copolymer hydrogels of *N*-isopropylacrylamide, trimethyl acrylamidopropyl ammonium iodide, and 3-dimethyl (methacryloyloxyethyl) ammonium propane sulfonate have been developed. The release of caffeine was found to increase with hydrogel swelling. The anionic solute phenol red was found to strongly interact with the cationic hydrogel, and its release was hence found to be very slow [117].

#### 4.2.4.5 Polyvinylpyrrolidone-Based Hydrogels

Polyvinylpyrrolidone iodine liposomal hydrogel has been suggested as a drug delivery platform for wound treatment in which antiseptic and moist treatment are desirable in the healing process. Compared to the normal PVP-iodine complex, the liposomal formulation was proven to enhance epithelization [118]. Ferrogels, gels containing ferromagnetic nanoparticles have been prepared based on polyvinylpyrrolidone via irradiation. Bleomycin A5 Hydrochloride, a wide spectrum anticancer drug was immobilized in the ferrogel and its release was studied in vitro [119]. A new micro particulate hydrogel has been obtained by gamma irradiation of poly [*N*-(2-hydroxyethyl)-DL-aspartamide]. With various concentrations of gastric enzymes, pepsin and alpha-chymotrypsin, the hydrogel degradation was not observed over a 24-h exposure period. The hydrogel was evaluated for oral delivery of an anti-inflammatory drug, diflunisal [120]. Polyvinylacetal diethylaminoacetate hydrogel has also been suggested for nasal delivery [121].

### *4.2.5 Superdisintegrants*

Superdisintegrants are crosslinked hydrophilic polymers with the ability to swell in an aqueous medium. Although they are not as potent as super water absorbent polymers (with swelling capacity of 100–1,000 g/g), they have enough potency (swelling capacity of 10–40 g/g) to fulfill their task in the pharmaceutical dosage forms. The swelling power of a superdisintegrant is controlled by its backbone structure, the crosslink density, and the amount of substitution.

#### 4.2.5.1 Hydrogels Based on Cellulose

Crosslinked carboxymethyl cellulose (sodium salt) is prepared by internal crosslinking (in the absence of a chemical crosslinker) and carboxymethylation of cellulose. In fact, crosslinking is induced by partially changing sodium carboxymethyl groups to their free acids followed by heating. It has an anionic backbone with sodium as counterion, which causes the polymer swelling to be very sensitive to the pH, salts (mono, di, and trivalence) and the ionic strength of the swelling medium. Swelling power of this polymer is significantly reduced at low pH and in concentrated solution of salts especially in the presence of di- and trivalent cations. It is used in oral pharmaceutical formulations as a disintegrant for capsules, tablets, and granules.

#### 4.2.5.2 Hydrogels Based on Polyvinylpyrrolidone

Crosslinked polyvinylpyrrolidone is prepared via a popcorn polymerization of vinyl pyrrolidone monomer. This polymerization method utilizes the excessive heat of polymerization to establish random crosslinking into the polymer structure. The polymer is essentially nonionic, and hence its swelling power is independent of the pH. The disintegrant is expected to reach its maximum swelling power independent of the type of salts in the swelling medium.

#### 4.2.5.3 Starch-Based Hydrogels

Similar to the crosslinked CMC, the crosslinked starch glycolate (sodium slat) is an anionic polymer and produced by crosslinking and carboxymethylation of potato starch. Although other sources of starch including maize, wheat, and rice can also be used, the sodium starch glycolate from potato is preferred. More details on this class of crosslinked hydrogels are found in Table 4.4 [29, 122].

**Table 4.4** Examples of commercial superdisintegrants

| | |
|---|---|
| Crosslinked carboxymethyl cellulose is used in more than 150 drugs in the US market | |
| *Sodium croscarmellose*<br>Ac-Di-Sol® (FMC Biopolymer);<br>Primellose® (DMV-Fonterra) | Diltiazem hydrochloride; clarithromycin (Biaxin Filmtab®); niacin (Niacor®); fenofibrate (Triglide®); sildenafil citrate (Viagra®); atorvastatin calcium (Lipitor®); celecoxib (Celebrex®); fexofenadine HCl (Allegra®); ibuprofen (Motrin®); oxazepam (Serax®) |
| Crosslinked polyvinylpyrrolidone is used in more than 100 drugs in the US market | |
| *Crospovidone*<br>Kollidone CL®, CL-M® (BASF);<br>Polyplasdone XL®, XL10® (ISP) | Amoxicillin (Amoxil®); rosuvastatin Calcium (Crestor®); diphenhydramine (Benadryl®); fenofibrate (Tricor®); metformin HCl (Glumetza®); alprazolam (Niravam®); omeprazole (Prilosec®) |
| Crosslinked starch glycolate is used in more than 155 drugs in the US market | |
| Primojel® (DMV-Fonterra) | Acyclovir (Zovirax®); theophylline (Theo-Dur®); diltiazem (Cardizem® LA); cimetidine (Tagamet®); fenofibrate (Lipofen®); metoprolol tartrate (Lopressor®) |

### 4.2.6 Ion Exchanging Hydrogels

Ion exchange resins are crosslinked polymers (some with hydrophilic and some with hydrophobic backbone) with anionic or cationic structures. While the crosslinked nature of the polymer allows absorption of the aqueous fluids into their structure, the ionic nature of these polymers allows exchanging their mobile ions with another cation or anion respectively. These hydrogels have found extensive applications in pharmaceutical industries as an active pharmaceutical ingredient to treat certain electrolyte imbalance (hyperkalimia), to reduce cholesterol (via sequestering bile acids), to taste-mask a drug, to control the drug release, to enhance drug stability, and to help dosage forms with their disintegration process. More details about this class of hydrogels can be found in Table 4.5 [29, 122].

### 4.2.7 Macroporous Hydrogels

One way to change the release properties of a typical hydrogel is to introduce porosity into its structure. The pores inside the hydrogel structure can be either isolated or interconnected. While both can offer a faster absorption and release compared to the conventional nonporous hydrogels, the latter offers a much faster absorption and release. Besides, the equilibrium swelling capacity of these hydrogels can be reached in seconds or minutes regardless of their size in the dry state. These hydrogels can be prepared using hydrophilic, ionic, nonionic, or even hydrophobic monomers through simultaneous polymerization and crosslinking processes. Acrylamide, acrylic or methacrylic acid and their salts, vinyl pyrrolidone, NIPAM, hydroxyethyl methacrylate, and more have already been

**Table 4.5** Examples of commercial ion-exchange resins

| |
|---|
| *Amberlite: This ion-exchange polymer is used for example in risperidone orally disintegrating tablets (Risperdal® M-Tab), propoxyphenenapsylate, and acetaminophen (Darvocet®-N100)* |
| *Amberlite® IRP64*: poly(methacrylic acid) crosslinked with divinyl benzene (DVB), not neutralized, with hydrogen as counterion, a weak acid |
| *Amberlite® IRP88* is a similar polymer with potassium as counterion, a weak acid |
| *Amberlite® IRP69* is sulfonated polystyrene crosslinked with DVB, a strong acid with sodium as counterion |
| *Cholestyramine: This ion-exchange resin is used for example in Questran® for oral suspension* |
| A chloride salt of a strong basic anion exchange resin, polystyrene crosslinked with DVB, a cholesterol lowering agent |
| *Sodium polystyrene sulfonate: Kionex®, and Kayexalate®* |
| A cation exchange resin prepared with an in vitro exchange capacity of approximately 3.1 mEq of potassium per gram, the sodium content is approximately 100 mg (4.1 mEq) per gram of the drug, administered orally or in an enema |
| *Colestipol hydrochloride: Colestid®* |
| A lipid lowering agent for oral use, colestipol is an insoluble, high molecular weight basic anion exchange copolymer of diethylenetriamine and 1-chloro-2, 3-epoxypropane |

used in preparation of superporous hydrogels [123–125]. Owing to their unique swelling properties, this class of hydrogels has been found to be attractive enough for more specific pharmaceutical and biomedical applications where another important property, mechanical strength is very much desirable. Hydrogels in general and porous hydrogels in particular suffer from weak mechanical strength in their wet or hydrated state. Approaches have been taken to enhance hydrogel mechanical properties, among which IPN structures comprising a synthetic monomer and a hydrocolloid have found to be the most effective [126–128]. With this approach, an aqueous monomer solution containing an iono-gelling hydrocolloid is polymerized in the presence of a chemical crosslinker and treated with salts afterward. Salts can change the semi-IPN structure of the hydrogel to a full IPN hydrogel with enhanced wet strength. Alternatively, various concentrations of different salts can be used to manipulate the hydrogel mechanical properties [129–131]. These hydrogels have so far been investigated as a controlled release platform for proteins [132–134], as a gastroretentive platform to enhance bioavailability of the drugs with narrow absorption window [127] as well as a tablet superdisintegrant [135].

## *4.2.8 Other Hydrogel Products*

### 4.2.8.1 Hydrogel Implants

Histrelin acetate (Supprelin LA®, Vantas) subcutaneous implant is a long term delivery platform for the nonapeptide histrelin acetate. The drug is used to treat the symptoms of advanced prostate cancer and is released from this synthetic nonbiodegradable platform over a 12-month period. The hydrogel platform

(3.5 cm × 3 mm cylinder) is composed of 2-hydroxyethyl methacrylate, 2-hydroxypropyl methacrylate, trimethylolpropane trimethacrylate, and other nonpolymeric additives [29].

#### 4.2.8.2 Hydrogel Inserts

The vaginal insert Cervidil® is composed of a crosslinked polyethylene oxide/urethane polymer (rectangle shape, 29 mm × 9.5 mm × 0.8 mm) and has been designed to release dinoprostone at about 0.3 mg/h in vivo. Once placed in a moist environment, the platform swells and releases the drug [29].

#### 4.2.8.3 Osmotic Devices

Ionsys™ provides 40 μg dose of fentanyl per activation, which takes about 10 min. The system has two hydrogel reservoirs. The anode hydrogel contains fentanyl HCl and the cathode hydrogel contains inactive excipients including polacrilin and poly(vinyl alcohol) [29].

#### 4.2.8.4 Osmotic Implants

Viadur® (leuprolide acetate implant) is a sterile nonbiodegradable implant (45 mm × 4 mm, 1.1 g) that has been designed to deliver leuprolide acetate over a 12-month period. The implant utilizes Alza's Duros technology and is inserted subcutaneously. The platform is composed of a polyurethane rate controlling membrane, an elastomeric piston, and a polyethylene diffusion moderator [29]. The osmotic force, which drives long-term delivery of the active, is originated from the osmotic tablets composed of sodium chloride, sodium carboxymethyl cellulose, and povidone.

#### 4.2.8.5 Osmotic Tablets

Paliperidone is an atypical antipsychotic medication for the acute and maintenance treatment of schizophrenia. Invega® is an osmotically driven delivery system (in tablet form), which uses osmotic pressure to deliver paliperidone at a controlled rate. The delivery system is composed of a trilayer core (osmotically active), subcoat, and a semipermeable membrane and has two laser-drilled orifices on the drug layer. In an aqueous environment, water enters the tablet through the semipermeable membrane at a controllable rate. The hydrophilic polymers of the core generally poly(ethylene oxide) hydrate and swell and create a gel mass containing paliperidone, which is pushed out of the tablet orifices [29]. Concerta®, Ditropan®XL, and Glucophage®XR utilize a similar concept to deliver methylphenidate HCl (a central nervous system

stimulant), oxybutynin chloride (an antispasmodic, anticholinergic agent), and metformin HCl (an antidiabetic), respectively.

#### 4.2.8.6 Tissue Expanders

The idea of growing extra skin for reconstructing purposes is a neat one. Conventionally, a silicone rubber is inserted subcutaneously, and then is filled with saline to stretch the skin and to induce its growth. Silicone expanders are used for breast reconstruction and deformities, damaged skins, burns, scars, skin cancer, and more. In order to stretch the tissue to the desired size, the balloon needs to be filled with saline over and over, which may cause infection and rejection by patients. Osmed, a Germany based company has utilized a similar concept except the balloon is self inflated and it is not filled with fluids. The Osmed expander is a crosslinked copolymer of methyl methacrylate and *N*-vinyl pyrrolidone similar to the materials used in soft contact lenses. It absorbs the fluid from surrounding tissues and swells to 3–12 times its own volume. The slow swelling expanders are supplied as rectangle, round and cylinder with swelling time ranging from 10 to 180 days, while the faster ones are supplied as semi sphere, sphere and pin with swelling time of a few days [136–138]. Alternatively, the liquid contents of a conventional silicone expander can be converted to a semisolid mass to minimize the fluid leakage from the device. Hydrogels based on crosslinkable macromonomers with polymerizable end-groups are under development for breast reconstruction applications [139].

#### 4.2.8.7 Contact Lenses

A contact lens material should have a combination of properties such as ease of manufacturing, FDA acceptability, wetability, and permeability. There are generally three types of contact lenses, i.e., hard, soft, and gas permeable (GP or RGP). Hard lenses are originally based on poly(methyl methacrylate) and their service temperature is below the polymer glass transition temperature. To make the lens material, methyl methacrylate monomer is polymerized in bulk in the presence of crosslinker and initiator via a radiation technique (ultraviolet or infrared). Hard lenses prepared in this way are then cut with a precision lathe. Hard lenses are now obsolete and have been replaced by soft and gas permeable lenses. Soft contact lenses are typically formed via a simultaneous polymerization and cast molding or spin casting. These are generally based on 2-hydroxyethyl methacrylate with either *N*-vinyl pyrrolidone or methacrylic acid monomer, crosslinked with ethylene glycol dimethacrylate. Alternatively, soft lenses are manufactured based on polydimethylsiloxane, so called siloxane lenses. Focus Night and Day® (Ciba Vision), Acuvue Oasys® (Vistakon) and PureVision® (Bausch and Lomb) are silicon based hydrogel lenses. Some recently approved soft contact lenses by the FDA are Omafilcon A® (a copolymer of 2-hydroxyethyl methacrylate and 2-methacryloyloxyethyl phosphorylcholine

crosslinked with ethylene glycol dimethacrylate), Methafilcon A® (a hydrophilic copolymer of 2-hydroxyethyl methacrylate and methacrylic acid, crosslinked with ethylene glycol dimethacrylate), and Hioxifilcon A® (ultrahigh-molecular-weight random copolymer of 2-hydroxyethyl methacrylate and 2,3-dihydroxpropyl methacrylate (glycerol methacrylate) crosslinked with ethylene glycol dimethacrylate [140]). Some recently approved gas permeable contact lenses are Pahrifocon A® (a crosslinked copolymer of acrylate, silicone acrylate, and fluorosilicone acrylate monomers, dimers and oligomers), Hexafocon A®, Enflufocon B®, and Enflufocon A® (aliphatic fluoroitaconate siloxanyl methacrylate copolymer available with or without UV blocker) [140].

## 4.3 Conclusion

Swelling and mechanical features of hydrogel polymers have enabled them to find extensive applications in traditional, modern, and novel pharmaceutical area. Desirable hydrogel properties for a given application can be achieved by selecting a proper hydrogel material, crosslinking method, as well as processing techniques. These biocompatible materials are currently used in pharmaceutical dosage forms as superdisintegrant, ion exchangeable material, and controlled release platform. On the contrary, nondisposable hydrogels with longer term of service have found applications as biomedical inserts and implants. Superporous hydrogels are an exclusive class of hydrogels that can potentially be used for both short- and long term applications including superdisintegrant, controlled release platform, and a gastroretentive drug delivery system.

## References

1. Celia H, Special Delivery. http://pubs.acs.org/cen/coverstory/7838/7838scit1.html
2. Chen H et al (2007) Characterization of pH- and temperature-sensitive hydrogel nanoparticles for controlled drug release. PDA J Pharm Sci Technol 61(4):303–313
3. Satarkar NS, Hilt JZ (2008) Magnetic hydrogel nanocomposites for remote controlled pulsatile drug release. J Control Release 130(3):246–251
4. Huang G et al (2004) Controlled drug release from hydrogel nanoparticle networks. J Control Release 94(2–3):303–311
5. Kim JH, Lee TR (2006) Discrete thermally responsive hydrogel-coated gold nanoparticles for use as drug-delivery vehicles. Drug Dev Res 67(1):61–69
6. Okuyama Y et al (1993) Swelling controlled zero-order and sigmoidal drug-release from thermoresponsive poly(n-isopropylacrylamide-co-butyl methacrylate) hydrogel. J Biomater Sci Polym Ed 4(5):545–556
7. Jones DS et al (2008) Characterization of the physicochemical, antimicrobial, and drug release properties of thermoresponsive hydrogel copolymers designed for medical device applications. J Biomed Mater Res B Appl Biomater 85B(2):417–426

8. Jeong B, Bae YH, Kim SW (2000) Drug release from biodegradable injectable thermosensitive hydrogel of PEG-PLGA-PEG triblock copolymers. J Control Release 63 (1–2):155–163
9. Slepian MJ (1996) Polymeric endoluminal gel paving: therapeutic hydrogel barriers and sustained drug delivery depots for local arterial wall biomanipulation. Semin Interv Cardiol 1 (1):103–116
10. Mayo L et al (2008) A novel poloxamers/hyaluronic acid in situ forming hydrogel for drug delivery: rheological, mucoadhesive and in vitro release properties. Eur J Pharm Biopharm 70 (1):199–206
11. Zhao Y et al (2006) Study on preparation of the pH sensitive hydroxyethyl chitin/poly (acrylic acid) hydrogel and its drug release property. Sheng Wu Yi Xue Gong Cheng Xue Za Zhi 23(2):338–341
12. Bilia A et al (1996) In vitro evaluation of a pH-sensitive hydrogel for control of GI drug delivery from silicone-based matrices. Int J Pharm 130(1):83–92
13. Kim IS, Oh IJ (2005) Drug release from the enzyme-degradable and pH-sensitive hydrogel composed of glycidyl methacrylate dextran and poly(acrylic acid). Arch Pharm Res 28 (8):983–987
14. Ali Ael-H, Hegazy el-SA (2007) Radiation synthesis of poly(ethylene glycol)/acrylic acid hydrogel as carrier for site specific drug delivery. J Biomed Mater Res B Appl Biomater 81(1):168–174
15. Liu YY et al (2006) pH-responsive amphiphilic hydrogel networks with IPN structure: a strategy for controlled drug. Int J Pharm 308(1–2):205–209
16. Sadeghi M, Hosseinzadeh H (2008) Synthesis of starch-poly(sodium acrylate-co-acrylamide) superabsorbent hydrogel with salt and pH-responsiveness properties as a drug delivery system. J Bioact Comp Polym 23(4):381–404
17. Mundargi RC et al (2008) Sequential interpenetrating polymer network hydrogel microspheres of poly(methacrylic acid) and poly(vinyl alcohol) for oral controlled drug delivery to intestine. J Microencapsul 25(4):228–240
18. Bajpai SK, Saggu SPS (2007) Controlled release of an anti-malarial drug from a pH-sensitive poly(methacrylamide-co-methacrylic acid) hydrogel system. Desig Monom Polymer 10 (6):543–554
19. Varshosaz J, Hajian M (2004) Characterization of drug release and diffusion mechanism through hydroxyethylmethacrylate/methacrylic acid pH-sensitive hydrogel. Drug Deliv 11 (1):53–58
20. Jain SK et al (2007) Design and development of hydrogel beads for targeted drug delivery to the colon. AAPS PharmSciTech 8(3):E56
21. Jain SK et al (2007) Design and development of hydrogel beads for targeted drug delivery to the colon. AAPS PharmSciTech 8:E34–E41
22. Lin YW, Chen Q, Luo HB (2007) Preparation and characterization of *N*-(2-carboxybenzyl) chitosan as a potential pH-sensitive hydrogel for drug delivery. Carbohydr Res 342(1):87–95
23. Sun LP et al (2004) The synthesis of carboxymethylchitosan hydrogel and the application in drug controlled release systems. Acta Polymerica Sinica 2:191–195
24. Zhou YS et al (2008) A pH-sensitive water-soluble *N*-carboxyethyl chitosan/poly (hydroxyethyl methacrylate) hydrogel as a potential drug sustained release matrix prepared by photopolymerization technique. Polymer Adv Technol 19(8):1133–1141
25. Chen SC et al (2004) A novel pH-sensitive hydrogel composed of N, O-carboxymethyl chitosan and alginate crosslinked by genipin for protein drug delivery. J Control Release 96(2):285–300
26. Castelli F et al (2008) Differential scanning calorimetry study on drug release from an inulin-based hydrogel and its interaction with a biomembrane model: pH and loading effect. Eur J Pharm Sci 35(1–2):76–85
27. Varshosaz J, Falamarzian M (2001) Drug diffusion mechanism through pH-sensitive hydrophobic/polyelectrolyte hydrogel membranes. Eur J Pharm Biopharm 51(3):235–240

28. Kulkarni RV, Sa B (2008) Evaluation of pH-sensitivity and drug release characteristics of (Polyacrylamide-Grafted-Xanthan)-carboxymethyl cellulose-based pH-sensitive interpenetrating network hydrogel beads. Drug Develop Ind Pharm 34(12):1406–1414
29. http://www.rxlist.com
30. Bettini R et al (1994) Swelling and drug-release in hydrogel matrices – polymer viscosity and matrix porosity effects. Eur J Pharm Sci 2(3):213–219
31. Alvarez-Mancenido F et al (2006) Characterization of diffusion of macromolecules in konjac glucomannan solutions and gels by fluorescence recovery after photobleaching technique. Int J Pharm 316(1–2):37–46
32. Antony PJ, Sanghavi NM (1997) A new disintegrant for pharmaceutical dosage forms. Drug Dev Ind Pharm 23(4):413–415
33. Antony PJ, Sanghavi NM (1997) A new binder for pharmaceutical dosage forms. Drug Dev Ind Pharm 23(4):417–418
34. Deasy PB, Quigley KJ (1991) Rheological evaluation of deacetylated Gellan gum (Gelrite) for pharmaceutical use. Int J Pharm 73(2):117–123
35. Beck GM, Neau SH (2000) Optimization of lambda-carrageenan as a chiral selector in capillary electrophoresis separations. Chirality 12(8):614–620
36. Valenta C, Schultz K (2004) Influence of carrageenan on the rheology and skin permeation of microemulsion formulations. J Control Release 95(2):257–265
37. Binello A et al (2004) Synthesis of chitosan-cyclodextrin adducts and evaluation of their bitter-masking properties. Flav Fragr J 19(5):394–400
38. Chae SY, Jang MK, Nah JW (2005) Influence of molecular weight on oral absorption of water soluble chitosans. J Control Release 102(2):383–394
39. El Fattah EA et al (1998) Physical characteristics and release behavior of salbutamol sulfate beads prepared with different ionic polysaccharides. Drug Dev Ind Pharm 24(6):541–547
40. Felt O, Buri P, Gurny R (1998) Chitosan: a unique polysaccharide for drug delivery. Drug Dev Ind Pharm 24(11):979–993
41. George M, Abraham TE (2006) Polyionic hydrocolloids for the intestinal delivery of protein drugs: alginate and chitosan – a review. J Control Release 114(1):1–14
42. Singla AK, Chawla M (2001) Chitosan: some pharmaceutical and biological aspects – an update. J Pharm Pharmacol 53(8):1047–1067
43. Thanou M, Verhoef JC, Junginger HE (2001) Oral drug absorption enhancement by chitosan and its derivatives. Adv Drug Deliv Rev 52(2):117–126
44. Grant J, Cho J, Allen C (2006) Self-assembly and physicochemical and rheological properties of a polysaccharide-surfactant system formed from the cationic biopolymer chitosan and nonionic sorbitan esters. Langmuir 22(9):4327–4335
45. Harding SE (2006) Trends in mucoadhesive analysis. Trends Food Sci Technol 17 (5):255–262
46. Kas HS (1997) Chitosan: properties, preparations and application to microparticulate systems. J Microencapsul 14(6):689–711
47. Senel S, McClure SJ (2004) Potential applications of chitosan in veterinary medicine. Adv Drug Deliv Rev 56(10):1467–1480
48. Wu J et al (2007) Water soluble complexes of chitosan-g-MPEG and hyaluronic acid. J Biomed Mater Res A 80(4):800–812
49. Yu SY et al (2006) Stable and pH-sensitive nanogels prepared by self-assembly of chitosan and ovalbumin. Langmuir 22(6):2754–2759
50. Chan LW, Lee HY, Heng PWS (2002) Production of alginate microspheres by internal gelation using an emulsification method. Int J Pharm 242(1–2):259–262
51. Dusseault J et al (2006) Evaluation of alginate purification methods: effect on polyphenol, endotoxin, and protein contamination. J Biomed Mater Res A 76(2):243–251
52. Daraio ME, Francois N, Bernik DL (2003) Correlation between gel structural properties and drug release pattern in scleroglucan matrices. Drug Deliv 10(2):79–85

53. Deodhar UP, Paradkar AR, Purohit AP (1998) Preliminary evaluation of *Leucaena leucocephala* seed gum as a tablet binder. Drug Dev Ind Pharm 24(6):577–582
54. Rubinstein A, Glikokabir I (1995) Synthesis and swelling-dependent enzymatic degradation of Borax-modified guar gum for colonic delivery purposes. Stp Pharma Sciences 5 (1):41–46
55. Desai UR, Linhardt RJ (1995) Molecular-weight of heparin using C-13 nuclear-magnetic-resonance spectroscopy. J Pharm Sci 84(2):212–215
56. Fuchs T, Richtering W, Burchard W (1995) Thermoreversible gelation of a polysaccharide with immunological activity – rheology and dynamic light-scattering. Macromol Symp 99:227–238
57. Munzberg J, Rau U, Wagner F (1995) Investigations on the regioselective hydrolysis of a branched beta-1,3-glucan. Carbohydr Polymers 27(4):271–276
58. Song KW, Kim YS, Chang GS (2006) Rheology of concentrated xanthan gum solutions: steady shear flow behavior. Fibers & Polymers 7(2):129–138
59. Tobyn MJ et al (1996) Prediction of physical properties of a novel polysaccharide controlled release system 1. Int J Pharm 128(1–2):113–122
60. Uekama K et al (1995) Modification of rectal absorption of morphine from hollow-type suppositories with a combination of alpha-cyclodextrin and viscosity-enhancing polysaccharide. J Pharm Sci 84(1):15–20
61. Liu WG, Griffith M, Li FF (2008) Alginate microsphere-collagen composite hydrogel for ocular drug delivery and implantation. J Mater Sci Mater Med 19(11):3365–3371
62. Bajpai SK, Sharma S (2006) Investigation of pH-sensitive swelling and drug release behavior of barium alginate/carboxymethyl guar gum hydrogel beads. J Macromol Sci Part A-Pure Appl Chem 43(10):1513–1521
63. Soppimath KS, Kulkarni AR, Aminabhavi TM (2000) Controlled release of antihypertensive drug from the interpenetrating network poly(vinyl alcohol)-guar gum hydrogel microspheres. J Biomater Sci Polym Ed 11(1):27–43
64. Soppirnath KS, Aminabhavi TM (2002) Water transport and drug release study from crosslinked polyacrylamide grafted guar gum hydrogel microspheres for the controlled release application. Eur J Pharm Biopharm 53(1):87–98
65. Knapczyk J (1993) Chitosan hydrogel as a base for semisolid drug forms. Int J Pharm 93 (1–3):233–237
66. Dai YN et al (2008) Swelling characteristics and drug delivery properties of nifedipine-loaded pH sensitive alginate-chitosan hydrogel beads. J Biomed Mater Res B Appl Biomater 86B(2):493–500
67. Bodek KH (2000) Evaluation of properties microcrystalline chitosan as a drug carrier. Part 1. In vitro release of diclofenac from mictocrystalline chitosan hydrogel. Acta Pol Pharm 57 (6):431–440
68. Kubota N (1993) Molecular-weight dependence of the properties of chitosan and chitosan hydrogel for use in sustained-release drug. Bull Chem Soc Jpn 66(6):1807–1812
69. Liu TY et al (2006) Synthesis and characterization of amphiphatic carboxymethyl-hexanoyl chitosan hydrogel: water-retention ability and drug encapsulation. Langmuir 22(23):9740–9745
70. Qiu LY (2004) Preparation and evaluation of chitosan-coated polyphosphazene hydrogel beads for drug controlled release. J Appl Polym Sci 92(3):1993–1999
71. Taleb MFA (2008) Radiation synthesis of polyampholytic and reversible pH-responsive hydrogel and its application as drug delivery system. Polym Bull 61(3):341–351
72. Vodna L, Bubenikova S, Bakos D (2007) Chitosan based hydrogel microspheres as drug carriers. Macromol Biosci 7(5):629–634
73. Yao KD et al (1994) pH-dependent hydrolysis and drug-release of chitosan polyether interpenetrating polymer network hydrogel. Polym Int 34(2):213–219
74. Ishihara M et al (2006) Chitosan hydrogel as a drug delivery carrier to control angiogenesis. J Artif Organs 9(1):8–16

75. Mohamadnia Z et al (2007) pH-sensitive IPN hydrogel beads of carrageenan-alginate for controlled drug delivery. J Bioact Compat Polym 22(3):342–356
76. Liu JH, Li L, Cai YY (2006) Immobilization of camptothecin with surfactant into hydrogel for controlled drug release. Eur Polym J 42(8):1767–1774
77. Makino K et al (2001) Design of a rate- and time-programming drug release device using a hydrogel: pulsatile drug release from kappa-carrageenan hydrogel device by surface erosion of the hydrogel. Colloids Surf B Biointerfaces 20(4):355–359
78. Coviello T et al (2003) Structural and rheological characterization of Scleroglucan/borax hydrogel for drug delivery. Int J Biol Macromol 32(3–5):83–92
79. Coviello T et al (2003) Scleroglucan/borax: characterization of a novel hydrogel system suitable for drug delivery. Biomaterials 24(16):2789–2798
80. Coviello T et al (2005) A new scleroglucan/borax hydrogel: swelling and drug release studies. Int J Pharm 289(1–2):97–107
81. Palleschi A et al (2006) Investigation on a new scleroglucan/borax hydrogel: structure and drug release. Int J Pharm 322(1–2):13–21
82. Hayashi K et al (2007) Development of new drug delivery system for implant bone augmentation using a basic fibroblast growth factor-gelatin hydrogel complex. Dent Mater J 26 (2):170–177
83. David L et al (2008) Hyaluronan hydrogel: an appropriate three-dimensional model for evaluation of anticancer drug sensitivity. Acta Biomater 4(2):256–263
84. Luo Y, Kirker KR, Prestwich GD (2000) Crosslinked hyaluronic acid hydrogel films: new biomaterials for drug delivery. J Control Release 69(1):169–184
85. Sungthongjeen S et al (1999) Studies on pectins as potential hydrogel matrices for controlled-release drug delivery. Drug Dev Ind Pharm 25(12):1271–1276
86. Sutar PB et al (2008) Development of pH sensitive polyacrylamide grafted pectin hydrogel for controlled drug delivery system. J Mater Sci Mater Med 19(6):2247–2253
87. Mishra RK, Datt M, Banthia AK (2008) Synthesis and characterization of pectin/PVP hydrogel membranes for drug delivery system. AAPS PharmSciTech 9(2):395–403
88. Munjeri O, Collett JH, Fell JT (1997) Hydrogel beads based on amidated pectins for colon-specific drug delivery: the role of chitosan in modifying drug release. J Control Release 46 (3):273–278
89. Ramaraj B, Radhakrishnan G (1994) Interpenetrating hydrogel networks based on gelatin and polyacrylamide – synthesis, swelling, and drug-release analysis. J Appl Polym Sci 52 (7):837–846
90. Wang N, Wu XS (1997) Preparation and characterization of agarose hydrogel nanoparticles for protein and peptide drug delivery. Pharm Dev Technol 2(2):135–142
91. Chen F, Wu Z, Jin Y (2005) Application research on dextran-based hydrogel and its drug controlled release. Zhongguo Xiu Fu Chong Jian Wai Ke Za Zhi 19(11):919–922
92. Vervoort L et al (1997) Inulin hydrogels as carriers for colonic drug targeting: I. Synthesis and characterization of methacrylated inulin and hydrogen formation. Pharm Res 14 (12):1730–1737
93. Vervoort L et al (1999) Inulin hydrogels as carriers for colonic drug targeting. Rheological characterization of the hydrogel formation and the hydrogel network. J Pharm Sci 88 (2):209–214
94. Kuzma P et al (1996) Subcutaneous hydrogel reservoir system for controlled drug delivery. Macromol Symp 109:15–26
95. Eljarrat-Binstock E et al (2007) Preparation, characterization, and sterilization of hydrogel sponges for iontophoretic drug-delivery use. Polymer Adv Technol 18:720–730
96. Arica MY et al (2005) Novel hydrogel membrane based on copoly(hydroxyethyl methacrylate/p-vinylbenzylpoly(ethylene oxide)) for biomedical applications: properties and drug release characteristics. Macromol Biosci 5(10):983–992
97. Blanco MD, Rego JM, Huglin MB (1994) Drug-release with simultaneous dimensional changes from a new copolymeric hydrogel. Polymer 35(16):3487–3491

98. De Giglio E et al (2009) Electrosynthesis of hydrogel films on metal substrates for the development of coatings with tunable drug delivery performances. J Biomed Mater Res A 88(4):1048–1057
99. Eljarrat-Binstock E et al (2004) Hydrogel probe for iontophoresis drug delivery to the eye. J Biomater Sci Polym Ed 15(4):397–413
100. Eljarrat-Binstock E et al (2005) Transcorneal and transscleral iontophoresis of dexamethasone phosphate using drug loaded hydrogel. J Control Release 106(3):386–390
101. Eljarrat-Binstock E et al (2004) Delivery of gentamicin to the rabbit eye by drug-loaded hydrogel iontophoresis. Invest Ophthalmol Vis Sci 45(8):2543–2548
102. Gulsen D, Chauhan A (2005) Dispersion of microemulsion drops in HEMA hydrogel: a potential ophthalmic drug delivery vehicle. Int J Pharm 292(1–2):95–117
103. Gayet JC, Fortier G (1995) Drug-release from new bioartificial hydrogel. Artif Cells Blood Substit Immobil Biotechnol 23(5):605–611
104. Gayet JC, Fortier G (1996) High water content BSA-PEG hydrogel for controlled release device: evaluation of the drug release properties. J Control Release 38(2–3):177–184
105. Qiu B et al (2003) A hydrogel prepared by in situ crosslinking of a thiol-containing poly (ethylene glycol)-based copolymer: a new biomaterial for protein drug delivery. Biomaterials 24(1):11–18
106. Missirlis D, Tirelli N, Hubbell JA (2005) Amphiphilic hydrogel nanoparticles. Preparation, characterization, and preliminary assessment as new colloidal drug carriers. Langmuir 21 (6):2605–2613
107. Shekunov BY et al (2007) Structure and drug release in a crosslinked poly(ethylene oxide) hydrogel. J Pharm Sci 96(5):1320–1330
108. Shekunov BY, Taylor P, Grossmann JG (1999) Structural phenomena in hydrogel-drug systems. J Crystal Growth 198:1335–1339
109. Lin H et al (2006) Synthesis, characterization and drug release of temperature-sensitive PLGA-PEG-PLGA hydrogel. Chem J Chinese Universities-Chinese 27(7):1385–1388
110. Varshosaz J, Koopaie N (2002) Crosslinked poly (vinyl alcohol) hydrogel: study of swelling and drug release behaviour. Iranian Polym J 11(2):123–131
111. Wang N, Wu XS, Li JK (1999) A heterogeneously structured composite based on poly(lactic-co-glycolic acid) microspheres and poly(vinyl alcohol) hydrogel nanoparticles for long-term protein drug delivery. Pharm Res 16(9):1430–1435
112. Ramaraj B, Radhakrishnan G (1994) Hydrogel capsules for sustained drug-release. J Appl Polym Sci 51(6):979–988
113. Mandal TK et al (2002) Poly(d, l-lactide-co-glycolide) encapsulated poly(vinyl alcohol) hydrogel as a drug delivery system. Pharm Res 19(11):1713–1719
114. Tada D et al (2005) Drug release from hydrogel containing albumin as crosslinker. J Biosci Bioeng 100(5):551–555
115. Stanojevic M et al (2006) An investigation into the influence of hydrogel composition on swelling behavior and drug release from poly(acrylamide-co-itaconic acid) hydrogels in various media. Drug Deliv 13(1):1–7
116. Barthus RC, Lira LM, de Torresi SIC (2008) Conducting polymer-hydrogel blends for electrochemically controlled drug release devices. J Braz Chem Soc 19(4):630–636
117. Lee WF, Chiu RJ (2002) Thermoreversible hydrogel. XVII. Investigation of the drug release behavior for [N-isopropylacrylamide-co-trimethyl acrylamidopropyl ammonium iodide-co-3-dimethyl (methacryloyloxyethyl) ammonium propane sulfortate] copolymeric hydrogels. J Appl Polym Sci 86(7):1592–1598
118. Reimer K et al (2000) An innovative topical drug formulation for wound healing and infection treatment: in vitro and in vivo investigations of a povidone-iodine liposome hydrogel. Dermatology 201(3):235–241
119. Chen J et al (2005) Preparation and characterization of magnetic targeted drug controlled-release hydrogel microspheres. Macromol Symp 225:71–80

120. Giammona G et al (1997) A hydrogel based on a polyaspartamide: characterization and evaluation of in-vivo biocompatibility and drug release in the rat. J Pharm Pharmacol 49 (11):1051–1056
121. Aikawa K et al (1998) Drug release from pH-response polyvinylacetal diethylaminoacetate hydrogel, and application to nasal delivery. Int J Pharm 168(2):181–188
122. http://www.drugs.com
123. Chen J, Park H, Park K (1999) Synthesis of superporous hydrogels: hydrogels with fast swelling and superabsorbent properties. J Biomed Mater Res 44(1):53–62
124. Chen J, Park K (1999) Superporous hydrogels: fast responsive hydrogel systems. J Macromol Sci-Pure Appl Chem A36(7–8):917–930
125. Chen J, Park K (2000) Synthesis and characterization of superporous hydrogel composites. J Control Release 65(1–2):73–82
126. Omidian H, et al (2005) Hydrogels having enhanced elasticity and mechanical strength properties in US patent 6,960,617
127. Omidian H, Rocca JG (2006) Formation of strong superporous hydrogels in US patent 7,056,957
128. Omidian H, Rocca JG, Park K (2006) Elastic, superporous hydrogel hybrids of polyacrylamide and sodium alginate. Macromol Biosci 6(9):703–710
129. Omidian H, Park K (2008) Swelling agents and devices in oral drug delivery. J Drug Deliv Sci Technol 18(2):83–93
130. Omidian H, Park K, Rocca JG (2007) Recent developments in superporous hydrogels. J Pharm Pharmacol 59(3):317–327
131. Omidian H, Rocca JG, Park K (2005) Advances in superporous hydrogels. J Control Release 102(1):3–12
132. Dorkoosh FA et al (2001) Development and characterization of a novel peroral peptide drug delivery system. J Control Release 71(3):307–318
133. Dorkoosh FA et al (2002) Intestinal absorption of human insulin in pigs using delivery systems based on superporous hydrogel polymers. Int J Pharm 247(1–2):47–55
134. Dorkoosh FA et al (2002) Evaluation of superporous hydrogel (SPH) and SPH composite in porcine intestine ex-vivo: assessment of drug transport, morphology effect, and mechanical fixation to intestinal wall. Eur J Pharm Biopharm 53(2):161–166
135. Yang SC et al (2004) Application of poly(acrylic acid) superporous hydrogel microparticles as a super-disintegrant in fast-disintegrating tablets. J Pharm Pharmacol 56(4):429–436
136. Wiese KG (1996) Tissue expander inflating due to osmotic driving forces of a shaped body of hydrogel and an aqueous solution. US Patent #5,496,368
137. Wiese KG et al (2001) Biomaterial properties and biocompatibility in cell culture of a novel self-inflating hydrogel tissue expander. J Biomed Mater Res 54(2):179–188
138. Osmed (GMBH), Hydrogel competence: self-inflating tissue expander. http://www.osmed.biz
139. Akina, Tissue expanding hydrogel (Resitex). http://www.akinainc.com
140. List of contact lenses allowed to be sold in the United States. Food and Drug Administration Website, http://www.fda.gov/cdrh/contactlenses/lenslist.html

# Chapter 5
# Biodegradable Polymers in Drug Delivery Systems

**Jamie Tsung and Diane J. Burgess**

**Abstract** This chapter is focused on the use of biodegradable polymers in long acting injectable drug delivery systems with an emphasis on marketed products. An overview is provided of how the chemical structures and physical properties of these polymers impact functionality of drug delivery systems and how to strategically select polymers for different applications. Detailed examples of biodegradable drug delivery systems are discussed with respect to routes of administration and disease states. The reader will gain information on polymer selection for different applications and on how to integrate knowledge of materials science and formulations to strategically design drug delivery systems for different pathological states.

## 5.1 Introduction

During the past several decades, considerable research and development efforts have focused on biodegradable polymers for biomedical applications [1]. Medical applications of biodegradable polymers range from sutures in wound management to antiadhesive coating agents in stent devices [18, 26, 31–33, 41, 53]. The first suture using a synthetic polymer, polyglycolide suture (Dexon™), was introduced in 1969. Owing to the availability of safety and long-term clinical data, and their predicable degradation profiles, biodegradable polymers have been utilized in various controlled drug delivery systems [13, 29].

Controlled drug delivery can involve both rate and target control [6, 42], allowing for predictable dissolution rates, optimizing drug release to achieve concentrations

J. Tsung
Shire HGT, Cambridge, MA 02139, USA

D.J. Burgess (✉)
Department of Pharmaceutical Sciences, University of Connecticut, Storrs, CT, USA
e-mail: DJ burgess@uconn.edu

J. Siepmann et al. (eds.), *Fundamentals and Applications of Controlled Release Drug Delivery*, Advances in Delivery Science and Technology,
DOI 10.1007/978-1-4614-0881-9_5, 

within the therapeutic index in vivo, and targeting of specific cells, tissues, and organs. Consequently, controlled drug delivery is able to reduce the frequency of administration, reduce systemic side effects, and increase patient compliance. Controlled drug delivery is flexible and can utilize various routes of administration routes, including the oral, buccal, transdermal, ocular, nasal, pulmonary, and parenteral routes. However, the need for biodegradable polymeric delivery systems is mainly in the parenteral area.

Numerous parenteral, polymeric controlled delivery technologies have been successfully developed and validated, and many products are currently on the market, including nanoparticle systems, microspheres, hydrogel implants, and prodrugs [22, 38, 40, 47]. These systems are administered via intravenous, subcutaneous, and intramuscular injection. Biodegradable polymer delivery systems degrade safely in the body, eliminating the need for surgical extraction. In addition, biodegradable polymers tend to have improved biocompatibility with respect to foreign body response compared to nondegradable polymers.

In 1989, the US Food and Drug Administration (FDA) approved the first biodegradable polymeric controlled drug delivery system Lupron® Depot for the treatment of advanced prostate cancer [2]. Lupron® Depot is leuprolide encapsulated into poly(D,L-lactide-*co*-glycolide) (PLGA) microspheres. The depot is a suspension dosage form administered intramuscularly, providing long term leuprolide delivery. PLGA slowly hydrolyzes in the body, delivering leuprolide over periods of weeks to months. In recent years, numerous biodegradable polymeric delivery systems including Trelstar® Depot, Zoladex®, and Eligard® have been introduced into the market. Section 5.3 includes a detailed discussion of these delivery systems.

The aim of this chapter is to provide an overview of applications of biodegradable polymers in marketed parenteral drug delivery systems. Most of these applications are in the form of particulate and in situ controlled drug delivery systems. Formulation design and selection of biodegradable polymers as well as strategies for controlled delivery and targeting delivery are discussed.

## 5.2 Classification of Biodegradable Polymers

A polymer is a large molecule composed of many repeating smaller structural units called monomers that are connected by covalent chemical bonds. Biodegradation is the chemical breakdown of materials in a physiological environment where the material is degraded by enzymes or is hydrolysed [14, 46]. Depending on the source, biodegradable polymers are classified as either synthetic or natural (biologically derived). Examples of both kinds are listed in Table 5.1.

There are several requirements that must be met for biodegradable polymers to be used in parenteral drug delivery systems, as discussed by Naira and Laurencin [33]. Biodegradable polymers used in parenteral drug delivery systems should be naturally and completely eliminated from the body and the polymers and degradants

**Table 5.1** Examples of natural and synthetic biodegradable polymers

| Natural biodegradable polymers | Synthetic biodegradable polymers |
|---|---|
| Proteins: collagen, gelatin, albumin, elastin, fibrin | Polyesters: Poly(glycolic acid), Poly(lactic acid), Poly (lactic-glycolic acid), Poly(caprolactone) (PCL) |
| Polysaccharides: chitosan, dextran, alginate, hyaluronic acid | Polyanhydrides |
| | Polyorthoesters |
| | Polyurethanes |
| | Tyrosine-derived polycarbonates |
| | Polyphosphazenes |

should be nontoxic and non immunogenic. They should also be compatible with the therapeutic agent(s) and excipients, and should not interfere with the therapeutic effects of the drug. From a manufacturing and CMC (chemistry, manufacturing and controls) standpoint, the polymer should be easy to synthesize and characterize, batches should be reproducible, and the polymer should be stable and easily sterilized. The manufacturing process should be simple and economic to manufacture and scale-up. From a business standpoint, polymers should be applicable to various drugs, including small molecules, proteins, and nucleic acid-based drugs.

### *5.2.1 Natural Polymers*

Natural polymers, listed in the left column of Table 5.1, are present in plants or animals, as proteins and polysaccharides [41]. Most natural polymers are water-soluble and must be crosslinked to from a water insoluble polymer network. The extent of crosslinking can affect drug release rates from delivery systems prepared using these polymers. The crosslinking process can involve heat and/or the application of chemical agents, such as glutaraldehyde and 1-ethyl-3-(3-dimethylaminopropyl) carbodiimide (EDC, carbodiimide) [34]. EDC reacts with the amine and carboxyl groups on the polymer to form amide groups. Glutaraldehyde reacts with the amine groups on polymer to form a Schiff base.

Natural polymers vary in molecular weight and composition and hence can exhibit considerable lot to lot variability. They are less pure and their physicochemical properties are less easy to control when compared to synthetic polymers. In addition, they can elicit a strong immunogenic response. Most natural polymers undergo enzymatic degradation in vivo. Degradation of natural polymers depends on the degree of crosslinking and other physicochemical properties of natural polymers such as purity, and molecular weight, as well as the availability and concentration of enzymes at the local in vivo site. These conditions affect the drug release profile from delivery systems prepared using natural polymers. Natural polymers typically lack a reproducible degradation rate and typically have a short drug release half life. Collagen and gelatin are the most common natural polymers used in marketed products, and these are discussed below.

#### 5.2.1.1 Collagen

Collagen is a fibrous protein found in connective tissue. Collagen consists of three polypeptide chains intertwined to form a right handed triple helix (tertiary structure). Each of the individual polypeptide chains forms a left handed helix (secondary structure). There are more than 22 different types of collagen currently identified in the human body. Type I collagen is the most abundant protein present in mammals and is the most thoroughly studied protein. The three polypeptide subunits of Type I collagen have similar amino-acid compositions. Each polypeptide is composed of about 1,050 amino acids, containing approximately 33% glycine, 25% proline, and 25% hydroxyproline with a relative abundance of lysine.

Native collagen is water insoluble, and for many pharmaceutical applications collagen is modified to improve its water solubility. Collagen undergoes enzymatic degradation in the body via enzymes, such as collagenases and metalloproteinases. Drug release from collagen matrices is controlled by varying the degree of crosslinking and other physical properties such as porosity, density, and degree of degradation by enzymes in vivo.

Collagen is a major component of the extracellular matrix and natural collagen is, therefore, an ideal matrix material for tissue engineering and wound dressing applications. Product examples include AlloDerm® and Sulmycin® implants, applications of which are discussed in Sect. 5.3.

#### 5.2.1.2 Gelatin

Gelatin, denatured collagen, is a modified natural polymer formed by hydrolysis of fibrous insoluble collagen. Gelatin is typically isolated from bovine or porcine skin or bone by partial acid hydrolysis (Type A) or partial alkaline hydrolysis (Type B) [43]. This processing breaks up the collagen tripolypeptide, generating single polypeptide chains.

Structurally, gelatin molecules contain repeating sequences of glycine–X–Y triplets, where X and Y are frequently proline and hydroxyproline. These sequences are responsible for gelatin's ability to form a gel when saturated by water. Gelatin is zwitterionic, since it contains amino acids bearing acidic carboxyl (glutamic and aspartic acid) side chains, and basic ε-amino (lysine), guanidinium (arginine) and imidazole (histidine) groups. The isoelectric point (pI) of gelatin molecules is defined as the pH value at which the net average charge due to ionization of the acidic and basic groups is zero.

Similar to collagen, preparation of gelatin often presents lot-to-lot variability including a distribution of polypeptide fragments of different sizes, different isoelectric points (pI), and different gelling properties. Consequently, the physiochemical properties of gelatin vary depending on the method of extraction, the amount of thermal denaturation employed, and electrolyte content of the resulting material. To overcome the variable nature of gelatin preparations, manufactured recombinant

**Table 5.2** A list of the pros and cons of synthetic versus natural polymers

| Classification of polymer | Pro | Con |
|---|---|---|
| Natural | Hydrophilic | Possible immunogenicity |
| | Biocompatible | Require purification |
| | Cell/tissue specific binding affinity | Lot-to-lot variation |
| | Safe | Less controlled raw material specifications |
| | Readily available | Less controlled degradation |
| | | Short release profile |
| Synthetic | Design desired physicochemical feature, such as copolymer | Require ligands attached to achieve cell/tissue specific binding affinity |
| | Easy to add functional groups to allow crosslinking and surface modification of chemical moieties to improve functionality of polymer | Require synthesis |
| | Precise controlled release profile | Scale up challenges |
| | No immunogenicity | Hydrophobic |
| | Control of mechanical and physical properties of polymer such as branching | |

gelatins have been introduced [35]. Recombinant technology eliminates many of the variables and drawbacks associated with tissue derived material. This allows the production of gelatins with defined molecular weights and pIs, guaranteed lot to lot reproducibility, and the ability to tailor the molecule to match a specific application.

Gelatin is usually crosslinked to form a water insoluble polymer network. Gelatin has relatively low antigenicity, so it is useful in parenteral dosage forms. Gelatins have been used commercially as plasma expanders, vaccine bases, and absorbable sponges (e.g., Gelfoam® or Spongel®).

### *5.2.2 Synthetic Polymers*

In the first half of twentieth century, development of materials synthesized from glycolic acid and other α-hydroxy acids was abandoned because the resulting polymers were unstable for long-term industrial uses. However, this instability, leading to biodegradation, has proven to be immensely important in medical applications over the last three decades. The second column of Table 5.1 lists common synthetic biodegradable polymers currently in use for research and commercial applications [16]. Synthetic polymers have predictable and reproducible degradation rates and controlled release profiles that overcome some of the disadvantages of natural polymers.

Table 5.2 lists the pros and cons of natural and synthetic polymers [29]. Synthetic polymers which contain only a single type of repeating unit are known

as homopolymers, while polymers containing a mixture of repeating units are known as copolymers [23]. The physical properties of polymers depend on the structure of the polymer, including the type of monomer, the length of the chain and arrangement of monomers within the polymer. For example, custom design of the branching of the polymer chains can alter intermolecular forces and consequently affect bulk physical polymer properties. In general, long-chain branches may increase polymer strength, toughness, and the glass transition temperature ($T_g$) due to an increase in the number of entanglements per chain. Similarly, altering monomer arrangement in a copolymer can be used to control physicochemical and mechanical properties, such as crystallinity, tensile strength, and degradation profile. Depending on comonomer content and method of synthesis, alternating, random, and block copolymers, and grafted copolymers can be produced [23].

A disadvantage of synthetic polymers is that they usually cannot bind with receptor binding ligands on cells. To overcome this obstacle, research on the conjugation of polymers with receptor binding ligands and natural polymers coated on synthetic polymers is gaining attention to achieve site specific delivery [12, 51].

The most common synthetic polymers used in marketed drug delivery applications are discussed below. Other listed in Table 5.1, e.g., poly(orthoesters), have not yet been commercialized.

#### 5.2.2.1 Poly(α-esters)

Polyesters and their copolymers are the most commonly used polymers in parenteral drug delivery systems. The major disadvantages of this family of polymers should be addressed, including release of acidic degradation products, processing difficulties and limited range of mechanical properties. Degradation of polyesters is mainly by hydrolysis of ester linkages in the presence of water to release acidic degradation products. In general, incorporation of a buffer in polyester formulations containing protein and other acid labile therapeutics can improve the local environment by helping prevent acid catalyzed degradation. The limited range of mechanical properties can be addressed by incorporating other polymers.

PLA, PGA, and PLGA (Fig. 5.1(1))

Poly(lactic acid) (PLA) and poly(glycolic acid)(PGA) are homopolymers. The PLA homopolymer is stiff due to its highly crystalline nature, while PGA homopolymer is soft due to low crystallinity. Depending on the ratio of lactide to glycolide used for polymerization, different forms of poly(D,L-lactide-*co*-glycolide) (PLGA) ranging from mostly PLA to mostly PGA can be obtained [52].

The degradation period of PLGA is between days and years and is a function of the polymer's molecular weight and the ratio of lactic acid to glycolic residues [40]. The higher the content of lactide units, the higher the molecular weight and crystalline content, and this results in slower degradation. PLGA undergoes hydrolysis in the body to produce the original monomers, lactic acid and glycolic acid.

1. Poly(lactic-*co*-glycolic acid) (PLGA).

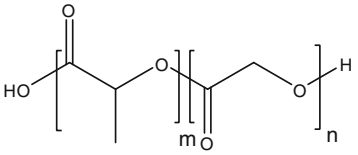


m: number of units of lactide
n: number of units of glycolde

2. Polycaprolactone (PCL)

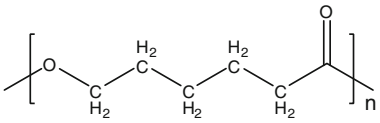


n: number of units of caprolactone

3. Poly [bis(p-carboxyphenoxy) propane-sebacic acid (PCPP-SA)

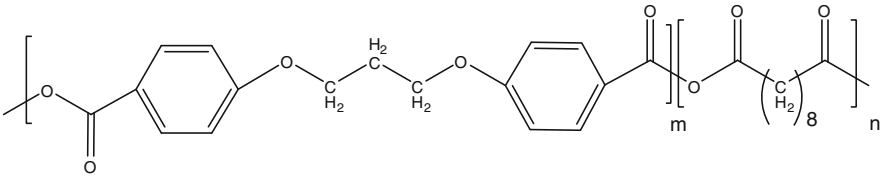


m: number of units of bis(p-carboxyphenoxy)propane
n: number of units of sebacic acid

**Fig. 5.1** Structures of biodegradable polymers. (**1**) PLGA. (**2**) Poly(ε-caprolactone). (**3**) Poly [(carboxyphenoxy propane)-(sebacic acid)] (PCPP-SA)

The acidic environment resulting from degradation can be overcome by formulating with a buffer to balance the pH and improve drug stability (e.g., for protein or peptide drugs) [50]. Since the two monomers are by-products of metabolic pathways in the body, there is minimal systemic toxicity associated with using PLGA for drug delivery or biomaterial applications.

Polymers prepared from glycolic acid and lactic acid are extensively used in biomedical applications, such as grafts, sutures and implants. Examples include polyglycolide suture (DEXON™) and PLGA used in sutures, surgical pins, and staples (i.e. Vicryl®, Quiet™ sutures or staples) [40, 52].

## Poly(ε-caprolactone) PCL

PCL is an aliphatic poly(α-hydroxy acid) and semicrystalline polymer (Fig. 5.1(2)). The monomeric unit ε-caprolactone is relatively inexpensive and much research is

focused on polycaprolactone. The degradation of poly(α-hydroxy acids) depends on chemical hydrolysis of hydrolytically labile aliphatic ester linkages. Owing to its slow degradation, high permeability to many drugs and nontoxicity, PCL was initially investigated as a long term drug delivery vehicle, for example, the long-term contraceptive device Capronor®. This biodegradable PCL capsule device was implanted subdermally and was capable of long term zero order controlled release of levonorgestrel. PCL alone is stiff and has a slow degradation profile. A block copolymer of ε-caprolactone with glycolide offers reduced stiffness compared with pure PGA, and is sold as a monofilament suture by Ethicon, Inc., under the trade name Monocryl™. In 2009, the FDA also approved the commercial Monocryl Plus antibacterial suture (poliglecaprone 25).

#### 5.2.2.2 Polyanhydrides

Polyanhydrides are characterized by aliphatic anhydride bonds that connect the monomer units of the polymer chain [21]. The hydrolytically labile backbone coupled with the hydrophobicity of the polymer precludes water penetration into the matrix, allowing polyanhydrides to undergo surface erosion. In vivo, polyanhydrides degrade into nontoxic diacid monomers that can be metabolized and eliminated from the body.

Aliphatic polyanhydrides were introduced in 1932 as fiber forming polymers for textile applications. Owing to their hydrolytic instability and surface eroding nature, Langer et al. investigated this class of polymers for controlled drug delivery applications in the 1980s. Owing to its safe degradation, poly[(carboxyphenoxy propane)-(sebacic acid)] (PCPP-SA) (Fig. 5.1(3)) was used as a localized delivery vehicle for controlled delivery of the chemotherapeutic agent carmustine (BCNU) in the treatment of brain cancer (Gliadel®). A copolymer of 1:1 sebacic acid and erucic acid dimer is used in the polyanhydride implant (Septacin®) that contains gentamicin sulfate and was developed for sustained local delivery in the treatment of osteomyelitis.

## 5.3 Biodegradable Polymeric Drug Delivery

Biodegradable polymeric drug delivery systems are beneficial in treating many disease states, and are presented in various dosage forms. Table 5.3 lists currently marketed biodegradable polymeric drug delivery systems, indications for use, and durations of action.

**Table 5.3** Biodegradable drug delivery systems on the market

| Polymer | Product name | Therapeutic | Treatment | Duration of action | Delivery systems |
|---|---|---|---|---|---|
| PLA | Lupron Depot® | Leuprolide acetate | Peptide prostate cancer, endometriosis | 1, 3, and 4 Months | Microparticles |
| PLA | Atridox® | Doxycycline hyclate | Chronic adult periodontitis | 7 Days | In situ forming implant |
| PLGA | Trelstar Depot® | Triptorelin pamoate | Prostate cancer | 1 and 3 Months | Microgranule suspension |
| PLGA | Risperdal® Consta® | Risperidone | Schizophrenia | 2 Weeks | Microparticles |
| PLGA | Somatuline® LA | Lanreotide | Acromegaly | 2 Weeks | Microparticles |
| PLGA | Arestin® | Minocycline | Periodontitis | 3 Weeks | Microparticles |
| PLGA | ProFACT Depot ® | Buserelin acetate | Endometriosis and uterine leiomyoma | 1 Month | Implant (Rod) |
| PLGA | SuprecureMP | Buserelin acetate | Endometriosis and uterine leiomyoma | 1 Month | Microparticles |
| PLGA | Eligard® | Leuprolide acetate | Advanced prostate cancer | 1, 3, 4 and 6 Months | In situ forming implant |
| PLGA | Zoladex® | Goserelin | Breast and prostate cancer | 3 Month | Implant (rod) |
| PLGA | Ozurdex® | Dexamethasone | Macular edema following branch retinal vein occlusion (BRVO) or central retinal vein occlusion (CRVO) | 3 Months | Intravitreal implant |
| PLGA | Vivitrol® | Naltrexone | Medication for alcohol and opioid dependence | 1 Month | Implant |
| PLGA – Glucose | Sandostatin LAR® Depot | Octreotide | Acromegaly | 1 Month | In situ forming implant |
| Polyanhydride PCPP:SA (80:20) | Gliadel® | Carmustine | Brain cancer | 2–3 Weeks | Surgical implant |
| Collagen | CollaRx® | Gentamicin | Diabetic foot ulcer | 7 Days | Surgical implant |

### 5.3.1 Mechanism of Release from Polymeric Drug Delivery Systems

Drug release from biodegradable delivery systems occurs by a combination of drug diffusion, osmosis and polymer degradation or bioerosion. In general, degradation of polymers includes bulk erosion and surface erosion [3]. Bulk erosion leads to multiple channels of drug diffusion out of a polymeric system and consequently unpredictable or undesirable release profiles can be obtained, such as burst effects. Therefore, drugs with narrow therapeutic windows should not be used with polymers that undergo bulk erosion. On the contrary, surface erosion of polymeric drug delivery systems can display nearly zero order release kinetics, and if release occurs primarily by diffusion of drug near the surface, then approximately constant release rates are achievable.

Natural polymers are mainly degraded by enzymatic degradation and the degradation products are amino acids or sugars. On the contrary, most synthetic biodegradable polymers are degraded by hydrolytic degradation with little enzyme involvement, and the ultimate degradation products are monomers. Hydrolysis depends on the site of administration and manufacturing procedure as well as the physical properties of these polymers, such as hydrophobicity, crystallinity, glass transition temperature ($T_g$), impurities, molecular weight, polydispersity, degree of crosslinking, and geometry. In general, slow degradation can be achieved by selection of polymers with high molecular weight, high degree of crystallinity, high $T_g$, and high degree of crosslinking.

### 5.3.2 Selection of Biodegradable Polymer in Controlled Drug Delivery

The science of drug delivery systems is multidisciplinary, integrating polymer science, pharmaceutical science, clinical and molecular biology. A general knowledge of the indication of treatment, properties of excipients and therapeutic drugs, and how the characteristics of the drug carrier impact the in vivo and in vitro situation is imperative. It is necessary to know the intended use of the drug and the target drug product profile including desired frequency and duration of the drug to be administered as well as the desired drug release profile in vivo. With knowledge of the target drug product profile in mind, a design space can be formulated. For example, selection of excipients includes consideration of drug-excipient incompatibility as well as the toxicity profile and clinical outcome. The physicochemical and mechanical properties of polymers impact the drug delivery system and its in vivo performance. For example, choice of the molecular weight of PLGA and the ratio of the two comonomers affects the drug release profile. Particle size and surface charge of the delivery system can have an impact on drug targeting and pharmacokinetics. The manufacturing process should be robust and a correlation

between the scale-down and scale-up model should be established. Understanding of the impact of key process parameters and critical attributes of the product is required. Chemistry, manufacturing, and control (CMC) issues as well as clinical concerns of safety and efficacy are key to successful drug product development.

Selection of a biodegrable polymer for a particular application depends on the desired controlled formulation or dosage form, location and frequency of administration, and duration of action. For example, drug delivery systems for central nervous system (CNS) chemotherapy require well controlled release profiles, such as a zero order release profiles and avoidance of burst release and local toxicity. Biodegradable polymers with surface erosion should, therefore, be considered for application to CNS chemotherapy [27]. Biodegradable polymers with bulk erosion profiles, such as PLA or PLGA, may provide first order release profiles and are suitable for long-term treatments as well as those requiring higher therapeutic concentrations. For local drug delivery with short-term application within weeks, natural polymers such as gelatin or collagen can be considered since natural polymers have relatively short time degradation profiles.

### *5.3.3 Overview of Controlled Drug Delivery*

Rate controlled drug delivery pre-designates the rate at which drug is delivered to the body. For example, release of active therapeutics may be extended over a long period (sustained release), it may be constant (zero order release), or it may be triggered by the environment (e.g., pulsatile release or feedback release).

Site specific or targeted delivery offers the advantages of reduced body burden and lower chance of systemic toxicity of the drugs, which is especially useful for highly toxic drugs such as anticancer agents [27, 28]. Site specific or targeted delivery includes passive and active targeting, as originally proposed by Paul Ehrlich [45]. Ehrlich suggested that drugs with special affinities, “magic bullets”, would directly reach the target pathological area following administration due to interactions between the drug and cells at the local site. This idea has led to the development of various targeted drug delivery systems that utilize targeting moieties to facilitate transport of drugs to or near to the physiological treatment site following systemic administration. Targeting moieties that identify certain cell lines or tissues are attached to the surface of “active” targeted drug delivery systems, or they may be attached directly to the drug. These targeting moieties include antibodies, enzymes, protein A, lectins, and sugars.

Active targeting is difficult due to the macrophages of the reticuloendothelial system (RES), which may remove particulate delivery systems from the vascular circulation, preventing them from reaching the target tissue site. Hydrophilic polymers on the surface of drug delivery systems provide a steric effect, which reduces protein adsorption on the surface of the polymer, consequently increasing their circulating half life [20, 23, 49]. An example is pegylated Stealth® liposomes. In this system, the flexible and relatively hydrophilic poly(ethylene glycol) (PEG)

chains induce a steric effect at the surface of the particles that reduces protein adsorption and RES uptake.

Passive targeting occurs when the drug carrier distributes naturally in vivo after administration, without using a specific targeting moiety. For example, particles in the size range 7–12 μm are usually filtered by the capillaries in the lung and, therefore, passively target the lung. Particles in the size range 0.3–2 μm are easily and rapidly taken up by macrophage cells and accumulate in the reticuloendothelial systems (RES). Consequently, diseases of the RES can be targeted by particles of this size.

Site specific delivery or active targeting can be achieved using a targeting moiety on the surface of the drug carrier that targets a specific regional pathophysiological site. Site specific delivery also can be achieved using a localized delivery device that delivers the drug carrier to a given region of the body. For example, a microsphere suspension can be placed and retained at the angioplasty site of an injured artery via a balloon catheter [10, 19, 25]. The polymer used for particulate preparation, together with physicochemical properties of the dosage form (the particle size and porosity), dictates the release rate. In general, natural polymers have short degradation rates between days and weeks while synthetic polymeric microspheres can have degradation rates between months and years [15]. Drug release from carriers is dependent on the mechanism of release, diffusion of the drug through the polymer matrix and the size and the surface area of the carrier. In general, nanoparticulate systems have faster release rates compared to microsphere systems due to their larger surface area. Nanoparticulates with hydrophilic chains on the particle surface have a long circulation time in vivo.

### *5.3.4 Particulate Polymeric Drug Delivery Systems*

Multiparticulate systems (microspheres, nanoparticles, micelles) can be efficiently localized at treatment areas and have less risk of dose dumping compared to large hydrogel implants [8]. These systems are also easy to administer to patients and depending on the application can be designed for long term release, minimizing the frequency of administration. The physicochemical characteristics of particulate systems, e.g., particle size, surface charge and surface hydrophobicity, and inclusion of targeting moieties, affect their distribution in the body. Colloidal systems easily travel in the blood circulation system to the targeted organs/tissues and are easily administrated via injection without the need for surgical incision. Microspheres and other large particulate systems are typically administered via subcutaneous or intramuscular injection for both local and systemic delivery.

Microspheres are solid spheres with particle sizes in the range 1–1,000 μm [7]. There are two types of microspheres, microcapsules and micromatrices. Microcapsules are vesicular systems where the drug is encapsulated in a cavity surrounded by a distinct polymeric membrane. Micromatrices are monolithic systems where drug is dispersed throughout the particles. Microspheres have the

ability to encapsulate a variety of drugs, including hydrophilic and hydrophobic agents, and small molecules and macromolecules, and can achieve sustained release of the agents over a period of days to years. A unique advantage of particulate systems is the ability to blend microspheres prepared with different types of polymers to modify the release profile.

### 5.3.5 *In Situ Injectable Implant Drug Delivery Systems*

In situ implant drug delivery consists of biodegradable polymers dissolved in biocompatible solvent systems, with drug either dissolved or suspended in the polymer solution [36]. Once the liquid polymer system is injected in the body, the polymer solidifies upon contact with the aqueous body fluids. The drug becomes encapsulated within the polymer matrix as it solidifies forming a depot system. The advantage of in situ injectable implants is that they combine long-term delivery with ease of administration. In addition, the manufacturing process is simple, cost effective and exhibits low batch-to-batch variation. Several mechanisms can be used to achieve solidification in vivo of injectable implants, including use of thermoplastic pastes, in situ crosslinking, in situ precipitation, and in situ solidifying organogels [17].

ATRIGEL® technology uses in situ precipitation, which is the most commercially available process and technology [11]. The biodegradable polymers include polyhydroxyacids, polyanhydrides, polyorthoesters and others. Solvents used to dissolve the polymers range from hydrophilic solvents such as *N*-methyl-2-pyrrolidone (NMP), to hydrophobic solvents such as triacetin and ethyl acetate. Of the latter NMP is the most frequently used due to its good solvency and safety/toxicology profile. Seven products have already been approved by the FDA using ATRIGEL® technology [11]. This technology can be used for parenteral as well as local drug delivery. An example of a parenteral product is Eligard®, an injectable leuprolide acetate suspension for prostate cancer treatment. Eligard® provides systemic release of leuprolide acetate and a range of drug release durations (1, 3, and 4 months) are available. Atridox® provides localized subgingival delivery of doxycycline for periodontal treatment. Nutropin® Depot is an injectable PLGA-encapsulated leuprolide acetate formulation for treatment of prostate cancer.

### 5.3.6 *Biodegradable Implant Drug Delivery Systems*

Biodegradable implants incorporating antibiotic and anti-inflammatory therapeutic agents are used for wound treatment. Collagen has been extensively investigated for the application of localized antibiotic delivery to wound areas, such as the Sulmycin® and Collatamp®G implants [48]. In 2009, the FDA approved commercial Monocryl™ plus antibacterial sutures based on poliglecaprone 25.

A synthetic polyanhydride copolymer (sebacic acid and erucic acid dimer; 1:1) is used in an implant, Septacin®, containing gentamicin sulfate for sustained local delivery to the site of infection for the treatment of osteomyelitis. To achieve prolonged drug delivery, formulation scientists have utilized different types of gentamicin salts in the collagen delivery system Septocoll® [44].

Gliadel® utilizes poly[(carboxyphenoxy propane)-(sebacic acid)] (PCPP-SA) as a localized delivery vehicle for the controlled delivery of the chemotherapeutic agent carmustine (BCNU) for the treatment of brain cancer. Ozurdex™ is a poly (D,L-lactide-*co*-glycolide) (PLGA) intravitreal implant containing the anti-inflammatory agent dexamethasone. Ozurdex™ eye implants used to treat retinal disease are placed at the rear of the eye to treat swelling caused by problems with retinal veins [24]. Profact® Depot is PLGA with encapsulated buserelin acetate for treatment of endometriosis. Zoladex® is PLGA with encapsulated goserelin for treatment of breast and prostate cancer.

Risperdal® Consta® PLGA microspheres contain risperidone, which are administered intramuscularly every two weeks for the treatment of schizophrenia and for the longer term treatment of Bipolar I Disorder.

### *5.3.7 Nucleic Acid Delivery*

The success of biodegradable polymers in controlled drug delivery systems has led to promising applications in nonviral nucleic acid delivery. Quoting Leaf Huang, "the goal in developing non-viral nucleic acid vectors is to design a system that simultaneously achieves high transfection efficiency, prolonged gene expression and low toxicity" [9]. However, toxicity remains a challenge in this area as a result of the toxicity associated with cationic polymers and lipids. Accordingly, anionic delivery systems have been developed which combine low toxicity with similar or better transfection when compared to cationic systems [37].

Nucleic acid delivery has two essential requirements, namely therapeutic nucleic acids that can be expressed at a target cell, and a safe and efficient delivery system that can deliver therapeutic nucleic acid to the specific tissue or cell. Cationic polymers are mostly used in nucleic acid delivery because they can easily complex with the anionic nucleic acid molecules and condense nucleic acids into nanoparticles in the 100–300 nm range [39]. The resulting polyplexes protect nucleic acids from degradation by nucleases. Cationic polyplexes can also interact with the negatively charged cell surface and thereby can be taken up by cells via endocytosis. Once inside the cell, the polyplexes osmotically swell and eventually burst the vesicles, which then release the nucleic acids into the cytoplasm. The nucleic acids are then free to enter the nucleus.

Polylysine and chitosan are biodegradable cationic polymers commonly used in polyplexes. The physical properties of these cationic polymers [such as the molecular weight and the structure of the polymers (branched versus linear, etc.)] impact their transfection efficiency and cytotoxicity. The surface properties of complexes

also impact transfection efficiency [30]. For example, PEG conjugated with cationic polymers results in improved half-life of polyplexes, and further conjugation of ligands onto PEG-cationic polymer conjugates can improve the transfection efficiency by reducing nonspecific cellular uptake.

## 5.4 Future Directions in Controlled Drug Delivery

Significant effort is being devoted to developing tailor-made polymers with desirable functional groups to overcome the limitations of the current biodegradable polymers. Scientists are developing novel synthetic polymers with unique functional groups to increase the diversity of the polymer's structure or adapt available polymers to synthesize more desired block or graft copolymers. Furthermore, by understanding the physical properties of polymers and the impact of functional groups on the delivery system, a polymer library can be developed as a basis for synthesis of new biodegradable polymers with the desired properties.

Polymeric drug delivery has demonstrated success in various applications and provides advantages for various therapies. The future of drug delivery includes combination devices that have incorporated therapeutic agents and mediate local drug release at the device implant site [4, 5]. New tailor-made biodegradable polymers will address the needs of drug delivery for nucleic acid therapy, to improve transfection efficiency and reduce cytotoxicity.

## References

1. Amass W, Amass A, Tighe B (1999) A review of biodegradable polymers: uses, current developments in the synthesis and characterization of biodegradable polyesters, blends of biodegradable polymers and recent advances in biodegradation studies. Polym Int 47:89–144
2. Anderson JM, Shive MS (1997) Biodegradation and biocompatibility of PLA and PLGA microspheres. Adv Drug Deliv Rev 28:5–24
3. Brem H, Langer R (1996) Polymer-based drug delivery to the brain. Sci Med 3:52–61
4. Bhardwaj U, Sura R, Papadimitrakopoulos F, Burgess DJ (2007) Controlling acute inflammation with fast releasing dexamethasone-PLGA microsphere/PVA hydrogel composites for implantable devices. J Diabetes Sci Technol 1:8–17
5. Bhardwaj U, Papadimitrakopoulos F, Burgess DJ (2008) A review of the development of a vehicle for localized and controlled drug delivery for implantable biosensors. J Diabetes Sci Technol 2:1016–1029
6. Burgess DJ, Davis SS, Tomlinson E (1987) Potential use of albumin microspheres as a drug delivery systems. I. Preparation and in vitro release of steroids. Int J Pharm 39:129–136
7. Burgess DJ, Hickey AJ (1994) Microsphere technology and applications. In: Swarbrick J, Boylan JC (eds) Encyclopedia of pharmaceutical technology. Marcel Dekker, New York, pp 1–29
8. Burgess DJ, Hickey A (2005) Microspheres: design and manufacturing. In: Burgess DJ (ed) Injectable dispersed systems: formulation, processing and performance. Taylor & Francis, Boca Raton, FL, pp 305–339
9. Celia MH (2001) Gene delivery – without viruses. Chem Eng News 79:35–41

10. Dev V, Eigler N, Fishbein MC, Tian Y, Hickey A, Rechavia E, Forrester JS, Litvack F (1997) Sustained local drug delivery to the arterial wall via biodegradable microspheres. Cathet Cardiovasc Diagn 41:324–332
11. Dunn R (2003) Application of the ATRIGEL® implant drug delivery technology for patient-friendly, cost-effective product development. Drug Deliv Technol 3:6
12. Duncan R (2007) Designing polymer conjugates as lysosomotropic nanomedicines. Biochem Soc Trans 35:56–60
13. Gilding DK, Reed AM (1979) Biodegradable polymers for use in surgery polyglycolic/poly (lactic acid) homo and copolymers: 1. Polymer 20:1459–1464
14. Gopferich A (1998) Mechanisms of polymer degradation and elimination. In: Wiseman DM, Kost J, Domb AJ (eds) Handbook of biodegradable polymers. Harwood Academic Publishers, Amsterdam, pp 451–472
15. Groves MJ (1999) Parenteral drug delivery systems. In: Mathiowitz E (ed) Encyclopedia of controlled drug delivery, vol 1. Wiley, New York, pp 743–777
16. Gunatillake PA, Adhikari R (2003) Biodegradable synthetic polymers for tissue engineering. Eur Cell Mater 5:1–16
17. Hatefi A, Amsden B (2002) Biodegradable injectable in situ forming drug delivery systems. J Control Release 80:9–28
18. Holy E, Fialkov JA, Davies JE, Shoichet MS (2003) Use of a biomimetic strategy to engineer bone. J Biomed Mater Res A 15:447–453
19. Humphrey WR, Erickson LA, Simmons CA, Northrup JL, Wishka DG, Morris J, Labhasetwar V, Song C, Levy RJ, Shebuski RJ (1997) The effect of intramural delivery of polymeric nanoparticles loaded with the antiproliferative 2-aminochromone U-86983 on neointimal hyperplasia development in balloon-injured porcine coronary arteries. Adv Drug Deliv Rev 24:87–108
20. Illum L, Davis SS, Müller RH, Mak E, West P (1987) The organ distribution and circulation time of intravenously injected colloidal carriers sterically stabilized with a blockcopolymer – poloxamine 908. Life Sci 40:367–374
21. Jain JP, Modi S, Domb AJ, Kumar N (2005) Role of polyanhydrides as localized drug carriers. J Control Release 103:541–563
22. Jeong SH, Park K (2006) Hydrogel drug delivery systems. In: Uchegbu IF, Schatzlein AG (eds) Polymers in drug delivery. Taylor & Francis, New York, pp 49–62
23. Kumar NJ, Ravikumar MN, Domb AJ (2001) Biodegradable block copolymers. Adv Drug Deliv Rev 53:23–44
24. Kimura H, Ogura Y (2001) Biodegradable polymers for ocular drug delivery. Ophthalmologica 215:143–155
25. Labhasetwar V, Song C, Levy RJ (1997) Nanoparticle drug delivery system for restenosis. Adv Drug Deliv Rev 24:63–85
26. Langer R (1990) New methods of drug delivery. Science 249:1527–1533
27. Lawrence KF, Saltzman WM (1997) Polymeric implants for cancer chemotherapy. Adv Drug Deliv Rev 26:209–230
28. Leach KJ (1999) Cancer drug delivery to treat – local and systemic. In: Mathiowitz E (ed) Encyclopedia of controlled drug delivery, vol 1. Wiley, New York, pp 119–142
29. Lewis DH (1990) Controlled release of bioactive agents from lactide/glycolide polymers. In: Chasin M, Langer R (eds) Biodegradable polymers as drug delivery systems. Marcel Dekker, New York, pp 1–8
30. Lynch J, Behan N, Birkinshaw C (2007) Factors controlling particle size during nebulization of DNA–polycation complexes. J Aerosol Med 20:257–268
31. Ma PX, Zhang R (2001) Microtubular architecture of biodegradable polymer scaffolds. J Biomed Mater Res 15:469–477
32. Middleton JC, Tipton AJ (2000) Synthetic biodegradable polymers as orthopedic devices. Biomaterials 21:2335–2346

33. Naira LS, Laurencin CT (2007) Biodegradable polymers as biomaterials. Prog Polym Sci 32:762–798
34. Okada H, Toguchi H (1995) Biodegradable microspheres in drug delivery. Crit Rev Ther Drug Carrier Syst 12:1–99
35. Olsen D, Yang C, Bodo M, Chang R, Leigh S, Baez J, Carmichael D, Perälä M, Hämäläinen E, Jarvinen M, Polarek J (2003) Recombinant collagen and gelatin for drug delivery. Adv Drug Deliv Rev 55:1547–1567
36. Packhaeuser CB, Schnieders J, Oster CG, Kissel T (2004) In situ forming parenteral drug delivery systems: an overview. Eur J Pharm Biopharm 58:445–455
37. Patil SD, Rhodes DG, Burgess DJ (2005) DNA-based therapeutics and DNA delivery systems: a comprehensive review. AAPS J 7:E61–E77
38. Pawar T, Ben-Ari A, Domb AJ (2004) Protein and peptide parenteral controlled delivery. Expert Opin Biol Ther 4:1203–1212
39. Peniston QP, Johnson E (1980) Process for the manufacture of chitosan. US Patent No. 4,195,175, 5 pp
40. Perrin DA, English JP (1997) Polyglycolide and polylactide. In: Wiseman DM, Kost J, Domb AJ (eds) Handbook of biodegradable polymers. Harwood Academic Publishers, Amsterdam, pp 3–25
41. Piskin E (1994) Biodegradable polymers as biomaterials. J Biomater Sci Polym Ed 6:775–795
42. Robinson JR, Lee VH (1987) Influence of drug properties and routes of drug administration on the design of sustained and controlled release systems. In: Robinson JR, Lee VHL (eds) Controlled drug delivery: fundamentals and applications, 2nd edn. Marcel Dekker, New York, pp 3–94
43. Rowe RC, Sheskey PJ, Weller PJ (2003) Handbook of pharmaceutical excipients, 4th edn. The Pharmaceutical Press, London
44. Ruszczak Z, Friess W (2003) Collagen as a carrier for on-site delivery of antibacterial drugs. Adv Drug Deliv Rev 55:1679–1698
45. Scholes PD, Coombes AGA, Davies MC, Illum I, Davis SS (1997) Particle engineering of biodegradable colloids for site-specific drug delivery. In: Park K (ed) Controlled drug delivery: challenges and strategies. American Chemical Society, Washington, DC, pp 73–106
46. Shalaby SW, Burg KJL (2003) Absorbable/biodegradable polymers: technology evolution. In: Shalaby SW, Burg KJL (eds) Absorbable and biodegradable polymers. CRC, Boca Raton, FL, pp 3–14
47. Shi Y, Li L (2005) Current advances in sustained-release systems for parenteral drug delivery. Expert Opin Drug Deliv 2:1039–1058
48. Singh MP, Stefko J, Lumpkin JA, Rosenblatt J (1995) The effect of electrostatic charge interaction on release rates of gentamicin from collagen matrices. Pharm Res 12:1205–1210
49. Stolnik S, Dunn SE, Garnett M, Davies MC, Combos AG, Taylor DC, Purkiss SC, Tadros TF, Davis SS, Illum L (1994) Surface modification of poly(lactide-co-glycolide) nanospheres by biodegradable poly(lactide)-poly(ethylene glycol) copolymers. Pharm Res 11:1800–1808
50. Schwendeman SP, Cardamone M, Brandon MR, Klibanov A, Langer R (1996) The stability of proteins and their delivery from biodegradable polymer microspheres. In: Cohen S, Bernstein H (eds) Microparticulate systems for the delivery of proteins and vaccines. Marcel Dekker, New York, pp 1–49
51. Tsung MJ, Burgess DJ (2001) Preparation and characterization of gelatin surface modified PLGA microspheres. AAPS PharmSci 3(2):E11
52. Vert M (2003) Polyglycolide and copolyesters with lactide in biopolymers. In: Yoshiharu D, Steinbüchel A (eds) Biopolymers, volume 4, polyesters III – applications and commercial products. Wiley-VCH, Weinheim, pp 179–202
53. Zaikov GE, Livshits VS (1984) Biodegradable polymers for medicinal use (review). I. Classification. Pharma Chem J 18:235–244

# Part III
# Temporal Delivery Systems and Mechanisms

# Chapter 6
# Diffusion Controlled Drug Delivery Systems

**Juergen Siepmann, Ronald A. Siegel, and Florence Siepmann**

**Abstract** This chapter presents an overview on the different types of drug delivery systems that are predominantly governed by diffusion. The systems are classified according to their physical structure (reservoir devices versus monolithic systems), as well as according to the ratio of "initial drug loading and drug solubility." For various cases, mathematical models are briefly presented considering different device geometries. These theories are mechanistically realistic and enable quantitative description of the resulting release kinetics. Effects of formulation parameters on drug release can also be predicted quantitatively. Practical examples are given to illustrate the applicability of the presented theories and the benefits of understanding how a diffusion-controlled drug delivery system works.

## 6.1 Introduction

Diffusion plays a major role in most controlled drug delivery systems. Often, the overall release rate is affected by several physical and chemical phenomena, e.g., a combination of water diffusion, drug dissolution, drug diffusion, polymer swelling, polymer dissolution, and/or polymer degradation. In this chapter, predominantly diffusion-controlled drug delivery systems are treated. Obviously, diffusion is the

J. Siepmann (✉) • F. Siepmann
INSERMU1008, College of Pharmacy, Université Lille Nord de France,
3 Rue du Prof. Laguesse, 59006 Lille, France
e-mail: juergen.siepmann@univ-lille2.fr; florence.siepmann@univ-lille2.fr

R.A. Siegel
Departments of Pharmaceutics and Biomedical Engineering, University of Minnesota,
Minneapolis, MN 55419, USA

Department of Pharmaceutics WDH 9-177, University of Minnesota, 308 Harvard St. S.E.,
Minneapolis, MN 55455, USA
e-mail: siege017@umn.edu

J. Siepmann et al. (eds.), *Fundamentals and Applications of Controlled Release Drug Delivery*, Advances in Delivery Science and Technology,
DOI 10.1007/978-1-4614-0881-9_6, 

mass transport mechanism when other processes are not involved in the control of drug release. Alternatively, diffusion is dominant if the impact of all other phenomena is negligible. If several processes take place in series and one of these steps is much slower than all the others, this slowest process is dominant. For the quantitative description of the overall release rate, only the slowest step needs to be taken into account. This is for instance the case if rapid drug dissolution is followed by slow drug diffusion through a polymeric network. Also, if a matrix forming material starts to degrade only after complete drug exhaust, then degradation is not involved in the control of drug release, and there is no need to consider it in a mathematical model quantifying drug release.

Diffusional mass transport is of fundamental importance for numerous processes in the body and nature in general. Adolf Eugen Fick (1829–1901) was the first to describe this very important phenomenon in a quantitative way. His historical contribution, published in 1855 and titled "Ueber Diffusion" (translated from German: "About Diffusion") in Poggendorff's Annalen der Physik [1], is translated into English in ref. [2]. The basic idea is that a solute diffuses from regions of higher concentration to adjacent regions of lower concentration. Considering diffusion in a single direction, $x$, Fick's First Law (FFL) relates diffusion flux, $J$ (mass flow per unit area) to the gradient in solute concentration, $c$, according to

$$J = -D\frac{\partial c}{\partial x}, \tag{6.1}$$

where $D$ is the diffusion coefficient, or diffusivity. Assuming that the solute is neither created nor consumed during the process, the local change in concentration with time in a thin sliver of solution between points $x$ and $x + \mathrm{d}x$ is determined by mass balance according to the difference in flux into the sliver at $x$ and out at $x + \mathrm{d}x$. As this sliver becomes infinitely small, this mass balance can be written as

$$\frac{\partial c}{\partial t} = -\frac{\partial J}{\partial x}. \tag{6.2}$$

Combining (6.1) and (6.2) we arrive at Fick's second law, also known as the diffusion equation

$$\frac{\partial c}{\partial t} = \frac{\partial}{\partial x}D\left(\frac{\partial c}{\partial x}\right). \tag{6.3}$$

Considering all three spatial dimensions, $x$, $y$, and $z$, and allowing the diffusion coefficient to vary with position, time, and/or solute concentration (6.3) generalizes to:

$$\frac{\partial c}{\partial t} = \frac{\partial}{\partial x}\left(D\frac{\partial c}{\partial x}\right) + \frac{\partial}{\partial y}\left(D\frac{\partial c}{\partial y}\right) + \frac{\partial}{\partial z}\left(D\frac{\partial c}{\partial z}\right). \tag{6.4}$$

These forms can be simplified if the diffusivity is independent of time, space, and concentration. For example (6.3) becomes

$$\frac{\partial c}{\partial t} = D\frac{\partial^2 c}{\partial x}. \tag{6.5}$$

The diffusion equation can be solved when initial and boundary conditions are specified. In this chapter, we explore analytical solutions of the diffusion equation that are applicable to controlled drug release systems. The initial condition refers to the initial drug distribution in the system, before the release process commences. Boundary conditions refer to the conditions at the drug delivery system's boundaries during drug release; these specify drug concentrations or concentration gradients at the device's surfaces. The term "analytical solution" refers to an explicit mathematical expression satisfying the diffusion equation, along with the prescribed initial and boundary conditions. The analytical solution is used to calculate drug release from the delivery system as a function of time.

An extensive collection of analytical solutions of Fick's second law of diffusion for different geometries and initial and boundary conditions is provided by Crank [3]. If the analytical solution for a specific type of drug delivery system with its set of initial and boundary conditions cannot be found in Crank textbook [3], an analogous expression for heat transfer might be found in the book of Carslaw and Jaeger [4]. Only a handful of basic analytical solutions of Fick's law of diffusion allowing for the quantitative description of drug release from specific types of delivery systems are included in this chapter. In all these cases, constant diffusion coefficients are considered. For more complex systems, the reader is referred to Crank [3], Carslaw and Jaeger [4], Vergnaud [5], Cussler [6], and Singh and Fan [7].

For delivery systems with time, position and/or concentration dependent diffusion coefficients, generally no analytical solution of Fick's law is available. The same is true for devices with complex shapes. In these cases, numerical techniques can be used to calculate mass transport. The basic idea is to make some approximations, e.g., replacing derivatives by finite differences calculated on a space and/or time grid. The resulting equations can be solved on a computer, but error due to discretization is introduced. To limit the importance of this error, the time and space steps need to be small, resulting in a significant number of required calculation steps. However, nowadays such numerical solutions can be calculated very rapidly and accurately using a standard personal computer. Numerical packages which utilize finite differences or the finite element method are available for calculations based on Fick's law, with suitable initial and boundary conditions.

Depending on the inner structure of the drug delivery system and its initial drug loading compared to the drug's solubility, four major types of devices can be distinguished, as illustrated in Fig. 6.1 [8]. While these devices can be realized in many geometries, spherical systems are presented as examples. If the drug and the release rate controlling material (often a polymer) are separated according to a core–shell structure, the drug being located in the center and the release rate controlling material forming a membrane surrounding this drug depot, then the device is called a "reservoir system." On the contrary, if drug is more or less homogeneously distributed in a continuous matrix formed by the release rate controlling material, or matrix, the device is called a "monolithic system."

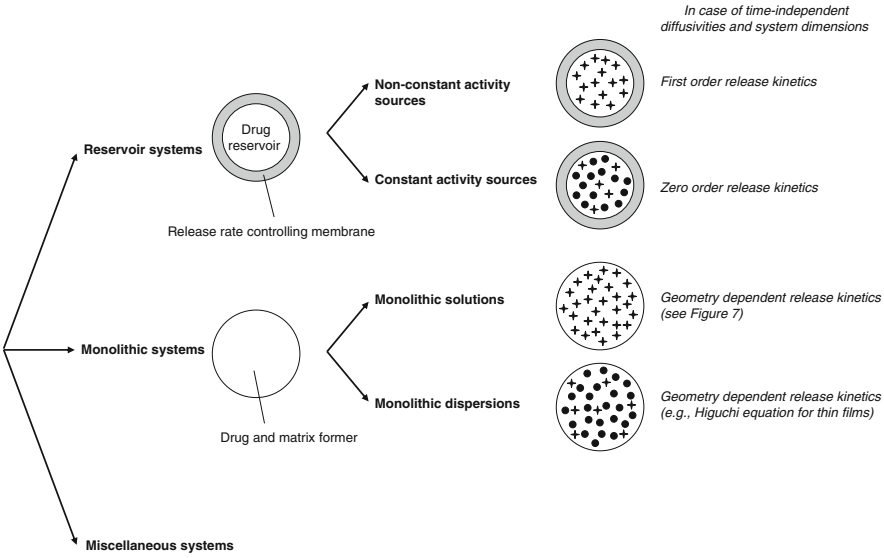


**Fig. 6.1** Classification scheme for predominantly diffusion-controlled drug delivery systems according to their physical structure and initial drug loading. *Stars* indicate molecularly dispersed (dissolved) drug molecules. *Black circles* represent nondissolved drug excess (e.g., drug crystals). Adapted from ref. [8]

Reservoir systems can be further classified as having either a "nonconstant activity source" or a "constant activity source." In the first case, drug concentration in the reservoir is below its solubility. Thus, drug molecules that are released across the membrane are not replaced, and the drug concentration at the inner membrane's surface decreases with time. In reservoir systems with a constant activity source, an excess of drug is provided in the depot and released drug molecules are rapidly replaced by dissolution of the remaining nondissolved drug excess. Consequently, the drug concentration at the inner membrane's surface remains constant as long as drug is present in excess. When the reservoir's drug concentration falls below solubility, the reservoir becomes a nonconstant activity source.

Similarly, two subtypes of monolithic systems can be distinguished according to the initial drug loading:drug solubility ratio. In monolithic solutions, the initial drug loading is below drug solubility and the drug is dissolved in the matrix. In monolithic dispersions, the initial drug loading is above drug solubility and the drug is partially dissolved (molecularly dispersed, stars in Fig. 6.1), the remainder being dispersed in the form of solid drug crystals and/or amorphous particles (black circles in Fig. 6.1) throughout the system. Drug can diffuse out of the device only after it is dissolved.

In the following sections, each of the four cases is treated in more detail. We note that this classification does not include all diffusion controlled systems, however. For example, a slightly more complex formulation is a monolithic system containing dissolved and/or dispersed drug, surrounded by a release-rate controlling membrane. Treatment of such a system is possible but will be more complicated.

## 6.2 Reservoir Devices

Upon contact with aqueous body fluids water penetrates into the dosage form and dissolves drug. If all drug is rapidly dissolved, the system acts as a reservoir device with a nonconstant activity source. If only part of the drug is dissolved due to limited solubility, the dosage form acts as a reservoir device with a constant activity source. Note that the relevant solubility is that of the drug in the wetted depot at body temperature, not the drug's solubility in the pure release medium or the drug solubility in the dry depot. In practice, it is often difficult to know the exact drug solubility in the system's core upon water penetration at 37°C and caution should be paid, since dissolution of other core compounds (e.g., sucrose and acid) might significantly affect the solubility of the drug [9, 10]. However, the ratio of the initial drug loading to drug solubility in water at 37°C can give a good first indication.

Once dissolved, drug molecules diffuse out through the release rate controlling membrane, due to the concentration gradient across the membrane. Thus, three mass transport processes occur in series: (1) water diffusion, (2) drug dissolution, and (3) drug diffusion. Often, drug diffusion is much slower than the other steps and is therefore rate controlling, and the mathematical description of drug diffusion through the membrane is sufficient to characterize release. This simplification is often acceptable, but not always [11]. In this chapter, drug diffusion is considered to be the slowest process.

### *6.2.1 Nonconstant Activity Sources*

The conditions for drug diffusion through the release rate controlling membrane of a reservoir device with a "nonconstant activity source" are illustrated in Fig. 6.2. In the surrounding bulk fluid, perfect sink conditions are considered, meaning that

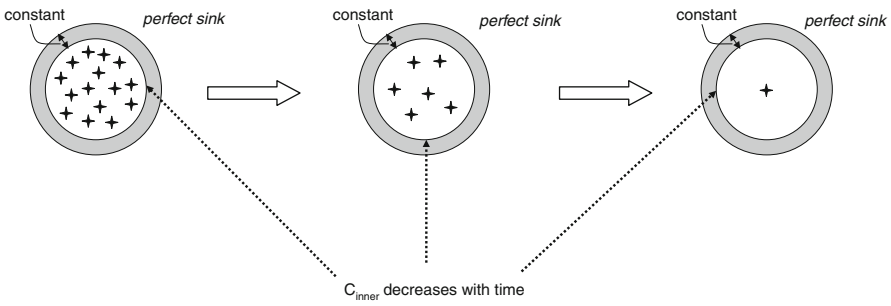


**Fig. 6.2** Reservoir devices with a nonconstant activity source: schematic presentation of the conditions for drug diffusion through the release-rate controlling membrane surrounding the drug reservoir. *Stars* indicate molecularly dispersed (dissolved) drug molecules; $c_{inner}$ denotes the drug concentration at the inner membrane's surface. The membrane thickness and permeability are considered to be time-independent

the drug concentration in the surrounding bulk fluid is negligible at all times. Thus, already released drug does not significantly slow down the release of drug still remaining in the dosage form. The mathematical treatment of drug release under *nonsink* conditions is more complex and the reader is referred to Crank [3] or Fan and Singh [7] for more details. In Fig. 6.2, stars represent dissolved (molecularly dispersed) drug molecules in the wetted system core. If the release rate controlling membrane does not significantly swell or shrink, does not dissolve, and does not significantly change in drug permeability during the release period, then the length of the diffusion pathway to be overcome (membrane thickness) is time-independent and the apparent diffusion coefficient of drug in the membrane remains constant.

When the membrane is very thin compared to other dimensions of the device, the "film" approximation is useful. In this case, the amount of drug transported through the membrane can be quantified according to Fick's law as follows:

$$\frac{M_t}{M_\infty} = 1 - \exp\left(-\frac{ADKt}{VL}\right), \tag{6.6}$$

where $M_t$ and $M_\infty$ denote the cumulative amounts of drug released at times $t$ and infinity (release completed), respectively, $A$ is the total surface area of the device, $D$ is the diffusion coefficient of the drug within the membrane, $V$ is the volume of the reservoir, $K$ is the partition coefficient of the drug between the membrane and the reservoir, and $L$ is the thickness of the membrane. Thus, drug release follows first-order kinetics.

For a spherical reservoir surrounded by a thin membrane,

$$\frac{M_t}{M_\infty} = 1 - \exp\left[-\frac{3DKR_o t}{(R_o - R_i) \times R_i^2}\right], \tag{6.7}$$

where $R_i$ and $R_o$ are the inner and outer radii of the device. This expression results from substituting $L = R_o - R_i$, $A = 4\pi R_i^2$, and $V = (4/3)\pi R_i^3$ into (6.6).

A practical example of a reservoir dosage form with a nonconstant activity source is illustrated in Fig. 6.3. The system consists of diltiazem HCl-layered beads, which are coated with a 90:10 blend of ethylcellulose and poly(vinyl alcohol)-poly (ethylene glycol) graft copolymer [12]. Diltiazem HCl is freely water soluble and the polymer coating does not significantly swell or shrink during drug release. In coated dosage forms attention must be paid to potential crack formation that might occur during drug release. Osmotically driven penetration of water into the system can lead to a significant internal hydrostatic pressure acting against the release rate controlling membrane. If the latter is too fragile to withstand this pressure, crack formation occurs [13] and drug diffusion occurs both through the cracks and the remaining intact film coating. The internal hydrostatic pressure might also lead to significant convective drug transport through the newly created channels, i.e., a "pushing out effect" [14]. Presence of high amounts of freely water soluble

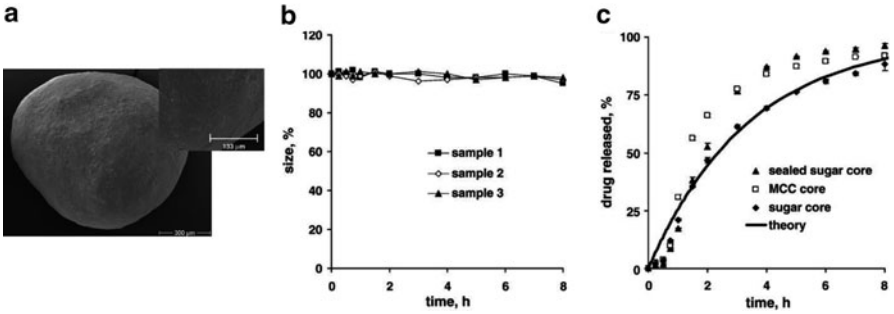


**Fig. 6.3** Example for a predominantly diffusion-controlled drug delivery system of the reservoir type with a nonconstant activity source: diltiazem HCl-layered beads coated with a 90:10 blend of ethylcellulose and poly(vinyl alcohol)-poly(ethylene glycol)-graft copolymer: (**a**) SEM picture of a pellet's surface after 2 h exposure to 0.1 N HCl (sugar core), (**b**) changes in the size of single pellets ($n = 3$) upon exposure to 0.1 N HCl (sugar cores), and (**c**) theoretically predicted (*curve*) and experimentally confirmed (*symbols*) drug release kinetics in 0.1 N HCl (reprinted from ref. [12] with permission)

compounds (drugs and/or excipients) in the core, or poor mechanical stability of the film coating, increases the probability of crack formation. The full mathematical description of mass transport in these systems is complex and beyond the scope of this chapter.

Various experimental techniques have been used to determine whether crack formation occurs during drug release. For example, scanning electron microscopy (SEM) can be very helpful. However, great care must be taken with respect to potential artifact creation. If the membrane takes up significant amounts of water, structural changes of the system during drying in preparation for SEM must be avoided. Figure 6.3a shows examples of SEM pictures, illustrating diltiazem HCl-layered sugar cores coated with 90:10 ethylcellulose–poly(vinyl alcohol)-poly(ethylene glycol)-graft copolymer after 2 h exposure to 0.1 N HCl. No evidence of crack formation is visible in these pictures.

Changes in pellet size during drug release might also indicate occurrence or absence of crack formation in the film coating. A steadily increasing pellet size can be indicative of penetration of significant amounts of water into the system. Subsequent abrupt and rapid decrease in pellet size would suggest crack formation [13] and pressure driven ejection of fluid from the device. If, on the contrary, the system size remains nearly constant during the observation period, this might serve as an indication for the absence of crack formation. Caution must be paid, however, since nonflexible membranes can crack without any prior significant increase in system size and without significant "pushing out" and shrinkage effect. The combination of different techniques, including SEM and monitoring of system dimensions, is, therefore, highly recommended to minimize the risk of erroneous conclusions.

Changes in size of individual diltiazem HCl loaded pellets upon exposure to 0.1 N HCl are illustrated in Fig. 6.3b. As can be seen, no significant changes were

observed over the time course of this study. It is important that the sizes of single coated reservoir devices, instead of the mean size of an ensemble of devices, are tracked through time, since increasing and decreasing sizes of single systems might compensate each other. These observations provide support for the presence of an intact film coating, which controls drug release predominantly by diffusion.

To verify this hypothesis, the theoretically predicted drug release kinetics was calculated using (6.7). The curve in Fig. 6.3c shows the theoretically predicted release rate of diltiazem HCl from pellets coated with 90:10 ethylcellulose:poly (vinyl alcohol)-poly(ethylene glycol)-graft copolymer blends. The reservoir was considered to be a "well stirred" compartment, and the effects of excipients including sugar, microcrystalline cellulose (MCC) and a "sealed" sugar core (sucrose starter core coated with ethylcellulose in this case) were not considered. The symbols represent the independent, experimentally measured drug release kinetics from three types of pellets, consisting of: (1) a sugar, MCC or sealed sugar bead as starter core (as indicated in the diagram), (2) a diltiazem HCl layer, and (3) an ethylcellulose:poly(vinyl alcohol)-poly(ethylene glycol)-graft copolymer coating. Reasonable agreement is observed between the theoretical prediction based on a simple first order equation and the independent experiments.

The experimentally observed lag time for drug release seen in Fig. 6.3c might be explained at least partially by the time needed for water to penetrate into the system, the fact that the film coating might be initially free of drug, and/or hindrance of drug diffusion due to osmotically driven water influx. The type of starter core does not very much affect the resulting drug release kinetics in this case.

Using (6.7), the impact of formulation parameters such as the film coating thickness and pellet size can be predicted. If a quantitative relationship between the apparent drug diffusivity in the membrane and the latter's composition is available (see Sect. 6.4), then the effects of the coating's formulation on drug release can also be quantitatively predicted.

### *6.2.2 Constant Activity Sources*

Figure 6.4 depicts drug diffusion through a membrane surrounding a drug reservoir containing a significant excess of undissolved drug, which provides a constant activity source. Stars represent dissolved drug molecules and black circles represent nondissolved drug excess, e.g., drug crystals or amorphous drug particles. Not all of the drug can be dissolved upon water penetration into the core due to the limited solubility of the drug. Consequently, a saturated drug solution is provided at the membrane's inner surface as long as nondissolved drug excess is present in the depot. Drug molecules that are released through the membrane are rapidly replaced by the compensating dissolution of the drug excess. (As discussed above, drug dissolution is considered to be fast compared to drug diffusion in these cases.) If perfect sink conditions are provided in the surrounding bulk fluid, this leads to a

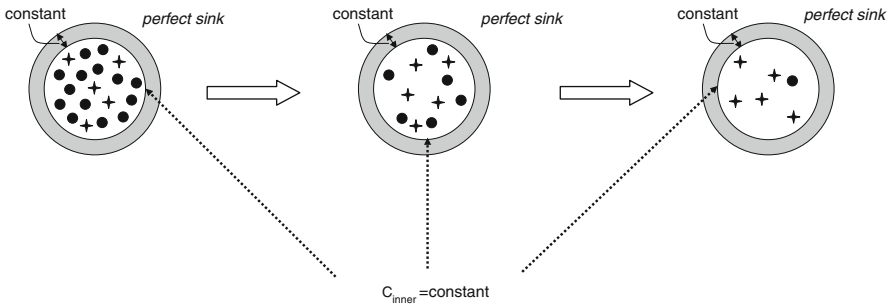


**Fig. 6.4** Reservoir devices with a constant activity source: schematic presentation of the conditions for drug diffusion through the release-rate controlling membrane surrounding the drug reservoir. *Stars* indicate molecularly dispersed (dissolved) drug molecules, *black circles* represent nondissolved drug excess (e.g., drug crystals), and $c_{inner}$ denotes the drug concentration at the inner membrane's surface (saturation concentration) as long as drug excess is provided. The membrane thickness and permeability are considered to be time-independent

constant drug concentration difference between the inside and outside of the device. If in addition the dimensions and composition of the membrane do not change during drug release, the concentration gradient of drug inside the membrane is constant, and drug is released at a constant rate, i.e., with zero-order release kinetics. According to geometry, one of the following equations can be used:

$$\text{Slab (thin film with negligible edge effects)}: \quad \frac{\mathrm{d}M_t}{\mathrm{d}t} = \frac{ADKc_\mathrm{s}}{L}. \tag{6.8}$$

$$\text{Sphere}: \quad \frac{\mathrm{d}M_t}{\mathrm{d}t} = \frac{4\pi DKc_\mathrm{s}R_\mathrm{o}R_\mathrm{i}}{R_\mathrm{o} - R_\mathrm{i}}. \tag{6.9}$$

$$\text{Cylinder}: \quad \frac{\mathrm{d}M_t}{\mathrm{d}t} = \frac{2\pi HDKc_\mathrm{s}}{\ln(R_\mathrm{o}/R_\mathrm{i})}, \tag{6.10}$$

where $c_\mathrm{s}$ is the concentration of saturated drug solution in the reservoir. In (6.10) $R_\mathrm{i}$ and $R_\mathrm{o}$ are the inner and outer radii, respectively, and $H$ is the length of the cylinder.

A practical example of a reservoir device with a "constant activity source" is illustrated in Fig. 6.5. The system consists of spherical theophylline matrix cores coated with a 85:15 ethylcellulose:poly(vinyl alcohol)-poly(ethylene glycol)-graft copolymer blend [15]. Again, it is important to know whether or not crack formation occurs during drug release. As can be seen in Fig. 6.5a,b, there is no evidence for crack formation, either from SEM pictures taken 2 h after exposure to 0.1 N HCl, or from monitoring the size of single pellets upon exposure to the release medium. Clearly, the resulting release follows near-zero order kinetics over 8 h (Fig. 6.5c),

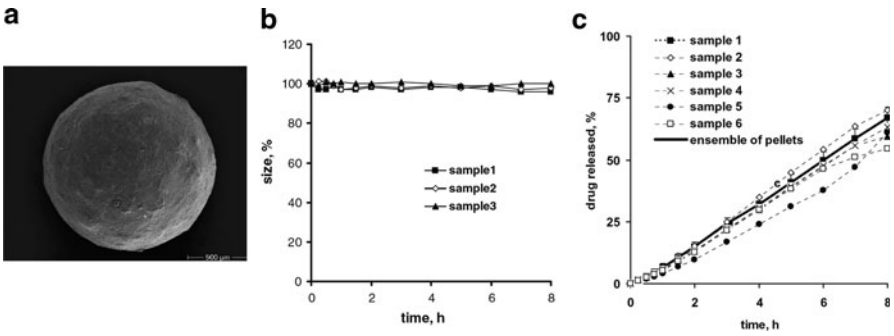


**Fig. 6.5** Example for a predominantly diffusion-controlled drug delivery system of the reservoir type with a constant activity source: theophylline matrix cores coated with a 85:15 blend of ethylcellulose and poly(vinyl alcohol)-poly(ethylene glycol)-graft copolymer: (**a**) SEM picture of a pellet's surface after 2 h exposure to 0.1 N HCl. (**b**) Changes in the size of single pellets ($n = 3$) upon exposure to 0.1 N HCl. (**c**) Drug release kinetics from single pellets (*thin curves*, $n = 6$) and an ensemble of pellets (*thick curve*) in 0.1 N HCl (reprinted from ref. [15] with permission)

as expected for a reservoir device with a constant activity source. Release profiles from single pellets are very similar to the release profile from the ensemble of pellets, indicating that the underlying drug release mechanisms are likely to be the same and that the interpellet variability of film coating thickness is small.

In other systems, drug release from individual units of a multiparticulate dosage form might differ substantially [16]. The release rates of all individual dose units might eventually sum up to a more or less constant release rate of the ensemble of dose units. When developing multiparticulate dose forms (e.g., coated pellets or minitablets), drug release from single units should be monitored to minimize the risk of erroneous conclusions regarding mechanism.

Zero-order release from a reservoir device with constant activity source occurs when a steady state drug concentration profile exists in the rate controlling membrane. For a thin film this profile will be linear, as illustrated in Fig. 6.6 by the black curves. (For simplicity, a partition coefficient of 1 between the membrane and the reservoir is assumed.) In practice, steady state might be more or less rapidly reached and deviations from zero order release kinetics might be observed at early time points. For example, significant amounts of drug might diffuse into the membrane during long term storage. In the extreme case, the membrane is saturated with drug. Upon exposure to the release medium the real concentration gradient at the system's surface is steeper than the gradient at steady state (red versus black curves in Fig. 6.6), resulting in higher initial drug release rates. This phenomenon is called the "burst effect." After a certain time, steady state is reached and zero-order release is observed (i.e., the red and black cumulative drug release curves become parallel). The extent of such a burst effect depends on the type of drug, and the type and thickness of the membrane.

By contrast, immediately after coating of the dosage form, the release rate controlling membrane will be essentially free of drug (green curve in Fig. 6.6).

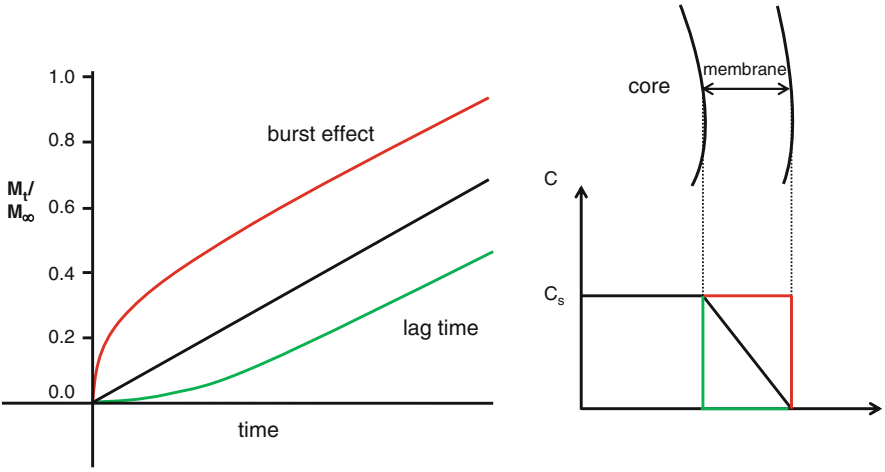


**Fig. 6.6** Schematic presentation of burst and lag-time effects potentially observed with predominantly diffusion-controlled drug delivery systems of the reservoir type (in this example with a constant activity source): the steady state case (marked in *black*) represents the expected zero-order kinetics. In the case of a burst effect (marked in *red*), drug diffused into the membrane to a significant extent during storage. In the case of a lag time (marked in *green*), the membrane is initially free of drug

Hence, the concentration gradient at the system's surface is initially lower than in the steady state and the initial drug release rate is lower (green versus black curves). After a time lag, drug concentration gradient reaches steady state, release rate is constant, and the cumulative drug release curve is parallel to the others in Fig. 6.6.

For thin film coated devices with membrane surface area $A$, the following equations can be used to calculate the cumulative amounts of drug released at time $t$, $M_t$, once steady state is reached:

$$\text{Lag} - \text{time systems}: \quad M_t = \frac{AKDc_s}{L}\left(t - \frac{L^2}{6D}\right). \tag{6.11}$$

$$\text{Burst effect systems}: \quad M_t = \frac{AKDc_s}{L}\left(t + \frac{L^2}{3D}\right). \tag{6.12}$$

An interesting aspect of these relations is that while steady state release depends on both partition and diffusion coefficient, the burst or lag time parameters depend only on the diffusion coefficient. If the membrane film thickness is well determined, then accurate measurements under burst or lag conditions enable the diffusion coefficient to be estimated. Other techniques for estimating the diffusion coefficient of drug in the membrane are presented in Sect. 6.4.

## 6.3 Monolithic Devices

In monolithic devices, drug is dissolved or dispersed thoughout the release controlling matrix. According to the ratio "initial drug loading:drug solubility," monolithic solutions and monolithic dispersions can be distinguished. Drug solubility in the wetted monolith at body temperature is decisive, as discussed above for reservoir systems.

### *6.3.1 Monolithic Solutions*

Figure 6.7 illustrates monolithic solutions of different geometries: thin slabs with negligible edge effects, spheres, and cylinders. These geometries cover many pharmaceutical dosage forms. Stars represent dissolved drug molecules. Initial drug distributions are assumed to be homogenous in all cases and perfect sink conditions are assumed throughout release. Fick's second law of diffusion can be

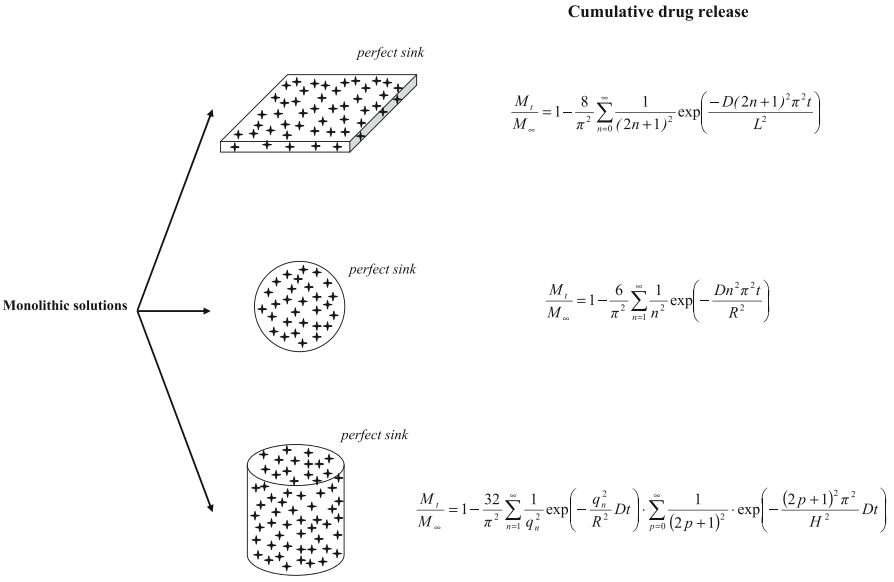


**Fig. 6.7** Drug release kinetics from diffusion-controlled delivery systems of the "monolithic solution" type with different geometry: thin films with negligible edge effects, spheres, and cylinders (with radial and axial diffusion). *Stars* indicate molecularly dispersed (dissolved) drug molecules. The *equations* represent analytical solutions of Fick's second law of diffusion considering the given initial and boundary conditions and allowing for the quantification of the cumulative amounts of drug released as a function of time. The *variables* are explained in the text

solved considering these initial and boundary conditions, leading to the following expressions for the fraction of drug released at time $t$, $M_t/M_\infty$:

$$\textit{Slabs}: \quad \frac{M_t}{M_\infty} = 1 - \frac{8}{\pi^2}\sum_{n=0}^{\infty}\frac{1}{(2n+1)^2}\exp\left[\frac{-D(2n+1)^2\pi^2 t}{L^2}\right], \tag{6.13}$$

where $L$ is the thickness of the slab and release is assumed to occur from both faces of the slab. The slab is assumed to be sufficiently thin that release through its edges is negligible.

$$\textit{Spheres}: \quad \frac{M_t}{M_\infty} = 1 - \frac{6}{\pi^2}\sum_{n=1}^{\infty}\frac{1}{n^2}\exp\left(-\frac{Dn^2\pi^2 t}{R^2}\right), \tag{6.14}$$

where $R$ the radius of the sphere.

*Cylinders*:

$$\frac{M_t}{M_\infty} = 1 - \frac{32}{\pi^2}\sum_{n=1}^{\infty}\frac{1}{q_n^2}\exp\left(-\frac{q_n^2}{R^2}Dt\right)\cdot\sum_{p=0}^{\infty}\frac{1}{(2p+1)^2}\times\exp\left[-\frac{(2p+1)^2\pi^2}{H^2}Dt\right], \tag{6.15}$$

where $R$ and $H$ denote the radius and height of the cylinder, $n$ and $p$ are summation indices, and $q_n$ is the $n$'s root of the zero-order Bessel function of the first kind $[J_0(q_n) = 0]$. The last expression is valid when release is permitted in both the radial direction and through the ends of the cylinder.

Simple but accurate approximations, listed below, can be used in place of infinite series during the early and late stages of drug release:

$$\text{Thin slabs, first 60\% of drug release:} \quad \frac{M_t}{M_\infty} = 4\sqrt{\frac{Dt}{\pi L^2}}. \tag{6.16}$$

$$\text{Thin slabs, last 60\% of drug release:} \quad \frac{M_t}{M_\infty} = 1 - \frac{8}{\pi^2}\exp\left(\frac{-\pi^2 Dt}{L^2}\right). \tag{6.17}$$

Figure 6.8 illustrates all three solutions: the exact one [black curve (6.13)], the early time approximation [dotted curve (6.16)] and the late time approximation [dashed curve (6.17)]. The approximations are valid provided the slab is very thin, and release through edges can be neglected.

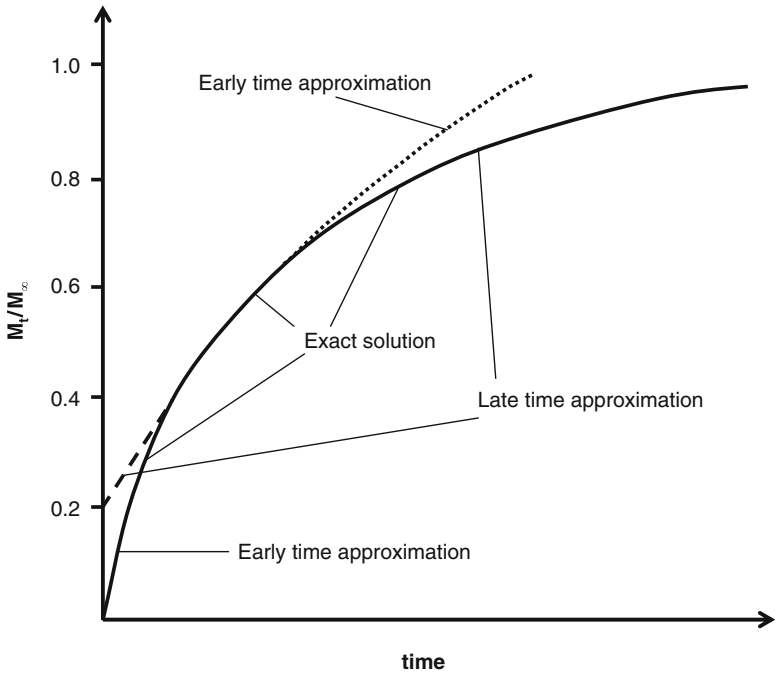


**Fig. 6.8** Drug release from monolithic solutions exhibiting film geometry with negligible edge effects under perfect sink conditions: analytical solution [*solid curve* (6.13)], early time approximation [*dotted curve* (6.16)] and late time approximation [*dashed curve* (6.17)]

$$\text{Spheres, first 40\% of drug release:} \quad \frac{M_t}{M_\infty} = 6\sqrt{\frac{Dt}{R^2\pi}} - \frac{3Dt}{R^2}. \tag{6.18}$$

$$\text{Spheres, last 40\% of drug release:} \quad \frac{M_t}{M_\infty} = 1 - \frac{6}{\pi^2} \times \exp\left(\frac{-\pi^2 Dt}{R^2}\right). \tag{6.19}$$

$$\text{Cylinders, first 40\% of drug release:} \quad \frac{M_t}{M_\infty} = 4\sqrt{\frac{Dt}{R\pi^2}} - \frac{Dt}{R^2}. \tag{6.20}$$

$$\text{Cylinders, last 40\% of drug release:} \quad \frac{M_t}{M_\infty} = 1 - 0.6196 \times \exp\left(-\frac{5.784Dt}{R^2}\right). \tag{6.21}$$

The approximate expressions for cylinders apply when release is mostly in the radial direction and axial release through the ends can be ignored.

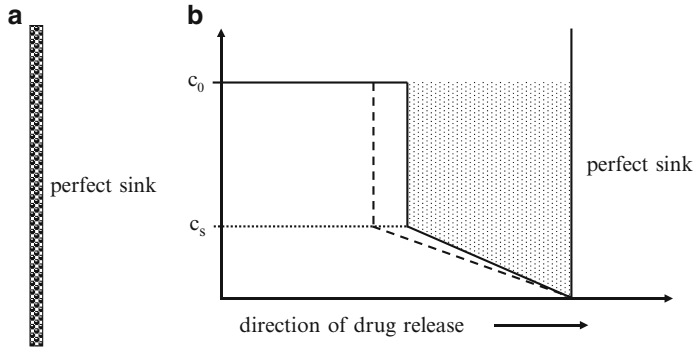


**Fig. 6.9** Schematic presentation of: (**a**) a thin ointment film/matrix system containing finely dispersed drug and being exposed to perfect sink conditions and (**b**) the drug concentration–distance profiles within the film during drug release, considered for the derivation of the Higuchi equation (6.22)

### *6.3.2 Monolithic Dispersions*

In the case of monolithic dispersions, a fraction of the drug is dissolved in the matrix and the remainder is dispersed in the form of crystalline and/or amorphous particles (nondissolved drug). Only dissolved drug is available for diffusion, but it can be rapidly replaced by dissolution of neighboring solid drug, where available. The exact mathematical treatment of this type of drug delivery system is rather complex and the reader is referred to the literature for details [7, 17–19]. A simple and accurate solution is available, however, for thin slabs (release through both faces and negligible edge effects) initially containing a large initial excess of drug (Fig. 6.9a). This is the celebrated Higuchi equation [20], according to which

$$M_t = 2A\sqrt{(2c_0 - c_s)c_s Dt}, \tag{6.22}$$

where $c_0$ is the initial total concentration of drug, dissolved and undissolved, in the monolith and $c_s$ is the solubility of drug in the monolith's matrix material under the conditions encountered upon administration. [The Higuchi equation was initially developed for ointment bases containing finely suspended drug. For ointments spread over the skin, the prefactor 2 is dropped, as in (3.10)].

The derivation of the Higuchi equation rests on a few simple assumptions. Initially, dissolved drug is at concentration $c_s$ throughout the monolith and excess undissolved solid drug is at concentration $c_0 - c_s$. At the first stage, dissolved drug at and near the surface is released, but it is immediately replaced by neighboring solid drug. This "store" of excess drug is rapidly depleted at the surface, however. In the next stage, dissolved drug that is initially a little further inside diffuses out, also to be replaced by its local solid excess, which is then depleted. With subsequent similar stages, a "moving front" of dissolution is established inside the monolith, as illustrated in Fig. 6.9b. At a given time, this front separates the monolith into a core

containing both dissolved and solid drug and a peripheral layer containing only dissolved drug. Since dissolution is rapid, drug concentration is $c_s$ at the moving front. Assuming release is into a perfect sink, drug concentration is zero at the edge of the device. To make further progress, Higuchi assumed that the front moves slowly enough that a linear concentration profile of dissolved drug, similar to the profile that would be assumed at steady state, is maintained in the peripheral layer. Release from the monolith is due to diffusion of dissolved drug down this concentration gradient, and drug release is matched at a given time by further dissolution and movement of the front. This sequence of events is illustrated in Fig. 6.9b, where the concentration profile at one time, given by the solid line, is followed at a later time by the profile depicted by the dashed line. Equation (6.22) results from these assumptions, and noticing that the total amount released at a given time (solid line) is given by the area of the stippled trapezoid in Fig. 6.9b.

The Higuchi equation is most applicable when (1) the initial drug concentration is much higher than drug solubility ($c_s/c_0 \ll 1$), (2) perfect sink conditions are maintained throughout the experiment, (3) the slab is thin, so edge effects are negligible, (4) the suspended drug is in a fine state, with particles much smaller in diameter than the thickness of the slab, (5) swelling or dissolution of the slab matrix is negligible, and (6) diffusivity of the drug in the matrix is constant. When the first condition is not satisfied, more precise expressions are available [18, 19], but the error in predicting cumulative release from a slab using the simple Higuchi equation is at most 13%. A simple fix, which brings error down to less than 0.5% in all cases, is offered by Bunge [21]

$$\frac{M_t}{M_\infty} = 2\sqrt{\left(2 - 0.727\frac{c_s}{c_0}\right)\left(\frac{c_s}{c_0}\right)\left(\frac{Dt}{L^2}\right)}. \tag{6.23}$$

When other conditions are not satisfied, more detailed computational methods are typically needed to properly model release. Finally, it should be noted that the assumption of rapid dissolution of drug from suspended particles may not always be correct, and Frenning has considered the case where the kinetics of dissolution at particle surfaces is a contributing factor [22].

The Higuchi equation has been extended to other geometries. We present here solutions, valid for $c_s/c_0 \ll 1$, for slabs, spheres, and cylinders (only radial release considered) [17, 19], in terms of fraction released, $M_t/M_\infty$:

$$\text{Slab (two faces):} \quad \frac{M_t}{M_\infty} = 2\sqrt{\left(2 - \frac{c_s}{c_0}\right)\left(\frac{c_s}{c_0}\right)\frac{Dt}{L^2}}, \quad 0 < t < \frac{L^2}{8D}\left(\frac{c_0}{c_s}\right). \tag{6.24}$$

$$\text{Sphere:} \quad \left[1 - \left(1 - \frac{M_t}{M_\infty}\right)^{2/3}\right] - \frac{2}{3}\left(\frac{M_t}{M_\infty}\right) = 2\left(\frac{c_s}{c_0}\right)\frac{Dt}{R^2}, \quad 0 < t < \frac{R^2}{6D}\left(\frac{c_0}{c_s}\right). \tag{6.25}$$

$$\text{Cylinder:} \quad \frac{M_t}{M_\infty} + \left(1 - \frac{M_t}{M_\infty}\right) \ln\left(1 - \frac{M_t}{M_\infty}\right) = 4\left(\frac{c_s}{c_0}\right)\frac{Dt}{R^2}, \quad 0 < t < \frac{R^2}{4D}\left(\frac{c_0}{c_s}\right). \tag{6.26}$$

The upper time limits correspond to points where the moving dissolution front(s) reaches the center of the device, and only dissolved drug remains. Afterwards, infinite series expressions are needed to describe release. Typically, this amounts to a very small part of the release process, especially when $c_s/c_0 \ll 1$. Notice that $M_t/M_\infty$ is an implicit, not explicit function of $t$ for the sphere and the cylinder. It is simple, however, to plot $M_t/M_\infty$ versus $t$ by letting $M_t/M_\infty$ run from 0 to 1, and determining the corresponding values of $t$.

The Higuchi equation has also been extended to consider porous structures, as discussed in Chap. 9.

## 6.4 Determination of Diffusion Coefficients and Other Parameters

The models of controlled released described in this chapter include the diffusion coefficient, partition coefficient, and drug solubility (in a reservoir or in a matrix), as parameters. These physicochemical quantities depend on the drug and the membrane or matrix material and may also vary with temperature and hydration of the material. The other important parameter is the system size (thickness for a slab, radius for a sphere, and radius and height for a cylinder). System geometry and size are set by the formulator.

The literature on determining the physicochemical parameters is extensive, and we focus here on simple techniques.

### *6.4.1 Solubility and Partition Coefficient*

Solubility is a thermodynamic property of drug and its surrounding medium. It should be measured at the relevant temperature (usually body temperature), and with the medium saturated by relevant body fluid or a simulated body fluid such as phosphate buffered saline.

A simple way to determine solubility of drug in a liquid medium is to disperse an excess of solid drug, preferably prepared as a fine powder, in the liquid and agitate the dispersion at the relevant temperature. At various times, the dispersion is removed and solid drug is removed by centrifugation and/or filtration. Concentration of the remaining dissolved drug will increase with time until it reaches a plateau, which can be taken as the saturation concentration, or solubility.

To determine solubility of a drug in the material constituting the membrane or release matrix, thin samples of the material, of uniform volume, can be added to the liquid dispersion. Following agitation, samples are removed at different times and quickly washed to remove excess drug on the surface. The drug is then extracted from a given sample and assayed. When the amount of drug assayed divided by volume of the material sample reaches a constant value, this ratio is taken as the solubility of drug in the material.

The partition coefficient, which is also a thermodynamic quantity, is estimated as the ratio of drug solubilities in the membrane/matrix material and the release medium. It can also be estimated by equilibrating the material samples with subsaturated drug solutions, and measuring the ratio of concentration of drug in the sample to the concentration of drug in the release medium, both measured after equilibrium has been reached. An elaboration of this technique is discussed below.

### *6.4.2 Diffusion Coefficient*

The diffusion coefficient of drug in the matrix material is a measure of the mobility of drug in the material. In recent years, sophisticated tools such as pulsed field gradient NMR and fluorescence recovery after photobleaching (FRAP) have been developed to measure diffusivities [23–26]. However, the required equipment is generally expensive and special skills are required for data analysis. Also, these techniques require that drug molecules be deuterated (NMR) or fluorescently tagged (FRAP) so that they can be distinguished from the background medium. If the partition coefficient of a drug in a membrane is known, then the diffusion coefficient of that drug in the membrane can be determined from the steady state rate of drug permeation across the membrane in a side-by-side diffusion cell [27], using (6.8). If the membrane is drug-free at the beginning of the permeation experiment, then $D$ and $K$ can be determined simultaneously from the time lag expression (6.11).

A simple alternative is to measure drug release kinetics from a thin film with an initially homogenous and subsaturated drug distribution (monolithic solution) into a well stirred release medium that provides perfect sink conditions. Figure 6.10 schematically shows such a setup. The film should be sufficiently thin that edge effects are minimal. Also, the film must not be soluble in the release medium, and film floating or folding during the experiment must be avoided, assuring that the entire film surface is always completely exposed to the bulk fluid. Thin films can often be rapidly prepared by casting or spraying drug–polymer solution onto a surface, followed by solvent evaporation. Release periods are generally short, e.g., 8 h, when using very thin films. Drug loading should be very low to assure complete drug dissolution in the system and to avoid changes in the film properties due to drug release, e.g., by creating cavities. Ideally, initial drug content should not exceed 0.5% of the total film weight. Under these conditions release kinetics are

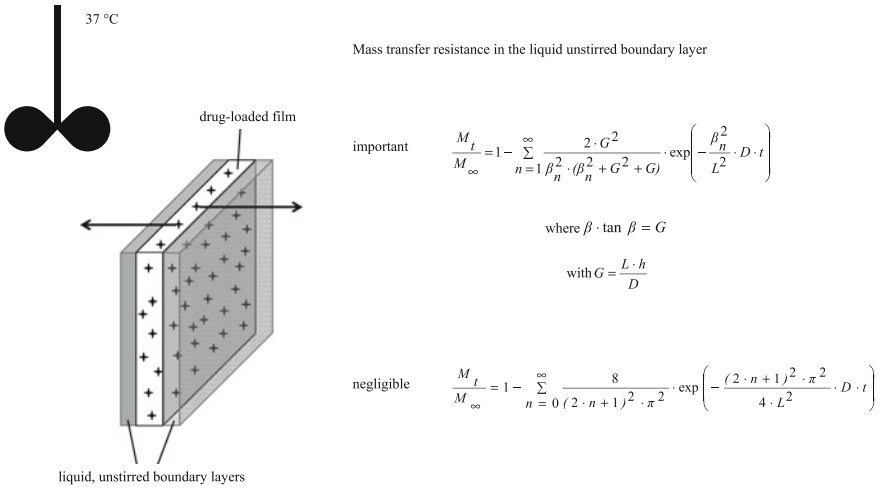


**Fig. 6.10** Illustration of an experimental method allowing for the determination of apparent drug diffusivities in polymeric systems: drug release from a thin film with negligible edge effects and homogeneous, molecular distribution (monolithic solution) is measured under perfect sink conditions. Depending on whether the mass transfer resistance within the liquid, unstirred boundary layer at the film's surface is of importance or not, one of the two analytical solutions of Fick's second law indicated in the diagram can be applied

described by (6.13), provided film thickness does not change substantially with time. This proviso can be checked by measuring film thickness before and after release. Fitting (6.13) to sets of experimentally measured drug release kinetics from thin films allows for the determination of the apparent diffusion coefficient of the drug in the respective system. Figure 6.11 shows an example of such a fit. The drug is theophylline, and the film is based on ethylcellulose, plasticized with 17.5% tributyl citrate. The drug-loaded film was exposed to well-agitated phosphate buffer pH 7.4 at 37°C [28]. Ideally, the entire drug release period is covered by at least 12 experimental data points. As it can be seen in Fig. 6.11, good agreement between theory and experiment was obtained in this example. The determined apparent diffusion coefficient in this case was equal to $1.2(\pm 0.1) \times 10^{-10}$ cm$^2$/s.

It should be noted that unstirred boundary layers are neglected in the derivation of (6.13). To be more accurate, a boundary layer mass transfer coefficient, illustrated in Fig. 6.10 in grey should be included in the release kinetics equation. The mass transfer coefficient, which we denote by $h$ (cm/s), depends on the partition coefficient of drug between release medium and the matrix, and the unstirred layer thickness, which in turn depends on the rate of agitation of the release medium. In the presence of significant external mass transfer resistance, it can be shown that

$$\frac{M_t}{M_\infty} = 1 - \sum_{n=1}^{\infty} \frac{2G^2}{\beta_n^2(\beta_n^2 + G^2 + G)} \times \exp(-\beta_n^2 Dt/L^2), \tag{6.27}$$

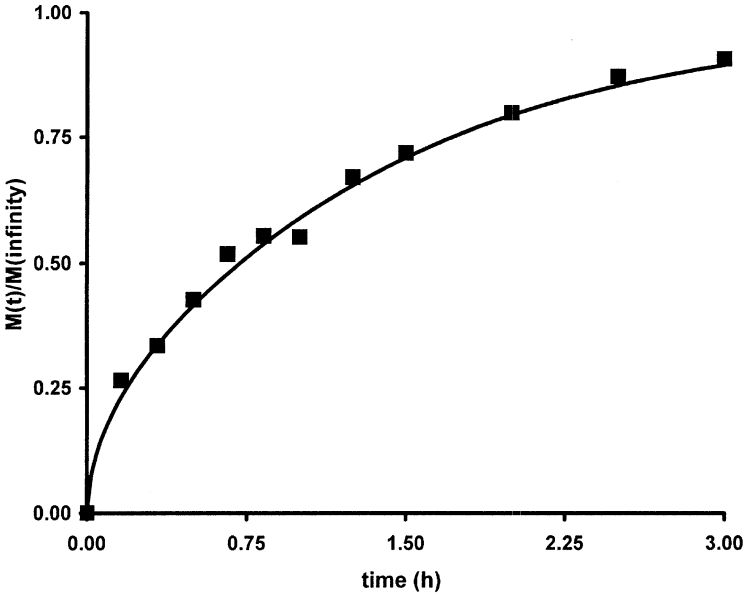


**Fig. 6.11** Example for the determination of an apparent drug diffusivity in a polymeric system: Fitting of an appropriate analytical solution of Fick's second law (6.13) (*curve*) to the experimentally measured release of theophylline from thin ethylcellulose films, plasticized with 17.5% tributyl citrate in phosphate buffer pH 7.4. Reprinted with permission from ref. [28]

where the $\beta_n s$ are the positive roots of

$$\beta \tan \beta = G, \tag{6.28}$$

with

$$G = \frac{Lh}{D}. \tag{6.29}$$

In practice, the mass transfer resistance due to diffusion within polymeric films used to control drug release is often much higher than the mass transfer resistance provide by the liquid unstirred boundary layers in well-agitated release media in vitro, and (6.13) can be used without introducing a significant error. To be certain, it is helpful to measure drug release from the thin films at different agitation speeds: if beyond a certain agitation speed no significant impact is observed on release kinetics, then the data gathered at that speed can be fitted to (6.13). (Note: conditions for drug release in vivo might be different and the presence of liquid unstirred boundary layers might be of importance. For drug diffusivity determination, however, the release medium should be well agitated.)

Both (6.13) and (6.22) assume that drug release is into a perfect sink, with essentially zero drug concentration. This condition is well approximated if the

release medium is exchanged sufficiently rapidly to preserve sink conditions, or if the volume of the release medium is so large that drug concentration in the medium is negligible. If release is into a constant volume without exchange, then the analysis must be modified to take into consideration that perfect sink conditions do not hold. In the absence of mass transfer resistance, release from a slab into medium with volume $V$ of drug is given by Crank [3] as

$$\frac{M_t}{M_\infty} = 1 - \sum_{n=1}^{\infty} \frac{2\alpha(1+\alpha)}{1+\alpha+\alpha^2 q_n^2} \exp(-Dq_n^2 t/L^2), \tag{6.30}$$

where the $q_n s$ are the positive roots of

$$\tan q = -\alpha q, \tag{6.31}$$

with

$$\alpha = V/KAL. \tag{6.32}$$

This last parameter is equal to the ratio of the amounts of drug in the release medium and that remaining in the slab at equilibrium. For large values of $\alpha$, virtually all drug is released and (6.13) holds.

In principle (6.13) and (6.30) can be used to simultaneously estimate the drug's diffusion and partition coefficients, since both parameters impinge on the shape of the release curve. Conversely, these parameters can be measured by introducing a drug-free slab into a subsaturated drug medium and measuring the kinetics of drug uptake by the slab, which is readily monitored by assaying the drop in concentration in the external medium with time. Once again (6.13) can be used, but now $M_t/M_\infty$ refers to fractional uptake of drug by the slab. More directly, the partition coefficient can be determined from fraction of drug remaining in the medium, $r$, according to

$$K = \left(\frac{1}{r} - 1\right)\frac{V}{AL}. \tag{6.33}$$

As already indicated, use of (6.13) to determine diffusivity assumes that $L$ is known and measured. Thus, either the film must not significantly swell, or swelling must be more rapid than drug diffusion. In the later case, $L$ should be taken as the measured thickness following release. The diffusion coefficient then refers to drug in the swollen matrix. If swelling and diffusion processes occur over comparable time scales, then (6.13) will not be valid.

Using the just described straightforward and inexpensive technique enables rapid determination of drug diffusivities, and quantitative evaluation of the impact of formulation parameters is feasible (e.g., using films of different composition). Figure 6.12 shows some examples. The dependence of the apparent diffusion coefficient of theophylline in ethylcellulose films has been determined as a function of the following: (a) type of plasticizer (at a constant plasticizer content of 20%),

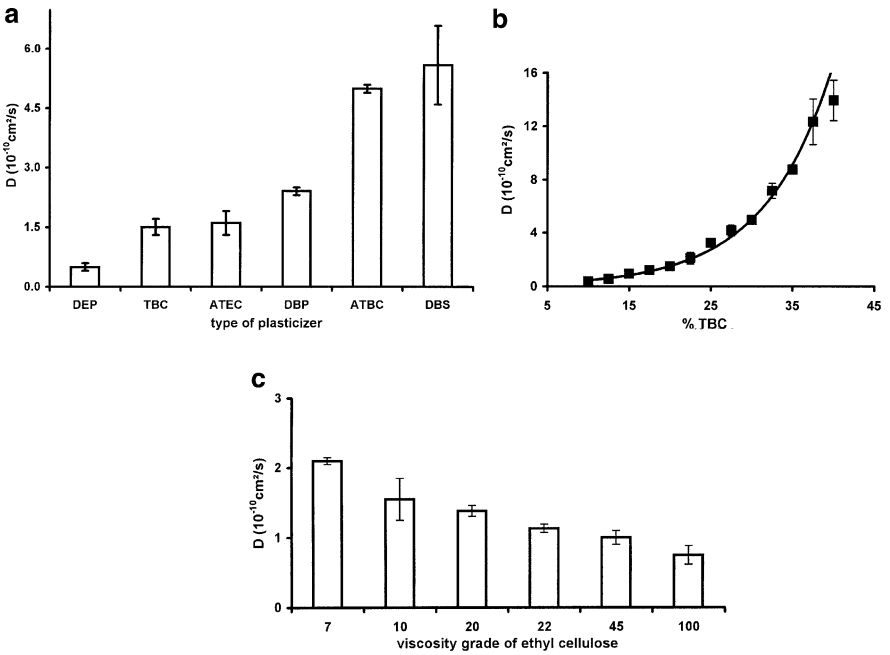


**Fig. 6.12** Examples for the dependence of the apparent diffusion coefficient of a drug (theophylline) in a polymeric system (ethylcellulose) on formulation parameters, such as the: (**a**) type of plasticizer (20% plasticizer content), (**b**) the percentage of plasticizer (tributyl citrate), and (**c**) the average polymer molecular weight (expressed as the viscosity of a 5% solution in 80% toluene and 20% ethanol, measured at 25°C, in cP, using an Ubbelohde viscosimeter). Reprinted with permission from ref. [28]

(b) the percentage of plasticizer (in this example tributyl citrate, TBC), and (c) the average polymer molecular weight (here expressed as the viscosity of a 5% solution in 80% toluene and 20% ethanol, measured at 25°C, in cp, using an Ubbelohde viscosimeter: increasing viscosity indicates increasing polymer molecular weight). Clearly, the type of plasticizer significantly affects the resulting drug diffusivity, due to different interactions with the polymer chains (Fig. 6.12a). With increasing plasticizer content, the mobility of the polymer chains increases, and thus the mobility of the drug molecules increases (Fig. 6.12b). By contrast, with increasing polymer molecular weight, the degree of polymer chain entanglement increases, resulting in reduced macromolecular mobility and reduced drug mobility (Fig. 6.12c).

Knowing the diffusion coefficient of a particular drug in a specific polymeric system permits quantitative prediction of the resulting drug release kinetics using the above described equations. Ideally, a quantitative relationship between the diffusion coefficient and the formulation parameter can be established, either empirically or using a theoretical model. For example, the following expression correlates theophylline diffusivity with tributyl citrate content in ethylcellulose films:

$$D(\%\ \mathrm{TBC}) = 0.135 \times \exp(0.121 \times \%\ \mathrm{TBC}) \times 10^{-10}\mathrm{cm}^2/\mathrm{s}. \qquad (6.34)$$

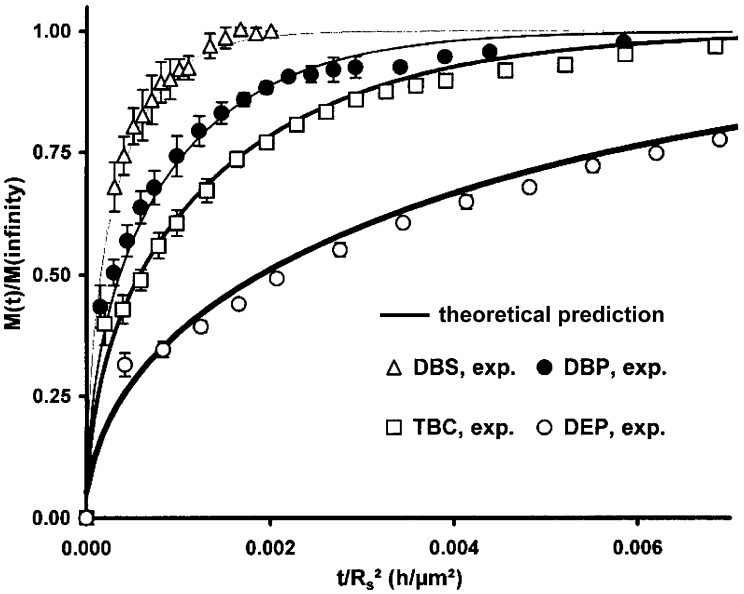


**Fig. 6.13** Theoretical prediction (*curves*) and independent experimental verification (*symbols*) of the release of theophylline from microparticles based on ethylcellulose, plasticized with 20% dibutylsebacate (DBS), dibutyl phthalate (DBP), tributyl citrate (TBC), or diethyl phthalate (DEP). The diffusion coefficients determined with thin films were used to predict the release kinetics form the spherical microparticles using (6.14). The data is normalized to the system's radius. Reprinted with permission from ref. [28]

Using such correlations, diffusion coefficients can be theoretically predicted for arbitrary plasticizer contents within the range of validity, reducing the number of required experiments.

Provided diffusion is the rate limiting process for drug release, drug diffusion coefficients determined in thin films can also be expected to be valid in delivery systems based on the same polymer matrix material but of different geometry. Figure 6.13 shows a comparison of quantitative predictions and experimental measurements of release of theophylline from spherical microparticles based on ethylcellulose, plasticized with 20% dibutylsebacate, dibutyl phthalate, tributyl citrate, or diethyl phthalate. Diffusion coefficients used in the theoretical predictions [curves in Fig. 6.13 (6.14)] were determined using thin films of the same composition as the respective microparticles. The good agreement between theory and independent experiments illustrates the applicability of this diffusivity measurement technique.

Certain drugs act as plasticizers for specific polymers. In these cases, drug diffusivity in the polymeric network increases with increasing drug content [29]. Figure 6.14 shows three examples for such systems: metoprolol tartrate, chlorpheniramine maleate, and ibuprofen in combination with Eudragit RS [30]. In Fig. 6.14a,

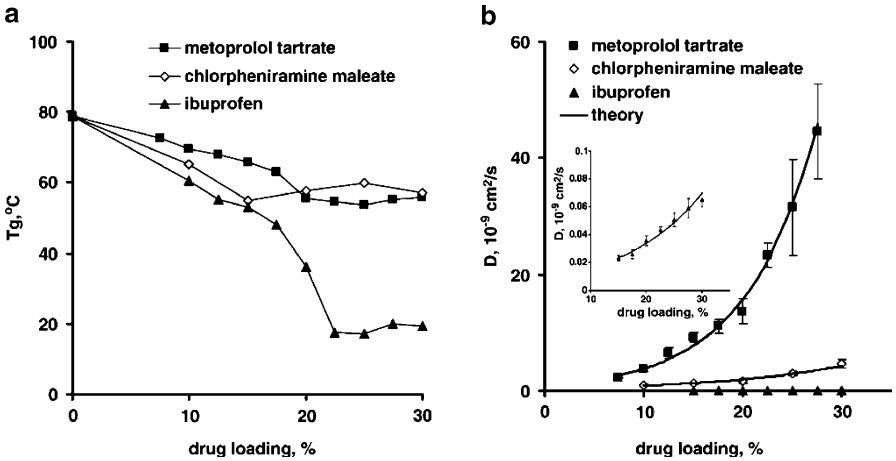


**Fig. 6.14** Examples for drugs acting as plasticizers for certain polymers: (**a**) Effects of the initial loading of metoprolol tartrate, chlorpheniramine maleate, and ibuprofen in Eudragit RS films on the glass transition temperature of the system. (**b**) Dependence of the apparent diffusion coefficient of the drug within the film on the initial drug loading. All films were transparent and did not show any evidence for the presence of drug crystals or amorphous particles. Reprinted with permission from ref. [30]

the decrease in glass transition temperature of the systems with increasing drug content is illustrated, whereas Fig. 6.14b shows an increase in apparent diffusion coefficient of these drugs with increasing drug content. It should be pointed out that (6.13), which was used to determine these drug diffusivities, was derived under the assumption of time independent $D$ values. In the case of plasticizing drugs, this assumption is likely to be not fully fulfilled since drug content is time-dependent (though perhaps partially be compensated by time-dependent water contents) and the determined values should be regarded as "time-averaged" diffusivities. Nevertheless, the obtained information can be very helpful in optimizing this type of controlled drug delivery system and in understanding their mechanism.

## 6.5 Summary

In this chapter, we discussed modeling of drug delivery from systems in which drug diffusion is the rate-limiting process. Distinctions were made between reservoir systems and monoliths, and between systems in which drug is completely dissolved in the device and those in which an undissolved excess of drug exists. Equations were presented for ideal device geometries, and it was assumed that important system parameters were constant. More complex systems might require numerical investigation. We also showed examples of experiments that can be carried out to investigate diffusion-controlled drug release. A wealth of literature exists on this

topic, and this chapter should be regarded more as an introduction than a comprehensive description.

Throughout this chapter, we tacitly assumed that all drug incorporated into a device is available for release. In fact, there are cases where drug may be trapped inside a device, such that its release will not occur within the time frame of interest, or over. This may occur if drug is surrounded by impermeable material, or if it is tightly bound to a component of the device. A fraction of drug molecules might even degrade before release. More detailed descriptions are required in these cases. Drug trapping is discussed in Chap. 9, where porous media are considered.

## References

1. Fick A (1855) Ueber diffusion. Poggendor Ann Phys 94:59–86
2. Fick A (1995) On liquid diffusion. J Membr Sci 100:33–38
3. Crank J (1975) The mathematics of diffusion. Clarendon Press, Oxford
4. Carslaw HS, Jaeger JC (1959) Conduction of heat in solids. Clarendon Press, Oxford
5. Vergnaud JM (1993) Controlled drug release of oral dosage forms. Ellis Horwood, Chichester
6. Cussler EL (1984) Diffusion: mass transfer in fluid systems. Cambridge University Press, New York
7. Fan LT, Singh SK (1989) Controlled release: a quantitative treatment. Springer-Verlag, Berlin
8. Siepmann J, Siepmann F (2008) Mathematical modeling of drug delivery. Int J Pharm 364:328–343
9. Badawy SI, Hussain MA (2007) Microenvironmental pH modulation in solid dosage forms. J Pharm Sci 96:948–959
10. Thoma K, Ziegler I (1998) The pH-independent release of fenoldopam from pellets with insoluble film coats. Eur J Pharm Biopharm 46:105–113
11. Kreye F, Siepmann F, Siepmann J (2011) Drug release mechanisms of compressed lipid implants. Int J Pharm 404:27–35
12. Muschert S, Siepmann F, Leclercq B, Carlin B, Siepmann J (2009) Prediction of drug release from ethylcellulose coated pellets. J Control Rel 135:71–79
13. Lecomte F, Siepmann J, Walther M, MacRae RJ, Bodmeier R (2005) pH-sensitive polymer blends used as coating materials to control drug release from spherical beads: elucidation of the underlying mass transport mechanisms. Pharm Res 22:1129–1141
14. Marucci M, Ragnarsson R, Axelsson A (2007) Evaluation of osmotic effects on coated pellets using a mechanistic model. Int J Pharm 336:67–74
15. Muschert S, Siepmann F, Leclercq B, Carlin B, Siepmann J (2009) Drug release mechanisms from ethylcellulose: PVA-PEG graft copolymer-coated pellets. Eur J Pharm Biopharm 72:130–137
16. Borgquist P, Nevsten P, Nilsson B, Wallenberg LR, Axelsson A (2004) Simulation of the release from a multiparticulate system validated by single pellet and dose release experiments. J Control Rel 97:453–465
17. Tanquary AC, Lacey RE (1974) Controlled release of biologically active agents. Plendon Press, New York
18. Paul DR, McSpadden SK (1976) Diffusional release of solute from a polymer matrix. J Membr Sci 1:33–48
19. Kim C-J (2000) Controlled release dosage form design. Technomic, Lancaster, PA
20. Higuchi T (1961) Rate of release of medicaments from ointment bases containing drugs in suspensions. J Pharm Sci 50:874–875

21. Bunge AL (1998) Release rates from topical formulations containing drugs in suspension. J Control Rel 52:141–148
22. Frenning G (2003) Theoretical investigation of drug release from planar matrix systems: effects of a finite dissolution rate. J Control Rel 92:331–339
23. Ferrero C, Massuelle D, Jeannerat D, Doelker E (2008) Towards elucidation of the drug release mechanism from compressed hydrophilic matrices made of cellulose ethers. I. Pulse-field-gradient spin-echo NMR study of sodium salicylate diffusivity in swollen hydrogels with respect to polymer matrix physical structure. J Control Rel 128:71–79
24. Snaar JE, Bowtell R, Melia CD, Morgan S, Narasimhan B, Peppas NA (1998) Self-diffusion and molecular mobility in PVA-based dissolution-controlled systems for drug delivery. Magn Reson Imaging 16:691–694
25. Vermonden T, Jena SS, Barriet D, Censi R, van der Gucht J, Hennink WE, Siegel RA (2010) Macromolecular diffusion in self-assembling biodegradable thermosensitive hydrogels. Macromolecules 43:782–789
26. Brandl F, Kastner F, Gschwind RM, Blunk T, Teßmar J, Göpferich A (2010) Hydrogel-based drug delivery systems: comparison of drug diffusivity and release kinetics. J Control Rel 142:221–228
27. Stringer JL, Peppas NA (1996) Diffusion of small molecular weight drugs in radiation-crosslinked poly(ethylene oxide) hydrogels. J Control Rel 42:195–202
28. Siepmann J, Lecomte F, Bodmeier R (1999) Diffusion-controlled drug delivery systems: calculation of the required composition to achieve desired release profiles. J Control Rel 60:379–389
29. Wu C, McGinity JW (1999) Non-traditional plasticization of polymeric films. Int J Pharm 177:15–27
30. Siepmann F, Le Brun V, Siepmann J (2006) Drugs acting as plasticizers in polymeric systems: a quantitative treatment. J Control Rel 115:298–306

# Chapter 7
# Swelling Controlled Drug Delivery Systems

**Juergen Siepmann and Florence Siepmann**

**Abstract** This chapter provides an introduction to the physical phenomena, which can be involved in the control of drug release from swellable delivery systems, namely, water diffusion, polymer chain relaxation, drug dissolution and diffusion, as well as polymer dissolution. Emphasis is placed on a mechanistic understanding of the occurring mass transport processes and on physically realistic mathematical theories. Several practical examples are given, illustrating the key properties of swelling-controlled drug delivery systems.

## 7.1 Introduction

The term "swelling-controlled drug delivery system" can be defined in a strict sense, referring only to devices, in which a swelling step is the only release rate-controlling phenomenon. Alternatively, the term "swelling-controlled drug delivery system" can be defined in a broader sense to include devices in which a swelling step is of importance, but also in which other mass transport processes can play a role (e.g., drug dissolution, drug diffusion, and polymer dissolution). This broader interpretation is commonly applied in the literature and also in this chapter.

Often, swelling-controlled drug delivery systems are based on hydrophilic polymers, such as hydroxypropyl methylcellulose [1–5]. Figure 7.1 illustrates the key features of polymer swelling: in the dry state (nonswollen state), the polymer network is dense and the mobility of the macromolecules is very much restricted. Upon contact with water, the polymer chains "relax," with two major consequences: (1) the mobility of the macromolecules significantly increases and (2) the volume of the system increases. Obviously, the conditions for drug transport

J. Siepmann (✉) • F. Siepmann
INSERMU1008, College of Pharmacy, University of Lille Nord de France,
3 Rue du Prof. Laguesse, 59006 Lille, France
e-mail: juergen.siepmann@univ-lille2.fr; florence.siepmann@univ-lille2.fr

J. Siepmann et al. (eds.), *Fundamentals and Applications of Controlled Release Drug Delivery*, Advances in Delivery Science and Technology,
DOI 10.1007/978-1-4614-0881-9_7, 

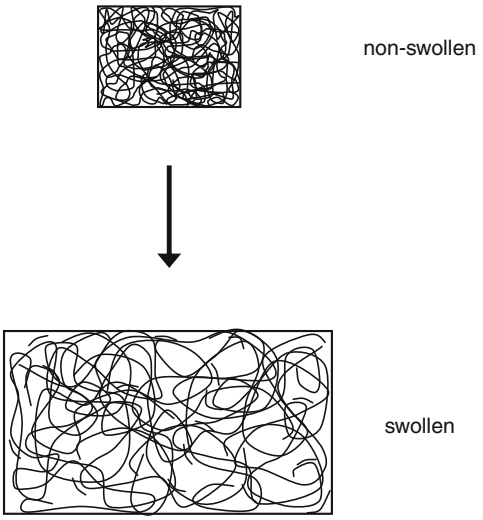


**Fig. 7.1** Schematic illustration of a macromolecular network in the nonswollen state (dense network structure, low polymer chain mobility) and in the swollen state (less dense network structure, high polymer chain mobility, and increased system volume)

in these two states (nonswollen versus swollen) are fundamentally different, and the change in physical state of the polymer can be used to accurately control the release rate of an incorporated drug.

## 7.2 Drug Release Mechanisms

In order to induce the polymer chain relaxation process, a minimum water concentration is required. The latter is a function of the physicochemical characteristics of the polymer (e.g., chemical structure of its backbone and potential side chains, average polymer molecular weight), and temperature. In a dry, nonswollen polymer network, incorporated drug is not mobile and is effectively entrapped. When the system comes into contact with aqueous fluids, water diffuses into the device due to concentration gradient. As soon as the minimum water content required to induce polymer chain relaxation is achieved at a certain position, the system swells at this location. Thus, two phenomena occur in a sequence: (1) water diffusion and (2) polymer chain relaxation. If one of these processes is much slower than the other, that process controls water penetration kinetics into the device.

Figure 7.2 illustrates an example of a system in which *water diffusion* into a thin, polymeric film is dominant [6]. Both surfaces of the film are exposed to the aqueous bulk fluid. Polymer chain relaxation is assumed to be very rapid and the volume increase is assumed to be negligible. While these conditions do not hold in many pharmaceutically relevant polymeric systems, the figure is useful in illustrating the nature of solvent diffusion. Water concentration is plotted as a function of position in the film and is scaled such that "1" indicates a fully swollen polymer network and "0" indicates a completely dry polymeric network. The curves show the calculated

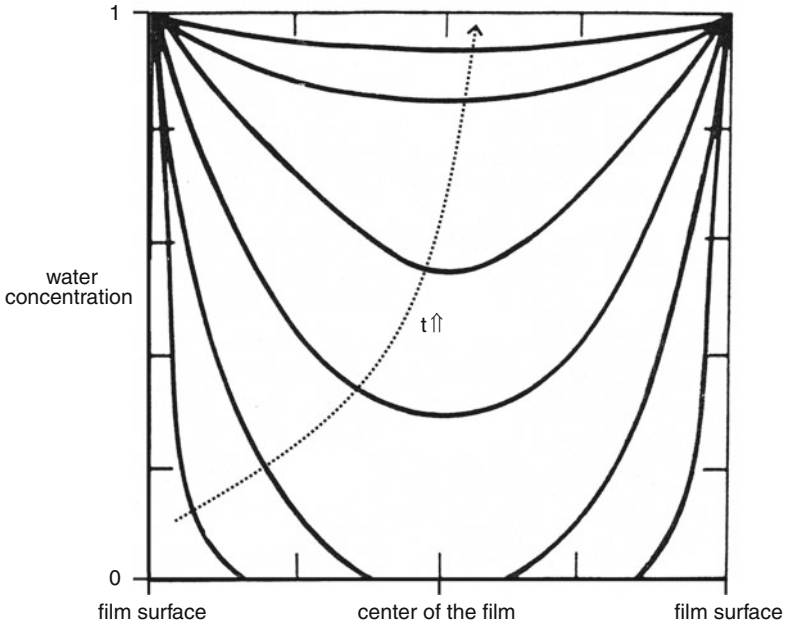


**Fig. 7.2** *Diffusion*-controlled penetration of a liquid into a thin, polymeric film: concentration–position profiles of a liquid (e.g., release medium) at different time points within the system. Two surfaces of the film are exposed to the bulk fluid (*left-* and *right-hand side*). The profiles have been calculated using Fick's second law of diffusion, considering constant diffusion coefficients and system dimensions (no polymer dissolution, no significant volume increase upon liquid penetration into the system). Water concentration "1" indicates that the polymeric system is saturated with liquid. Water concentration "0" indicates that the system is free of liquid. Adapted from ref. [6]

water concentration–time profiles upon exposure to the aqueous bulk fluid. The applied theory is based on Fick's second law of diffusion (see Chap. 6) and assumes that water diffusivity is constant. In this case, the water uptake rate monotonically decreases with time.

In contrast, if water diffusion into the polymeric network is much more rapid than subsequent polymer chain relaxation, then water concentration–position profiles, such as those illustrated in Fig. 7.3, can be observed [6]. In this example, only one side of the polymeric film is exposed to water. The film is divided into a swollen region on the left and a nonswollen, dry region on the right, separated by a narrow swelling zone within which there is a steep gradient in water concentration. In the swollen region, water diffusion is rapid, and water content is maximal at every position in that region. In the swelling zone, polymer chain relaxation takes place, resulting in increased macromolecular mobility and volume expansion. With time, this swelling zone moves toward the center of the film. If the film is homogenous, the swelling front moves at a constant velocity, since the conditions for polymer swelling are time independent: in this case, zero-order uptake kinetics are observed. If drug is incorporated in such a system, it is generally immobilized

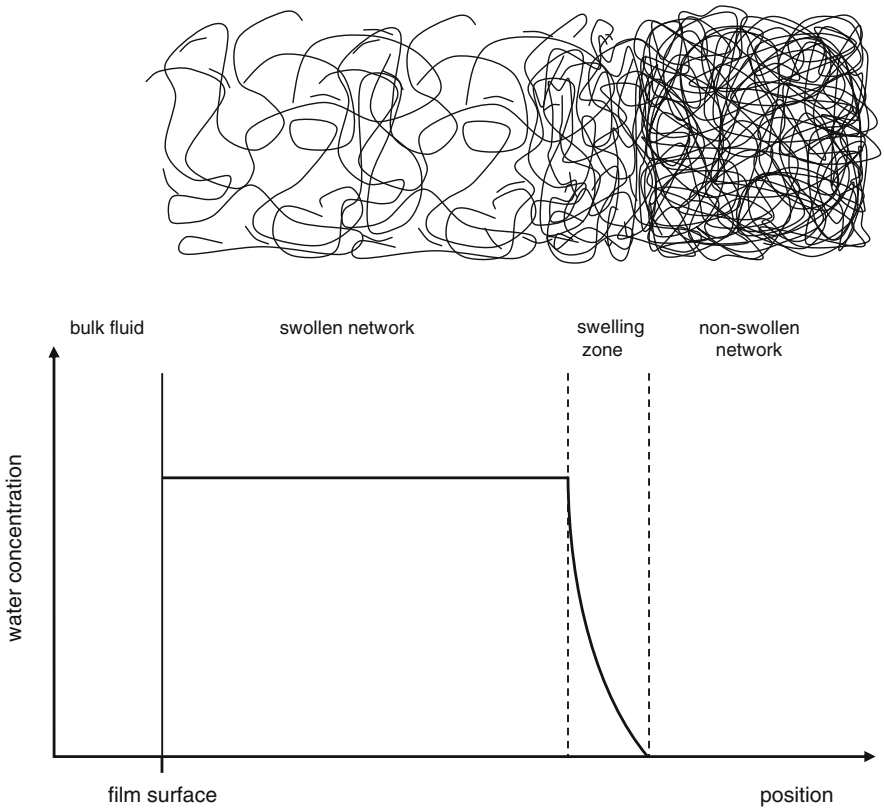


**Fig. 7.3** Polymer relaxation-controlled penetration of a liquid into a thin, polymeric film: concentration–position profile of a liquid (e.g., release medium) at a given time point within the system. One surface of the film is exposed to the bulk fluid (*left-hand side*). Three different zones can be distinguished inside the film: (1) swollen network (high liquid content, high mobility of macromolecules and liquid molecules); (2) swelling zone (polymer chain relaxation); and (3) nonswollen network (low mobility of macromolecules, "free" of liquid). Adapted from ref. [6]

until the surrounding polymer chains undergo chain relaxation. If drug dissolution and diffusion through the swollen polymeric network are rapid compared to polymer chain relaxation and swelling front movement, then drug release will be controlled by swelling and its rate will also be constant. Swelling plus drug diffusion are schematically illustrated in Fig. 7.4a,b, with crosses representing drug molecules, which are immobilized in the nonswollen, dry polymeric network, but become mobile in the swelling zone. Diffusion of drug then occurs down its concentration gradient in the swollen region.

Peppas and coworkers [7] reported an example of this type of "purely swelling"-controlled drug delivery system: they studied theophylline release from poly (HEMA-co-NVP) [poly(2-hydroxyethylmethacrylate-*co*-*N*-vinylpyrrolidone)] disks

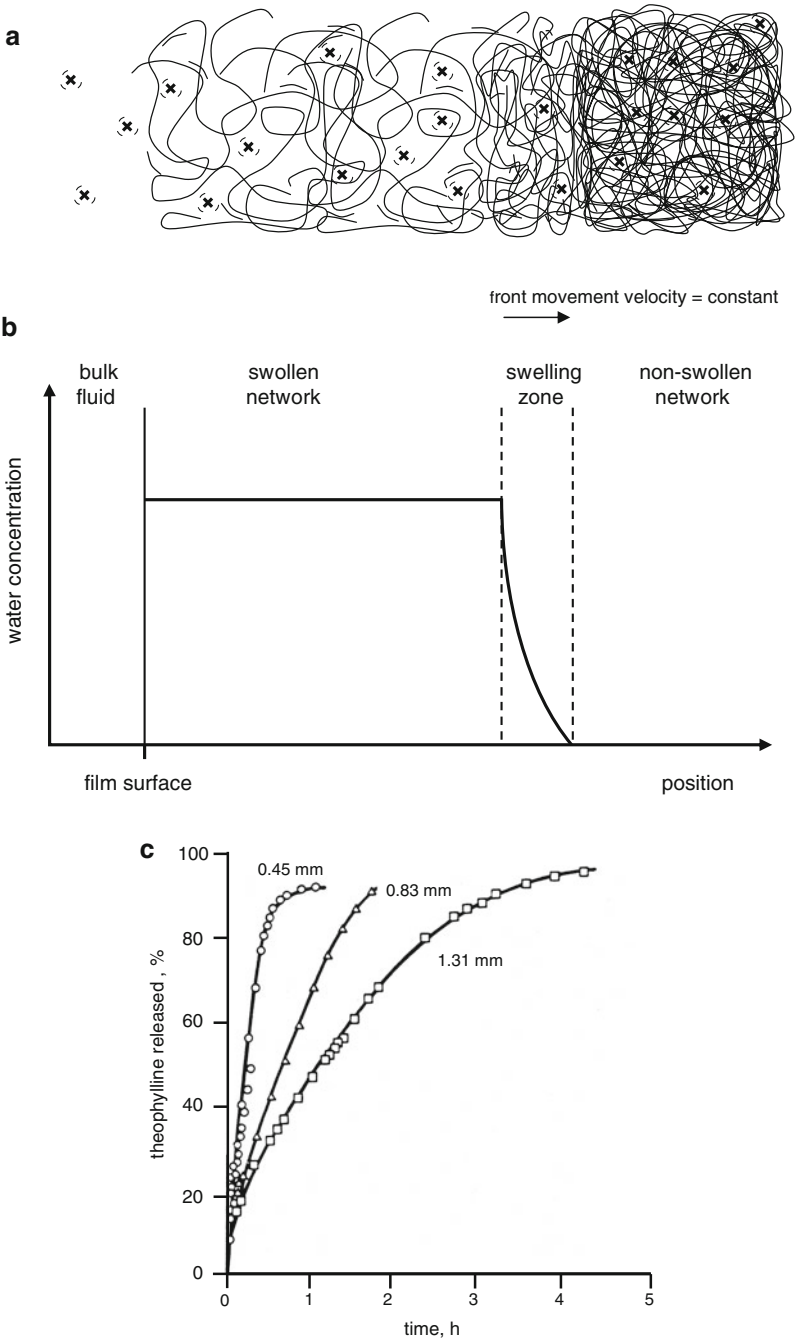


**Fig. 7.4** Polymer relaxation-controlled release of theophylline from poly(HEMA-co-NVP) disks: (**a**) schematic illustration of the polymer chain density and mobility as well as theophylline (*crosses*) location and mobility and (**b**) schematically illustrated liquid concentration–position profile inside the system. Since polymer chain relaxation is the slowest process, the swelling front moves inward at a constant velocity. (**c**) Experimentally measured drug release kinetics from disks of different thickness (indicated in the diagram). Adapted from ref. [6]

into distilled water. The symbols in Fig 7.4c illustrate the obtained experimental results. As can be seen, the release rate of the drug is nearly constant or zero order during major parts of the release period, particularly for the thinnest sample. The *relative* drug release rate decreased with increasing device thickness because it takes more time for the swelling front to move throughout the entire system, which is required for all drug to be released. Moreover, the thicker samples displayed a slight slowing down of release with time, probably due to drug diffusion becoming increasingly more rate limiting. (Recall from Chaps. 2 and 6 that diffusion is slower at greater distances.)

Zero order drug release kinetics result if the polymer relaxation process is the slowest step in the series of physicochemical phenomena involved in the control of drug release and if the surface area of the swelling front is time independent. The latter condition is, for example, fulfilled in the case of thin films with negligible edge effects. When plotting the cumulative amount of drug release versus time, a straight line is obtained and drug release can be quantified according to the following equation:

$$\frac{M_t}{M_\infty} = kt, \tag{7.1}$$

where $M_t$ and $M_\infty$ denote the absolute cumulative amounts of drug released at time $t$ and infinite time, respectively; $k$ is a rate constant. However, if the dosage form is sufficiently thick or has a different geometry, e.g., that of a sphere or a cylinder, then the surface area of the swelling front generally decreases with time. Thus, the release rate decreases with time, although the underlying drug release mechanism may still be characterized as "pure polymer chain relaxation control." It can be shown that this decrease in surface area with time leads to the following expressions which fit release kinetics over a substantial portion of the release process:

$$\text{For a cylinder:} \quad \frac{M_t}{M_\infty} = kt^{0.89} \tag{7.2}$$

$$\text{For a sphere:} \quad \frac{M_t}{M_\infty} = kt^{0.85} \tag{7.3}$$

In a more general form, (7.1)–(7.3) can be written as follows:

$$\frac{M_t}{M_\infty} = kt^n. \tag{7.4}$$

This power law approximation was introduced into the pharmaceutical field by Nicholas Peppas to describe drug release from a dosage form. Both the exponent $n$ and the prefactor $k$ depend on dosage form geometry, the relative importance of relaxation and diffusion, and structural factors governing diffusion and relaxation rates. Equations (7.1)–(7.3) are special cases of (7.4) corresponding to

**Table 7.1** Release exponent $n$ of the Peppas equation and drug release mechanism from polymeric-controlled delivery systems with different geometries

| Thin film | Exponent, $n$ cylinder | Sphere | Drug release mechanism |
|---|---|---|---|
| 0.5 | 0.45 | 0.43 | Fickian diffusion |
| $0.5 < n < 1.0$ | $0.45 < n < 0.89$ | $0.43 < n < 0.85$ | Anomalous transport |
| 1.0 | 0.89 | 0.85 | Polymer swelling |

predominantly swelling controlled drug release from slabs, cylinders, and spheres. Table 7.1 lists the respective $n$ values. Caution should be paid that no other phenomena, e.g., limited drug solubility or inhomogeneous initial drug distribution, are of importance, as they may lead to similar $n$ values as pure swelling control.

If diffusional mass transport (e.g., of dissolved drug or water) is the dominant drug release mechanism, then similar equations can be obtained (being simplified approximate solutions of Fick's law of diffusion): $n = 0.5$ for thin films with negligible edge effects, $n = 0.45$ for cylinders, and $n = 0.43$ for spheres (Table 7.1). However, again caution should be paid because the superposition of other phenomena besides pure diffusion might occasionally lead to the comparable $n$-values [8]. When $n$ values are observed between 0.5 and 1 for slabs, 0.45 and 0.89 for cylinders, and 0.43 and 0.85 for spheres, diffusional mass transport and polymer chain relaxation may both be rate controlling processes. In such cases, transport is commonly called "anomalous."

## 7.3 Moving Boundaries

If the polymer chains are soluble in water, erosion might also play a significant rate-controlling role for drug release. Upon contact with aqueous media, liquid penetrates into the system, leading to steadily increasing water concentrations. As soon as the water content is high enough, the polymer chains start to disentangle from the network and diffuse through the liquid unstirred boundary layer surrounding the device into the surrounding fluid. Figure 7.5 schematically illustrates these processes: in the dry state, the polymer chains are highly entangled and exhibit low mobility. Upon contact with aqueous media, water content significantly increases, resulting in increased macromolecular mobility, and the chains start to perform reptational (snake-like) motions through each other. Due to these movements, polymer chains disentangle at certain positions and re-entangle at others. If the water content is high enough (polymer content low enough), then the number of disentanglements exceeds the number of new entanglements, and the network erodes into the bulk fluid. The front separating the bulk fluid and the system is called the "erosion front."

The black diamonds in Fig. 7.5 represent nondissolved drug particles, whereas the crosses represent dissolved, individual drug molecules. Often, the incorporated

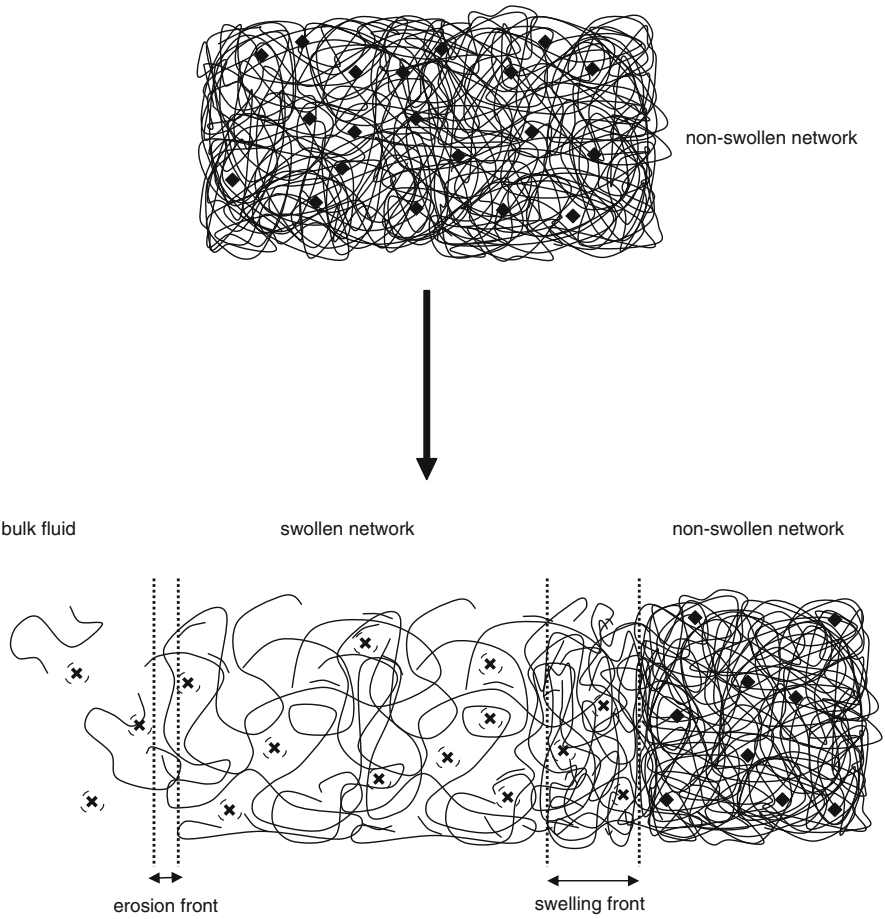


**Fig. 7.5** Schematic presentation of a drug-loaded polymeric network in the nonswollen state (*top*) and upon liquid penetration into the system (*bottom*). If the polymer is soluble in water, an erosion front separates the bulk fluid from the swollen polymeric network. *Crosses* represent dissolved drug molecules, *black diamonds* nondissolved drug particles

drug is initially present in the form of solid particles inside a polymeric matrix, e.g., as drug crystals and/or amorphous aggregates. Upon contact with aqueous fluids, these particles start to dissolve. The kinetics of this process can be described using the Noyes–Whitney equation [9]. When the drug dissolution step is much more rapid than the other mass transport steps, it can be considered as being essentially instantaneous when predicting release rate. Figure 7.5 shows a schematic illustration of the different zones, which can be distinguished in this type of swellable drug delivery systems: drug particles (black diamonds) are incorporated in the initially dry polymeric network, which is dense and poorly permeable

(upper cartoon). Upon contact with aqueous media, water diffuses into the system, resulting in: (1) polymer swelling and (2) drug dissolution. Once dissolved, the drug molecules (crosses) diffuse out into the release medium. If the polymer is water soluble, polymer dissolution takes place at the system's surface and two *moving* boundaries can be distinguished: (1) the erosion front, separating the bulk fluid and the delivery device and (2) the swelling front, separating the swollen polymeric network containing only dissolved drug and the still dry polymeric network containing drug particles. (The terms "swelling front" and "swelling zone" are often used as synonyms.) The swelling front continuously moves inward upon contact with the release medium, whereas the erosion front generally first moves outward due to system swelling, and then inward due to subsequent erosion of swollen polymer.

When drug loading greatly exceeds its solubility in the swollen network, not all of the drug can instantaneously dissolve: dissolved and nondissolved drug now coexist in the swollen polymeric network, as illustrated in Fig. 7.6. In this case, a third moving boundary, called the "diffusion front" is present. Only dissolved drug (crosses) is available for diffusion, whereas nondissolved drug excess (black diamonds) is not able to diffuse. In most cases, the existence of the diffusion front is due to the limited *solubility* of the drug, an equilibrium property, and not to a kinetic limitation in the dissolution process. Consequently, drug molecules that diffuse out of the swollen polymeric network are rapidly replaced by partial dissolution of the remaining drug excess, as discussed in the lead up to the Higuchi equation in Chap. 6.

Colombo et al. [10] reported a very nice example of a system allowing experimental observation of these different fronts and their movements. The idea is to use a drug, which changes its color depending on its physical state. Buflomedil pyridoxal phosphate is such a drug: its dry particles are light yellow, whereas concentrated drug solutions are orange and less concentrated drug solutions are yellow. Different amounts of this drug were incorporated into hydroxypropyl methylcellulose (HPMC) tablets, which were placed between two transparent Plexiglas plates and exposed to distilled water in a USP paddle apparatus. At predetermined time points, photographs were taken. Figure 7.7 shows an example of such a picture, illustrating a tablet initially containing 60% buflomedil pyridoxal phosphate after a 4-h exposure to water. As it can be seen, the still dry tablet core (white) can be easily distinguished from the swollen tablet region, still containing nondissolved drug particles (light yellow). The swelling front separates these two regions. The diffusion front is also clearly visible, separating the swollen region containing dissolved and nondissolved drug from the swollen region containing only dissolved drug (orange). Even the decrease in the buflomedil pyridoxal phosphate concentration within the swollen tablet region containing only dissolved drug can be nicely observed (orange to yellow to transparent). Finally, the erosion front separating the bulk fluid from the swollen tablet region is readily visible. Using this experimental setup, the movements of these fronts during drug release can be described in a quantitative manner, allowing deeper insight into the importance of the contributing physical phenomena.

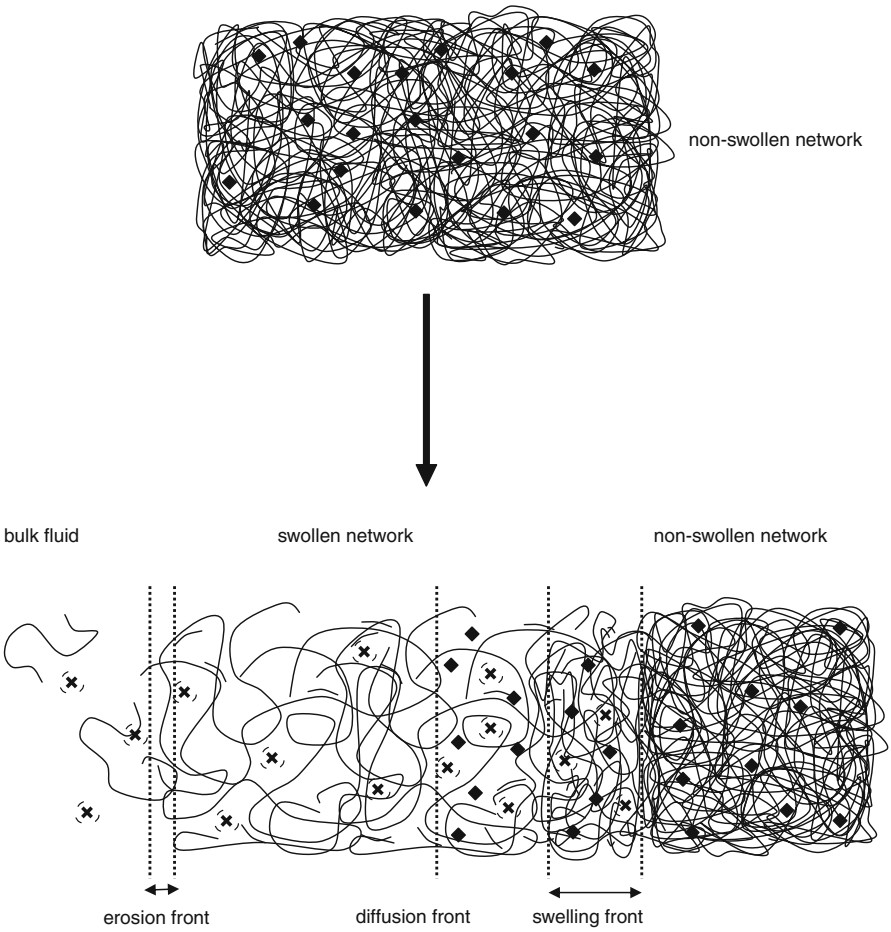


**Fig. 7.6** Schematic presentation of a drug-loaded, polymeric network in the nonswollen state (*top*) and upon liquid penetration into the system (*bottom*). The drug is present as solid particles (*black diamonds*, e.g., crystals or amorphous aggregates) and as dissolved molecules (*crosses*). An additional front can be distinguished: the diffusion front, separating the swollen network containing only dissolved drug and the swollen network containing dispersed and dissolved drug

## 7.4 Mechanistic Mathematical Theories

Different mathematical theories have been proposed to model drug release from swelling controlled drug delivery systems [11, 12]. An interesting early theory for polymeric tablets, considering: (1) water diffusion, (2) drug diffusion, (3) polymer swelling, (4) a moving swelling front, and (5) a moving "bulk fluid-tablet" front, was presented by Peppas et al. [13]. The model allows quantitative prediction of drug and water concentration–position profiles at arbitrary time points following exposure of a uniformly loaded, planar dosage form, with release occurring through

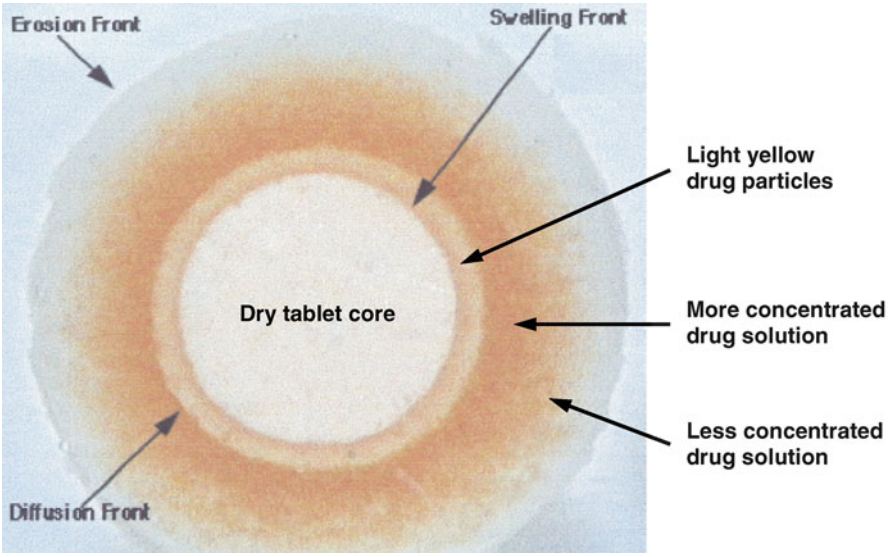


**Fig. 7.7** Photograph of an HPMC matrix tablet loaded with buflomedil pyridoxal phosphate upon a 4-h exposure to distilled water. The tablet was fixed between two Plexiglas disks; the ensemble was placed in a USP dissolution apparatus 2. Drug particles are *light yellow*; drug solutions are *orange* to *yellow* (with decreasing concentration). The use of this colored drug allows visualizing the positions of the swelling and diffusion fronts (indicated in the diagram). Adapted from ref. [10]

one planar face. Predictions were in good agreement with experimental results obtained with HPMC-based matrix tablets containing KCl as a model drug.

The experimental setup illustrated in Fig. 7.8 was used to expose tablets prepared by direct compression to a well stirred 0.1 N HCl bath at 37°C. Tablets were fixed in Plexiglas holders so that water penetration into the system and drug release out of the device were restricted to one surface only. At predetermined time points, tablets were removed, deep frozen, and cut in a microtome. The obtained 250 μm thick slices were analyzed for their water, polymer, and KCl content. Figure 7.8 shows an example for the experimentally determined composition of the swollen region of such tablets after a 5-h exposure to 0.1 N HCl (symbols). The "bulk fluid-tablet" interface is located on the left-hand side, and the still dry tablet region on the right-hand side. As can be seen, the water content steeply decreases from the tablet surface toward the dry tablet side (filled circles). In contrast, the KCl (filled squares) and HPMC (filled triangles) contents significantly increase in the swollen tablet region in the direction of the dry part of the system. The solid curves in Fig. 7.8 show the theoretically calculated water and KCl concentration–position profiles in the system at this time point. Good agreement between the theory and the experiments was obtained (symbols and solid curves in Fig. 7.8).

Later, Siepmann, and Peppas developed the so-called "sequential layer model" in order to quantify drug release from hydrophilic, cylindrical matrix tablets [14–17], taking into account the following phenomena.

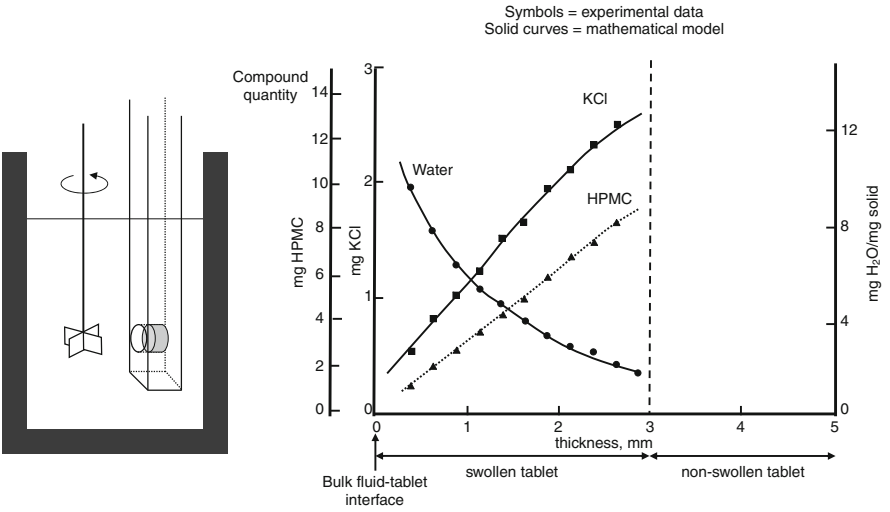


**Fig. 7.8** Experiment and theory: On the *left-hand side*, the experimental setup used by Peppas et al. [13] to monitor water and KCl transport in HPMC matrix tablets (fixed in a Plexiglas holder) is schematically illustrated. On the *right-hand side*, the experimentally measured water, HPMC, and KCl concentration–position profiles in the systems after a 5-h exposure to the release medium are shown as *symbols*. The *solid curves* show the theoretically calculated water and KCl profiles, according to their model. Adapted from ref. [13]

1. Upon exposure to the release medium, steep water concentration gradients are formed at the "bulk fluid-tablet" interface, resulting in water diffusion into the device. This mass transport step is described considering: (1) the exact geometry of the system; (2) axial and radial diffusion within the cylinders; and (3) significant dependence of the water diffusion coefficient on the degree of swelling of the polymeric network.
2. Due to the penetration of water into the tablet, the hydrophilic polymer HPMC swells, resulting in significant changes in the polymer and drug concentrations and in increasing system dimensions.
3. Upon contact with water, the drug dissolves and diffuses out of the tablet into the bulk fluid.
4. With increasing water content, the diffusion coefficient of the drug significantly increases.
5. In the case of drugs with limited water solubility, dissolved and nondissolved drug coexist within the tablet. Only dissolved drug is considered to be able to diffuse.
6. Given high initial drug loadings, the inner structure of the tablet significantly changes during drug release, becoming more porous and less restrictive for diffusional mass transport.
7. Depending on the chain length and degree of substitution of the hydrophilic polymer, the latter dissolves more or less rapidly.

The resulting set of partial differential equations is rather complex and no analytical solution can be derived. Instead, the model can be solved numerically, e.g., using finite differences. For details, the reader is referred to the literature [14, 18]. Briefly, derivatives are approximated by finite differences to simplify the equations. The introduced error is negligible if the considered time and position steps are sufficiently small. A standard personal computer can perform the required calculations very rapidly, when drug is initially homogeneously distributed within the tablet, since the system is then highly symmetric. Alternatively, finite element multiphysics platforms, such as COMSOL®, can be used to integrate model equations.

Figure 7.9a shows a schematic of a cylindrical tablet. Since drug is uniformly loaded and the system is cylindrically symmetric, there are no angular ($\theta$) gradients in concentration, and this coordinate can be neglected. It is, therefore, sufficient to calculate the changes in water, drug, and polymer concentration in the highlighted two-dimensional rectangle to describe the mass transport processes occurring in the upper half of the tablet (Fig. 7.9b). Due to the symmetry plane at $z = 0$, transport processes above and below this plane are "mirror images," so only $z \geq 0$ needs to be considered. In order to account for the swelling of the matrix, beginning at the interface with the bulk fluid, onion-like "sequential layers" are considered, as illustrated in Fig. 7.9c. Upon contact with water, the outermost tablet layer starts to swell. With time, water penetrates into the deeper tablet layers, which then swell. Polymer dissolution at the interface "tablet-release medium" is taken into account according to reptation theory [19]. The critical polymer concentration, below which macromolecular chain disentanglement from the network occurs, can be determined according to Ju et al. [20–22], as a function of the average polymer molecular weight: with increasing chain length, the degree of entanglement increases. Thus, higher water contents are required to induce macromolecular disentanglement and matrix dissolution. In other words, the polymer disentanglement concentration decreases with increasing polymer molecular weight, as illustrated in Fig. 7.10.

Radial and axial transport of water and drug in the cylindrical tablets are quantified according to Fick's second law of diffusion and taking into account time- and position-dependent diffusion coefficients [18]:

$$\frac{\partial c_k}{\partial t} = \frac{1}{r}\left\{\frac{\partial}{\partial r}\left(rD_k\frac{\partial c_k}{\partial r}\right) + \frac{\partial}{\partial z}\left(rD_k\frac{\partial c_k}{\partial z}\right)\right\}. \tag{7.5}$$

Here, $c_k$ and $D_k$ are the concentration and diffusion coefficient of the diffusing species ($k = 1$ for water, $k = 2$ for the drug), respectively; $r$ and $z$ represent the radial and axial coordinates, and $t$ denotes time. The dependence of the diffusivities on the water content of the system is considered using a Fujita type [23] relationship:

$$D_k = D_{k,\mathrm{crit}} \exp\left\{-\beta_k\left(1 - \frac{c_1}{c_{1\mathrm{crit}}}\right)\right\}, \tag{7.6}$$

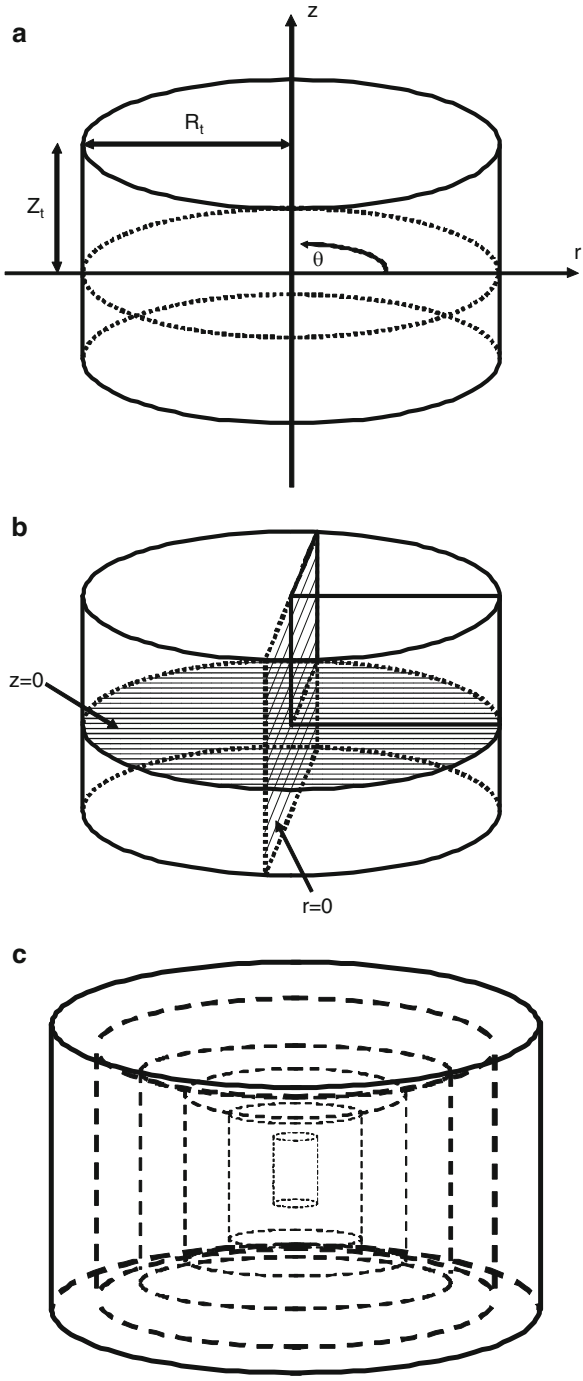


**Fig. 7.9** Schematic presentations of: (**a**) cylindrical HPMC tablet for mathematical analysis; (**b**) the symmetry planes, which can help to facilitate the mathematical modeling; and (**c**) the "sequential layer" structure considered in the mathematical theory proposed by Siepmann et al. [14]. Reprinted from ref. [14], with permission from Elsevier

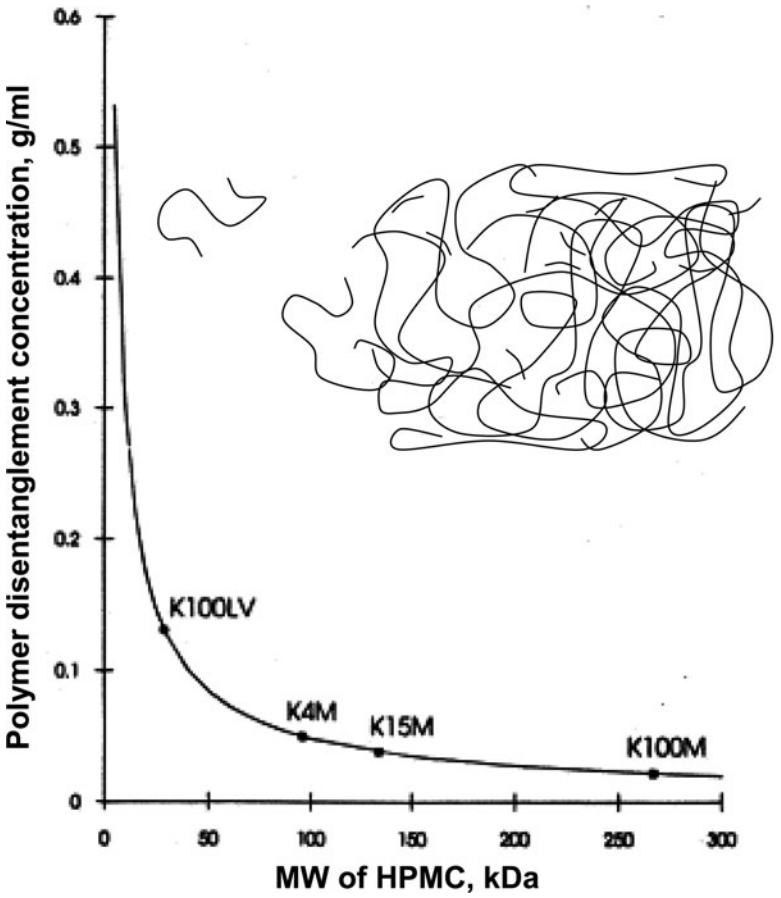


**Fig. 7.10** Dependence of the polymer disentanglement concentration (polymer concentration, below which polymer chain disentanglement starts) on the average polymer molecular weight of HPMC. The *symbols* represent experimentally measured results, obtained with commercially available products. Adapted from ref. [21]

where $\beta_1$ and $\beta_2$ are dimensionless constants characterizing the dependence of the water and drug diffusivity on the degree of tablet swelling; $D_{1,\text{crit}}$ and $D_{2,\text{crit}}$ are the diffusion coefficients of water and drug at the bulk fluid-tablet interface, where polymer chain disentanglement occurs. The model assumes that there is no volume contraction upon mixing of drug, polymer, and water so that the total volume of the system is given by the sum of the volumes of the single components at all time points. For the definition of the boundary conditions, the water concentration at the surface of the matrix, $c_{1\text{crit}}$, is calculated from the polymer disentanglement concentration [20, 21, 24–26], and the drug concentration at the surface of the tablet is assumed to be equal to zero (perfect sink condition). Due to the mirror image assumption, concentration gradients at $z = 0$ are taken to be zero.

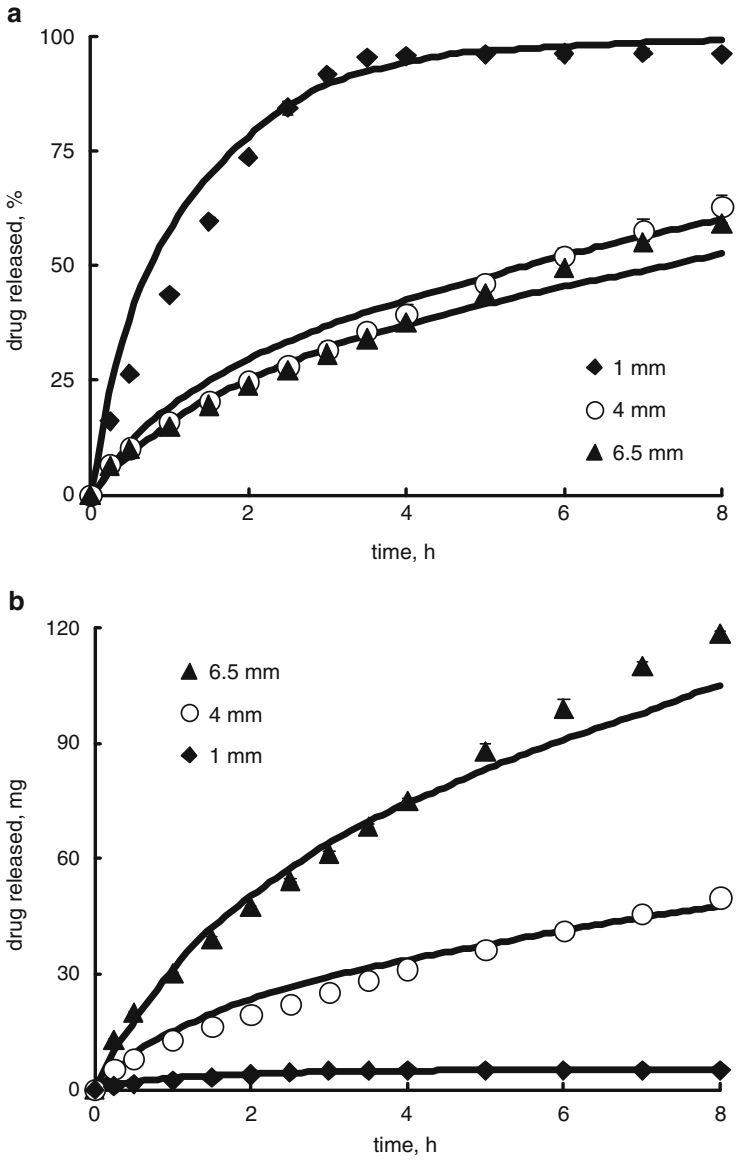


**Fig. 7.11** Mathematical modeling of drug release from HPMC matrix tablets: theoretical prediction (*curves*, calculated using the "sequential layer model") of the effects of varying the tablet radius on the: (**a**) *relative* amount of theophylline released, (**b**) *absolute* amount of theophylline released as a function of the exposure time to phosphate buffer, pH 7.4. The *symbols* represent the *independent* experimental results. The initial tablet height was 2.6 mm in all cases; the initial tablet radius was varied from 1 mm (*filled diamonds*) to 4 mm (*open circles*) to 6.5 mm (*filled triangles*). Reprinted from ref. [27], with permission from Elsevier

The sequential layer model has been shown to be applicable to different types of hydrophilic matrix tablets, enabling further insight into the underlying drug release mechanisms. The model also allows for the quantitative prediction of the effects of formulation parameters on the resulting drug release rate [27]. One example of such a prediction is illustrated in Fig. 7.11, in which the sequential layer model was used to predict the impact of varying the initial radius of HPMC-based matrix tablets loaded with 50% theophylline on the resulting drug release kinetics in phosphate buffer, pH 7.4. The curves show the theoretically predicted release profiles from tablets with an initial height of 2.6 mm. The tablet radius was varied from 1 to 6.5 mm, as indicated. The relative and absolute cumulative amounts of drug released are plotted as a function of exposure time to the release medium. Clearly, the initial radius had a pronounced effect on both types of release profiles. With increasing initial tablet radius, the relative surface area decreases, hence the relative release rate decreases. In contrast, the absolute surface area and absolute amount of drug available for diffusion increase, resulting in increased absolute drug release rate. These theoretical predictions were confirmed by independent experimental results (symbols in Fig. 7.11), demonstrating the validity and practical benefit of the theory.

Thus, this type of mechanistically realistic mathematical model, besides providing mechanistic insights, can also help to facilitate device optimization by simulating the effects of parameter variations in silico.

## References

1. Colombo P, Santi P, Siepmann J, Colombo G, Sonvico F, Rossi A, Strusi OL (2008) Swellable and rigid matrices: controlled release matrices with cellulose ethers. In: Augsburger LL, Hoag SW (eds) Pharmaceutical dosage forms: tablets, vol 2: rational design and formulation, 3rd edn. Informa Healthcare, New York
2. Chirico S, Dalmoro A, Lamberti G, Russo G, Titomanlio G (2007) Analysis and modeling of swelling and erosion behavior for pure HPMC tablet. J Control Rel 122:181–188
3. Viridén A, Larsson A, Wittgren B (2010) The effect of substitution pattern of HPMC on polymer release from matrix tablets. Int J Pharm 389:147–156
4. Williams HD, Ward R, Culy A, Hardy IJ, Melia CD (2010) Designing HPMC matrices with improved resistance to dissolved sugar. Int J Pharm 401:51–59
5. Escudero JJ, Ferrero C, Jimenez-Castellanos MR (2010) Compaction properties, drug release kinetics and fronts movement studies from matrices combining mixtures of swellable and inert polymers. II. Effect of HPMC with different degrees of methoxy/hydroxypropyl substitution. Int J Pharm 387:56–64
6. Baker RW, Lonsdale HK (1974) Controlled release: mechanisms and rates. In: Tanquary AC, Lacey RE (eds) Controlled release of biologically active agents. Plenum Press, New York
7. Korsmeyer RW, Peppas NA (1984) Solute and penetrant diffusion in swellable polymers. III. Drug release from glassy poly5HEMA-co-NVP copolymers. J Control Rel 1:89–98
8. Siepmann J, Peppas NA (2001) Modeling of drug release from delivery systems based on hydroxypropyl methylcellulose (HPMC). Adv Drug Deliv Rev 48:139–157
9. Noyes AA, Whitney WR (1897) Über die Auflösungsgeschwindigkeit von festen Stoffen in ihren eigenen Lösungen. Z Phys Chem 23:689–692

10. Colombo P, Bettini R, Peppas NA (1999) Observation of swelling process and diffusion front position during swelling in hydroxypropyl methyl cellulose (HPMC) matrices containing a soluble drug. J Control Rel 61:83–91
11. Siepmann J, Siepmann F (2008) Mathematical modeling of drug delivery. Int J Pharm 364:328–343
12. Kaunisto E, Marucci M, Borgquist P, Axelsson A (2011) Mechanistic modelling of drug release from polymer-coated and swelling and dissolving polymer matrix systems. Int J Pharm 418:54–77
13. Peppas NA, Gurny R, Doelker E, Buri P (1980) Modelling of drug diffusion through swellable polymeric systems. J Membr Sci 7:241–253
14. Siepmann J, Podual K, Sriwongjanya M, Peppas NA, Bodmeier R (1999) A new model describing the swelling and drug release kinetics from hydroxypropyl methylcellulose tablets. J Pharm Sci 88:65–72
15. Siepmann J, Kranz H, Bodmeier R, Peppas NA (1999) HPMC-matrices for controlled drug delivery: a new model combining diffusion, swelling and dissolution mechanisms and predicting the release kinetics. Pharm Res 16:1748–1756
16. Siepmann J, Kranz H, Peppas NA, Bodmeier R (2000) Calculation of the required size and shape of hydroxypropyl methylcellulose matrices to achieve desired drug release profiles. Int J Pharm 201:151–164
17. Siepmann J, Peppas NA (2000) Hydrophilic matrices for controlled drug delivery: an improved mathematical model to predict the resulting drug release kinetics (the "Sequential Layer" model). Pharm Res 17:1290–1298
18. Crank J (1975) The mathematics of diffusion. Clarendon Press, Oxford
19. De Gennes PG (1971) Reptation of a polymer chain in the presence of fixed obstacles. J Chem Phys 55:572–579
20. Ju RTC, Nixon PR, Patel MV (1995) Drug release from hydrophilic matrices. 1. New scaling laws for predicting polymer and drug release based on the polymer disentanglement concentration and the diffusion layer. J Pharm Sci 84:1455–1463
21. Ju RTC, Nixon PR, Patel MV, Tong DM (1995) Drug release from hydrophilic matrices. 2. A mathematical model based on the polymer disentanglement concentration and the diffusion layer. J Pharm Sci 84:1464–1477
22. Ju RTC, Nixon PR, Patel MV (1975) Diffusion coefficients of polymer chains in the diffusion layer adjacent to a swollen hydrophilic matrix. J Pharm Sci 86:1293–1298
23. Fujita H (1961) Diffusion in polymer-diluent systems. Fortschr Hochpolym Forsch 3:1–47
24. Narasimhan B, Peppas NA (1996) Disentanglement and reptation during dissolution of rubbery polymers. J Polym Sci Polym Phys 34:947–961
25. Narasimhan B, Peppas NA (1996) On the importance of chain reptation in models of dissolution of glassy polymers. Macromolecules 29:3283–3291
26. Narasimhan B, Peppas NA (1997) Molecular analysis of drug delivery systems controlled by dissolution of the polymer carrier. J Pharm Sci 86:297–304
27. Siepmann J, Streubel A, Peppas NA (2002) Understanding and predicting drug delivery from hydrophilic matrix tablets using the "sequential layer" model. Pharm Res 19:306–314

# Chapter 8
# Degradable Polymeric Carriers for Parenteral Controlled Drug Delivery

**C. Wischke and S.P. Schwendeman**

**Abstract** Drug loaded carriers from degradable polymers, namely, injectable microparticles, injectable in situ forming implants, and preformed implants, are established in the clinic for parenteral controlled drug delivery. This chapter provides an overview on several factors influencing release behavior such as drug properties, effects of environmental conditions, osmotically mediated mechanisms, and the selection of the carrier type. Moreover, degradation and erosion of the polymeric matrices are discussed in detail in view of their impact on drug release for different relevant polymer classes and groups of bioactive molecules. Additionally, carrier type-specific issues are included based on the knowledge gained to date from available parenteral controlled release products, as obtained from a comprehensive review of the scientific and patent literature. In particular, preparation techniques and related mechanisms, and both advantages and challenges associated with degradable polymer based delivery systems are described. Strategies to establish a continuous drug release are examined based on rational evaluation of specific polymer classes and carrier types.

C. Wischke (✉)
Department of Pharmaceutical Sciences, University of Michigan, 428 Church Street, Ann Arbor, MI 48109-1065, USA

*Present address*: Center for Biomaterial Development and Berlin-Brandenburg Center for Regenerative Therapies, Helmholtz-Zentrum Geesthacht, Kantstr. 55, 14513 Teltow, Germany
e-mail: christian.wischke@berlin.de

S.P. Schwendeman
Department of Pharmaceutical Sciences, University of Michigan, 428 Church Street, Ann Arbor, MI 48109-1065, USA

J. Siepmann et al. (eds.), *Fundamentals and Applications of Controlled Release Drug Delivery*, Advances in Delivery Science and Technology,
DOI 10.1007/978-1-4614-0881-9_8, © Controlled Release Society 2012

## 8.1 Introduction

Polymer-based controlled release formulations for parenteral administration are of ongoing academic and industrial interest. Microencapsulation concepts developed in the 1980s and 1990s of the last century [1] led to injectable particulate depot formulations, e.g., for leuprolide acetate (Lupron® Depot, Enantone®, Trenantone®) and goserelin acetate (Zoladex®) as peptide drugs, that are accepted standard therapies in the clinic. Preformed drug loaded implants can be injected subcutaneously or administered during surgery for a local drug release, e.g., carmustine loaded wafers (Gliadel®) in the treatment of glioblastoma, one of the most aggressive types of cancer. More recently, in situ forming implants have received US FDA approval and are available for treatment of prostate cancer with leuprolide (Eligard®) and of periodontal disease with doxycycline (Atridox®). Commercial success of such matrix polymer based drug delivery systems is expected to depend not only on their clinical performance in the respective therapeutic application but also on several other aspects such as the convenience of treatment for the patient and/or marketing strategies, to name only two.

Clinically, there is a clear trend toward therapies that would allow the body to regain full functionality, e.g., of damaged tissues. These regenerative therapies mostly are cell-based concepts; however, a prolonged local release of bioactive molecules including small chemical entities as well as more complex substances such as growth factors or chemokines may be desired and is addressed in present research [2, 3]. Additionally, also for the long-term treatment of chronical diseases, intense research activities can be expected in the pharmaceutical industry to provide controlled release formulations as successors of initial oral dosage forms. The motivation for such efforts may often be associated with product lifetime management and endeavors to extend the time of exclusive marketing. This may be possible when new intellectual property is generated by new controlled release formulations.

Independent from the motivation to sustain drug release, this goal can be achieved by embedding the drug into polymeric matrices, which govern the release rates of encapsulated drugs. These matrices typically consist of degradable polymers, which slowly degrade under physiological conditions and thus avoid accumulation of exhausted drug carriers in the body or the need of a second surgery for explantation. In this context, degradability is often a strong benefit in terms of patients' convenience, marketing, and hospitalization costs. Additionally, there are applications where therapeutic success is generally linked to the implant's capability to initially induce ingrowth of tissue and serve as a structural cell support, but subsequently degrade as required for full regeneration, e.g., tissue engineering scaffolds for critical bone defects [4]. However, degradation of the drug carrier results in dynamic alterations of polymer properties with substantial effects on the polymer's ability to retain embedded drugs in the matrix.

The term degradation (or biodegradation if driven by contributions of living cells) usually refers to a breakdown of polymers at the molecular level, i.e., chain cleavage that leads to degradation products that are safely eliminated by the body. By contrast, the term erosion refers to the process of polymer mass loss, which includes

not only degradation but several other processes, such as water uptake leading to microscopic or macroscopic changes of the structural integrity of the drug carrier and eventual removal of degraded or nondegraded material to the surrounding medium [5–7]. Erosion, typically initiated by degradation of medical implants, may follow different pathways and is typically of major relevance for drug release kinetics.

In principle, drug release from hydrophobic polymers can be controlled by diffusion and/or degradation of the matrix, typically by spontaneous hydrolysis. In addition, osmotically mediated mechanisms may be involved. In all cases, the uptake of distinct quantities of water into the matrix is required to enable drug diffusion and hydrolytic cleavage of polymer chains. For polymers with a higher water uptake that form gels in a physiological environment, swelling may control drug release rates. However, for many controlled release implants and particles from less hydrophilic polymers, the extent of water uptake is rather low. In this case, the type of erosion mechanism may largely depend on the involved rates of two mechanisms, water uptake and hydrolytic degradation, and which of them is dominating over the other.

While several additional aspects such as drug characteristics, matrix shape, and microstructure may impact drug release, a detailed understanding of the inherent properties of matrix polymers is required to design drug releasing particles or implants with the desired release rates. In this chapter, temporal controlled injectable and implantable delivery systems are reviewed, which involve degradation and erosion of the polymer matrix.

## 8.2 Factors Influencing Drug Release from Degradable Polymer Matrices

### *8.2.1 Overview*

A central goal in controlled drug delivery is to establish the desired release kinetics of a certain drug for a specific application. Several factors may affect drug release rates, and the most important aspects of these are summarized in Fig. 8.1. In general, factors controlling drug release behavior can be classified into two major groups, i.e., (1) physical processes and chemical/physicochemical molecular properties associated with the involved materials and (2) the environmental conditions as well as properties related to the engineered shape of the drug carrier. Importantly, stability of the bioactive compound under the conditions used for incorporation in the polymer matrix as well as in the microenvironment provided during release is the most important precondition, which is of relevance particularly for proteins [8–12]. Although each of these aspects is worth discussion in length, this chapter mainly focuses on the effects of polymer properties and degradation/erosion on controlled drug release. Other important parameters or processes that contribute to the release profile are only briefly mentioned in the following subsections.

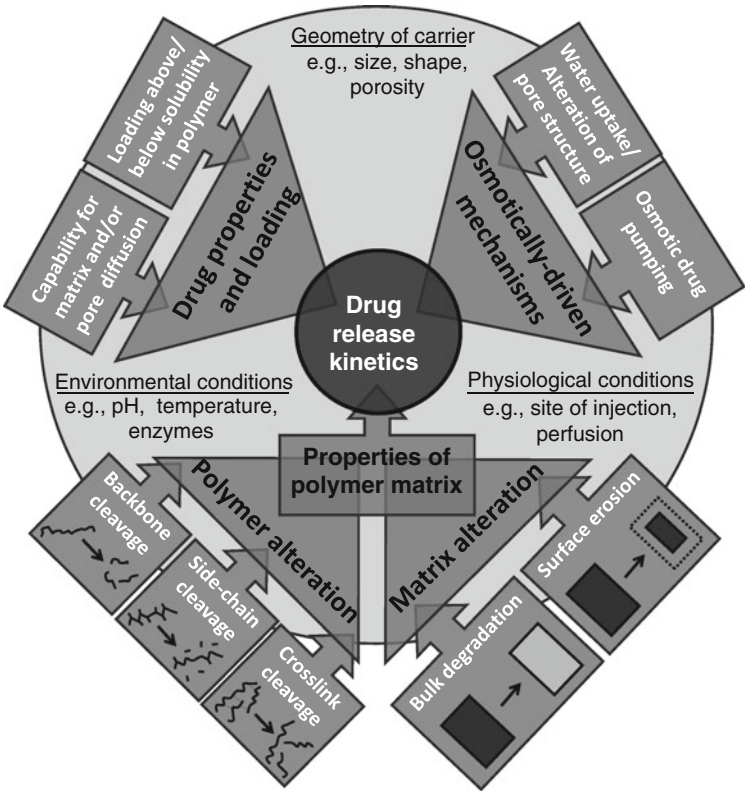


**Fig. 8.1** Scheme of major factors that may influence drug release rates from drug carriers based on degradable polymers

### *8.2.2 Indication and Required Release Rates Define Preferred Carrier Type*

At the starting point of any project aiming to design controlled release carriers, two things will typically be known – the drug and its clinical application. Against the background of the drug's pharmacokinetics (e.g., minimal effective concentration, clearance), the specific application will define several requirements such as (1) the desired release rates, duration of release and total dose, (2) the route of administration (e.g., sc, im, ip, or site of surgical placement), (3) type of drug carrier (e.g., particles or implants), (4) specific shapes or dimensions of the carrier (e.g., particle size distribution or shape of implants such as polymeric stents), and (5) other design criteria.

Depending on these application-dictated requirements, a specific drug carrier may be selected that fits the indication of interest, e.g., implant rods [13, 14] or injectable 20–100 μm microparticles as local drug depots [15, 16], phagocytozable

microparticles of 1–10 μm for vaccine targeting into antigen presenting cells [17, 18], nanoparticles of <200 nm for cancer therapy [19] hypothesized to accumulate in tumor tissue by the enhanced permeation and retention (EPR) effect [20], or even actively moving matrices such as self-anchoring implants [21–23].

Obviously, the three dimensional geometry of the carrier is of major importance. Larger diffusion lengths, such as present when increasing the diameter of spherical microparticles, often result in slower release, for low-molecular-weight hydrophobic drugs, as shown for unimodal microparticles of different sizes [24]. By contrast, release of large macromolecular drugs from PLGA implants has shown surprisingly little device size dependence [25]. Macroscopic implants such as rods can be expected to show substantially different release by drug diffusion when the aspect ratio of implant length and diameter is altered. Moreover, a porous ultrastructure of the polymeric matrix may enable diffusion through macro- or micropores at much higher rates than through a dense matrix.

### *8.2.3 Effect of Environmental Conditions on Release*

The drug release rates that finally can be realized from a specific carrier are largely affected by environmental or physiological conditions, drug physicochemical properties, matrix ultrastructure and shape, contributions of osmotically driven mechanisms, and, importantly, biodegradation and erosion pathways of the polymeric matrix. While release assays may not in all cases be designed to fully display in vivo conditions, modifications in experimental conditions certainly can alter drug release. Typically, standard conditions will be at 37°C in a suitable buffer at physiological pH value. However, particularly for hydrophobic drugs with low solubility, the set up of the assay, the volume of release medium, the presence of solubilizing surfactants, and the intensity of agitation may play a significant role [16]. Also, alterations of microparticle mass per volume of release medium changed release rates in selected cases indirectly due to an accumulation of degradation products and pH drop in the bulk fluid when studying suspension concentrations in the typically employed range [26].

Physiological or pathological environmental conditions during in vivo studies may sometimes result in a faster drug release than in vitro, e.g. due to the presence of enzymes, which in some cases are known accelerators of polymer degradation [27]. Such enzymes or alternative substances that catalyze polymer breakdown [28] or plasticize the matrix polymer may be included in in vitro studies. However, besides single catalytic substances that could be employed in release assays, polymeric drug carriers may additionally be faced with a complex interplay of immune cells and soluble factors when exposed to a physiological environment in vivo. Additionally, different injection sites may provide substantial differences in environmental conditions such as blood perfusion, capillary distances, or interstitial fluid volumes, which potentially lead to intra- and interindividual alterations in drug release rates.

### 8.2.4 Impact of Drug Properties

The physicochemical properties of the drug molecules are another key factor when discussing release rates. For example, low solubility drugs are typically characterized by lower diffusion rates due to a lower concentration gradient of the drug from the inside to the outside the matrix. The diffusion of encapsulated substances may also depend strongly on the drugs' hydrodynamic radii, or more simply, their molecular weights. Diffusion mechanisms of molecules encapsulated in a polymer matrix include jumps between cavities in the free volume of the polymer and movements of these cavities due to wriggling of polymer chains in a rubbery or swollen state [29]. Large substances such as proteins do often not show release by diffusion through a dense, nonporous polymer matrix. This is because proteins do not generally partition in the polymer phase and because their molecular size may be substantially larger than the physically entangled mesh of the matrix polymer.

Noncovalent binding between drug and polymer may reduce release rates or cause incomplete release until complete erosion of the polymer. For example, hydrophobic moieties of drug and polymer may interact by hydrophobic binding. Basic drugs that possess ionizable amine groups may undergo ionic interactions with carboxyl functions that are initially present or emerge from polymer degradation. Besides, as discussed later, drug molecules may interact by different pathways with the polymer degradation.

### 8.2.5 Contributions of Osmotically Mediated Mechanisms

Although thematically overlapping with certain aspects of what has briefly been summarized above, osmotically driven mechanisms are major contributors to drug release profiles. In the polymer matrix, osmotic pressure builds up by encapsulated highly water-soluble compounds, resulting in water influx. Such water penetration through the polymer phase and/or pore network can result in rupture of pore walls for rapid release out of the polymer and/or release by osmotic convective mass transfer. Osmotically active substances may not only be hydrophilic drug molecules, but also several types of excipients. For instance, this includes salts, polyols, or sugars commonly used to shield therapeutic proteins from interfaces during microencapsulation and release, to act as cryo- or lyoprotectors, to enhance microviscosity, or to modify the particle microstructure [8–12, 16].

For some matrix polymers, particularly those with a substantial degree of swelling, water uptake into the polymer phase potentially increases the overall diameter of the drug carrier. At the same time, along with the swelling of the polymer phase of a porous matrix, polymer free drug loaded micropores and cavities may lose some of their volume after being occupied by swollen polymer. As an example from commonly used PLGA materials, free carboxyl end groups and low molecular weight promote water uptake. Therefore, on the one hand, swelling of the matrix

material could facilitate movement of dissolved drug out of large interconnective pores. Also, a higher swellability of the particle core compared to the shell may result in osmotically driven breakage of the particles. This was shown for microparticles prepared in a two step procedure with coating of water soluble polymers with nonsoluble PLGA [30] as well as for phase segregated microparticles as obtained by blending immiscible polymers with different hydrophilicities and molecular weights [31, 32]. On the other hand, substantial swelling that first occurs at the particle surface may lead to closure of micropores and a swelling-controlled release mechanism from polymer matrices of relative hydrophilicity.

Recently, attention has been drawn to a mechanism that affects drug release from amorphous polymers with a glass transition in the range of body temperature – the pore closing mechanism [33, 34]. Such polymers such as PLGA, at least after the onset of degradation and/or plastification in an aqueous environment, show self-healing phenomena. Among other preconditions [35, 36], chain mobility and polymer interdiffusion is required to take place at relevant rates for self healing, which can be the case when exceeding the glass transition temperature $T_g$ of linear, physically entangled polymers. Also, prone from plasticization by water after immersing the polymer into the release medium, $T_g$ reduction to physiological temperature is a major contributor. As a consequence, initially rough macroporous particle surfaces can become smooth in the first days of incubation, which is linked to a reduced drug diffusion and possibly the end of the initial release period [33, 37].

Moreover, polymer properties have a very important impact on drug release rates from degradable matrices. This includes several aspects, e.g. polymer hydrophilicity/hydrophobicity, drug–polymer interactions, polymer mesh width and drug diffusibility, polymer morphology and physical state, and, importantly, the polymer degradation and erosion behavior.

## 8.3 Principles of Polymer Degradation and Erosion

### *8.3.1 Principles of Polymer Degradation*

The degradation, i.e., the molecular breakdown of polymers is governed by both their chemical composition, architecture and morphology as well as a complex interplay of environmental conditions and device properties. For example, in hydrolytically degrading (co)polymers, the uptake of water into the matrix is an essential precondition for chain cleavage and is affected by the matrix hydrophilicity as a function, e.g., of the type of monomer, comonomer mixture, and end-capping. Moreover, for semicrystalline polymers water uptake and degradation preferentially occurs in amorphous domains which are less organized and show higher water and drug diffusivities. This makes polymer crystallinity a decisive matter also in terms of drug release. Additionally, several other aspects influence water uptake of produced devices such as the temperature, the matrix porosity, or the incorporation of substances like drugs or additives with distinct capacities for inducing osmotic pressure.

In principle, three concepts of polymer degradation with relevance for controlled drug release can be differentiated [38]. First, linear polymers as most often used for controlled drug release matrices can degrade into mono- or oligomers by random or selective scission of bonds in the polymer main chain (Fig. 8.1). All commercialized drug loaded implants and microparticle products based on polyesters or polyanhydrides follow this pathway. Second, linear polymers may contain side chains that, after cleavage, convert into hydrophilic or charged groups attached to the polymer backbone, which enable aqueous solubility of the polymer. Besides other pathways [39, 40], this mechanism is discussed as the major pathway in polyalkylcyanoacrylate degradation in vivo [41–43]. Third, polymer networks may disintegrate into water-soluble linear polymer chains by selective degradation of netpoints. Polyacrylate-based networks crosslinked with hydrolytically cleavable copolyester segments are examples for hydrophobic matrices following this principle [44]. Additionally, alginate hydrogels with ionic crosslinking [45], modified gelatin with weak covalent crosslinks [46], or poly(ethylene glycol) hydrogels crosslinked by enzyme sensitive peptides [47] are other examples for this principle. However, hydrogel matrices with high diffusion rates for small molecular drugs may not in all cases be useful for a prolonged drug release without additional modifications.

Besides the overall chemical composition, the sequence structure of copolymers can substantially influence the polymer degradation. This is particularly true when bonds associated with certain monomers in copolymers undergo faster degradation than others, i.e., they represent weak links. When these weak links are arranged in distinct blocks in the polymer chain, selective degradation of such blocks will occur first. Mass loss and complete erosion of such block copolymer samples in aqueous media may be substantially slower than in the case of copolymers with a random distribution of the weak links, where possibly shorter chains are produced from initial degradation. Typical examples for weak links are glycolide–glycolide diads in lactide–glycolide copolymers, which are more sensitive for hydrolytic degradation [48, 49]. In block copolymers with poly(ε-caprolactone) (PCL) and poly(p-dioxanone) (PPDO) segments, PCL blocks were shown to be weak links in the presence of enzymes as relevant for in vivo conditions [27].

The three dimensional architecture of the polymer molecules should also be taken into account when discussing degradation properties. While mostly linear polymers are synthesized by using mono- or possibly bifunctional starter molecules, star shaped or branched polymers can be obtained when employing starter molecules with three or more reactive moieties. One example with relevance in the field of controlled release is glucose-PLGA, which bears multiple chains of lactide–glycolide on a central glucose molecule. Typically, a faster degradation and mass loss can be observed for branched compared to linear polymers of a similar molecular weight (Fig. 8.2). This was suggested to advantageously contribute to the aim of a continuous release of encapsulated drugs by reducing intermediate “lag” phases of low release [50, 51]. A faster degradation of branched molecules may be explained by a faster gain of the critical oligomer size for aqueous solubility due to the shorter initial length of each arm. Another theoretical explanation, i.e. a higher water uptake due to a larger number of hydrophilic end groups, could not be

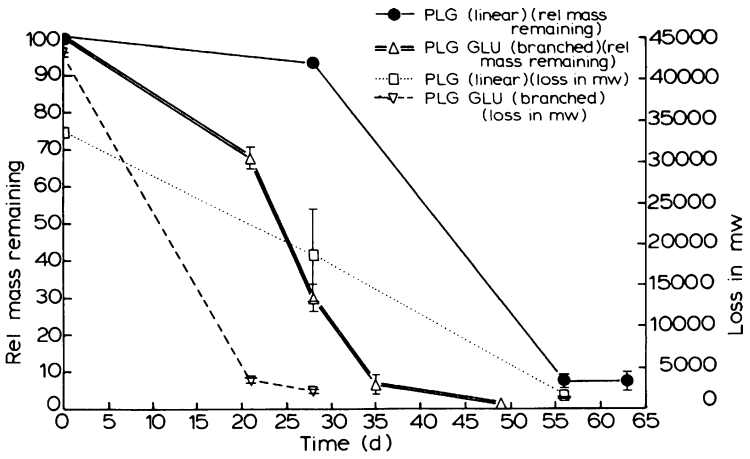


**Fig. 8.2** Impact of architecture of 55:45 PLGA on polymer in vivo degradation behavior in rats. Comparison of relative mass loss (*left ordinate*) and decrease in molecular weight (*right ordinate*) for linear PLGA and star-shaped glucose-PLGA. Figure reprinted from [51], Copyright 1991, with permission from Elsevier

confirmed [51], since free carboxyl groups of linear PLGA appear to attract more water than hydroxyl terminated branched PLGA. Besides, it may be hypothesized on whether there is a larger polymer free volume in branched PLGA because of a limited packing density of the arms. In this case, a higher diffusivities for water and other substances might occur, which possibly may facilitate degradation.

In contrast to small molecule or protein drugs with a defined chemical structure and molecular weight, polymers synthetically obtained by macromolecular chemistry are characterized by a certain distribution of molecular weights. The polydispersity (PD) as calculated by dividing the weight average molecular weight $M_w$ by the number average molecular weight $M_n$ serves as a measure to describe the molecular weight distribution and the content of low molecular weight components. Preferentially, the PD is in the range of 1.2–2.5 for uniform chain lengths [52]. When polymer chains with a lower degree of polymerization are present in mixture with high molecular weight polymers, the short chains at identical degradation rates statistically reach faster the critical molecular weight for aqueous solubility of oligomers. Thus, microvoids are created in the matrix, which enhance the water uptake. In addition, the oligomers may act as catalysts for degradation, and can result in an overall faster and/or inhomogeneous degradation of the entire matrix.

Depending on the matrix size, average diffusion pathlengths for polymer degradation products out of the matrix can differ by orders of magnitude. Autocatalytic activity of acidic polymer degradation products trapped inside the matrix is a common observation for polyester materials [53, 54]. While a pH drop due to accumulation of these acidic degradation products has also been observed for very small microparticles [55], this effect is typically more pronounced for larger matrices.

Such accumulation of catalytic polymer degradation products can result in different local degradation rates at different spatial positions of polymeric implants [48, 56–58], which determine the overall erosion characteristics of the sample.

### 8.3.2 Principles of Erosion Triggering Mass Loss

Polymer erosion, i.e., the release of degraded or nondegraded polymeric material, resulting in mass loss of the sample, may in principle derive from degradation induced by exposure to different factors including, e.g., heat, light, or oxidative stress. However, physiologic triggers such as spontaneous hydrolysis in an aqueous environment or enzyme and cellular attacks may be the most common pathways for polymers designed for medical applications. For polymer erosion that relies on aqueous hydrolysis, four different steps can be differentiated, i.e., (1) wetting of the polymer surface including a possible internal porous structure, (2) water uptake with a material-specific rate into the polymer bulk, (3) degradation of the polymer following a characteristic pathway with a material- and possibly geometry dependent rate, and (4) if possible, diffusion controlled removal of degradation products. A major aspect in this context is the speed and extent of water uptake compared to the degradation rate and water consumption during hydrolysis [59, 60].

On the one hand, diffusion of water into the matrix may take place at very low rates and, if exceeded by the degradation rate of the polymer, the combination of both leads to a surface-erosion mechanism of the drug carrier. In such a strictly surface-eroding material, the water uptake into the bulk will be low. The average molecular weight of the polymer sample remains high over a long period of time due to nonattacked polymer in the matrix core, while the device mass decreases continuously.

On the other hand, there is the predominantly used group of bulk degrading polymers for controlled release matrices, e.g., copolymers synthesized from dilactides and diglycolide (PLGA). In these materials, water uptake is most commonly faster than biodegradation. This means that degradation is not confined to the matrix surface but rather the entire polymer matrix is subjected to degradation at the same time. This is typically reflected in a decrease of the average molecular weight of the matrix without major initial mass loss, followed by a fast mass loss once the polymer degradation products in the matrix core reach a critical chain length (Fig. 8.3). Owing to osmotic activity of the degradation products and increased hydrophilicity of the polymer as the molecular weight decreases, the water uptake into the bulk may increase over time [61, 62].

When devices are characterized by a geometry and/or microstructure that allows easy diffusion of degradation products out of the matrix, the decrease of molecular weight during bulk degradation may be homogeneous throughout the matrix [63, 64]. However, mostly this is not the case for bulk degrading materials, particularly for larger sized implants [48, 56]. This is well known to be initiated by an accumulation of degradation products [53], which autocatalyze degradation and lead to a heterogeneous bulk degradation.

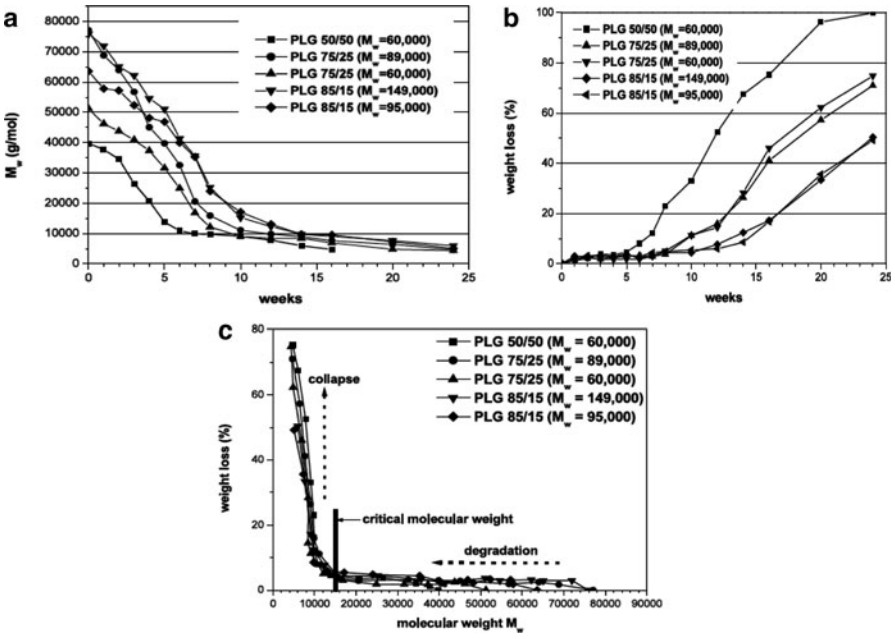


**Fig. 8.3** Typical pattern of bulk degrading materials consisting of the following stages: (1) hydration of the polymer matrix (data not shown), (2) decrease in average molecular weight (panel **a**) without major mass loss (panel **b**), and (3) collapse of the bulk eroding matrix with massive mass loss upon degradation to critical molecular weight (panel **c**; also see discussion in the text). Data for PLGA microparticles. Figures reprinted from [62], Copyright 2002, with permission from Elsevier

The critical molecular weight at which mass loss occurs was found to be 10–25 kDa for PLGA in some studies [62]. However, others reported much lower values such as 4 kDa [65] to be the critical PLGA molecular weight. When analyzing the aqueous solubility of 1 kDa PLGA oligomers (~14-mers; no PD reported), only ~70% dissolved in distilled water [66], suggesting that significant solubility may be achieved only for rather short oligomers. This is in line with data from the degradation of poly(D,L-lactide), where aqueous solubility was only observed for a degree of polymerization lower than 8 [67]. In this context, it is important to consider (1) differences in the analytical techniques to determine average molecular weights (relative values as calculated compared e.g. to polystyrene standards vs. the absolute values as obtained by multidetector GPC), (2) the polydispersity, PD, of the polymer, (3) the solubility of the endcapping moiety, and (4) that discussing $M_n$ values might be more relevant in view of the initiation of matrix mass loss by aqueous solubility of degradation products (the cited studies typically providing only relative $M_w$).

Since the matrix degradation/erosion pathway depends on several factors such as the water uptake rate, degradation rate, and matrix dimensions, different erosion profiles may be observed for one material when changing, e.g., environmental conditions or matrix dimensions. For instance, incorporation of acidic substances

into the matrix acting as catalysts can increase the degradation rate, thus changing degradation pattern and drug release to a surface erosion controlled mechanism for certain polymers [68]. Also, in principle, classically bulk eroding polyester materials such as PLGA may be surface eroding when the matrix dimensions are dramatically increased or the rate constant of degradation rises strongly by changing to a highly basic pH. Similarly, classically surface eroding materials may become bulk eroding when the matrix dimensions are reduced below a critical length scale [59, 60, 69]. However, limitations in the therapeutically suitable sizes of drug carriers and in vivo environmental conditions may not allow free alteration of the erosion behavior of a given polymer by these strategies. Therefore, careful selection of polymer properties, including building blocks and matrix characteristics, remains the most feasible strategies to tailor polymer degradation/erosion and drug release.

It is important to stress again that the degradation/erosion pathway of hydrolytically degradable materials is not necessarily an irrevocable consequence of the employed linkages between the building blocks such as ester bonds. On the contrary, in pure water the mechanism depends on water uptake and degradation rates. Recently published reports indicate that surface erosion can be realized for polyesters when the water uptake rates are reduced by erasing the relative hydrophilicity of polyesters. In order to do so, hydrophobic alkanediol starter molecules were used to first synthesize polyester macrodiols, which subsequently were linked together with hydrophobic diacids [70]. Similar effects might possibly be observed when coencapsulating hydrophobic additives in the matrix.

As described above, the degradation/erosion pathway can also be a function of environmental conditions [59], which include in vivo the presence of enzymes and cells. For PLGA, a spontaneous hydrolysis is assumed to be rate limiting. However, occasionally observed higher degradation rates in vivo are repeatedly assigned to enzymatic catalysis [71, 72], but may also be based on other factors, e.g. inflammatory cell/tissue responses or plasticization of the polymer by molecules present in vivo. At least for poly(L-lactide), there are some reports on enzymatic acceleration of polymer degradation [73]. Also, for other polyesters or copolyesters that include ε-caprolactone as building blocks, an enzymatically catalyzed surface erosion was observed [74, 75].

### *8.3.3 Drug Effects on Polymer Degradation*

The incorporation of any substances including drugs into a polymer matrix may change the polymers degradation behavior. This is very obvious in the case of embedded highly soluble drugs or additives of similar properties, which may change the osmotic pressure in the matrix and increase water uptake. Accordingly, an increased catalytic degradation of PLGA implants was observed depending on the loading with a water-soluble *N*-acetyl cysteine, which enhanced water uptake. Additionally, the free carboxyl groups of the drug may have contributed to polymer degradation by acidic catalysis [76]. Moreover, water uptake resulted in a $T_g$

reduction, i.e., plasticization with increased chain flexibility and in turn higher water and drug diffusion coefficients.

For basic drugs, e.g., thioridazine, an amine catalyzed hydrolysis of the polymer matrix during the particle preparation and a faster release were observed, which could be reduced by performing the o/w emulsification at lower temperatures or erasing the drug's basicity by the formation of salts [77, 78]. Similarly, drug induced PLGA degradation could be overcome for basic metoclopramide by using its salt form for the preparation of in situ implants [78]. In another study with different amine drugs molecularly dispersed in poly(lactic acid) (PLA), it was shown that an accelerated release correlated well with the ability of the drug to catalyze the polymer degradation, but not with the $T_g$ reduction, the drug's $pK_a$, or the drug's octanol–water partition coefficient [79, 80].

Another drug, namely, haloperidol, was suggested to change the type of matrix erosion from bulk-to surface erosion [81]. It is interesting to speculate as to whether high loading of the hydrophobic drug may have altered the water uptake and, as a consequence, slowed down polymer degradation in the matrix core.

## 8.4 Drug Release Characteristics of Degradable Polymeric Carriers

### *8.4.1 Polymers in Commercial Parenteral Drug Delivery Products*

A summary of commercial controlled drug release products for parenteral administration that are based on degradable polymer matrices is provided in Table 8.1. The employed carrier strategies include microparticles, preformed implants, and in situ forming implants. Importantly, in all but one of the so far commercialized products, PLA/PLGA is used as matrix polymer. This can be explained from a historical point of view, since there was substantial experience with PLA/PLGA as suture material when research on controlled release implants and microparticles was initiated. However, the approval of at least one non-PLA/PLGA product indicates that regulatory requirements and economic aspects can both be fulfilled when introducing new degradable polymers for use in humans. Also, there are significant efforts to get to the market an injectable viscous poly(ortho ester). This viscous mixture consists of ~6 kDa polymer, drug, and 550 kDa methoxy poly (ethylene glycole) to further reduce the viscosity [82]. Progress toward commercialization of this material can be seen from a recently completed Phase III study on APF 530 (granisetrone) for the prevention of nausea and vomiting in patients receiving chemotherapy [83] and the submitted new drug application for subcutaneously injected APF 530, a serotonin antagonist specifically binding to 5-$HT_3$ receptors [84].

**Table 8.1** Degradable controlled release products for parenteral administration

| Drug | Product | Indication | Matrix polymer | References |
|---|---|---|---|---|
| *Microparticles* | | | | |
| Octreotide | Sandostatin LAR® Depot | Acromegaly; diarrhea associated with metastatic carcinoid tumors; diarrhea associated with Vasoactive intestinal peptide secreting tumors | PLGA-glucose | [51, 104, 218–222] |
| Lanreotide acetate | Somatuline® LA | Acromegaly; thyrotropic adenomas; neuroendocrinic tumors | PLGA | [223] |
| Leuprolide acetate | Enantone®/ Trenantone® (Europe) Lupron Depot® (USA) Prostap® (GB) | Prostate cancer; endometriosis; uterine fibroids; central precocious puberty[a] | PLGA/PLA | [1, 93, 110, 215, 224–231] |
| Triptorelin acetate | Decapeptyl®, Gonapeptyl® | Prostate cancer; endometriosis; uterine fibroids; central precocious puberty[a] | PLGA | [232–234] |
| Triptorelin pamoate | Trelstar™ Depot | Prostate cancer; endometriosis; uterine fibroids; central precocious puberty[a] | PLGA | [235, 236] |
| Triptorelin embonate | Pamorelin® | Prostate cancer; endometriosis; uterine fibroids; central precocious puberty[a] | PLGA | Not available |
| Buserelin acetate | Suprecur® MP | Endometriosis, uterine myoma | PLGA | [103] |
| Naltrexone | Vivitrol® | Alcohol dependence | 75:25 PLGA | [98, 237] |
| Risperidone | Risperdal® Consta® | Schizophrenia | 75:25 PLGA | [238–243] |
| Minocycline hydrochloride | Arestin® | Peridontal disease | PLGA | [244] |
| Exenatide | Exenatide Once Weekly[b] | Type 2 diabetes | PLGA | [245, 246] |

| | | | | |
|---|---|---|---|---|
| *Preformed implants* | | | | |
| Buserelin acetate | Profact® Depot | Prostate cancer | 75:25 PLGA | [132, 247–250] |
| Goserelin acetate | Zoladex® | Prostate cancer, | 50:50 PLGA | [61] |
| Carmustin | Gliadel® | Brain tumors (glioblastoma) | 20:80 Poly[1,3-bis(*p*-carboxyphenoxy) propane-*co*-sebacic acid], p(CPP-SA), (Polifeprosan 20) | [117, 134, 135, 137, 138, 251, 252] |
| *In situ forming implants* | | | | |
| Doxycycline | Atridox® | Peridontal disease | PLA | [158, 159, 198, 199, 253] |
| Leuprolide acetate | Eligard® | Prostate cancer | PLGA[c] | [158, 159, 170, 187, 197, 254–258] |

[a]Approved indications may differ depending on the respective product and approving country
[b]Approval pending
[c]Employed PLGA comonomer ratios differ (1 Month: 50:50 PLGA, 7.5 mg drug; 3 months: 75:25 PLGA, 22.5 mg drug; 6 months 85:15, 45 mg drug)

Obviously, the largest number of degradable parenteral controlled release products are based on microparticles as drug carriers. Beneficial aspects of microparticles as drug depots compared to preformed implants include their injectability through needles of smaller diameters as well as the advantages of all multiple unit dosage forms, i.e., a possibly better average reproducibility of their properties. As an alternative delivery concept that benefits from an easy injectability along with a simple preparation procedure, in situ forming implants have received market approval for multiple products. In situ implants are formed in the tissue after injection, mostly due to polymer precipitation from organic solutions as recently summarized [16, 85, 86].

Besides preformed implants in the classical rod-like shape with the single functionality to act as drug depot, processing of drug loaded degradable polymers into advanced shapes may open new fields of application that combine drug release and a supporting function. Particularly the stent technology for the treatment of coronary artery diseases is demanding such degradable material concepts [87]. Therefore, there are some approaches in preclinical or early clinical research toward stents that are solely based on degradable polymers [88] such as PLA, poly(anhydride esters) [89, 90], tyrosine derived polycarbonates [90, 91], or shape-memory polymers [92].

## *8.4.2 Microparticles*

### 8.4.2.1 Microencapsulation Techniques

Parenteral administration of microparticles into a tissue require injectability through standard needles. Therefore, particle sizes below 100 μm are typically preferred. Smaller particles below 10 μm can be subject to phagocytosis and immunological processing. Thus, such small particles may be undesired for sustained release formulations as local depots unless antigen presenting cell targeting is desired. The employed microencapsulation technique can largely affect the particle properties such as the morphology, which may be capsular, multivesicular, or monolithic.

A summary of the most commonly employed microencapsulation techniques is provided in Fig. 8.4. Out of these methods, emulsion techniques are most often used at least in the laboratory scale due to their versatility in adaption for drugs of different physicochemical properties. Water soluble compounds that exhibit no major solubility in carrier solvents such as methylene chloride or ethyl acetate can be dispersed in the polymer phase as an aqueous drug solution. This $w_1/o$ emulsion is subsequently dispersed in an external aqueous phase resulting in a $w_1/o/w_2$ emulsion, where the o-phase solvent is removed by extraction/evaporation. This technique was mainly advanced in the development of Lupron Depot® for a peptide drug [1, 93] (see Table 8.1). It may result in multivesicular or capsular morphology and is useful also for other water-soluble compounds including proteins. However, molecules such as proteins, which may be more critical due to physical or chemical instabilities in the dissolved state during emulsification [8], may benefit from

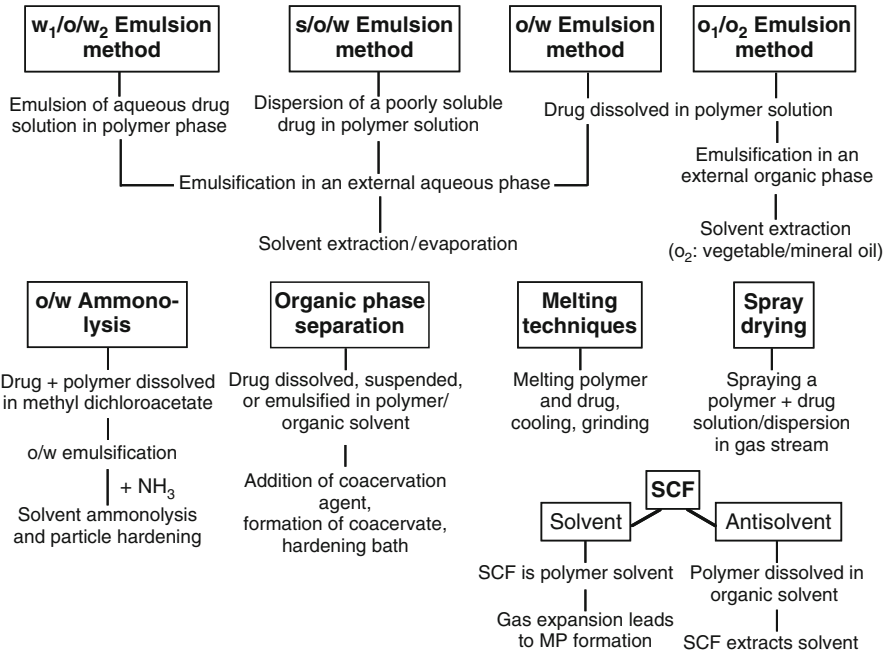


**Fig. 8.4** Summary of the principles of the most common techniques for the microencapsulation of drugs (*SCF* supercritical fluids, *MP* microparticle). Modified figure adapted from [16], Copyright 2008, with permission from Elsevier

alternative techniques that avoid the exposure of dissolved drug to physical or chemical stress. This was realized by encapsulation methods, where solid compounds are suspended in the polymer phase. This suspension may then be dispersed in an external aqueous phase (s/o/w technique) [94], an external oil phase (s/o/o technique) [95], or subjected to spray drying or spray congealing methods [96].

Drugs that dissolve well in polymer solutions can be embedded into microparticles by even more techniques. For those molecules that show poor aqueous solubility, the most easy microencapsulation methods involve o/w emulsions of a drug–polymer solution in an aqueous continuous phase [97] such as industrially used for the preparation of Vivitrol® [98]. Also, the o/w ammonolysis technique [99] may be suitable in selected cases. Possible leakage of drugs with higher solubility in to external aqueous phases may be overcome by $o_1/o_2$ emulsion methods [100], spray drying [101], or organic phase separation techniques [102]. Some of these techniques are also used for hydrophilic molecules such as peptides. For example, buserelin acetate was loaded in Supracur MP® by spray drying [103] and coacervation techniques were used to manufacture octreotide loaded Sandostatin LAR® Depot [104, 105]. Drugs that are compatible with a molten polymer may be molecularly distributed and, after solidification of the polymer, ground into drug-loaded particles [106]. Also, the solvent or antisolvent properties of supercritical fluids for polymers were suggested to be used in microencapsulation processes [107]. A more comprehensive summary of all preparation techniques has been given recently [16].

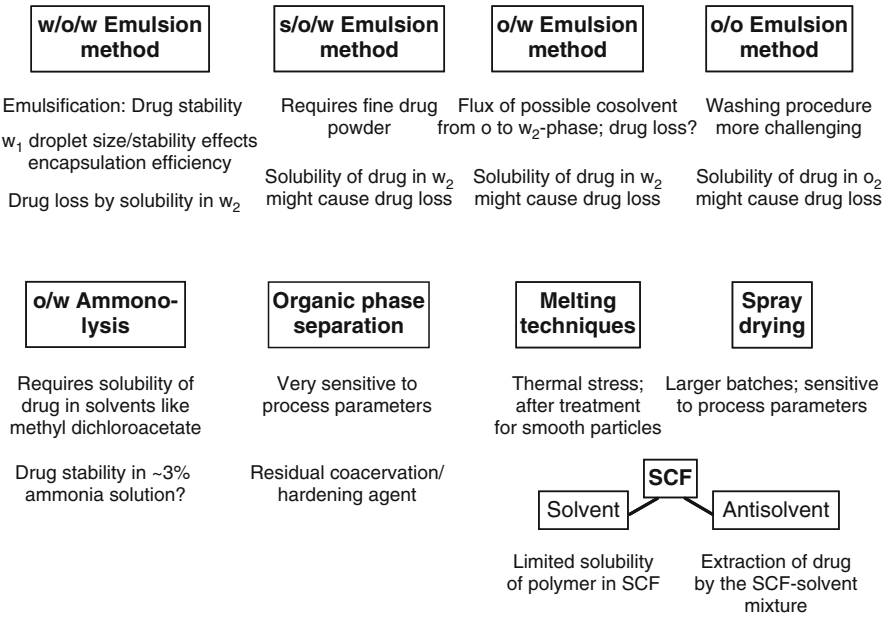


**Fig. 8.5** Selected challenges commonly associated with specific encapsulation techniques (*SCF* supercritical fluids). Modified figure adapted from [16], Copyright 2008, with permission from Elsevier

Obviously, there is no microencapsulation technique that will be likewise suitable for all types of drugs and polymers. Some very common challenges of the different methods are briefly summarized in Fig. 8.5. Generally, emulsion methods are faced with issues of solubility and distribution of drugs and solvents between the different employed phases. As drug solubility in the continuous phase may result in drug loss and poor encapsulation efficiencies, proper selection of the dispersion medium including analysis of solubilization by the employed stabilizer (s) is essential to obtain high encapsulation efficiencies. Moreover, due to a limited, but still relevant solubility of polymer solvents in the continuous phase, drugs dissolved in that solvent (e.g., o/w and $o_1/o_2$ techniques) may follow the solvent flux and distribute into the continuous phase. Additionally, organic phase separation techniques are frequently faced with the issue of residual, commonly nonvolatile coacervation agent.

Spray-drying appears as an elegant approach as it involves gas rather than solvents for particle dispersion, so that drug loss may certainly not be a major issue. However, solvent flux to the gas interface and hardening of the particles has to occur very rapidly, possibly making spray drying harder to control and less flexible in view of formulation parameters compared to emulsion techniques. Also, the absence of surfactants coated to the particle surface may result in particle aggregation and poor dispersibility of particles from hydrophobic polymers. Additionally, at least under laboratory conditions, typically larger batch sizes and more

specific equipment are required. The same may be true for techniques employing supercritical fluids, which so far are industrially applied to extract substances from biological matrices, e.g., essential oils. This is because they can penetrate well through materials and have good solvent power under specific conditions [108]. Therefore, although acting as antisolvents for most polymers and inducing precipitation of microparticles, supercritical fluids may at the same time well dissolve drugs, which could result in poor encapsulation efficiency.

#### 8.4.2.2 Drug Release from Microparticles

Microparticles are generally characterized by a large ratio of surface area and volume. For drugs that are suitable to diffuse through a totally hydrated microparticle matrix, short diffusion pathways may result in release over days to months depending on the microparticle morphology and the physicochemical properties of the drug. By contrast, molecules that cannot permeate through a compact polymer matrix such as proteins above a certain hydrodynamic radius may, after initial burst, not be further released until breakdown of the dense matrix [109]. Therefore, a controlled induction of a defined level of porosity during microparticle preparation along with suitable properties of the degradable matrix polymer may be the key to establish a continuous release of such encapsulated compounds. Some general approaches involving additives to improve release profiles may be generally applicable for both microparticles and implants have intensively been reviewed in the literature [8, 10–12, 16]. Some additive strategies are discussed for implants in Sect. 8.4.3.2.

Among the commercially successful microparticle products (Table 8.1), the formulations of leuprolide acetate based on 14 kDa PLGA 75:25 (Enantone® and Lupron Depot® 1-Month SR formulations) or 15 kDa PLA (Trenantone® and Lupron Depot® 3-Month SR or 4-Month SR formulations) are best described in the scientific literature and provide a valuable knowledge of most of the basic aspects of microencapsulation. Often, release profiles from dense microparticles are characterized by a more or less pronounced burst release followed by a "lag" phase of almost no release. Depending on the degradation/erosion profile of the matrix polymer, the onset of a "log" phase with an exponentially accelerated release can be observed after a certain time. Different approaches have been used to overcome "lag" phases such as blending the matrix polymer with small portions of low molecular weight polymers [25]. During the development of Lupron Depot®, PLGA/PLA oligomers were consciously avoided, as they also may enhance burst release [110]. In contrast, a distinct level of porosity with pores of ~1 μm in diameter created in the microparticle surface, but not in the core, was achieved during the $w_1/o/w_2$ solvent extraction/evaporation and lyophilization process (Fig. 8.6a) [110]. As a consequence, the effective surface for a diffusion-controlled drug release from the top layers of the microparticles is much larger than the outer particle surface. This may explain why the lag phase is relatively short until degradation/erosion of the polymer bulk contributes to the leuprolide release profile in vivo (Fig. 8.6b).

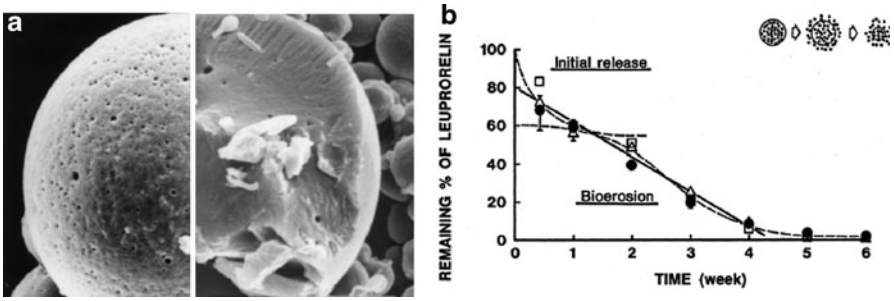


**Fig. 8.6** Characteristics of leuprolide acetate loaded PLGA microparticles (Enantone®, Lupron Depot® 1-Month SR). (**a**) Surface structure and cross section of 20–30 μm microparticles. Figures adapted from [215] and reprinted with kind permission from Springer Science + Business Media. (**b**) In vivo release after subcutaneous injection in rats for doses of 0.9 (●), 3 (△), or 9 (□) mg/rat ($n = 5$, mean ± SD). Figure adapted from [110], Copyright 1997, with permission from Elsevier

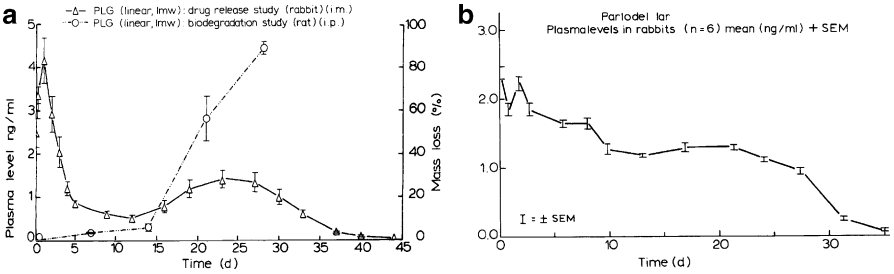


**Fig. 8.7** Effect of PLGA architecture on the in vivo release of bromocriptine from microparticles. (**a**) Bromocriptine plasma levels in rabbits and polymer mass loss in rats for linear, low-molecular-weight PLGA. (**b**) Bromocriptine plasma levels in rabbits for Parlodel® LAR microparticles prepared from branched PLGA-glucose. Figures reprinted from [51], Copyright 1991, with kind permission from Elsevier

Another approach to smoothen the release profile was developed for bromocriptine, which was released in a characteristic biphasic manner in vivo from microparticles prepared from linear standard PLGA. After a high burst release and a pronounced "lag" phase, a second phase of increased release rates correlated with the onset of mass loss, i.e., the erosion of the microparticle matrices (Fig. 8.7a). The development of branched PLGA employing glucose as a polyol starter molecule in polymer synthesis provided materials that faster reach aqueous solubility of degradation products than linear polymers of the same average molecular weight (Fig. 8.2). As a consequence, a reduced or absent "lag" phase was observed until polymer degradation contributed to the bromocriptine release from Parlodel® LAR microparticles (Fig. 8.7b). While Parlodel® LAR is no longer on the market,

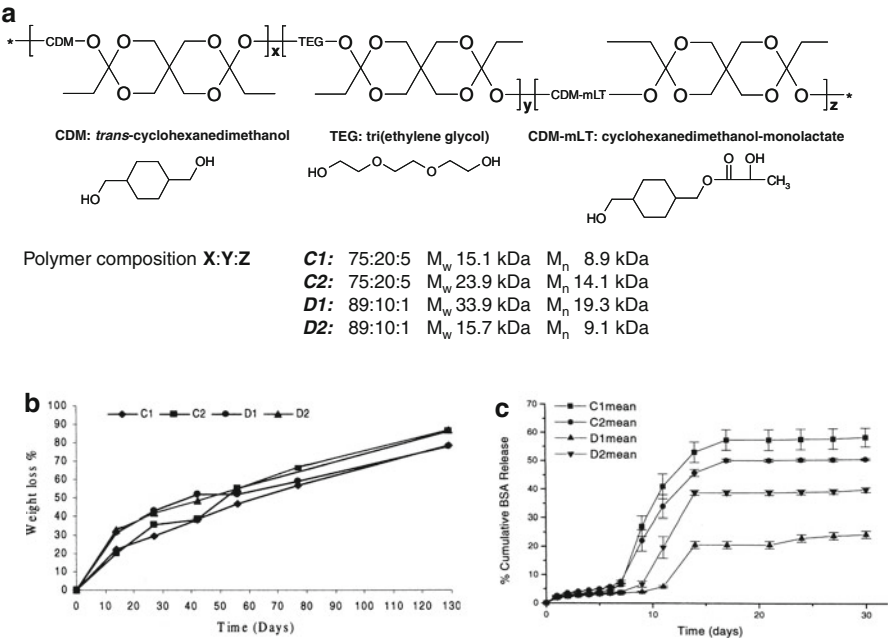


**Fig. 8.8** Properties of w/o/w microparticles from a series of class IV polyorthoesters for the release of bovine serum albumin. (**a**) Scheme of involved building blocks. Based on the reaction of the diketene acetal 3,9-diethylidene-2,4,8,10-tetraoxaspiro[5.5]undecane (DETOSU) with different diols, the copolymers C1, C2, D1, and D2 with molecular compositions were obtained. CDM is a rigid diol with a hydrophobic core, while TEG is flexible, hydrophilic and attracts water. CDM-mLT contains lactide as a latent acid to catalyze the degradation of polyorthoester linkages. (**b**) Weight loss of microparticles prepared from the polymers C1, C2, D1, and D2 during *in vitro* degradation in pH 7.4 PBS buffer at 37°C. (**c**) Cumulative in vitro release of bovine serum albumin (BSA) from microparticles in pH 7.4 PBS buffer at 37°C. Figures adapted from [216], Copyright 2001, with permission from Elsevier

the technology platform of branched PLGA-glucose remains of economical relevance, since the copolymer is used in the Sandostatin LAR® Depot (Table 8.1).

One may expect that classical surface eroding materials such as polyorthoesters can also be used to overcome discontinuous release profiles, particularly for large molecules such as proteins. Bovine serum albumin (BSA) was encapsulated by a w/o/w method into multivesicular microparticles from a series of class IV polyorthoesters. This class of polyorthoesters is often termed as "autocatalyzed," since these copolymers include small quantities of latent acids such as lactic acid (Fig. 8.8a) in the backbone which, upon cleavage, catalyze the hydrolysis of otherwise relatively stable orthoester linkages. Additionally, the polymer hydrophilicity, water uptake, and degradation rate can be altered by conducting copolymerization with different ratios of different diol compounds such as hydrophilic, flexible triethylene glycol and hydrophobic, rigid *trans*-cyclohexanedimethanol (Fig. 8.8a). During

**Table 8.2** Potential advantages and challenges associated with microparticles as drug carriers

| Potential advantages | Potential challenges |
|---|---|
| Easy adjustment of doses | Burst release |
| Injection through small needles | Nonlinear release profiles |
| No local anesthesia required | Hard to remove from the body when treatment must be stopped for medical reasons |
| No dose dumping due to failure in single carrier | |
| Selection from variety of biodegradable polymers | Complex and expensive preparation |
| Some preparation techniques conducted under mild conditions | Large surface may promote aggregation |
| | Limited drug loading levels |
| High acceptance by patients | Dispersion medium required that increases injection volume; resuspension issues |

degradation, an almost linear mass loss without an induction period and with practically no difference between the different microparticle formulations was observed (Fig. 8.8b). Along with practically no change of the remaining polymer mass (data not shown), this indicates a surface eroding behavior. However, since BSA was entrapped in the multivesicular structure in the particle core and did not diffuse through the dense particle shell, an induction period of ~7 days was observed before the onset of (incomplete) protein release (Fig. 8.8c). Decreasing pH due to the latent acid and potential protein aggregation may have supported this behavior. The most hydrophilic, low molecular weight polymer C1 provided highest release of ~60% of its payload during day 7 and day 14 of the study. Generally, non linear release may illustrate that surface eroding materials will not necessarily overcome any issues of discontinuous release profiles from microparticles.

Microparticles as drug carriers have several advantages but are also faced with challenges. Similar to oral multiple unit dosage forms such as pellets, they provide the total drug dosage subdivided into numerous individual matrices. In theory, when considering the properties of a single carrier, i.e., one microparticle compared to one preformed implant, there is a reduced risk for microparticles that failure in the integrity of one individual carrier unit could have toxic effects by dose dumping in a patient. By contrast, it can be speculated that in some cases different release rates of different particle fractions may have advantageously summed up to a linear release profile when particles of nonhomogeneous properties were provided in experimental studies. The same can be achieved by blending particles of different defined release properties (see Sect. 8.5.3) [24]. Another advantageous property of microparticles is their easy adaption of the administered dose to the clinical need by simply injecting a larger or smaller quantity of individual microparticles. By doing so, the relative drug release in vivo may be identical as shown in Fig. 8.6b for a tenfold increase in administered dose of leuprolide loaded microparticles. This is, from an industrial point of view, highly lucrative since one formulation with ~10% (w/w) of peptide payload can be marketed in different strengths (Lupron Depot® 1-Month SR 3.75/7.5/11.25/15 mg). These and other potential advantages but also some challenges of microparticles as drug carriers are summarized in Table 8.2.

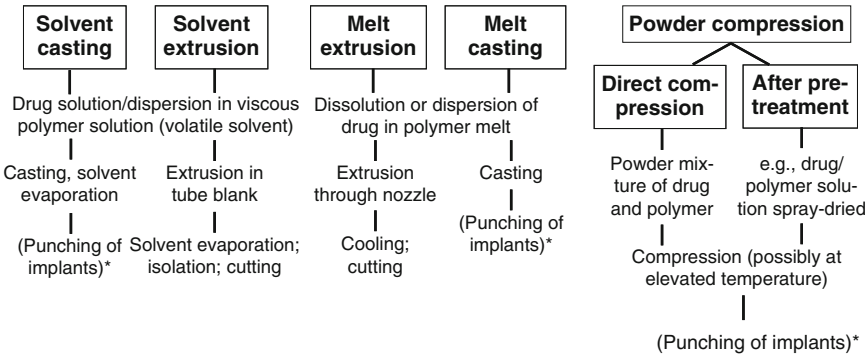


*(If no implant-specific casting/compression mold was used in previous step)*

**Fig. 8.9** Summary of the principles of some common preparation techniques for implants

## *8.4.3 Preformed Implants*

### 8.4.3.1 Preparation Techniques

Implants from solid polymers are typically prepared either in a rod-like shape for subcutaneous injection or as disks/wafers for implantation such as during open surgery. Polymer processing to form the implants can in principle be conducted starting from a polymer solution, melt, or powdered material. Although not an exhaustive list, some commonly employed methods are summarized in Fig. 8.9. Drug material dissolved or suspended in a more or less viscous polymer solution can be casted in dishes or extruded into tube blanks such as a silicone tubing [76]. Also, molten or plasticized polymers with molecularly dispersed or suspended drug can be slowly extruded at elevated temperatures using plastic syringes and syringe pumps for processing in an easy laboratory screening method [111, 112]. However, for industrial fabrication of drug loaded implants such as Parlodel® Depot, a more sophisticated setup for hot melt extrusion with well controlled process parameters may be preferred [113], e.g. by using twin screw extruders. Injection molding, which is used to fabricate devices of complex shape for numerous technical fields and employs higher pressure to transfer the plasticized material into a mold, has for example been discussed for peptide loaded implantable rods [114] and industrially applied for gentamicin loaded biodegradable beads [115]. Another concept that avoids organic solvents involves powder mixtures of polymer and drug that are either directly compressed into disks or after a specific pretreatment. The pretreatment may be useful to establish a more homogeneous drug loading and may involve casting of drug/polymer solutions, solvent evaporation, and grinding [116] or, as finally used in the manufacturing of Gliadel®, spray drying into drug loaded microparticles before final compression [117].

It has to be pointed out that each preparation technique may be associated with certain challenges (Fig. 8.10) and that the product properties, e.g., of an implant rod

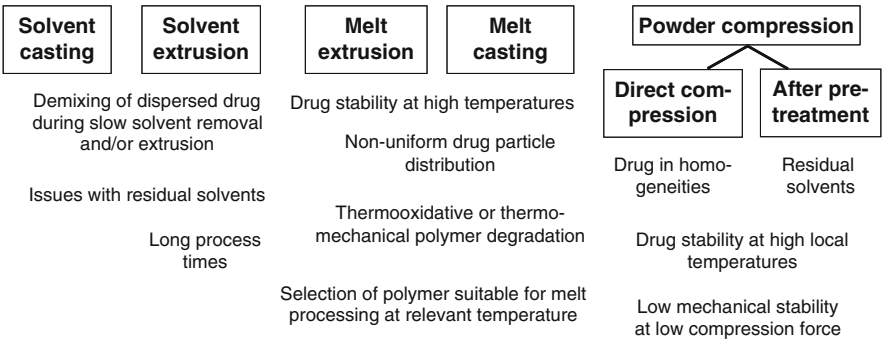


**Fig. 8.10** Selected challenges that commonly are associated with specific implant preparation techniques

may strongly differ when prepared by different techniques. For example, the porosity of implants from poly[1,3-bis(p-carboxyphenyl)propane-*co*-sebacic acid] 20:80 p(CPP-SA), a polyanhydride known as surface eroding material, strongly increased depending on the preparation technique in the following order: melt-molding < compression molding < solvent casting. As a consequence, no erosion front as a classical marker of surface erosion could be observed in samples prepared by solvent casting [118].

The use of organic solvents allows shaping of implants at low temperatures and thus may be of interest particularly for temperature sensitive compounds. However, slow solvent removal and hardening of implants may be associated with some disadvantages [119] such as demixing of suspended drug particles, Ostwald ripening of precipitating drug aggregates upon gradual solvent removal, and possibly in homogeneities of the product. While an expected higher porosity after solvent removal may be advantageous to enhance the release of large molecular weight drugs by pore diffusion, high levels of porosity may be associated with poor mechanical stability of implants. Also, the long process times associated with a typically slow solvent evaporation may not be preferred in the pharmaceutical industry. Moreover, due to the implant size with larger diffusion lengths than for microparticles, residual solvents may be more critical for such bulky drug carriers. Table 8.3 summarizes the relevance of vapor pressure for the evaporation process, as well as the ICH solvent classification and ppm limits, of good polymer solvents. It can be concluded that acetone advantageously combines high vapor pressure and noncritical solvent limits with high solvent strength, e.g., for PLGA, which allows use of concentrated polymer solutions in solvent extrusion processes.

Implant manufacturing at elevated temperatures using molten or plasticized matrix polymers is of high relevance for industrial applications as it is a one step process, which is fast and can be operated in a continuous process. However, a dramatic decrease in polymer molecular weight due to thermooxidative or thermomechanical degradation was reported in some studies for both extrusion [120] and injection molding [121] at least for PLA. Besides the matrix polymer, embedded drugs may be subject to degradation. In contrast to that assumption, stability of

**Table 8.3** Properties of good solvents for polymers such as PLGA

| Solvent (S) | Evaporation process Vapor pressure (hPa, 20°C) | Residual solvent guidance[a] Solvent class | Limit (ppm) |
|---|---|---|---|
| Acetone | 233 | 3 | 5,000 |
| Acetonitrile | 97 | 2 | 410 |
| Chloroform | 211 | 2 | 60 |
| Dimethylformamide (DMF) | 3.8 | 2 | 880 |
| Dimethylsulfoxide (DMSO) | 56 | 3 | 5,000 |
| Ethyl acetate | 94 | 3 | 5,000 |
| Methylene chloride | 475 | 2 | 600 |
| N-Methylpyrrolidone (NMP) | 0.3 | 2[b] | 530[b] |
| Tetrahydrofurane (THF) | 173 | 2 | 720 |

[a]According to [259]

[b]It appears that the limit for NMP set in the guideline may not necessarily be critical for FDA approval at least in selected cases. Approved products (e.g., Eligard®) can be directly injected and contain much larger quantities of NMP. Also, the permitted daily exposure of 5.3 mg/day for NMP according to the guideline is likely exceeded for the first days after injection by this product

substances as labile as peptides and proteins was reported for melt extrusion with PLGA at temperatures in the range of 70–100°C. For example, 100% of BSA were released from a class IV polyorthoester implant prepared by suspension of polymer powder in the polymer at 70°C and subsequent extrusion, indicating the absence of insoluble protein aggregates at least for BSA processing in the solid state [114]. As reported recently, the activity of released lysozyme after melt extrusion with PLGA at 100°C was ~93%, but only ~63% when extruded at 105°C [112]. For vapreotide pamoate, a peptide that is an analog of somatostatin and contains a labile disulfide bond, systematic studies on the effect of extrusion temperature and process time revealed stability for up to two hours at temperatures below 100°C [122]. For injection molding as compared to extrusion processes, higher process temperatures may have to be applied. Additionally, samples are exposed to much stronger shear forces and possibly higher local heat produced during ejection of the plasticized polymer through the nozzle. Extrusion processes are also well known to have difficulties with nonuniform distribution of suspended particles, e.g., higher concentration of particles in the center than at the edges [123, 124].

In their plasticized state during extrusion and injection molding, polymers typically orientate into the thermodynamically preferred random coil. However, when discharged through a nozzle, polymer chains may experience longitudinal orientation. For materials that are suitable to form polymer crystallites such as poly(L-lactide), this orientation of polymer chains may support chain interaction and theoretically may increase polymer crystallinity. Furthermore, polymer crystallites in hydrophobic polymers are often not instantly hydrated and act as diffusion barriers for incorporated drugs under release conditions. Therefore, manufacturing derived alterations of matrix crystallinity may be relevant not only in terms of the mechanical features of an implant, but also regarding the drug release and degradation/erosion properties. Compared to melt extrusion, injection molding typically involves a faster cooling and solidification of possibly well oriented polymer chains as a shell at the wall of

the mold. This may explain why a core–shell implant architecture with higher shell-crystallinity was observed for an industrially manufactured implant bead from a polyanhydride material at relatively low process temperatures, i.e., under conditions where a fast solidification at the wall of the mold can be expected [115]. In this specific case, the oriented crystallites in the shell of the beads advantageously provided mechanical strength against cracking of the implants in an aqueous environment, which otherwise was possibly induced by the osmotic pressure associated with drug loading. Generally, it may be considered that cracking of melt-processed devices could also be a consequence of residual, processing-induced stress. For instance, this stress may be derived from differences in the molecular chain orientation with oriented chains in the shell and relaxed chains in the core zones of the implant (flow-induced residual stress). Also, local differences in the thermo mechanical history such as cooling rates and the capability for contraction of material after initial solidification of the shell may result in built in thermally induced residual stress. Tempering of implants at temperatures only slightly below the peak of a broad melting phase transition of the material, i.e., at conditions suitable to relieve residual stress in melt-processed devices, resulted in the absence of major cracks and a reduction in drug release rates due to a smaller available surface [125]. This supports a possible contribution of residual stress to the observed implant cracking in the aforementioned example. Besides, it should be noted that tempering was associated with a reduction in molecular weight, which may also have contributed to the relief of residual stress. Overall, this example may illustrate the relevance of process parameters on implant properties.

#### 8.4.3.2 Drug Release from Preformed Implants

When comparing microparticles and implants as possible drug carrier, it is very obvious that different release rates can be expected even if both carriers were prepared from identical polymers and had a similar level of porosity. Very often, the percentaged drug release from implants will be slower due to longer diffusion lengths. Also, when considering a possibly higher amount of drug incorporated in one dose, implants may allow drug release over a longer period of time. Therefore, in addition to the properties of the matrix polymer, the surface area/volume ratio and the porosity, which are both associated with the implant shape and method of processing shape, may be major contributors to the observed release pattern. It has already been highlighted in Fig. 8.1 and discussed for microparticles in Sect. 8.4.2.2, that the properties of the incorporated drugs are obviously relevant in terms of release profiles. For example, when 10 wt.% of two small molecular weight drugs, either hydrophilic *N*-acetylcysteine or hydrophobic 2-methoxyestradiol, were incorporated in rod-shaped PLGA implants prepared under identical conditions by a solvent extrusion process, only ~20% of 2-methoxyestradiol was released over 4 weeks [14], whereas the same percent release of *N*-acetylcysteine occurred in only a few hours [76]. Also, as already reported for microparticles, proteins may not be

released from PLGA implants after initial burst if not supplemented with tailored quantities of suitable additives [9].

Generally, the incorporation of additives may serve multiple goals. For example, osmotically active agents may be used to increase osmotic pressure, water uptake, and porosity for an accelerated drug release. Additives may also be used to decrease drug solubility by formation of poorly soluble drug salts or they may catalyze hydrolytic polymer degradation. Lag phases for the release of hydrophobic drugs may often be overcome by adding to the polymer matrix various water-soluble leaching agents such as polymer, sugars, or salts [14]. Porosity derived from leaching molecules or osmotically active agents increases the water uptake of the matrix and thus the available volume of aqueous medium to dissolve the drug. The incorporation of solubilizing agents for hydrophobic drugs, which range from micelle forming surfactants to, e.g., cyclodextrins to mask hydrophobic drug moieties, may also contribute to an enhanced drug release. Furthermore, mixtures of matrix polymers of different molecular weight remain a repeatedly successful strategy to adjust release rates [14]. For highly water soluble drugs, precipitation into less water soluble ion pairs (e.g., amine drugs with fatty acids; acidic drugs with quaternary ammonium compounds such as SDS analogs) [126] or similar masking approaches may reduce drug solubility, drug-derived osmotic pressure, water influx, and water (or drug) associated plasticization of the polymeric matrix. Also, catalytic effects of the drug on polymer degradation may be overcome by employing multivalent salts, for example, as was performed with *N*-acetylcysteine (e.g., $Ca^{2+}$) compared to the drug in its free-acidic form (Fig. 8.11) [76].

For proteins, incorporation of bases can modify the microclimate in the proximity of these labile molecules in the polymeric matrix and circumvent pH-induced protein aggregation due to initially present acidic impurities as well as from polymer degradation products [127] as shown, e.g., for BSA [128], BMP-2 [9], rhbFGF [9, 13], rht-PA [129], and tetanus toxoid [130]. Additionally, by neutrolizing acidic degradation products, incorporated bases also alter the porosity and water uptake, which often contribute to increased protein release [128, 131].

When employing PLGA, the properties of the implant matrix such as its hydrophilicity or the degradation speed can be modified by the polymer's molecular weight, architecture, end groups, and comonomer ratio. Since glycolide–glycolide diads are weak links in these copolymers, a decreasing molar content of glycolide allows for longer degradation times due to different mechanisms (increased steric hindrance to nucleophilic attack by water, lower relative hydrophilicity of the material, and slower water uptake). Therefore, as exemplarily shown by data from the preclinical evaluation of buserelin acetate loaded implantable rods (Fig. 8.12a), a more constant and longer-lasting drug release may be achieved by PLGA matrices with a higher lactide content. By contrast, the 50:50 PLGA implants were associated with a faster initial water uptake (increase in wet mass) and a subsequent degradation triggered mass loss (Fig. 8.12b). This leads to shorter release periods in vivo (Fig. 8.12a) and possibly a temporarily limited pharmacological effect (Fig. 8.12c) [132].

Larger molecules such as proteins cannot diffuse through dense polymer matrices as for instance created by melt extrusion processes. In order to control the

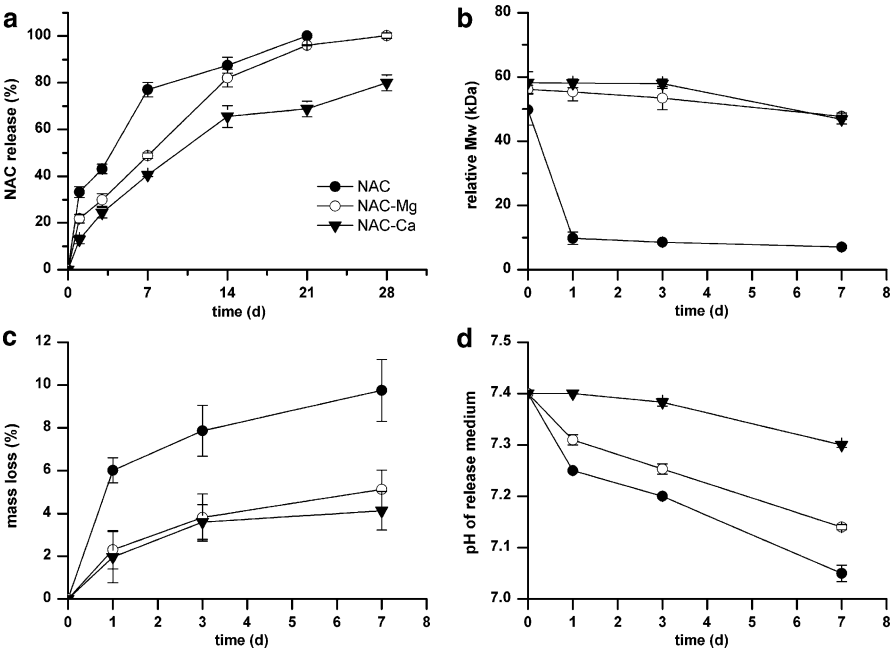


**Fig. 8.11** Properties of PLGA 50:50 implant rods prepared by a solvent extrusion process and loaded with 10 wt.% of free *N*-acetylcysteine (NAC) (●), NAC-$Mg^{2+}$ (○), or NAC-$Ca^{2+}$ (▼) as observed under in vitro release conditions. (**a**) Cumulative drug release, (**b**) Decrease the polymers relative average molecular weight as determined by comparison to polystyrene standards, (**c**) Mass loss of implants corresponding to released drug (compare panel **a**) and escape of water-soluble polymer degradation products, (**d**) pH changes in the release medium. Figures adapted from [76] with kind permission from Springer Science+Business Media

release by mechanisms other than a controlled induction of porosity by additives and polymer blends, predominantly surface eroding polymers such as class IV polyorthoester were evaluated. When FITC-BSA was embedded in such a material by melt extrusion, congruent curves for the cumulative percent protein release and the implants' percent mass were observed (Fig. 8.13a) [114]. However, it is not clear from the experimental description if all of the incorporated protein was quantitatively released in the native state and/or if insoluble protein aggregates may have been formed. As can be seen from Fig. 8.13a, there was a pronounced initial lag phase, which, interestingly, resulted in a similar release pattern for this specific composition, as previously discussed for microspheres from poly (orthoesters) (Fig. 8.8). According to the theory of pure surface erosion [6], the molecular weight of the bulk material should be constant for an extended period of time, while degradation-induced mass loss from the implant surface should occur in a linear manner upon contact with water. Obviously, both mass loss (Fig. 8.13a) and decrease in molecular weight (Fig. 8.13b) did not strictly follow that rule for the presented samples.

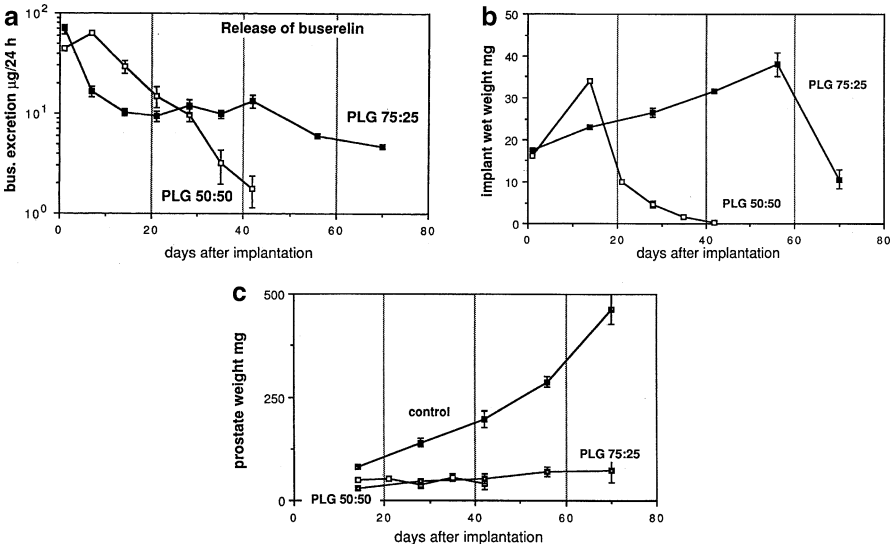


**Fig. 8.12** Impact of PLGA comonomer molar ratio on the in vivo characteristics of buserelin acetate loaded implantable rods in rats (data from the formulation and preclinical studies of Profact® Depot). (**a**) Release rate of buserelin as determined by the urinary excretion. In rats, about 30% of the dose released per day is excreted in the urine. (**b**) Implant weight in the dry state (day 0) and in the wet state as recovered at different time points from subcutaneous tissue. Wet implant weight is affected by two interfering processes–water uptake and erosion-derived mass loss. (**c**) Biological effect on prostate weight as exemplary androgen dependent organs. The control shows the normal increase in prostate weight in young male rats. Figures reproduced from [132] with permission from W. Zuckschwerdt Verlag GmbH

It is generally known that the concept of surface eroding materials involves hydrophobic repeating units, which limit the water uptake into the bulk. These repeating units are typically connected by hydrolytically sensitive bonds. In case of class IV polyorthoesters, additional autocatalysis is enabled by latent acids polymerized into the polymer backbone. However, a small amount of water will typically be taken up in the bulk polymer, which may be different for different families of class IV polyorthoesters depending on the employed copolymer types and ratios. This low water content in the polymer bulk may induce degradation and result in a molecular weight decrease at low rates as illustrated in Fig. 8.13b. For larger devices such as implants, an erosion zone at the implant surface can be distinguished where degradation occurs at much higher rates than in the bulk due to the presence of larger quantities of water. As a consequence, large molecules such as proteins, which previously were entrapped in the polymer, can be released from the surface erosion zone. Therefore, the rates of protein release and mass loss of the implant are closely related to the movement of the erosion front toward the core of the matrix system [133]. However, since the hydration of the erosion zone and a local reduction of the molecular weight to water soluble products are required first, lag phases may also occur for polyorthoesters. These lag phases may not

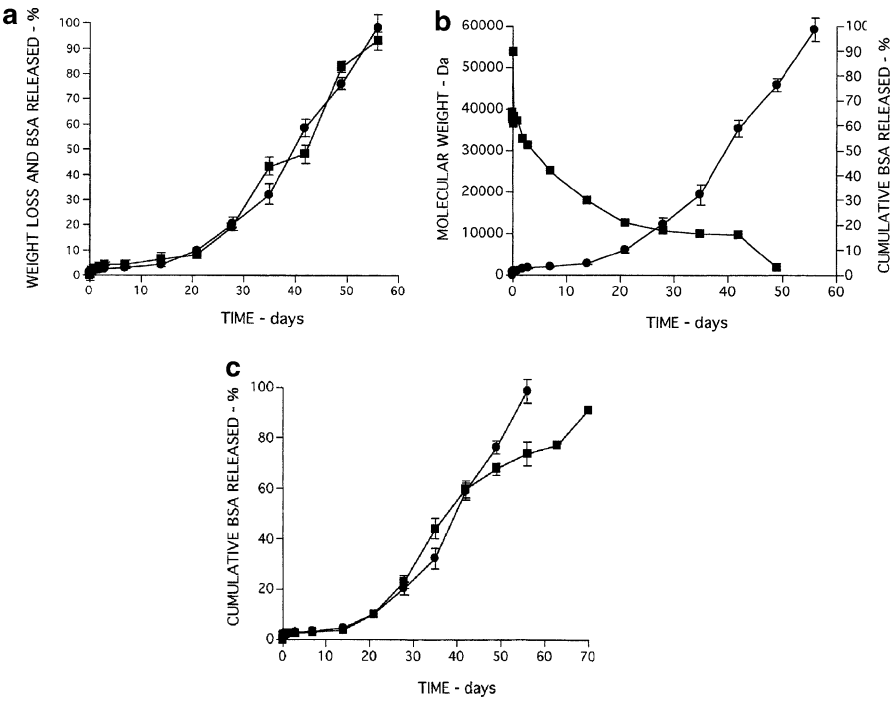


**Fig. 8.13** In vitro study on model protein loaded implant rods (10 × 1 mm) from class IV polyorthoester consisting of 3,9-diethylidene-2,4,8,10-tetraoxaspiro[5.5]undecane (DETOSU), 1,4-pentanediol, and 1,6 hexanediol glycolide (100/95/5). Samples loaded with 15 wt.% of dispersed FITC-BSA were prepared with a twin screw extruder at 70°C. (**a**) FITC-BSA release (●) and weight loss (■) of implants (61.5 kDa initial polymer molecular weight). (**b**) FITC-BSA release (●) and change of the average molecular weight (■) of implants (61.5 kDa initial polymer molecular weight). (**c**) Effect of the initial average molecular weight, either 12 kDa (■) or 61.5 kDa (●) on the FITC-BSA release. Release studies were conducted in 10 mM phosphate buffer pH 7.4 at 37°C. Figures reprinted from [114], Copyright 2001, with kind permission from Elsevier

always be as long as found in Fig. 8.13b and certainly depend on the material's sensitivity to hydrolysis. The fact that a polymer of identical composition but much lower molecular weight resulted in the identical release profile (Fig. 8.13c) stresses that surface erosion rather than bulk degradation was the driving mechanism of release for proteins, which were unable to diffuse through the bulk polymer.

Polyanhydrides, as a second major class of surface eroding materials, have intensively been studied for the controlled release of a small hydrophilic molecule, carmustine, which eventually resulted in regulatory approval of thin wafer implants (Gliadel®) for the treatment of glioblastoma in the brain. As these tumors tend to recur very close to their original location, the wafers are used to line the wall of the surgical cavity. From there, the drug is transported by diffusion or other mechanisms up to 10 mm or even longer distances into the brain tissue as shown in some animal trials providing high local drug concentrations [117, 134]. Gliadel® implants are

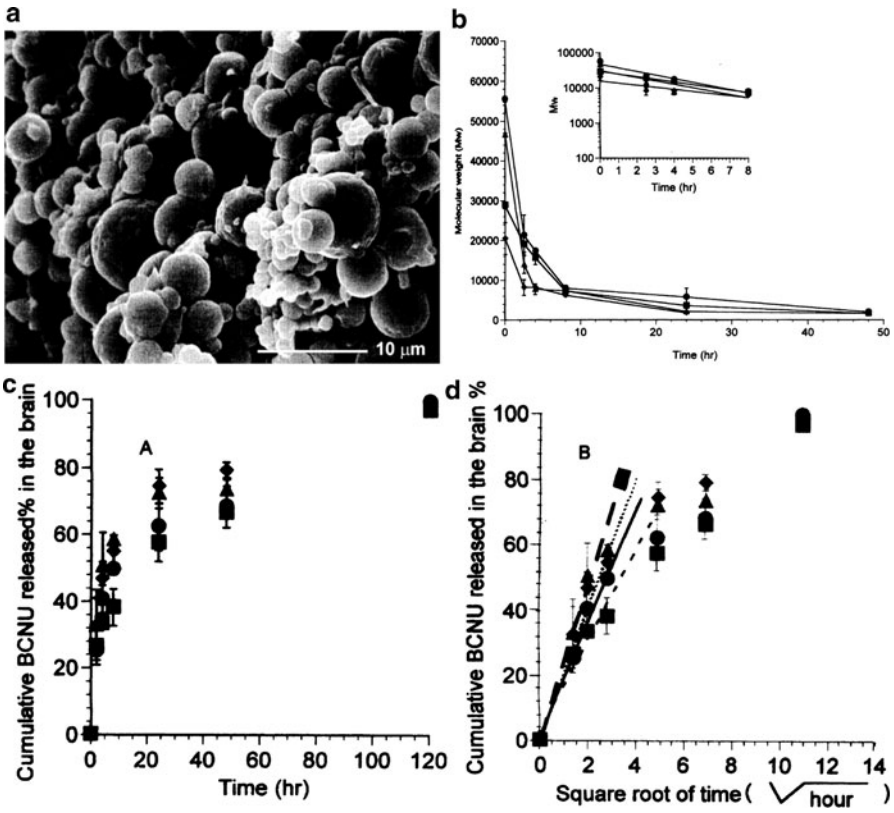


**Fig. 8.14** Properties of carmustine (BCNU) loaded Gliadel® wafers prepared by compression of spray dried 20:80 poly[1,3-bis(p-carboxyphenyl)propane-*co*-sebacic acid] / carmustine microparticles. (**a**) SEM of cryofractured wafer. Figure adapted from [135] and reprinted with kind permission from Springer Science+Business Media. (**b–d**) Effect of the initial average molecular weight of 20 kDa (◆), 29 kDa (■), 47 kDa (▲), and 55 kDa (●) on the decrease of the average molecular weight (**b**) and the cumulative drug release as plotted linearly (**c**) or over the square root of the time (**d**) in a rat brain in vivo study. Figures reprinted from [138], Copyright 1996, with permission from Elsevier

produced by spray drying drug–polymer solutions, forming 5–10 μm particles, which subsequently are compressed into wafers. An SEM image of Gliadel® wafers (Fig. 8.14a) illustrates that highly porous devices are obtained, in which the structure of individual microparticles is almost unchanged [135]. Owing to the prominent hydrolytic instability, low mechanical strength, and a tendency to spontaneous depolymerization in organic solutions at least for some families of polyanhydrides including p(CPP-SA) as used for the matrix of Gliadel® [136], materials have to be handled under moisture free conditions and stored at −20°C [137]. For wafers prepared from p(CPP-SA) of different initial molecular weight, a very fast degradation with a decrease in the average molecular weight to a plateau value of ~8 kDa was observed within 8 h in vivo (Fig. 8.14b) [138]. Carmustine release was practically

**Table 8.4** Potential advantages and challenges associated with preformed implants as drug carriers

| Potential advantages | Potential challenges |
|---|---|
| Reliable manufacturing processes | Implantation with large needle injectors |
| Possibly best control for continuous release | Implantation may require anesthesia |
| High potential for long-term release | Irritation of tissue due to implant size |
| No resuspension/dissolution step prior to administration | |
| Explantation possible | |

independent of the initial molecular weight (Fig. 8.14c). Moreover, the drug release was assumed to be mainly diffusion controlled, since it conformed to a linear square root of the time relationship, at least during the initial hours of strong molecular weight decrease (Fig. 8.14d). Independence of release rates from the polymer's initial average molecular weight may not necessarily have been expected for a compact polyanhydride implant of similar size. This finding for porous wafers has to be attributed to the low drug diffusion length from the small individual microparticle compartments toward the well-hydrated interconnective porous network. Overall, the presented examples of biodegradable implants stress that the feasibility for a controlled drug release cannot solely be discussed in the light of matrix material properties such as prevalence to surface or bulk erosion, but also involves numerous aspects of polymer processing.

Even though preformed degradable implants may presently not be the most intensively used commercial controlled release carrier (Table 8.1), they combine several advantages (Table 8.4) and, therefore, remain a promising carrier particularly for controlled release applications over months. With their mostly relatively low surface area to volume ratio, implants may be useful particularly for drugs, where a major burst release has to be excluded. Implant manufacturing may be realized by robust industrial processes, which, particularly for extrusion methods, allow high output. For the clinician, error prone resuspension or dilution steps as for microparticles or in situ implants can be excluded with preformed implants. Obviously, however large implant diameters for a subcutaneous and possibly painful insertion are expected to be associated with a significantly lower acceptance by patients.

## *8.4.4 In Situ Forming Drug Depots*

### 8.4.4.1 Strategies to form In Situ Drug Depots

In situ forming drug depots are based on injectable formulations such as more or less viscous polymer solutions that form a depot during and/or after administration. Thereby, a variety of material concepts and underlying mechanisms may be employed,

ranging from organic-solvent exchange with precipitation of hydrophobic polymers to stimuli sensitive intermolecular bonding of hydrophilic or amphiphilic molecules.

In situ forming gels, i.e., solvent rich matrices consisting of hydrophilic or amphiphilic molecules, may employ various mechanisms of intermolecular binding including (1) thermosensitive materials gelling upon decrease in temperature; materials range from block copolymers studied in water [139] to small molecules evaluated in different solvents including biocompatible vegetable oils [140, 141], (2) thermosensitive materials, which gel upon increase in temperature; gelation occurs, e.g. due to the formation of block copolymer micelles and possibly intermicelle bonding in water [142, 143] or due to a partial dehydration of polymers enabling hydrophobic chain–chain interactions [144, 145], (3) covalent crosslinking of network precursors, e.g. by enzymatic reactions [146], by photopolymerization using acrylate chemistry [147, 148], or by reaction of thiol group-containing polymers with vinylsulfone crosslinkers to thioether networks [149], (4) ionic crosslinking, e.g. of charged polymers [150] or nanoparticles [151], or (5) pH changes, e.g. for charged polymers such as chitosan that may precipitate to gel-like matrices when the pH is increased from acidic conditions to its isoelectric point.

Other concepts of in situ forming depots employ polymers that are semisolid at ambient temperature such as some class IV polyorthoesters (Biochronomer™) of low molecular weight (1–6 kDa), which are synthesized by combining DETUSO (see Fig. 8.8) with highly flexible diols [82, 152]. In order to improve injectability, up to 20% of methoxypolyethylene glycol (550 kDa) was suggested to be used for reduction of viscosity [153]. As mentioned in Sect. 8.4.1, there are efforts to transfer an injectable granisetrone formulation based on this technology into clinical use. Theoretically, polymers that can be handled as a liquid at temperatures (slightly) above physiological temperatures and solidify when cooled to body temperature by phase transition to a glassy or semicrystalline state could also be used for in situ forming depots [85, 154]. Classical PLGA or PCL may not be usable since liquefaction typically cannot be obtained at temperatures suitable for injection without tissue damage. However, there are examples of low molecular weight copolyesters obtained, e.g., by copolymerization of ε-caprolactone with L-lactide and propylene glycol [155] or with 1,4 dioxanone and propylene glycole [156] as well as low-molecular-weight polyanhydrides [157] that were discussed for solvent-free in situ forming implants that solidify after cooling to body temperature.

The class of in situ forming drug carriers that has advanced to clinical use employs organic solvents and mostly relies on standard PLGA as also used for preformed implants. After injection of a viscous polymer solution or emulsion, solvent exchange with water leads to liquid–liquid phase separation and the precipitation of the matrix polymer. Depending on the properties of the polymer solvent, some patented drug delivery technologies can be differentiated: Atrigel® [158, 159] uses solutions of PLGA in totally water-miscible solvents (e.g., NMP, DMSO) and is employed in Eligard® and Atridox® (see Table 8.1). By contrast, partially water-miscible solvents such as ethyl benzoate, benzyl benzoate, or triacetin are employed in the Alzamer® system for in situ forming PLGA implants [160, 161]. The Saber® system does not rely on PLGA but involves a viscous sugar derivative,

sucrose acetate isobutyrate, plus some organic solvent such as ethanol for easier injectability and subsequent viscosity increase [162, 163].

By combining the concepts of microparticulate carriers and in situ forming depots, in situ forming microparticles [164] were proposed to overcome issues associated with conventional microparticle formulations such as the cost intensive preparation, drying, and potentially difficult resuspension. Also, in contrast to in situ forming implants, in situ forming microparticles showed lower myotoxicity [165], easier injectability depending on the type of solvent and suspension medium [166], and a more reproducible surface area as opposed to the irregular shape obtained for in situ implants. The concept of dropping aliquots of drug plus PLGA/NMP into aqueous medium [261] was revived and advanced by either using o/o emulsions, which were preformed and stored until administration [167–169] or by preparing o/w or o/o emulsions in two compartment systems (syringes attached to each other with a syringe connector) directly before administration [164]. Natural vegetable oils or partially synthetic oils are commonly employed as continuous phase in the o/o microparticle formulations. Importantly, there is an increasing number of allergies that may be associated with the standard oil for injection, peanut oil, due to occasionally present residual plant proteins as impurities. Therefore, great care must be exercised when selecting a vegetable oil as carrier for in situ implants (for further discussion see [16]).

After injection, the partitioning of the biocompatible solvent [170] into the tissue causes the hardening of the polymer solution or the emulsion droplets in vivo. In contrast to the preparation of preformed implants or microparticles, where a loss of drug during the manufacturing process is uncritical in terms of pharmacology, drug leakage during carrier formation of in situ depot systems is inevitably linked to burst release issues and potentially even to dose dumping with possible toxic effects.

#### 8.4.4.2 In Situ Depot Formation by Liquid–Liquid Phase Separation and Drug Release Characteristics

When polymers such as PLGA are dissolved in a good solvent and are subsequently brought into contact with a nonsolvent, solvent exchange and a liquid–liquid phase separation occurs, finally resulting in the formation of a polymer precipitate. This technology is, for example, widely used for the preparation of membranes by transferring thin films of polymer solution into a bath of nonsolvent. Several process parameters may be changed to alter the properties of the resulting membrane, e.g., the polymer concentration, type, molecular weight, comonomer ratio, solvent, or the nonsolvent. The strongest differences in membrane morphology for a given polymer are commonly observed by changing the solvent–nonsolvent system.

For in situ implants for biological applications, water is the only relevant nonsolvent. Some additives dissolved in water, at least those salts and proteins

**Table 8.5** Aqueous solubility of polymer solvents used for in situ implants and selected references on in situ implant studies

| Solvent | Solubility in water (%) | Selected references |
|---|---|---|
| *N*-Methylpyrrolidone (NMP) | Miscible | [172, 174, 179, 187, 188] |
| Dimethylsulfoxide (DMSO) | Miscible | [180, 181] |
| PEG, PEG-dimethylether (PEG-DME) | Miscible | [182, 183] |
| Glycofurol[a] | Miscible | [184, 185] |
| Triacetin[b] | ≈7 | [160, 172, 174] |
| Triethyl citrate | ≈5.7 | [160] |
| Ethyl benzoate | ≈0.4 | [172, 174] |
| Benzyl benzoate | ≈0.15 | [78, 174–178, 260] |

[a]Polyethylene glycol monotetrahydrofurfuryl ester
[b]Glycerol triacetate

possibly present under physiological conditions, had only minor effects on phase separation kinetics [171]. This stresses the role of the organic carrier solvent for the polymer and that its careful selection were major steps in the development of advanced technologies for in situ forming implants.

Mechanistically, the liquid–liquid phase separation process and the properties of an obtained polymeric device from drug loaded polymer solutions is based on the following two aspects [171, 172]: First is the thermodynamic state of the initial system as determined by the ternary composition containing polymer, solvent, and nonsolvent. Commonly, the system is initially in a more or less nonsolvent free, homogeneous state beyond the ternary composition region where polymer precipitation occurs. The polymer type and concentration as well as the solvent properties determine how much nonsolvent has to enter the system to induce phase separation. Second, the kinetics of mass transfer during solvent exchange and polymer precipitation is crucial, and involves the following processes:

- Diffusion of water into to polymer solution. Water uptake is limited by i) the solubility of water in the solvent (Table 8.5), ii) water solubility in the polymer, iii) the presence of additives including drugs of specific physicochemical properties, and iv) the formation of a precipitated polymer shell acting as a diffusion barrier. This may result in the development of a two-phase system consisting of a polymer- and solvent-rich continuous phase that contains nonsolvent (water)-rich, polymer-poor zones. For polymers that can interact well with water, such as PLGA of relatively low molecular weight and containing free hydrophilic carboxyl groups, the water uptake may be higher than the loss of solvent resulting in swollen, gel-like structures.
- Solvent removal from the polymer solution into the nonsolvent bath or, in vivo, into the tissue. Solvent removal is limited by the solvent solubility in the nonsolvent and the properties of the precipitated polymer shell that again acts as a diffusion barrier. Solvent removal rates are related to the solvents aqueous solubility and the water uptake.
- Polymer precipitation to form solid implants. Precipitation occurs first at the interfaces of solvent-rich and nonsolvent (water) rich phases when the ternary

composition of polymer, solvent, and nonsolvent is shifted toward a thermodynamically unstable state. As a trend, solvents characterized by a high water miscibility may lead to a fast phase separation and hardening of the implant, while those of low water uptake may stay liquid or semiliquid over extended periods of time.

- Drug distribution between the phases. Drugs with distinct aqueous solubility may rapidly partition into the water rich phase until final hardening of the polymer rich phase occurs. Depending on the drug's physicochemical properties such as the hydrodynamic radius as well as on the hydration of the polymeric bulk matrix, a diffusion of polymer-entrapped drug may or may not be enabled.

Against this background, it may be obvious that a solvent's affinity for water is of large relevance when discussing implant properties derived from polymer precipitation. NMP as the standard solvent for in situ forming implants is freely miscible with water and, therefore, may be exchanged at high rates. Other explored solvents (Table 8.5) are only partially soluble in water, and therefore slower solidification is expected for such in situ implants.

In a number of fundamental studies [171, 172], water uptake of in situ implants was fastest when using NMP as polymer solvent compared to triacetin and ethyl benzoate, which follows their order of aqueous solubilities (Fig. 8.15a). Also, drug release profiles of a model protein were dramatically altered with release rates decreasing in the same order. A more continuous release of lysozyme was observed for partially water miscible solvents, which may be a consequence of different release mechanisms (Fig. 8.15b). This assumption is based on obvious differences in implant morphology with generally highly porous, i.e., rapidly phase separated samples for NMP (Fig. 8.15c) [172, 173] compared to much denser, possibly semiliquid and persistently solvent containing implants from triacetin (Fig.8.15d) and ethyl benzoate (Fig. 8.15e) [172]. However, it needs to be stressed that protein stability, as always challenging in controlled release systems, may be a serious issue for proteins exposed to such a mixed milieu of water, solvent, and polymer. Particularly critical may be the dissolution of proteins and their diffusion at the boundary of solvent rich to nonsolvent rich zones. Upon hardening of the matrix, negligible diffusion of proteins in precipitated PLGA is expected, which correlates well with the lack of major subsequent release from the NMP formulation after 4 days [172]. The fast protein release before that time point was discussed to occur for the NMP formulation from the lumen of interconnective pores that arise from nonsolvent rich zones. By contrast, due to the absence of major porous structures for ethyl benzoate, in this case protein release was assumed to occur by protein diffusion in the polymer rich phase, which was enabled by the prolonged persistence of the solvent rich matrix in a semiliquid state [172].

When determining the release of human growth hormone from in situ implants in vivo, a solvent with very low aqueous solubility, benzyl benzoate, resulted in the most continuous serum levels [174]. In vitro, however, a perfectly linear drug release from benzyl benzoate based in situ implants was observed for small hydrophobic molecules [175] and peptides [176] only. Larger molecules such as

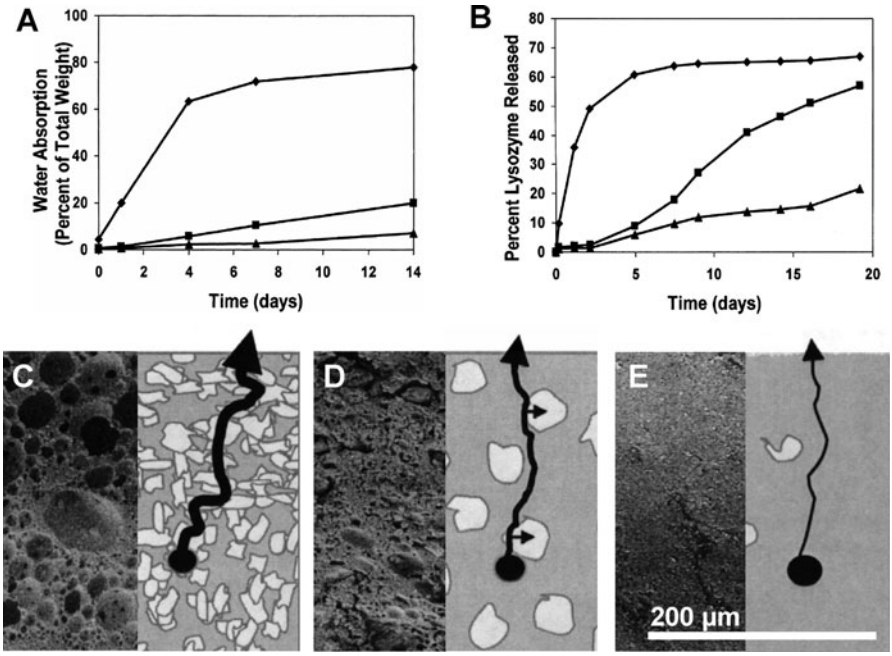


**Fig. 8.15** Phase inversion dynamics, protein release, implant morphology, and postulated release mechanism for in situ implants prepared from NMP (◆), triacetin (■), or ethyl benzoate (▲) as solvents, 50 wt.% Resomer® RG 502 (PLGA 50:50) as polymer, and PBS buffer as nonsolvent. (**a**) Water uptake, (**b**) release of lysozyme, (**c**–**e**) SEM images and scheme of matrix structure and postulated preferred pathway of protein release for NMP (**c**), triacetin (**d**), and ethyl benzoate (**e**) as solvents. *Gray* regions in schemes indicate the polymer-rich phase, *bright* areas represent water-filled pores, and *arrow thickness* indicates release rates. Figures adapted from [172], Copyright 1999, with permission from Elsevier

insulin [177] and lysozyme [178], at least at low polymer concentrations, resulted in burst release with little or no subsequent protein release over weeks to months. This illustrates the relevance of the environmental conditions as well as other formulation parameters such as the polymer type and concentration in addition to the aforementioned importance of the properties of the polymer solvent.

Unfortunately, structural integrity of proteins formulated into in situ implants was not in the focus of the several studies cited above. However, there are data, for example, for benzyl benzoate systems suggesting enzymatic activity of lysozyme recovered from the release medium after 14 days to be lower than freshly dissolved protein but significantly higher than that of lysozyme solutions stored under identical conditions [178]. Other reports showed a partial or total loss of activity depending on the type of enzyme, but suggested cellular bioactivity and in vivo bioactivity of several growth factors tested within one or two weeks of release from PLGA/NMP systems [179]. Because of protein instability during in situ formation, considerable research is necessary before this system may become a viable strategy for delivery of a successful commercial biotechnology derived drug product.

Besides NMP, other water-miscible solvents (Table 8.5) have been explored for their capability to form in situ forming implants, including DMSO [180, 181], PEG and PEG-DME [182, 183], and glycofurol [184, 185]. A linear in vitro release and an in vivo efficiency of experimental therapeutic proteins were observed only in selected cases [184].

As pointed out before, besides solvent exchange kinetics, the initial thermodynamic state of the polymer solution as characterized by the polymer type, comonomer ratio, molecular weight, concentration, solvent type, and possibly the presence of nonsolvents is decisive for the properties of the prepared implants. For a given PLGA concentration, polymer precipitation from DMSO solutions was found to occur at about half of the percentage water uptake compared to precipitation of NMP polymer solutions [186]. When considering the limited availability of free water and interindividual differences in water diffusion rates at subcutaneous or intramuscular application sites, such differences in the initial thermodynamic state may largely affect solidification rates. It should be noted that commonly employed solvents clearly differ in their solvent power for relevant polymers, and thus in the thermodynamic state of the polymer solutions prepared at identical polymer concentration. Increasing the polymer concentration or the average molecular weight accelerated the polymer precipitation at the interface of the polymer solution and the aqueous surroundings and reduced solvent mediated burst release of hydrophobic drugs [186]. A continuous release of hydrophobic fenretinide without a lag phase or major burst release could be established by in situ implants from low average molecular weight PLGA with carboxyl end groups, which were shown to swell much more than their analoges prepared from PLGA bearing ethyl end groups [262]. The solidification at the implant surface due to fast precipitation has to be distinguished from the much slower process of implant hardening throughout the entire matrix. Thus, the overall solvent exchange and precipitation speed may be reduced for higher polymer concentration or higher average molecular weight, if a rapidly formed implant skin acts as diffusion barrier. This can lead to changes in the implant morphologies ranging from a structure with thin implant skins and finger-like macrovoids (high water uptake and fast overall precipitation) to sponges of homogeneous internal pore sizes with dense skin layers (slow precipitation) [171, 173]. The incorporation of additives, such as osmotically active sugars, salts, or water-soluble polymers may alter solvent exchange, polymer precipitation, and implant morphologies according to these principles with larger implant porosity for samples of faster water influx (Fig. 8.16) [185]. However, relatively small modifications in the polymer concentration or drug payload may not result in major changes in the efficacy of in situ forming implants in vivo [187].

So far, there are only limited noninvasive techniques available to characterize the implant formation/solidification particularly in an in vivo scenario. By benchtop magnetic resonance imaging, the implant position and fate including solidification and degradation could be visualized [188]. Electron paramagnetic resonance (EPR) spectroscopy was employed to test the microenvironment such as microviscosity around encapsulated spin probes in vitro. A fast solidification and complete solvent exchange was observed within a few hours for PEG 400 as a polar protic solvent of high water affinity. By contrast, ~30% of NMP as a polar aprotic solvent remained

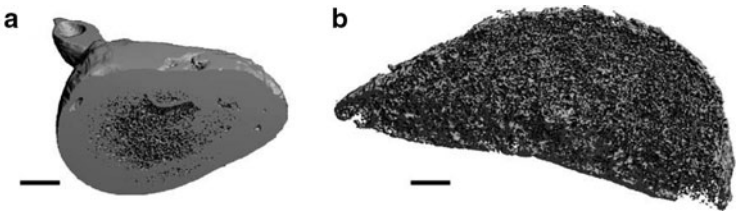


**Fig. 8.16** Effect of osmotically effective additives on the microstructure of in situ implants as visualized by microcomputed tomography. Implants were prepared from 10% (w/v) 50:50 PLGA in glycofurol either without (**a**) or with (**b**) spiking of polymer solutions with sodium chloride/water prior to injection (scale bars: 1 mm). Figures reprinted from [185], Copyright 2009, with permission from Elsevier

in the implants after 24 h as detected by EPR spectroscopy [188]. In an in vivo study, about 10% NMP was left at the same time in the identically prepared implants [189]. By using diagnostic ultrasound, a leakage of material from the liquid core due to swelling induced pressure was observed after 1–4 days in vitro and depended on the employed average molecular weight of the polymer [190]. Generally, this illustrates that similar to partially miscible solvents discussed above, a full solidification of in situ forming implants from fully water miscible solvents does not necessarily occur instantly and may also depend on the polymer concentration, type, and injection volume.

Different polymer types and morphologies, such as amorphous PLGA compared to semicrystalline poly(ε-caprolactone) (PCL), may translate in the formation of specific microstructures of in situ formed implants. Similar to what previously has been found for preformed implants from poly(L-lactic acid) [191], crystallization of PCL during solvent exchange of ethyl benzoate-based in situ implants resulted in an accelerated protein release. This finding was related to the formation of a porous microstructure for PCL in situ implants rather than for amorphous PLGA systems due to the PCL crystallization process. For PCL, the protein was excluded from crystalline domains and therefore was transfered into the nonsolvent rich aqueous phase [192]. Moreover, it has been reported that PLGA with a nonuniform distribution of glycolide and an average length of glycolide building blocks >~3 might exhibit some tendency to gelation in benzyl benzoate and other rather weak polymer solvents. This phenomenon may occur during storage and after injection, possibly due to polymer segment association that is not preferred in good solvents [193].

Finally, changes in drug properties may affect their release rates from in situ implants. Complexation of therapeutic proteins such as insulin with ions such as zinc has been known for decades to sustain their release from injectable depots, where an equilibrium between the complexed and the free, soluble form of the protein exists. This concept has also been applied to reduce the availability of leuprolide in its soluble form and, by this means, to reduce the burst release compared to the commercial Atrigel® formulation [194]. For human growth hormone, it has been found that zinc complexation could decrease the dissolution rate. In an in vivo study with protein quantification by an immunochemiluminometric assay, a direct comparison of two

**Table 8.6** Potential advantages and challenges associated with in situ-forming drug carriers

| Potential advantages | Potential challenges |
|---|---|
| Simple and low-cost preparation process | Burst release triggered by solvent exchange |
| Very mild preparation conditions | Nonlinear release profiles |
| Injection through medium-sized needles | Irritation of tissue due to solvent |
| No local anesthesia required | Polymer degradation when stored in organic solution with water impurities and drugs |
| Adaption of implant shape to cavities at application site | Multistep resuspension procedure for commercial (dry state) products |
| Individual sterilization of involved compounds | |

protein pretreatment protocols was reported, i.e., complexation and lyophilization (reduced solubility) vs. compression with 5% stearic acid and grinding (reduced accessible surface area). Interestingly, a similarly sustained protein release was shown for both samples compared to untreated human growth hormone [174]. For metoclopramide as a basic low molecular weight drug, formation of a drug salt reduced the drug release by impeding base-catalyzed polymer degradation [78].

Generally, drug carriers prepared by techniques that involve solvents have to pass residual solvent determination to exclude toxicity. Obviously, the evaluation of solvent related toxicity is particularly important when directly injecting relatively large quantities of solvent in the body. The analyzed water miscible solvents were mostly biocompatible when administered subcutaneously or intramuscularly as shown, for example, for DMSO and NMP [170, 181]. However, there are also some studies showing that creatine kinase was released at higher levels after injection of blank NMP based in situ forming implants compared to in situ forming microparticles [165]. Also, a higher in vitro hemolysis was observed for NMP compared to PEG-DMA [183]. By contrast, no hemolysis was found in vivo when volumes as large as 0.8 ml of different solvents were infused in several swine arteries; however, a stronger tendency to induce vasospasms was observed for DMSO rather than for NMP [195].

In summary (see Table 8.6), in situ forming implants advantageously reduce manufacturing costs as they do not require processing into a certain shape. For labile bioactive molecules, excluding high energy input, exposure to elevated temperature, or shear forces during preparation of in situ implants may be advantageous compared to polymer processing to a preformed shape. Still, great care should be applied to exclude instability (e.g. protein aggregation) of incorporated macromolecules in mixed systems of water and organic solvents. Additionally, for drugs that dissolve well in the employed organic solvent, a significant burst release and a nonlinear release profile may be obtained. As polymers may be unstable until administration, or solvents may leak from prefilled syringes when stored over a long time in the dissolved state, commercial products will provide the drug and polymer as powders in multicompartment syringes. Dissolution of polymers and suspension of drugs is required in a multistep procedure for these products, which might be associated with handling errors by patients and clinicians. Clinical data support the

assumption solvent that distribution in the tissue may be associated with local transient burning [196]. However, it has to be mentioned that compared to preformed implants, e.g., for leuprolide, which mostly are administered intramuscularly, the subcutaneous injection of in situ forming implants might be less painful [197]. Moreover, it should be noted that the capability to adapt a shape that fits to the geometry of the application site such as periodontal pockets [198, 199], is a unique feature of in situ forming implants.

## 8.5 Strategies to Control Drug Release Rates from Degradable Polymers Toward Zero Order Profiles

### *8.5.1 Relevance of In Vitro Zero Order Release and Common Limitations*

Most commonly, research on controlled release formulations aims to provide delivery systems that show zero order drug release [200], i.e., constant release rates over time. This is particularly important for drugs that are characterized by a narrow therapeutic window between the minimum effective concentration and the minimum toxic concentration. However, since the therapeutic window is an in vivo characteristic, the determination of release profiles in vitro strongly requires considerations on the relevance of the chosen parameters compared to in vivo conditions. In other words, particularly for degradable matrix polymers, e.g. plasticization, potential catalytic activities of enzymes, or possible alterations in local environment due to cellular immune response, may have to be included when translating an in vitro zero order release profile into an assumed in vivo behavior.

Also, in many cases, a zero order profile may not be required to achieve the desired pharmacological effects in vivo. It has already been described in the first studies on controlled release microparticles, e.g., for hydrophilic nafarelin as a LHRH agonist, that a triphasic in vitro and at least biphasic in vivo profile could strongly suppress testosterone production in male monkeys [201]. Similarly, nonlinear nafarelin release from microparticles in female monkeys showed suppressive effects on progesterone plasma levels and ovulation (Fig. 8.17) [202]. In this context, it should be noted that high plasma concentrations from drug released during burst or "log" phases may be acceptable in the case of LHRH agonists for pharmacological reasons, but can be more critical for other classes of bioactive molecules.

Besides the release rates, the drug's pharmacokinetics should also be taken into account. Particularly for hydrophobic drugs, accumulation in deep compartments such as the fatty tissue may occur. As a consequence, (1) the determined plasma concentration may not reflect the true amount of the released drug, (2) a possible release of the correct dose may not result in efficacy, and (3) the drug may be available for pharmacological effects even after exhaustion of the drug carrier due to a gradual distribution from the deep compartment into other compartments.

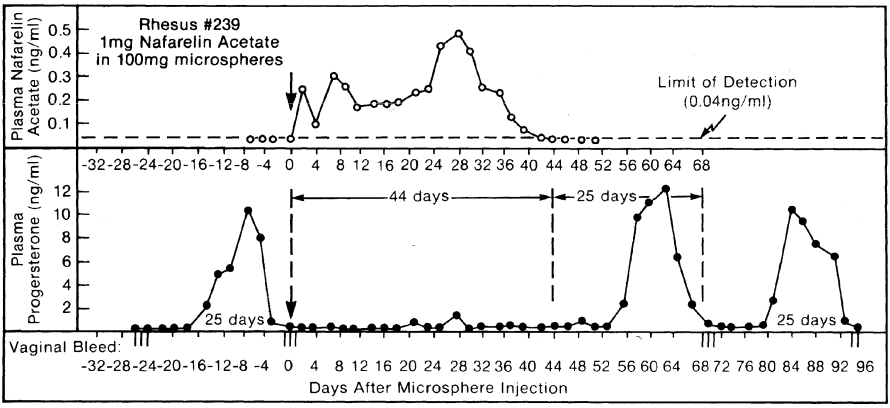


**Fig. 8.17** Release of nafarelin acetate (LHRH agonist) from PLGA microparticles in female rhesus monkeys. Drug plasma profile and effects on progesterone levels and interruption of menstrual cycles. Figure reprinted from [217], Copyright Harper & Row 1984, with permission from Wolters Kluwer Health

Compared to the total amount of literature on parenteral drug depots from degradable polymers, the aim of an in vitro zero order release has been achieved only in a limited number of setups. Often, a strong liberation of drug is observed in the initial hours of release. This burst release may be a consequence of several factors such as (1) poor embedding of drug particles in the matrix, e.g., due to high loading levels [97], (2) poor solubility of many drugs in the matrix polymer [203], (3) drug transport to the matrix's surface caused by solvent diffusion during preparation of the carrier, e.g., for emulsion based microparticle preparation techniques [204] or for drug loading of implants by swelling and drying [21] [205], and (4) dynamic pore formation and closure, which transiently controls diffusion paths [37]. Approaches to overcome undesired high initial release include strategies to improve miscibility of the drug and the polymer, to reduce diffusion to interfaces by advanced carrier processing techniques [203, 206], or to eventually wash off drug from the carrier's surface [207]. For controlling the subsequent sustained release, different strategies that rely on the usage of additives specifically tailored for a certain drug have been discussed above. However, some more general approaches that may enable a prolonged period of continuous release are again highlighted below.

### *8.5.2 Timely Separation of Diffusion-Controlled Drug Release and Collapse of Bulk-degrading Matrices*

Depending on the drugs physicochemical properties and the characteristics of the respective polymer matrix, drugs with and without capacity for matrix diffusion have to be differentiated (Fig. 8.1). In both cases, the employed loading levels are often higher than the drug solubility in the polymer phase, so that the incorporated

drug is dispersed as drug solid particles (e.g., amorphous and/or crystalline) in the matrix. For diffusible drugs and matrix polymers of relative hydrophilicity such as bulk eroding PLA/PLGA, this means that the drugs can be solubilized and slowly released upon hydration of the matrix. Thereby, drug release may take place before or simultaneously to polymer degradation. When the initial drug concentration is higher than the drug solubility and when the accessible surface area of the drug carrier does not change, constant release rates may be obtained only the case of certain geometries, e.g., coated hemispherical implants, which provide for a steadily increased area normal to transport as the increased diffusion path increases.

As noted before, drug diffusivity will be affected by polymer properties such as the polymer free volume, but also by the drug's hydrodynamic radius. In addition to the drug/polymer properties on the molecular level, processing-derived properties of the carrier such as the surface area and the porosity will impact the release kinetics. Furthermore, environmental conditions can control the drug diffusion in solution but also in the polymer phase (e.g., temperature) or can support the removal of the boundary layer (e.g., intensity of shaking, tissue perfusion). By using fluorescent probes, the dramatic impact of temperature on probe diffusion coefficient in the PLGA phase ranging over three orders of magnitude between 22.5 °C and 43 °C was shown [208].

When aiming to control drug diffusion rates through the polymer phase, attention should be paid to the polymer's wet state glass transition, which occurs close to body temperature for most PLGA qualities. Enhanced plasticization may therefore sensitively translate into increased drug diffusion rates. Importantly, for degradable polymers, material properties, properties of the prepared carrier matrix, and in many cases also microenvironmental conditions dynamically change over time, i.e., enable higher drug diffusion rates. In some cases this may compensate the lower diffusion rates, which occur upon exhaustion of undissolved drug particles in late stages of the release. In other cases, polymer degradation driven increases in drug diffusivity may result in a secondary, possibly less controlled rapid release phase. Therefore, by selecting a combination of a hydrophilic, diffusible drug and a bulk degrading material with low degradation rates, a timely separation of drug release and degradation may be achieved and late state dose dumping linked to polymer degradation/ matrix erosion may be avoided. Additionally, employing slowly degrading polymers such as PLA may reduce the burst release of hydrophilic compounds [209].

### *8.5.3 Blending Approaches for Bulk Degrading Carriers*

Major challenges in the development of controlled release carriers are "lag phases". Most commonly, the "lag phase" is considered as a slow release or even as an absence of reasonable drug release due to poor drug diffusion in an initially dense matrix. Upon degradation-driven increase in matrix porosity, the "lag phase" may be followed by a rapid release phase. This translates into an "S" shaped release curve. An alternative explanation for the beginning of the lag phase for

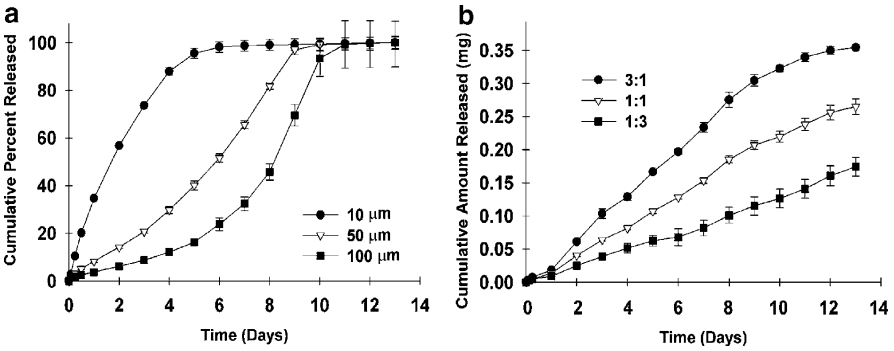


**Fig. 8.18** Blending approach to modify the release of piroxicam from uniformly sized PLGA microparticles. (**a**) Cumulative percentile release from different microparticle sizes (10, 50, and 100 µm in diameter). (**b**) Cumulative release of drug mass as obtained by different mixing ratios of 10 µm and 50 µm microparticles shown in panel **a**. Figures adapted from [24], Copyright (2002), with permission from Elsevier

initially porous materials involves spontaneous pore closing as driving mechanism. The pore closing phenomenon has been shown for polymers, which have a wet-state glass transition temperature at about body temperature as it is the case for most PLGA qualities [15, 34, 37].

Typically, lag phases in diffusion controlled release systems are observed for larger molecules or hydrophobic drugs, which require the access of larger volumes of water for drug solubilization or larger pore diameters for drug diffusion. Therefore, blending of high average molecular weight polymer with a small portion of a low average molecular weight polymer was one of the first methods identified to ensure continuous release of peptides [25] and hydrophobic drugs [210]. By employing this approach, the low molecular weight component presumably reaches more rapidly the critical chain length for aqueous solubility, is removed from the matrix, and leaves a porous structure. These pores enable a higher water influx, lower diffusion length from bulk to pore, and, thus, higher drug release rates. This effect could potentially also be achieved by blending the matrix polymer, preferentially in a water free preparation technique, with water soluble polymers [211, 212] or other porogens [131], which gradually leach out during release [16].

Diffusion lengths of both water entering the matrix and dissolved drug being released clearly depend on the surface area/volume ratio, e.g., for nonporous particulate drug carriers. High surface area/volume ratios, i.e., small particle sizes are often associated with higher (initial) release rates. Larger particles may show a lag phase (Fig. 8.18a) [24]. By blending preformed, uniformly sized polymer microparticles of different radii and drug diffusion lengths, linear release profiles can be established (Fig. 8.18b). Others have reported modified peptide release by mixing microparticles of different individual release profiles, which were manufactured from PLGA blends at different blending ratios and PLGA molecular weights [213].

By contrast, for peptides and proteins, which exhibit limited or no matrix diffusion, remarkably little size dependence of PLGA release after the initial

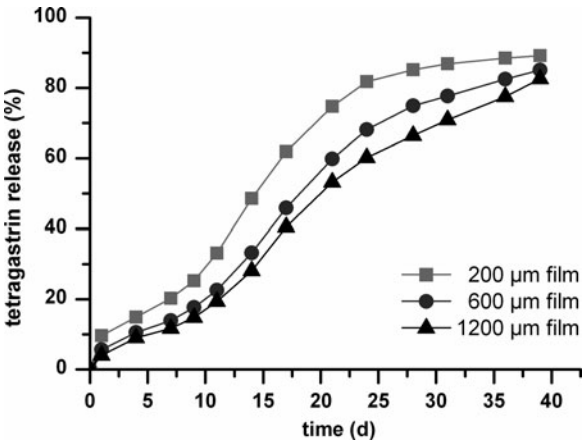


**Fig. 8.19** Virtual independence of implant thickness (200–1,200 µm) on release kinetics of tetragastrin (tetra peptide, $M_w$ 731 Da) after initial burst release from 50:50 PLGA ($M_w$ ~15 kDa, high PD) films prepared by melt compression. Graphical illustration of data from [25]

burst has long been understood [25], as shown in Fig. 8.19 for tetragastrin. As we know, the erosion time of PLGA matrices may be insubstantially different for microparticles compared to millimeter scale implants. Therefore, unlike the piroxicam case (see Fig. 8.18), one should not be confused into thinking control of the implant size is a rational means of controlling the release of peptides and proteins, which most often rely on erosion-controlled release.

### *8.5.4 Employing Surface Eroding Carriers*

For drugs that do not easily diffuse in bulk degrading materials or at least for carriers from these materials that do not have a porous microstructure, a zero order drug release will unlikely be found. Particularly for protein drugs with sensitivity to acidic microenvironment, prolonged exposure to acidic products of polymer degradation such as present inside bulk eroding poly(α-hydroxy esters) may induce protein instability in many cases. Therefore, surface eroding polyorthoesters or polyanhydrides are often believed to be a guarantee for zero order release profiles, since degradation products are not accumulated and drug diffusion is not the controlling mechanism of release. However, a perfect zero order release may theoretically only be observed for certain matrix geometries with a minimal change in surface area during erosion [214]. This condition is best fulfilled for, e.g., films rather than microparticles. Additionally, in previous sections some examples were provided illustrating that the release of drugs was not zero order as desired for the entire time frame from administration to exhaustion (Figs. 8.8, 8.13 and 8.14). Unfortunately, for different reasons including patent strategies, the surface eroding polyorthoesters or polyanhydrides are presently not commercially available, which limits their broad exploration for release of nonmatrix diffusing drugs.

## 8.6 Conclusion

Degradable, polymer-based drug carriers remain a scientifically and commercially important strategy to control the release of bioactive molecules over time periods ranging from several days to several months. The therapeutic aim and drug properties strongly determine the choice of carrier type such as microparticles, preformed implants, or in situ implants. Drug release from these carriers is governed by a complex interplay of parameters including drug properties, polymer degradation/erosion characteristics, and osmotically driven mechanisms, as well as environmental conditions and processing-derived device properties. Importantly, when changing from stable small molecule drugs to substances as sensitive as proteins, stability of the encapsulated compound may become the most challenging task for these formulations. Additives as possibly required to stabilize proteins may often be relevant also in terms of water uptake and degradation of the polymeric carrier. Therefore, a careful selection of the degradable matrix polymer is essential to control the rate and overall duration of drug release. It again has to be pointed out that besides the polymer properties, also processing parameters, additives, and drug properties have to be similarly weighted in view of release rates. Therefore, a mechanistic and empirical understanding of the involved processes for different carrier types as reported here is essential to establish specific release profiles from degradable drug carriers.

## References

1. Ogawa Y, Yamamoto M, Okada H, Yashiki T, Shimamoto T (1988) A new technique to efficiently entrap leuprolide acetate into microcapsules of polylactic acid or copoly(lactic/glycolic) acid. Chem Pharm Bull 36:1095–1103
2. Hou Q, Chau DY, Pratoomsoot C, Tighe PJ, Dua HS, Shakesheff KM, Rose FR (2008) In situ gelling hydrogels incorporating microparticles as drug delivery carriers for regenerative medicine. J Pharm Sci 97:3972–3980
3. Harrison BS, Eberli D, Lee SJ, Atala A, Yoo JJ (2007) Oxygen producing biomaterials for tissue regeneration. Biomaterials 28:4628–4634
4. Wenk E, Meinel AJ, Wildy S, Merkle HP, Meinel L (2009) Microporous silk fibroin scaffolds embedding PLGA microparticles for controlled growth factor delivery in tissue engineering. Biomaterials 30:2571–2581
5. Tamada JA, Langer R (1993) Erosion kinetics of hydrolytically degradable polymers. Proc Natl Acad Sci USA 90:552–556
6. Gopferich A (1996) Mechanisms of polymer degradation and erosion. Biomaterials 17:103–114
7. Gopferich A (1996) Polymer degradation and erosion: mechanisms and applications. Eur J Pharm Biopharm 42:1–11
8. Schwendeman SP, Cardamone M, Klibanov AM, Langer R, Brandon MR (1996) Stability of proteins and their delivery from biodegradable polymer microspheres. In: Cohen S, Bernstein H (eds) Microparticulate systems for the delivery of proteins and vaccines. Marcel Decker, New York, pp 1–49

9. Zhu G, Mallery SR, Schwendeman SP (2000) Stabilization of proteins encapsulated in injectable poly (lactide- co-glycolide). Nat Biotechnol 18:52–57
10. Perez C, Castellanos IJ, Costantino HR, Al-Azzam W, Griebenow K (2002) Recent trends in stabilizing protein structure upon encapsulation and release from bioerodible polymers. J Pharm Pharmacol 54:301–313
11. Giteau A, Venier-Julienne MC, Aubert-Pouessel A, Benoit JP (2008) How to achieve sustained and complete protein release from PLGA-based microparticles? Int J Pharm 350:14–26
12. van der Walle CF, Sharma G, Ravi Kumar M (2009) Current approaches to stabilising and analysing proteins during microencapsulation in PLGA. Expert Opin Drug Deliv 6:177–186
13. Zhong Y, Zhang L, Ding AG, Shenderova A, Zhu G, Pei P, Chen RR, Mallery SR, Mooney DJ, Schwendeman SP (2007) Rescue of SCID murine ischemic hindlimbs with pH-modified rhbFGF/poly(DL-lactic-co-glycolic acid) implants. J Control Release 122:331–337
14. Desai KG, Mallery SR, Schwendeman SP (2008) Effect of formulation parameters on 2-methoxyestradiol release from injectable cylindrical poly(DL-lactide-co-glycolide) implants. Eur J Pharm Biopharm 70:187–198
15. Wang J, Wang BM, Schwendeman SP (2004) Mechanistic evaluation of the glucose-induced reduction in initial burst release of octreotide acetate from poly(D, L-lactide-co-glycolide) microspheres. Biomaterials 25:1919–1927
16. Wischke C, Schwendeman SP (2008) Principles of encapsulating hydrophobic drugs in PLA/PLGA microparticles. Int J Pharm 364:298–327
17. Wischke C, Borchert HH, Zimmermann J, Siebenbrodt I, Lorenzen DR (2006) Stable cationic microparticles for enhanced model antigen delivery to dendritic cells. J Control Release 114:359–368
18. Schlosser E, Mueller M, Fischer S, Basta S, Busch DH, Gander B, Groettrup M (2008) TLR ligands and antigen need to be coencapsulated into the same biodegradable microsphere for the generation of potent cytotoxic T lymphocyte responses. Vaccine 26:1626–1637
19. Arias JL, Gallardo V, Ruiz MA (2009) Engineering of poly(butylcyanoacrylate) nanoparticles for the enhancement of the antitumor activity of gemcitabine. Biomacromolecules 10:2310–2318
20. Iwai K, Maeda H, Konno T (1984) Use of oily contrast medium for selective drug targeting to tumor: enhanced therapeutic effect and X-ray image. Cancer Res 44:2115–2121
21. Wischke C, Neffe AT, Steuer S, Lendlein A (2009) Evaluation of a degradable shape-memory polymer network as matrix for controlled drug release. J Control Release 138:243–250
22. Wischke C, Neffe AT, Lendlein A (2010) Controlled drug release from shape-memory polymers. Adv Polym Sci 226:177–205
23. Wischke C, Lendlein A (2010) Shape-memory polymers as drug carriers – a multifunctional system. Pharm Res 27(4):527–529
24. Berkland C, King M, Cox A, Kim K, Pack DW (2002) Precise control of PLG microsphere size provides enhanced control of drug release rate. J Control Release 82:137–147
25. Hutchinson FG (1986) Continuous release pharmaceutical compositions. European Patent EP 58 481
26. Klose D, Siepmann F, Willart JF, Descamps M, Siepmann J (2010) Drug release from PLGA-based microparticles: effects of the "microparticle:bulk fluid" ratio. Int J Pharm 383:123–131
27. Kulkarni A, Reiche J, Hartmann J, Kratz K, Lendlein A (2008) Selective enzymatic degradation of poly(epsilon-caprolactone) containing multiblock copolymers. Eur J Pharm Biopharm 68:46–56
28. Elkharraz K, Faisant N, Guse C, Siepmann F, Arica-Yegin B, Oger JM, Gust R, Goepferich A, Benoit JP, Siepmann J (2006) Paclitaxel-loaded microparticles and implants for the treatment of brain cancer: preparation and physicochemical characterization. Int J Pharm 314:127–136

29. Zhao ZJ, Wang Q, Zhang L, Liu YC (2007) A different diffusion mechanism for drug molecules in amorphous polymers. J Phys Chem B 111:4411–4416
30. Schwendeman SP, Tobio M, Joworowicz M, Alonso MJ, Langer R (1998) New strategies for the microencapsulation of tetanus vaccine. J Microencapsul 15:299–318
31. Domb AJ (1993) Degradable polymer blends.1. Screening of miscible polymers. J Polym Sci A Polym Chem 31:1973–1981
32. Matsumoto A, Matsukawa Y, Horikiri Y, Suzuki T (2006) Rupture and drug release characteristics of multi-reservoir type microspheres with poly(dl-lactide-co-glycolide) and poly(dl-lactide). Int J Pharm 327:110–116
33. Wang J (2000) Characterization of microsphere drug delivery systems during encapsulation and initial drug release. The Ohio State University, Columbus
34. Kang J, Schwendeman SP (2007) Pore closing and opening in biodegradable polymers and their effect on the controlled release of proteins. Mol Pharm 4:104–118
35. Wool RP, Oconnor KM (1981) A theory of crack healing in polymers. J Appl Phys 52:5953–5963
36. Wool RP (2008) Self-healing materials: a review. Soft Matter 4:400–418
37. Wang J, Wang BM, Schwendeman SP (2002) Characterization of the initial burst release of a model peptide from poly(D, L-lactide-co-glycolide) microspheres. J Control Release 82:289–307
38. Heller J (1980) Controlled release of biologically-active compounds from bioerodible polymers. Biomaterials 1:51–57
39. Leonard F, Kulkarni RK, Brandes G, Nelson J, Cameron JJ (1966) Synthesis and degradation of poly (alkyl a-cyanoacrylates). J Appl Polym Sci 10:259–272
40. Ryan B, McCann G (1996) Novel sub-ceiling temperature rapid depolymerization-repolymerization reactions of cyanoacrylate polymers. Macromol Rapid Commun 17:217–227
41. Lenaerts V, Couvreur P, Christiaens-Leyh D, Joiris E, Roland M, Rollman B, Speiser P (1984) Degradation of poly (isobutyl cyanoacrylate) nanoparticles. Biomaterials 5:65–68
42. Scherer D, Robinson JR, Kreuter J (1994) Influence of enzymes on the stability of polybutyl-cyanoacrylate nanoparticles. Int J Pharm 101:165–168
43. Nicolas J, Couvreur P (2009) Synthesis of poly(alkyl cyanoacrylate)-based colloidal nanomedicines. Wiley Interdiscip Rev Nanomed Nanobiotechnol 1:111–127
44. Wischke C, Neffe AT, Steuer S, Lendlein A (2010) AB-polymer Networks with Cooligoester and Poly(n-butyl acrylate) Segments as a Multifunctional Matrix for Controlled Drug Release. Macromol Biosci 10:1063–1072
45. Augst AD, Kong HJ, Mooney DJ (2006) Alginate hydrogels as biomaterials. Macromol Biosci 6:623–633
46. Madaghiele M, Piccinno A, Saponaro M, Maffezzoli A, Sannino A (2009) Collagen- and gelatine-based films sealing vascular prostheses: evaluation of the degree of crosslinking for optimal blood impermeability. J Mater Sci Mater Med 20(10):1979–1989
47. Kraehenbuehl TP, Ferreira LS, Zammaretti P, Hubbell JA, Langer R (2009) Cell-responsive hydrogel for encapsulation of vascular cells. Biomaterials 30:4318–4324
48. Li SM, Garreau H, Vert M (1990) Structure-property relationships in the case of the degradation of massive poly(alpha -hydroxy acids) in aqueous media. Part 2 degradation of/actide-g/yco/ide copo/ymers. PLA37.5GA25 and PLA75GA25. J Mater Sci Mater Med 1:131–139
49. Park TG (1995) Degradation of poly(lactic-co-glycolic acid) microspheres: effect of copolymer composition. Biomaterials 16:1123–1130
50. Maniar M, Xie XD, Domb AJ (1990) Polyanhydrides. V. Branched polyanhydrides. Biomaterials 11:690–694
51. Kissel T, Brich Z, Bantle S, Lancranjan I, Nimmerfall F, Vit P (1991) Parenteral depot-systems on the basis of biodegradable polyesters. J Control Release 16:27–41

52. Jerome C, Lecomte P (2008) Recent advances in the synthesis of aliphatic polyesters by ring-opening polymerization. Adv Drug Deliv Rev 60:1056–1076
53. Ding AG, Schwendeman SP (2004) Determination of water-soluble acid distribution in poly (lactide-co-glycolide). J Pharm Sci 93:322–331
54. Siepmann J, Elkharraz K, Siepmann F, Klose D (2005) How autocatalysis accelerates drug release from PLGA-based microparticles: a quantitative treatment. Biomacromolecules 6:2312–2319
55. Li L, Schwendeman SP (2005) Mapping neutral microclimate pH in PLGA microspheres. J Control Release 101:163–173
56. Li SM, Garreau H, Vert M (1990) Structure-property relationships in the case of the degradation of massive aliphatic poly-(alpha-hydroxy acids) in aqueous media. Part 1 poly (DL-lactic acid). J Mater Sci Mater Med 1:123–130
57. Li S (1999) Hydrolytic degradation characteristics of aliphatic polyesters derived from lactic and glycolic acids. J Biomed Mater Res 48:342–353
58. Lu L, Garcia CA, Mikos AG (1999) In vitro degradation of thin poly(DL-lactic-co-glycolic acid) films. J Biomed Mater Res 46:236–244
59. von Burkersroda F, Schedl L, Gopferich A (2002) Why degradable polymers undergo surface erosion or bulk erosion. Biomaterials 23:4221–4231
60. Rothstein SN, Federspiel WJ, Little SR (2009) A unified mathematical model for the prediction of controlled release from surface and bulk eroding polymer matrices. Biomaterials 30:1657–1664
61. Furr BJA, Hutchinson FG (1992) A biodegradable delivery system for peptides: preclinical experience with the gonadotrophin-releasing hormone agonist Zoladex. J Control Release 21:117–128
62. Husmann M, Schenderlein S, Luck M, Lindner H, Kleinebudde P (2002) Polymer erosion in PLGA microparticles produced by phase separation method. Int J Pharm 242:277–280
63. Grizzi I, Garreau H, Li S, Vert M (1995) Hydrolytic degradation of devices based on poly (DL-lactic acid) size-dependence. Biomaterials 16:305–311
64. Witschi C, Doelker E (1998) Influence of the microencapsulation method and peptide loading on poly(lactic acid) and poly(lactic-co-glycolic acid) degradation during in vitro testing. J Control Release 51:327–341
65. Bhardwaj R, Blanchard J (1998) In vitro characterization and in vivo release profile of a poly (D, L-lactide-co-glycolide)-based implant delivery system for the alpha-MSH analog, melanotan-I. Int J Pharm 170:109–117
66. Liggins RT, Burt HM (2001) Paclitaxel loaded poly(L-lactic acid) microspheres: properties of microspheres made with low molecular weight polymers. Int J Pharm 222:19–33
67. Vidil C, Braud C, Garreau H, Vert M (1995) Monitoring of the poly(D, L-lactic acid) degradation by-products by capillary zone electrophoresis. J Chromatogr A 711:323–329
68. Joshi A, Himmelstein KJ (1990) Kinetics of controlled release from acid catalyzed polymeric matrices. Polym Prepr 31:175–176
69. Gopferich A, Tessmar J (2002) Polyanhydride degradation and erosion. Adv Drug Deliv Rev 54:911–931
70. Xu XJ, Sy JC, Shastri VP (2006) Towards developing surface eroding poly(alpha-hydroxy acids). Biomaterials 27:3021–3030
71. Alexis F (2005) Factors affecting the degradation and drug-release mechanism of poly(lactic acid) and poly (lactic acid)-co-(glycolic acid). Polym Int 54:36–46
72. Zolnik BS, Burgess DJ (2008) Evaluation of in vivo-in vitro release of dexamethasone from PLGA microspheres. J Control Release 127:137–145
73. Hakkarainen M (2002) Aliphatic polyesters: abiotic and biotic degradation and degradation products. Adv Polym Sci 157:113–138
74. Pitt CG, Hendren RW, Schindler A, Woodward SC (1984) The enzymatic surface erosion of aliphatic polyesters. J Control Release 1:3–14

75. Liu F, Zhao ZX, Yang J, Wei J, Li SM (2009) Enzyme-catalyzed degradation of poly(L-lactide)/poly(epsilon-caprolactone) diblock, triblock and four-armed copolymers. Polym Degrad Stabil 94:227–233
76. Desai KG, Mallery SR, Schwendeman SP (2008) Formulation and characterization of injectable poly(DL-lactide-co-glycolide) implants loaded with N-acetylcysteine, a MMP inhibitor. Pharm Res 25:586–597
77. Maulding HV, Tice TR, Cowar DR, Fong JW, Pearson JE, Nazareno JP (1986) Biodegradable microcapsules: acceleration of polymeric excipient hydrolytic rate by incorporation of a basic medicament. J Control Release 3:103–117
78. Wang L, Venkatraman S, Kleiner L (2004) Drug release from injectable depots: two different in vitro mechanisms. J Control Release 99:207–216
79. Cha Y, Pitt CG (1988) A one-week subdermal delivery system for l-methadone based on biodegradable microcapsules. J Control Release 8:69–78
80. Cha Y, Pitt CG (1989) The acceleration of degradation controlled drug delivery from polyester microspheres. J Control Release 8:259–265
81. Siegel SJ, Kahn JB, Metzger K, Winey KI, Werner K, Dan N (2006) Effect of drug type on the degradation rate of PLGA matrices. Eur J Pharm Biopharm 64:287–293
82. Heller J, Barr J (2005) Biochronomer technology. Expert Opin Drug Deliv 2:169–183
83. APF530 study (2009) APF530 or Palonosetron Combined With Dexamethasone in Preventing Nausea and Vomiting in Patients Receiving Chemotherapy for Cancer (NCT00343460). U.S. National Institutes of Health. http://www.ClinicalTRials.gov
84. AP Pharma (2010) Press release: A.P. Pharma Receives FDA Complete Response Letter for APF530. http://www.appharma.com/PDFs/03-19-10%20Complete%20Response%20Letter.pdf. Accessed 18 Jun 2010
85. Packhaeuser CB, Schnieders J, Oster CG, Kissel T (2004) In situ forming parenteral drug delivery systems: an overview. Eur J Pharm Biopharm 58:445–455
86. Exner AA, Saidel GM (2008) Drug-eluting polymer implants in cancer therapy. Expert Opin Drug Deliv 5:775–788
87. Wykrzykowska JJ, Onuma Y, Serruys PW (2009) Advances in stent drug delivery: the future is in bioabsorbable stents. Expert Opin Drug Deliv 6:113–126
88. Su S-H (2007) Mini Review of the fully biodegradable polymeric stents. Recent Pat Eng 1:244–250
89. ANZHSN (2007) Biodegradable stents for coronary artery disease. Australian Government, Department of Health and Aging. http://www.surgeons.org/AM/Template.cfm?Section=ASERNIP_S_NET_S_Database&Template=/CM/ContentDisplay.cfm&ContentFileID=24135
90. Ramcharitar S, Serruys PW (2008) Fully biodegradable coronary stents: progress to date. Am J Cardiovasc Drugs 8:305–314
91. Weber N, Pesnell A, Bolikal D, Zeltinger J, Kohn J (2007) Viscoelastic properties of fibrinogen adsorbed to the surface of biomaterials used in blood-contacting medical devices. Langmuir 23:3298–3304
92. Lendlein A, Behl A, Hiebl B, Wischke C (2010) Shape-memory polymers as technology platform for biomedical applications. Expert Rev Med Dev 7:357–379
93. Okada H, Ogawa Y, Yashiki T (1987) Prolonged release microcapsule and its production. United States Patent US 4,652,441
94. Castellanos IJ, Cuadrado WO, Griebenow K (2001) Prevention of structural perturbations and aggregation upon encapsulation of bovine serum albumin into poly(lactide-co-glycolide) micropheres using the solid-in-oil-in water technique. J Pharm Pharmacol 53:1099–1107
95. Carrasquillo KG, Carro JC, Alejandro A, Toro DD, Griebenow K (2001) Reduction of structural perturbations in bovine serum albumin by non-aqueous microencapsulation. J Pharm Pharmacol 53:115–120

96. Johnson OL, Cleland JL, Lee HJ, Charnis M, Duenas E, Jaworowicz W, Shepard D, Shahzamani A, Jones AJ, Putney SD (1996) A month-long effect from a single injection of microencapsulated human growth hormone. Nat Med 2:795–799
97. Wakiyama N, Juni K, Nakano M (1981) Preparation and evaluation in vitro of polylactic acid microspheres containing local anesthetics. Chem Pharm Bull 29:3363–3368
98. Dean RL (2005) The preclinical development of Medisorb Naltrexone, a once a month long acting injection, for the treatment of alcohol dependence. Front Biosci 10:643–655
99. Sah H, Lee B (2006) Development of new microencapsulation techniques useful for the preparation of PLGA microspheres. Macromol Rapid Commun 27:1845–1851
100. Wada R, Hyon SH, Ikada Y (1990) Lactic-acid oligomer microspheres containing hydrophilic drugs. J Pharm Sci 79:919–924
101. Bodmeier R, Chen HG (1988) Preparation of biodegradable Poly (+/−) lactide microparticles using a spray-drying technique. J Pharm Pharmacol 40:754–757
102. Leelarasamee N, Howard SA, Malanga CJ, Luzzi LA, Hogan TF, Kandzari SJ, Ma JK (1986) Kinetics of drug release from polylactic acid-hydrocortisone microcapsules. J Microencapsul 3:171–179
103. Lill N, Sandow J (1995) Langwirkende bioabbaubare Mikropartikel und ein Verfahren zur Herstellung. European Patent
104. Bodmer D, Fong JW, Kissel T, Maulding HV, Nagele O, Pearson JE (1996) Sustained release formulations of water soluble peptides. United States Patent US 5,538,739
105. Kissel T, Maretschek S, Packhaeuser CB, Schnieders J, Seidel N (2006) Microencapsulation techniques for parenteral depot systems and their application in the pharmaceutical industry. In: Benita S (ed) Microencapsulation: methods and industrial application. CRC, Boca Raton, FL
106. Smith A, Hunneyball IM (1986) Evaluation of poly(lactic acid) as a biodegradable drug delivery system for parenteral administration. Int J Pharm 30:215–220
107. Mishima K (2008) Biodegradable particle formation for drug and gene delivery using supercritical fluid and dense gas. Adv Drug Deliv Rev 60:411–432
108. Williams JR, Clifford AA, Al-Saidi SH (2002) Supercritical fluids and their applications in biotechnology and related areas. Mol Biotechnol 22:263–286
109. Wischke C, Borchert HH (2006) Influence of the primary emulsification procedure on the characteristics of small protein-loaded PLGA microparticles for antigen delivery. J Microencapsul 23:435–448
110. Okada H (1997) One- and three-month release injectable microspheres of the LH-RH superagonist leuprorelin acetate. Adv Drug Deliv Rev 28:43–70
111. Zhou T, Lewis H, Foster RE, Schwendeman SP (1998) Development of a multiple-drug delivery implant for intraocular management of proliferative vitreoretinopathy. J Control Release 55:281–295
112. Ghalanbor Z, Korber M, Bodmeier R (2010) Improved lysozyme stability and release properties of poly(lactide-co-glycolide) implants prepared by hot-melt extrusion. Pharm Res 27:371–379
113. Breitenbach J (2002) Melt extrusion: from process to drug delivery technology. Eur J Pharm Biopharm 54:107–117
114. Rothen-Weinhold A, Schwach-Abdellaoui K, Barr J, Ng SY, Shen HR, Gurny R, Heller J (2001) Release of BSA from poly(ortho ester) extruded thin strands. J Control Release 71:31–37
115. Li LC, Deng J, Stephens D (2002) Polyanhydride implant for antibiotic delivery – from the bench to the clinic. Adv Drug Deliv Rev 54:963–986
116. Grossman SA, Reinhard C, Colvin OM, Chasin M, Brundrett R, Tamargo RJ, Brem H (1992) The intracerebral distribution of BCNU delivered by surgically implanted biodegradable polymers. J Neurosurg 76:640–647
117. Chasin B, Hollenbeck G, Brem H, Grossman S, Colvin M, Langer R (1990) Interstitial drug therapy for brain tumors: a case study. Drug Dev Ind Pharm 16:2579–2594

118. Akbari H, D'Emanuele A, Attwood D (1998) Effect of fabrication technique on the erosion characteristics of polyanhydride matrices. Pharm Dev Technol 3:251–259
119. Laurencin CT, Ibim SEM, Langer RS (1995) Poly(anhydrides). In: Hollinger JO (ed) Biomedical applications of synthetic biodegradable polymers. CRC, Boca Raton, FL, pp 59–102
120. Weiler W, Gogolewski S (1996) Enhancement of the mechanical properties of polylactides by solid-state extrusion.1. Poly(D-lactide). Biomaterials 17:529–535
121. Gogolewski S, Jovanovic M, Perren SM, Dillon JG, Hughes MK (1993) The effect of melt-processing on the degradation of selected polyhydroxyacids – polylactides, polyhydroxybutyrate, and polyhydroxybutyrate-co-valerates. Polym Degrad Stabil 40:313–322
122. Rothen-Weinhold A, Besseghir K, Vuaridel E, Sublet E, Oudry N, Gurny R (1999) Stability studies of a somatostatin analogue in biodegradable implants. Int J Pharm 178:213–221
123. Leighton D, Acrivos A (1987) The shear-induced migration of particles in concentrated suspensions. J Fluid Mech 181:415–439
124. Nott PR, Brady JF (1994) Pressure-driven flow of suspensions – simulation and theory. J Fluid Mech 275:157–199
125. Deng J, Li L, Stephens D, Tian Y, Robinson D (2004) Effect of postmolding heat treatment on in vitro properties of a polyanhydride implant containing gentamicin sulfate. Drug Dev Ind Pharm 30:341–346
126. Choi SH, Park TG (2000) Hydrophobic ion pair formation between leuprolide and sodium oleate for sustained release from biodegradable polymeric microspheres. Int J Pharm 203:193–202
127. Schwendeman SP (2002) Recent advances in the stabilization of proteins encapsulated in injectable PLGA delivery systems. Crit Rev Ther Drug Carrier Syst 19:73–98
128. Zhu G, Schwendeman SP (2000) Stabilization of proteins encapsulated in cylindrical poly (lactide-co-glycolide) implants: mechanism of stabilization by basic additives. Pharm Res 17:351–357
129. Kang JC, Schwendeman SP (2002) Comparison of the effects of Mg(OH)(2) and sucrose on the stability of bovine serum albumin encapsulated in injectable poly(D, L-lactide-co-glycolide) implants. Biomaterials 23:239–245
130. Jiang WL, Schwendeman SP (2008) Stabilization of tetanus toxoid encapsulated in PLGA microspheres. Mol Pharm 5:808–817
131. Zhang Y, Zale S, Sawyer L, Bernstein H (1997) Effects of metal salts on poly(DL-lactide-co-glycolide) polymer hydrolysis. J Biomed Mater Res 34:531–538
132. Sandow J, von Rechenberg W, Seidel H, Keil M (1989) Experimental studies on tissue tolerance and on biodegradation of polylactide/glycolide-buserelin implants in rats. In: Aumüller G (ed) New aspects in the regulation of prostatic function. W. Zuckerschwerdt Verlag GmbH, Munich, pp 157–166
133. Siepmann J, Gopferich A (2001) Mathematical modeling of bioerodible, polymeric drug delivery systems. Adv Drug Deliv Rev 48:229–247
134. Lin SH, Kleinberg LR (2008) Carmustine wafers: localized delivery of chemotherapeutic agents in CNS malignancies. Expert Rev Anticancer Ther 8:343–359
135. Dang W, Daviau T, Brem H (1996) Morphological characterization of polyanhydride biodegradable implant gliadel during in vitro and in vivo erosion using scanning electron microscopy. Pharm Res 13:683–691
136. Kumar N, Langer RS, Domb AJ (2002) Polyanhydrides: an overview. Adv Drug Deliv Rev 54:889–910
137. Domb AJ, Israel ZH, Elmalak O, Teomim D, Bentolila A (1999) Preparation and characterization of carmustine loaded polyanhydride wafers for treating brain tumors. Pharm Res 16:762–765
138. Dang WB, Daviau T, Ying P, Zhao Y, Nowotnik D, Clow CS, Tyler B, Brem H (1996) Effects of GLIADEL(R) wafer initial molecular weight on the erosion of wafer and release of BCNU. J Control Release 42:83–92

139. Jeong B, Bae YH, Lee DS, Kim SW (1997) Biodegradable block copolymers as injectable drug-delivery systems. Nature 388:860–862
140. Couffin-Hoarau AC, Motulsky A, Delmas P, Leroux JC (2004) In situ-forming pharmaceutical organogels based on the self-assembly of L-alanine derivatives. Pharm Res 21:454–457
141. Motulsky A, Lafleur M, Couffin-Hoarau AC, Hoarau D, Boury F, Benoit JP, Leroux JC (2005) Characterization and biocompatibility of organogels based on L-alanine for parenteral drug delivery implants. Biomaterials 26:6242–6253
142. Jeong B, Bae YH, Kim SW (1999) Thermoreversible gelation of PEG-PLGA-PEG triblock copolymer aqueous solutions. Macromolecules 32:7064–7069
143. Gong C, Shi S, Wu L, Gou M, Yin Q, Guo Q, Dong P, Zhang F, Luo F, Zhao X, Wei Y, Qian Z (2009) Biodegradable in situ gel-forming controlled drug delivery system based on thermosensitive PCL-PEG-PCL hydrogel. Part 2: sol-gel-sol transition and drug delivery behavior. Acta Biomater 5:3358–3370
144. Sarkar N (1979) Thermal gelation properties of methyl and hydroxypropyl methylcellulose. J Appl Polym Sci 24:1073–1087
145. Tate MC, Shear DA, Hoffman SW, Stein DG, LaPlaca MC (2001) Biocompatibility of methylcellulose-based constructs designed for intracerebral gelation following experimental traumatic brain injury. Biomaterials 22:1113–1123
146. Park KM, Shin YM, Joung YK, Shin H, Park KD (2010) In situ forming hydrogels based on tyramine conjugated 4-Arm-PPO-PEO via enzymatic oxidative reaction. Biomacromolecules 11(3):706–712
147. Slepian MJ, Hubbell JA (1997) Polymeric endoluminal gel paving: hydrogel systems for local barrier creation and site-specific drug delivery. Adv Drug Deliv Rev 24:11–30
148. Ramakumar S, Roberts WW, Fugita OE, Colegrove P, Nicol TM, Jarrett TW, Kavoussi LR, Slepian MJ (2002) Local hemostasis during laparoscopic partial nephrectomy using biodegradable hydrogels: initial porcine results. J Endourol 16:489–494
149. Qiu B, Stefanos S, Ma JL, Lalloo A, Perry BA, Leibowitz MJ, Sinko PJ, Stein S (2003) A hydrogel prepared by in situ cross-linking of a thiol-containing poly(ethylene glycol)-based copolymer: a new biomaterial for protein drug delivery. Biomaterials 24:11–18
150. Cohen S, Lobel E, Trevgoda A, Peled Y (1997) A novel in situ-forming ophthalmic drug delivery system from alginates undergoing gelation in the eye. J Control Release 44:201–208
151. Packhaeuser CB, Kissel T (2007) On the design of in situ forming biodegradable parenteral depot systems based on insulin loaded dialkylaminoalkyl-amine-poly(vinyl alcohol)-g-poly (lactide-co-glycolide) nanoparticles. J Control Release 123:131–140
152. Heller J, Barr J, Ng SY, Shen HR, Schwach-Abdellaoui K, Gurny R, Vivien-Castioni N, Loup PJ, Baehni P, Mombelli A (2002) Development and applications of injectable poly(ortho esters) for pain control and periodontal treatment. Biomaterials 23:4397–4404
153. Barr J, Woodburn KW, Ng SY, Shen HR, Heller J (2002) Post surgical pain management with poly(ortho esters). Adv Drug Deliv Rev 54:1041–1048
154. Hatefi A, Amsden B (2002) Biodegradable injectable in situ forming drug delivery systems. J Control Release 80:9–28
155. Bezwada RS (1995) Liquid copolymers of epsilon-caprolactone and lactide. United States Patent US 5,422,033
156. Bezwada RS, Arnold SC, Shalaby SW, Williams BL (1997) Liquid absorbable polymers for parenteral applications. United States Patent US 5,653,992
157. Jain JP, Modi S, Kumar N (2008) Hydroxy fatty acid based polyanhydride as drug delivery system: synthesis, characterization, in vitro degradation, drug release, and biocompatibility. J Biomed Mater Res A 84A:740–752
158. Dunn RL, English JP, Cowsar DR, Vanderbilt DP (1990) Biodegradable in situ forming implants and methods of producing the same. United States Patent US 4,938,763
159. Dunn RL, Tipton AJ (1997) Polymeric compositions useful as controlled release implants. United States Patent US 7,702,716

160. Shah NH, Railkar AS, Chen FC, Tarantino R, Kumar S, Murjani M, Palmer D, Infeld MH, Malick AW (1993) A biodegradable injectable implant for delivering micromolecules and macromolecules using poly(lactic-co-glycolic) acid (plga) copolymers. J Control Release 27:139–147
161. Brodbeck KJ, Gaynor-Duarte AT, Shen TT (2000) Gel compositions and methods. United States Patent US 6,130,200
162. Tipton AJ (1999) High viscosity liquid controlled delivery system as a device. United States Patent US 5,968,542
163. Burns PJ, Gibson JW, Tipton AJ (2000) Compositions suitable for controlled release of the hormone GNRH and its analogs. United States Patent US 6,051,558
164. Bodmeier R (1998) Verfahren zur in-situ Herstellung von Partikeln. German Patent Application Publication DE 197 24 784
165. Kranz H, Brazeau GA, Napaporn J, Martin RL, Millard W, Bodmeier R (2001) Myotoxicity studies of injectable biodegradable in-situ forming drug delivery systems. Int J Pharm 212:11–18
166. Rungseevijitprapa W, Bodmeier R (2009) Injectability of biodegradable in situ forming microparticle systems (ISM). Eur J Pharm Sci 36:524–531
167. Jain RA, Rhodes CT, Railkar AM, Malick AW, Shah NH (2000) Controlled release of drugs from injectable in situ formed biodegradable PLGA microspheres: effect of various formulation variables. Eur J Pharm Biopharm 50:257–262
168. Jain RA, Rhodes CT, Railkar AM, Malick AW, Shah NH (2000) Comparison of various injectable protein-loaded biodegradable poly(lactide-co-glycolide) (PLGA) devices: in-situ-formed implant versus in-situ-formed microspheres versus isolated microspheres. Pharm Dev Technol 5:201–207
169. Jain RA, Rhodes CT, Railkar AM, Malick AW, Shah NH (2000) Controlled delivery of drugs from a novel injectable in situ formed biodegradable PLGA microsphere system. J Microencapsul 17:343–362
170. Royals MA, Fujita SM, Yewey GL, Rodriguez J, Schultheiss PC, Dunn RL (1999) Biocompatibility of a biodegradable in situ forming implant system in rhesus monkeys. J Biomed Mater Res 45:231–239
171. Graham PD, Brodbeck KJ, McHugh AJ (1999) Phase inversion dynamics of PLGA solutions related to drug delivery. J Control Release 58:233–245
172. Brodbeck KJ, DesNoyer JR, McHugh AJ (1999) Phase inversion dynamics of PLGA solutions related to drug delivery – Part II. The role of solution thermodynamics and bath-side mass transfer. J Control Release 62:333–344
173. Astaneh R, Erfan M, Moghimi H, Mobedi H (2009) Changes in morphology of in situ forming PLGA implant prepared by different polymer molecular weight and its effect on release behavior. J Pharm Sci 98:135–145
174. Brodbeck KJ, Pushpala S, McHugh AJ (1999) Sustained release of human growth hormone from PLGA solution depots. Pharm Res 16:1825–1829
175. Chen SB, Singh J (2005) Controlled delivery of testosterone from smart polymer solution based systems: in vitro evaluation. Int J Pharm 295:183–190
176. Singh S, Singh J (2007) Phase-sensitive polymer-based controlled delivery systems of leuprolide acetate: in vitro release, biocompatibility, and in vivo absorption in rabbits. Int J Pharm 328:42–48
177. Kang F, Singh J (2005) In vitro release of insulin and biocompatibility of in situ forming gel systems. Int J Pharm 304:83–90
178. Singh S, Singh J (2004) Controlled release of a model protein lysozyme from phase sensitive smart polymer systems. Int J Pharm 271:189–196
179. Yewey GL, Duysen ED, Cox SM, Dunn RL (1997) Delivery of proteins from a controlled release injectable implant. In: Sanders LM, Hendren RW (eds) Protein delivery: physical systems. Plenum, New York, pp 93–117

180. Dunn RL, Yewey GL, Fujita SM, Josephs KR, Whitman SL, Southard GL, Dernell WS, Straw RC, Withrow SJ, Powers BE (1996) Sustained release of cisplatin in dogs from an injectable implant delivery system. J Bioact Compat Pol 11:286–300
181. Fang F, Gong CY, Dong PW, Fu SZ, Gu YC, Guo G, Zhao X, Wei YQ, Qian ZY (2009) Acute toxicity evaluation of in situ gel-forming controlled drug delivery system based on biodegradable poly(epsilon-caprolactone)-poly(ethylene glycol)-poly(epsilon-caprolactone) copolymer. Biomed Mater 4:025002
182. Schoenhammer K, Petersen H, Guethlein F, Goepferich A (2009) Injectable in situ forming depot systems: PEG-DAE as novel solvent for improved PLGA storage stability. Int J Pharm 371:33–39
183. Schoenhammer K, Petersen H, Guethlein F, Goepferich A (2009) Poly(ethyleneglycol) 500 dimethylether as novel solvent for injectable in situ forming depots. Pharm Res 26:2568–2577
184. Eliaz RE, Kost J (2000) Characterization of a polymeric PLGA-injectable implant delivery system for the controlled release of proteins. J Biomed Mater Res 50:388–396
185. Krebs MD, Sutter KA, Lin ASP, Guldberg RE, Alsberg E (2009) Injectable poly(lactic-co-glycolic) acid scaffolds with in situ pore formation for tissue engineering. Acta Biomater 5:2847–2859
186. Shively ML, Coonts BA, Renner WD, Southard J, Bennett AT (1995) Physicochemical characterization of a polymeric injectable implant delivery system. J Control Release 33:237–243
187. Ravivarapu HB, Moyer KL, Dunn RL (2000) Parameters affecting the efficacy of a sustained release polymeric implant of leuprolide. Int J Pharm 194:181–191
188. Kempe S, Metz H, Pereira PG, Mader K (2010) Non-invasive in vivo evaluation of in situ forming PLGA implants by benchtop magnetic resonance imaging (BT-MRI) and EPR spectroscopy. Eur J Pharm Biopharm 74:102–108
189. Kempe S, Metz H, Mader K (2008) Do in situ forming PLG/NMP implants behave similar in vitro and in vivo? A non-invasive and quantitative EPR investigation on the mechanisms of the implant formation process. J Control Release 130:220–225
190. Solorio L, Babin BM, Patel RB, Mach J, Azar N, Exner AA (2010) Noninvasive characterization of in situ forming implants using diagnostic ultrasound. J Control Release 143 (2):183–190
191. Miyajima M, Koshika A, Okada J, Ikeda M, Nishimura K (1997) Effect of polymer crystallinity on papaverine release from poly (L-lactic acid) matrix. J Control Release 49:207–215
192. DesNoyer JR, McHugh AJ (2001) Role of crystallization in the phase inversion dynamics and protein release kinetics of injectable drug delivery systems. J Control Release 70:285–294
193. Wang L, Kleiner L, Venkatraman S (2003) Structure formation in injectable poly(lactide-co-glycolide) depots. J Control Release 90:345–354
194. Astaneh R, Nafissi-Varcheh N, Erfan M (2007) Zinc-leuprolide complex: preparation, physicochemical characterization and release behaviour from in situ forming implant. J Pept Sci 13:649–654
195. Dudeck O, Jordan O, Hoffmann KT, Okuducu AF, Tesmer K, Kreuzer-Nagy T, Rufenacht DA, Doelker E, Felix R (2006) Organic solvents as vehicles for precipitating liquid embolics: a comparative angiotoxicity study with superselective injections of swine rete mirabile. Am J Neuroradiol 27:1900–1906
196. AGL9909 study (2000) A six-month, open label, fixed dose study to evaluate the safety, tolerance, pharmacokinetics and endocrine efficacy of two doses of LA-2550 22.5mg in patients with advanced prostate cancer, Eligard® product information. http://products.sanofi-aventis.us/eligard/eligard_225.html. Accessed 23 Jan 2008
197. Cox MC, Scripture CD, Figg WD (2005) Leuprolide acetate given by a subcutaneous extended-release injection: less of a pain? Expert Rev Anticancer Ther 5:605–611
198. Kim TS, Klimpel H, Fiehn W, Eickholz P (2004) Comparison of the pharmacokinetic profiles of two locally administered doxycycline gels in crevicular fluid and saliva. J Clin Periodontol 31:286–292

199. Southard GL, Dunn RL, Garrett S (1998) The drug delivery and biomaterial attributes of the ATRIGEL technology in the treatment of periodontal disease. Expert Opin Investig Drugs 7:1483–1491
200. Langer R (1980) Polymeric delivery systems for controlled drug release. Chem Eng Commun 6:1–48
201. Sanders LM, McRae GI, Vitale KM, Kell BA (1985) Controlled delivery of an LHRH analogue from biodegradable injectable microspheres. J Control Release 2:187–195
202. Sanders LM, Kent JS, McRae GI, Vickery BH, Tice TR, Lewis DH (1984) Controlled release of a luteinizing hormone-releasing hormone analogue from poly(d, l-lactide-co-glycolide) microspheres. J Pharm Sci 73:1294–1297
203. Allison SD (2008) Analysis of initial burst in PLGA microparticles. Expert Opin Drug Deliv 5:615–628
204. Jalil R, Nixon JR (1989) Microencapsulation using poly(L-lactic acid). I: microcapsule properties affected by the preparative technique. J Microencapsul 6:473–484
205. Wischke C, Neffe AT, Steuer S, Lendlein A (2010) Comparing techniques for drug loading of shape-memory polymer networks-effect on their functionalities. Eur J Pharm Sci. doi:10.1016/j.ejps.2010.06.003
206. Yeo Y, Park K (2004) Control of encapsulation efficiency and initial burst in polymeric microparticle systems. Arch Pharm Res 27:1–12
207. Bodmeier R, McGinity JW (1987) The preparation and evaluation of drug-containing poly (dl-lactide) microspheres formed by the solvent evaporation method. Pharm Res 4:465–471
208. Kang JC, Schwendeman SP (2003) Determination of diffusion coefficient of a small hydrophobic probe in poly(lactide-co-glycolide) microparticles by laser scanning confocal microscopy. Macromolecules 36:1324–1330
209. Luan X, Bodmeier R (2006) In situ forming microparticle system for controlled delivery of leuprolide acetate: influence of the formulation and processing parameters. Eur J Pharm Sci 27:143–149
210. Bodmeier R, Oh KH, Chen H (1989) The effect of the addition of low-molecular weight poly (Dl-Lactide) on drug release from biodegradable poly(Dl-Lactide) drug delivery systems. Int J Pharm 51:1–8
211. Lavelle EC, Yeh MK, Coombes AG, Davis SS (1999) The stability and immunogenicity of a protein antigen encapsulated in biodegradable microparticles based on blends of lactide polymers and polyethylene glycol. Vaccine 17:512–529
212. Jiang WL, Schwendeman SP (2001) Stabilization and controlled release of bovine serum albumin encapsulated in poly(D, L-lactide) and poly(ethylene glycol) microsphere blends. Pharm Res 18:878–885
213. Ravivarapu HB, Burton K, DeLuca PP (2000) Polymer and microsphere blending to alter the release of a peptide from PLGA microspheres. Eur J Pharm Biopharm 50:263–270
214. Langer RS, Peppas NA (1981) Present and future applications of biomaterials in controlled drug delivery systems. Biomaterials 2:201–214
215. Okada H, Heya T, Ogawa Y, Toguchi H, Shimamoto T (1991) Sustained pharmacological activities in rats following single and repeated administration of once-a-month injectable microspheres of leuprolide acetate. Pharm Res 8:584–587
216. Chia HH, Yang YY, Chung TS, Ng S, Heller J (2001) Auto-catalyzed poly(ortho ester) microspheres: a study of their erosion and drug release mechanism. J Control Release 75:11–25
217. Kent JS, Sanders L, Tice TR, Lewis DH (1984) Microencapsulation of the peptide narfalin acetate for controlled release. In: Zatuchni GI, Goldsmith A, Shelton JD, Sciarra JJ (eds) Long-acting contraceptive delivery systems. Harper & Row, Philadelphia, pp 169–179
218. Bodmer D, Kissel T, Traechslin E (1992) Factors influencing the release of peptides and proteins from biodegradable parenteral depot systems. J Control Release 21:129–137
219. Bodmer D, Fong JW, Kissel T, Maulding HV, Nagele O, Pearson JE (1996) Octreotidepamoat und dessen Verwendung zur Herstellung von pharmazeutischen Formulierungen. Swiss Patent CH 686 252

220. Bodmer D, Fong JW, Kissel T, Maulding HV, Nagele O, Pearson JE (1997) Sustained release formulations of water soluble peptides. United States Patent US 5,639,480
221. Lambert O, Ausborn M, Petersen H, Löffler R, Bonny J-D (2004) Pharmaceutical composition comprising microparticles. International Publication WO 2004/045633
222. Petersen H, Ahlheimer M (2007) Sustained release formulation comprising octreotide and two or more polylactide-co-glycolide polymers. International Publication WO 2007/071395
223. Pellet M, Roume C (2002) Sustained release compositions and the process for their preparation. US Patent US 6,475,507
224. Okada H, Ionoue Y, Ogawa Y, Toguchi H (1992) Three-month release injectable microspheres of leuprolin acetate. Proc Int Symp Control Rel Bioact Mater 19:52
225. Okada H, Yamamoto M, Heya T, Inoue Y, Kamei S, Ogawa Y, Toguchi H (1994) Drug-delivery using biodegradable microspheres. J Control Release 28:121–129
226. Ogawa Y, Yamamoto M, Takada S, Okada H, Shimamoto T (1988) Controlled-release of leuprolide acetate from polylactic acid or copoly(lactic/glycolic) acid microcapsules: influence of molecular weight and copolymer ratio of polymer. Chem Pharm Bull 36:1502–1507
227. Okada H, Heya T, Ogawa Y, Shimamoto T (1988) One-month release injectable microcapsules of a luteinizing hormone-releasing hormone agonist (leuprolide acetate) for treating experimental endometriosis in rats. J Pharmacol Exp Ther 244:744–750
228. Ogawa Y, Okada H, Heya T, Shimamoto T (1989) Controlled release of LHRH agonist, leuprolide acetate, from microcapsules: serum drug level profiles and pharmacological effects in animals. J Pharm Pharmacol 41:439–444
229. Ogawa Y (1992) Monthly microcapsule-depot form of LHRH agonist, leuprolide acetate (Enantone® Depot): formulation and pharmacokinetics in animals. Eur J Hosp Pharm 2:120–127
230. Yamamoto M, Takada S, Ogawa Y (1994) Sustained release microcapsule. United States Patent US 5,330,767
231. Takechi N, Ohtani S, Nagai A (2002) Production of microspheres. European Patent EP 779 072
232. Nerlich B, Mank R, Gustafsson J, Hörig J, Köchling W (1996) Mikroverkapselung wasserlöslicher Wirkstoffe. European Patent EP 579 347
233. Mank R, Gustafsson J, Hörig J, Köchling W, Nerlich B (1996) Microencapsulation of water-soluble medicaments. United States Patent US 5,503,851
234. Klippel KF, Winkler CJ, Jocham D, Rubben H, Moser B, Gulati A (1999) Effectiveness and tolerance of 1 dosage forms (subcutaneous and intramuscular) of decapeptyl depot in patients with advanced prostate carcinoma. Urologe A 38:270–275
235. Orsolini P (1992) Method for preparing a pharmaceutical composition in the form of microparticles. United States Patent US 5,134,122
236. Orsolini P (1993) Pharmaceutical composition in the form of microparticles. United States Patent US 5,225,205
237. Bartus RT, Emerich DF, Hotz J, Blaustein M, Dean RL, Perdomo B, Basile AS (2003) Vivitrex, an injectable, extended-release formulation of naltrexone, provides pharmacokinetic and pharmacodynamic evidence of efficacy for 1 month in rats. Neuropsychopharmacology 28:1973–1982
238. Rickey ME, Ramstack JM, Lewis DH, Mesens J (1998) Preparation of extended shelf-life biodegradable, biocompatible microparticles containing a biologically active agent. United Staes Patent US 5,792,477
239. Wright SG, Rickley ME, Ramstack JM, Lyons SL, Hotz JM (2001) Method for preparing microparticles having a selected polymer molecular weight. United States Patent US 6,264,987
240. Mesens J, Rickey ME, Atkins TJ (2003) Microencapsulated 3-Piperidinyl substituted 1,2-benzisooxazoles and 1,2-benzisothiazoles. United States Patent US 6,544,559
241. Ramstack JM, Riley MG, Zale SE, Hotz JM, Johnson OL (2003) Preparation of injectable suspensions having improved injectability. United States Patent US 6,667,061

242. Lyons SL, Wright SG (2004) Apparatus and method for preparing microparticles. United States Patent US 6,713,090
243. Lyons SL, Wright SG (2005) Method and apparatus for preparing microparticles using in-line solvent extraction. United States Patent US 6,939,033
244. Lawter JR, Lanzilotti MG (1996) Phase separation-microencapsulated pharmaceuticals compositions useful for alleviating dental disease. United States Patent US 5,500,228
245. Gedulin BR, Smith P, Prickett KS, Tryon M, Barnhill S, Reynolds J, Nielsen LL, Parkes DG, Young AA (2005) Dose-response for glycaemic and metabolic changes 28 days after single injection of long-acting release exenatide in diabetic fatty Zucker rats. Diabetologia 48:1380–1385
246. Iwamoto K, Nasu R, Yamamura A, Kothare PA, Mace K, Wolka AM, Linnebjerg H (2009) Safety, tolerability, pharmacokinetics, and pharmacodynamics of exenatide once weekly in Japanese patients with type 2 diabetes. Endocr J 56:951–962
247. Sandow J, Seidel HR, Krauss B, Jerabek-Sandow G (1987) Pharmacokinetics of LHRH agonist in different deliver systems and the relation to endocrine function. In: Klijn JGM (ed) Hormonal manipulation of cancer: peptides, growth factors, and new (anti)steroidal agents. Raven, New York
248. Waxman JH, Sandow J, Abel P, Farah N, O'Donoghue EP, Fleming J, Cox J, Sikora K, Williams G (1989) Two-monthly depot gonadotropin releasing hormone agonist (buserelin) for treatment of prostatic cancer. Acta Endocrinol (Copenh) 120:315–318
249. Sandow J, Stoeckemann K, Jerabek-Sandow G (1990) Pharmacokinetics and endocrine effects of slow release formulations of LHRH analogues. J Steroid Biochem Mol Biol 37:925–963
250. Behre HM, Sandow J, Nieschlag E (1992) Pharmacokinetics of the gonadotropin-releasing hormone agonist buserelin after injection of a slow-release preparation in normal men. Arzneimittelforschung 42:80–84
251. Tamada J, Langer R (1992) The development of polyanhydrides for drug delivery applications. J Biomater Sci Polym Ed 3:315–353
252. Brem H, Gabikian P (2001) Biodegradable polymer implants to treat brain tumors. J Control Release 74:63–67
253. Greenstein G, Polson A (1998) The role of local drug delivery in the management of periodontal diseases: a comprehensive review. J Periodontol 69:507–520
254. Ravivarapu HB, Moyer KL, Dunn RL (2000) Sustained suppression of pituitary-gonadal axis with an injectable, in situ forming implant of leuprolide acetate. J Pharm Sci 89:732–741
255. Perez-Marreno R, Chu FM, Gleason D, Loizides E, Wachs B, Tyler RC (2002) A six-month, open-label study assessing a new formulation of leuprolide 7.5 mg for suppression of testosterone in patients with prostate cancer. Clin Ther 24:1902–1914
256. Dunn R, Garrett J, Ravivarapu H, Chandrashekar B (2003) Polymeric delivery formulations of leuprolide with improved efficacy. United States Patent US 6,565,874
257. Sartor O (2003) Eligard: leuprolide acetate in a novel sustained-release delivery system. Urology 61:25–31
258. Perez-Marrero I, Tyler RC (2004) A subcutaneous delivery system for the extended release of leuprolide acetate for the treatment of prostate cancer. Expert Opin Pharmacother 5:447–457
259. ICH (2003) Guidance for industry, Q3C impurities: Residual solvents. U.S. Department of Health and Human Services, Food and Drug Administration (FDA). http://www.fda.gov/downloads/RegulatoryInformation/Guidances/ucm128317.pdf and http://www.fda.gov/downloads/RegulatoryInformation/Guidances/ucm128282.pdf%20
260. Wang LW, Venkatraman S, Gan LH, Kleiner L (2005) Structure formation in injectable poly (lactide-co-glycolide) depots. II. Nature of the gel. J Biomed Mater Res B 72B:215–222
261. Lambert WJ, Peck KD (1995) Development of an in situ forming biodegradable poly-lactide-co-glycolide system for the controlled release of proteins. J Control. Rel. 33:189–195
262. Wischke C, Zhang Y, Mittal S, Schwendeman S (2010) Development of PLGA-based injectable delivery systems for hydrophobic fenretinide. Pharm. Res. 27:2063–2074

# Chapter 9
# Porous Systems

**Ronald A. Siegel**

**Abstract** Porous systems play a significant role in controlled release. Porous membranes and matrices can be used to store drug prior to release, and pore structure plays a significant role in determining release kinetic profiles. In this chapter we review methods used to measure pore structure and mathematical models used to relate pore structure to drug transport properties. Steric and hydrodynamic interactions between drug and pore walls, pore tortuosity, and variation in pore width are identified as factors affecting transport. Percolation theory, which addresses connectedness of random pore networks and its effect on overall releasability of drug and release rate, is discussed. Concepts developed for porous systems can be applied, with some modifications, to transport in other heterogeneous systems, such as tissue interstitium and hydrogels.

## 9.1 Introduction

Porous systems are ubiquitous in natural world and in technology. Examples from nature include volcanic rocks such as pumice, oil sediments, soils, dry wood, leaves, bone, and the glomeruli of the kidney. The cell's plasma membrane is studded with channel proteins that open and shut to admit certain ions and exclude others, and its nuclear membrane contains a lattice of pores that regulate traffic of macromoleculles between the nucleus and the cytoplasm. In the industrial world, porous systems are used for filtration, dialysis, reverse osmosis, adsorption, catalysis, flow control, mixing, and other applications where a large surface area/volume ratio is required.

R.A. Siegel (✉)
Departments of Pharmaceutics and Biomedical Engineering, University of Minnesota, Minneapolis, MN 55419, USA

Department of Pharmaceutics WDH 9-177, University of Minnesota, 308 Harvard St. S.E., Minneapolis, MN 55455, USA
e-mail: siege017@umn.edu

J. Siepmann et al. (eds.), *Fundamentals and Applications of Controlled Release Drug Delivery*, Advances in Delivery Science and Technology,
DOI 10.1007/978-1-4614-0881-9_9, 

Paper is a porous medium that is designed to absorb and retain inks or graphite particles. Solid foams, cardboards, and aerogels are porous systems that are useful due to their mechanical and acoustic properties. Porosity may be an intentional property or it may be a side effect of manufacture, as in compacted powders.

Porosity plays a major role in many controlled release systems [1]. A typical controlled release system consists of a solid substrate, or matrix, into which drug is incorporated. Often, the matrix material is impermeable to the drug, and release occurs through a system of water filled pores. Pores are formed either as a result of phase separation or spinodal decomposition during preparation, by dissolution and leaching of pore forming soluble excipients, or by the drug itself which, upon release, leaves behind a void space. In recent years, advances in lithographic, electrochemical, and block polymer self assembly have produced highly reproducible, regular porous structures that can be used to precisely control release rate.

In this chapter, we first present examples of porous media relevant to controlled release. We then briefly review techniques for characterizing pore size distributions and pore structure. Finally, we discuss some mathematical approaches used to predict diffusional release from porous media.

There is no strict definition of a porous medium, and we prefer to work with the idea that the medium has one or more components that admit drug diffusion and others that serve as barriers to diffusion. In this respect, many of the concepts developed in this chapter can also be applied to other heterogeneous media, such as the stratum corneum of skin or the extracellular interstitial medium between living cells.

## 9.2 Example of Porous Media Relevant to Controlled Release

A very simple example of a porous system is the common laboratory filter membrane. Such membranes are composed of interwoven polymer fibers with gaps or pores between the fibers that permit passage of water and small molecules, but reject larger molecules. Placing a drug solution on one side of the membrane and a receiving medium on the other side, drug diffuses through the membrane at a rate that depends on the relative size of the drug molecule compared to a typical distance between the fibers. The fiber network is usually sufficiently dense to suppress convection, allowing diffusion control of drug transport.

Traditional filters and dialysis membranes are characterized by random porosity. Consequently, their selectivity by molecular size is not absolute, and size cutoff specifications are fuzzy. In fact, cutoffs are typically specified in terms of molecular weight, not diameter. For several decades, radiation track etched polycarbonate (Nuclepore®) membranes were regarded as the best alternative, since the etched micron sized pores were relatively monodisperse [2, 3]. However, these membranes, besides having pores that are too large to provide size selectivity, are characterized by randomly positioned pores, and their porosity (volume or area fraction of pores in the membrane) must be kept low in order to avoid pore overlap.

Since the 1990s, there have been major advances in fabrication of micro- and nanoporous arrays with high pore density. Solid state microporous arrays can be

formed by a number of traditional chemical and plasma etching, and electron beam techniques, many of which were originally developed for the microelectronics industry but are now also used in microelectromechanical systems (MEMS) and microfluidics [4]. For example, a microporous array can be fabricated by placing a thin silicon wafer under a patterned mask that blocks reactive ions, except in an array of gaps introduced into the mask. The silicon under the gaps is etched away upon exposure to plasma, leaving behind an array of pores. Alternatively, an array of microposts can be formed by a mask/etch process. A microporous sheet can then be formed by pouring a thin layer of polymer, such as poly(dimethylsiloxane) (PDMS), to a level below the tips of the posts, curing the PDMS, and peeling off the cured sheet, which now contains a pore array. Under proper conditions, the silicon post array acts as a "master" from which identical microporous membranes can be cast repetitively.

Anopore® membranes are 60 μm thick aluminum oxide sheets containing a dense honeycomb array of near-regular cylindrical pores whose diameters can be as small as 20 nm. These regular structures are manufactured electrochemically under strong electric fields.

It has long been known that block polymers self-assemble into regular arrays whose structure and periodicity depend on the mutual compatibility of the polymer blocks and their lengths. Lamellar, hexagonal, cubic, and gyroid morphologies have been predicted and demonstrated in 3D block polymer materials [5]. When solutions of block polymers are spun onto a surface and the solvent is evaporated, they self-assemble into thin films that also exhibit 2D spatial periodicity. In one example [6], a polymer solution consisting of long polystyrene (PS) and short poly (lactic acid) (PLA) blocks, separated by an even shorter polyisoprene (PI) block, is spun onto a thin wafer. Following solvent evaporation these block polymers form hexagonal arrays, with PLA cylinders, lined by PI, dispersed in a PS continuum. Upon exposure to strong base the PLA cylinders are etched away, leaving behind an ultrathin (~100 nm thick), nanoporous (~40 nm diameter) array on top of the wafer. Using a combination of chemical and plasma etching techniques, an array of micropores is introduced into the underlying wafer. The result is an asymmetric membrane with a nanoporous carpet lying on top of a microporous substrate. The latter provides mechanical support to the former. If the nanopore diameters can be further reduced, then selectivity based on size is possible in this system. It is interesting to note that nuclear pores in the eukaryotic cell are of comparable diameters to the nanopores in this block polymer-based system.

In the past two decades, there has been extensive research into mesoporous silica nanoparticles (MSNs) [7, 8]. These nanoparticles, of diameter ~100 nm, are formed by condensation of silica around arrays of cylindrical micelle templates, followed by removal of the template. These structured particles contain arrays of rigid, parallel, cylindrical pores of diameter ~2–4 nm that extend from one end to the other. Pore diameter can be further reduced, if desired, by functionalizing the silica pore walls. Drug can be rapidly loaded into the pores by diffusion, and its partitioning into the MSN can be encouraged by functionalizing the pore walls with moieties that favor drug association. MSNs coated with lipid bilayer membranes, which hold hydrophilic drugs inside but release the drug when the membrane is destabilized (e.g., due to lowering of pH in an endosome), are under investigation [9].

In the forgoing examples, pores are of cylindrical shape. As is discussed below, a critical parameter affecting diffusion through narrow pores is the ratio of molecular diameter to pore diameter. The same holds true for narrow slit-like pores, which have been studied thoroughly in the past decade. In one example, very thin (~10 nm), sacrificial oxide layers are grown on micron sized walls of cavities etched into silicon wafers. The coated cavities are then backfilled with polysilicon, and the oxide is removed, leaving behind nanoscale, slit-like gaps that serve as channels for diffusion of drug [10].

We now turn to more traditional porous polymeric systems which, though more heterogeneous in their pore structure, are much cheaper to produce on a mass scale. A simple general procedure is to mix a polymer with an additive, which might be a gas, liquid, or solid under conditions, e.g., temperature or vapor pressure, where the components are compatible. If external conditions are changed so that the polymer and additive become incompatible, then the system will phase separate into polymer rich and additive rich domains. Upon removal of the additive, either by evaporation or liquid leaching, the domain structure becomes a randomly porous structure [11]. The resulting pore structure depends on whether coagulation of the polymer occurs by a nucleation/growth mechanism or by spinodal decomposition, and random, periodic, and cellular morphologies are possible, depending on processing conditions.

Another method is to prepare a multiphase mixture with interfaces stabilized by surfactants. By removing of one of the phases and "hardening" the other, a porous medium results. For example [12], drug-loaded porous microspheres can be formed by dissolving the drug in the internal aqueous phase of a water-in-oil-in-water (w/o/w) emulsion, in which the "oil" phase consists of droplets of an organic polymer solution and even smaller droplets of an internal aqueous phase, all suspended in a continuous aqueous medium. The phases are stabilized by emulsifying agents or surfactants. Under vigorous stirring, the organic solvent is removed by evaporation, and the resulting microspheres are then removed from the continuous phase, followed by drying of the internal aqueous phase, which leaves the drug behind in pores. This process can be adapted to spray systems, in which the evaporation steps are fast.

More direct methods for producing porosity are to blow a foam in a polymer solution or melt, followed by hardening of the polymer around the air bubbles or by suspending pore-forming agents, such as salts or incompatible polymers, in the initial polymeric preparation, followed by liquid leaching. Solid particles of the drug itself may constitute the pore-forming agent. Again, these procedures may be amenable to spray processing.

## 9.3 Characterization of Porous Materials

The definition of a pore is ambiguous, since it refers to void space within solid material, which also cannot be defined rigorously. The inferred porosity of a material and details regarding pore structure depend on the methods used to

probe these properties. Furthermore, different probes provide different information about a porous medium [13].

Perhaps the most straightforward way to estimate void volume in a dry porous solid is to measure the amount of helium (He) that is introduced into it at a specified pressure. Since He is an inert gas, it interacts minimally with the solid component, and the pore volume can be calculated using either the ideal gas law or, more accurately, the van der Waals equation of state for He. This measure of porosity accounts for all pores except those whose diameters are less than that of a helium atom.

If instead of helium nitrogen gas ($N_2$) is used, an estimate of the internal surface area of the porous media can be made. As a highly polarizable molecule, $N_2$ adsorbs readily to most surfaces, so the first introduction of $N_2$ coats all pore walls, except those that are not accessible to the gas because they are surrounded by nitrogen impermeable material. Using Brunauer–Emmet–Teller (BET) analysis, it is possible to ascertain both the internal surface area of a porous solid and the affinity of the solid for $N_2$.

While He and $N_2$ absorption isotherms are useful for determining pore volume and internal surface area of a porous solid, they cannot generally be used to determine pore sizes. Traditionally, mercury (Hg) intrusion measurements have been used for this purpose. As a liquid, Hg possesses a surface tension with air, $\gamma$, and a contact angle at the Hg/air/solid interface, $\theta$. According to the Washburn equation, the pressure (excess of atmospheric pressure) required to drive Hg through a pore of diameter $R_\mathrm{p}$ is given by

$$\Delta P = 4\gamma \cos\theta / R_\mathrm{p}. \tag{9.1}$$

By plotting pressure versus the amount of Hg introduced, the distribution of pore diameters is determined. The Washburn equation predicts that large pores are filled before small pores. Unfortunately, this procedure cannot be accurate in general, since some large pores may be initially inaccessible, and can only be reached after initial penetration of surrounding smaller pores [1, 14, 15]. Moreover, the Washburn equation does not account for compressibility of the porous medium [16].

Various imaging and microscopy techniques can be used to characterize pore structure, including serial section microtomy, optical laser scanning confocal microscopy (LSCM), confocal Raman microscopy (CRM), scanning electron microscopy (SEM), transmission electron microscopy (TEM), and magnetic resonance imaging (MRI). Atomic force microscopy (AFM) can also be used to probe the surface terrain of a material and ascertain the location and sometimes the depth of nanopores. These techniques, together with present day data storage and computational capabilities, make it possible to reconstruct many of the details of pore structure, going beyond simple measures such as porosity and specific surface area. For example, many porous systems contain large pore bodies connected by relatively narrow throats. As is discussed below, these details are often crucial in determining transport processes in porous media.

## 9.4 Mathematical Models

The variety of pore morphologies and arrangements or topologies that are possible in porous media is such that no single mathematical description or model of diffusion inside the medium covers all possibilities. Hence, it is necessary to have at least an approximate idea as to how a medium is structured before modeling can be pursued. As indicated above, it is conceivable that a porous medium's structure can be characterized with great accuracy by imaging/reconstruction algorithms, and this structure can be used with powerful and computationally intensive (e.g., finite element modeling) software packages to make predictions of release behavior. However, such a procedure may provide little insight into factors governing diffusional release. Here we discuss some relatively simple models.

### *9.4.1 Tubular Pores*

The simplest model of a porous medium is a planar membrane containing a collection of circular cylindrical tubes passing from one face of a membrane, of thickness $L$, to the other, with longitudinal axes perpendicular to the membrane surfaces [2, 17–19]. Figure 9.1a is a rendering of such a membrane. Let $A_p$ be the area of a single pore. For a circular pore with radius $R_p$, $A_p = \pi R_p^2$. If there are, on average, $n$ such pores per unit area of membrane, then the *porosity*, $\varepsilon$, of the membrane is given by $\varepsilon = nA_p = n\pi R_p^2$. Not all of the pore space is equally available, however, and we must be concerned with the freedom of a molecule to place itself fully inside the pore, considering steric or other interactions with the pore wall.

For pores whose radii are in the nanometer scale, a critical parameter determining accessibility of the pore to a solute molecule is the ratio of the molecule's radius, $a$, to the pore radius, $\lambda = a/R_p$. Since the center of the molecule cannot come any closer to the wall than a single molecular radius, the available porosity is

$$\varepsilon_s = n\pi\left(R_p - a\right)^2 = n\pi a^2(1-\lambda)^2 = \varepsilon(1-\lambda)^2. \tag{9.2}$$

For drugs that are much smaller than the pore diameter ($\lambda \ll 1$), the factor $(1-\lambda)^2$ is not significant, but it can be important for large molecules or narrow pores.

The parameter $\varepsilon_s$ is analogous to the partition coefficient, $K$, discussed in Chap. 6, and the two quantities are equal, provided drug is allowed only in the pores and all pore space is accessible to solute. As calculated above, $\varepsilon_s$ is affected only by steric interaction between drug molecule and pore wall. In fact, there are other interactions, such as van der Waals, hydrophobic, and dielectric and electrical forces, the latter being particularly important when both pore wall and drug are charged. Charged pore walls attract oppositely charged drug molecules and repel

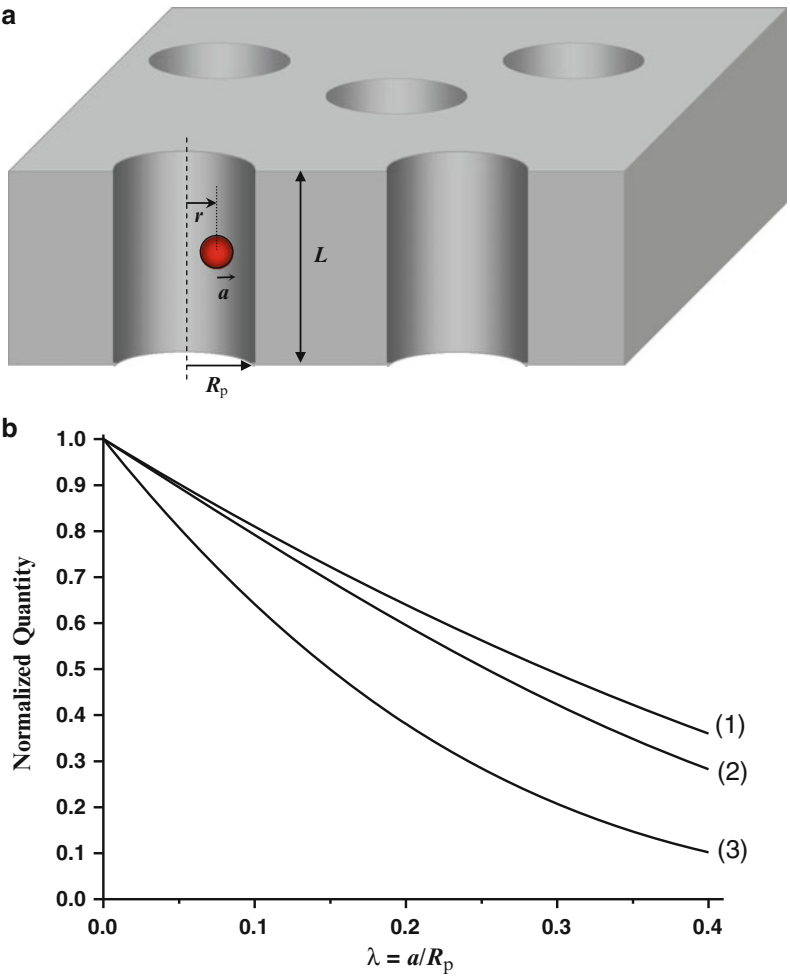


**Fig. 9.1** (**a**) Schematic of simple, straight, cylindrical pores crossing a membrane, with spherical molecules inside. Pore length and radius are $L$ and $R_p$, respectively, and diffusing molecule is of radius $a$ centered at distance $r$ from centerline (*dashed*) of pore. (**b**) Plot of normalized quantities $\varepsilon_s/\varepsilon$ (*curve* 1), $D_{eff}/D_0$ (*curve* 2), and their product $(\varepsilon_s/\varepsilon)(D_{eff}/D_0)$ (*curve* 3) as a function of ratio of molecular radius to pore radius ($a/R_p$)

similarly charged molecules. The forces between pore wall and drug are attenuated by thermal excitation, and electrical forces on a charged solute are partially screened by neighboring ions of opposite charge.

Again assuming circular symmetry of the pore, these forces can be represented by a potential energy of interaction, $U$, between the molecule and the pore wall, which depends on the radial position, $r$, of the molecule's center from the centerline

of the pore, with $0 < r < R_p(1-\lambda)$. The "partition coefficient" of drug in the membrane is then given, according to statistical thermodynamics, by

$$K = \frac{2\varepsilon}{R_p^2}\int_0^{R_p(1-\lambda)} r e^{-U(r)/k_B T} dr, \tag{9.3}$$

which reduces to the earlier expression when there are no forces ($U = 0$). In this expression, $k_B$ is Boltzmann's constant and $T$ is temperature (°K). We shall not indulge in detailed calculations here, but note in the electrostatic case that positive $U$ (similarly charged wall and drug) leads to decreased $K$ while negative $U$ (opposite charges) leads to increased $K$. The electrostatic range of influence of the wall on the drug molecule in aqueous solution is characterized, roughly, by the Debye length, $\ell_D = \sqrt{RT\varepsilon_w\varepsilon_0/1,000F^2(2I)}$, where $R$ is the gas constant, $F$ is Faraday's constant, $\varepsilon_0$ is the dielectric permittivity of vacuum, $\varepsilon_w$ is the dielectric constant of water (~80) and $I$ is the ionic strength of the solution. Under physiological conditions, $I = 155$ mM and $\ell_D \approx 8$ Å, so electrostatic effects are confined to within a few nanometers of the pore wall.

The partitioning properties of nonspherical molecules into pores are also of interest. An extreme but illuminating case is a long, thin rod-like molecule that does not interact with the wall in any way other than sterically. Assume that the rod's radius is much smaller than that of the pore, but that its length is larger than the pore diameter. The rod can fit easily into the pore by orienting itself closely parallel to the pore's longitudinal axis, and therefore would seemingly be able to partition easily. However, this orientation is very particular. Outside the membrane, the rod is free to orient in any direction; hence, there is a high entropy cost associated with entering the pore. Similarly, linear polymer molecules that assume a random coil configuration whose radius of gyration is comparable to or larger than the pore radius could seemingly uncoil and form a "straight line" in a narrow pore, but doing so would come with considerable cost in conformational entropy. In both cases, the partition coefficient is greatly reduced [20, 21].

Finally, reversible or irreversible adsorption of molecules, such as proteins, may reduce $\varepsilon_s$ or $K$, especially when pore walls are hydrophobic. Globular proteins typically consist of a core containing hydrophobic residues surrounded by a surface containing polar residues, many of which are charged. Upon encountering a hydrophobic surface, the protein rearranges or unfolds such that its core residues adsorb onto the surface. The polar/charged residues project into the pore lumen, introducing extra steric and ionic interactions to other diffusing molecules, especially other proteins.

We now turn to wall effects on the diffusion coefficient. In dilute solution, the diffusion constant is given by the Stokes–Einstein relation, $D_0 = k_B T/6\pi a\eta$, where $\eta$ is the solvent viscosity. This equation is derived by balancing the thermal "force," $k_B T$, against the viscous drag, $6\pi a\eta$, presented by the medium. Drag is due to a solvent fluid shear profile that extends away from the molecule, from the molecule's surface to infinity. While the shear field decays away from the surface, it remains significant over a considerable distance. The presence of a rigid wall

close to the moving molecule constrains the shear field, and provides extra resistance to the molecule's motion. Calculations of this effect are complicated, and exact results are not available [22]. For spherical molecules that do not interact other than sterically with the wall, a useful expression due to Faxén [23],

$$D_{\text{eff}}/D_0 = 1 - 2.104\,\lambda + 2.09\,\lambda^3 - 0.95\,\lambda^5, \tag{9.4}$$

accounts reasonably well for cylindrical wall drag, provided $\lambda < 0.4$. Here, $D_{\text{eff}}$ is the so called effective diffusion constant, which can be substituted for $D$ in any of the expressions modeling drug release by diffusion given in Chap. 6. Similarly, the expression

$$\varepsilon_s D_{\text{eff}} = (1-\lambda)^2(1 - 2.104\,\lambda + 2.09\,\lambda^3 - 0.95\,\lambda^5)\varepsilon D_0 \tag{9.5}$$

would replace the product $KD$ in that chapter. Expressions for $\varepsilon_s/\varepsilon$, $D_{\text{eff}}/D_0$, and $\varepsilon_s D_{\text{eff}}/\varepsilon D_0$ as a function $\lambda$, which reflect the effects the cylindrical pore wall, are plotted in Fig. 9.1b.

The Faxén expression was derived by considering drag effects on spherical molecules positioned at the centerline of the pore. It should be modified for nonspherical molecules or when there are nonsteric interactions between the pore wall and the solute, but precise calculations are difficult.

The discussion so far applies, strictly speaking, to dilute solutions, where solute molecules are rarely close enough to each other to interact. Many controlled release systems, however, are concentrated. While concentration affects diffusion and partition coefficients in general, the effects tend to be of extra significance in systems with nanoscale pores, where close proximity of pore walls may augment energetic and hydrodynamic interactions between solute molecules [24]. The normal formulation of Fick's laws of diffusion, which assumes that solute molecule executes independent random walks, breaks down. In the limit where $\lambda > 1/2$, solute molecules must move single file through the pores. At high concentrations, entry of drug into cylindrical pores becomes difficult since the pores are already occupied by other molecules, and the rate of drug permeation tends to saturate.

It is interesting to note that saturation of transport at high solute concentrations has been also observed in microfabricated 2D "slit pores" (see above) when the slit width is of comparable dimension to that of a large solute (e.g. a protein), but the lateral dimension is much larger. In this case, single file diffusion cannot explain the behavior, but one can imagine that the energetic and viscous interactions between highly concentrated solute molecules can lead to highly correlated motions resembling single file diffusion [25–27].

### *9.4.2 Tortuous Pathways*

Thus far, we have only considered the effects of pore width on partitioning and diffusion of drug. Another potential factor is pore length. In Fig. 9.1a, pores were

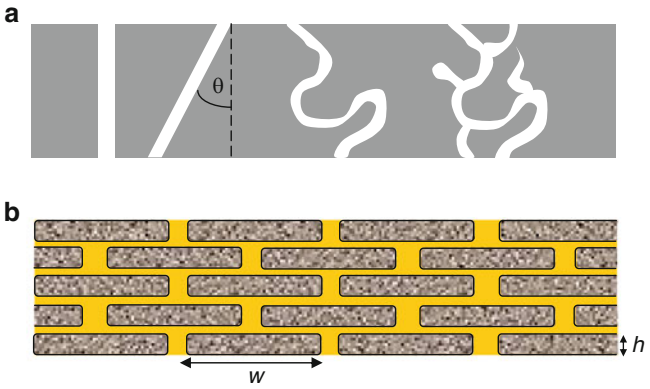


**Fig. 9.2** (**a**) Various pore structures. *From left*: A straight pore as a 2D analog of the pores in Fig. 9.1; a "tilted" pore illustrating the simplest kind of increase in path length, with tortuosity factor 1/cos $\theta$; a curved, tortuous single path from face to face; a tangle of curved pores with intersections and dead ends. (**b**) Brick and mortar representation of stratum corneum

drawn to be perpendicular to the membrane surfaces, with lengths the same as the membrane thickness, denoted by $L$ in Chap. 6. In Fig. 9.2a, pores are still depicted as tubes, but they do not connect the two faces of the membrane by a perpendicular path. In this case, the path length is increased. We shall denote this increase in length by a "tortuosity factor," $\tau$, such that the "effective thickness" of the membrane becomes $\tau L$. This product can replace $L$ or $R$ in the equations for drug release presented in Chap. 6. For example, the expression (6.10) for release across a membrane becomes

$$M_t = \frac{A\varepsilon_s D_{\text{eff}} c_s}{\tau L}\left(t - \frac{\tau^2 L^2}{6D_{\text{eff}}}\right) \tag{9.6}$$

and the Higuchi equation (6.24) becomes

$$\frac{M_t}{M_\infty} = 2\sqrt{\left(2 - \frac{\varepsilon_s c_s}{c_0}\right)\left(\frac{\varepsilon_s c_s}{c_0}\right)\left(\frac{D_{\text{eff}} t}{\tau^2 L^2}\right)}. \tag{9.7}$$

This expression combines the effects of porosity, pore width, and tortuosity.

In the past, tortuosity has referred to any feature of a porous network that slows down diffusion, and the effective diffusion constant was defined as $D_{\text{eff}} = \varepsilon D/\tau$ [28], where here the steric and hydrodynamic factors discussed above are not considered. For example, the Higuchi equation often appears with $\tau$ in the denominator instead of $\tau^2$. This definition is not tenable, however, since porosity by itself has no bearing on time lag while both $D/\tau$ and $D/\tau^2$ appear in (9.6). Neither of these combinations can account for both steady state and lag properties [1].

The basic idea behind tortuosity is that molecules pass through channels that do not direct them straight toward the release surface. For a straight pore making

angle $\theta$ with the line directly connecting the two faces of a planar slab, $\tau = 1/\cos\theta$. However, as shown in Fig. 9.2a, the direction of a pore may change with position. More generally, tubular pores can meet at junction points, where molecules switch direction as they move from one pore to another, and some tubular channels may lead to nowhere. Thus, tortuosity is often a statistical characteristic. For a membrane or monolithic system with well-connected pore network whose pores are uniformly distributed in diameter and direction, it can be shown that $\tau = \sqrt{3}$ [1, 29].

Another example of a tortuous diffusion network is the stratum corneum, the outer epithelial layer of the skin. As described in Chap. 2, the stratum corneum consists of multiple layers of desiccated, proteinaceous cells surrounded by lipids through which lipophilic drugs diffuse, arranged in a "brick and mortar" fashion. Similar barrier structures with tortuous paths for diffusion have been created by dispersing clay platelets in polymer films [55, 56]. Figure 9.2b is a simplified rendering, in 2D, of such structures, in which the "bricks" are uniform and regularly spaced with successive layers in alternating register. The mortar separating any two bricks is assumed to be narrow compared to the brick dimensions. Let $h$ and $w$ be the vertical and lateral dimensions of a brick, respectively, and assume that each mortar channel crossing a layer begins and ends at the center of bricks of the previous and following layers. If there are $m$ such layers, then the overall thickness of the "membrane" will be $mh$. However, the shortest "zig-zag" path that a diffusing drug molecule can take has length $m(h + w/2)$. Because of the symmetry of this geometry, it can be shown that tortuosity is $\tau = 1 + w/2h$. Clearly, very high tortuosities result given wide, thin bricks. More complicated results have been derived for similar structures with variable brick thicknesses and offsets between layers [57], and for 3D brick and mortar structures [58, 59].

### *9.4.3 Variations in Pore Diameter*

In addition to tortuosity, there are other means by which pore structure can affect the rate of transport and release. Consider a medium containing relatively large, varicose pores connected by relatively narrow throats, as illustrated in Fig. 9.3a. Most of the time spent by a diffusing solute is in the large pores. To move from one large pore to the next, a molecule must find a throat and pass through it. However, the solute must do so by executing a random walk, and it may require considerable time to find a throat. Even after it enters that throat, the molecule may pass part way and then return, again at random, to the original pore, where it gets "lost" again. Thus, one may expect longer confinement in a pore body if its surface area is large compared to the total surface area of the exits to the throats from that pore and if the throats are long [30–33]. Under these circumstances, solute is "well mixed" in the pore, with nearly uniform concentration. This argument does not rely on any steric or hydrodynamic interactions between the solute and the pore wall, which were previously discussed.

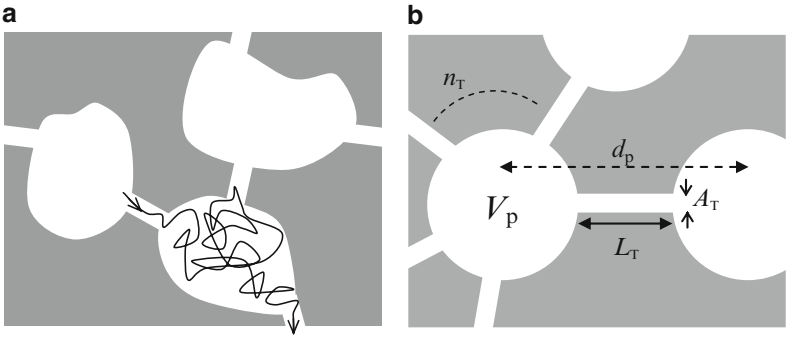


**Fig. 9.3** (**a**) Schematic of Brownian motion (diffusion) of a single molecule in a porous medium with varicose pores and narrow throats. Upon entering the pore, the molecule makes numerous unsuccessful attempts to leave that pore, even occasionally venturing part way into one of its connecting throats but not making a full crossing. Eventually, the molecule crosses a throat into another pore. (**b**) Two dimensional rendering of model for retarded diffusion in porous media with varicose pore bodies and narrow throats. Pores of "volume" $V_p$ are each surrounded by $n_T$ throats of length $L_T$ and "area" $A_T$. Pore centers are separated by distance $d_p$

A simple mathematical model of the effect of pore constrictions or throats is illustrated in Fig. 9.3b [31]. The pore's volume is denoted by $V_p$, and $n_T$ throats of area $A_T$ and length $L_T$ emanate from the pore. Using simple dimensional analysis, we estimate the average time it takes for a molecule to leave the pore and reach one of its neighbors as being approximately $t_P = V_p/n_T(A_T D/L_T)$. Now, let us assume that the pore centers are spaced, on average, at distance $d_P$ from their nearest neighbors. Again using dimensional analysis, the effective solute diffusion coefficient in this porous medium, $D_{eff}$ can be estimated according to $t_P = \omega d_P^2/D_{eff}$, where $\omega$ depends on the arrangement of the pores. Equating these two time estimates, we find that

$$D_{eff}/D = \frac{\omega n_T A_T d_P^2}{L_T V_P}. \tag{9.8}$$

Further, if we define the total throat volume per pore as $V_T = n_T A_T L_T/2$ (denominator signifies that each throat connects two pores), then we obtain the relation

$$D_{eff}/D = \frac{\omega}{2(\tau')^2}\frac{V_T}{V_P}, \tag{9.9}$$

where $\tau' = L_T/d_p$ is an apparent tortuosity factor which may be significant if throats connecting pores are twisted. Because these relations were derived rather crudely, they cannot be exact, and more detailed computational tools would be needed for

specific pore/throat configurations. Nevertheless, these relations suggest that the effective diffusion coefficient of a solute in a constricted porous medium can vary substantially due to pore and throat geometric factors. Of course, when throats are extremely narrow, steric and hydrodynamic factors also need to be accounted for.

The analysis to this point has dealt with pores that are accessible to the releasing surfaces of a monolithic device or to both sides of a membrane through which drug passes by diffusion. Clearly there are porous structures where this is not the case. Pores can be isolated from all channels leading to a device surface, and hence they become irrelevant for drug release, assuming that the matrix material is otherwise impermeable to drug. In the next section, we discuss concepts from percolation theory, in which the effects of random positioning of pores in a medium is shown to affect not only the accessibility of pore space, but also the rate of drug release by diffusion.

### *9.4.4 Percolation Theory*

Percolation theory was developed initially to account for the connectedness of pores in rock, as a function of porosity [34, 60]. Later, it was extended to other phenomena such as electrical conduction in heterogeneous materials [46], mechanical strength of composite materials [61], tertiary oil recovery [62], groundwater flow [63], compaction of materials including pharmaceuticals [64, 65], and even forest fires and the spread of disease through random contacts [34, 60]. It also turns out that percolation phenomena are analogous to certain types of physical phase transitions [60]. The theory has been developed by mathematicians [35], physicists [36], and chemical engineers [37]. Because diffusion through random porous systems has elements in common with conduction, percolation concepts also apply to controlled release systems [31, 38–41]. In the following discussion, we restrict attention to *site* percolation theory.

The simplest predictions of percolation theory relate to pore connectedness. Figure 9.4 illustrates a sequence of equatorial cross sections of simulated spherical porous matrices of different porosities that are set up by random assignment of pores onto a 3D simple cubic (sc) lattice of sites that is embedded in the spherical geometry. The "radius," $N$, of each sphere was taken to be 50 lattice sites. The porosity, $\varepsilon$, of a matrix determines the probability that any site is assigned as a pore. Yellow pores are connected to the surface of the sphere through a sequence of neighboring pores while black pores cannot make such a connection to the surface. Connectedness of pores to the surface is determined by the following algorithm. First, all pores at the surface are colored yellow. Next, pores that share a cubic face with any one of the surface pores are colored yellow. This second step is repeated over and over, connecting interior pores sharing cubic faces with already yellowed pores, until no new pores are available to be added by this process. The remaining pores, which do not share cubic faces with yellow pores, are colored black. (Since

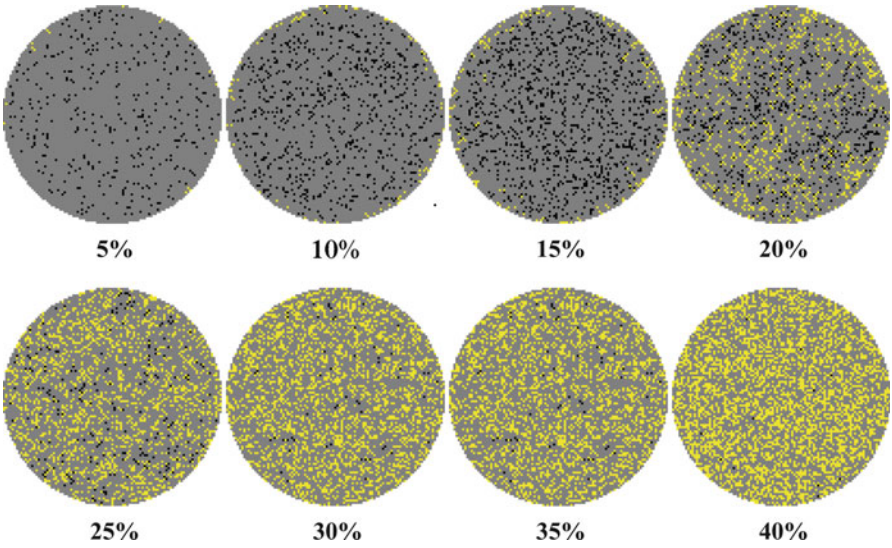


**Fig. 9.4** Model pore networks based on simple cubic lattice embedded in a sphere. Pictured are equatorial cross sections with *gray* lattice sites designating impermeable polymer matrix, *yellow* sites designating pores belonging to clusters connected to the surface, and *black* sites designating pores belonging to clusters that are isolated from the surface. Pore clusters calculated using site percolation procures, with body-centered cubic (bcc) connectivity

each cross section shown in Fig. 9.4 is a 2D slice, it should be kept in mind that pores that are not apparently connected by 2D paths might be connected by paths in 3D that go outside the slice.) At low porosities, say $\varepsilon = 0.05$, only pores near the surface are colored yellow. As $\varepsilon$ increases, the yellow pores invade further into the center of the sphere, until nearly all of the pores are seen to be connected to the surface when $\varepsilon = 0.4$.

The porous structures illustrated in Fig. 9.4 might be due to solid drug particles that are randomly deposited in a polymer matrix during formation of a spherical device. In this case, the yellow sites would refer to drug that is releasable from the device while the black sites would indicate drug that is trapped inside the device, assuming that the polymer is completely impermeable to drug. If the polymer is slightly permeable, then the yellow pores would indicate rapidly releasable drug while the black pores would signify drug that is released much more slowly. In the following, we assume that release from a pore is either all or none.

Figure 9.5a shows the predicted fraction of drug release, $F_\infty$, from the model spherical systems, as a function of $\varepsilon$. In the limit of low porosity ($\varepsilon \to 0$), $F_\infty \to \varepsilon \times$ (surface fraction of lattice sites) while $F_\infty \to 1$ when $\varepsilon \to 1$. Most interesting, however, is the rapid rise in $F_\infty(\varepsilon)$ over an intermediate range of porosities. This transition is due to the growth and coalescence of clusters of connected pores, until eventually one of these clusters extends, or "percolates" throughout the matrix. For values of $\varepsilon$ below the transitional range, pores are mostly disconnected from each

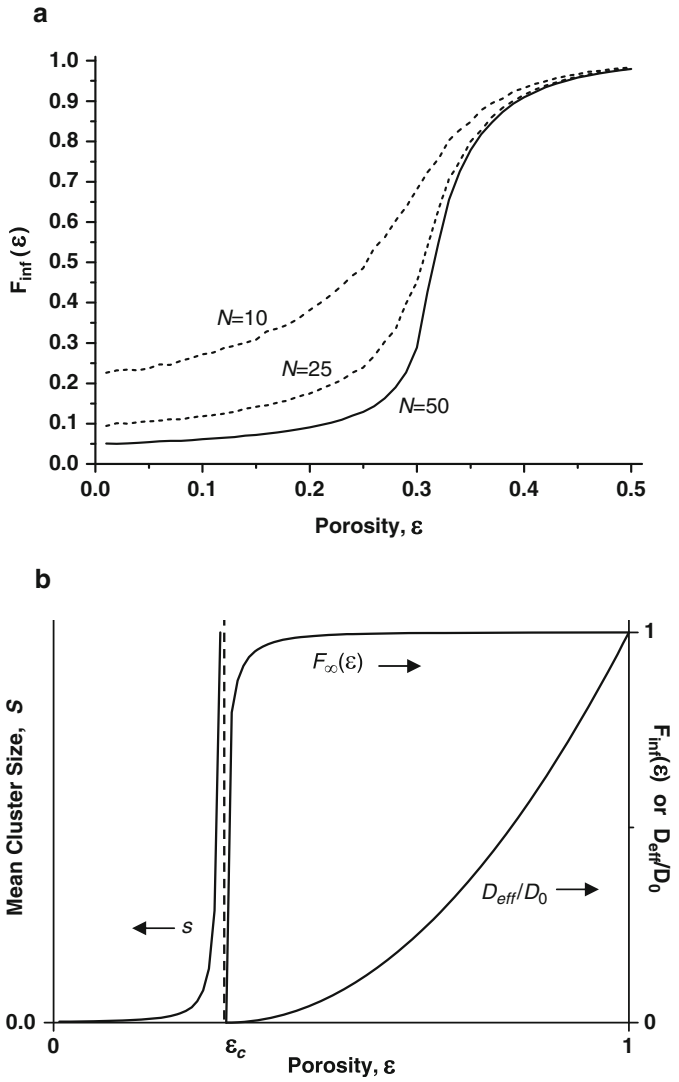


**Fig. 9.5** (**a**) Calculation of fraction of releasable drug, $F_\infty(\varepsilon)$, for finite, simple cubic lattices embedded in spheres, as illustrated in Fig. 9.4. $N$ denotes radius of sphere in lattice units. (**b**) Behaviors of $F_\infty(\varepsilon)$ and $D_{\text{eff}}/D_0$ above the percolation threshold $\varepsilon_c$ and average cluster size, $S(\varepsilon)$ below $\varepsilon_c$ for infinite 3D lattices. Precise value of $\varepsilon_c$ depends on lattice type, but general shapes of curves are universal across lattices of given dimension

other and no percolating cluster exists. Moving through the transitional range, more pore clusters are recruited into the percolating cluster, until all belong. At any stage, contributions to $F_\infty(\varepsilon)$ include the percolating cluster, plus nonpercolating clusters containing at least one site on the surface.

Figure 9.5a also shows predictions for spherical systems of smaller radius relative to pore size, i.e., smaller $N$. As this number decreases, the fraction of pores at or near the surface increases and the fraction of releasable drug increases. The transition range becomes less well defined.

For an infinitely extended lattice, it can be shown that a definite threshold value of $\varepsilon$, called the *percolation threshold*, exists at which a pore cluster of infinite extent appears. Below that threshold, denoted by $\varepsilon_c$, all pore clusters are isolated, so $F_\infty(\varepsilon \leq \varepsilon_c) \rightarrow 0$ since the surface/volume ratio of the lattice becomes vanishingly small, and the fraction of finite pore clusters intersecting the surface must also vanish. For the finite size devices, with "lattice" site size determined by the ratio between device diameter and a typical pore diameter, $F_\infty > 0$ for all porosities and the threshold is diffuse, becoming sharper as device diameter increases or pore diameter related to drug particle size decreases. The threshold value, $\varepsilon_c$, is a useful concept even for finite size systems, since near that point behavior tends to change radically.

Close inspection of Fig. 9.4 reveals that near the percolation threshold the connected paths from internal pores to the surface are very tortuous. In this regime, an initial rapid burst release of drug from the surface is followed by much slower diffusion. In addition to the tortuous pathways, much of the pore space available to a diffusing molecule consists of "dead ends" into which the molecule may wander (see also the rightmost pore structure in Fig. 9.2a). These dead ends "distract" the molecule from its most direct path to the surface, and time is lost while the molecule finds its way back to the more direct path. This delay in finding the "proper way out" is similar to that which occurs in a large pore body when a molecule is trying to find a throat through which it can escape, as previously described. Delay due to dead ends also finds analogy in gel permeation chromatography, in which small molecules wander into and linger in gel interstices while larger molecules are sterically prohibited from doing so, the result being that the larger molecules are convected more rapidly through the column by the carrier solvent and are eluted more rapidly.

While the simple cubic lattice with a fraction of lattice sites containing pores is an idealization of true pore space, results can be generalized to other geometric partitionings of a matrix. A critical parameter for a given scheme is the average number of nearest neighbor "sites" that can potentially contain pores, which we denote by $\bar{z}$. In the simple cubic lattice, each lattice site has exactly six nearest neighbors, $\bar{z} = 6$. Another regular structure, the hexagonal close packed (hcp) lattice, can be visualized as a stack of closely packed cannonballs, with cannonballs in each layer surrounded by six others forming a hexagon and each cannonball "resting" in a valley formed by a triangle of cannonballs in the underlying layer. For hcp, each site has 12 nearest neighbors, so $\bar{z} = 12$.

A well-studied nonregular geometric model is the Voronoi tessellation, in which "seed" points are distributed at random in a three dimensional medium, which is then partitioned into cells, each cell containing all points that are closest to a particular seed point. Cells are irregular polyhedra bounded by polygons with varying numbers of edges, and different cells have different number of nearest

neighbors. It has been shown that for a completely random Voronoi tessellation in 3D, $\bar{z} = 15.56$ [42].

Percolation threshold values, $\varepsilon_c$, have been tabulated by computer for all regular 3D lattices and the Voronoi tesselation. For example, values of $\varepsilon_c$ for sc, hcp, and Voronoi lattices are, respectively, 0.312, 0.199, and 0.145. For values of $\bar{z}$ ranging from 4 to 42, a useful empirical correlation is [40]

$$\varepsilon_c \approx \frac{1}{1 + 0.356\bar{z}}. \tag{9.10}$$

Models based on regular lattices or Voronoi tesselations do not exactly reproduce percolation thresholds observed in most porous systems, since real systems are not configured according to these models. Other "continuum" percolation models have been proposed [43, 44]. All such models still make assumptions regarding pore sizes, shapes, and configurations, and therefore can only make specialized predictions. One interesting observation is that the percolation threshold decreases as pores become more oblong at constant $\varepsilon$, since the chance of pore intersection increases [45, 66]. In the end, the percolation threshold $\varepsilon_c$ of a family of porous media characterized by certain rules of formation is particular to these rules, which are often not well understood. It is prudent, when dealing with complex real systems, to treat $\varepsilon_c$ as a free parameter. The power of percolation theory lies in its descriptions of behaviors near threshold, which are relatively insensitive to the particular value of $\varepsilon_c$, as is now discussed.

For infinite lattices, over a range or porosities just above $\varepsilon_c$, a power law relates fraction of pore space available for release to total porosity:

$$F_\infty(\varepsilon) = A(\varepsilon - \varepsilon_c)^\beta \quad \varepsilon_c \leq \varepsilon \ll 1, \tag{9.11}$$

where $\beta = 0.40$ for all 3D cases, including Voronoi tessellations and other models. A different value $\beta =$ applies to 2D systems, which do not concern us here. The fact that $\beta$ only depends on dimension, but not the details of lattice structure or configuration of pores, indicates that a kind of "universality" exists in percolation phenomena. It should be noted, however, that $\varepsilon_c$, the prefactor $A$, and the range of validity of the power law depend on the particular lattice or other space partitioning structure. Universality of the power law exponent, but not the critical point or the prefactor, is related to universal behaviors that have been revealed in physics when comparing disparate critical phenomena, such as vaporization of liquids and ferromagnetism.

Just below the percolation threshold and onset of the infinite cluster, the average finite cluster size grows rapidly, and another power law behavior has been determined. Denoting average cluster size by $S(\varepsilon)$, the universal expression, with $\varepsilon$ close to $\varepsilon_c$, is

$$S = A_S(\varepsilon_c - \varepsilon)^{-\gamma} \quad 0 \ll \varepsilon < \varepsilon_c, \tag{9.12}$$

where $\gamma = 1.8$ for 3D ($\gamma = 2.4$ for 2D). The coefficient $A_S$ is system dependent. In *finite*-size systems below the percolation threshold, these clusters account for the releasable drug as determined by $F_\infty(\varepsilon)$. A similar power law accounts for rapid decrease in finite cluster size above $\varepsilon_c$ due to recruitment of finite clusters into the growing infinite cluster.

Another "universal" behavior of interest refers to the ratio of the effective diffusion coefficient of solute in the random pore structure and the diffusion coefficient of solute in water [46, 47]. Again, a power law relation is seen for $\varepsilon_c \leq \varepsilon \ll 1$:

$$\frac{D_{\text{eff}}(\varepsilon)}{D_0} = A_D(\varepsilon - \varepsilon_c)^\mu, \tag{9.13}$$

where $\mu = 2.0$ for all 3D systems but $A_D$ is system dependent. (For 2D, $\mu = 1.3$.) In addition to pore topology (e.g., the number of nearest neighbors), pore/throat geometry and pore wall hydrodynamic interactions (for narrow pores) are factors influencing $A_D$.

Plots comparing $F_\infty(\varepsilon)$, $S(\varepsilon)$, and $D_{\text{eff}}(\varepsilon)/D_0$ for infinite lattices are shown in Fig. 9.5b. The sharp rise of $F_\infty(\varepsilon)$ and the much gentler rise of $D_{\text{eff}}(\varepsilon)/D_0$ reflect tortuosity of the percolating pore cluster and the predominance of dead-end pores near the percolation threshold.

Although power law behaviors apply, strictly speaking, only to infinite systems, they ultimately must be compared against finite sized systems. The larger the system with respect to pore diameter, the better the theory is supposed to hold. Several studies testing percolation theory have been carried out in the controlled release arena [31, 38–41, 67–69]. Here we summarize the results of two carefully constructed studies by Hastedt and Wright [40, 41]. These authors mixed various proportions of micronized solid benzoic acid (BzA) and poly(vinyl stearate) (PVS) particles, both with average diameter ~10 μm, in a die, and were compressed to form solid monolithic tablets of thickness 500 μm. Assuming random mixing, device thickness was approximately 50 times that of the particle, which is a suitably large ratio to apply power law predictions. PVS is water insoluble and BzA has a low solubility in water, so the Higuchi model was used to account for release. Porosity in the monolith was accounted for by the volume of the drug particles, plus a small void volume (0.02) that was measured by helium intrusion.

The authors found that release rate data fit well to (9.13), with the proper value of $\mu$, above an apparent percolation threshold of $\varepsilon_c = 0.09$. This threshold is much lower than would be predicted by the sc, hcp, or Voronoi models or any reasonable model that assumes random juxtaposition of BzA and PVS particles. Two possible explanations were offered. First, it was thought that the mixing of BzA and PVS particles was not completely random. As already discussed, nonrandom mixing, and nonspherical shapes of particle aggregates, may lower the percolation threshold. Second, it was noted that PVS is not completely impermeable to BzA, as the authors demonstrated by measuring the diffusion coefficient of BzA in a thin membrane containing pure PVS. Indeed, their experiments showed nearly complete

release even at very low inclusion of BzA, with $\varepsilon < \varepsilon_c$. Thus, release was not exclusively through the BzA created pores. Instead, drug most likely was able to traverse from "isolated" BzA pores into other pores, albeit slowly, eventually reaching the surface, where drug was released.

It is usually desirable, when formulating a drug delivery system, to have all drug released, as was observed in Hastedt and Wright's work, and it appears that the matrix must be extremely impermeable to drug in order for strict percolation theory to apply. For small but finite matrix permeabilities, "effective medium" theory [36, 46], which provides a means for averaging fast transport through pores and slow transport through the matrix material, can be used to estimate drug release kinetics.

One example, where "strict" percolation theory may apply, is in the release of paclitaxel (PTX) from coated stents that are used to treat cardiac angioplasty [48]. Here, the drug particles, along with a block polymer matrix material, polystyrene-*b*-isobutylene-*b*-polystyrene (SIBS), are dissolved in a common solvent and sprayed onto stent struts (see Chap. 14). Upon evaporation of solvent, the initial solution phase separates, with PTX nanodomains dispersed in SIBS. These domains are imaged using AFM. Below 25% PTX incorporation, release is incomplete while release is virtually complete above that loading. At low loadings, only drug at or close to the surface is released while drug that is deeper in the coating is trapped by surrounding SIBS. At the higher loadings, all drug appears to be available for release through a connected series of neighboring pores.

We conclude this section with a perspective. As already described, percolation theory makes interesting qualitative predictions regarding ultimate release fraction and release kinetics from porous systems. However, it is also pointed out that its utilization requires determination of the percolation threshold for a given family of porous systems. Pore sizes need to be much smaller than overall system size, and the matrix must be highly impermeable to drug in order for percolation effects to be fully manifested. When these conditions are fulfilled, there is a sharp rise in the fraction of drug that is releasable just above the percolation threshold. Leaving aside the observation that nonreleased drug is wasted drug, one should be aware of the quality control pitfalls that are likely to present themselves near the percolation threshold. Small changes in porosity may lead to large changes in fraction released. Thus, it might be recommended that once the percolation threshold is determined, one should strive to formulate with $\varepsilon$ sufficiently larger than $\varepsilon_c$ that $F_\infty(\varepsilon)$ is close to 1. The gentler rise of $D_{\text{eff}}(\varepsilon)/D_0$ is such that one can still control the release rate by varying porosity over this "safe" range, although it should not be expected that effects will be as dramatic as they would be closer to $\varepsilon_c$.

When the matrix possesses a limited but finite permeability to drug, the percolation threshold gains a new significance. When individual drug particles/pores or clusters are isolated from each other, most drug must diffuse through the matrix material to be released, and one can use the solubility/diffusivity properties of drug in the matrix to make predictions. Drug that belongs to clusters intersecting with the surface is released in a burst, however. The strength of the burst depends on the cluster size distribution. Approaching $\varepsilon_c$ from below, average cluster size increases

and the size distribution broadens, and one may again expect quality control problems when $\varepsilon$ is too close to $\varepsilon_c$. Once $\varepsilon_c$ is determined, it is safest to stay away from it.

## 9.5 Concluding Remarks

The emphasis in the chapter has been on porous systems with complicated structural characteristics and randomness. Models have been qualitative in nature, and have primarily been developed to illustrate means by which pore structure can influence availability of drug for release, as well as release kinetics. As noted at the beginning, progress in methods for precisely characterizing the internal pore structure of a medium, and in computational power, may permit designers to obtain much more accurate predictions. We believe that qualitative modeling and quantitative characterization/computational approaches have complementary value. The former provides initial guidance while the latter enable fine tuning.

We have already noted that lessons learned from porous media can be applied to other drug delivery issues, such as transport across the skin and through tissue interstitium. These systems can all be regarded as *structured media*. In concluding this chapter, we briefly comment on diffusion through hydrogels, which constitute another important class of structured media encountered frequently in drug delivery applications.

As discussed elsewhere in this book, hydrogels are water-swollen polymer networks. Water soluble drugs passing through hydrogels diffuse more slowly than in bulk water because their pathways are obstructed by polymer chains and due to hydrodynamic interactions between the diffusing drug and the less mobile polymer. The analogy to diffusion in porous media is evident, but there are two more aspects that need to be considered in hydrogels. First, a substantial portion of hydrogel water is often "bound" to polymer chains and thus has different properties than bulk water. Second, and perhaps more importantly, hydrogel chains execute thermal "breathing" motions which may open and close water spaces available for drug diffusion. These fluctuations in time add a new statistical layer to analyzing transport. A large amount of data is now available for testing theories of partitioning and diffusion in hydrogels that take into account obstructions, hydrodynamic interactions, and chain fluctuations, as summarized in extensive reviews [49–52]. Such theories are most appropriate for drugs which have little affinity for the polymer.

There are of course cases in which drug binding to polymer in the hydrogel provides a means for controlling release rate, and building solute binding specificity is an active area of research, particularly for hydrogels intended for tissue engineering applications (see Chap. 17) [53].

Finally, we note that pore structure in controlled release systems may evolve with time. Bulk degrading polymers often feature growth of internal pores with time, prior to disintegration of the polymer mass. Similarly, porous systems have

also been designed with osmotically active agents incorporated into pores that are isolated from the surface. As water enters the pores, the latter swell until the surrounding polymer bursts, opening new channels for drug release [54].

If solid drug is incorporated into a surface eroding polymer in order to achieve zero order release, then this should occur below the percolation threshold in order to guarantee erosion control. Otherwise, pathways for direct diffusional release are available.

## References

1. Siegel RA (1989) Modeling of drug release from porous polymers. In: Rosoff M (ed) Controlled release of drugs: polymers and aggregate systems. VCH, New York, pp 1–51
2. Bean CP (1972) The physics of porous membranes–neutral pores. In: Eisenmann G (ed) Membranes. Marcel Dekker, New York, pp 1–54
3. Deen WM, Bohrer MP, Epstein NB (1981) Effects of molecular size and configuration on diffusion in microporous membranes. AIChE J 27:952–959
4. Madou M (2002) Fundamentals of microfabrication, 2nd edn. CRC, New York
5. Mueller A, Hillmyer M, Bates FS (2009) Ordered network mesostructures in block polymer materials. Macromolecules 42:7221–7250
6. Nuxoll EE, Hillmeyer MA, Wang R, Leighton C, Siegel RA (2009) Composite block polymer-microfabricated silicon nanoporous membrane. ACS Appl Mater Interf 1:889–893
7. Anglin EJ, Cheng L, Freeman WR, Sailor MJ (2008) Porous silicon in drug delivery devices and materials. Adv Drug Deliv Rev 60:1266–1277
8. Slowing II, Vivero-Escoto JL, Wu C-W, Lin VS-Y (2008) Mesoporous silica nanoparticles as controlled release drug delivery and gene transfection carriers. Adv Drug Deliv Rev 60: 1278–1288
9. Cauda V, Engelke H, Sauer A, Arcizet D, Bräuchle C (2010) Colchicine-loaded lipid bilayer-coated 50 nm mesoporous nanoparticles efficiently induce microtubule depolymerization upon cell uptake. Nano Letters 10:2484–2492
10. Martin F, Walczak R, Boiarski A, Cohen M, West T, Cosentino C, Ferrari M (2005) Tailoring width of microfabricated nanochannels to solute size can be used to control diffusion kinetics. J Control Release 102:123–133
11. Baker RW (2004) Membrane technology and applications. Wiley, Chichester
12. Li M, Rouaud O, Poncelet D (2008) Microencapsulation by solvent evaporation: state of the art for process engineering approaches. Int J Pharm 363:26–39
13. Martin AN (2011) Micromeritics. In: Sinko P (ed) Martin's physical pharmacy and pharmaceutical sciences. Kluwer, Philadelphia, pp 442–468
14. Chandler R, Koplik J, Lerman K, Willemsen JF (1982) Capillary displacement and percolation in porous media. J Fluid Mech 119:249–267
15. Lane A, Shah N, Connor WC (1986) Measurement of the morphology of high-surface-area solids: porosimetry as a percolation process. J Coll Interf Sci 109:235–242
16. Miller ES, Peppas NA, Winslow DN (1983) Morphological changes of ethylene/vinyl acetate-based controlled delivery systems during release of water-soluble solutes. J Membr Sci 14:79–92
17. Lightfoot EN, Bassingthwaighte JB, Grabowski EF (1976) Hydrodynamic models for diffusion in microporous membranes. Ann Biomed Eng 4:78–90
18. Malone DM, Anderson JL (1978) Hindered diffusion of particles through small pores. Chem Eng Sci 33:1429–1440

19. Deen WM (1989) Hindered transport of large molecules in liquid-filled pores. AIChE J 33: 1409–1423
20. Cassasa EF (1967) Equilibrium distribution of flexible polymer chains between a macroscopic solution phase and small voids. J Poly Sci Polym Lett 5:773–777
21. Davidson MG, Suter UW, Deen WM (1987) Hydrodynamic partitioning of flexible macromolecules between bulk solution and cylindrical pores. Macromolecules 20:1141–1146
22. Brenner H, Gaydos LJ (1977) The constrained Brownian movement of spherical particles in cylindrical pores of comparable radius. J Coll Interf Sci 58:312–356
23. Faxen H (1923) Die Bewegung einer Einer Starren Kuegel laengs der Achse mit zaeher Fluessigkeit gefuellten Rohres. Ark Mat Astron Fys 17:1
24. Glandt ED (1981) Noncircular pores in model membranes: a calculation of the effect of pore geometry on the partition of a solute. J Membr Sci 8:331–336
25. Cosentino C, Amato F, Walczak R, Boiarski A, Ferrari M (2005) Dynamic model of biomolecular diffusion through two-dimensional nanochannels. J Phys Chem B 109:7358–7364
26. Pricl S, Ferrone M, Fermeglia M, Amato F, Cosentino C, Ming-Cheng Cheng M, Walczak R, Ferrari M (2006) Multiscale modeling of protein transport in silicon membrane nanochannels. Part 1. Derivation of molecular parameters from computer simulations. Biomed Microdevices 8:277–290
27. Amato F, Cosentino C, Pricl S, Ferrone M, Fermeglia M, Ming-Cheng Cheng M, Walczak R, Ferrari M (2006) Multiscale modeling of protein transport in silicon membrane nanochannels. Part 2. From molecular parameters to a perdictive continuum diffusion model. Biomed Microdevices 8:291–298
28. Higuchi T (1963) Mechanism of sustained-action medication. Theoretical analysis of solid drugs dispersed in solid matrices. J Pharm Sci 52:1145–1149
29. Pismen LM (1974) Diffusion in porous media of a random structure. Chem Eng Sci 29: 1227–1236
30. Siegel RA, Langer R (1986) A new Monte Carlo approach to diffusion in constricted porous geometries. J Coll Interf Sci 109:426–440
31. Siegel RA, Langer R (1990) Mechanistic studies of macromolecular drug release from macroporous polymers. II. Models for the slow kinetics of drug release. J Control Release 14:153–167
32. Dudko OK, Berezhkovskii AM, Weiss GH (2005) Time-dependent diffusion coefficients in periodic porous media. J Phys Chem B 109:21296–21299
33. Maknovskii YA, Berezhkovskii AM, Zitserman VYu, Zitserman VY (2009) Time-dependent diffusion in tubes with periodic partitions. J Chem Phys 131:104705
34. Broadbent S, Hammersley J (1957) Percolation processes: crystals and mazes. Proc Cambr Philos Soc 53:629–641
35. Bollobas B, Riordan O (2006) Percolation. Cambridge University Press, Cambridge
36. Stauffer D, Aharony A (1994) Introduction to percolation theory. CRC, New York
37. Sahimi M (1994) Applications of percolation theory. Taylor and Francis, Boca Raton, FL
38. Saltzman M, Langer R (1989) Transport rates of proteins in porous materials with known microgeometry. Biophys J 55:163–171
39. Siegel RA, Kost J, Langer RA (1989) Mechanistic studies of macromolecular drug release from macroporous polymers. I. Experiments and preliminary theory concerning completeness of drug release. J Control Release 8:223–236
40. Hastedt JE, Wright JL (1990) Diffusion in porous materials above the percolation threshold. Pharm Res 7:893–901
41. Hastedt JE, Wright JL (2006) Percolative transport and cluster diffusion near and below the percolation threshold of a porous polymeric matrix. Pharm Res 23:2427–2440
42. Winterfeld PH, Scriven LE, Davis HT (1981) Percolation and conduction on 3D Voronoi and regular networks: a second case study in topological disorder. J Phys C Solid State Phys 17:3429–3439
43. Powell MJ (1979) Site percolation in randomly packed spheres. Phys Rev B 20:4194–4198

44. Vicsek T, Kertesz J (1981) Monte Carlo renormalization-group approach to percolation in a continuum: test of universality. J Phys A Math Gen 14:L31–L37
45. Boissonade J, Barreau F, Carmona F (1983) The percolation of fibers with random orientations: a Monte Carlo study. J Phys A Math Gen 16:2777–2787
46. Kirkpatrick S (1973) Percolation and conduction. Rev Mod Phys 574:574–588
47. Brandt WW (1975) Use of percolation theory to estimate effective diffusion coefficients of particles migrating on various ordered lattices and in a random network structure. J Chem Phys 63:5162–5167
48. Barocas V, Drasler W, Girton T, Guler I, Knapp DR, Moeller J, Parsonage E (2009) A dissolution-diffusion model for the TAXUS™ drug-eluting stent with surface burst estimated from continuum percolation. J Biomed Mater Res B Appl Biomater 90B:267–274
49. Schnitzer JE (1988) Analysis of steric partition behavior of molecules in membranes using statistical physics. Application to gel chromatography and electrophoresis. Biophys J 54: 1065–1076
50. Lustig SR, Peppas NA (1988) Solute diffusion in swollen membranes. IX. Scaling laws for solute diffusion in gels. J Appl Polym Sci 36:735–747
51. Amsden B (1998) Solute diffusion within hydrogels. Mechanisms and models. Macromolecules 31:8382–8395
52. Masaro L, Zhu XX (1999) Physical models of diffusion for polymer solutions, gels, and solids. Progr Polym Sci 24:731–775
53. Sakiyama-Elbert SE, Hubbell JA (2000) Controlled release of nerve growth factor from a heparin-containing fibrin-based cell ingrowth matrix. J Control Release 69:149–158
54. Amsden BG, Cheng Y-L (1994) Enhancement of fraction released above percolation threshold from monoliths containing osmotic excipients. J Control Release 33:99–105
55. Eitzman DM, Melkote RR, Cussler EL (1996) Barrier membranes with tipped flakes. AIChE J 42:2–9
56. DeRocher JP, Gettlefinger BT, Wang J, Nuxoll EE, Cussler EL (2005) Barrier membranes with different sizes of aligned flakes. J Membr Sci 254:21–30
57. Lape NK, Nuxoll EE, Cussler EL (2004) Polydisperse flakes in barrier films. J Membr Sci 236:29–37
58. Fredrickson GH, Bicerano J (1999) Barrier properties of oriented disc composites. J Chem Phys 110:2181–2188
59. Liu Q, Cussler EL (2006) Barrier membranes made with lithographically printed flakes. J Membr Sci 285:56–67
60. Shante VKS, Kirkpatrick S (1971) An introduction to percolation theory. Adv. Phys. 20: 325–357
61. Nan C-W, Shen Y, Ma J (2010) Physical composites near percolation. Annu Rev Mater Res 40:131–151
62. Larson RG, Scriven LE, Davis HT (1977) Percolation theory of residual phases in porous media. Nature 268: 409–413
63. Berkowitz B, Balgerg I (1993) Percolation theory and its application to groundwater hydrology. Water Resourc Res 29:775–794
64. Holman LE, Leuenberger H (1988) The relationship between solid fraction and mechanical properties of compacts–the percolation theory approach. Int J Pharmaceut 46:35–44
65. Kuentz M, Leuenberger H (1999) Pressure susceptibility of polymer tablets as a critical property: a modified Heckel equation. J Pharm Sci 88:174–179
66. Balberg I, Binenbaum N, Wagner N (1984) Percolation thresholds in the three-dimensional sticks system. Phys Rev Lett 52:1465–1468
67. Leuenberger H, Bonny JD, Kolb M (1995) Percolation effects in matrix-type controlled release systems. Int J Pharmaceut 115:217–224
68. Tongwen X, Binglin H (1998) Mechanism of sustained drug release in diffusion-controlled polymer matrix–aplication of percolation theory. Int J Pharmaceut 170:139–149
69. Adrover A, Massimiliano G, Grassi M (1996) Analysis of controlled release in disordered structures: the percolation model. J Membr Sci 113:21–30

# Part IV
# Spatial Delivery Systems and Mechanisms

# Chapter 10
# Targeted Delivery Using Biodegradable Polymeric Nanoparticles

**Elias Fattal, Hervé Hillaireau, Simona Mura, Julien Nicolas, and Nicolas Tsapis**

**Abstract** Biodegradable polymeric nanoparticles have been extensively used for targeted drug delivery mostly because of their potentialities to carry multifunctional properties. This chapter shows that nanoparticles can be made of different types of materials and prepared by multiple preparation methods that allow for the entrapment of all types of drugs, small and large, hydrophilic and lipophilic. Moreover, this chapter makes clear that polymer chemistry and the discovery of new grafting methods have opened the way to modification, leading to the covalent linkage on their surface by either poly(ethylene glycol) for long blood circulation time, or ligands for specific biorecognition. The future of such targeting systems relies on the discovery of new and specific targets that will permit the use of targeted nanoparticles in several therapeutic applications.

## Abbreviations

| | |
|---|---|
| Apo E | Apolipoprotein E |
| Av | Avidin |
| BSA | Bovine serum albumin |
| cLABL | Cyclo-(1,12)-penITDGEATDSGC |
| CS | Chitosan |
| CuAAC | Copper-catalyzed azide-alkyne cycloaddition |
| DCC | Dicyclocarbodiimide |
| DLS | Dynamic light scattering |

E. Fattal (✉) • H. Hillaireau • S. Mura • J. Nicolas • N. Tsapis
Laboratoire de Physico-Chimie, Pharmacotechnie et Biopharmacie, Université Paris-Sud 11, UMR CNRS 8612, Faculté de Pharmacie, 5 rue Jean-Baptiste Clément, 92296 Châtenay-Malabry Cedex, France
e-mail: elias.fattal@u-psud.fr

J. Siepmann et al. (eds.), *Fundamentals and Applications of Controlled Release Drug Delivery*, Advances in Delivery Science and Technology,
DOI 10.1007/978-1-4614-0881-9_10, 

| | |
|---|---|
| DMAP | 4-Dimethylaminopyridine |
| EDC | 1-Ethyl-3-[3-(dimethylamino)propyl]carbodiimide |
| EGF | Epithelial growth factor |
| EGFR | Epidermal growth factor receptor |
| FA | Folic acid |
| HA | Hyaluronic acid |
| HAS | Human serum albumin |
| HER2 | Human epidermal receptor-2 |
| ICAM-1 | Intercellular adhesion molecule-1 |
| Mal | Maleimide |
| MPS | Mononuclear phagocyte system |
| $M_W$ | Molecular weight |
| NAv | Neutravidin |
| NCs | Nanocapsules |
| NHS | *N*-hydroxysuccinimide |
| NPs | Nanoparticles |
| NSs | Nanospheres |
| PACA | Poly(alkylcyanoacrylate) |
| PBLG | Poly(benzyl L-glutamate) |
| PCL | Poly(ε-caprolactone) |
| PCS | Photon correlation spectroscopy |
| PDS | Pyridyl disulfide |
| PEG | Poly(ethylene glycol) |
| PEI | Polyethyleneimine |
| PEO | Poly(ethyleneoxide) |
| PHDCA | Poly(hexadecylcyanoacrylate) |
| PLA | Poly(lactic acid) or polylactide |
| PLGA | Poly(lactide-*co*-glycolide) |
| PLL | Poly-L-lysine |
| PMMA | Poly(methylmethacrylate) |
| polyHis | Polyhistidine |
| PPO | Poly(propylene oxide) |
| PS | Polystyrene |
| PVL | Poly(δ-valerolactone) |
| QELS | Quasi-elastic light scattering |
| ROP | Ring-opening polymerization |
| SEM | Scanning electron microscopy |
| siRNA | Small interfering ribonucleic acid |
| Sulfo-MBS | m-maleimidobenzoyl-*N*-hydroxy-sulfosuccinimide ester |
| TEM | Transmission electron microscopy |
| Tf | Transferrin |
| TMCC | 2-Methyl, 2-carboxytrimethylene carbonate |

## 10.1 Introduction

Over the past decades, there has been a considerable interest in the development of biodegradable nanoparticles (NPs) as drug delivery systems. Various polymers such as poly(lactide-*co*-glycolide) (PLGA), polylactide (PLA), or poly(alkylcyanoacrylate) (PACA) have been used for targeted drug delivery, increasing the therapeutic efficiency and reducing side effects. NPs are defined as submicron (around 100 nm) colloidal systems, generally made of a biodegradable polymer. NPs were first developed in the mid-1970s by Birrenbach and Speiser [1]. Later on, their application for the design of drug delivery systems was made available by the use of biodegradable polymers, considered to be highly suitable for human applications [2]. At that time, research on colloidal carriers was focusing only on liposomes but no one was able to make available stable systems for clinical applications. In a few experiments, NPs have been shown to be more active than liposomes due to their better stability [3, 4]. This is the reason why many drugs were associated to NPs in the last decades (e.g. antibiotics, cytostatics, nucleic acids). Nevertheless, the ability to deliver high effective dosages to specific sites in the human body has become the holy grail of drug delivery research. This is the reason why specific targeting of NPs to the active site is the only solution that guarantees a marked drug efficacy. Attempts to attach ligands to particle surface have been achieved. This chapter focuses on the state of the art regarding the design of targeted delivery systems using biodegradable polymer NPs.

## 10.2 Methods for Nanoparticle Preparation

Depending on the process used for their preparation, nanospheres (NSs) or nanocapsules (NCs) can be independently obtained. NSs are matrix systems in which the drug is dispersed throughout the whole matrix, whereas NCs are vesicular systems in which the drug is confined in a cavity surrounded by a unique polymeric membrane. Several methods have been developed so far for their preparation. They can be classified into two main categories according to whether their formation requires a polymerization reaction, or whether it is achieved directly from a natural macromolecule or a preformed polymer.

### *10.2.1 Nanoparticles Obtained by Monomer Polymerization*

Nanoparticle preparation methods based on monomer polymerization generally consists in either introducing a monomer into the dispersed phase of an emulsion, an inverse microemulsion or dissolving the monomer in a nonsolvent of the polymer.

In these systems, polymerization reactions occur in two steps: a nucleation step followed by a growth step. The first type of NP prepared by such methods was proposed by Birrenbach and Speiser [1]. These particles consisted of crosslinked poly(acrylamide) and were obtained by polymerization of acrylamide and *N, N′*-methylenebisacrylamide in inverse microemulsions. Polymerization was carried out by gamma irradiation. Later, Kopf et al. [5] used the same procedure to encapsulate drugs. Similarly, Kreuter and Speiser [6] developed poly(methylmethacrylate) (PMMA) NPs by dispersion polymerization of methyl methacrylate. The monomer was dissolved in an aqueous medium before being polymerized. This method allowed avoiding the use of large quantities of organic solvent and anionic surfactants. These systems were, however, inappropriate for drug delivery purposes, especially for intravascular administration, because of the very slow biodegradability of the polymers used. To broaden the spectrum of NPs for drug delivery, Couvreur et al. [2, 7] developed NSs consisting of PACA. These polymers, used for several years as surgical glues, are bioresorbable [8]. In contrast to other acrylic derivatives requiring an energy input for polymerization that can affect drug stability, alkylcyanoacrylates can be readily polymerized without such a contribution. These NPs are prepared by anionic emulsion polymerization of alkylcyanoacrylate dispersed in an acidic aqueous phase. The size of the NPs obtained is approximately 200 nm, but it can be reduced to 30–40 nm using a non-ionic surfactant in the polymerization medium [9] or by adding $SO_2$ to the monomer [10]. The dominant mechanism of particle degradation was found to be a surface erosion process [11]. Freeze fracture studies have revealed that the internal structure of these NSs consisted in a matrix of a dense polymeric network [12]. Molecular weight ($M_w$) determinations made by size exclusion chromatography suggested that NSs are built up from an entanglement of numerous small oligomeric subunits rather than from the wrapping of one or a few long polymer chains [13]. The anionic emulsion polymerization has been successfully used to obtain NPs of poly(dialkylmethilidene malonate), a biomaterial displaying a great potential as alternative drug delivery system [14, 15]. Alternatively to anionic polymerization, radical polymerization has been developed for PACA NP production [16]. Finally, to obtain PACA NCs, Al Khouri-Fallouh et al. [17] proposed an original method in which the monomer is solubilized in an oil-containing alcoholic phase and is then dispersed in an aqueous solution of surfactants. In contact with water, the alcoholic phase is dispersed and favors the formation of a very fine oil-in-water emulsion. The monomer, insoluble in water, polymerizes at the oil–water interface, yielding the nanocapsule wall. This simple process was designed to encapsulate large quantities of lipophilic drugs.

Other authors have suggested processes adapted to hydrophilic drugs in which alkylcyanoacrylates are polymerized in inverse water-in-oil emulsion or microemulsion to form NCs [18–20] (Fig. 10.1). These methods require a tedious washing step to remove oils and obtain an aqueous dispersion of NCs.

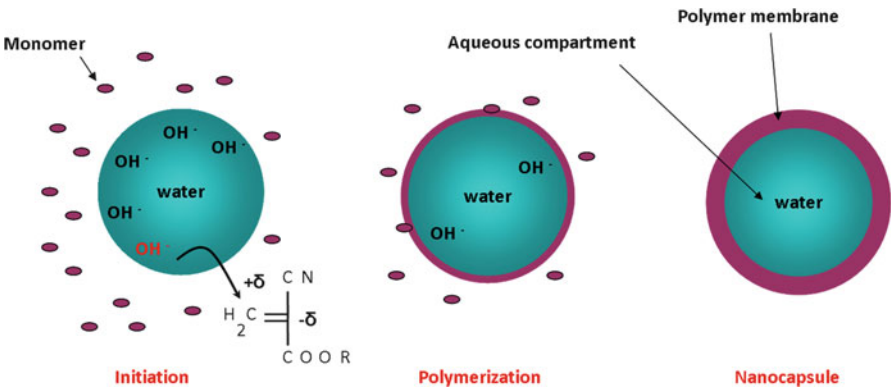


**Fig. 10.1** Formation of alkylcyanoacrylate nanocpasules with aqueous cores

### *10.2.2 Nanoparticles Obtained from Preformed Polymers*

With the exception of alkyl-2-cyanoacrylates and dialkylmethylidene malonate, most of the monomers suitable for a micellar polymerization process in an aqueous phase lead to slowly biodegradable or nonbiodegradable polymers. In addition, residual molecules in the polymerization medium (monomers, oligomers, surfactants) can be more or less toxic, and a tedious purification of colloidal material is thus needed. To avoid these limitations, methods have been proposed using preformed polymers or natural macromolecules. In general, NPs are formed by precipitation of synthetic polymers or by denaturation, solidification, or crosslinking of natural biomacromolecules, mainly proteins and polysaccharides.

#### 10.2.2.1 Nanoparticles Prepared with Synthetic Preformed Polymers

Two methodologies have been proposed for the preparation of NPs from preformed synthetic polymers. The first is based on the emulsification of non water-miscible organic solutions of preformed polymers in an aqueous phase containing surfactants, followed by the removal of solvents under reduced pressure (Fig. 10.2). This method, named solvent emulsion–evaporation, is derived from the preparation of pseudolatex or artificial latex developed by Vanderhoff et al. [21]. It has been applied to PLA by Vanderhoff et al. [21] and then by Krause et al. [22] and by Tice and Gilley [23]. The main advantage is that PLA polymers are generally considered as biodegradable, biocompatible, and well tolerated. Poly(β-hydroxybutyrate) is also considered as a very promising biodegradable polymer that has been used as a material for producing NPs by solvent evaporation process [24, 25]. With this polymer, high pressure emulsification reduced particle size down to 170 nm. Biodegradable NSs of PLA were prepared by emulsion, microfluidization, and solvent evaporation method using

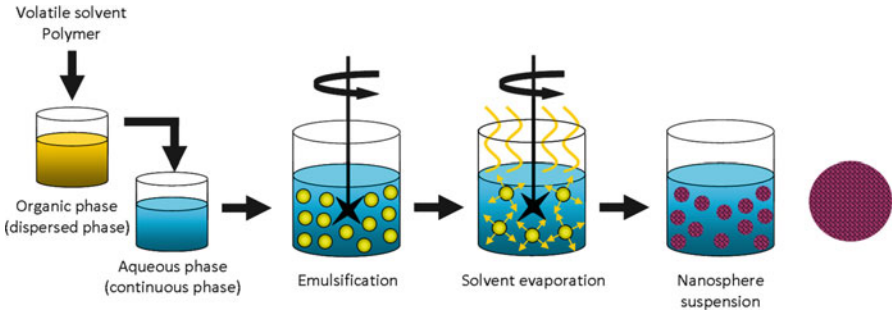


**Fig. 10.2** Preparation of nanospheres by solvent emulsion evaporation

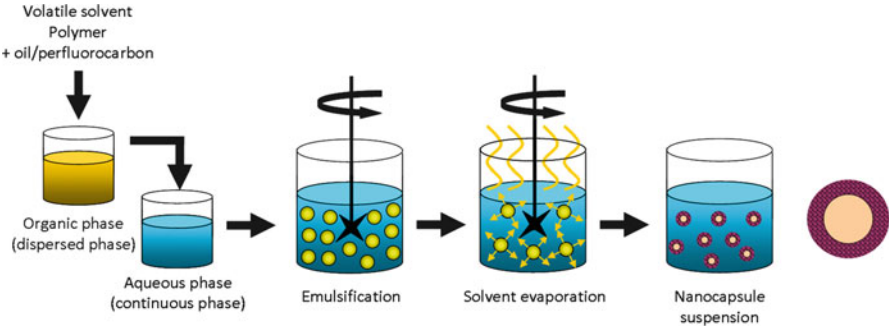


**Fig. 10.3** Preparation of oil–perfluorocarbon nanocapsules by solvent emulsion evaporation

human serum albumin as stabilizer [26]. Alternatively, PLGA can be selected to increase the rate of polymer degradation [27].

The solvent emulsion–evaporation process has also been modified to yield capsules with a oil or perfluorcarbon core surrounded by a polymer shell [28, 29]. The oil/perfluorcarbon is simply mixed in the organic solvent under the miscibility limit, along with the polymer (Fig. 10.3). The rest of the process remains identical.

To encapsulate hydrophilic drugs, a double emulsion (water-in-oil-in-water) is formed with the drug dissolved in the internal aqueous phase (Fig. 10.4).

When the solvent is partially miscible with water, the emulsification–diffusion process can be used to obtain NPs [30]. The aqueous phase is saturated with the solvent and the organic phase saturated with water. After emulsification, water is added in excess to promote solvent diffusion in the aqueous phase and polymer precipitation [31] (Fig. 10.5). The solvent emulsification–diffusion process has also been modified to generate capsules with an oily core by adding oil in the organic phase [32, 33].

Another interesting technology, applicable to a wide range of polymers, is based on the selection of salts producing the salting out of acetone from water [34, 35]. Saturated aqueous solution prevents acetone from being miscible with water.

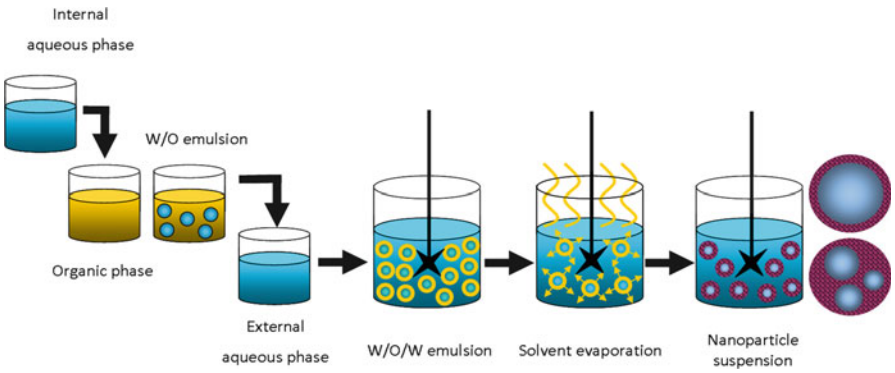


**Fig. 10.4** Preparation of nanoparticles containing internal water cavities by double emulsion solvent evaporation process

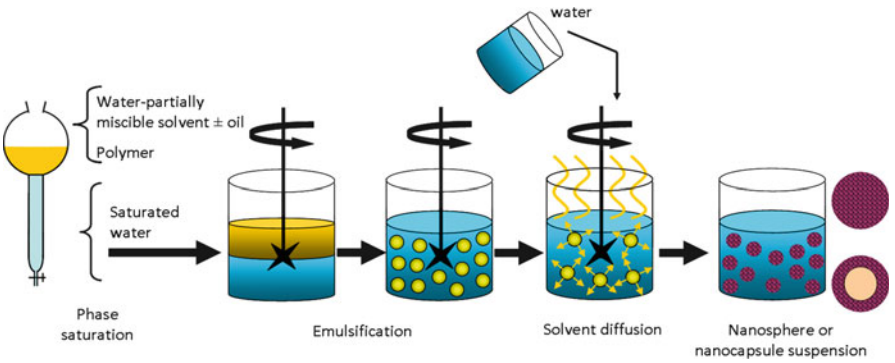


**Fig. 10.5** Preparation of nanoparticles by emulsification–diffusion

After the preparation of an oil-in-water emulsion, water is added in a sufficient amount to allow complete diffusion of acetone into the aqueous phase, inducing the formation of NSs (Fig. 10.6). This process does not require a temperature increase and, therefore, may be useful for heat sensitive drugs [35]. The method has allowed to prepare PLA, PMMA, and ethylcellulose NSs [34].

The second methodology for obtaining NSs from synthetic polymers has been proposed by Fessi et al. [36] and is called "nanoprecipitation." It is based on the precipitation of a polymer in solution following the addition of a nonsolvent of the polymer. Therefore, this method allows the formation of NSs without prior emulsification (Fig. 10.7). The choice of the polymer/solvent/nonsolvent system is obviously extremely important, since it governs the production of NPs [36]. The solvent and the nonsolvent of the polymer must be mutually miscible. The progressive addition of the polymer solution to the not solvent generally leads to the formation of NSs close to 200 nm in size. The NPs appear to be formed by a

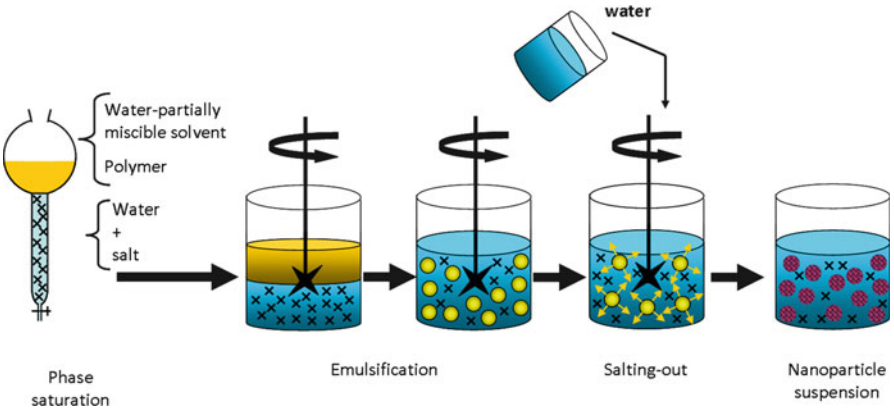


**Fig. 10.6** Preparation of nanoparticles by salting-out

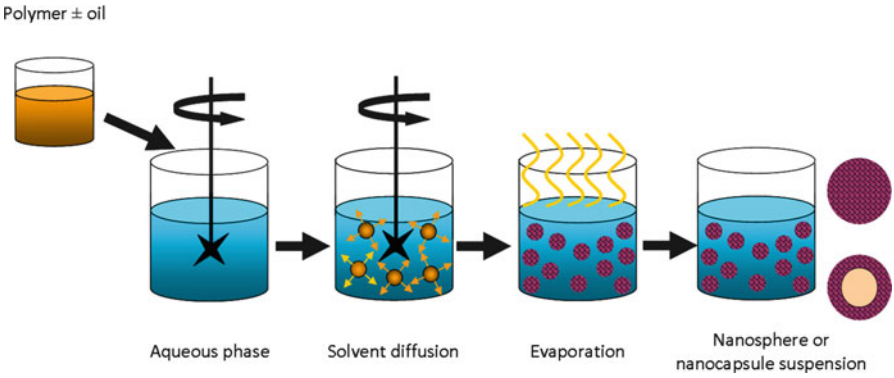


**Fig. 10.7** Preparation of nanoparticles by nanoprecipitation

mechanism comparable to the "diffusion and standing" process found in spontaneous emulsification. This phenomenon, beyond the scope of this chapter, has been explained by local variations of the interfacial tension between the two nonmiscible liquids due to the reciprocal diffusion of the third liquid. This method has been successfully applied to various polymeric materials such as PLA and PLGA, poly(ε-caprolactone) (PCL), ethylcellulose, PACA, and polystyrene (PS). Several parameters such as polymer concentration and respective volumes of the two phases can be adjusted to optimize NPs formation [37]. NCs may also be obtained by a very similar procedure [38] (Fig. 10.7). The method differs from the preparation method of NSs by the introduction of a fourth component of an oily nature miscible with the polymer solvent but not miscible with the polymer solvent/nonsolvent mixture. The polymer is deposited at the interface between the finely dispersed oily droplets and the water phase, thus forming NPs with a shell-like wall and a size around 200 nm (Fig. 10.7).

#### 10.2.2.2 Nanoparticles Produced from Natural Macromolecules

The first method for preparing NPs from a natural macromolecule was developed by Scheffel et al. [39]. These particles were obtained by thermal denaturation of albumin. In fact, this process was already developed earlier to prepare microspheres [40]. It is based on the heating of an oily emulsion containing very small droplets of an aqueous solution of albumin, which induces the denaturation of the protein leading to NPs. Methods for preparing albumin NPs by heat denaturation were later optimized by Gallo et al. [41]. Such methodology is obviously only applicable to drug molecules that are not heat sensitive.

For this reason, methods based on the desolvation/resolvation properties of proteins have been proposed [42, 43]. Gelatin NPs have been synthesized by the slow addition of a desolvating agent to a gelatin solution, which induces progressive modifications of the protein's tertiary structure that turn it into a hydrophobic material [42]. After partial resolvation of the polymer, NPs may be obtained. This operation is performed under turbidimetric control before the particles are hardened by chemical crosslinking using glutaraldehyde. This process offers the advantage of producing NPs directly in suspension in an aqueous medium, but the use of potentially toxic compounds (glutaraldehyde, desolvating agents) requires purification. Thus, Stainmesse et al. [44] proposed a simpler, single step technique consisting of pouring an aqueous solution of the protein (i.e. gelatin or albumin) into a heated nonsolvent.

Yoshioka et al. [45] used a slightly different method in which droplets of an aqueous solution of gelatin from a water-in-oil emulsion were hardened by cooling below the gelation point and subsequent crosslinking with glutaraldehyde. A water-in-oil emulsion system has been used also by Edman et al. [46] and Artursson et al. [47] to produce carbohydrate NPs. In this method, natural polysaccharides (starch) were derivatized with acrylic acid glucidyl ester and emulsified. Upon addition of a diamine, the water phase droplets are polymerized to yield NPs whose size was around 500 nm.

A new concept was then proposed for preparing NPs by a gelification process [48]. In fact, this method is based on the control of the gelification of alginate by calcium ions. After strengthening the microgels formed using poly-L-lysine, small particles of well-defined sizes (250–850 nm) may be obtained. The main interest of those NPs is that they are characterized by an unusual high surface hydrophilicity.

Other authors have used electrostatic interactions to associate polyelectrolytes of opposite charges and obtain NPs. In particular, this process has been used to encapsulate nucleic acids (DNA, siRNA, or antisense oligonucleotides) using for example polyethyleneimine (PEI) as a polycation [49, 50]. The very same concept has been used to prepare insulin-loaded NPs formed by ionic interactions between cationic chitosan (CS) and anionic tripolyphosphate [51].

This general overview of the state of the art shows that an impressive number of technologies are available for the preparation of NPs. These methods follow a wide variety of principles and employ macromolecular materials of synthetic or natural origin. Some of these processes present drawbacks from a technological standpoint,

while others are probably unsuitable for the formulation of certain drugs. However, the diversity of the methodologies proposed let suppose that a suitable formulation process should exist for any biologically active molecule that would need to be administered under the form of NPs.

## 10.3 Basic Characterization of Nanoparticles

NPs may be characterized in terms of average diameter, size distribution and surface charge by several experimental techniques. The main one is dynamic light scattering (DLS), sometimes referred to as photon correlation spectroscopy (PCS) or quasi-elastic light scattering (QELS). This technique allows the diffusion coefficient of NPs to be determined by shining a laser through a NP suspension and the intensity fluctuations of the scattered light to be analyzed. This yields the diffusion coefficient of the particles related to their Brownian motion and hence the particle size using the Stokes–Einstein relationship. Several models allow the particle mean diameter and the width of the size distribution to be obtained, sometimes expressed as polydispersity index. The diameter measured in DLS is the hydrodynamic diameter and takes into account the solvatation/hydration layer at the surface of NPs. Therefore, the hydrodynamic diameter may vary with nanoparticle concentration, as well as with the concentrations and types of ions in the medium. The obtained size may be larger than measured by electron microscopy when, for example, particles are removed from their native environment. Scanning electron microscopy (SEM) or transmission electron microscopy (TEM) is indeed relevant to evaluate nanoparticle size distribution and the resulting polydispersity index. For SEM, NPs are deposited on a carbon conductive tape either freeze dried or as a suspension that is left to dry. Samples are then coated by a thin layer of metal before being examined. For TEM, suspensions are deposited on a copper grid and optionally contrasted by uranyl acetate of phosphotungstic acid depending on their surface charge. Nanoparticle surface charge is assessed by electrophoretic mobility measurements, and thanks to the Smoluchowski equation, the zeta potential of NPs is obtained. In absolute value, the larger is the zeta potential, the better the colloidal stability.

## 10.4 Fate of Nanoparticles After Intravenous Administration

### *10.4.1 Uptake by Phagocytic Cells*

After intravenous administration, NPs are mainly taken up by phagocytosis primarily in specialized cells also called professional phagocytes: mostly in macrophages from the mononuclear phagocyte system (MPS), monocytes, neutrophils and dendritic cells [52]. Other types of cells (fibroblasts, epithelial and endothelial cells),

referred to as para- and nonprofessional phagocytes, may display some phagocytic activity, but to a lower extent [53]. The phagocytic pathway of entry into cells can be described using three distinct steps (1) recognition by opsonization in the bloodstream, (2) adhesion of the opsonized particles to the macrophages, and (3) ingestion of the particle. Opsonization is an important process occurring before the phagocytosis itself. It consists in tagging the foreign NPs by proteins called opsonins, making the former visible to macrophages. This typically takes place in the bloodstream rapidly after introduction of the particles. Major opsonins include immunoglubulins (IgG and IgM) as well as complement components (C3, C4, C5) [54], in addition to other blood serum proteins (including laminin, fibronectin, C-reactive protein, type-I collagen) [55]. Opsonized particles then attach to the macrophage surface through specific receptor-ligand interactions. The major and best-studied receptors for this purpose include the Fc receptors (FcR) and the complement receptors (CR). FcRs bind to the constant fragment of particle-adsorbed immunoglobulins, the best understood interaction involving IgG and FcγR; CRs mostly bind to C3 fragments [52, 56]. Other receptors, including the mannose/fructose and scavenger receptors can be involved in the phagocytosis [52] while new opsono-receptors such as CD44 are still being discovered [57]. Receptor ligation is the beginning of a signaling cascade mediated by Rho-family GTPases [58], which triggers actin assembly, forming cell surface extensions (pseudopodia) that zipper up around the particle and engulf it.

The resulting phagosome will ferry the particle throughout the cytoplasm. As actin is depolymerized from the phagosome, the newly denuded vacuole membrane becomes accessible to early endosomes [59]. Through a series of fusion and fission events, the vacuolar membrane and its contents will mature, fusing with late endosomes and ultimately lysosomes to form a phagolysosome. The rate of these events depends on the surface properties of the ingested particle, typically from half to several hours [52]. The phagolysosomes become acidified due to the vacuolar proton pump ATPase located in the membrane and acquire many enzymes, including esterases and cathepsins [60]. The enzymatic content of these intracellular vesicles is a key issue for synthetic polymeric NPs, since polymer biodegradability is required in pharmaceutical applications, both to ensure drug release and to avoid accumulation of the ingested material, which can lead to further toxicities. This explains the wide use of the biodegradable PLGA and PACA. PLGA chains are degraded through a hydrolytic mechanism facilitated by low pH [61], whereas PACA is bioeroded intracellularly, i.e. the alkyl groups are hydrolyzed by esterases, which increases the hydrophilicity of the polymer backbone until it becomes water soluble [8].

### *10.4.2 Escaping Phagocytic Cells*

Several strategies have been developed to interfere with the binding of opsonins to make NPs “invisible” to the MPS. This process, called “dysopsonization,” varies according to different parameters, of which the size plays a major role; smaller

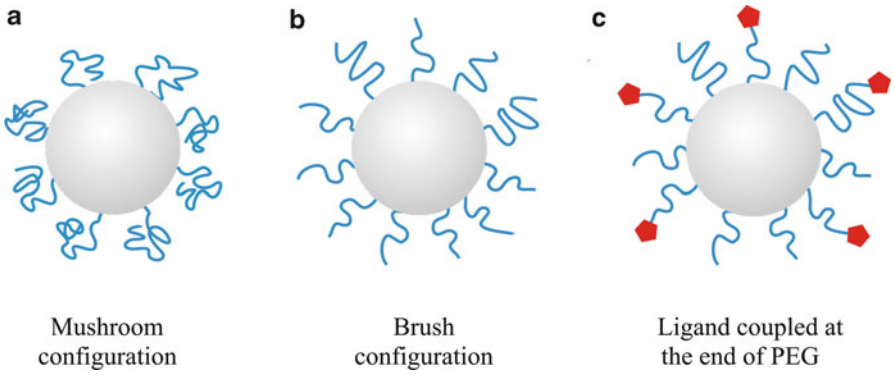


**Fig. 10.8** Different conformation of PEG onto nanoparticle surface

particles attach less proteins [62]. Moreover, NPs with hydrophobic surface [63] or that are positively charged [64] are more prone to opsonization. Shielding the surface with hydrophilic polymers such as poly(ethyleneglycol) (PEG) reduces opsonization [55]. It is conferred by PEG coating (or PEGylation) due to the formation of a dense, hydrophilic cloud at the surface of NPs. Indeed, water molecules form hydrogen bonds with the oxygen from PEG ether groups, leading to the creation of a hydrated layer around the particle that prevents interaction with proteins. When opsonins are attracted to the NP surface, hydrophilic PEG molecules adopt in solution an extended conformation, which starts to be compressed [65]. This compression causes the transition of PEG to a higher energy conformation and leads to the creation of an opposite repulsive force that, when it is high enough, can balance and overcome the attractive forces between NPs and opsonins. However, PEG's ability to reduce plasma protein adsorption and interaction with macrophages of MPS is strictly dependent on different parameters such as the molecular weight ($M_W$). Many authors reported that PEG with a minimum $M_W$ of 2,000 Da is required to achieve stealth properties. Indeed, PEG polymers with high $M_W$ show higher flexibility than smaller PEG chains and can guarantee a more efficient protection [66–68]. Moreover, an optimal surface stabilization can be conferred using a mixture of PEG with different $M_W$s, where the short PEG chains are interdigitated between higher $M_W$ PEG chains [69]. In addition, the surface chain density and the configuration of polymer chains are critical points to cover all the surface of the NPs and provide an efficient steric protection [70–73]. At low density, polymer chains show a large range of motion and assume a mushroom configuration in which PEG molecules are disposed close to NPs surface, which is favorable for protein repulsion (Fig. 10.8a). However, the low density of PEG molecules leaves enough spaces between chains making the surface still accessible to proteins adsorption [65]. When increasing chain density, the range of motion of PEG chains is reduced and they exhibit a brush configuration (Fig. 10.8b). The high density provides a complete coverage, but the reduced mobility of PEG chains decreases the steric hindrance properties of the PEG layer [74]. Therefore, an optimal surface

coverage can be achieved with an intermediate configuration between the mushroom and the extended one where the density is enough to ensure complete surface coverage but enough freedom to preserve molecule motion. According to the area occupied by each PEG chain, [75], the optimal surface density should correspond to a distance of around 1 nm between two PEG chains to prevent the adsorption of small proteins and around 2 nm for larger proteins [76]. Moreover, as described below, PEG end groups can be used for nicely coupling ligands to their extremities (Fig. 10.8c).

Surface coverage of NPs has been achieved by physical adsorption of the commercially available poloxamer copolymers that are made of poly(ethylene oxide) and poly(propylene oxide) (PPO). Their block structure allows their adsorption onto NPs surface via their hydrophobic PPO block, while the PEO block, soluble in the surrounding medium, forms a hydrophilic brush-like surface [74]. However, a drawback of polymer adsorption approach is their desorption and displacement by blood components after injection leaving some nonprotected spaces available for opsonin binding [77]. To overcome this issue, an alternative was proposed using amphiphilic diblock copolymers R-PEG in which PEG is linked to a biodegradable polymer (R) such as PLGA, PLA, PCL, or PACA. The two portions of the copolymer have different solubility: PEG is soluble in water while R is soluble in organic solvents. During preparation of NPs, the PEG chains migrate toward the water phase to form the external layer of the stealth® NPs whose cores are mainly composed of R chains. In recent studies, surface properties of biodegradable PLGA NPs have been successfully modified using PEGylated phospholipids [78, 79]. PEGylation or carbohydrates [80]. This coating provides steric protection against protein adsorption [81]. Carbohydrates show biodegradability and biocompatibility, and present many reactive groups for ligand coupling. As for PEG, surface modification can be achieved by adsorption or the use of polysaccharides coupled to biodegradable polymers. The most used polysaccharides are dextran, chitosan, and heparin. It is reported that dextran and its derivatives could induce strong complement activation due to the high availability of hydroxyl groups. However, complement activation can be decreased by grafting sulfonate groups near to the hydroxyl groups or by grafting dextran chains in a brush and flexible conformation [82, 83].

### *10.4.3 Extravasation from Leaky Endothelium*

PEGylation results in the so-called stealth® or long circulating NPs [55]. However, NPs obtained with copolymers show longer circulation time than similar NPs with surface absorbed PEG [84–87]. Moreover, their administration results in a low uptake by the liver and higher level of targeted organ accumulation compared to non-surface-modified NPs [66, 86, 88–90]. As a result, these NPs can exploit abnormalities of tumor vasculature, namely, hypervascularization, aberrant vascular architecture, and extensive production of vascular permeability factors that induce NP extravasation within tumor tissues [91]. In addition, solid tumors tend

to lack functional lymphatics and extravasated NPs are retained within the tumor site for prolonged periods of time. However, this strategy poses a limit to the maximum size of the particles of about 100–300 nm, since larger particles would be less likely to pass through the fenestrations passively. Moreover, such an approach relies exclusively on the presence of vascular fenestrations whose size is known to change over time, being negligibly small at an early stage of the disease. In addition, the extent of extravasation is affected by the type of tumor and the site of tumor growth [92] and is potentially reduced by antiangiogenic therapies. Other parameters such as particle geometry, which might be different from one material to another, are still under debate regarding the ideal particle shape that would allow the leaky endothelium to be crossed [93].

## 10.5 Ligand Coupling to Nanoparticles

### *10.5.1 General Considerations*

As described before, the most convenient covalent coupling strategy employed with polymeric nanocarriers relies on the synthesis of amphiphilic block copolymers whereby the hydrophobic part is generally a biodegradable polymer and the hydrophilic part is a PEG chain at the extremity of which is attached the ligand. The latter can be either linked to the amphiphilic copolymer prior to self assembly into NPs (Fig. 10.9a), at the surface of preformed NPs (Fig. 10.9b), or being already coupled to the PEG chain prior synthesis of the block copolymer (Fig. 10.9a). The choice of synthetic route is mainly governed by the size of the ligand to be attached: whereas a small ligand such as folic acid (FA) can be linked either to the copolymer prior NP formation or at the surface of preformed NPs, the linkage of bulky ligands (e.g. peptide or protein) is restricted to the second pathway for obvious self-assembly and hydrophilic-lipophilic balance reasons. Importantly, here, the PEG chain not only acts as a spacer between the NP core and the ligand but also confers steric stabilization and stealth properties to the resulting nanocarriers as described above.

Some examples also reported the direct coupling of peptides (without a PEG spacer) to the core polymer, followed by self-assembly into the corresponding functionalized NPs (Fig. 10.9c).

Noncovalent functionalization for preparing targeted NPs can be envisioned using different strategies. The most widely employed route involves avidin (Av)/steptavidin/neutravidin–biotin couples, which exhibit the strongest noncovalent biological interaction known to date [94, 95]. In this case, the biotin-binding protein can be either (1) attached to the surface of the NPs, either at the extremity of PEG chains (Fig. 10.10a) or directly to the core of the NPs (Fig. 10.10b) and subsequently incubated with a biotinylated ligand or (2) functionalized by the desired ligand, by biotinylation (Fig. 10.10c) or by standard coupling chemistry (Fig. 10.10d) and linked to preformed biotinylated NPs.

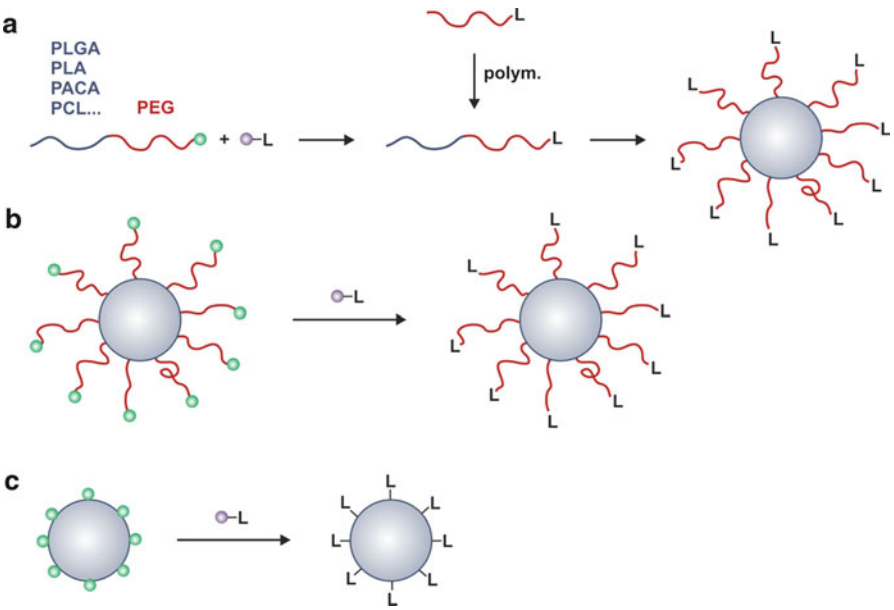


**Fig. 10.9** Synthetic routes for achieving ligand-functionalized nanoparticles by covalent coupling (*L* ligand)

The simple adsorption of a PEG-based surfactant at the surface of NPs and their subsequent coupling with the desired ligand, or the simple adsorption of ligands at the surface of the NPs have also been investigated, although possible desorption upon in vivo injection can represent an issue.

## *10.5.2 Covalent Coupling Strategies*

A wide range of ligation strategies has been used so far to achieve targeted NPs. Most of them employ traditional coupling chemistries that take advantage of functional groups already present in the structures of polymers and biologically active ligands. In addition, the establishment of novel coupling approaches has been recently witnessed, a typical example being the use of click chemistry.

### 10.5.2.1 Traditional Coupling Reactions

The most representative example in this field is certainly the amidation reaction between an amine moiety and a carboxylic acid group, performed under standard dicyclocarbodiimide (DCC) coupling conditions. This reaction often occurs in

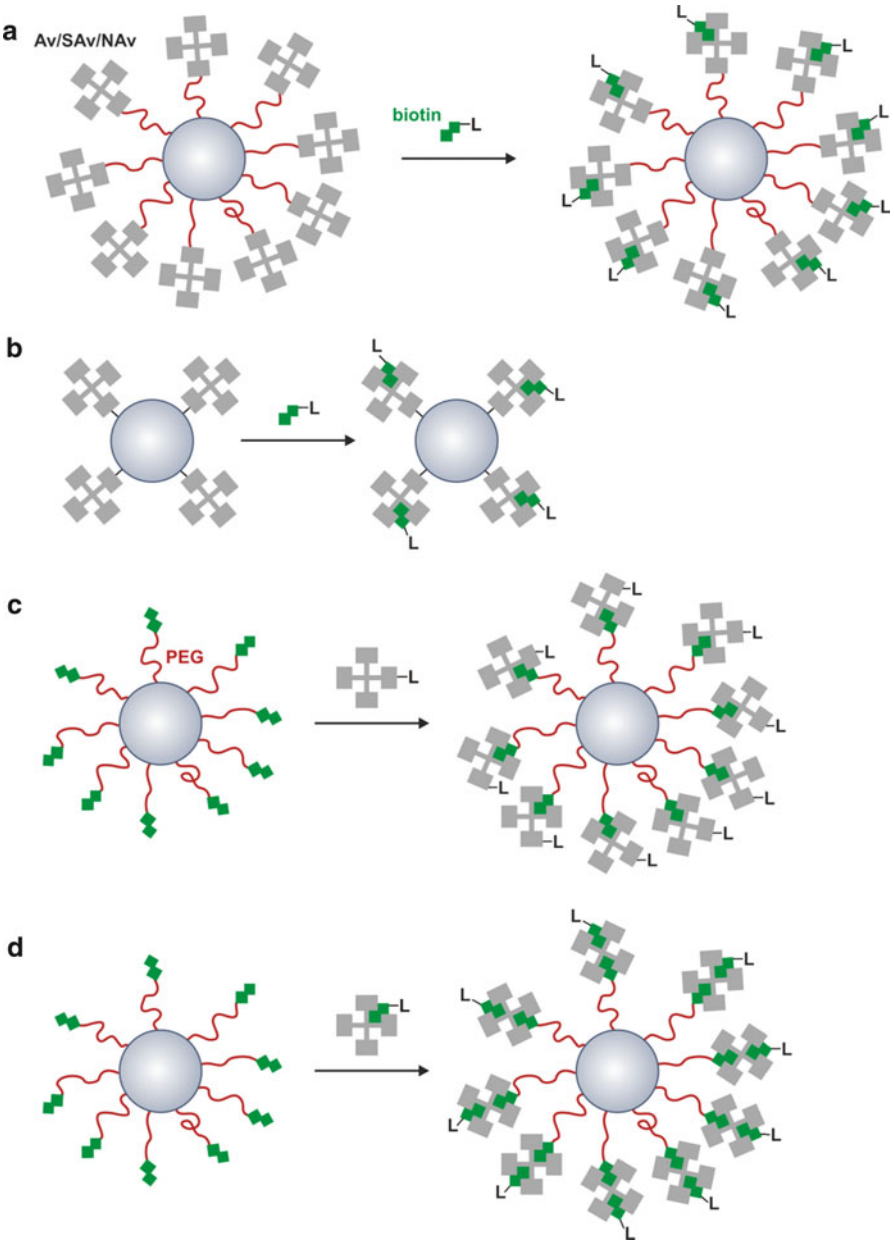


**Fig. 10.10** Synthetic routes for achieving functionalized NPs by noncovalent coupling using avidin/streptavidin/neutravidin–biotin interactions (*L* ligand, *Av* avidin, *SAV* streptavidin, *NAv* neutravidin)

the presence of NHS to prepare an activated ester in situ, prone to react with amine-containing moieties.

The amidation pathway for targeted NPs was reported with PLGA, PLA, PCL, poly (δ-valerolactone) PVL, PACA, poly(benzyl L-glutamate) (PBLG), polyethyleneimine (PEI), or polyhistidine (polyHis) NPs covered by PEG chains using $H_2N$–PEG [96–109] or NHS–PEG [110–127] reactive moieties for coupling. FA [96–102, 104, 105, 107–109, 114–116, 120, 121, 126, 128], RGD peptide [122–124], RNA aptamers [110–113], cyclo-(1,12)-penITDGEATDSGC (cLABL) peptide [126], Epidermal growth factor (EGF) [117, 118, 125], anti-epidermal growth factor receptor (anti-EGFR) antibody [119], galactose [97], or biotin [101] were selected as the ligand of interest. PEI-*b*-PLA NPs were also derivatized with FA by amidation [129].

Thiol/maleimide (Mal) coupling, which leads to a thioether bond, is also a route of interest for targeted NPs. Typical examples are the use of thiolated OX26 antibody, [130] bovine serum albumin (BSA) [131] or RGD peptide [132] followed by their linkage at the surface of preformed Mal-PEG-*b*-PCL or Mal-PEG-*b*-PLA NPs. The anti-human epidermal receptor-2 (HER2) antibody was also thiolated upon reaction with 2-iminothiolane and further linked to maleimide-decorated PEG-*b*-PLA NPs [133]. The reverse strategy, which consists of the synthesis of thiolated NPs, was reported using PLA as the biodegradable polymer, anti-HER2 or anti-CD20 monoclonal antibodies as the ligands, and *m*-maleimidobenzoyl-*N*-hydroxy-sulfosuccinimide ester (sulfo-MBS) as the crosslinker [134–136]. One can also take advantage of the maleimide function to perform a Diels–Alder coupling. This was demonstrated by the synthesis of a poly(TMCC-*co*-LA)-*g*-PEG-furan, further conjugated to a maleimido-antibody (anti-HER2) to yield functionalized NPs [137].

Interestingly, this coupling strategy was also used in combination with the amidation pathway to prepare functionalized human serum albumin (HSA) or gelatin NPs. The studies reported the dual coupling via the heterobifunctional NHS-PEG-Mal, used here as a spacer between the core of the NP and the desired ligand [138–144]. This was successfully applied to OX26, R17217, and trastuzumab antibodies [138, 142, 143], EGFR [140], as well as to Apo E [139, 141, 144]. FA was also attached via its native carboxylic acid group to hydroxyl-terminated HO-PEG-*b*-PCL-based [145] and polyHis-*b*-PEG-OH [116] NPs under DCC/DMAP assistance or under its amino form at the surface of activated PEO-*b*-PPO-*b*-PEO/PEG shell crosslinked NCs exhibiting reactive *p*-nitro phenyl ester functional groups [146].

The amination coupling pathway between amino containing ligands and aldehyde terminated polymers has been reported with CS and glycyrrhizine [147], PACA-*b*-PEG and the transferrin ligand [148], PBLG-*b*-PEG and the GRGDS peptide [149] and with PCL-*b*-PEG and the GRGDS peptide [150, 151]. Another study reported the coupling of RGD peptide to PLA-*b*-PEG, previously activated by methyl sulfonyl chloride [128]. Eventually, the reaction between a pyridyl-disulfide-terminated (poly-L-lysine) PLL and a thiolated transferrin, giving rise to a disulfide bridge, was reported [152]. This route required the previous thiolation of transferrin (Tf) by a dithiopyridin linker. Interestingly, PLGA NPs were functionalized by the

Tf ligand via an epoxy linker [153]. The same ligand was also anchored to gelatin NPs following an identical ligation strategy [154].

The core polymer of the NPs can also be directly functionalized by the ligand. This strategy was applied to PLGA, PLA/PLL, or CS NPs where the authors took advantage of native functional groups already present within the polymer structure for further coupling to peptides, antibodies, or organic molecules via DCC chemistry [155–164]. Branched polyester copolymers of hydroxy-acid and allyl glycidyl ether were derivatized with a known potent nonselective selectin ligand by esterification via an acyl chloride formation [165, 166].

#### 10.5.2.2 Other Coupling Strategies

Copper(I)-catalyzed Huisgen 1,3-dipolar cycloaddition reaction between an azide and an alkyne, named copper catalyzed azide-alkyne cycloaddition (CuAAC), belongs to the class of chemical reactions, often referred as "click" chemistry [167], that share several very important features (1) a very high efficiency in terms of both conversion and selectivity, (2) mild experimental conditions, (3) a simple workup, and (4) little or no by-products. Click chemistry has recently received a tremendous interest in many research areas [168–172] and can be readily performed in aqueous solutions, thus representing a relevant approach if functionalization of preformed NPs is envisioned. However, in contrast to traditional coupling approaches using native ligand functional groups (amine, thiol, carboxylic acid, etc.), the click chemistry pathway requires both the NP/copolymer and the ligand to be previously derivatized with alkyne and azide functionalities prior coupling reaction. Click chemistry for surface functionalized NPs was applied to PEGylated PACA copolymers/NPs exhibiting azide moieties at the extremity of the PEG chains, acting here as a clickable scaffold. Model and biologically active alkyne derivatives were quantitatively coupled either to the copolymer in homogeneous medium followed by self-assembly in aqueous solution or directly at the surface of preformed azido-decorated NPs in aqueous dispersed medium, both yielding highly functionalized NPs [173, 174]. Recently, Lu et al. have derivatized a poly(2-methyl-2-carboxytrimethylene carbonate-*co*-D,L-lactide) (poly(TMCC-*co*-LA)) copolymer with azido-PEG pendant chains via 1-ethyl-3-[3-(dimethylamino)propyl]carbodiimide (EDC) chemistry to form the corresponding amphiphilic copolymer able to self-assemble into well-defined NPs [175]. Then, alkyne modified KGRGDS peptides were synthesized and coupled to the azide functionalized NPs via click chemistry. Very recently, a difunctional initiator has allowed ring opening polymerization (ROP) of lactide and controlled/living radical polymerization of PEG-based macromonomers (bearing glucopyranoside molecules linked by click chemistry) to be sequentially performed by divergent chain growth [176]. The amphiphilic feature of such a comb-shaped construct led to well defined NPs decorated with sugar moieties, the accessibility of which was accessed by concanavalin.

Photografting was investigated as an original approach to design targeted NPs [177–179]. Garinot et al. reported the synthesis of PCL-*b*-PEG-*g*-GRGDS NPs

achieved by grafting of RGD molecules to PCL-*b*-PEG copolymer [179]. This covalent coupling required first the derivatization of PEG chain ends with NHS groups, prone to react with the peptide terminal free amines. Another route relied on the use of *O*-succinimidyl 4-(*p*-azidophenyl) butanoate upon irradiation [177, 178].

### *10.5.3 Noncovalent Ligations*

Avidin, neutravidin and streptavidin exhibit four biotin-binding sites that can be exploited for conjugation purposes with NPs. To immobilize the biotin-binding protein at their surface, a convenient strategy is to use an heterobifunctional PEG spacer [141], bearing on one side a NHS group for coupling to the NPs and on the other side a maleimide moiety suitable for conjugation to the biotin binding protein via sulfhydryl modification. Linkage to NPs is then achieved by amidation whereas the protein is linked via a thioether bond. Targeted NPs are eventually obtained by simple incubation with the desired biotinylated ligand (here a biotinylated Apo E), the synthesis of which is usually achieved by traditional coupling chemistry (biotin display a primary carboxylic acid function far from its binding site). The coupling of biotin-binding proteins to the NPs can also be directly obtained by standard DCC assisted coupling chemistry [180, 181]. In this case, NPs are previously activated with DCC and further reacted with the protein. In these examples, NPs should present suitable functional groups at their surface such as $NH_2$ or COOH for the coupling to take place. It has also been reported the covalent linkage of neutravidin at the surface of gelatin NPs by thiolation and subsequent incubation with biotinylated epithelial growth factor (EGF) or Apo E [182–184].

The reverse strategy, which consists in the preparation of biotinylated NPs [185, 186], requires the coupling of the ligand to the biotin binding protein by traditional coupling chemistry, whereas biotin is inserted at the extremity of PEG chains surrounding the NPs. This was exemplified by the design of OX-26-decorated PEGylated-chitosan NPs [185] and anti-VCAM-1 functionalized poly(sebacid acid)-PEG NPs[186] with Av and streptavidin as the biotin-binding protein, respectively.

Eventually, the synthetic route, which consists in the biotinylation of both the NPs and the ligands, has been employed. The binding is performed upon incubation with a biotin binding protein, and this has been exemplified with PEI-*b*-PEG-biotin, Tf-biotin and Av [187].

Even though covalent linkages or biotin-based bindings are believed to be the most robust approaches regarding the stability of the corresponding nanocarriers, other noncovalent routes have been used to prepare targeted NPs. For instance, Blackwell et al. reported the simple adsorption of monoclonal antibody recognizing E- and P-selectin adsorbed at the surface of PS NPs [188].

Interestingly, different routes have been proposed to obtain hyaluronic acid (HA)-coated PCL NSs (1) coating the core by chain entanglement with HA, (2) coating the NSs by a simple HA adsorption or (3) coating the NSs by electrostatic

interactions between negatively charged HA and a cationic surfactant (stearylamine or benzalkonium chloride). The best results in term on HA coating were shown when the positively charged surfactant was used [189].

Eventually, some authors performed the coupling reaction on the Pluronic surfactant, previously adsorbed at the surface of PS [190] or PLGA [191] NPs. Whereas Gullbert et al. reported the preparation of RGD- and RGDE-Pluronic-coated PS NPs via a pyridyl disulfide (PDS) functionalization [190], Chittasupho et al. proposed the synthesis of NHS-Pluronic followed by coupling of the cLABL peptide via its terminal amine group [191].

## 10.6 Ligand Targeted Nanoparticles

### *10.6.1 Folate Receptor Targeting*

FA has been widely studied as a targeting ligand for nanocarriers, especially for anticancer strategies [192]. Indeed, FA binds with a low affinity to the reduced folate carrier present in virtually all cells, but with a high affinity (in the nanomolar range) to the glycosylphosphatidylinositol-linked folate receptor (FR), which exhibits very limited distribution [193]. In particular, FR is often overexpressed on the surface of cancer cells but highly restricted in normal tissues [194]. Moreover, FR has the ability to transport both FA and the FA-linked cargo by receptor mediated endocytosis with subsequent endosomal escape into the cytosol [193, 195], thus avoiding lysosomal degradation. FA has been successfully coated onto PEGylated polymer NPs by conjugation of the activated *N*-hydroxysuccinimide FA with the aminated PEG-poly(hexadecyl cyanoacrylate) (PHDCA) copolymer. Surface plasmon resonance revealed that FA bound to these particles had a tenfold higher apparent affinity for FR compared to free FA [104]. FA was also associated to PLGA NPs by coating a poly(L-lysine)-*b*-PEG-FA conjugate. Such particles showed a preferential uptake by the FR-overexpressing carcinoma KB cells compared to simple PLL-*b*-PEG-coated PLGA NPs, which was not the case in the presence of an excess of free FA in the medium, nor in the case of the lung adenocarcinoma, FA-deficient, A549 cells [98]. The same approach was used to coat PEI/siRNA polyplexes with FA. These FA-decorated polyplexes significantly increased gene inhibition on KB cells compared to FA-coated lipoplexes, but not on A549 cells [196]. These successful examples of FR targeting are slowly translating from in vitro to in vivo. For instance, PLGA NPs have recently been decorated by FA via the use of PLA-*b*-PEG-FA or PLA-*b*-PEG-biotin conjugates. These particles were found to increase paclitaxel delivery to tumors and to enhance its activity on a mice xenograft model [197]. Further studies may, however, be needed before polymeric NPs can fully demonstrate in vivo the relevance of FR targeting.

### *10.6.2 Transferrin Receptor Targeting*

Tf receptors (TfR) are known to be overexpressed in several malignant tissues compared to healthy ones [198] (typically two- to tenfold more [199]). Tf was, therefore, studied as targeting ligand to specific cell populations to increase cellular uptake of anticancer drugs loaded onto NPs. PLGA NPs were thereby conjugated with Tf and exhibited a twofold greater in vitro uptake by MCF-7 cells as well as a reduced exocytosis, compared to unconjugated PLGA particles. Competition experiments with free Tf confirmed the involvement of TfR in the uptake process [153]. In vivo studies performed in S-180 solid tumor bearing mice showed a promising accumulation in the tumor of paclitaxel after intravenous administration of Tf-conjugated to PEG-*b*-PACA NPs loaded with this drug [200]. Interestingly, in addition to cancer cells, TfR are also known to be highly expressed in some healthy tissues such as brain capillaries where they are known to mediate transcytosis [201]. TfR targeting has, thus, been investigated to enhance the delivery of drugs across the blood–brain barrier, which is almost impermeable to most of the available therapeutic molecules. Tf was conjugated to PEG-coated albumin NPs, which significantly increased the delivery of AZT to rat brain, the proportion of the drug located in this tissue being doubled as compared to the same particles devoid of ligand [202]. However, the use of Tf as a ligand for NP decoration may be hindered by a competition with the corresponding endogenous pool of ligands [201]. This is the reason why monoclonal antibodies (mAb) have been employed such as the mouse OX26 directed against the rat TfR. This mAb binds to a TfR epitope distinct from the Tf binding site, thus preventing competition with endogenous Tf [203]. Using the Av-biotin technology, chitosan NSs were also conjugated with PEG bearing the OX26 mAb. These functionalized CS-PEG-biotin-Av/OX26 NPs were able to translocate into the brain tissue after intravenous administration to mice [185].

### *10.6.3 Targeting of Cell Adhesion Molecules*

Cell adhesion molecules (CAMs) have been investigated for the targeting of various endothelial cells, especially for anticancer strategies directed against angiogenesis. In particular, the $\alpha_v\beta_3$ integrin, highly expressed on neovascular endothelial cells, is usually targeted using the RGD peptide [204]. PEGylated PLGA based NPs, when decorated with RGD and RGD peptidomimetic were notably found to efficiently deliver paclitaxel to HUVEC cells via $\alpha_v\beta_3$ binding. These particles also enhanced paclitaxel activity on transplantable lymphoid tumor bearing mice, in terms of tumor growth as well as survival rates [178]. RGD targeting has also been applied to nucleic acid delivery. Interestingly, while PEGylated PEI based polyplexes were found to exhibit a lower cell uptake compared to the parent polyplexes, conjugation of an RGD peptide at the extremity of the PEG chains was able to restore the original uptake levels, but this time through specific

receptor-mediated endocytosis. This allowed efficient in vitro luciferase gene inhibition by siRNA, as well as in vivo accumulation in cancer cells, after intravenous administration to mice [122]. RGD-grafted chitosan NPs have also been recently demonstrated to preferentially accumulate in vitro into $\alpha_v\beta_3$-expressing cells, but also to significantly enhance tumor growth inhibition by specific delivery of siRNA to mice [205].

ICAM-1 is another particularly interesting target for altered endothelial cells, especially for the treatment of inflammatory diseases [206]. PEGylated PLGA NPs bearing mAb to Intercellular Adhesion Molecule-1 (ICAM-1) and other CAMs were demonstrated to selectively adhere to inflamed endothelium, both under in vitro flow conditions and in vivo on mice, thus mimicking leukocytes [207]. As for cell internalization, endothelial cells did not internalize ICAM-1 mAb but mAb-coated PS NPs or multivalent mAb conjugates. Indeed, the uptake was found to require ICAM-1 clustering [208]. ICAM-1 targeting was also investigated using the cyclic peptide cLABL, which was associated to PLGA NPs by coupling it to the poloxamer used for the particle coating. These particles allowed an in vitro delivery of doxorubicin to ICAM-1-overexpressing A549 cells [191].

### *10.6.4 Targeting of Human Epidermal Receptors*

The EGFR and HER-2 play a critical role in cell growth and proliferation in response to the binding of growth factor ligands [204]. Some mAbs targeting these receptors have been approved for cancer treatment, including cetuximab (EGFR, colorectal, and head/neck cancers) and trastuzumab (HER-2, breast cancer). The latter has been conjugated to PLA NPs, either through direct coupling via thiolation, or using the avdin-biotin technology. In both cases, this strategy enhanced the delivery to the HER-2 expressing SKOV-3 ovarian cancer cells by up to tenfold [209, 210]. Trastuzumab was also used to decorate HSA NPs, allowing a specific uptake on several HER-2-positive breast cancer cell lines [142], and an efficient delivery of the Plk1 antisense oligonucleotide to BT-474 cells [211]. Besides mAbs, "natural" ligands such as EGF were also investigated for the targeting of EGRF. Gelatin NPs decorated with EGF through Av-Biotin interaction were found to be selectively taken up by A549 cells [183]. Noteworthy, they were efficiently delivered as a nebulized aerosol to mice and were accumulated in EGFR-positive cancer cells in the lung tissue [184].

### *10.6.5 Targeting of the Prostate-Specific Membrane Antigen*

Prostate specific membrane antigen (PSMA) is abundantly expressed in cancer situations, making it the most appealing antigen for targeted treatments of prostate cancers. The A10 aptamer, which recognizes the extracellular domain of PSMA

[212], was grafted onto PEG-*b*-PLGA NPs loaded with docetaxel [111] or with a cisplatin prodrug [213]. These particles bound specifically to LNCaP prostate epithelial cells, significantly enhancing the drug cytotoxicity. They also allow a higher tumor regression after a single intratumoral injection to mice, compared to untargeted NPs, and a 100% survival rate over 109 days [111].

### *10.6.6 Targeting Using Cell Penetrating Peptides*

Cell penetrating peptides (CPPs), also known as protein transduction domains, have also raised increasing attention due to their ability to translocate across membranes [214, 215]. The most commonly studied CPP for NP functionalization is the HIV-1 transactivating transcriptional activator peptide (TAT). Remarkably, ultrasmall superparamagnetic iron oxide particles (USPIO) coated with TAT were shown to efficiently tag progenitor cells [216]. Polyplexes based on DNA and a PEI-PEG-TAT conjugate also led to interesting transfection efficiency after intratracheal instillation to mice [217]. Although promising, the mechanism of CPP-mediated targeting and uptake remains to be fully elucidated.

## 10.7 Conclusions

This chapter has extensively described different aspects of targeted delivery using biodegradable polymer NPs. Most of the studies dealing with NPs have proved over the past years to have a dramatic impact in medicine by improving the biodistribution and the target site accumulation while reducing side effects of systematically applied therapeutics. As shown in this chapter, attempts to increase the amount of drug that actually reaches the target tissue was carried out using ligand-addressed nanoparticles. However, one of the main issues to be solved is tissue targeting specificity. Indeed, as exemplified, in the field of tumor targeting by nanotechnologies for instance, rather ubiquitous receptors were addressed such as the folic acid, hyaluronic acid, transferrin, or epithelial growth factor receptors. Future prospects should include targeting more specific receptors or designing multifunctional nanoparticles, combining imaging and triggered drug delivery. One example could be the design of polymeric nanocarriers containing ultrasound contrast agents that can be visualized under ultrasound imaging, which can release their drug content at the target site by ultrasound energy.

## References


1. Birrenbach G, Speiser P (1976) Polymerized micelles and their use as adjuvants in immunology. J Pharm Sci 65:1763–1766
2. Couvreur P, Kante B, Roland M, Guiot P, Bauduin P, Speiser P (1979) Polycyanoacrylate nanocapsules as potential lysosomotropic carriers: preparation, morphological and sorptive properties. J Pharm Pharmacol 31:331–332
3. Fattal E, Rojas J, Roblot-Treupel L, Andremont A, Couvreur P (1991) Ampicillin-loaded liposomes and nanoparticles: comparison of drug loading, drug release and in vitro antimicrobial activity. J Microencapsul 8:29–36
4. Fattal E, Rojas J, Youssef M, Couvreur P, Andremont A (1991) Liposome-entrapped ampicillin in the treatment of experimental murine listeriosis and salmonellosis. Antimicrob Agents Chemother 35:770–772
5. Kopf H, Joshi RK, Soliva M, Speiser P (1977) Study of micelle polymerization in the presence of low molecular weight drugs, Part 2: Mode of binding of incorporated low molecular weight model substances to polyacrylamide-based nanoparticles. Pharm Ind 39:993–997
6. Kreuter J, Speiser PP (1976) In vitro studies of poly(methyl methacrylate) adjuvants. J Pharm Sci 65:1624–1627
7. Couvreur P, Roland M, Speiser P (1982) Biodegradable submicroscopic particles containing a biologically active substance and composition containing them. US Patent 4329332
8. Lenaerts V, Couvreur P, Christiaens-Leyh D, Joiris E, Roland M, Rollman B, Speiser P (1984) Degradation of poly (isobutyl cyanoacrylate) nanoparticles. Biomaterials 5:65–68
9. Seijo B, Fattal E, Roblot-Treupel L, Couvreur P (1990) Design of nanoparticles of less than 50 nm in diameter, preparation, characterization and drug loading. Int J Pharm 62:1–7
10. Lenaerts V, Raymond P, Juhasz J, Simard MA, Jolicoeur C (1989) New method for the preparation of cyanoacrylic nanoparticles with improved colloidal properties. J Pharm Sci 78:1051–1052
11. Muller RH, Lherm C, Herbort J, Couvreur P (1990) In vitro model for the degradation of alkylcyanoacrylate nanoparticles. Biomaterials 11:590–595
12. Rollot JM, Couvreur P, Roblot-Treupel L, Puisieux F (1986) Physicochemical and morphological characterization of polyisobutyl cyanoacrylate nanocapsules. J Pharm Sci 75:361–364
13. Lescure F, Seguin C, Breton P, Bourrinet P, Roy D, Couvreur P (1994) Preparation and characterization of novel poly(methylidene malonate 2.1.2.)-made nanoparticles. Pharm Res 11:1270–1277
14. De Keyser JL, Poupaert JH, Dumont P (1991) Poly(diethyl methylidenemalonate) nanoparticles as a potential drug carrier: preparation, distribution and elimination after intravenous and peroral administration to mice. J Pharm Sci 80:67–70
15. Mbela TKM, Poupaert JH, Dumont P, Hoemer SA (1993) Development of poly (dialkylmethylidene malonate) nanoparticles as drug carriers. Int J Pharm 92:71–79
16. Chauvierre C, Labarre D, Couvreur P, Vauthier C (2003) Radical emulsion polymerization of alkylcyanoacrylates initiated by the redox system dextran−cerium(IV) under acidic aqueous conditions. Macromolecules 36:6018–6027
17. al Khouri N, Fessi H, Roblot-Treupel L, Devissaguet JP, Puisieux F (1986) An original procedure for preparing nanocapsules of polyalkylcyanoacrylates for interfacial polymerization. Pharm Acta Helv 61:274–281
18. El-Samaligy MS, Rohdewald P, Mahmoud HA (1986) Polyalkyl cyanoacrylate nanocapsules. J Pharm Pharmacol 38:216–218
19. Gasco M, Trotta M (1986) Nanoparticles from microemulsions. Int J Pharm 29:267–268
20. Lambert G, Fattal E, Pinto-Alphandary H, Gulik A, Couvreur P (2000) Polyisobutylcyanoacrylate nanocapsules containing an aqueous core as a novel colloidal carrier for the delivery of oligonucleotides. Pharm Res 17:707–714
21. Vanderhoff JW, El Aasser MS, Ugelstad J (1979) Polymer emulsification process. U.S. Patent

22. Krause HJ, Schwartz A, Rohdewald P (1986) Interfacial polymerization, a useful method for the preparation of polymethylcyanoacrylate nanoparticles. Drug Dev Ind Pharm 12:527–552
23. Tice TR, Gilley RM (1985) Preparation of injectable controlled release microcapsules by a solvent-evaporation process. J Control Release 2:343–352
24. Koosha F, Muller RH, Davis SS, Davis MC (1989) The surface chemical structure of poly (b-hydroxybutyrate) microparticles produced by solvent evaporation process. J Control Release 9:149–153
25. Koosha F, Muller RH, Washington C (1987) Production of polyhydroxybutyrate (PHB) nanoparticles for drug targeting. J Pharm Pharmacol 39:136P
26. Verrecchia T, Huve P, Bazile D, Veillard M, Spenlehauer G, Couvreur P (1993) Adsorption/desorption of human serum albumin at the surface of poly(lactic acid) nanoparticles prepared by a solvent evaporation process. J Biomed Mater Res 27:1019–1028
27. Gomez-Gaete C, Tsapis N, Besnard M, Bochot A, Fattal E (2007) Encapsulation of dexamethasone into biodegradable polymeric nanoparticles. Int J Pharm 331:153–159
28. Losa C, Marchal-Heussler L, Orallo F, Vila Jato JL, Alonso MJ (1993) Design of new formulations for topical ocular administration: polymeric nanocapsules containing metipranolol. Pharm Res 10:80–87
29. Pisani E, Tsapis N, Paris J, Nicolas V, Cattel L, Fattal E (2006) Polymeric nano/microcapsules of liquid perfluorocarbons for ultrasonic imaging: physical characterization. Langmuir 22:4397–4402
30. Leroux JC, Allemann E, Doelker E, Gurny R (1995) New approach for the preparation of nanoparticles by an emulsification–diffusion method. Eur J Pharm Biopharm 41:14–18
31. Quintanar-Guerrero D, Allemann E, Doelker E, Fessi H (1998) Preparation and characterization of nanocapsules from preformed polymers by a new process based on emulsification-diffusion technique. Pharm Res 15:1056–1062
32. Moinard-Checot D, Chevalier Y, Briancon S, Beney L, Fessi H (2008) Mechanism of nanocapsules formation by the emulsion-diffusion process. J Colloid Interface Sci 317:458–468
33. Mosqueira VC, Legrand P, Pinto-Alphandary H, Puisieux F, Barratt G (2000) Poly(D, L-lactide) nanocapsules prepared by a solvent displacement process: influence of the composition on physicochemical and structural properties. J Pharm Sci 89:614–626
34. Allémann E, Gurny R, Doelker E (1992) Preparation of aqueous polymeric nanodispersions by a reversible salting-out process: influence of process parameters on particle size. Int J Pharm 87:247–253
35. Ibrahim H, Bindschaedler C, Doelker E, Buri P, Gurny R (1992) Aqueous nanodispersions prepared by a salting-out process. Int J Pharm 87:239–246
36. Fessi H, Devissaguet JP, Puisieux F, Thies C (1991) Process for the preparation of dispersible colloidal systems of a substance in the form of nanocapsules. US Patent 5049322
37. Legrand P, Lesieur S, Bochot A, Gref R, Raatjes W, Barratt G, Vauthier C (2007) Influence of polymer behaviour in organic solution on the production of polylactide nanoparticles by nanoprecipitation. Int J Pharm 344:33–43
38. Fessi H, Puisieux F, Devissaguet JP, Ammoury N, Benita S (1989) Nanocapsules formation by interfacial polymer deposition following solvent displacement. Int J Pharm 55:R1–R4
39. Scheffel U, Rhodes BA, Natarajan TK, Wagner HN (1972) Albumin microspheres for study of the reticulo-endothelial system. J Nucl Med 13:498–503
40. Zolle I, Rhodes BA, Wagner HN Jr (1970) Preparation of metabolizable radioactive human serum albumin microspheres for studies of the circulation. Int J Appl Radiat Isot 21:155–167
41. Gallo JM, Hung CT, Perrier DG (1984) Analysis of albumin microsphere preparation. Int J Pharm 22:63–74
42. Marty JJ, Oppenheim RC, Speiser P (1978) Nanoparticles – a new colloidal drug delivery system. Pharm Acta Helv 53:17–23

43. Oppenheim RC, Marty JJ, Stewart NF (1978) The labelling of gelatin nanoparticles with 99mTechnetium and their in vivo distribution after intravenous infection. Aust J Pharm Sci 7:113–117
44. Stainmesse S, Fessi H, Devissaguet JP, Puisieux F (1989) Process for the preparation of dispersible colloidal systems of a substance in the form of nanoparticles. US Patent 374246.
45. Yoshioka T, Hashida M, Muranishi S, Sezaki H (1981) Specific delivery of mitomycin C to the liver, spleen and lung: nano- and microspherical carriers of gelatin. Int J Pharm 8:131–141
46. Edman P, Ekman B, Sjoholm I (1980) Immobilization of proteins in microspheres of biodegradable polyacryldextran. J Pharm Sci 69:838–842
47. Artursson P, Edman P, Laakso T, Sjoholm I (1984) Characterization of polyacryl starch microparticles as carriers for proteins and drugs. J Pharm Sci 73:1507–1513
48. Rajaonarivony M, Vauthier C, Couarraze G, Puisieux F, Couvreur P (1993) Development of a new drug carrier made from alginate. J Pharm Sci 82:912–917
49. Boussif O, Lezoualc'h F, Zanta MA, Mergny MD, Scherman D, Demeneix B, Behr JP (1995) A versatile vector for gene and oligonucleotide transfer into cells in culture and in vivo: polyethylenimine. Proc Natl Acad Sci USA 92:7297–7301
50. Gomes dos Santos AL, Bochot A, Tsapis N, Artzner F, Bejjani RA, Thillaye-Goldenberg B, de Kozak Y, Fattal E, Behar-Cohen F (2006) Oligonucleotide-polyethylenimine complexes targeting retinal cells: structural analysis and application to anti-TGFbeta-2 therapy. Pharm Res 23:770–781
51. Fernandez-Urrusuno R, Calvo P, Remunan-Lopez C, Vila-Jato JL, Alonso MJ (1999) Enhancement of nasal absorption of insulin using chitosan nanoparticles. Pharm Res 16:1576–1581
52. Aderem A, Underhill DM (1999) Mechanisms of phagocytosis in macrophages. Annu Rev Immunol 17:593–623
53. Rabinovitch M (1995) Professional and non-professional phagocytes: an introduction. Trends Cell Biol 5:85–87
54. Vonarbourg A, Passirani C, Saulnier P, Simard P, Leroux JC, Benoit JP (2006) Evaluation of pegylated lipid nanocapsules versus complement system activation and macrophage uptake. J Biomed Mater Res A 78:620–628
55. Owens DE 3rd, Peppas NA (2006) Opsonization, biodistribution, and pharmacokinetics of polymeric nanoparticles. Int J Pharm 307:93–102
56. Groves E, Dart AE, Covarelli V, Caron E (2008) Molecular mechanisms of phagocytic uptake in mammalian cells. Cell Mol Life Sci 65:1957–1976
57. Vachon E, Martin R, Plumb J, Kwok V, Vandivier RW, Glogauer M, Kapus A, Wang X, Chow CW, Grinstein S, Downey GP (2006) CD44 is a phagocytic receptor. Blood 107:4149–4158
58. Caron E, Hall A (1998) Identification of two distinct mechanisms of phagocytosis controlled by different Rho GTPases. Science 282:1717–1721
59. Swanson JA, Baer SC (1995) Phagocytosis by zippers and triggers. Trends Cell Biol 5:89–93
60. Claus V, Jahraus A, Tjelle T, Berg T, Kirschke H, Faulstich H, Griffiths G (1998) Lysosomal enzyme trafficking between phagosomes, endosomes, and lysosomes in J774 macrophages. Enrichment of cathepsin H in early endosomes. J Biol Chem 273:9842–9851
61. Shive MS, Anderson JM (1997) Biodegradation and biocompatibility of PLA and PLGA microspheres. Adv Drug Deliv Rev 28:5–24
62. Fang C, Shi B, Pei Y-Y, Hong M-H, Wu J, Chen H-Z (2006) In vivo tumor targeting of tumor necrosis factor-[alpha]-loaded stealth nanoparticles: effect of MePEG molecular weight and particle size. Eur J Pharm Sci 27:27–36
63. Carrstensen H, Müller RH, Müller BW (1992) Particle size, surface hydrophobicity and interaction with serum of parenteral fat emulsions and model drug carriers as parameters related to RES uptake. Clin Nutr 11:289–297
64. Miller CR, Bondurant B, McLean SD, McGovern KA, O'Brien DF (1998) Liposome−cell interactions in vitro: effect of liposome surface charge on the binding and endocytosis of conventional and sterically stabilized liposomes. Biochemistry 37:12875–12883

65. Jeon SI, Lee JH, Andrade JD, De Gennes PG (1991) Protein-surface interactions in the presence of polyethylene oxide. I. Simplified theory. J Colloid Interface Sci 142:149–158
66. Gref R, Minamitake Y, Peracchia MT, Trubetskoy V, Torchilin V, Langer R (1994) Biodegradable long-circulating polymeric nanospheres. Science 263:1600–1603
67. Leroux JC, De Jaeghere F, Anner B, Doelker E, Gurny R (1995) An investigation on the role of plasma and serum opsonins on the internalization of biodegradable poly(D, L-lactic acid) nanoparticles by human monocytes. Life Sci 57:695–703
68. Peracchia TM (2003) Stealth nanoparticles for intravenous administration. STP Pharma Sci 13:7
69. Pavey KD, Olliff CJ (1999) SPR analysis of the total reduction of protein adsorption to surfaces coated with mixtures of long- and short-chain polyethylene oxide block copolymers. Biomaterials 20:885–890
70. Dunn SE, Brindley A, Davis SS, Davies MC, Illum L (1994) Polystyrene-poly (ethylene glycol) (PS-PEG2000) particles as model systems for site specific drug delivery. 2. The effect of PEG surface density on the in vitro cell interaction and in vivo biodistribution. Pharm Res 11:1016–1022
71. Peracchia MT, Vauthier C, Passirani C, Couvreur P, Labarre D (1997) Complement consumption by poly(ethylene glycol) in different conformations chemically coupled to poly (isobutyl 2-cyanoacrylate) nanoparticles. Life Sci 61:749–761
72. Stolnik S, Daudali B, Arien A, Whetstone J, Heald CR, Garnett MC, Davis SS, Illum L (2001) The effect of surface coverage and conformation of poly(ethylene oxide) (PEO) chains of poloxamer 407 on the biological fate of model colloidal drug carriers. Biochim Biophys Acta 1514:261–279
73. Vonarbourg A, Passirani C, Saulnier P, Benoit J-P (2006) Parameters influencing the stealthiness of colloidal drug delivery systems. Biomaterials 27:4356–4373
74. Storm G, Belliot SO, Daemen T, Lasic DD (1995) Surface modification of nanoparticles to oppose uptake by the mononuclear phagocyte system. Adv Drug Deliv Rev 17:31–48
75. Gref R, Lück M, Quellec P, Marchand M, Dellacherie E, Harnisch S, Blunk T, Müller RH (2000) Stealth' corona-core nanoparticles surface modified by polyethylene glycol (PEG): influences of the corona (PEG chain length and surface density) and of the core composition on phagocytic uptake and plasma protein adsorption. Colloids Surf B Biointerfaces 18:301–313
76. Vittaz M, Bazile D, Spenlehauer G, Verrecchia T, Veillard M, Puisieux F, Labarre D (1996) Effect of PEO surface density on long-circulating PLA-PEO nanoparticles which are very low complement activators. Biomaterials 17:1575–1581
77. Neal JC, Stolnik S, Schacht E, Kenawy ER, Garnett MC, Davis SS, Illum L (1998) In vitro displacement by rat serum of adsorbed radiolabeled poloxamer and poloxamine copolymers from model and biodegradable nanospheres. J Pharm Sci 87:1242–1248
78. Díaz-López R, Libong D, Tsapis N, Fattal E, Chaminade P (2008) Quantification of pegylated phospholipids decorating polymeric microcapsules of perfluorooctyl bromide by reverse phase HPLC with a charged aerosol detector. J Pharm Biomed Anal 48:702–707
79. Díaz-López R, Tsapis N, Santin M, Bridal SL, Nicolas V, Jaillard D, Libong D, Chaminade P, Marsaud V, Vauthier C, Fattal E (2010) The performance of PEGylated nanocapsules of perfluorooctyl bromide as an ultrasound contrast agent. Biomaterials 31:1723–1731
80. Lemarchand C, Gref R, Couvreur P (2004) Polysaccharide-decorated nanoparticles. Eur J Pharm Biopharm 58:327–341
81. Labarre D, Vauthier C, Chauvierre C, Petri B, Müller R, Chehimi MM (2005) Interactions of blood proteins with poly(isobutylcyanoacrylate) nanoparticles decorated with a polysaccharidic brush. Biomaterials 26:5075–5084
82. Lemarchand C, Gref R, Passirani C, Garcion E, Petri B, Müller R, Costantini D, Couvreur P (2006) Influence of polysaccharide coating on the interactions of nanoparticles with biological systems. Biomaterials 27:108–118

83. Passirani C, Barratt G, Devissaguet J-P, Labarre D (1998) Interactions of nanoparticles bearing heparin or dextran covalently bound to poly(methyl methacrylate) with the complement system. Life Sci 62:775–785
84. Bazile D, Prud'homme C, Bassoullet MT, Marlard M, Spenlehauer G, Veillard M (1995) Stealth Me.PEG-PLA nanoparticles avoid uptake by the mononuclear phagocytes system. J Pharm Sci 84:493–498
85. Esmaeili F, Ghahremani MH, Esmaeili B, Khoshayand MR, Atyabi F, Dinarvand R (2008) PLGA nanoparticles of different surface properties: preparation and evaluation of their body distribution. Int J Pharm 349:249–255
86. Gref R, Domb A, Quellec P, Blunk T, Müller RH, Verbavatz JM, Langer R (1995) The controlled intravenous delivery of drugs using PEG-coated sterically stabilized nanospheres. Adv Drug Deliv Rev 16:215–233
87. Peracchia MT, Harnisch S, Pinto-Alphandary H, Gulik A, Dedieu JC, Desmaele D, d'Angelo J, Muller RH, Couvreur P (1999) Visualization of in vitro protein-rejecting properties of PEGylated stealth polycyanoacrylate nanoparticles. Biomaterials 20:1269–1275
88. Calvo P, Gouritin B, Brigger I, Lasmezas C, Deslys J-P, Williams A, Andreux JP, Dormont D, Couvreur P (2001) PEGylated polycyanoacrylate nanoparticles as vector for drug delivery in prion diseases. J Neurosci Methods 111:151–155
89. Kim SY, Lee YM (2001) Taxol-loaded block copolymer nanospheres composed of methoxy poly(ethylene glycol) and poly([var epsilon]-caprolactone) as novel anticancer drug carriers. Biomaterials 22:1697–1704
90. Peracchia MT, Fattal E, Desmaele D, Besnard M, Noel JP, Gomis JM, Appel M, d'Angelo J, Couvreur P (1999) Stealth PEGylated polycyanoacrylate nanoparticles for intravenous administration and splenic targeting. J Control Release 60:121–128
91. Matsumura Y, Maeda H (1986) A new concept for macromolecular therapeutics in cancer chemotherapy: mechanism of tumoritropic accumulation of proteins and the antitumor agent Smancs. Cancer Res 46:6387–6392
92. Hobbs SK, Monsky WL, Yuan F, Roberts WG, Griffith L, Torchilin VP, Jain RK (1998) Regulation of transport pathways in tumor vessels: role of tumor type and microenvironment. Proc Natl Acad Sci USA 95:4607–4612
93. Decuzzi P, Pasqualini R, Arap W, Ferrari M (2009) Intravascular delivery of particulate systems: does geometry really matter? Pharm Res 26:235–243
94. Savage MD, Mattson G, Desai S, Nielander GW, Morgensen S, Conklin EJ (1992) Avidin-biotin chemistry: a handbook. Pierce Chemical Co, Rockford, IL
95. Wilchek M, Bayer EA (1990) Introduction to avidin-biotin technology. Methods Enzymol 184:5–13
96. Cho KC, Kim SH, Jeong JH, Park TG (2005) Folate receptor-mediated gene delivery using folate-poly(ethylene glycol)-poly(L-lysine) conjugate. Macromol Biosci 5:512–519
97. Jeong Y-I, Seo S-J, Park I-K, Lee H-C, Kang I-C, Akaike T, Cho C-S (2005) Cellular recognition of paclitaxel-loaded polymeric nanoparticles composed of poly([gamma]-benzyl L-glutamate) and poly(ethylene glycol) diblock copolymer endcapped with galactose moiety. Int J Pharm 296:151–161
98. Kim SH, Jeong JH, Chun KW, Park TG (2005) Target-specific cellular uptake of PLGA nanoparticles coated with poly(L-lysine)−poly(ethylene glycol)−folate conjugate. Langmuir 21:8852–8857
99. Nie Y, Zhang Z, Li L, Luo K, Ding H, Gu Z (2009) Synthesis, characterization and transfection of a novel folate-targeted multipolymeric nanoparticles for gene delivery. J Mater Sci Mater Med 20:1849–1857
100. Park EK, Kim SY, Lee SB, Lee YM (2005) Folate-conjugated methoxy poly(ethylene glycol)/poly([var epsilon]-caprolactone) amphiphilic block copolymeric micelles for tumor-targeted drug delivery. J Control Release 109:158–168
101. Patil YB, Toti US, Khdair A, Ma L, Panyam J (2009) Single-step surface functionalization of polymeric nanoparticles for targeted drug delivery. Biomaterials 30:859–866

102. Prabaharan M, Grailer JJ, Pilla S, Steeber DA, Gong S (2009) Folate-conjugated amphiphilic hyperbranched block copolymers based on Boltorn® H40, poly(l-lactide) and poly(ethylene glycol) for tumor-targeted drug delivery. Biomaterials 30:3009–3019
103. Salem AK, Cannizzaro SM, Davies MC, Tendler SJB, Roberts CJ, Williams PM, Shakesheff KM (2001) Synthesis and characterisation of a degradable poly(lactic acid)−poly(ethylene glycol) copolymer with biotinylated end groups. Biomacromolecules 2:575–580
104. Stella B, Arpicco S, Peracchia MT, Desmaële D, Hoebeke J, Renoir M, d'Angelo J, Cattel L, Couvreur P (2000) Design of folic acid-conjugated nanoparticles for drug targeting. J Pharm Sci 89:1452–1464
105. Stella B, Marsaud V, Arpicco S, Geraud G, Cattel L, Couvreur P, Renoir J-M (2007) Biological characterization of folic acid-conjugated poly(H2NPEGCA-co-HDCA) nanoparticles in cellular models. J Drug Target 15:146–153
106. Yang X, Deng W, Fu L, Blanco E, Gao J, Quan D, Shuai X (2008) Folate-functionalized polymeric micelles for tumor targeted delivery of a potent multidrug-resistance modulator FG020326. J Biomed Mater Res A 86A:48–60
107. Yoo HS, Park TG (2004) Folate receptor targeted biodegradable polymeric doxorubicin micelles. J Control Release 96:273–283
108. Zhao H, Yung LYL (2008) Selectivity of folate conjugated polymer micelles against different tumor cells. Int J Pharm 349:256–268
109. Zhou J, Romero G, Rojas E, Ma L, Moya S, Gao C (2010) Layer by layer chitosan/alginate coatings on poly(lactide-co-glycolide) nanoparticles for antifouling protection and Folic acid binding to achieve selective cell targeting. J Colloid Interface Sci 345:241–247
110. Cheng J, Teply BA, Sherifi I, Sung J, Luther G, Gu FX, Levy-Nissenbaum E, Radovic-Moreno AF, Langer R, Farokhzad OC (2007) Formulation of functionalized PLGA-PEG nanoparticles for in vivo targeted drug delivery. Biomaterials 28:869–876
111. Farokhzad O, Cheng J, Teply B, Sherifi I, Jon S, Kantoff P, Richie J, Langer R (2006) Targeted nanoparticle-aptamer bioconjugates for cancer chemotherapy in vivo. Proc Natl Acad Sci USA 103:6315–6320
112. Farokhzad OC, Jon S, Khademhosseini A, Tran T-NT, LaVan DA, Langer R (2004) Nanoparticle-aptamer bioconjugates. Cancer Res 64:7668–7672
113. Gu F, Zhang L, Teply BA, Mann N, Wang A, Radovic-Moreno AF, Langer R, Farokhzad OC (2008) Precise engineering of targeted nanoparticles by using self-assembled biointegrated block copolymers. Proc Natl Acad Sci USA 105:2586–2591
114. Kim D, Gao ZG, Lee ES, Bae YH (2009) In vivo evaluation of doxorubicin-loaded polymeric micelles targeting folate receptors and early endosomal pH in drug-resistant ovarian cancer. Mol Pharm 6:1353–1362
115. Kim D, Lee ES, Oh KT, Gao ZG, Bae YH (2008) Doxorubicin-loaded polymeric micelle overcomes multidrug resistance of cancer by double-targeting folate receptor and early endosomal pH. Small 4:2043–2050
116. Lee ES, Na K, Bae YH (2003) Polymeric micelle for tumor pH and folate-mediated targeting. J Control Release 91:103–113
117. Lee H, Hoang B, Fonge H, Reilly R, Allen C (2010) Distribution of polymeric nanoparticles at the whole-body, tumor, and cellular levels. Pharm Res 27:2343–2355
118. Lee H, Hu M, Reilly RM, Allen C (2007) Apoptotic epidermal growth factor (EGF)-conjugated block copolymer micelles as a nanotechnology platform for targeted combination therapy. Mol Pharm 4:769–781
119. Noh T, Kook YH, Park C, Youn H, Kim H, Oh ET, Choi EK, Park HJ, Kim C (2008) Block copolymer micelles conjugated with anti-EGFR antibody for targeted delivery of anticancer drug. J Polym Sci Part A: Polym Chem 46:7321–7331
120. Pan J, Feng S-S (2008) Targeted delivery of paclitaxel using folate-decorated poly(lactide)-vitamin E TPGS nanoparticles. Biomaterials 29:2663–2672
121. Pan J, Feng S-S (2009) Targeting and imaging cancer cells by folate-decorated, quantum dots (QDs)-loaded nanoparticles of biodegradable polymers. Biomaterials 30:1176–1183

122. Schiffelers RM, Ansari A, Xu J, Zhou Q, Tang Q, Storm G, Molema G, Lu PY, Scaria PV, Woodle MC (2004) Cancer siRNA therapy by tumor selective delivery with ligand-targeted sterically stabilized nanoparticle. Nucleic Acids Res 32:e149
123. Wang Y, Wang X, Zhang Y, Yang S, Wang J, Zhang X, Zhang Q (2009) RGD-modified polymeric micelles as potential carriers for targeted delivery to integrin-overexpressing tumor vasculature and tumor cells. J Drug Target 17:459–467
124. Wang Z, Chui W-K, Ho PC (2009) Design of a multifunctional PLGA nanoparticulate drug delivery system: evaluation of its physicochemical properties and anticancer activity to malignant cancer cells. Pharm Res 26:1162–1171
125. Zeng F, Lee H, Allen C (2006) Epidermal growth factor-conjugated poly(ethylene glycol)-block- poly(δ-valerolactone) copolymer micelles for targeted delivery of chemotherapeutics. Bioconjug Chem 17:399–409
126. Zhang N, Chittasupho C, Duangrat C, Siahaan TJ, Berkland C (2007) PLGA nanoparticle–peptide conjugate effectively targets intercellular cell-adhesion molecule-1. Bioconjug Chem 19:145–152
127. Zhang Z, Huey Lee S, Feng S-S (2007) Folate-decorated poly(lactide-co-glycolide)-vitamin E TPGS nanoparticles for targeted drug delivery. Biomaterials 28:1889–1899
128. Hu Z, Luo F, Pan Y, Hou C, Ren L, Chen J, Wang J, Zhang Y (2008) Arg-Gly-Asp (RGD) peptide conjugated poly(lactic acid)–poly(ethylene oxide) micelle for targeted drug delivery. J Biomed Mater Res A 85A:797–807
129. Jeong JH, Kim SH, Kim SW, Park TG (2005) In vivo tumor targeting of ODN-PEG-folic acid/PEI polyelectrolyte complex micelles. J Biomater Sci Polym Ed 16:1409–1419
130. Pang Z, Lu W, Gao H, Hu K, Chen J, Zhang C, Gao X, Jiang X, Zhu C (2008) Preparation and brain delivery property of biodegradable polymersomes conjugated with OX26. J Control Release 128:120–127
131. Lu W, Zhang Y, Tan Y-Z, Hu K-L, Jiang X-G, Fu S-K (2005) Cationic albumin-conjugated pegylated nanoparticles as novel drug carrier for brain delivery. J Control Release 107:428–448
132. Nasongkla N, Shuai X, Ai H, Weinberg BD, Pink J, Boothman DA, Gao J (2004) cRGD-functionalized polymer micelles for targeted doxorubicin delivery. Angew Chem Int Ed 43:6323–6327
133. Debotton N, Parnes M, Kadouche J, Benita S (2008) Overcoming the formulation obstacles towards targeted chemotherapy: in vitro and in vivo evaluation of cytotoxic drug loaded immunonanoparticles. J Control Release 127:219–230
134. Cirstoiu-Hapca A, Bossy-Nobs L, Buchegger F, Gurny R, Delie F (2007) Differential tumor cell targeting of anti-HER2 (Herceptin®) and anti-CD20 (Mabthera®) coupled nanoparticles. Int J Pharm 331:190–196
135. Cirstoiu-Hapca A, Buchegger F, Bossy L, Kosinski M, Gurny R, Delie F (2009) Nanomedicines for active targeting: Physico-chemical characterization of paclitaxel-loaded anti-HER2 immunonanoparticles and in vitro functional studies on target cells. Eur J Pharm Sci 38:230–237
136. Nobs L, Buchegger F, Gurny R, Allémann E (2005) Biodegradable nanoparticles for direct or two-step tumor immunotargeting. Bioconjug Chem 17:139–145
137. Shi M, Ho K, Keating A, Shoichet MS (2009) Doxorubicin-conjugated immuno-nanoparticles for intracellular anticancer drug delivery. Adv Funct Mater 19:1689–1696
138. Anhorn MG, Wagner S, Jr K, Langer K, von Briesen H (2008) Specific targeting of HER2 overexpressing breast cancer cells with doxorubicin-loaded trastuzumab-modified human serum albumin nanoparticles. Bioconjug Chem 19:2321–2331
139. Kreuter J, Hekmatara T, Dreis S, Vogel T, Gelperina S, Langer K (2007) Covalent attachment of apolipoprotein A-I and apolipoprotein B-100 to albumin nanoparticles enables drug transport into the brain. J Control Release 118:54–58

140. Magadala P, Amiji M (2008) Epidermal growth factor receptor-targeted gelatin-based engineered nanocarriers for DNA delivery and transfection in human pancreatic cancer cells. AAPS J 10:565–576
141. Michaelis K, Hoffmann MM, Dreis S, Herbert E, Alyautdin RN, Michaelis M, Kreuter J, Langer K (2006) Covalent linkage of apolipoprotein E to albumin nanoparticles strongly enhances drug transport into the brain. J Pharmacol Exp Ther 317:1246–1253
142. Steinhauser I, Spänkuch B, Strebhardt K, Langer K (2006) Trastuzumab-modified nanoparticles: optimisation of preparation and uptake in cancer cells. Biomaterials 27:4975–4983
143. Ulbrich K, Hekmatara T, Herbert E, Kreuter J (2009) Transferrin- and transferrin-receptor-antibody-modified nanoparticles enable drug delivery across the blood-brain barrier (BBB). Eur J Pharm Biopharm 71:251–256
144. Zensi A, Begley D, Pontikis C, Legros C, Mihoreanu L, Wagner S, Büchel C, von Briesen H, Kreuter J (2009) Albumin nanoparticles targeted with Apo E enter the CNS by transcytosis and are delivered to neurones. J Control Release 137:78–86
145. Chen S, Zhang X-Z, Cheng S-X, Zhuo R-X, Gu Z-W (2008) Functionalized amphiphilic hyperbranched polymers for targeted drug delivery. Biomacromolecules 9:2578–2585
146. Bae KH, Lee Y, Park TG (2007) Oil-encapsulating PEO-PPO-PEO/PEG shell cross-linked nanocapsules for target-specific delivery of paclitaxel. Biomacromolecules 8:650–656
147. Lin A, Liu Y, Huang Y, Sun J, Wu Z, Zhang X, Ping Q (2008) Glycyrrhizin surface-modified chitosan nanoparticles for hepatocyte-targeted delivery. Int J Pharm 359:247–253
148. Li Y, Ogris M, Wagner E, Pelisek J, Rüffer M (2003) Nanoparticles bearing polyethyleneglycol-coupled transferrin as gene carriers: preparation and in vitro evaluation. Int J Pharm 259:93–101
149. Xiong X-B, Mahmud A, Uludağ H, Lavasanifar A (2008) Multifunctional polymeric micelles for enhanced intracellular delivery of doxorubicin to metastatic cancer cells. Pharm Res 25:2555–2566
150. Xiong X-B, Ma Z, Lai R, Lavasanifar A (2010) The therapeutic response to multifunctional polymeric nano-conjugates in the targeted cellular and subcellular delivery of doxorubicin. Biomaterials 31:757–768
151. Xiong X-B, Mahmud A, Uludağ H, Lavasanifar A (2007) Conjugation of arginine-glycine-aspartic acid peptides to poly(ethylene oxide)-b-poly(ε-caprolactone) micelles for enhanced intracellular drug delivery to metastatic tumor cells. Biomacromolecules 8:874–884
152. Wagner E, Zenke M, Cotten M, Beug H, Birnstiel ML (1990) Transferrin-polycation conjugates as carriers for DNA uptake into cells. Proc Natl Acad Sci USA 87:3410–3414
153. Sahoo SK, Labhasetwar V (2005) Enhanced antiproliferative activity of transferrin-conjugated paclitaxel-loaded nanoparticles is mediated via sustained intracellular drug retention. Mol Pharm 2:373–383
154. Sahoo SK, Ma W, Labhasetwar V (2004) Efficacy of transferrin-conjugated paclitaxel-loaded nanoparticles in a murine model of prostate cancer. Int J Cancer 112:335–340
155. Acharya S, Dilnawaz F, Sahoo SK (2009) Targeted epidermal growth factor receptor nanoparticle bioconjugates for breast cancer therapy. Biomaterials 30:5737–5750
156. Choi S-W, Kim J-H (2007) Design of surface-modified poly(D, L-lactide-co-glycolide) nanoparticles for targeted drug delivery to bone. J Control Release 122:24–30
157. Costantino L, Gandolfi F, Tosi G, Rivasi F, Vandelli MA, Forni F (2005) Peptide-derivatized biodegradable nanoparticles able to cross the blood-brain barrier. J Control Release 108:84–96
158. Dawson GF, Halbert GW (2000) The in vitro cell association of invasin coated polylactide-co-glycolide nanoparticles. Pharm Res 17:1420–1425
159. Fernandes JC, Wang H, Jreyssaty C, Benderdour M, Lavigne P, Qiu X, Winnik FM, Zhang X, Dai K, Shi Q (2008) Bone-protective effects of nonviral gene therapy with folate-chitosan DNA nanoparticle containing interleukin-1 receptor antagonist gene in rats with adjuvant-induced arthritis. Mol Ther 16:1243–1251

160. Kocbek P, Obermajer N, Cegnar M, Kos J, Kristl J (2007) Targeting cancer cells using PLGA nanoparticles surface modified with monoclonal antibody. J Control Release 120:18–26
161. Liu P, Li Z, Zhu M, Sun Y, Li Y, Wang H, Duan Y (2010) Preparation of EGFR monoclonal antibody conjugated nanoparticles and targeting to hepatocellular carcinoma. J Mater Sci Mater Med 21:551–556
162. Mansouri S, Cuie Y, Winnik F, Shi Q, Lavigne P, Benderdour M, Beaumont E, Fernandes JC (2006) Characterization of folate-chitosan-DNA nanoparticles for gene therapy. Biomaterials 27:2060–2065
163. Sahu S, Mallick S, Santra S, Maiti T, Ghosh S, Pramanik P (2010) In vitro evaluation of folic acid modified carboxymethyl chitosan nanoparticles loaded with doxorubicin for targeted delivery. J Mater Sci Mater Med 21:1587–1597
164. Tosi G, Costantino L, Rivasi F, Ruozi B, Leo E, Vergoni AV, Tacchi R, Bertolini A, Vandelli MA, Forni F (2007) Targeting the central nervous system: In vivo experiments with peptide-derivatized nanoparticles loaded with Loperamide and Rhodamine-123. J Control Release 122:1–9
165. Banquy X, Gg L, Rabanel J-M, Argaw A, J-Fo B, Hildgen P, Giasson S (2008) Selectins ligand decorated drug carriers for activated endothelial cell targeting. Bioconjug Chem 19:2030–2039
166. Hammady T, Rabanel J-M, Dhanikula RS, Leclair G, Hildgen P (2009) Functionalized nanospheres loaded with anti-angiogenic drugs: cellular uptake and angiosuppressive efficacy. Eur J Pharm Biopharm 72:418–427
167. Kolb HC, Finn MG, Sharpless KB (2001) Click chemistry: diverse chemical function from a few good reactions. Angew Chem Int Ed 40:2004–2021
168. Binder WH, Sachsenhofer R (2007) 'Click' chemistry in polymer and materials science. Macromol Rapid Commun 28:15–54
169. Kolb HC, Sharpless KB (2003) The growing impact of click chemistry on drug discovery. Drug Discov Today 8:1128–1137
170. Le Droumaguet B, Nicolas J (2010) Recent advances in the design of bioconjugates from controlled/living radical polymerization. Polym Chem 1:563–598
171. Le Drournaguet B, Velonia K (2008) Click chemistry: a powerful tool to create polymer-based macromolecular chimeras. Macromol Rapid Commun 29:1073–1089
172. Lutz J-F (2007) 1,3-dipolar cycloadditions of azides and alkynes: a universal ligation tool in polymer and materials science. Angew Chem Int Ed 46:1018–1025
173. Le Droumaguet B, Souguir H, Brambilla D, Verpillot R, Nicolas J, Taverna M, Couvreur P, Andrieux K (2011) Selegiline-functionalized, PEGylated poly(alkyl cyanoacrylate) nanoparticles to target the amyloid-β peptide. Int J Pharm 416:457–464
174. Nicolas J, Bensaid F, Desmaele D, Grogna M, Detrembleur C, Andrieux K, Couvreur P (2008) Synthesis of highly functionalized poly(alkyl cyanoacrylate) nanoparticles by means of click chemistry. Macromolecules 41:8418–8428
175. Lu J, Shi M, Shoichet MS (2008) Click chemistry functionalized polymeric nanoparticles target corneal epithelial cells through RGD-cell surface receptors. Bioconjug Chem 20:87–94
176. Jubeli E, Moine L, Barratt G (2010) Synthesis, characterization, and molecular recognition of sugar-functionalized nanoparticles prepared by a combination of ROP, ATRP, and click chemistry. J Polym Sci Part A: Polym Chem 48:3178–3187
177. Danhier F, Ucakar B, Magotteaux N, Brewster ME, Préat V (2010) Active and passive tumor targeting of a novel poorly soluble cyclin dependent kinase inhibitor, JNJ-7706621. Int J Pharm 392:20–28
178. Danhier F, Vroman B, Lecouturier N, Crokart N, Pourcelle V, Freichels H, Jérôme C, Marchand-Brynaert J, Feron O, Préat V (2009) Targeting of tumor endothelium by RGD-grafted PLGA-nanoparticles loaded with Paclitaxel. J Control Release 140:166–173
179. Garinot M, Fiévez V, Pourcelle V, Stoffelbach F, des Rieux A, Plapied L, Theate I, Freichels H, Jérôme C, Marchand-Brynaert J, Schneider Y-J, Préat V (2007) PEGylated PLGA-based nanoparticles targeting M cells for oral vaccination. J Control Release 120:195–204

180. Haun JB, Hammer DA (2008) Quantifying nanoparticle adhesion mediated by specific molecular interactions. Langmuir 24:8821–8832
181. Lin A, Sabnis A, Kona S, Nattama S, Patel H, Dong J-F, Nguyen KT (2010) Shear-regulated uptake of nanoparticles by endothelial cells and development of endothelial-targeting nanoparticles. J Biomed Mater Res A 93A:833–842
182. Tseng C-L, Su W-Y, Yen K-C, Yang K-C, Lin F-H (2009) The use of biotinylated-EGF-modified gelatin nanoparticle carrier to enhance cisplatin accumulation in cancerous lungs via inhalation. Biomaterials 30:3476–3485
183. Tseng C-L, Wang T-W, Dong G-C, Yueh-Hsiu Wu S, Young T-H, Shieh M-J, Lou P-J, Lin F-H (2007) Development of gelatin nanoparticles with biotinylated EGF conjugation for lung cancer targeting. Biomaterials 28:3996–4005
184. Tseng C, Wu S, Wang W, Peng C, Lin F, Lin C, Young T, Shieh M (2008) Targeting efficiency and biodistribution of biotinylated-EGF-conjugated gelatin nanoparticles administered via aerosol delivery in nude mice with lung cancer. Biomaterials 29:3014–3022
185. Aktaş Y, Yemisci M, Andrieux K, Gürsoy RN, Alonso MJ, Fernandez-Megia E, Novoa-Carballal R, Quiñoá E, Riguera R, Sargon MF, Çelik HH, Demir AS, Hıncal AA, Dalkara T, Çapan Y, Couvreur P (2005) Development and brain delivery of chitosan−PEG nanoparticles functionalized with the monoclonal antibody OX26. Bioconjug Chem 16:1503–1511
186. Deosarkar SP, Malgor R, Fu J, Kohn LD, Hanes J, Goetz DJ (2008) Polymeric particles conjugated with a ligand to VCAM-1 exhibit selective, avid, and focal adhesion to sites of atherosclerosis. Biotechnol Bioeng 101:400–407
187. Vinogradov S, Batrakova E, Li S, Kabanov A (1999) Polyion complex micelles with protein-modified corona for receptor-mediated delivery of oligonucleotides into cells. Bioconjug Chem 10:851–860
188. Blackwell JE, Dagia NM, Dickerson JB, Berg EL, Goetz DJ (2001) Ligand coated nanosphere adhesion to E- and P-selectin under static and flow conditions. Ann Biomed Eng 29:523–533
189. Barbault-Foucher S, Gref R, Russo P, Guechot J, Bochot A (2002) Design of poly-epsilon-caprolactone nanospheres coated with bioadhesive hyaluronic acid for ocular delivery. J Control Release 83:365–375
190. Gullberg E, Keita ÅV, SaY S, Andersson M, Caldwell KD, Söderholm JD, Artursson P (2006) Identification of cell adhesion molecules in the human follicle-associated epithelium that improve nanoparticle uptake into the Peyer's patches. J Pharmacol Exp Ther 319:632–639
191. Chittasupho C, Xie S-X, Baoum A, Yakovleva T, Siahaan TJ, Berkland CJ (2009) ICAM-1 targeting of doxorubicin-loaded PLGA nanoparticles to lung epithelial cells. Eur J Pharm Sci 37:141–150
192. Chavanpatil MD, Khdair A, Panyam J (2006) Nanoparticles for cellular drug delivery: mechanisms and factors influencing delivery. J Nanosci Nanotechnol 6:2651–2663
193. Hilgenbrink A, Low P (2005) Folate receptor-mediated drug targeting: from therapeutics to diagnostics. J Pharm Sci 94:2135–2146
194. Weitman SD, Lark RH, Coney LR, Fort DW, Frasca V, Zurawski VR, Kamen BA (1992) Distribution of the folate receptor GP38 in normal and malignant cell lines and tissues. Cancer Res 52:3396–3401
195. Rothberg KG, Ying YS, Kolhouse JF, Kamen BA, Anderson RG (1990) The glycophospholipid-linked folate receptor internalizes folate without entering the clathrin-coated pit endocytic pathway. J Cell Biol 110:637–649
196. Kim S, Jeong J, Cho K, Kim S, Park T (2005) Target-specific gene silencing by siRNA plasmid DNA complexed with folate-modified poly(ethylenimine). J Control Release 104:223–232
197. Patil YB, Toti US, Khdair A, Ma L, Panyam J (2008) Single-step surface functionalization of polymeric nanoparticles for targeted drug delivery. Biomaterials 30:859–866
198. Qian ZM, Li H, Sun H, Ho K (2002) Targeted drug delivery via the transferrin receptor-mediated endocytosis pathway. Pharmacol Rev 54:561–587

199. Vasir JK, Labhasetwar V (2007) Biodegradable nanoparticles for cytosolic delivery of therapeutics. Adv Drug Deliv Rev 59:718–728
200. Xu Z, Gu W, Huang J, Sui H, Zhou Z, Yang Y, Yan Z, Li Y (2005) In vitro and in vivo evaluation of actively targetable nanoparticles for paclitaxel delivery. Int J Pharm 288:361–368
201. Jones AR, Shusta EV (2007) Blood–brain barrier transport of therapeutics via receptor-mediation. Pharm Res 24:1759–1771
202. Mishra V, Mahor S, Rawat A, Gupta PN, Dubey P, Khatri K, Vyas SP (2006) Targeted brain delivery of AZT via transferrin anchored pegylated albumin nanoparticles. J Drug Target 14:45–53
203. Lee HJ, Engelhardt B, Lesley J, Bickel U, Pardridge WM (2000) Targeting rat anti-mouse transferrin receptor monoclonal antibodies through blood–brain barrier in mouse. J Pharmacol Exp Ther 292:1048–1052
204. Byrne JD, Betancourt T, Brannon-Peppas L (2008) Active targeting schemes for nanoparticle systems in cancer therapeutics. Adv Drug Deliv Rev 60:1615–1626
205. Han HD, Mangala LS, Lee JW, Shahzad MMK, Kim HS, Shen D, Nam EJ, Mora EM, Stone RL, Lu C, Lee SJ, Roh JW, Nick AM, Lopez-Berestein G, Sood AK (2010) Targeted gene silencing using RGD-labeled chitosan nanoparticles. Clin Cancer Res 16:3910–3922
206. Ding B-S, Dziubla T, Shuvaev VV, Muro S, Muzykantov VR (2006) Advanced drug delivery systems that target the vascular endothelium. Mol Interv 6:98–112
207. Sakhalkar H, Dalal M, Salem A, Ansari R, Fu A, Kiani M, Kurjiaka D, Hanes J, Shakesheff K, Goetz D (2003) Leukocyte-inspired biodegradable particles that selectively and avidly adhere to inflamed endothelium in vitro and in vivo. Proc Natl Acad Sci USA 100:15895–15900
208. Muro S, Dziubla T, Qiu W, Leferovich J, Cui X, Berk E, Muzykantov VR (2006) Endothelial targeting of high-affinity multivalent polymer nanocarriers directed to intercellular adhesion molecule 1. J Pharmacol Exp Ther 317:1161–1169
209. Nobs L, Buchegger F, Gurny R, Allemann E (2004) Poly(lactic acid) nanoparticles labeled with biologically active neutravidin (TM) for active targeting. Eur J Pharm Biopharm 58:483–490
210. Nobs L, Buchegger F, Gurny R, Allemann E (2006) Biodegradable nanoparticles for direct or two-step tumor immunotargeting. Bioconjug Chem 17:139–145
211. Steinhauser I, Langer K, Strebhardt K, Spänkuch B (2008) Effect of trastuzumab-modified antisense oligonucleotide-loaded human serum albumin nanoparticles prepared by heat denaturation. Biomaterials 29:4022–4028
212. Lupold S, Hicke B, Lin Y, Coffey D (2002) Identification and characterization of nuclease-stabilized RNA molecules that bind human prostate cancer cells via the prostate-specific membrane antigen. Cancer Res 62:4029–4033
213. Dhar S, Gu FX, Langer R, Farokhzad OC, Lippard SJ (2008) Targeted delivery of cisplatin to prostate cancer cells by aptamer functionalized Pt(IV) prodrug-PLGA-PEG nanoparticles. Proc Natl Acad Sci USA 105:17356–17361
214. Patel LN, Zaro JL, Shen W-C (2007) Cell penetrating peptides: intracellular pathways and pharmaceutical perspectives. Pharm Res 24:1977–1992
215. Torchilin VP (2008) Tat peptide-mediated intracellular delivery of pharmaceutical nanocarriers. Adv Drug Deliv Rev 60:548–558
216. Lewin M, Carlesso N, Tung CH, Tang XW, Cory D, Scadden DT, Weissleder R (2000) Tat peptide-derivatized magnetic nanoparticles allow in vivo tracking and recovery of progenitor cells. Nat Biotechnol 18:410–414
217. Kleemann E, Neu M, Jekel N, Fink L, Schmehl T, Gessler T, Seeger W, Kissel T (2005) Nano-carriers for DNA delivery to the lung based upon a TAT-derived peptide covalently coupled to PEG-PEI. J Control Release 109:299–316

# Chapter 11
# Liposomes in Drug Delivery

**Vladimir Torchilin**

**Abstract** Liposomes, phospholipid bubbles with a bilayered membrane structure, are considered as promising pharmaceutical carriers for different applications. Currently, liposomes are used experimentally and clinically to deliver various pharmaceuticals including drugs and diagnostic agents as well as genes and related products. Research in the field of liposomes aims now at the development of various liposome-based multifunctional nanopreparations for therapy and diagnostics or for both simultaneously (theranostics). This chapter briefly addresses the basic properties of liposomes as drug delivery systems and the development and current status of some liposomal products.

## 11.1 Liposomes: Brief Overview of Preparation and Properties

Liposomes are artificial phospholipid vesicles, which can be obtained by a variety of methods from lipid dispersions in water. Over the years since their discovery in early 1960s, various preparations methods, properties, and biomedical applications of liposomes have been thoroughly investigated and discussed in detail in multiple monographs, see for example [90, 155, 156, 289, 315]. The most frequently used methods for liposome preparation include ultrasonication, reverse phase evaporation, detergent removal from mixed lipid-detergent micelles by dialysis or gel filtration, freeze–thawing, extrusion, and lipid film hydration. To increase liposome membrane stability and slow down their disintegration and release of incorporated drugs, various amounts of cholesterol are incorporated into the liposomal membrane. Liposome size depends on their composition, preparation method, and intended use, and can vary from around 80 nm or even less to greater than 1 μm

V. Torchilin (✉)
Center for Pharmaceutical Biotechnology and Nanomedicine, Northeastern University, 360 Huntington Avenue, Boston, MA 02115, USA
e-mail: v.torchilin@neu.edu

J. Siepmann et al. (eds.), *Fundamentals and Applications of Controlled Release Drug Delivery*, Advances in Delivery Science and Technology,
DOI 10.1007/978-1-4614-0881-9_11, 

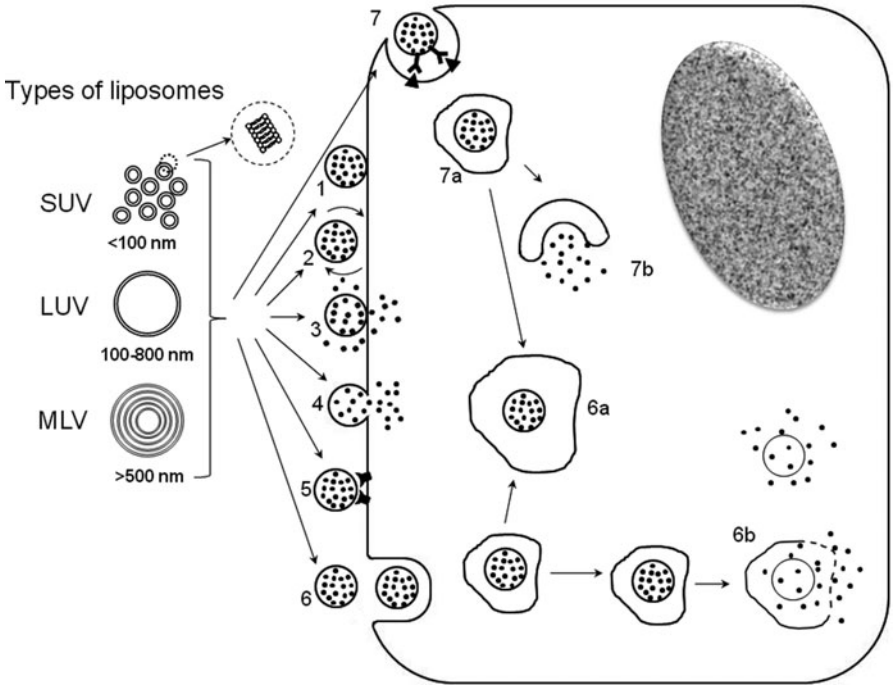


**Fig. 11.1** Liposome–cell interaction. Drug-loaded liposomes can adsorb on the cell surface specifically (**1**) or nonspecifically (**2**). Liposome can also fuse with the cell membrane releasing its contents inside cell cytoplasm (**3**). It can also be destabilized by certain cell membrane components when adsorbed on the surface so that the released drug can enter cell via micropinocytosis (**4**). Liposome can undergo the direct or transfer protein-mediated exchange of lipid components with the cell membrane (**5**). It can also be subjected to a specific or nonspecific endocytosis (**6**). In this case, a liposome can be delivered by the endosome into the lysosome (**6a**) or, en route to lysosome, liposome can provoke endosome destabilization, which results in drug liberation into the cell cytoplasm (**6b**). Drug-loaded liposome modified with certain viral components can specifically interact with cells, provoke endocytosis, and, via the interaction of viral components with the inner membrane of the endosome, allow for the drug efflux into the cell cytoplasm (**7**)

in diameter: SUVs are small unilamellar vesicles below 100 nm in size and are formed by a single bilayer, LUVs are large unilamellar vesicles ranging in size from 100 to 800 nm, and MLVs are multilamellar vesicles with the size from 500 to 5,000 nm and consisting of several concentric bilayers (see Fig. 11.1). The encapsulation efficacy for different substances is variable. Thus, the use of the reverse phase evaporation method [265] permits inclusion of 50 and more percent of the substance to be encapsulated from the water phase into the liposomes. In general, the trap volume for smaller liposomes is rather small (it can go below 1 l/mol lipid for liposomes smaller in size than 200 nm), while relatively high drug/lipid ratios are usually required. Although some liquid preparations of liposomes demonstrate good stability, methods have been developed to obtain lyophilized liposomal

preparations using various cryoprotective agents, such as mannose [174]. The release rate of different compounds from liposomes in vitro is usually under 1% per hour, assuming that the incubation temperature sufficiently differs from the phase transition temperature of a given phospholipid, since the maximal permeability of liposomes is observed at temperatures close to the phase transition temperature of the liposomal phospholipid. In vivo, the release rate can vary from minutes to hours and depends on the liposome composition and location in the body.

Liposomes are in general biocompatible, cause no or very little antigenic, pyrogenic, allergic, and toxic reactions (unless contain impurities or contaminations), easily undergo biodegradation, protect the host from any undesirable effects of the encapsulated drug, and protect an entrapped drug from premature inactivation by the physiological medium. Different methods of liposomal content delivery into the cytoplasm have been elaborated. (The principal mechanisms of liposome–cell interaction are presented in Fig. 11.1.) Thus, the liposome could be rendered pH sensitive by being prepared from pH-sensitive components and, taken up by a cell, it fuses with the endovacuolar membrane under the action of lowered pH inside the endosome, destabilizing the latter and releasing the liposomal contents into the cytoplasm [38]. The method described seems to be very promising for intracellular protein drug delivery, which opens unique opportunities in enzyme therapy of diseases caused by inherited disturbances in normal functioning of intracellular enzymes, e.g. in liver cells [49, 86]. Liposomes have also been shown to fuse with microscopic pores on the cell surface appearing as a result of a natural or artificially induced ischemia [133, 134] and deliver their contents into the cell cytoplasm. Liposomes modified on the surface with cell-penetrating peptides, such as TAT-peptide [283], also deliver their cargo directly into the cytoplasm [285].

Liposomes loaded with drugs can incorporate these drugs in a variety of fashions: water-soluble drugs are entrapped in the liposomal inner aqueous space (and, in case of multilammellar liposomes, into the aqueous space between bilayers), while less soluble drugs may be incorporated in the phospholipid membrane (see Fig. 11.2).

In vivo, liposomes are rapidly eliminated from the systemic circulation by cells of the mononuclear phagocyte system (MPS), first of all by Kupffer cells of the liver [244]. Many studies have shown that within the first 15–30 min after intravenous administration of liposomes, between 50 and 80% of the dose is adsorbed by the cells of MPS.

Clinical applications of liposomes are multiple and well known (see some examples in Table 11.1). Doxorubicin in polyethylene glycol(PEG)-coated liposomes was successfully used for the treatment of solid tumors in patients with breast carcinoma metastases, since such preparation significantly reduced cardiac toxicity of doxorubicin [195, 211, 261]. The same set of indications was targeted by combination therapy involving liposomal doxorubicin and paclitaxel [240] or Doxil/Caelyx® (doxorubicin in PEG-liposomes) and carboplatin [83]. Caelyx® is also approved for the treatment of ovarian cancer and is in a Phase II study for patients with squamous cell cancer of the head and neck [102, 121]. Clinical trials

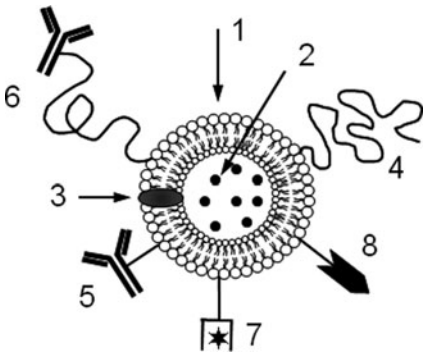


**Fig. 11.2** Attachment of various modifiers to the liposome surface. **1** – liposome; **2** – soluble drug in inner aqueous space; **3** – insoluble drug in the membrane; **4** – targeting ligand attached to a distal end of protective polymer chain; **5** – stimuli-sensitive or cell-penetrating function on the surface of liposomes; **6** – contrast moiety attached to the liposome surface for liposome visualization in the body

**Table 11.1** Some liposomal drugs approved for clinical application or under clinical evaluation (in different countries, same drug could be approved for different indications)

| Active drug (and product name for liposomal preparation where available) | Indications | Reference |
|---|---|---|
| Daunorubicin (DaunoXome) | Kaposi's sarcoma | [39] |
| Doxurubicin (Mycet) | Combinational therapy of ovarian cancer | [2, 14] |
| Doxorubicin in PEG-liposomes | Refractory Kaposi's sarcoma | [39, 71] |
| Annamycin | Doxorubicin-resistant tumors | [24] |
| Amphotericin B (AmBisome) | Fungal infections | [154] |
| Cytarabine (DepoCyt) | Lymphomatous meningitis | [18] |
| Vincristine (Onco TCS) | Non-Hodgkin's lymphoma | [233] |
| Lurtotecan (NX211) | Ovarian cancer | [44] |
| Nystatin (Nyotran) | Topical anti-fungal agent | [95] |
| All-trans retinoic acid (Altragen) | Acute promyelocytic leukemia; non-Hodgkin's; Kaposi's sarcoma | [23, 294] |
| Cytarabine/Daunorubicin (CPX-351) | Leukemia | [272] |
| Platinum compounds (Aroplatin) | Solid tumors | [52] |
| Cisplatin | Germ cell cancers, small-cell lung carcinoma | [119, 138] |
| Photosensitizers | Photodynamic therapy of skin cancer | [17] |
| E1A gene | Various tumors | [325] |
| DNA plasmid encoding HLA-B7 and β2 microglobulin (Allovectin-7) | Metastatic melanoma | [84] |
| Liposomes for various drugs and | Broad applications | [322, 332] |
| BLP 25 vaccine Stimuvax® | Nonsmall-cell lung cancer vaccine | [230] |

showed the impressive effect of doxorubicin in PEG-liposomes against unresectable hepatocellular carcinoma [237], cutaneous T-cell lymphoma [313], and sarcoma [250]. See also the recent review on the successful use of Caelyx® in the treatment of ovarian cancer in [210]. Liposomal lurtotecan was found to be effective in patients with topotecan resistant ovarian cancer [242]. Among other indications, one may notice the use of the liposomal amphotericin B for the treatment of visceral leishmaniasis [260] and long acting analgesia with liposomal bupivacaine in healthy volunteers [87].

## 11.2 Liposomes In Vivo: Achievements and Problems

As was said, liposomes are eliminated from the blood by the cells of the MPS, primarily in the liver. Liposomes of larger size are captured by MPS organs faster, and the preparations intended for clinical application are based on SUVs, although their longevity is also not very high. To increase liposomal drug accumulation in the desired areas, the use of targeted liposomes with surface-attached ligands capable of recognition and binding to cells of interest was attempted (see Fig. 11.2). Antibodies (immunoglobulins of the IgG class) and their fragments, which are the most widely used targeting moieties for liposomes, can be attached to liposomes without affecting liposomes' integrity or antibody properties, by covalent binding to the liposome surface or by the insertion into the liposomal membrane upon premodification with hydrophobic residues [277].

*Long-circulating liposomes*. It has been clearly demonstrated that liposomes, similar to macromolecules and other nanoparticulates, are capable of accumulating in various pathological areas with compromised vasculature (such as tumor, infarcts, and inflammations) via the so-called enhanced permeability and retention (EPR) effect [175, 326]. Thus, the longer circulation of liposomes should enhance this means of target accumulation, allowing for more passages through the target region and longer time for accumulation. Different methods have been suggested to achieve long circulation of liposomes in vivo, including coating the liposome surface with inert, biocompatible polymers, such as PEG. One of the hypotheses explaining the prolonged circulation of PEGylated liposomes was that PEG forms a protective layer over the liposome surface and slows down liposome recognition by opsonins and subsequent clearance [19, 143], see Fig. 11.2. Alternatively, PEG may prevent liposome-cell interaction and thus slow down the capture of liposomes by cells.

Doxorubicin, incorporated into long-circulating PEGylated liposomes (Doxil®) demonstrates good activity in EPR-based tumor therapy and strongly diminishes the toxic side effects (cardiotoxicity) of the original drug [80]. Evidently, long-circulating liposomes can be easily adapted for the delivery of various pharmaceuticals to tumor and other "leaky" areas. It should be mentioned however, that some recent evidence shows that PEG-liposomes, previously considered to be biologically inert, still can induce certain side reactions via activation of the complement system [187, 188].

Long circulating liposomes are now investigated in detail and widely used in biomedical in vitro and in vivo studies and have also found their way into clinical practice [80, 155]. Long circulating liposomes demonstrate dose independent, nonsaturable, log linear kinetics, and increased bioavailability [5]. Attempts have been made to attach PEG to the liposome surface in a removable fashion to facilitate liposome capture by the cell after PEG-liposomes accumulate in target site via the EPR effect [175], and PEG coating is detached under the action of local conditions (e.g. decreased pH in tumors). New detachable PEG conjugates are described in [328], where the detachment process is based on mild thiolysis of the dithiobenzylurethane linkage between PEG and an amino-containing substrate, such as PE. Low pH-degradable PEG-lipid conjugates based on the hydrazone linkage between PEG and lipid have also been described [125, 235].

Although PEG remains the gold standard in liposome steric protection, attempts continue to identify other polymers that could be used to prepare long circulating liposomes. Earlier studies with various water soluble flexible polymers have been summarized [288, 314]. More recent papers describe long-circulating liposomes prepared using poly(*N*-(2-hydroxypropyl)methacrylamide)) [312], poly-*N*-vinylpyrrolidones [286], L-amino acid-based biodegradable polymer–lipid conjugates [185], and polyvinyl alcohol [267].

*Targeting of long-circulating liposomes*. Further development of liposomal carriers has involved attempts to combine the properties of long-circulating liposomes and targeted liposomes in one preparation, since longevity should also allow for the better interaction of targeted liposomes with the target [1, 20, 282]. Currently, various advanced technologies for the preparation of targeted long-circulating liposomes are used, and the targeting moiety is usually attached above the protecting polymer layer, to minimize the steric hindrances for the interaction with the target, by coupling it with the distal water-exposed terminus of a liposome-grafted polymer molecule [20, 101, 284], see Fig. 11.2.

Multiple studies in this direction relate to cancer targeting, which utilizes a variety of monoclonal antibodies. Internalizing antibodies are required to achieve an improved therapeutic efficacy of antibody-targeted liposomal drugs, as was shown using B-lymphoma cells and internalizable epitopes (CD19) [231]. An interesting concept was developed to target HER2-The overexpressing tumors using anti-HER2 liposomes [205]. Antibody CC52 against rat colon adenocarcinoma CC531 attached to PEGylated liposomes provided specific accumulation of liposomes in a rat model of metastatic CC531 [127]. Nucleosome specific antibodies capable of recognition of various tumor cells via tumor cell surface bound nucleosomes improved Doxil® targeting to tumor cells and increased its cytotoxicity [59, 172]. The same 2C5 antibody successfully targeted doxorubicin loaded PEGylated liposomes into human brain U-87 tumor intracranial xenograft in nude mice and significantly enhanced the therapeutic outcome [98]. The general applicability of doxorubicin loaded PEGylated liposomes modified with 2C5 antibody for the successful treatment of various experimental tumors, including highly metastatic ones in mice, has been confirmed in a set of recent experiments [62, 63]. GD2-targeted immunoliposomes with the novel

antitumor drug, fenretinide, inducing apoptosis in neuroblastoma and melanoma cell lines, demonstrated strong antineuroblastoma activity both in vitro and in vivo in mice [215]. EGFR-overexpressing colorectal tumor cells were effectively targeted with liposomes bearing Fab′ from humanized anti-EGFR monoclonal antibody [177, 178]. Anti-P-selecting antibody modified liposomes were shown to target the areas of inflammation after an acute myocardial infarction and can delivery pro-angiogenic drugs to this area [241]. The combination of a targeting antibody and an endosome disruptive peptide on the same liposome has been shown to improve the cytosolic delivery of liposomal drug and its cytotoxicity. For example, diphtheria toxin A chain incorporated together with the pH-dependent fusogenic peptide diINF-7 into liposomes was specifically active against ovarian carcinoma [182]. (See some examples of antibody targeted liposomes used for tumor targeting in Table 11.2.)

Transferrin (Tf) receptors (TfR) are overexpressed on the surface of many tumor cells, and antibodies against TfR as well as Tf itself are among promising ligands for liposome targeting to tumors [105]. Coupling of Tf to PEG on PEGylated liposomes is used to combine longevity and targetability for drug delivery into solid tumors [116], including delivery of hypericin for photodynamic therapy [46, 81] and intracellular delivery of cisplatin [115]. Increase in the expression of the TfR was also discovered in postischemic cerebral endothelium and used to deliver Tf-modified PEG-liposomes to postischemic brain in rats [196]. Tf [123] as well as anti-TfR antibodies [271, 318] were also used to facilitate gene delivery into cells by cationic liposomes. Immunoliposomes with OX26 monoclonal antibody to the rat TfR concentrate on brain microvascular endothelium [112]. Targeting tumors with folate modified liposomes also represents a popular approach, since folate receptor (FR) is frequently overexpressed in tumor cells [79, 169]. Early studies demonstrated the possibility of delivery of macromolecules [160] and liposomes [162] into living cells utilizing FR endocytosis, which could bypass multidrug resistance. Liposomal daunorubicin [192], doxorubicin [201], and 5-fluorouracyl [99] were delivered into tumor cells in vitro and in vivo via FR and demonstrated increased cytotoxicity. The application of folate modified doxorubicin loaded liposomes for the treatment of acute myelogenous leukemia was combined with the induction of FR using all-trans retinoic acid [202]. Folate targeted liposomes have been suggested as delivery vehicles for boron neutron capture therapy [256] and used also for targeting tumors with haptens for tumor immunotherapy [170]. Within the frame of gene therapy, folate targeted liposomes were utilized for both gene targeting to tumor cells [217] as well as for targeting tumors with antisense oligonucleotides [159].

PEG-liposomes were also targeted by RGD peptides to integrins of tumor vasculature and, being loaded with doxorubicin, demonstrated increased efficiency against C26 colon carcinoma in mice [236]. Epidermal growth factor receptor (EGFR)-targeted immunoliposomes were specifically delivered to variety of tumor cells overexpressing EGFR [176]. Mitomycin C in long-circulating hyaluronan-targeted liposomes increases its activity against tumors that overexpress hyaluronan receptors [209]. Cisplatin-loaded liposomes specifically binding chondroitin sulfate overexpressed in many tumor cells were used for successful

**Table 11.2** Examples of antibodies (or their fragments) used to target liposomal anticancer drugs to tumors

| Targeting agent | Drug | Model | Reference |
|---|---|---|---|
| Recombinant human anti-HER2-Fab′ or scFv | Doxorubicin | HER2-overexpressing human breast cancer | [204] |
| Anti-HER2 | Paclitaxel | HER2-overexpressing human breast cancer | [321] |
| Anti-HER2 Fab′ or scFv | – | Human breast BT-474 | [139, 140] |
| Anti-$GD_2$ and anti-$GD_2$-Fab′ | Doxorubicin | Human neuroblastoma | [206] |
| Anti $GD_2$ | Fenretinide | Human melanoma | [199] |
| Anti-nucleosome 2C5 mAb | | Murine LLC, 4T1, C26 | [58] |
| Anti-nucleosome 2C5 mAb | Doxorubicin | Human BT-20, MCF-7, PC3 | [59, 172]; [61] |
| Anti-hu CEA 21B2 and anti-hu CEA 21B2 Fab′ | – | CEA-positive human gastric cancer, MKN45 | [181] |
| AntiCD19 | Doxorubicin | Namala hu-B-cell lymphoma | [6, 167, 232]; [33, 34, 168] |
| Anti-$\beta_1$-integrin Fab′ | Doxorubicin | Human non-small cell lung carcinoma | [259] |
| CC52 | Floxuridine (analog) | Rat colon carcinoma | [146] |
| Anti-idiotype mAb, S5A8 | Doxorubicin | Murine D-cell lymphoma | [292] |
| Anti-human E-selectin | – | Activated human endothelial cells | [132] |
| Anti-ganglioside $G_{M3}$(DH2) or anti-$L^{Ex}$(SH1) | Doxorubicin | B16BL6 mouse melanoma and HRT-18 human colorectal adenocarcinoma | [189] |
| Anti-ED-B scFv | Fluorodeoxyuridylate (analog) | In vitro Caco-2 cells and In vivo murine F9 teratocarcinoma | [180] |
| Anti-MT1-MMP-Fab′ | Doxorubicin | Human HT1080 fibrosarcoma | [9, 104] |
| C225 mAb or Fab′ | Doxorubicin | Human MDA-MB-468 Adenocarcinoma, U87 glioblastoma | [177] |
| OX26 mAb | Daunomycin | RBE4 brain capillary cells, rat biodistribution | [238] |
| Anti-Thy-1.1 OX7 mAb | Doxorubicin | Rat mesamgial cells, biodistribution | [296] |
| Anti CD74 LL1 | Doxorubicin | Raji human B-lymphoma | [173] |
| chTNT | Doxorubicin | Human non-small lung carcinoma H460 | [200] |

suppression of tumor growth and metastases in vivo [161]. Tumor selective targeting of PEGylated liposomes was also achieved by grafting these liposomes with basic fibroblast growth factor-binding peptide [274].

Recently, attempts have been made to target liposomes and other pharmaceutical nanocarriers to cancer cells by residues of ascorbic acid attached to the liposome surface [42]. Another recent approach suggests the use of phage coat fusion proteins as targeting ligands for liposomes, purified from phage preparations specifically selected against target cells and incorporated into the liposome membrane via the hydrophobic fragment of the protein [118]. If successful, such an approach can substitute expensive and unstable monoclonal antibodies with cheap, stable, and easy to prepare phage proteins.

In general, the conjugation methodology for attaching specific ligands to the liposome surface is based on several chemical reactions, which are efficient and selective: reaction between activated carboxyl groups and amino groups yielding an amide bond; reaction between pyridyldithiols and thiols yielding disulfide bonds; and reaction between maleimide derivatives and thiols yielding thioether bonds. Other approaches also exist, for example, yielding the carbamate bond via the reaction of *p*-nitrophenylcarbonyl- and amino groups [284] (review in [144, 290]). Several recent reviews [251, 252, 276] cover a broad variety of aspects relating to the use of antibody-modified liposome for cancer chemotherapy.

One has to note here that despite a sufficient number of successful experiments with targeting PEGylated liposomes using various specific ligands, certain problems exist complicating this approach. First, in general, the attachment of various ligands, such as whole antibody molecules, to PEG-liposomes can significantly affect the longevity of the final preparation, and the optimal composition should be searched for in each individual case, allowing for good targeting and sufficiently long liposome circulation. Second, keeping in mind the adjuvant properties of liposomes, ligands attached to PEG-liposomes could present an immunological problem and each such preparation should be thoroughly checked in this respect. Third, the possibility of a by-stander effect should be always taken into account. All of these problems hinder clinical application of targeted long-circulating liposomes as pharmaceutical drug carriers, although multiple efforts aim to overcome them.

*Bringing liposomes inside cells.* In many cases, drug loaded liposomes should bring the drug inside cells and allow for its release from the endosomes into cell cytoplasm to escape the lysosomal degradation. To achieve this, the liposome could be made pH-sensitive, i.e. made of pH-sensitive components and, after being endocytosed, it interacts with the endovacuolar membrane under the action of lowered pH inside the endosome, releasing its content into the cytoplasm [129] (Fig. 11.1). Long circulating PEGylated pH-sensitive liposomes, although having a decreased pH-sensitivity, still effectively deliver their contents into cytoplasm (recent review in [247]). Antisense oligos could be delivered into cells by anionic pH-sensitive PE-containing liposomes, which are stable in blood, but undergo a phase transition at acidic endosomal pH and facilitate release of the oligo into cell cytoplasm [69].

pH-sensitive liposomal additives were described containing oleyl alcohol [258] and mono-stearoyl derivative of morpholine [8]. Serum stable, long-circulating PEGylated pH-sensitive liposomes were prepared using the combination of PEG and pH-sensitive terminally alkylated copolymer of *N*-isopropylacrylamide and methacrylic acid [221]. The combination of liposome pH-sensitivity and specific ligand targeting for cytosolic drug delivery was described for both folate and Tf-targeted liposomes [124, 297]. Liposomes that can carry on their surface multiple functionalities, such as a targeting ligand and a residue of a cell penetrating peptide allowing for an effective intracellular delivery, and that demonstrate different properties depending on the specific conditions of surrounding tissues (e.g. lowered pH in tumors), have also been described [125, 126, 235].

Another approach to intracellular drug delivery is based on the use of certain viral proteins demonstrating a unique ability to penetrate into cells ("protein transduction" phenomenon). Recent data assume more than one mechanism for cell penetrating peptides and proteins (CPP) and CPP-mediated intracellular delivery of various molecules and particles. TAT-mediated intracellular delivery of large molecules and nanoparticles was proved to proceed via energy dependent macropinocytosis with subsequent enhanced escape from endosome into the cell cytoplasm [309], while individual CPPs or CPP-conjugated small molecules penetrate cells via electrostatic interactions and hydrogen bonding and do not seem to depend on energy [220]. It was demonstrated that relatively large particles, such as liposomes, could be delivered into various cells by multiple TAT-peptide or other CPP molecules attached to the liposome surface [85, 287, 293]. Complexes of TAT–peptide–liposomes with a plasmid (plasmid pEGFP-N1 encoding for the Green Fluorescence Protein, GFP) were used for successful in vitro transfection of various tumor and normal cells as well as for in vivo transfection of tumor cells in mice bearing Lewis lung carcinoma [285]. TAT-peptide liposomes have also been successfully used for transfection of intracranial tumor cell in mice via intracarotid injection [97].

An interesting example of intracellular targeting of liposomes was described recently, where liposomes containing in their membrane mitochondriotropic amphiphilic cations with delocalized positive charge, were shown to specifically target mitochondria in intact cells [21, 22, 208].

## 11.3 Administration Routes for Liposome-Based Preparations

Liposomes as a dosage form allow for a broad variety of administration routes, each having its own limitations. Some aspects of parenteral (intravenous) administration have been already discussed. Oral administration requires high liposome stability and drug loaded liposome delivery from the gut to the blood with subsequent drug release [219]. Chitosan coated insulin liposomes were shown to cause hypoglycemic effect in mice upon oral administration [316]. A hypocalcemic

effect of liposomal salmon calcitonin upon oral administration was also demonstrated [320]. Liposomes containing gangliosides GM1 and GM type III can survive the GI tract [266]. PEG coated liposomes were used for oral delivery of recombinant human epidermal growth factor for gastric ulcer healing [163]. PEG-liposomes are also considered for oral vaccines – ovalbumin in PEG-coated liposomes induces the best mucosal immune response of all carriers tested [186].

After liposome drying methods were developed [299], aerosolized liposomal preparations were suggested for lung delivery. Thus, a combined aerosol of liposomal paclitaxel and cyclosporin A gives better results in the treatment of pulmonary metastases of renal cell carcinoma in mice than each preparation alone [148]. Spray dried powder formulations of liposomes and disaccharides were used as carriers for superoxide dismutase [165]. Improved delivery of rifampicin by aerosolized liposomes to alveolar macrophages could be useful in the treatment of tuberculosis [308]. Aerosolized liposomal budesonide was effective against experimental asthma in mice [145]. Aerosols of liposomal 9-nitrocamptothecin were nontoxic and efficiently treated melanoma and osteosarcoma lung metastases in mice [82]. Liposomal paclitaxel in aerosol effectively treated pulmonary metastases in murine renal carcinoma model [149]. Nebulization was recently suggested to deliver liposomal aerosols [48]. In this particular case, a dispersion of a physical mixture of drugs and phospholipids in saline, which spontaneously formed liposomes with the drug inside, was used. Liposomes for drug delivery to the lungs by nebulization have also been described [329].

Over the years, topical delivery of liposomes was tried for different purposes and in different models [28]. In general, liposomes were found to increase skin penetration of many hydrophilic substances [304]. Highly flexible liposomes, Transferosomes that follow the transepidermal water activity gradient in the skin have been proposed; diclofenac in Transferosomes demonstrated good results when tested in mice, rats, and pigs [29–31]. Deformable liposomes have also been used for skin delivery of ketotifen [64, 65]. The concept of increased deformability of transdermal liposomes was supported by the results of transdermal delivery of pergolide in liposomes, where elastic vesicles were shown to be more efficient [110]. The combination of liposomes and iontophoresis for transdermal delivery also yielded promising results [307].

Because subcutaneous administration of liposomes results in their uptake by draining lymphatic capillaries at the injection site, and because active capture of liposomes by macrophages occurs in regional lymph nodes, plain and ligand targeted liposomes were suggested as good means to target lymphatics for therapeutic and diagnostic applications after subcutaneous administration [198]. Liposomes have been used for lymphatic delivery of methotrexate [137] and for magnetic resonance imaging, using gadolinium (Gd) loaded liposomes [78]. An interesting example of a new approach is a combination of radiofrequency tumor ablation with intravenous liposomal doxorubicin, which resulted in better tumor accumulation of liposomes and increased necrosis in tumors [3, 4].

Liposomes loaded with various drugs and decorated with various targeting moieties, such as sugar residues, have also been utilized for nasal [51] and ocular [27, 50, 106] drug delivery.

According to [41], the following quality control assays should be applied to liposomal formulations for use in humans:

- Basic characterization assays, such as pH; osmolarity; trapped volume; phospholipid concentration; phospholipid composition; phospholipid acyl chain composition; cholesterol concentration; active compound concentration; residual organic solvents and heavy metals; active compound/phospholipid ratio; and proton or ion gradient before and after remote loading.
- Physical characterization assays, such as appearance; vesicle size distribution; submicron range; micron range; electrical surface potential and surface pH; zeta potential; thermotropic behavior, phase transition, and phase separation; and percentage of free drug.
- Chemical stability assays, such as phospholipid hydrolysis; nonesterified fatty acid concentration; phospholipid acyl chain autoxidation; cholesterol autoxidation; and active compound degradation.
- Microbiological assays, such as sterility; and pyrogenicity (endotoxin level).

## 11.4 A Special Case of Liposomal Peptide and Protein Drugs

Proteins and peptides intended as therapeutic agents often demonstrate low biological stability. Processes inactivating various biologically active proteins and peptides in vivo include: conformational protein transformation into inactive form under the action of temperature, pH, high salt concentration, or detergents; dissociation of protein subunits or, in case of enzymes, enzyme–cofactor complexes, or association of protein or peptide molecules with formation of inactive associates; noncovalent complexation with ions or low molecular weight and high molecular weight compounds; proteolytic degradation under the action of endogenous proteases. Rapid elimination and widespread distribution into nontargeted organs and tissues requires administration of a protein or peptide drug in large quantities, which is often not economical and sometimes complicated due to nonspecific toxicity. Another very important factor is the immune response of the macroorganism to foreign proteins containing different antigenic determinants.

One of the technologies to improve pharmacological properties of proteins and peptides is their incorporation into liposomes (see schematics in Fig. 11.3). Liposomal forms of various enzymes have been prepared and investigated: glucose oxidase, glucose-6-phosphate dehydrogenase, hexokinase, β-galactosidase, β-glucuronidase, glucocerebrosidase, α-mannosidase, amiloglucosidase, hexoseaminidase A, peroxidase, β-D-fructofuranosidase, neuraminidase, superoxide dismutase, catalase, asparaginase, cytochrome oxidase, ATPase, dextranase, as well as many other enzymes from different sources (see recent review in [281]).

From the clinical point of view, the potential ability of liposome encapsulated enzymes to enter the cytoplasm or lysosomes of live cells is of primary importance

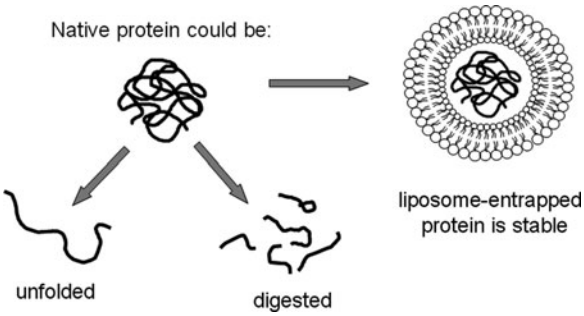


**Fig. 11.3** Liposomes as carriers for proteins and peptides. Native proteins and peptides easily lose their activity in vivo via unfolding or proteolytic degradation (cased by body temperature, oxidation or reduction, influence of various ions, body enzymes and inhibitors, etc.). Immobilization of proteins and peptides into liposomes stabilizes them significantly slowing down many of the inactivation processes

for the treatment of inherited diseases caused by abnormal functioning of some intracellular enzymes, especially in the liver and CNS cells. The use of liposome-immobilized enzymes instead of their native precursors opens new opportunities for enzyme therapy [88, 91] especially in the treatment of diseases localized in liver cells that are natural targets for liposomes. Thus, the biodistribution of liposomes made of phosphatidylcholine, phosphatidic acid and cholesterol, and containing β-fructofuranosidase, has been studied [93]. It was shown that after 6 h, 45% of the enzyme activity accumulated in the liver. The enzyme preserves its activity for a long time – 25% of the administered activity can be found in the liver after 48 h. Similar data have been obtained for intravenously administered liposome encapsulated α-mannosidase [207] and neuraminidase [92].

β-Glucuronidase in charged liposomes composed mainly from phosphatidylcholine dipalmitoyl, also demonstrated fast accumulation in the liver of experimental mice. The enzyme remained active more than a week, associated with the lysosomes of liver cells [255]. Rats with dextran overloaded livers treated with liposome immobilized dextranase (intravenous injection) demonstrated a decrease in the dextran content by 70% in 2 days [37]. The ability of liposome immobilized β-galactosidase to degrade $GM_1$-ganglioside in lysosomes of feline fibroblasts with pathological accumulation of this substrate, has been demonstrated [218]. The native enzyme was unable to penetrate cells. β-galactosidase containing liposomes administered as a single injection, after preliminary injection of liposomes with galactocerebroside into experimental mice, causes the break-down of 70–80% of intracellular galactocerebroside [298].

An increase in the circulation half life of liposomal L-asparaginase and a decrease in its antigenicity and susceptibility toward proteolytic degradation, together with an increase in the efficacy of experimental tumor therapy in mice have been shown [72]. Use of the liposome encapsulated asparaginase improves survival of animals with P1534 tumors compared to free enzyme. It is also important that encapsulation into liposomes prevents the production

of antiasparaginase antibodies. Palmitoyl-L-asparaginase was also incorporated into liposomes and demonstrated prolonged persistence in blood by almost tenfold, decrease in acute toxicity, and improved antitumor activity in vivo [122].

Liposome entrapped SOD reduces ischemia–reperfusion oxidative stress in gerbil brain upon intraperitoneal bolus injection by increasing enzyme activity and decreasing membrane peroxidation in various regions of the brain [253]. Liposomes can also be used for transmembrane intracellular delivery of superoxide dismutase and catalase [75, 76]. This is extremely important for the elimination of oxygen derived free radicals inside cells, as their increased generation causes the toxic effect of ischemia on endothelial and many other cells. Spray-dried powder formulations of the active SOD in DPPC liposomes mixed with disaccharides have been recently described [165]. Experimental thrombolytic therapy with liposome incorporated tissue-type plasminogen activator in rabbits with jugular vein thrombosis clearly demonstrated the benefits of the liposomal enzyme over the native one: significantly lower dose of the liposomal enzyme was required to provide the same degree of lysis [109]. A recent review [60] describes a variety of application of liposomes for the delivery of antithrombotic drugs.

The use of liposomes for the transfer of therapeutic enzymes through the "blood–brain" barrier, which permits delivery of these enzymes into cells of the central nervous system, also seems very attractive. It has been already shown that horse radish peroxidase, encapsulated into liposomes made of phosphatidylcholine, cholesterol, and phosphatidic acid acquires the ability to cross the hematoencephalic barrier, whereas the native enzyme cannot. The presence of peroxidase in brain cells was proved by histochemical methods [319]. The same authors have shown that after injection of the liposomal glucose oxidase into rat tail vein, up to 5% of the enzymatic activity can be discovered in brain tissues [190].

Antibody directed enzyme prodrug therapy (ADEPT) allows for specific generation of active cytotoxic molecules from their prodrugs in the vicinity of tumor cells. For this purpose, a conjugate of a tumor specific antibody with an enzyme responsible for the conversion of a prodrug into the active drug is targeted toward tumor, accumulates there, and converts inactive prodrug into a cytotoxic molecule right at the site of its action [13, 45, 245]. In order to increase the efficiency of the required enzyme in the tumor, it was suggested to use immunoliposomes loaded with the required enzyme (immuno-enzymosomes) [74, 257]. Experiments have been performed with tumor-specific liposomes bearing β-glucuronidase capable of activating anthracycline prodrugs [257, 306].

Eventually, it was found that encapsulation into liposomes could affect certain properties of enzymes or even cause certain undesirable side effects. Thus, liposomal DNAase I can provoke neoplastic transformation in embryonic Syrian hamster cells in culture [327]. It was also shown that the liposomal membrane can influence catalytic properties of the liposome-immobilized β-D-galactoside 2→3 sialyltransferase [311]. The probability of similar effects should always be taken into account with liposome-immobilized enzymes (especially, membrane enzymes). Special attention has also been paid to the immunological properties of liposome-immobilized enzymes. The ability of liposomes to demonstrate in some

cases adjuvant properties is already well known; see further. The authors of [111] demonstrated the possibility of enhanced immune response development in mice receiving intravenously administered liposomes with immobilized bovine β-glucuronidase, despite the expected protection of the intraliposomal enzyme from contact with immunocompetent cells.

An attempt to improve the bioavailability of the oral liposomal insulin by coating insulin containing liposomes with chitosan for better mucoadhesion in the GI tract turned out to be successful in rats and resulted in an efficient and long-lasting lowering of glucose level [269]. Similar results have been also obtained with insulin-containing liposomes coated with PEG or mucin [117], and were explained by better interaction of polymer coated liposomes with the mucus layer and better retention of insulin under aggressive conditions of the stomach and GI (general issues associated with the preparation of the liposomal dosage form with improved mucoadhesion for oral and pulmonary administration of peptide drugs have been reviewed in [268]). The efficiency of the oral administration of the liposomal insulin in liposomes of different phospholipid composition was also confirmed [141]. However, high variability of effects following oral administration of the liposomal insulin still represents a challenge. Buccal delivery of liposomal insulin, which showed encouraging results in rabbit experiments [323], might represent an interesting alternative.

Incorporation of recombinant interleukin-2 into liposomes increased its blood circulation time by eightfold [128]. Liposomal preparations of GM-CSF and TNF-alpha demonstrated improved pharmacokinetics and biological activity on the background of reduced toxicity in mice [131]. Liposomal muramyl tripeptide was successfully used in patients with relapsed osteosarcoma [142]. Mannosilated liposomes with muramyl dipeptide significantly inhibited liver metastases in tumor-bearing mice [197]. PEG-coated liposomes have also been proposed for oral delivery of recombinant human epidermal growth factor [163]. Liposomal delivery of the peptide inhibitor of the transcription factor nuclear factor-kappaB was shown to significantly inhibit proliferation of vascular smooth muscle cells [243]. Liposomal recombinant human TNF strongly suppressed parasitemia and protects against *Plasmodium berghei k173*-induced experimental cerebral malaria in mice [214]. The possibility of the topical delivery of liposomal interferon was considered [55] and the details of dermal penetration of liposomal gamma-interferon, highlighting the key role of the transfollicular route, were investigated [54]. Topical delivery growth hormone-releasing peptide in mice was suggested [73]; such liposomes for peptide delivery may be further improved by modification with hyaluronic acid, which increases their bioadhesion [324]. Topical delivery of liposomal enkephalin has also been demonstrated [307]. Antimicrobial and antiendotoxin cationic peptide, CM3, incorporated into liposomes was suggested for aerosol delivery, and corresponding models describing its potential distribution in lungs of patients with different breathing patterns have been developed [153]. Liposomes with calcitonin have been developed for intranasal delivery [158].

Natural hemoglobin was incorporated into liposomes of different compositions (hemosomes). It was shown that the maximal quantity of hemoglobin obtained

**Table 11.3** Some examples of proteins and peptides in liposomes

| Protein/peptide | Reference |
|---|---|
| β-Fructofuranosidase | [93] |
| α-Mannosidase | [207] |
| Neuraminidase | [92] |
| β-Glucorunidase | [111, 255] |
| Dextranase | [37] |
| β-Galactosidase | [218, 298] |
| L-Asparaginase | [72, 122] |
| SOD | [75, 76, 165, 253] |
| Catalase | [75] |
| Tissue-type plasminogen activator | [109] |
| Horse radish peroxidase | [319] |
| Glucose oxidase | [190] |
| Insulin | [117, 141, 269, 323] |
| Interleukin-2 | [128] |
| GM-CSF | [131] |
| TNF-α | [131, 214] |
| Muramyl tripeptid | [142, 197] |
| Human epidermal growth factor | [163] |
| Interferon | [54, 55] |
| Growth hormone-releasing peptide | [73, 324] |
| Enkephalin | [307] |
| Cationic peptide CM3 | [153] |
| Calcitonin | [158] |
| Hemoglobin | [130, 228, 262, 263, 295] |
| Cilosporin | [56] |

from lysed erythrocytes incorporated into negatively charged liposomes [263]. The authors of [130] have stabilized hemosomes with carboxymethylchitin. Stabilized hemosomes bind oxygen in the same way as human blood hemolysates. Acute toxicity of hemosomes was moderate – in mice, the $LD_{5O}$ was 13.8 ml hemosomes per kg weight. Polymerizable liposomes [107, 295] have also been used for hemosome preparation. Stable polymerized hemosomes are capable of reversible binding of molecular oxygen in physiological conditions even at high flow rates [295]. Incorporation of allosteric effectors into hemosomes permits almost quantitative conversion of immobilized hemoglobin into the oxy-form [107]. To make long circulating hemosomes, technology of PEG postinsertion was developed, in which the resulting liposomes do not lose any hemoglobin and circulate longer in rabbits [11]. PEGylated liposomal hemoglobin was found to be stable upon storage for 1 year even at room temperature [227], and circulate long in rabbits when labeled with $^{99m}$Tc (half clearance time of 48 h) [212]. Good microvascular perfusion was achieved with liposomal hemoglobin in hamsters [228]. Hemoglobin vesicles suspended in recombinant human serum albumin helped treat hemorrhagic shock in rats [226]. However, some side effects were found for PEG-hemosomes. Thus, they are phagocytosed by human peripheral blood monocytes and macrophages via the

opsonin-independent pathway [246]. Liposomes can also cause undesirable changes in hemodynamics, including immediate hypersensitivity and cardiopulmonary distress [264] – this was shown in pigs receiving liposomal hemoglobin (complement activation related pseudo allergy). In addition, some studies show complement activation upon administration of PEGylated Hb-liposomes [262]. This certainly points to the necessity of detailed studies with protein/peptide loaded liposomes before suggesting their clinical application. Some examples of proteins and peptides loaded into liposomes are collected in Table 11.3.

## 11.5 Liposomes as Vehicles for Delivery of DNA and Related Materials

The use of liposomes for gene delivery is a big and well-elaborated area, which is only briefly addressed here. Although viral systems are currently the most common means for DNA delivery, nonviral systems have also been developed. Cationic lipid-based liposomes [70] are easy to prepare, reasonably cheap, and nonimmunogenic. Since many of the finer features of these delivery systems and mechanisms remain insufficiently understood, recent studies in this popular area concentrate on structure, function, structure–activity relationships, detailed mechanisms of liposome mediated gene delivery, and improved efficiency of transfection. Assembly of liposome/DNA complexes is discussed in [225]. To combine the longevity of liposomal preparations with efficient DNA delivery, precondensed DNA was encapsulated into PEGylated cationic liposomes [157]. Polycationic liposomes for gene delivery have been suggested, i.e. liposomes modified by cetylated polyethylene imine, which anchors in the membrane via cetyl residues and binds DNA via positive charges. Such liposomes demonstrate good loading with DNA and high transfection efficacy [184]. In vivo results with cationic liposome mediated gene delivery and future prospects of this technology are discussed in detail elsewhere [10, 273]. Gene transfer systems based on procationic–liposome–protamine–DNA complexes have been recently described [334]. Gene delivery into ischemic myocardium was also successfully performed by double-targeted liposomes modified by both antibody against cardiac myosin, specifically recognizing ischemic cells and TAT peptide [**I**].

Liposomes are also used for targeting of antisense oligonucleotides, in particular for neuroblastoma treatment, exemplified by coated cationic liposomes composed of a central core of a cationic phospholipid bound to oligonucleotide, and an outer shell of neutral lipid. Such liposomes are additionally modified with a monoclonal antibody against neuroectodermal antigens and target antigen positive cells both in vitro and in vivo [26]. Liposomes composed of ursodeoxycholic acid and cationic DOTAP effectively deliver oligonucleotides into HaCaT cells [222]. Combination of the proapoptotic peptide D-(KLAKLAK)2 and Bcl-2 antisense oligo G3139 in a single liposomal preparation resulted in a synergistic effect and improved cancer therapy in mice [**B**]. Reports have appeared on cationic liposome

mediated delivery of siRNA have appeared [136], in particular analyzing and comparing the i.v. and i.p. administration routes in adult mice [249]. Galactosylated cationic liposomes delivered siRNA into liver cells in mice [234]. Liposomes have also been used for intraperitoneal delivery of siRNA for therapy of advanced ovarian cancer [152]. Liposomes decorated with cell penetrating peptides appear to be a promising mean to effectively deliver siRNA inside cells and silence the target gene [330].

## 11.6 Liposomes as Immunological Adjuvants

Liposomes are known to be effective immunological adjuvant for various antigens (see [77, 89]). They are capable of inducing both humoral and cellular immune responses toward liposomal antigens. Liposomes with encapsulated protein or peptide antigen are phagocytosed by macrophages and eventually end up in lysosomes. There, proteins and peptides are degraded by lysosomal enzymes, and their fragments are then presented on the macrophage surface, associated with the MHCII complex. This results in stimulation of specific T-helper cells, and, via the lymphokine secretion and interaction of T cells with B cells that captured free antigen, stimulation of specific B cells and subsequent secretion of antibodies [77]. In some cases, however, a fraction of liposomal antigen can escape from endosomes into the cytoplasm (e.g. when pH-sensitive liposomes are used) and in this case the liberated antigen is processed and presented, associated with the MHCI complex, inducing cytotoxic T lymphocytes (CTL response). The ability to induce the CTL response provides liposomes with certain benefits when compared to traditional adjuvants, such as Freund's adjuvant, which do not induce significant CTL response.

A variety of protein antigens such as diphtheria toxoid [7], hepatitis B antigens [179, 229], influenza virus antigens [57, 291], tumor associated antigens [254], and many others [89], have been incorporated into liposomes). A pronounced immunoadjuvant effect of liposomes can also be seen when proteins (enzymes) or other immunogens are bound to the outer surface of liposomal membranes [108].

Liposomal antigens have been also used to enhance the mucosal immune response. The colonic/rectal IgA response to liposomal ferritin was significantly enhanced over the response to free antigen when cholera toxin was used as adjuvant [335]. The protective efficiency of 30 kDa secretory protein of *Mycobacterium tuberculosis* H37Ra against tuberculosis in mice was significantly enhanced by incorporating this protein into liposomes serving as adjuvant [248]. Synthetic human MUC1 peptides, which are considered as candidates for therapeutic cancer vaccines, were incorporated into liposomes or attached to the surface of liposomes and in both cases elicited strong antigen specific T-response [96]. Formaldehyde inactivated ricin toxoid in liposomes was used for intrapulmonary vaccination to create protection against inhaled ricin with good results [94]. Liposomes incorporating cell penetrating Antennapedia homeodomain fused to a poorly immunogenic CTL epitope, increased

immunogenicity of the construct and improved immune response (activation of CD8+ T cells), evidently because of protection the antigen by liposomes [36]. Various approaches to deliver liposomal proteins to the cytoplasm and Golgi of antigen presenting cells were reviewed recently [216]. In recent developments, liposomes were successfully used for the delivery of peptide vaccines and CTL epitopes to dendritic cells (DCs), improving the immune response [35, 40]. Liposomal formulations of peptide vaccines loaded and activated DCs, leading to protective antiviral and antitumor immune responses [171]. Liposomes successfully delivered CTL epitopes to DCs [35]. A hybrid CTL epitope delivery system was also suggested consisting of Antennapedia homeodomain peptide vector in liposomes [36]. Antigen in mannosylated liposomes enhances uptake and activation of DC and increases their ability to induce primed T-cell proliferation [40]. Modification with cell penetrating TAT peptide has also improved transfection of spleen-derived antigen-presenting cells in culture [203].

Oral delivery of antigens in liposomes (ovalbumin was used as a model antigen) was shown to effectively induce oral tolerance [183].

## 11.7 Liposomes in Medical Imaging

Use of liposomes for the delivery of imaging agents for all imaging modalities has a long history [278]. There exist several different methods to label/load the liposome with a contrast/reporter group: (a) Label is added to liposomes during the manufacturing process, either into the aqueous interior of liposome or into the liposome membrane; (b) Label is adsorbed onto the surface of preformed liposomes; (c) Label is incorporated into the lipid bilayer of preformed liposomes; (d) Label is loaded into preformed liposomes using membrane-incorporated transporters, ion channels, or concentration gradients. In any case, the labeling procedure should be simple and efficient, the reporter group should be affordable, stable, and safe/easy to handle, and the liposomes should be stable during storage and in vivo, with no release of free label.

Liposomal contrast agents have been used for experimental diagnostic imaging of liver, spleen, brain, cardio-vascular system, tumors, inflammations and infections [278, 279]. The relative efficacy of entrapment of contrast materials into different liposomes, as well as advantages and disadvantages of various liposome types, were elucidated quite a while ago [275].

Gamma-scintigraphy and MR imaging both require a sufficient quantity of radionuclide or paramagnetic metal to be associated with the liposome. There are two possible routes to improve the efficacy of liposomes as contrast media for gamma scintigraphy and MRI: to increase the quantity of carrier associated reporter metal (such as $^{111}$In or Gd), and/or enhance signal intensity. To increase the load of liposomes with reporter metals, amphiphilic chelating polymers containing a hydrophobic block for the firm incorporation into the liposomal membrane, and a hydrophilic block with multiple chelating groups, were introduced [67, 68, 280]. The polymers easily incorporate into the liposomal membrane and sharply

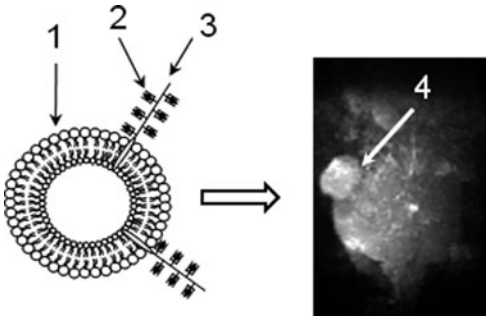


**Fig. 11.4** Magnetic resonance imaging of a model subcutaneous tumor in mice using Gd-loaded liposomes. Liposome (**1**; usually, PEGylated and modified with tumor-specific antibody) is loaded with Gd (**2**) via amphiphilic polymers (**3**) containing multiple chelating groups attached as side-groups to the main polymeric chain and terminal lipid group for anchoring in the liposome membrane. Such combination of longevity (due to attached PEG), targetability (due to attached antibody), and heavy Gd load (due to liposome-incorporated polychelating polymer) results in fast (less than 4 h) and efficient tumor (**4**) visualization. According to [66]

increase the number of chelated Gd or In atoms attached to a single lipid anchor. In the case of MRI, metal atoms chelated into these groups are directly exposed to the water environment, which enhances the signal intensity of the paramagnetic ions and leads to the corresponding enhancement of the vesicle contrast properties. The overall performance of chelating polymer-bearing liposomes might be further improved by additional incorporation of amphiphilic PEG into the liposome membrane due to the presence of increased amount of PEG-associated water protons in the close vicinity of chelated Gd ions located on the liposomal membrane. In addition to the enhanced relaxivity, the coating of liposome surface with PEG polymer can help in avoiding contrast agent uptake in the site of injection by resident phagocytic cells. This approach resulted in efficient liposomal contrast agents for the MR imaging of the blood pool [310]. The attachment of the target specific monoclonal antibody to PEGylated liposomes loaded with multiple reporter metal moieties via the liposome-incorporated polychelating polymers could bring to life efficient and target specific contrast agents, as was shown with Gd-loaded liposomes modified with anticancer 2C5 antibody [66], Fig. 11.4. MR imaging using pH responsive contrast liposomes allowed for visualization of pathological areas with decreased pH values [166]. Contrast agent loaded liposomes were also used for in vivo monitoring of tissue pharmacokinetics of liposomal drugs in mice [305]. Sterically stabilized superparamagnetic liposomes were suggested for MR imaging and cancer therapy [213].

Because of its short half life and ideal radiation energy, $^{99m}$Tc is the most clinically attractive isotope for gamma-scintigraphy. Recently, new methods for labeling preformed glutathione-containing liposomes with various $^{99m}$Tc and $^{186}$Re complexes were developed [15, 16], which are extremely effective and result in a very stable product.

CT contrast agents (primarily, heavily iodinated organic compounds) have been included in the inner water compartment of liposomes or incorporated into the liposome membrane. Thus, iopromide was incorporated into plain [223] and PEGylated liposomes [224] and demonstrated favorable biodistribution and imaging potential in rats and rabbits.

Recent interesting approaches suggest combining CT and MRI contrast properties in a single liposomal preparation, thus allowing for very effective multimodal imaging in vivo [331, 333].

Liposomes for sonography are prepared by incorporating gas bubbles (which are efficient reflectors of sound) into the liposome, or by forming the bubble directly inside the liposome as a result of a chemical reaction, such as bicarbonate hydrolysis yielding carbon dioxide. Gas bubbles stabilized inside the phospholipid membrane demonstrate good performance and low toxicity of these contrast agents in rabbit and porcine models. Recently, liposome application for ultrasound and gamma-scintigraphic imaging was discussed [43]. A review of data relating to the use of liposome-based imaging agents for cancer has been published [252].

## 11.8 Some Miscellaneous Applications

*Photo-dynamic therapy* (PDT) is a fast developing modality for treatment of superficial/skin tumors, where photosensitizing agents are used for photochemical eradication of malignant cells. In PDT, liposomes are used both as drug carriers and enhancers. Recent reviews on the use of liposomes in PDT are available [32, 47]. Targeting and controlled release of photosensitizing agent in tumors may still further increase the outcome of the liposome-mediated PDT. Benzoporphyrin derivative encapsulated in polycation liposomes modified with cetyl-polyethyleneimine was used for antiangiogenic PDT. This drug, when incorporated in such liposomes, was better internalized by human umbilical vein endothelial cells and was found in the intranuclear region and associated with mitochondria [270]. The commercial liposomal preparation of benzoporphyrin derivative monoacid ring A, known as Visudyne (Novartis), was active against tumors in sarcoma-bearing mice [113]. PDT with liposomal Photofrin® gives better results in mice with human gastric cancer that with a free drug [114]. Another porphyrin derivative, SIM01, incorporated in DMPC liposomes, also gives better results in PDT, mainly due to better accumulation in the tumor (human adenocarcinoma in nude mice) [25]. Similarly, liposomal *meso*-tetrakis-phenylporphyrin was very effective in PDT of human amelanotic melanoma in nude mice [120].

*Liposomal forms of "bioenergic" substrates*, such as ATP, are of clear interest, and some encouraging results with ATP-loaded liposomes in various in vitro and in vivo models have been reported. ATP-liposomes were shown to protect human endothelial cells from energy failure in a cell culture model of sepsis [100]. In a brain ischemia model, the use of the liposomal ATP increased the number of ischemic episodes

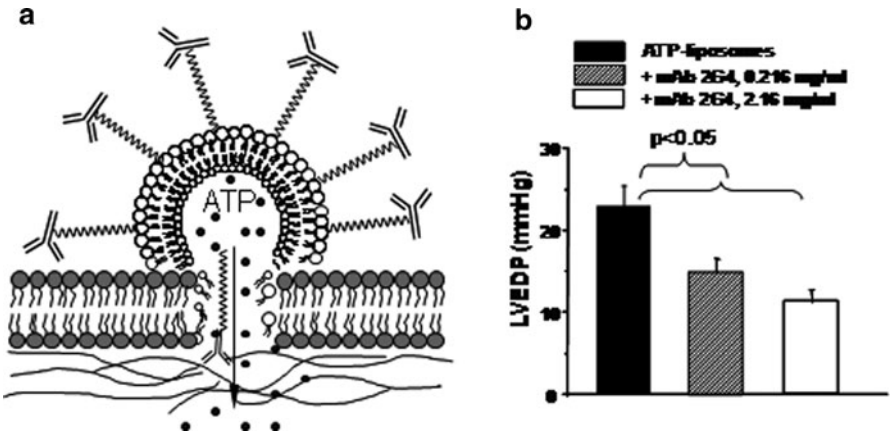


**Fig. 11.5** Use of liposome to transport ATP into hypoxic cells. Liposomes loaded with ATP and modified with monoclonal antibody 2G4-specific against cardiac myosin and recognizing ischemically damaged cardiomyocytes were shown to fuse with the sites of ischemically damaged membranes of cardiomyocytes and deliver ATP inside cells (**a**). As a result, damage to mechanical properties of cardiomyocytes (estimated as an initial left ventricle end diastolyc pressure, LVEDP, characterizing the ability of the heart to relax) in the model of isolated rat heart was significantly reduced (smaller LVEDP). Maximum reduction was achieved for antibody-targeted ATP-loaded liposomes, the effect being proportional to the quantity of the preparation used (**b**). According to [303]

tolerated before brain electrical silence and death [151]. In a hypovolemic shock-reperfusion model in rats, administration of ATP-liposomes provided effective protection to the liver [147]. ATP-liposomes also improved the rat liver energy state and metabolism during cold storage preservation [191]. Similar properties were also demonstrated for the liposomal coenzyme Q10 [193]. Interestingly, biodistribution studies with the ATP-liposomes demonstrated their significant accumulation in the damaged myocardium [317]. Recently, ATP-loaded liposomes were shown to effectively preserve mechanical properties of the heart under ischemic conditions in an isolated rat heart model [302]. ATP-loaded immunoliposomes were also prepared possessing specific affinity toward myosin, i.e. capable of specific recognition of hypoxic cells [164] and effectively protected infarcted myocardium in vivo [300, 303], Fig. 11.5; see recent summary [103]. Similarly, liposomes loaded with coenzyme Q10 effectively protected the myocardium in infarcted rabbits [301].

*Magnetic liposomes* with doxorubicin were intravenously administered to osteosarcoma-bearing hamsters. When the tumor implanted limb was placed between two poles of a 0.4 T magnet, application of the field for 60 min resulted in a fourfold increase in drug concentration in the tumor [194]. In the same osteosarcoma model with the magnet implanted into the tumor, magnetic liposomes loaded with adriamycin demonstrated better accumulation in tumor vasculature and tumor growth inhibition [150]. Upon intravenous injection in rats, liposomes loaded with $^{99m}$Tc-albumin and magnetite demonstrated a 25-fold increase in accumulated

radioactivity in right kidney, near which a SmCo magnet was implanted, compared to control left kidney [12].

*New generation liposomes* frequently demonstrate a combination of different attractive properties, such as simultaneous longevity and targetability, longevity and stimuli-sensitivity, targetability and contrast properties, etc. Liposomes are also described demonstrating sensitivity toward low temperatures and ultrasound [53]. Controlling liposomal drug release by low frequency ultrasound is also receiving increased attention [239] as are liposomes conjugated with acoustically active microbubbles [135].

## References


1. Abra RM, Bankert RB, Chen F, Egilmez NK, Huang K, Saville R, Slater JL, Sugano M, Yokota SJ (2002) The next generation of liposome delivery systems: recent experience with tumor-targeted, sterically-stabilized immunoliposomes and active-loading gradients. J Liposome Res 12:1–3
2. Adamo V, Lorusso V, Rossello R, Adamo B, Ferraro G, Lorusso D, Condemi G, Priolo D, Di Lullo L, Paglia A, Pisconti S, Scambia G, Ferrandina G (2008) Pegylated liposomal doxorubicin and gemcitabine in the front-line treatment of recurrent/metastatic breast cancer: a multicentre phase II study. Br J Cancer 98:1916–1921
3. Ahmed M, Liu Z, Lukyanov AN, Signoretti S, Horkan C, Monsky WL, Torchilin VP, Goldberg SN (2005) Combination radiofrequency ablation with intratumoral liposomal doxorubicin: effect on drug accumulation and coagulation in multiple tissues and tumor types in animals. Radiology 235:469–477
4. Ahmed M, Lukyanov AN, Torchilin V, Tournier H, Schneider AN, Goldberg SN (2005) Combined radiofrequency ablation and adjuvant liposomal chemotherapy: effect of chemotherapeutic agent, nanoparticle size, and circulation time. J Vasc Interv Radiol 16:1365–1371
5. Allen TM, Hansen C (1991) Pharmacokinetics of stealth versus conventional liposomes: effect of dose. Biochim Biophys Acta 1068:133–141
6. Allen TM, Mumbengegwi DR, Charrois GJ (2005) Anti-CD19-targeted liposomal doxorubicin improves the therapeutic efficacy in murine B-cell lymphoma and ameliorates the toxicity of liposomes with varying drug release rates. Clin Cancer Res 11:3567–3573
7. Allison AG, Gregoriadis G (1974) Liposomes as immunological adjuvants. Nature 252:252
8. Asokan A, Cho MJ (2003) Cytosolic delivery of macromolecules. II. Mechanistic studies with pH-sensitive morpholine lipids. Biochim Biophys Acta 1611:151–160
9. Atobe K, Ishida T, Ishida E, Hashimoto K, Kobayashi H, Yasuda J, Aoki T, Obata K, Kikuchi H, Akita H, Asai T, Harashima H, Oku N, Kiwada H (2007) In vitro efficacy of a sterically stabilized immunoliposomes targeted to membrane type 1 matrix metalloproteinase (MT1-MMP). Biol Pharm Bull 30:972–978
10. Audouy SA, de Leij LF, Hoekstra D, Molema G (2002) In vivo characteristics of cationic liposomes as delivery vectors for gene therapy. Pharm Res 19:1599–1605
11. Awasthi VD, Garcia D, Klipper R, Goins BA, Phillips WT (2004) Neutral and anionic liposome-encapsulated hemoglobin: effect of postinserted poly(ethylene glycol)-distearoylphosphatidylethanolamine on distribution and circulation kinetics. J Pharmacol Exp Ther 309:241–248
12. Babincova M, Altanerova V, Lampert M, Altaner C, Machova E, Sramka M, Babinec P (2000) Site-specific in vivo targeting of magnetoliposomes using externally applied magnetic field. Z Naturforsch C 55:278–281

13. Bagshawe KD, Springer CJ, Searle F, Antoniw P, Sharma SK, Melton RG, Sherwood RF (1988) A cytotoxic agent can be generated selectively at cancer sites. Br J Cancer 58:700–703
14. Balbi G, Visconti S, Monteverde A, Manganaro MA, Cardone A (2007) Liposomal doxorubicin: a phase II trial. Acta Biomed 78:210–213
15. Bao A, Goins B, Klipper R, Negrete G, Mahindaratne M, Phillips WT (2003) A novel liposome radiolabeling method using 99mTc-"SNS/S" complexes: in vitro and in vivo evaluation. J Pharm Sci 92:1893–1904
16. Bao A, Goins B, Klipper R, Negrete G, Phillips WT (2003) 186Re-liposome labeling using 186Re-SNS/S complexes: in vitro stability, imaging, and biodistribution in rats. J Nucl Med 44:1992–1999
17. Bendsoe N, Persson L, Johansson A, Axelsson J, Svensson J, Grafe S, Trebst T, Andersson-Engels S, Svanberg S, Svanberg K (2007) Fluorescence monitoring of a topically applied liposomal Temoporfin formulation and photodynamic therapy of nonpigmented skin malignancies. J Environ Pathol Toxicol Oncol 26:117–126
18. Benesch M, Urban C (2008) Liposomal cytarabine for leukemic and lymphomatous meningitis: recent developments. Expert Opin Pharmacother 9:301–309
19. Blume G, Cevc G (1993) Molecular mechanism of the lipid vesicle longevity in vivo. Biochim Biophys Acta 1146:157–168
20. Blume G, Cevc G, Crommelin MD, Bakker-Woudenberg IA, Kluft C, Storm G (1993) Specific targeting with poly(ethylene glycol)-modified liposomes: coupling of homing devices to the ends of the polymeric chains combines effective target binding with long circulation times. Biochim Biophys Acta 1149:180–184
21. Boddapati SV, D'Souza GG, Erdogan S, Torchilin VP, Weissig V (2008) Organelle-targeted nanocarriers: specific delivery of liposomal ceramide to mitochondria enhances its cytotoxicity in vitro and in vivo. Nano Lett 8:2559–2563
22. Boddapati SV, Tongcharoensirikul P, Hanson RN, D'Souza GG, Torchilin VP, Weissig V (2005) Mitochondriotropic liposomes. J Liposome Res 15:49–58
23. Boorjian SA, Milowsky MI, Kaplan J, Albert M, Cobham MV, Coll DM, Mongan NP, Shelton G, Petrylak D, Gudas LJ, Nanus DM (2007) Phase 1/2 clinical trial of interferon alpha2b and weekly liposome-encapsulated all-trans retinoic acid in patients with advanced renal cell carcinoma. J Immunother 30:655–662
24. Booser DJ, Esteva FJ, Rivera E, Valero V, Esparza-Guerra L, Priebe W, Hortobagyi GN (2002) Phase II study of liposomal annamycin in the treatment of doxorubicin-resistant breast cancer. Cancer Chemother Pharmacol 50:6–8
25. Bourre L, Thibaut S, Fimiani M, Ferrand Y, Simonneaux G, Patrice T (2003) In vivo photosensitizing efficiency of a diphenylchlorin sensitizer: interest of a DMPC liposome formulation. Pharmacol Res 47:253–261
26. Brignole C, Pagnan G, Marimpietri D, Cosimo E, Allen TM, Ponzoni M, Pastorino F (2003) Targeted delivery system for antisense oligonucleotides: a novel experimental strategy for neuroblastoma treatment. Cancer Lett 197:231–235
27. Budai L, Hajdu M, Budai M, Grof P, Beni S, Noszal B, Klebovich I, Antal I (2007) Gels and liposomes in optimized ocular drug delivery: studies on ciprofloxacin formulations. Int J Pharm 343:34–40
28. Cevc G (2004) Lipid vesicles and other colloids as drug carriers on the skin. Adv Drug Deliv Rev 56:675–711
29. Cevc G, Blume G (2001) New, highly efficient formulation of diclofenac for the topical, transdermal administration in ultradeformable drug carriers, Transfersomes. Biochim Biophys Acta 1514:191–205
30. Cevc G, Gebauer D (2003) Hydration-driven transport of deformable lipid vesicles through fine pores and the skin barrier. Biophys J 84:1010–1024
31. Cevc G, Schatzlein A, Richardsen H (2002) Ultradeformable lipid vesicles can penetrate the skin and other semi-permeable barriers unfragmented. Evidence from double label CLSM experiments and direct size measurements. Biochim Biophys Acta 1564:21–30

32. Chen B, Pogue BW, Hasan T (2005) Liposomal delivery of photosensitising agents. Expert Opin Drug Deliv 2:477–487
33. Cheng WW, Allen TM (2008) Targeted delivery of anti-CD19 liposomal doxorubicin in B-cell lymphoma: a comparison of whole monoclonal antibody, Fab' fragments and single chain Fv. J Control Release 126:50–58
34. Cheng WW, Das D, Suresh M, Allen TM (2007) Expression and purification of two anti-CD19 single chain Fv fragments for targeting of liposomes to CD19-expressing cells. Biochim Biophys Acta 1768:21–29
35. Chikh G, Schutze-Redelmeier MP (2002) Liposomal delivery of CTL epitopes to dendritic cells. Biosci Rep 22:339–353
36. Chikh GG, Kong S, Bally MB, Meunier JC, Schutze-Redelmeier MP (2001) Efficient delivery of Antennapedia homeodomain fused to CTL epitope with liposomes into dendritic cells results in the activation of CD8+ T cells. J Immunol 167:6462–6470
37. Colley CM, Ryman BE (1976) The use of a liposomally entrapped enzyme in the treatment of an artificial storage condition. Biochim Biophys Acta 451:417–425
38. Connor J, Huang L (1986) pH-sensitive immunoliposomes as an efficient and target-specific carrier for antitumor drugs. Cancer Res 46:3431–3435
39. Cooley T, Henry D, Tonda M, Sun S, O'Connell M, Rackoff W (2007) A randomized, double-blind study of pegylated liposomal doxorubicin for the treatment of AIDS-related Kaposi's sarcoma. Oncologist 12:114–123
40. Copland MJ, Baird MA, Rades T, McKenzie JL, Becker B, Reck F, Tyler PC, Davies NM (2003) Liposomal delivery of antigen to human dendritic cells. Vaccine 21:883–890
41. Crommelin DJ, Storm G (2003) Liposomes: from the bench to the bed. J Liposome Res 13:33–36
42. D'Souza GG, Wang T, Rockwell K, Torchilin VP (2008) Surface modification of pharmaceutical nanocarriers with ascorbate residues improves their tumor-cell association and killing and the cytotoxic action of encapsulated paclitaxel in vitro. Pharm Res 25:2567–2572
43. Dagar S, Rubinstein I, Onyuksel H (2003) Liposomes in ultrasound and gamma scintigraphic imaging. Methods Enzymol 373:198–214
44. Dark GG, Calvert AH, Grimshaw R, Poole C, Swenerton K, Kaye S, Coleman R, Jayson G, Le T, Ellard S, Trudeau M, Vasey P, Hamilton M, Cameron T, Barrett E, Walsh W, McIntosh L, Eisenhauer EA (2005) Randomized trial of two intravenous schedules of the topoisomerase I inhibitor liposomal lurtotecan in women with relapsed epithelial ovarian cancer: a trial of the national cancer institute of Canada clinical trials group. J Clin Oncol 23:1859–1866
45. Deonarain MP, Epenetos AA (1994) Targeting enzymes for cancer therapy: old enzymes in new roles. Br J Cancer 70:786–794
46. Derycke AS, De Witte PA (2002) Transferrin-mediated targeting of hypericin embedded in sterically stabilized PEG-liposomes. Int J Oncol 20:181–187
47. Derycke AS, de Witte PA (2004) Liposomes for photodynamic therapy. Adv Drug Deliv Rev 56:17–30
48. Desai TR, Hancock RE, Finlay WH (2002) A facile method of delivery of liposomes by nebulization. J Control Release 84:69–78
49. Desnick RJ, Thorpe SR, Fiddler MB (1976) Toward enzyme therapy for lysosomal storage diseases. Physiol Rev 56:57–99
50. Diebold Y, Jarrin M, Saez V, Carvalho EL, Orea M, Calonge M, Seijo B, Alonso MJ (2007) Ocular drug delivery by liposome-chitosan nanoparticle complexes (LCS-NP). Biomaterials 28:1553–1564
51. Ding WX, Qi XR, Fu Q, Piao HS (2007) Pharmacokinetics and pharmacodynamics of sterylglucoside-modified liposomes for levonorgestrel delivery via nasal route. Drug Deliv 14:101–104
52. Dragovich T, Mendelson D, Kurtin S, Richardson K, Von Hoff D, Hoos A (2006) A phase 2 trial of the liposomal DACH platinum L-NDDP in patients with therapy-refractory advanced colorectal cancer. Cancer Chemother Pharmacol 58:759–764

53. Dromi S, Frenkel V, Luk A, Traughber B, Angstadt M, Bur M, Poff J, Xie J, Libutti SK, Li KC, Wood BJ (2007) Pulsed-high intensity focused ultrasound and low temperature-sensitive liposomes for enhanced targeted drug delivery and antitumor effect. Clin Cancer Res 13:2722–2727
54. du Plessis J, Egbaria K, Ramachandran C, Weiner N (1992) Topical delivery of liposomally encapsulated gamma-interferon. Antiviral Res 18:259–265
55. Egbaria K, Ramachandran C, Kittayanond D, Weiner N (1990) Topical delivery of liposomally encapsulated interferon evaluated by in vitro diffusion studies. Antimicrob Agents Chemother 34:107–110
56. Egbaria K, Ramachandran C, Weiner N (1990) Topical delivery of ciclosporin: evaluation of various formulations using in vitro diffusion studies in hairless mouse skin. Skin Pharmacol 3:21–28
57. el Guink N, Kris RM, Goodman-Snitkoff G, Small PA Jr, Mannino RJ (1989) Intranasal immunization with proteoliposomes protects against influenza. Vaccine 7:147–151
58. Elbayoumi TA, Torchilin VP (2006) Enhanced accumulation of long-circulating liposomes modified with the nucleosome-specific monoclonal antibody 2C5 in various tumours in mice: gamma-imaging studies. Eur J Nucl Med Mol Imaging 33:1196–1205
59. Elbayoumi TA, Torchilin VP (2007) Enhanced cytotoxicity of monoclonal anticancer antibody 2C5-modified doxorubicin-loaded PEGylated liposomes against various tumor cell lines. Eur J Pharm Sci 32:159–168
60. Elbayoumi TA, Torchilin VP (2008) Liposomes for targeted delivery of antithrombotic drugs. Expert Opin Drug Deliv 5:1185–1198
61. Elbayoumi TA, Torchilin VP (2008) Tumor-specific antibody-mediated targeted delivery of Doxil((R)) reduces the manifestation of auricular erythema side effect in mice. Int J Pharm 357:272–279
62. Elbayoumi TA, Torchilin VP (2009) Tumor-specific anti-nucleosome antibody improves therapeutic efficacy of doxorubicin-loaded long-circulating liposomes against primary and metastatic tumor in mice. Mol Pharm 6:246–254
63. ElBayoumi TA, Torchilin VP (2009) Tumor-targeted nanomedicines: enhanced antitumor efficacy in vivo of doxorubicin-loaded, long-circulating liposomes modified with cancer-specific monoclonal antibody. Clin Cancer Res 15:1973–1980
64. Elsayed MM, Abdallah OY, Naggar VF, Khalafallah NM (2006) Deformable liposomes and ethosomes: mechanism of enhanced skin delivery. Int J Pharm 322:60–66
65. Elsayed MM, Abdallah OY, Naggar VF, Khalafallah NM (2007) Deformable liposomes and ethosomes as carriers for skin delivery of ketotifen. Pharmazie 62:133–137
66. Erdogan S, Medarova ZO, Roby A, Moore A, Torchilin VP (2008) Enhanced tumor MR imaging with gadolinium-loaded polychelating polymer-containing tumor-targeted liposomes. J Magn Reson Imaging 27:574–580
67. Erdogan S, Roby A, Sawant R, Hurley J, Torchilin VP (2006) Gadolinium-loaded polychelating polymer-containing cancer cell-specific immunoliposomes. J Liposome Res 16:45–55
68. Erdogan S, Roby A, Torchilin VP (2006) Enhanced tumor visualization by gamma-scintigraphy with 111In-labeled polychelating-polymer-containing immunoliposomes. Mol Pharm 3:525–530
69. Fattal E, Couvreur P, Dubernet C (2004) "Smart" delivery of antisense oligonucleotides by anionic pH-sensitive liposomes. Adv Drug Deliv Rev 56:931–946
70. Felgner PL, Ringold GM (1989) Cationic liposome-mediated transfection. Nature 337:387–388
71. Ferrandina G, Ludovisi M, Lorusso D, Pignata S, Breda E, Savarese A, Del Medico P, Scaltriti L, Katsaros D, Priolo D, Scambia G (2008) Phase III trial of gemcitabine compared with pegylated liposomal doxorubicin in progressive or recurrent ovarian cancer. J Clin Oncol 26:890–896

72. Fishman Y, Citri N (1975) L-asparaginase entrapped in liposomes: preparation and properties. FEBS Lett 60:17–20
73. Fleisher D, Niemiec SM, Oh CK, Hu Z, Ramachandran C, Weiner N (1995) Topical delivery of growth hormone releasing peptide using liposomal systems: an in vitro study using hairless mouse skin. Life Sci 57:1293–1297
74. Fonseca MJ, Jagtenberg JC, Haisma HJ, Storm G (2003) Liposome-mediated targeting of enzymes to cancer cells for site-specific activation of prodrugs: comparison with the corresponding antibody-enzyme conjugate. Pharm Res 20:423–428
75. Freeman BA, Turrens JF, Mirza Z, Crapo JD, Young SL (1985) Modulation of oxidant lung injury by using liposome-entrapped superoxide dismutase and catalase. Fed Proc 44:2591–2595
76. Freeman BA, Young SL, Crapo JD (1983) Liposome-mediated augmentation of superoxide dismutase in endothelial cells prevents oxygen injury. J Biol Chem 258:12534–12542
77. Friede M (1995) Liposomes as carriers of antigens. In: Philippot JR, Schuber F (eds) Liposomes as tools in basic research and industry. CRC, Boca Raton, pp 189–200
78. Fujimoto Y, Okuhata Y, Tyngi S, Namba Y, Oku N (2000) Magnetic resonance lymphography of profundus lymph nodes with liposomal gadolinium-diethylenetriamine pentaacetic acid. Biol Pharm Bull 23:97–100
79. Gabizon A, Shmeeda H, Horowitz AT, Zalipsky S (2004) Tumor cell targeting of liposome-entrapped drugs with phospholipid-anchored folic acid-PEG conjugates. Adv Drug Deliv Rev 56:1177–1192
80. Gabizon AA (2001) Pegylated liposomal doxorubicin: metamorphosis of an old drug into a new form of chemotherapy. Cancer Invest 19:424–436
81. Gijsens A, Derycke A, Missiaen L, De Vos D, Huwyler J, Eberle A, de Witte P (2002) Targeting of the photocytotoxic compound AlPcS4 to Hela cells by transferrin conjugated PEG-liposomes. Int J Cancer 101:78–85
82. Gilbert BE, Seryshev A, Knight V, Brayton C (2002) 9-nitrocamptothecin liposome aerosol: lack of subacute toxicity in dogs. Inhal Toxicol 14:185–197
83. Goncalves A, Braud AC, Viret F, Genre D, Gravis G, Tarpin C, Giovannini M, Maraninchi D, Viens P (2003) Phase I study of pegylated liposomal doxorubicin (Caelyx) in combination with carboplatin in patients with advanced solid tumors. Anticancer Res 23:3543–3548
84. Gonzalez R, Hutchins L, Nemunaitis J, Atkins M, Schwarzenberger PO (2006) Phase 2 trial of Allovectin-7 in advanced metastatic melanoma. Melanoma Res 16:521–526
85. Gorodetsky R, Levdansky L, Vexler A, Shimeliovich I, Kassis I, Ben-Moshe M, Magdassi S, Marx G (2004) Liposome transduction into cells enhanced by haptotactic peptides (Haptides) homologous to fibrinogen C-termini. J Control Release 95:477–488
86. Grabowsky GA, Desnick RJ (1981) Enzyme replacement in genetic diseases. In: Holcenberg JS, Roberts J (eds) Enzymes as drugs. Wiley, New York, p 167
87. Grant GJ, Barenholz Y, Bolotin EM, Bansinath M, Turndorf H, Piskoun B, Davidson EM (2004) A novel liposomal bupivacaine formulation to produce ultralong-acting analgesia. Anesthesiology 101:133–137
88. Gregoriadis G (1978) Liposomes in the therapy of lysosomal storage diseases. Nature 275:695–696
89. Gregoriadis G (1993) Liposomes as immunological adjuvants for peptide and protein antigens. In: Gregoriadis G, Florence AT, Patel HM (eds) Liposomes in drug delivery. Harwood Academic Publishers, Switzerland, pp 77–94
90. Gregoriadis G (2007) Liposome technology: Liposome preparation and related techniques, 3rd edn., 1–3. Informa Healthcare, New York, p 1240
91. Gregoriadis G, Dean MF (1979) Enzyme therapy in genetic diseases. Nature 278:603–604
92. Gregoriadis G, Putman D, Louis L, Neerunjun D (1974) Comparative effect and fate of non-entrapped and liposome-entrapped neuraminidase injected into rats. Biochem J 140:323–330

93. Gregoriadis G, Ryman BE (1972) Lysosomal localization of -fructofuranosidase-containing liposomes injected into rats. Biochem J 129:123–133
94. Griffiths GD, Phillips GJ, Bailey SC (1999) Comparison of the quality of protection elicited by toxoid and peptide liposomal vaccine formulations against ricin as assessed by markers of inflammation. Vaccine 17:2562–2568
95. Groll AH, Mickiene D, Petraitis V, Petraitiene R, Alfaro RM, King C, Piscitelli SC, Walsh TJ (2003) Comparative drug disposition, urinary pharmacokinetics, and renal effects of multilamellar liposomal nystatin and amphotericin B deoxycholate in rabbits. Antimicrob Agents Chemother 47:3917–3925
96. Guan HH, Budzynski W, Koganty RR, Krantz MJ, Reddish MA, Rogers JA, Longenecker BM, Samuel J (1998) Liposomal formulations of synthetic MUC1 peptides: effects of encapsulation versus surface display of peptides on immune responses. Bioconjug Chem 9:451–458
97. Gupta B, Levchenko TS, Torchilin VP (2007) TAT peptide-modified liposomes provide enhanced gene delivery to intracranial human brain tumor xenografts in nude mice. Oncol Res 16:351–359
98. Gupta B, Torchilin VP (2007) Monoclonal antibody 2C5-modified doxorubicin-loaded liposomes with significantly enhanced therapeutic activity against intracranial human brain U-87 MG tumor xenografts in nude mice. Cancer Immunol Immunother 56:1215–1223
99. Gupta Y, Jain A, Jain P, Jain SK (2007) Design and development of folate appended liposomes for enhanced delivery of 5-FU to tumor cells. J Drug Target 15:231–240
100. Han YY, Huang L, Jackson EK, Dubey RK, Gillepsie DG, Carcillo JA (2001) Liposomal atp or NAD+ protects human endothelial cells from energy failure in a cell culture model of sepsis. Res Commun Mol Pathol Pharmacol 110:107–116
101. Hansen CB, Kao GY, Moase EH, Zalipsky S, Allen TM (1995) Attachment of antibodies to sterically stabilized liposomes: evaluation, comparison and optimization of coupling procedures. Biochim Biophys Acta 1239:133–144
102. Harrington KJ, Lewanski C, Northcote AD, Whittaker J, Peters AM, Vile RG, Stewart JS (2001) Phase II study of pegylated liposomal doxorubicin (Caelyx) as induction chemotherapy for patients with squamous cell cancer of the head and neck. Eur J Cancer 37:2015–2022
103. Hartner WC, Verma DD, Levchenko TS, Bernstein EA, Torchilin VP (2009) ATP-loaded liposomes for treatment of myocardial ischemia. Wiley Interdiscip Rev Nanomed Nanobiotechnol 1:530–539
104. Hatakeyama H, Akita H, Ishida E, Hashimoto K, Kobayashi H, Aoki T, Yasuda J, Obata K, Kikuchi H, Ishida T, Kiwada H, Harashima H (2007) Tumor targeting of doxorubicin by anti-MT1-MMP antibody-modified PEG liposomes. Int J Pharm 342:194–200
105. Hatakeyama H, Akita H, Maruyama K, Suhara T, Harashima H (2004) Factors governing the in vivo tissue uptake of transferrin-coupled polyethylene glycol liposomes in vivo. Int J Pharm 281:25–33
106. Hathout RM, Mansour S, Mortada ND, Guinedi AS (2007) Liposomes as an ocular delivery system for acetazolamide: in vitro and in vivo studies. AAPS PharmSciTech 8:1
107. Hayward JA, Levine DM, Neufeld L, Simon SR, Johnston DS, Chapman D (1985) Polymerized liposomes as stable oxygen-carriers. FEBS Lett 187:261–266
108. Heath TD, Shek P, Papahadjopoulos D (1986) Production of immunogens by antigen conjugation to liposomes. The Regents of the University of California, United States
109. Heeremans JL, Prevost R, Bekkers ME, Los P, Emeis JJ, Kluft C, Crommelin DJ (1995) Thrombolytic treatment with tissue-type plasminogen activator (t-PA) containing liposomes in rabbits: a comparison with free t-PA. Thromb Haemost 73:488–494
110. Honeywell-Nguyen PL, Frederik PM, Bomans PHH, Junginger HE, Bouwstra JA (2002) Transdermal delivery of pergolide from surfactant-based elastic and rigid vesicles: characterization and in vitro transport studies. Pharmaceut Res (NY) 19:991–997
111. Hudson LD, Fiddler MB, Desnick RJ (1979) Enzyme therapy. X. Immune response induced by enzyme- and buffer-loaded liposomes in C3H/HeJ Gus(h) mice. J Pharmacol Exp Ther 208:507–514

112. Huwyler J, Wu D, Pardridge WM (1996) Brain drug delivery of small molecules using immunoliposomes. Proc Natl Acad Sci U S A 93:14164–14169
113. Ichikawa K, Takeuchi Y, Yonezawa S, Hikita T, Kurohane K, Namba Y, Oku N (2004) Antiangiogenic photodynamic therapy (PDT) using Visudyne causes effective suppression of tumor growth. Cancer Lett 205:39–48
114. Igarashi A, Konno H, Tanaka T, Nakamura S, Sadzuka Y, Hirano T, Fujise Y (2003) Liposomal photofrin enhances therapeutic efficacy of photodynamic therapy against the human gastric cancer. Toxicol Lett 145:133–141
115. Iinuma H, Maruyama K, Okinaga K, Sasaki K, Sekine T, Ishida O, Ogiwara N, Johkura K, Yonemura Y (2002) Intracellular targeting therapy of cisplatin-encapsulated transferrin-polyethylene glycol liposome on peritoneal dissemination of gastric cancer. Int J Cancer 99:130–137
116. Ishida O, Maruyama K, Tanahashi H, Iwatsuru M, Sasaki K, Eriguchi M, Yanagie H (2001) Liposomes bearing polyethyleneglycol-coupled transferrin with intracellular targeting property to the solid tumors in vivo. Pharm Res 18:1042–1048
117. Iwanaga K, Ono S, Narioka K, Kakemi M, Morimoto K, Yamashita S, Namba Y, Oku N (1999) Application of surface-coated liposomes for oral delivery of peptide: effects of coating the liposome's surface on the GI transit of insulin. J Pharm Sci 88:248–252
118. Jayanna PK, Torchilin VP, Petrenko VA (2009) Liposomes targeted by fusion phage proteins. Nanomedicine 5:83–89
119. Jehn CF, Boulikas T, Kourvetaris A, Possinger K, Luftner D (2007) Pharmacokinetics of liposomal cisplatin (lipoplatin) in combination with 5-FU in patients with advanced head and neck cancer: first results of a phase III study. Anticancer Res 27:471–475
120. Jezek P, Nekvasil M, Skobisova E, Urbankova E, Jirsa M, Zadinova M, Pouckova P, Klepacek I (2003) Experimental photodynamic therapy with MESO-tetrakisphenylporphyrin (TPP) in liposomes leads to disintegration of human amelanotic melanoma implanted to nude mice. Int J Cancer 103:693–702
121. Johnston SR, Gore ME (2001) Caelyx: phase II studies in ovarian cancer. Eur J Cancer 37 (Suppl 9):S8–S14
122. Jorge JC, Perez-Soler R, Morais JG, Cruz ME (1994) Liposomal palmitoyl-L-asparaginase: characterization and biological activity. Cancer Chemother Pharmacol 34:230–234
123. Joshee N, Bastola DR, Cheng PW (2002) Transferrin-facilitated lipofection gene delivery strategy: characterization of the transfection complexes and intracellular trafficking. Hum Gene Ther 13:1991–2004
124. Kakudo T, Chaki S, Futaki S, Nakase I, Akaji K, Kawakami T, Maruyama K, Kamiya H, Harashima H (2004) Transferrin-modified liposomes equipped with a pH-sensitive fusogenic peptide: an artificial viral-like delivery system. Biochemistry 43:5618–5628
125. Kale AA, Torchilin VP (2007) Design, synthesis, and characterization of pH-sensitive PEG-PE conjugates for stimuli-sensitive pharmaceutical nanocarriers: the effect of substitutes at the hydrazone linkage on the pH stability of PEG-PE conjugates. Bioconjug Chem 18:363–370
126. Kale AA, Torchilin VP (2007) Enhanced transfection of tumor cells in vivo using "Smart" pH-sensitive TAT-modified pegylated liposomes. J Drug Target 15:538–545
127. Kamps JA, Koning GA, Velinova MJ, Morselt HW, Wilkens M, Gorter A, Donga J, Scherphof GL (2000) Uptake of long-circulating immunoliposomes, directed against colon adenocarcinoma cells, by liver metastases of colon cancer. J Drug Target 8:235–245
128. Kanaoka E, Takahashi K, Yoshikawa T, Jizomoto H, Nishihara Y, Hirano K (2001) A novel and simple type of liposome carrier for recombinant interleukin-2. J Pharm Pharmacol 53:295–302
129. Karanth H, Murthy RS (2007) pH-sensitive liposomes–principle and application in cancer therapy. J Pharm Pharmacol 59:469–483
130. Kato A, Tanaka I, Arakawa M, Kondo T (1985) Liposome-type artificial red blood cells stabilized with carboxymethyl chitin. Biomater Med Devices Artif Organs 13:61–82

131. Kedar E, Palgi O, Golod G, Babai I, Barenholz Y (1997) Delivery of cytokines by liposomes. III. Liposome-encapsulated GM-CSF and TNF-alpha show improved pharmacokinetics and biological activity and reduced toxicity in mice. J Immunother 20:180–193
132. Kessner S, Krause A, Rothe U, Bendas G (2001) Investigation of the cellular uptake of E-Selectin-targeted immunoliposomes by activated human endothelial cells. Biochim Biophys Acta 1514:177–190
133. Khaw BA, daSilva J, Vural I, Narula J, Torchilin VP (2001) Intracytoplasmic gene delivery for in vitro transfection with cytoskeleton-specific immunoliposomes. J Control Release 75:199–210
134. Khaw BA, Torchilin VP, Vural I, Narula J (1995) Plug and seal: prevention of hypoxic cardiocyte death by sealing membrane lesions with antimyosin-liposomes. Nat Med 1:1195–1198
135. Kheirolomoom A, Dayton PA, Lum AF, Little E, Paoli EE, Zheng H, Ferrara KW (2007) Acoustically-active microbubbles conjugated to liposomes: characterization of a proposed drug delivery vehicle. J Control Release 118:275–284
136. Khoury M, Louis-Plence P, Escriou V, Noel D, Largeau C, Cantos C, Scherman D, Jorgensen C, Apparailly F (2006) Efficient new cationic liposome formulation for systemic delivery of small interfering RNA silencing tumor necrosis factor alpha in experimental arthritis. Arthritis Rheum 54:1867–1877
137. Kim CK, Han JH (1995) Lymphatic delivery and pharmacokinetics of methotrexate after intramuscular injection of differently charged liposome-entrapped methotrexate to rats. J Microencapsul 12:437–446
138. Kim ES, Lu C, Khuri FR, Tonda M, Glisson BS, Liu D, Jung M, Hong WK, Herbst RS (2001) A phase II study of STEALTH cisplatin (SPI-77) in patients with advanced non-small cell lung cancer. Lung Cancer 34:427–432
139. Kirpotin D, Park JW, Hong K, Zalipsky S, Li WL, Carter P, Benz CC, Papahadjopoulos D (1997) Sterically stabilized anti-HER2 immunoliposomes: design and targeting to human breast cancer cells in vitro. Biochemistry 36:66–75
140. Kirpotin DB, Drummond DC, Shao Y, Shalaby MR, Hong K, Nielsen UB, Marks JD, Benz CC, Park JW (2006) Antibody targeting of long-circulating lipidic nanoparticles does not increase tumor localization but does increase internalization in animal models. Cancer Res 66:6732–6740
141. Kisel MA, Kulik LN, Tsybovsky IS, Vlasov AP, Vorob'yov MS, Kholodova EA, Zabarovskaya ZV (2001) Liposomes with phosphatidylethanol as a carrier for oral delivery of insulin: studies in the rat. Int J Pharm 216:105–114
142. Kleinerman ES, Gano JB, Johnston DA, Benjamin RS, Jaffe N (1995) Efficacy of liposomal muramyl tripeptide (CGP 19835A) in the treatment of relapsed osteosarcoma. Am J Clin Oncol 18:93–99
143. Klibanov AL, Maruyama K, Torchilin VP, Huang L (1990) Amphipathic polyethyleneglycols effectively prolong the circulation time of liposomes. FEBS Lett 268:235–237
144. Klibanov AL, Torchilin VP, Zalipsky S (2003) Long-circulating sterically protected liposomes. In: Torchilin VP, Weissig V (eds) Liposomes: a practical approach, 2nd edn. Oxford University Press, New York, pp 231–265
145. Konduri KS, Nandedkar S, Duzgunes N, Suzara V, Artwohl J, Bunte R, Gangadharam PR (2003) Efficacy of liposomal budesonide in experimental asthma. J Allergy Clin Immunol 111:321–327
146. Koning GA, Gorter A, Scherphof GL, Kamps JA (1999) Antiproliferative effect of immunoliposomes containing 5-fluorodeoxyuridine-dipalmitate on colon cancer cells. Br J Cancer 80:1718–1725
147. Konno H, Matin AF, Maruo Y, Nakamura S, Baba S (1996) Liposomal ATP protects the liver from injury during shock. Eur Surg Res 28:140–145
148. Koshkina NV, Golunski E, Roberts LE, Gilbert BE, Knight V (2004) Cyclosporin A aerosol improves the anticancer effect of paclitaxel aerosol in mice. J Aerosol Med 17:7–14

149. Koshkina NV, Kleinerman ES, Waidrep C, Jia SF, Worth LL, Gilbert BE, Knight V (2000) 9-Nitrocamptothecin liposome aerosol treatment of melanoma and osteosarcoma lung metastases in mice. Clin Cancer Res 6:2876–2880
150. Kubo T, Sugita T, Shimose S, Nitta Y, Ikuta Y, Murakami T (2001) Targeted systemic chemotherapy using magnetic liposomes with incorporated adriamycin for osteosarcoma in hamsters. Int J Oncol 18:121–125
151. Laham A, Claperon N, Durussel JJ, Fattal E, Delattre J, Puisieux F, Couvreur P, Rossignol P (1988) Liposomally entrapped adenosine triphosphate. Improved efficiency against experimental brain ischaemia in the rat. J Chromatogr 440:455–458
152. Landen CN, Merritt WM, Mangala LS, Sanguino AM, Bucana C, Lu C, Lin YG, Han LY, Kamat AA, Schmandt R, Coleman RL, Gershenson DM, Lopez-Berestein G, Sood AK (2006) Intraperitoneal delivery of liposomal siRNA for therapy of advanced ovarian cancer. Cancer Biol Ther 5:1708–1713
153. Lange CF, Hancock RE, Samuel J, Finlay WH (2001) In vitro aerosol delivery and regional airway surface liquid concentration of a liposomal cationic peptide. J Pharm Sci 90:1647–1657
154. Lanternier F, Lortholary O (2008) Liposomal amphotericin B: what is its role in 2008? Clin Microbiol Infect 14(Suppl 4):71–83
155. Lasic DD, Martin FJ (1995) Stealth liposomes. CRC, Boca Raton, p 320
156. Lasic DD, Papahadjopoulos D (1998) Medical applications of liposomes. Elsevier, Amsterdam, p xiv, 79
157. Lasic DD, Vallner JJ, Working PK (1999) Sterically stabilized liposomes in cancer therapy and gene delivery. Curr Opin Mol Ther 1:177–185
158. Law SL, Shih CL (2001) Characterization of calcitonin-containing liposome formulations for intranasal delivery. J Microencapsul 18:211–221
159. Leamon CP, Cooper SR, Hardee GE (2003) Folate-liposome-mediated antisense oligodeoxynucleotide targeting to cancer cells: evaluation in vitro and in vivo. Bioconjug Chem 14:738–747
160. Leamon CP, Low PS (1991) Delivery of macromolecules into living cells: a method that exploits folate receptor endocytosis. Proc Natl Acad Sci U S A 88:5572–5576
161. Lee CM, Tanaka T, Murai T, Kondo M, Kimura J, Su W, Kitagawa T, Ito T, Matsuda H, Miyasaka M (2002) Novel chondroitin sulfate-binding cationic liposomes loaded with cisplatin efficiently suppress the local growth and liver metastasis of tumor cells in vivo. Cancer Res 62:4282–4288
162. Lee RJ, Low PS (1994) Delivery of liposomes into cultured KB cells via folate receptor-mediated endocytosis. J Biol Chem 269:3198–3204
163. Li H, Song JH, Park JS, Han K (2003) Polyethylene glycol-coated liposomes for oral delivery of recombinant human epidermal growth factor. Int J Pharm 258:11–19
164. Liang W, Levchenko T, Khaw BA, Torchilin V (2004) ATP-containing immunoliposomes specific for cardiac myosin. Curr Drug Deliv 1:1–7
165. Lo YL, Tsai JC, Kuo JH (2004) Liposomes and disaccharides as carriers in spray-dried powder formulations of superoxide dismutase. J Control Release 94:259–272
166. Lokling KE, Fossheim SL, Klaveness J, Skurtveit R (2004) Biodistribution of pH-responsive liposomes for MRI and a novel approach to improve the pH-responsiveness. J Control Release 98:87–95
167. Lopes de Menezes DE, Pilarski LM, Allen TM (1998) In vitro and in vivo targeting of immunoliposomal doxorubicin to human B-cell lymphoma. Cancer Res 58:3320–3330
168. Lopes de Menezes DE, Pilarski LM, Belch AR, Allen TM (2000) Selective targeting of immunoliposomal doxorubicin against human multiple myeloma in vitro and ex vivo. Biochim Biophys Acta 1466:205–220
169. Lu Y, Low PS (2002) Folate-mediated delivery of macromolecular anticancer therapeutic agents. Adv Drug Deliv Rev 54:675–693
170. Lu Y, Low PS (2002) Folate targeting of haptens to cancer cell surfaces mediates immunotherapy of syngeneic murine tumors. Cancer Immunol Immunother 51:153–162

171. Ludewig B, Barchiesi F, Pericin M, Zinkernagel RM, Hengartner H, Schwendener RA (2000) In vivo antigen loading and activation of dendritic cells via a liposomal peptide vaccine mediates protective antiviral and anti-tumour immunity. Vaccine 19:23–32
172. Lukyanov AN, Elbayoumi TA, Chakilam AR, Torchilin VP (2004) Tumor-targeted liposomes: doxorubicin-loaded long-circulating liposomes modified with anti-cancer antibody. J Control Release 100:135–144
173. Lundberg BB, Griffiths G, Hansen HJ (2007) Cellular association and cytotoxicity of doxorubicin-loaded immunoliposomes targeted via Fab' fragments of an anti-CD74 antibody. Drug Deliv 14:171–175
174. Madden TD, Bally MB, Hope MJ, Cullis PR, Schieren HP, Janoff AS (1985) Protection of large unilamellar vesicles by trehalose during dehydration: retention of vesicle contents. Biochim Biophys Acta 817:67–74
175. Maeda H, Sawa T, Konno T (2001) Mechanism of tumor-targeted delivery of macromolecular drugs, including the EPR effect in solid tumor and clinical overview of the prototype polymeric drug SMANCS. J Control Release 74:47–61
176. Mamot C, Drummond DC, Greiser U, Hong K, Kirpotin DB, Marks JD, Park JW (2003) Epidermal growth factor receptor (EGFR)-targeted immunoliposomes mediate specific and efficient drug delivery to EGFR- and EGFRvIII-overexpressing tumor cells. Cancer Res 63:3154–3161
177. Mamot C, Drummond DC, Noble CO, Kallab V, Guo Z, Hong K, Kirpotin DB, Park JW (2005) Epidermal growth factor receptor-targeted immunoliposomes significantly enhance the efficacy of multiple anticancer drugs in vivo. Cancer Res 65:11631–11638
178. Mamot C, Ritschard R, Kung W, Park JW, Herrmann R, Rochlitz CF (2006) EGFR-targeted immunoliposomes derived from the monoclonal antibody EMD72000 mediate specific and efficient drug delivery to a variety of colorectal cancer cells. J Drug Target 14:215–223
179. Manesis EK, Cameron CH, Gregoriadis G (1979) Hepatitis B surface antigen-containing liposomes enhance humoral and cell-mediated immunity to the antigen. FEBS Lett 102:107–111
180. Marty C, Odermatt B, Schott H, Neri D, Ballmer-Hofer K, Klemenz R, Schwendener RA (2002) Cytotoxic targeting of F9 teratocarcinoma tumours with anti-ED-B fibronectin scFv antibody modified liposomes. Br J Cancer 87:106–112
181. Maruyama K (2000) In vivo targeting by liposomes. Biol Pharm Bull 23:791–799
182. Mastrobattista E, Koning GA, van Bloois L, Filipe AC, Jiskoot W, Storm G (2002) Functional characterization of an endosome-disruptive peptide and its application in cytosolic delivery of immunoliposome-entrapped proteins. J Biol Chem 277:27135–27143
183. Masuda K, Horie K, Suzuki R, Yoshikawa T, Hirano K (2002) Oral delivery of antigens in liposomes with some lipid compositions modulates oral tolerance to the antigens. Microbiol Immunol 46:55–58
184. Matsuura M, Yamazaki Y, Sugiyama M, Kondo M, Ori H, Nango M, Oku N (2003) Polycation liposome-mediated gene transfer in vivo. Biochim Biophys Acta 1612:136–143
185. Metselaar JM, Bruin P, de Boer LW, de Vringer T, Snel C, Oussoren C, Wauben MH, Crommelin DJ, Storm G, Hennink WE (2003) A novel family of L-amino acid-based biodegradable polymer-lipid conjugates for the development of long-circulating liposomes with effective drug-targeting capacity. Bioconjug Chem 14:1156–1164
186. Minato S, Iwanaga K, Kakemi M, Yamashita S, Oku N (2003) Application of polyethyleneglycol (PEG)-modified liposomes for oral vaccine: effect of lipid dose on systemic and mucosal immunity. J Control Release 89:189–197
187. Moein Moghimi S, Hamad I, Bunger R, Andresen TL, Jorgensen K, Hunter AC, Baranji L, Rosivall L, Szebeni J (2006) Activation of the human complement system by cholesterol-rich and PEGylated liposomes-modulation of cholesterol-rich liposome-mediated complement activation by elevated serum LDL and HDL levels. J Liposome Res 16:167–174

188. Moghimi SM, Szebeni J (2003) Stealth liposomes and long circulating nanoparticles: critical issues in pharmacokinetics, opsonization and protein-binding properties. Prog Lipid Res 42:463–478
189. Nam SM, Kim HS, Ahn WS, Park YS (1999) Sterically stabilized anti-G(M3), anti-Le(x) immunoliposomes: targeting to B16BL6, HRT-18 cancer cells. Oncol Res 11:9–16
190. Naoi M, Yagi K (1980) Incorporation of enzyme through blood-brainbarrier into the brain by means of liposomes. Biochem Int 1:591–596
191. Neveux N, De Bandt JP, Chaumeil JC, Cynober L (2002) Hepatic preservation, liposomally entrapped adenosine triphosphate and nitric oxide production: a study of energy state and protein metabolism in the cold-stored rat liver. Scand J Gastroenterol 37:1057–1063
192. Ni S, Stephenson SM, Lee RJ (2002) Folate receptor targeted delivery of liposomal daunorubicin into tumor cells. Anticancer Res 22:2131–2135
193. Niibori K, Wroblewski KP, Yokoyama H, Crestanello JA, Whitman GJ (1999) Bioenergetic effect of liposomal coenzyme Q10 on myocardial ischemia reperfusion injury. Biofactors 9:307–313
194. Nobuto H, Sugita T, Kubo T, Shimose S, Yasunaga Y, Murakami T, Ochi M (2004) Evaluation of systemic chemotherapy with magnetic liposomal doxorubicin and a dipole external electromagnet. Int J Cancer 109:627–635
195. O'Shaughnessy JA (2003) Pegylated liposomal doxorubicin in the treatment of breast cancer. Clin Breast Cancer 4:318–328
196. Omori N, Maruyama K, Jin G, Li F, Wang SJ, Hamakawa Y, Sato K, Nagano I, Shoji M, Abe K (2003) Targeting of post-ischemic cerebral endothelium in rat by liposomes bearing polyethylene glycol-coupled transferrin. Neurol Res 25:275–279
197. Opanasopit P, Sakai M, Nishikawa M, Kawakami S, Yamashita F, Hashida M (2002) Inhibition of liver metastasis by targeting of immunomodulators using mannosylated liposome carriers. J Control Release 80:283–294
198. Oussoren C, Storm G (2001) Liposomes to target the lymphatics by subcutaneous administration. Adv Drug Deliv Rev 50:143–156
199. Pagnan G, Montaldo PG, Pastorino F, Raffaghello L, Kirchmeier M, Allen TM, Ponzoni M (1999) GD2-mediated melanoma cell targeting and cytotoxicity of liposome-entrapped fenretinide. Int J Cancer 81:268–274
200. Pan H, Han L, Chen W, Yao M, Lu W (2008) Targeting to tumor necrotic regions with biotinylated antibody and streptavidin modified liposomes. J Control Release 125:228–235
201. Pan XQ, Wang H, Lee RJ (2003) Antitumor activity of folate receptor-targeted liposomal doxorubicin in a KB oral carcinoma murine xenograft model. Pharm Res 20:417–422
202. Pan XQ, Zheng X, Shi G, Wang H, Ratnam M, Lee RJ (2002) Strategy for the treatment of acute myelogenous leukemia based on folate receptor beta-targeted liposomal doxorubicin combined with receptor induction using all-trans retinoic acid. Blood 100:594–602
203. Pappalardo JS, Quattrocchi V, Langellotti C, Di Giacomo S, Gnazzo V, Olivera V, Calamante G, Zamorano PI, Levchenko TS, Torchilin VP (2009) Improved transfection of spleen-derived antigen-presenting cells in culture using TATp-liposomes. J Control Release 134:41–46
204. Park JW, Hong K, Kirpotin DB, Colbern G, Shalaby R, Baselga J, Shao Y, Nielsen UB, Marks JD, Moore D, Papahadjopoulos D, Benz CC (2002) Anti-HER2 immunoliposomes: enhanced efficacy attributable to targeted delivery. Clin Cancer Res 8:1172–1181
205. Park JW, Kirpotin DB, Hong K, Shalaby R, Shao Y, Nielsen UB, Marks JD, Papahadjopoulos D, Benz CC (2001) Tumor targeting using anti-her2 immunoliposomes. J Control Release 74:95–113
206. Pastorino F, Brignole C, Marimpietri D, Sapra P, Moase EH, Allen TM, Ponzoni M (2003) Doxorubicin-loaded Fab' fragments of anti-disialoganglioside immunoliposomes selectively inhibit the growth and dissemination of human neuroblastoma in nude mice. Cancer Res 63:86–92

207. Patel HM, Ryman BE (1974) α-Mannosidase in zinc-deficient rats. Possibility of liposomal therapy in mannosidosis. Biochem Soc Trans 2:1014–1017
208. Patel NR, Hatziantoniou S, Georgopoulos A, Demetzos C, Torchilin VP, Weissig V, D'Souza GG (2010) Mitochondria-targeted liposomes improve the apoptotic and cytotoxic action of sclareol. J Liposome Res 20(3):244–249
209. Peer D, Margalit R (2004) Loading mitomycin C inside long circulating hyaluronan targeted nano-liposomes increases its antitumor activity in three mice tumor models. Int J Cancer 108:780–789
210. Perez-Lopez ME, Curiel T, Gomez JG, Jorge M (2007) Role of pegylated liposomal doxorubicin (Caelyx) in the treatment of relapsing ovarian cancer. Anticancer Drugs 18:611–617
211. Perez AT, Domenech GH, Frankel C, Vogel CL (2002) Pegylated liposomal doxorubicin (Doxil) for metastatic breast cancer: the Cancer Research Network, Inc., experience. Cancer Invest 20(Suppl 2):22–29
212. Phillips WT, Klipper RW, Awasthi VD, Rudolph AS, Cliff R, Kwasiborski V, Goins BA (1999) Polyethylene glycol-modified liposome-encapsulated hemoglobin: a long circulating red cell substitute. J Pharmacol Exp Ther 288:665–670
213. Plassat V, Martina MS, Barratt G, Menager C, Lesieur S (2007) Sterically stabilized superparamagnetic liposomes for MR imaging and cancer therapy: pharmacokinetics and biodistribution. Int J Pharm 344:118–127
214. Postma NS, Crommelin DJ, Eling WM, Zuidema J (1999) Treatment with liposome-bound recombinant human tumor necrosis factor-alpha suppresses parasitemia and protects against Plasmodium berghei k173-induced experimental cerebral malaria in mice. J Pharmacol Exp Ther 288:114–120
215. Raffaghello L, Pagnan G, Pastorino F, Cosimo E, Brignole C, Marimpietri D, Bogenmann E, Ponzoni M, Montaldo PG (2003) Immunoliposomal fenretinide: a novel antitumoral drug for human neuroblastoma. Cancer Lett 197:151–155
216. Rao M, Alving CR (2000) Delivery of lipids and liposomal proteins to the cytoplasm and Golgi of antigen-presenting cells. mangala.rao@na.amedd.army.mil. Adv Drug Deliv Rev 41:171–188
217. Reddy JA, Abburi C, Hofland H, Howard SJ, Vlahov I, Wils P, Leamon CP (2002) Folate-targeted, cationic liposome-mediated gene transfer into disseminated peritoneal tumors. Gene Ther 9:1542–1550
218. Reynolds GC, Baker HJ, Reynolds RH (1978) Enzyme replacement using liposome carriers in feline Gm1 gangliosidosis fibroblasts. Nature 275:754–755
219. Rogers JA, Anderson KE (1998) The potential of liposomes in oral drug delivery. Crit Rev Ther Drug Carrier Syst 15:421–480
220. Rothbard JB, Jessop TC, Lewis RS, Murray BA, Wender PA (2004) Role of membrane potential and hydrogen bonding in the mechanism of translocation of guanidinium-rich peptides into cells. J Am Chem Soc 126:9506–9507
221. Roux E, Passirani C, Scheffold S, Benoit JP, Leroux JC (2004) Serum-stable and long-circulating, PEGylated, pH-sensitive liposomes. J Control Release 94:447–451
222. Ruozi B, Battini R, Montanari M, Mucci A, Tosi G, Forni F, Vandelli MA (2007) DOTAP/UDCA vesicles: novel approach in oligonucleotide delivery. Nanomedicine 3:1–13
223. Sachse A, Leike JU, Rossling GL, Wagner SE, Krause W (1993) Preparation and evaluation of lyophilized iopromide-carrying liposomes for liver tumor detection. Invest Radiol 28:838–844
224. Sachse A, Leike JU, Schneider T, Wagner SE, Rossling GL, Krause W, Brandl M (1997) Biodistribution and computed tomography blood-pool imaging properties of polyethylene glycol-coated iopromide-carrying liposomes. Invest Radiol 32:44–50
225. Safinya CR (2001) Structures of lipid-DNA complexes: supramolecular assembly and gene delivery. Curr Opin Struct Biol 11:440–448

226. Sakai H, Masada Y, Horinouchi H, Yamamoto M, Ikeda E, Takeoka S, Kobayashi K, Tsuchida E (2004) Hemoglobin-vesicles suspended in recombinant human serum albumin for resuscitation from hemorrhagic shock in anesthetized rats. Crit Care Med 32:539–545
227. Sakai H, Tomiyama KI, Sou K, Takeoka S, Tsuchida E (2000) Poly(ethylene glycol)-conjugation and deoxygenation enable long-term preservation of hemoglobin-vesicles as oxygen carriers in a liquid state. Bioconjug Chem 11:425–432
228. Sakai H, Tsai AG, Rohlfs RJ, Hara H, Takeoka S, Tsuchida E, Intaglietta M (1999) Microvascular responses to hemodilution with Hb vesicles as red blood cell substitutes: influence of O2 affinity. Am J Physiol 276:H553–H562
229. Sanchez Y, Ionescu-Matiu I, Dreesman GR, Kramp W, Six HR, Hollinger FB, Melnick JL (1980) Humoral and cellular immunity to hepatitis B virus-derived antigens: comparative activity of Freund complete adjuvant alum, and liposomes. Infect Immun 30:728–733
230. Sangha R, Butts C (2007) L-BLP25: a peptide vaccine strategy in non small cell lung cancer. Clin Cancer Res 13:s4652–s4654
231. Sapra P, Allen TM (2002) Internalizing antibodies are necessary for improved therapeutic efficacy of antibody-targeted liposomal drugs. Cancer Res 62:7190–7194
232. Sapra P, Allen TM (2004) Improved outcome when B-cell lymphoma is treated with combinations of immunoliposomal anticancer drugs targeted to both the CD19 and CD20 epitopes. Clin Cancer Res 10:2530–2537
233. Sarris AH, Hagemeister F, Romaguera J, Rodriguez MA, McLaughlin P, Tsimberidou AM, Medeiros LJ, Samuels B, Pate O, Oholendt M, Kantarjian H, Burge C, Cabanillas F (2000) Liposomal vincristine in relapsed non-Hodgkin's lymphomas: early results of an ongoing phase II trial. Ann Oncol 11:69–72
234. Sato A, Takagi M, Shimamoto A, Kawakami S, Hashida M (2007) Small interfering RNA delivery to the liver by intravenous administration of galactosylated cationic liposomes in mice. Biomaterials 28:1434–1442
235. Sawant RM, Hurley JP, Salmaso S, Kale A, Tolcheva E, Levchenko TS, Torchilin VP (2006) "SMART" drug delivery systems: double-targeted pH-responsive pharmaceutical nanocarriers. Bioconjug Chem 17:943–949
236. Schiffelers RM, Koning GA, ten Hagen TL, Fens MH, Schraa AJ, Janssen AP, Kok RJ, Molema G, Storm G (2003) Anti-tumor efficacy of tumor vasculature-targeted liposomal doxorubicin. J Control Release 91:115–122
237. Schmidinger M, Wenzel C, Locker GJ, Muehlbacher F, Steininger R, Gnant M, Crevenna R, Budinsky AC (2001) Pilot study with pegylated liposomal doxorubicin for advanced or unresectable hepatocellular carcinoma. Br J Cancer 85:1850–1852
238. Schnyder A, Krahenbuhl S, Drewe J, Huwyler J (2005) Targeting of daunomycin using biotinylated immunoliposomes: pharmacokinetics, tissue distribution and in vitro pharmacological effects. J Drug Target 13:325–335
239. Schroeder A, Avnir Y, Weisman S, Najajreh Y, Gabizon A, Talmon Y, Kost J, Barenholz Y (2007) Controlling liposomal drug release with low frequency ultrasound: mechanism and feasibility. Langmuir 23:4019–4025
240. Schwonzen M, Kurbacher CM, Mallmann P (2000) Liposomal doxorubicin and weekly paclitaxel in the treatment of metastatic breast cancer. Anticancer Drugs 11:681–685
241. Scott RC, Wang B, Nallamothu R, Pattillo CB, Perez-Liz G, Issekutz A, Valle LD, Wood GC, Kiani MF (2007) Targeted delivery of antibody conjugated liposomal drug carriers to rat myocardial infarction. Biotechnol Bioeng 96:795–802
242. Seiden MV, Muggia F, Astrow A, Matulonis U, Campos S, Roche M, Sivret J, Rusk J, Barrett E (2004) A phase II study of liposomal lurtotecan (OSI-211) in patients with topotecan resistant ovarian cancer. Gynecol Oncol 93:229–232
243. Selzman CH, Shames BD, Reznikov LL, Miller SA, Meng X, Barton HA, Werman A, Harken AH, Dinarello CA, Banerjee A (1999) Liposomal delivery of purified inhibitory-kappaBalpha inhibits tumor necrosis factor-alpha-induced human vascular smooth muscle proliferation. Circ Res 84:867–875

244. Senior JH (1987) Fate and behavior of liposomes in vivo: a review of controlling factors. Crit Rev Ther Drug Carrier Syst 3:123–193
245. Senter PD, Saulnier MG, Schreiber GJ, Hirschberg DL, Brown JP, Hellstrom I, Hellstrom KE (1988) Anti-tumor effects of antibody-alkaline phosphatase conjugates in combination with etoposide phosphate. Proc Natl Acad Sci U S A 85:4842–4846
246. Shibuya-Fujiwara N, Hirayama F, Ogata Y, Ikeda H, Ikebuchi K (2001) Phagocytosis in vitro of polyethylene glycol-modified liposome-encapsulated hemoglobin by human peripheral blood monocytes plus macrophages through scavenger receptors. Life Sci 70:291–300
247. Simoes S, Moreira JN, Fonseca C, Duzgunes N, de Lima MC (2004) On the formulation of pH-sensitive liposomes with long circulation times. Adv Drug Deliv Rev 56:947–965
248. Sinha RK, Khuller GK (1997) The protective efficacy of a liposomal encapsulated 30 kDa secretory protein of Mycobacterium tuberculosis H37Ra against tuberculosis in mice. Immunol Cell Biol 75:461–466
249. Sioud M, Sorensen DR (2003) Cationic liposome-mediated delivery of siRNAs in adult mice. Biochem Biophys Res Commun 312:1220–1225
250. Skubitz KM (2003) Phase II trial of pegylated-liposomal doxorubicin (Doxil) in sarcoma. Cancer Invest 21:167–176
251. Sofou S (2007) Surface-active liposomes for targeted cancer therapy. Nanomed 2:711–724
252. Sofou S, Sgouros G (2008) Antibody-targeted liposomes in cancer therapy and imaging. Expert Opin Drug Deliv 5:189–204
253. Stanimirovic DB, Markovic M, Micic DV, Spatz M, Mrsulja BB (1994) Liposome-entrapped superoxide dismutase reduces ischemia/reperfusion 'oxidative stress' in gerbil brain. Neurochem Res 19:1473–1478
254. Steele G Jr, Ravikumar T, Ross D, King V, Wilson RE, Dodson T (1984) Specific active immunotherapy with butanol-extracted, tumor-associated antigens incorporated into liposomes. Surgery 96:352–359
255. Steger LD, Desnick RJ (1977) Enzyme therapy. VI: Comparative in vivo fates and effects on lysosomal integrity of enzyme entrapped in negatively and positively charged liposomes. Biochim Biophys Acta 464:530–546
256. Stephenson SM, Yang W, Stevens PJ, Tjarks W, Barth RF, Lee RJ (2003) Folate receptor-targeted liposomes as possible delivery vehicles for boron neutron capture therapy. Anticancer Res 23:3341–3345
257. Storm G, Vingerhoeds MH, Crommelin DJA, Haisma HJ (1997) Immunoliposomes bearing enzymes (immuno-enzymosomes) for site-specific activation of anticancer prodrugs. Adv Drug Del Rev 24:225–231, 227
258. Sudimack JJ, Guo W, Tjarks W, Lee RJ (2002) A novel pH-sensitive liposome formulation containing oleyl alcohol. Biochim Biophys Acta 1564:31–37
259. Sugano M, Egilmez NK, Yokota SJ, Chen FA, Harding J, Huang SK, Bankert RB (2000) Antibody targeting of doxorubicin-loaded liposomes suppresses the growth and metastatic spread of established human lung tumor xenografts in severe combined immunodeficient mice. Cancer Res 60:6942–6949
260. Sundar S, Jha TK, Thakur CP, Mishra M, Singh VP, Buffels R (2003) Single-dose liposomal amphotericin B in the treatment of visceral leishmaniasis in India: a multicenter study. Clin Infect Dis 37:800–804
261. Symon Z, Peyser A, Tzemach D, Lyass O, Sucher E, Shezen E, Gabizon A (1999) Selective delivery of doxorubicin to patients with breast carcinoma metastases by stealth liposomes. Cancer 86:72–78
262. Szebeni J, Alving CR (1999) Complement-mediated acute effects of liposome-encapsulated hemoglobin. Artif Cells Blood Substit Immobil Biotechnol 27:23–41
263. Szebeni J, Di Iorio EE, Hauser H, Winterhalter KH (1985) Encapsulation of hemoglobin in phospholipid liposomes: characterization and stability. Biochemistry 24:2827–2832
264. Szebeni J, Fontana JL, Wassef NM, Mongan PD, Morse DS, Dobbins DE, Stahl GL, Bunger R, Alving CR (1999) Hemodynamic changes induced by liposomes and liposome-encapsulated

hemoglobin in pigs: a model for pseudoallergic cardiopulmonary reactions to liposomes. Role of complement and inhibition by soluble CR1 and anti-C5a antibody. Circulation 99:2302–2309
265. Szoka F Jr, Papahadjopoulos D (1980) Comparative properties and methods of preparation of lipid vesicles (liposomes). Annu Rev Biophys Bioeng 9:467–508
266. Taira MC, Chiaramoni NS, Pecuch KM, Alonso-Romanowski S (2004) Stability of liposomal formulations in physiological conditions for oral drug delivery. Drug Deliv 11:123–128
267. Takeuchi H, Kojima H, Yamamoto H, Kawashima Y (2001) Evaluation of circulation profiles of liposomes coated with hydrophilic polymers having different molecular weights in rats. J Control Release 75:83–91
268. Takeuchi H, Yamamoto H, Kawashima Y (2001) Mucoadhesive nanoparticulate systems for peptide drug delivery. Adv Drug Deliv Rev 47:39–54
269. Takeuchi H, Yamamoto H, Niwa T, Hino T, Kawashima Y (1996) Enteral absorption of insulin in rats from mucoadhesive chitosan-coated liposomes. Pharm Res 13:896–901
270. Takeuchi Y, Ichikawa K, Yonezawa S, Kurohane K, Koishi T, Nango M, Namba Y, Oku N (2004) Intracellular target for photosensitization in cancer antiangiogenic photodynamic therapy mediated by polycation liposome. J Control Release 97:231–240
271. Tan PH, Manunta M, Ardjomand N, Xue SA, Larkin DF, Haskard DO, Taylor KM, George AJ (2003) Antibody targeted gene transfer to endothelium. J Gene Med 5:311–323
272. Tardi P, Johnstone S, Harasym N, Xie S, Harasym T, Zisman N, Harvie P, Bermudes D, Mayer L (2009) In vivo maintenance of synergistic cytarabine:daunorubicin ratios greatly enhances therapeutic efficacy. Leuk Res 33:129–139
273. Templeton NS (2002) Cationic liposome-mediated gene delivery in vivo. Biosci Rep 22:283–295
274. Terada T, Mizobata M, Kawakami S, Yamashita F, Hashida M (2007) Optimization of tumor-selective targeting by basic fibroblast growth factor-binding peptide grafted PEGylated liposomes. J Control Release 119:262–270
275. Tilcock C (1995) Imaging tools: liposomal agents for nuclear medicine, computed tomography, magnetic resonance, and ultrasound. In: Philippot JR, Schuber F (eds) Liposomes as tools in basic research and industry. CRC, Boca Raton, pp 225–240
276. Torchilin V (2008) Antibody-modified liposomes for cancer chemotherapy. Expert Opin Drug Deliv 5:1003–1025
277. Torchilin VP (1985) Liposomes as targetable drug carriers. Crit Rev Ther Drug Carrier Syst 2:65–115
278. Torchilin VP (1996) Liposomes as delivery agents for medical imaging. Mol Med Today 2:242–249
279. Torchilin VP (1997) Surface-modified liposomes in gamma- and MR-imaging. Adv Drug Deliv Rev 24:301–313
280. Torchilin VP (2000) Polymeric contrast agents for medical imaging. Curr Pharm Biotechnol 1:183–215
281. Torchilin VP (2005) Liposomal delivery of protein and peptide drugs. In: Mahato RI (ed) Biomaterials for delivery and targeting of proteins and nucleic acids, chapter 14. CRC, Boca Raton, pp 433–459
282. Torchilin VP, Klibanov AL, Huang L, O'Donnell S, Nossiff ND, Khaw BA (1992) Targeted accumulation of polyethylene glycol-coated immunoliposomes in infarcted rabbit myocardium. FASEB J 6:2716–2719
283. Torchilin VP, Levchenko TS (2003) TAT-liposomes: a novel intracellular drug carrier. Curr Protein Pept Sci 4:133–140
284. Torchilin VP, Levchenko TS, Lukyanov AN, Khaw BA, Klibanov AL, Rammohan R, Samokhin GP, Whiteman KR (2001) p-Nitrophenylcarbonyl-PEG-PE-liposomes: fast and simple attachment of specific ligands, including monoclonal antibodies, to distal ends of PEG chains via p-nitrophenylcarbonyl groups. Biochim Biophys Acta 1511:397–411

285. Torchilin VP, Levchenko TS, Rammohan R, Volodina N, Papahadjopoulos-Sternberg B, D'Souza GG (2003) Cell transfection in vitro and in vivo with nontoxic TAT peptide-liposome-DNA complexes. Proc Natl Acad Sci U S A 100:1972–1977
286. Torchilin VP, Levchenko TS, Whiteman KR, Yaroslavov AA, Tsatsakis AM, Rizos AK, Michailova EV, Shtilman MI (2001) Amphiphilic poly-N-vinylpyrrolidones: synthesis, properties and liposome surface modification. Biomaterials 22:3035–3044
287. Torchilin VP, Rammohan R, Weissig V, Levchenko TS (2001) TAT peptide on the surface of liposomes affords their efficient intracellular delivery even at low temperature and in the presence of metabolic inhibitors. Proc Natl Acad Sci U S A 98:8786–8791
288. Torchilin VP, Trubetskoy VS (1995) Which polymers can make nanoparticulate drug carriers long-circulating? Adv Drug Deliv Rev 16:141–155
289. Torchilin VP, Weissig V (2003) Liposomes: a practical approach. Practical approach series; 264, 2nd edn. Oxford University Press, New York, p xxiii
290. Torchilin VP, Weissig V, Martin FJ, Heath TD, Ne RRC (2003) Surface modifications of liposomes. In: Torchilin VP, Weissig V (eds) Liposomes: a practical approach, 2nd edn. Oxford University Press, New York, pp 193–229
291. Trudel M, Nadon F (1981) Virosome preparation: differences between influenza and rubella hemagglutinin adsorption. Can J Microbiol 27:958–962
292. Tseng YL, Hong RL, Tao MH, Chang FH (1999) Sterically stabilized anti-idiotype immunoliposomes improve the therapeutic efficacy of doxorubicin in a murine B-cell lymphoma model. Int J Cancer 80:723–730
293. Tseng YL, Liu JJ, Hong RL (2002) Translocation of liposomes into cancer cells by cell-penetrating peptides penetratin and tat: a kinetic and efficacy study. Mol Pharmacol 62:864–872
294. Tsimberidou AM, Tirado-Gomez M, Andreeff M, O'Brien S, Kantarjian H, Keating M, Lopez-Berestein G, Estey E (2006) Single-agent liposomal all-trans retinoic acid can cure some patients with untreated acute promyelocytic leukemia: an update of The University of Texas M D. Anderson Cancer Center Series. Leuk Lymphoma 47:1062–1068
295. Tsuchida E, Hasegawa E, Matsushita Y, Eshima K, Yuasa M, Nishide H (1985) Polymerized liposome as the carrier of heme. A physically stable oxygen carrier under physiological conditions. Chem Lett 13:969–972
296. Tuffin G, Waelti E, Huwyler J, Hammer C, Marti HP (2005) Immunoliposome targeting to mesangial cells: a promising strategy for specific drug delivery to the kidney. J Am Soc Nephrol 16:3295–3305
297. Turk MJ, Reddy JA, Chmielewski JA, Low PS (2002) Characterization of a novel pH-sensitive peptide that enhances drug release from folate-targeted liposomes at endosomal pHs. Biochim Biophys Acta 1559:56–68
298. Umezawa F, Eto Y, Tokoro T, Ito F, Maekawa K (1985) Enzyme replacement with liposomes containing beta-galactosidase from Charonia lumpas in murine globoid cell leukodystrophy (twitcher). Biochem Biophys Res Commun 127:663–667
299. van Winden EC (2003) Freeze-drying of liposomes: theory and practice. Methods Enzymol 367:99–110
300. Verma DD, Hartner WC, Levchenko TS, Bernstein EA, Torchilin VP (2005) ATP-loaded liposomes effectively protect the myocardium in rabbits with an acute experimental myocardial infarction. Pharm Res 22:2115–2120
301. Verma DD, Hartner WC, Thakkar V, Levchenko TS, Torchilin VP (2007) Protective effect of coenzyme Q10-loaded liposomes on the myocardium in rabbits with an acute experimental myocardial infarction. Pharm Res 24(11):2131–2137
302. Verma DD, Levchenk T, Bernstein EA, Torchilin V (2004) ATP-loaded liposomes effectively protect mechanical functions of the myocardium from global ischemia in an isolated rat heart model. In: 31st annual meeting of the Controlled Release Society, Honolulu 2004, Controlled Release Society, #572

303. Verma DD, Levchenko TS, Bernstein EA, Mongayt D, Torchilin VP (2006) ATP-loaded immunoliposomes specific for cardiac myosin provide improved protection of the mechanical functions of myocardium from global ischemia in an isolated rat heart model. J Drug Target 14:273–280
304. Verma DD, Verma S, Blume G, Fahr A (2003) Liposomes increase skin penetration of entrapped and non-entrapped hydrophilic substances into human skin: a skin penetration and confocal laser scanning microscopy study. Eur J Pharm Biopharm 55:271–277
305. Viglianti BL, Abraham SA, Michelich CR, Yarmolenko PS, MacFall JR, Bally MB, Dewhirst MW (2004) In vivo monitoring of tissue pharmacokinetics of liposome/drug using MRI: illustration of targeted delivery. Magn Reson Med 51:1153–1162
306. Vingerhoeds MH, Haisma HJ, Belliot SO, Smit RH, Crommelin DJ, Storm G (1996) Immunoliposomes as enzyme-carriers (immuno-enzymosomes) for antibody-directed enzyme prodrug therapy (ADEPT): optimization of prodrug activating capacity. Pharm Res 13:604–610
307. Vutla NB, Betageri GV, Banga AK (1996) Transdermal iontophoretic delivery of enkephalin formulated in liposomes. J Pharm Sci 85:5–8
308. Vyas SP, Kannan ME, Jain S, Mishra V, Singh P (2004) Design of liposomal aerosols for improved delivery of rifampicin to alveolar macrophages. Int J Pharm 269:37–49
309. Wadia JS, Stan RV, Dowdy SF (2004) Transducible TAT-HA fusogenic peptide enhances escape of TAT-fusion proteins after lipid raft macropinocytosis. Nat Med 10:310–315
310. Weissig VV, Babich J, Torchilin VV (2000) Long-circulating gadolinium-loaded liposomes: potential use for magnetic resonance imaging of the blood pool. Colloids Surf B Biointerfaces 18:293–299
311. Westcott KR, Hill RL (1985) Reconstitution of a porcine submaxillary gland beta-D-galactoside alpha 2–3 sialyltransferase into liposomes. J Biol Chem 260:13116–13121
312. Whiteman KR, Subr V, Ulbrich K, Torchilin VP (2001) Poly(HPMA)-coated liposomes demonstrate prolonged circulation in mice. J Liposome Res 11:153–164
313. Wollina U, Dummer R, Brockmeyer NH, Konrad H, Busch JO, Kaatz M, Knopf B, Koch HJ, Hauschild A (2003) Multicenter study of pegylated liposomal doxorubicin in patients with cutaneous T-cell lymphoma. Cancer 98:993–1001
314. Woodle MC (1998) Controlling liposome blood clearance by surface-grafted polymers. Adv Drug Deliv Rev 32:139–152
315. Woodle MC, Storm G (1998) Long circulating liposomes: old drugs, new therapeutics. Biotechnology intelligence unit. Springer, Berlin, 301 p
316. Wu ZH, Ping QN, Wei Y, Lai JM (2004) Hypoglycemic efficacy of chitosan-coated insulin liposomes after oral administration in mice. Acta Pharmacol Sin 25:966–972
317. Xu GX, Xie XH, Liu FY, Zang DL, Zheng DS, Huang DJ, Huang MX (1990) Adenosine triphosphate liposomes: encapsulation and distribution studies. Pharm Res 7:553–557
318. Xu L, Huang CC, Huang W, Tang WH, Rait A, Yin YZ, Cruz I, Xiang LM, Pirollo KF, Chang EH (2002) Systemic tumor-targeted gene delivery by anti-transferrin receptor scFv-immunoliposomes. Mol Cancer Ther 1:337–346
319. Yagi N, Naoi M, Sasaki H, Abe H, Konishi H, Arichi S (1982) Incorporation of enzyme into the brain by means of liposomes of novel composition. J Appl Biochem 4:121–125
320. Yamabe K, Kato Y, Onishi H, Machida Y (2003) Potentiality of double liposomes containing salmon calcitonin as an oral dosage form. J Control Release 89:429–436
321. Yang T, Choi MK, Cui FD, Kim JS, Chung SJ, Shim CK, Kim DD (2007) Preparation and evaluation of paclitaxel-loaded PEGylated immunoliposome. J Control Release 120:169–177
322. Yang T, Cui FD, Choi MK, Lin H, Chung SJ, Shim CK, Kim DD (2007) Liposome formulation of paclitaxel with enhanced solubility and stability. Drug Deliv 14:301–308
323. Yang TZ, Wang XT, Yan XY, Zhang Q (2002) Phospholipid deformable vesicles for buccal delivery of insulin. Chem Pharm Bull (Tokyo) 50:749–753

324. Yerushalmi N, Arad A, Margalit R (1994) Molecular and cellular studies of hyaluronic acid-modified liposomes as bioadhesive carriers for topical drug delivery in wound healing. Arch Biochem Biophys 313:267–273
325. Yoo GH, Hung MC, Lopez-Berestein G, LaFollette S, Ensley JF, Carey M, Batson E, Reynolds TC, Murray JL (2001) Phase I trial of intratumoral liposome E1A gene therapy in patients with recurrent breast and head and neck cancer. Clin Cancer Res 7:1237–1245
326. Yuan F, Leunig M, Huang SK, Berk DA, Papahadjopoulos D, Jain RK (1994) Microvascular permeability and interstitial penetration of sterically stabilized (stealth) liposomes in a human tumor xenograft. Cancer Res 54:3352–3356
327. Zajac-Kaye M, Ts'o PO (1984) DNAase I encapsulated in liposomes can induce neoplastic transformation of Syrian hamster embryo cells in culture. Cell 39:427–437
328. Zalipsky S, Qazen M, Walker JA 2nd, Mullah N, Quinn YP, Huang SK (1999) New detachable poly(ethylene glycol) conjugates: cysteine-cleavable lipopolymers regenerating natural phospholipid, diacyl phosphatidylethanolamine. Bioconjug Chem 10:703–707
329. Zaru M, Mourtas S, Klepetsanis P, Fadda AM, Antimisiaris SG (2007) Liposomes for drug delivery to the lungs by nebulization. Eur J Pharm Biopharm 67:655–666
330. Zhang C, Tang N, Liu X, Liang W, Xu W, Torchilin VP (2006) siRNA-containing liposomes modified with polyarginine effectively silence the targeted gene. J Control Release 112:229–239
331. Zheng J, Liu J, Dunne M, Jaffray DA, Allen C (2007) In vivo performance of a liposomal vascular contrast agent for CT and MR-based image guidance applications. Pharm Res 24:1193–1201
332. Zheng J, Liu J, Dunne M, Jaffray DA, Allen C (2007) In vivo performance of a liposomal vascular contrast agent for CT and MR-based image guidance applications. Pharm Res 24:1193–1201
333. Zheng J, Perkins G, Kirilova A, Allen C, Jaffray DA (2006) Multimodal contrast agent for combined computed tomography and magnetic resonance imaging applications. Invest Radiol 41:339–348
334. Zhong ZR, Liu J, Deng Y, Zhang ZR, Song QG, Wei YX, He Q (2007) Preparation and characterization of a novel nonviral gene transfer system: procationic-liposome-protamine-DNA complexes. Drug Deliv 14:177–183
335. Zhou F, Kraehenbuhl JP, Neutra MR (1995) Mucosal IgA response to rectally administered antigen formulated in IgA-coated liposomes. Vaccine 13:637–644

# Chapter 12
# Receptor Mediated Delivery Systems for Cancer Therapeutics

**Tamara Minko**

**Abstract** Directing anticancer agents specifically to tumors and/or cancer cells by targeting specific extracellular receptors fulfills the following three most important tasks: (1) preventing or at least substantially limiting adverse side effects on healthy tissues; (2) enhancing drug internalization by cancer cells; and (3) overcoming (at least in part) resistance mechanisms that are based on the active efflux of exogenous drugs from cancer cells. This review is focused on the last decade of accomplishments in the field of cancer-targeted drug delivery and describes different approaches to receptor-targeted delivery of anticancer agents. Mechanisms of receptor mediated endocytosis, targeting folate, carbohydrate (lactose, galactosamine, ascorbic acid, hyaluronic acid), peptide, and protein (somatostatin, growth factor, tissue factor, integrin, transferrin, vitamin, and luteinizing hormone-releasing hormone) receptors are discussed.

## 12.1 Introduction

The idea of drug targeting was first proposed by Paul Ehrlich more than a century ago as a concept of a "magic bullet" that selectively and effectively kills the "villain" and spares the "innocent bystander" [1]. Although the idea attracted the attention of several generations, real advances in its practical realization have been made only in the last decades. Targeting of physiologically active substances is important in treating all types of diseases in order to increase therapeutic efficiency and limit side effects. Targeting is exceptionally important in cancer chemotherapy, where highly toxic substances are usually used in order to effectively kill cancer cells.

T. Minko (✉)
Department of Pharmaceutics, Ernest Mario School of Pharmacy, Rutgers, The State University of New Jersey, 160 Frelinghuysen Rd, Piscataway, NJ 08854-8020, USA
e-mail: minko@rci.rutgers.edu

J. Siepmann et al. (eds.), *Fundamentals and Applications of Controlled Release Drug Delivery*, Advances in Delivery Science and Technology,
DOI 10.1007/978-1-4614-0881-9_12, 

In a previous review, we grouped cancer targeting approaches into two large clusters, "passive" and "active" targeting, and each cluster was subdivided into several distinct subclasses [2]. According to this classification, receptor-mediated targeting of cancer cells belongs to active targeting and covers two subclasses: "targeting specific organs" and "targeting cancer cells." In fact, cell surface plasma membrane receptors overexpressed in cancerous organs and/or specific cancer cells can be selected as targets. Choosing an entire organ with a tumor as the target to chemotherapy via certain organ-specific receptors ensures the delivery and accumulation of anticancer drug(s) in an entire organ, whereas targeting distinct cancer cells guarantees killing only cancer cells while minimizing adverse impact on normal cells in the same organ. Both approaches are currently being investigated, but with primary emphasis on targeting cancer cells. In addition to killing cancer cells inside the primary tumor, the latter approach permits effective preemption and killing of metastases.

Numerous approaches are currently being explored for ligand-mediated active targeting of anticancer drugs, other active components, and complex systems, to cancer cells, tumors, and entire organs with tumors. Most are based on the use of a targeting moiety as part of the delivery system, to redirect an entire entity or just anticancer drugs toward the cancer cells by interacting with specific receptors that are unique to cancer cells or are overexpressed in cancer cells. Such moieties include but are not limited to antibodies, polypeptides, oligosaccharides (carbohydrates), viral proteins, fusogenic residues, and molecules of endogenous origin [2–4]. Viral and immune-based targeting approaches are also used for drug and gene delivery [5–7].

In this chapter, we limit discussion to nonviral and nonimmune approaches to receptor-mediated targeted drug delivery. Directing anticancer agents specifically to tumors and/or cancer cells by targeting specific extracellular receptors accomplishes three critical tasks: (1) preventing or at least substantially limiting adverse side effects on healthy tissues; (2) enhancing drug internalization by cancer cells; and (3) overcoming (at least in part) resistance mechanisms that are based on active efflux of drugs from cancer cells. The first task is self explanatory and reflects Ehrlich's magic bullet, killing only malignant cells while leaving intact (or considerably less harmed) normal healthy cells. The second task is fulfilled because targeting of anticancer drugs to specific extracellular plasma membrane receptors changes the route of internalization of the drug (or complex system containing the drug) from "simple" diffusion (for low molecular weight drugs) or "nonspecific" endocytosis (for high molecular weight drugs or complex prodrug delivery systems) to receptor-mediated endocytosis, which is a much more efficient means of internalization.

The significance of the third task is often underestimated. Internalization of small drug molecules by receptor mediated endocytosis in membrane limited and protein coated organelles allows them to escape plasma membrane bound drug-efflux transporters tuned for free small molecules and therefore overcome one of the most important components of cellular drug resistance, termed by us as "pump resistance" [2, 8, 9].

Fulfillment of all three tasks by tumor targeted enhanced internalization converts an anticancer "magic bullet" into a "silver bullet" capable of killing multidrug-resistant cancer cells. As a side note, it should be stressed, however, that the other major mechanism of cellular anticancer drug resistance, which we designated as "nonpump resistance" [2, 8, 9], cannot be overcome simply by receptor targeting and require additional lines of attack.

In addition to tumors, receptor-mediated targeting is important in the delivery of therapeutics to the brain. In most cases, the blood–brain barrier (BBB) hinders delivery of drugs from blood to the brain parenchyma. Similar to receptor mediated endocytosis in cancer cells, receptor mediated transcytosis or carrier mediated transporter systems can be employed to facilitate drug delivery across the BBB. While BBB targeting lies outside the scope of this chapter, many of the relevant concepts are similar.

## 12.2 Receptor Mediated Endocytosis

Before reaching an intracellular site of action (i.e., cytoplasm, mitochondria, nuclei, etc.), an anticancer drug must cross the plasma membrane, travel through the cytoplasm, and possibly cross several intracellular membranes. It is very important that the drug preserve its activity during this journey. If drug is delivered into the systemic circulation as an inactive prodrug or is coupled with a carrier, then it needs to be separated from the carrier and/or converted to its active form. Only small lipophilic molecules can easily cross the plasma membrane. Water-soluble drugs can penetrate through the plasma membrane by diffusion (small drugs) or nonspecific endocytosis (large drugs or high molecular weight delivery systems). Both pathways possess very low efficiency and generally require a high concentration of the drug in the neighboring extracellular space. Entry of an anticancer agent into cancer cells by simple diffusion or endocytosis will result in relatively low cytotoxicity of the drug. Similarly, conjugation of a low molecular weight drug to a high molecular weight carrier should substantially decrease its cytotoxicity.

In multidrug-resistant cancer cells that overexpress drug-efflux transporters, a significant fraction of low molecular weight drug is pumped out from the cytoplasm by membrane based drug efflux transporters [10]. By contrast, high molecular weight drugs and drugs carried by high molecular weight carriers enter the cell by endocytosis in membrane coated vesicles. This mechanism prevents drug efflux by the plasma membrane pumps. Our experimental data have shown that low molecular weight doxorubicin (DOX) bound to a high molecular weight polymeric carrier demonstrates similar toxicity in multidrug-resistant cancer cells when compared with drug-sensitive cells [11]. These data confirm that high molecular weight drug conjugates can overcome drug-efflux pumps. However, "nonspecific" endocytosis cannot be considered a solution for effectively overcoming drug resistance in cancer cells because the cytotoxicity of high molecular weight drugs/systems delivered into cells by this mechanism still remains low.

As was already mentioned, interaction of a targeting ligand with its receptor substantially changes the internalization mechanism of anticancer drugs or systems bound to the ligand from "simple" diffusion or "simple" endocytosis to so-called receptor-mediated endocytosis [12–14]. The main steps of this process are shown schematically in Fig. 12.1. Interaction of a ligand-conjugated therapeutic payload (cargo) with its extracellular plasma membrane receptor leads to the formation of protein-coated pits – small areas of the plasma membrane coated with protein that invaginate into the cell cytoplasm, where they are pinched off to form protein-coated vesicles. In most cases, clathrin represents the main structural component of the coat [14].

Soon after formation, coated vesicles lose their coat and fuse with other such vesicles and specialized membrane organelles known as endosomes, forming so-called early endosomes. In most cases, the receptor–ligand pairs and the associated ligand payload remain intact in early endosomes. However, decreasing pH and any slight change in enzymatic environment inside the early endosome may lead to the partial dissociation of ligands from the ligand–receptor complexes. During the process of maturation of early endosomes into late endosomes, a change in intravesicular pH and penetration of enzymes from the Golgi apparatus leads to dissociation of ligand–receptor complexes and transporting ("sorting") of intact receptors in membrane-limited organelles back to the surface of the cell. Consequently, receptors can be recycled and participate in several rounds of endocytosis. However, some internalyzed receptors can remain in the endosomes and finally be proteolyzed. Therapeutic cargo may also be unbound from the ligand or ligand-containing carrier and be released from early or late stage endosomes.

Some early and almost all late endosomes contain membrane-limited vesicles inside their bodies. (For simplicity, these vesicles are not shown in Fig. 12.1.) As a result, late stage endosomes are referred to as multivesicular bodies. Late endosomes eventually interact with lysosomes. Two mechanisms of such interaction are generally distinguished as (1) so-called kissing, where exchange of contents between a lysosome and an endosome occurs via a small contact zone and internalized endosome content mostly remains inside the endosome, and (2) complete fusion to form a hybrid organelle with complete exchange of material between interacting bodies (Fig. 12.1). As a result of these processes, intravesicular pH further decreases (down to pH 4.5–5), and lysosomal enzymes attack endocytosed drug complexes. In most cases, the linkage between the ligand and therapeutic cargo breaks here and drug is released into the cytoplasm.

Even a simplified model of receptor mediated endocytosis shows the complexity of the process and raises several issues that should be addressed when designing a targeted drug delivery system (DDS). Most of these issues are related to the mechanism of drug release from the entire complex system. In general, two triggers are most commonly used to facilitate drug release from the DDS: a drop in pH and action of lysosomal enzymes.

Chemical design of the link between the drug and ligand-targeted carrier or simple ligand mainly depends on the mechanism of action of the anticancer drug. If the drug acts in the cytoplasm, then early release from endosomes is desired.

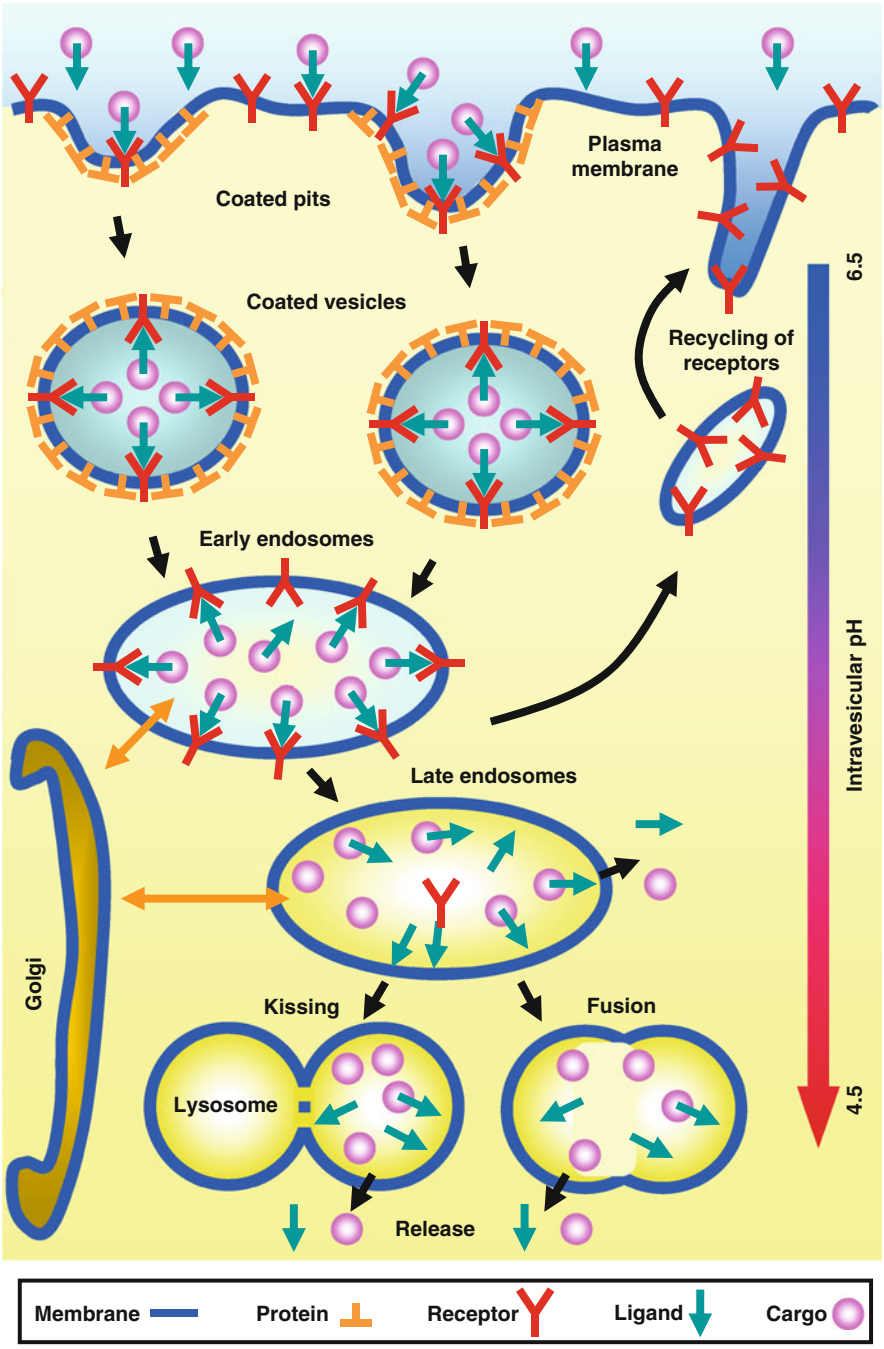


**Fig. 12.1** A simplified schema of receptor-mediated endocytosis. Drawings are not to scale

If, by contrast, the drug acts in the nucleus, then the drug (or drug/carrier complex) should be released from lysosomes near the nucleus. In some cases, an additional targeting ligand can be used to facilitate penetration of drug into the nucleus or other organelles [15, 16]. Specific types of bonds between the drug and carrier/ligand, and specific construction of an entire delivery system are used to achieve drug release from the DDS at a specific point of its intracellular journey. Examples include pH-degradable disulfide or hydrazone bonds [17–20] and special spacer sequences that are degraded by lysosomal enzymes [21, 22].

## 12.3 Receptor Mediated Tumor Targeting

### *12.3.1 Types of Receptor Targeted Anticancer DDSs*

By definition, a tumor-targeted system which utilizes targeting of extracellular receptors should kill cancer cells and be targeted to specific receptors predominately overexpressed in cancer cells. In most cases, these two goals are achieved by including such a DDS into two distinct moieties: an anticancer drug and a targeting ligand. In a simple case, a tumor targeted DDS consists of an anticancer agent and a targeting ligand conjugated to each other directly or via a biodegradable spacer (Fig. 12.2a, 1). Often, nontoxic biocompatible polymers are used to conjugate a targeting moiety and active component directly or in combination with biodegradable spacers. Several polymers have been successfully utilized as carriers to deliver a wide range of anticancer drugs [23]. Commonly used polymers include poly (ethyleneglycol) (PEG), *N*-(2-hydroxypropyl) methacrylamide (HPMA), and poly (lactide-co-glycolide) (PLGA) copolymers.

Unmodified linear polymers without side chains (e.g., PEG) have only two terminal ends available for conjugation and therefore they can be bound to no more than two active components of the DDS (Fig. 12.2a, 2). Consequently, one molecule of PEG based conjugate can deliver only two molecules, for instance, one molecule of anticancer agent and one molecule of a targeting moiety. In order to increase the loading capacity of such polymer, several modifications in architecture of carrier have been proposed [24]. A spacer can be conjugated to the linear polymer backbone (Fig. 12.2a, 3). Additional active components (drug, peptide, nucleic acid, etc.) can be bound to this spacer. If the polymer does not allow the conjugation of additional spacer(s) in the middle of its backbone (e.g., PEG), then branched spacers can be conjugated at the distal ends of the polymer (Fig. 12.2a, 4). We proposed citric acid as such a branched spacer and experimentally confirmed the efficacy of the approach [25].

Systems utilizing linear polymers and spacers to bind active components in one DDS can be successfully used when the payload does not possess electrical charge. However, utilization of such DDS for delivery of negatively charged (in neutral or alkaline conditions) nucleic acids represents a substantial challenge. Although

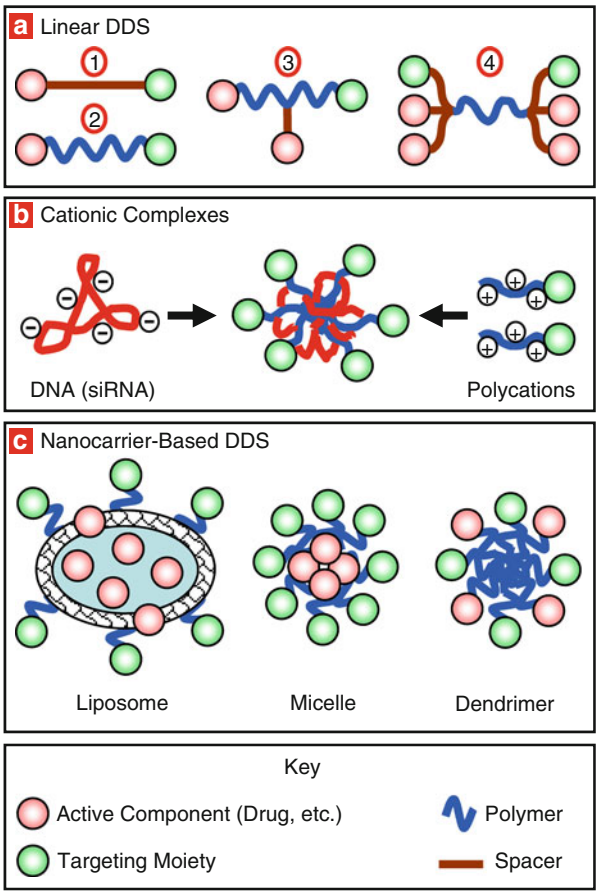


**Fig. 12.2** The most common architectures of tumor-targeted drug delivery systems

chunks of DNA or RNA can be made electrically neutral (e.g., by P-ethoxy modification of the DNA backbone of all bases) in order to be used in linear systems, another approach is more widely used. According to this approach, DNA or RNA molecules are complexated with tumor targeted polycations to form small nanoparticles (Fig. 12.2b) [26]. As will be shown later, such tumor-targeted nanoparticles have been successfully used to deliver DNA or small interfering DNA (siRNA) molecules specifically to tumor cells.

In addition to relatively simple linear polymeric systems, more complex DDS are often used for targeted delivery of different anticancer agents to cancer cells (Fig. 12.2c). Liposomes are employed for tumor targeted delivery of water-soluble (inside liposomes in the aqueous inner space) or lipophilic (in lipid membrane) anticancer agents and other active components in multifunctional DDS. Micelles can also be used to deliver preferably lipophilic compounds in their core or chemically conjugated hydrophilic substances. Dendrimers as cascade polymers have the high potential to deliver multiple copies of targeting moieties or anticancer

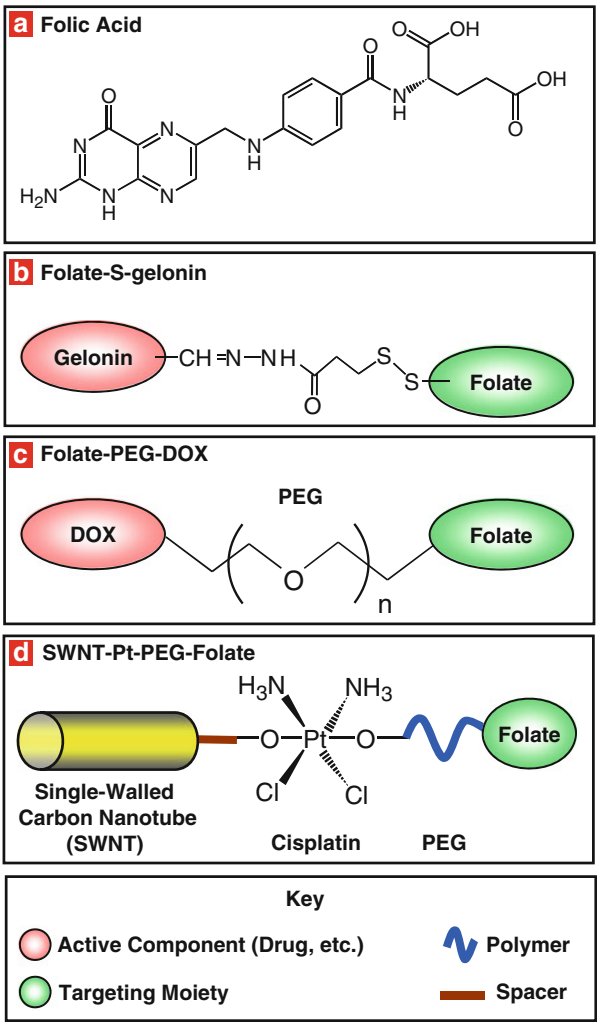


**Fig. 12.3** The chemical structure of folic acid and examples of tumor-targeted drug delivery systems utilizing folate as a targeting moiety

agents by conjugating them to the surface ends of polymeric branches or by forming complexes with nucleic acids. All of the above-mentioned DDS used for receptor-mediated tumor-targeted delivery is discussed in this chapter.

## *12.3.2 Targeting Folate Receptors*

Folic acid (FA, Fig. 12.3a), also known as vitamin $B_9$, vitamin $B_c$, or folacin, is essential for many bodily functions. It is used for DNA synthesis, repair and methylation, and acts as a cofactor in several biological reactions. Members of

the folate receptor (FR) family (also known as the membrane folate-binding proteins) bind folic acid and its reduced derivatives. Folate receptors are generally overexpressed in several human tumor cells [27] and even in the blood of cancer patients [28]. Although the exact mechanisms and physiological reasons for such overexpression are not clear, one can suggest that folate as a basic component of cell metabolism, DNA synthesis, and repair is required in increased amounts for rapidly dividing cancer cells to maintain DNA synthesis.

Ovarian carcinoma exhibits the highest level of expression of folate receptors among different cancers [29, 30]. Consequently, folate-targeted delivery systems should demonstrate greatest specificity, maximal therapeutic effect, and lowest adverse side effects in patients with ovarian carcinoma. Several DDS with folate-targeting moieties have been developed, evaluated, and tested during the last two decades after folate receptors were proposed and evaluated as a target for the cancer-specific delivery of therapeutics by receptor mediated endocytosis [31–33].

Many different types of DDS architecture have been employed to create tumor-targeted DDS using folate as a targeting moiety, from simple conjugation of anticancer agent directly to the targeting moiety, to robust complex DDS containing several components. One example of a "simple" DDS is presented in Fig. 12.3b. This DDS consists of folate conjugated to a protein drug (plant toxin gelonin) via carbohydrate residues, using a SH-folate intermediate [34]. This folate–gelonin conjugate retains over 99% of toxin activity when compared with unmodified gelonin and is able to bind folate receptors with the same affinity as free folic acid. As an indication of its anticancer activity, the conjugate exhibits prolonged inhibition of protein synthesis in FR-positive cell lines in vitro.

PEG is widely used as a carrier for folate receptor targeted DDS. Folate–polyethylene glycol–doxorubicin (Folate–PEG–DOX) [35] represents one example of such a conjugate (Fig. 12.3c). Doxorubicin and folate were conjugated to the alpha- and omega-terminal end groups of a PEG chain, respectively. Conjugation resulted in formation of nano-aggregates with an average size of 200 nm in diameter. Intracellular uptake of this conjugate by FR-positive cancer cells was significantly higher than by FR-negative cells, confirming the receptor-mediating character of uptake. As a result, cytotoxicity of the DDS in FR-positive cancer cells was substantially higher when compared with free DOX.

In addition to anticancer drugs, folate targeted PEG can be successfully used to deliver other types of active components. In one study [36], folate–PEG was attached on *baculovirus* surface to obtain efficiency and specificity of gene delivery. Conjugation of *baculovirus* to folate–PEG significantly enhanced its transduction efficiency compared to nontargeted PEG–baculovirus in FR-positive cancer cells. Enhanced transduction was not observed in FR-negative cells. Presence of free folate in the medium blocked transduction of folate–PEG–*baculovirus*, whereas transduction efficiency of PEG–*baculovirus* in the presence or absence of free folate was not changed significantly. All of these findings clearly show that folate–PEG–*baculovirus* is internalized by FR-positive cancer cells by receptor-mediated endocytosis.

For effective delivery of nucleic acids or anionic proteins, neutral folate–PEG conjugates should be modified to obtain positively charged polycations in order to form complexes by electrostatic interactions between these polycations and negatively charged nucleic acids or proteins. Examples of such folate targeted PEG polycations include but are not limited to folate–PEG–poly(L-lysine) [37], folate–poly(ethylene glycol) grafted trimethylchitosan [38], and folate–poly(ethylene glycol)–polyethylenimine [39, 40] conjugates. In addition to folate–PEG based DDS, folate modified cationic polyethylenimine [37] or amphiphilic block copolymers of polyethylenimine and poly(L-lactide) [40] were synthesized. All of these conjugates form stable electrostatic complexes with plasmids or minicircle DNA, small interfering RNA, and anionic proteins forming compact nanoscale-based cationic nanoparticles. Experiments confirmed that complexes of nucleotides with such polycations significantly exhibit enhanced uptake of FR-positive cancer cells by receptor mediated endocytosis, with specific activity of delivered nucleic acids preserved.

In addition to being conjugated directly to the payload or to other polymers, folate–PEG conjugates are being used to coat liposomes [41–43]. Such coating fulfills two major tasks: (1) protecting the payload from degradation in the bloodstream by masking of vehicles and preventing their uptake by the reticulo-endothelial system, and (2) targeting the entire delivery system specifically to cancer cells by folate. Similar to the stand alone folate–PEG conjugates, coating of liposomes or lipid vesicles by folate–PEG conjugates forces uptake of the vehicles by receptor mediated endocytosis, enhancing the specific activity of the payload.

In contrast to liposomes and lipid vesicles, which are bodies with a lipid membrane and aqueous inner space, micelles are liquid colloidal aggregates of surfactant molecules whose hydrophilic “head” regions contact the surrounding aqueous solvent and whose hydrophobic single tail regions segregate into the micelle interior. Folate as the targeting moiety can be linked to the hydrophilic heads of the micelles directly or via polymer spacers (e.g., PEG polymer micelle coating) while lipophilic drug can be incorporated into the lipophilic core of the micelle. Examples of recently developed folate targeted micelles include folate conjugated micelles [44] or lipid molecules [45], micellar nanoparticles self assembled from copolymer folate–chitosan [46], as well as polyelectrolyte complex micelles [47]. These micelles were intensively studied as vehicles and successfully used for solubilization of several anticancer drugs including 9-nitro-camptothecin, co-delivery of pyrrolidinedithiocarbamate and doxorubicin, and delivery of oligonucleotides. In addition to the effective targeted delivery of the payload specifically to FR-positive cancer cells, micelles allowed for overcoming of multiple drug resistance in cancer cells [46], probably by shielding the delivered drugs from membrane bound drug efflux pumps.

Dendrimers, which are repeatedly branched spherical large molecules, offer multiple sites for conjugation of different molecules. Consequently, they have attracted continuous attention as prospective drug delivery vesicles. These structures allow for binding of several copies of different active components of DDS, including folate as the targeting moiety, and anticancer drugs. In addition,

positively charged dendrimers can be successfully used to condense nucleic acids in order to form stable nanoparticles with charged oligonucleotides, chunks of DNA, and siRNA. Poly(amido amine) (PAMAM) dendrimers have been used recently as folate targeted delivery systems. These dendrimers were used to deliver antisense oligonucleotides (ASO) specifically to C6 glioma cells [48]. Conjugation of ASO to folate targeted dendrimers increased ASO transfection rates resulting in greater suppression of the targeted protein and inhibition of glioma cell growth when compared with oligofectamine.

Two approaches can be used to load drugs into dendrimers. First, hydrophobic drugs can be complexed in the hydrophobic dendrimer interior. Second, drug can be covalently conjugated to the dendrimer surface. These two approaches were experimentally compared for folate targeted delivery of methotrexate [49]. It was found that drug complexed inside the dendrimer was quickly released into phosphate-buffered saline. In contrast, covalently coupled drug conjugates were stable in water and buffered saline, and they provided efficient delivery of methotrexate inside FR-positive cancer cells via receptor-mediated endocytosis.

In addition to dendrimers, other approaches can be employed to develop tumor-targeted nanoparticles for delivering anticancer agents specifically to cancer cells. For instance, tumor-targeted nanoparticles were prepared from poly (3-hydroxybutyrate-co-3-hydroxyoctanoate) as a carrier, folate as a targeting moiety, and doxorubicin as an anticancer drug [50]. The resulting nanoparticles had average size around 240 nm and exhibited high encapsulation efficiency of DOX (>80%). These nanoparticles demonstrated relatively prolonged release of DOX (~50% release within 5 days). As with all folate targeted DDS, these nanoparticles showed excellent internalization by FR-positive cancer cells. In vivo experiments showed effective inhibition of tumor growth by DOX containing nanoparticles. In another study [51], a more complex DDS has been developed using an amine functionalized single walled carbon nanotube (SWNT) as a carrier connected via succinate to cisplatin as an anticancer drug (Fig 12.3d). PEG–folate conjugate was bound to the second axial ligand of cisplatin. This complex system effectively killed FR-positive cancer cells by releasing the drug after intracellular reduction of Pt(IV) to Pt(II).

### *12.3.3 Targeting Carbohydrate Receptors*

Several carbohydrate moieties including but not limited to lactose, ascorbic acid, hyaluronic acid, and galactosamine have recently been used to target tumor cells (Fig. 12.4). DDS targeted to carbohydrate receptors have been employed for tumor-specific delivery of several anticancer agents, anti-sense oligonucleotides (ASOs), siRNA, and plasmid DNA. A carbohydrate moiety is added to the DDS in order to achieve receptor-specific uptake by cancer cells [52]. Asialoglycoprotein receptor is one of the major receptors overexpressed in cancer cells targeted by carbohydrate moieties. Asialoglycoprotein receptors are lectins that bind glycoproteins. It should

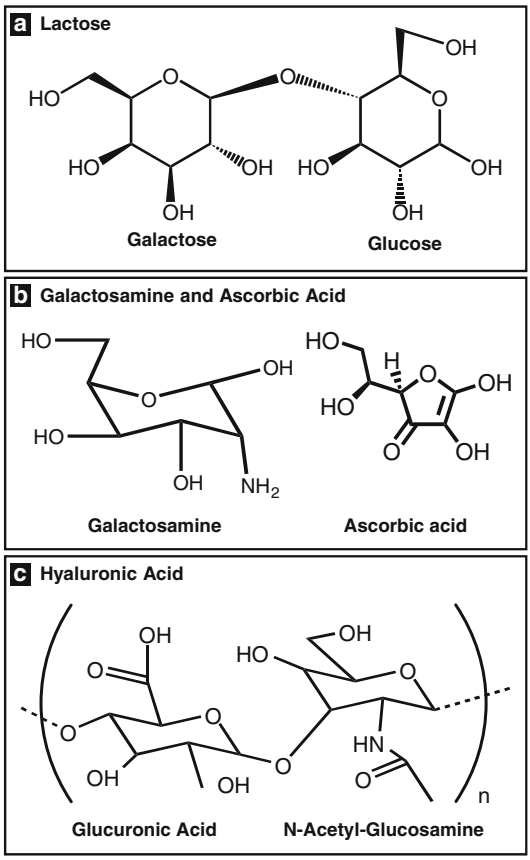


**Fig. 12.4** Examples of carbohydrate molecules used as cancer targeting moieties

be stressed that these receptors are also expressed in normal hepatocytes, which raises the question of nonspecific uptake of carbohydrate-targeted DDS by liver. For more details about using lectins and carbohydrates for tumor-specific delivery, the reader is referred to our previous publications [4, 53]. Here, we describe some recent advances.

### 12.3.3.1 Lactose

The main milk sugar lactose is formed by the condensation of galactose and glucose (Fig. 12.4a). It has been extensively used to target asialoglycoprotein receptors overexpressed in cancer cells. Novel polyion complex micelles of poly(L-lysine) and a lactosylated poly(ethylene glycol) were developed for the delivery of ASOs [54]. ASOs were conjugated to PEG via beta-propionate, a pH sensitive, acid labile linkage. These micelles demonstrated a more significant gene suppression effect in hepatoma cells compared to free ASO and ASO bound to the complex by non-acid labile linkages. These experimental findings confirmed that uptake of such DDS

is accomplished via receptor mediated endocytosis and that release of ASO from the system is achieved in response to pH decrease in the endosomal compartment.

Another lactose targeted DDS was constructed as a block copolymer of α-lactosyl-poly(ethylene glycol)-*block*-poly(2-(dimethylamino)ethyl methacrylate) [55]. This polyion copolymer formed complex micelles with plasmid DNA. The micelles were useful for selective transfection of human liver carcinoma cells. Transfection was inhibited by an excess of asialofetuin, a natural ligand against the asialoglycoprotein receptor, indicating that receptor-mediated endocytosis represents the major mechanism of the cellular uptake of these micelles.

Poly(L-lactic acid) nanoparticles coated with galactose-carrying polymer were used to deliver another anticancer drug, *trans*-retinoic acid [56]. Similar to other lactose-targeted DDS, the uptake of these nanoparticles was achieved by receptor targeted endocytosis.

#### 12.3.3.2 Galactosamine

Galactosamine, a hexosamine derived from galactose (Fig. 12.4b), has also been used to target asialoglycoprotein receptor in human hepatocellular carcinoma cells [57]. Micelles based on a diblock copolymer of poly(ethyl ethylene phosphate) and poly(epsilon-caprolactone) were synthesized, surface conjugated with galactosamine, and loaded with paclitaxel. The micelles were about 70 nm in the diameter, and they were negatively charged in aqueous solution. These micelles showed more pronounced anticancer activity in human hepatocellular carcinoma cells when compared with free drug and nontargeted nanoparticles, suggesting ligand–receptor interactions.

#### 12.3.3.3 Ascorbic Acid

Another carbohydrate-targeting moiety is ascorbic acid (Fig. 12.4b), one form of which is commonly known as vitamin C. Ascorbic acid was used to target certain tumor cells that have a higher ascorbic acid uptake than normal cells [58]. Polymeric nanoparticles functionalized with L-ascorbic acid 6-stearate were used to deliver the antitumor agent *trans*-dehydrocrotonin. This system demonstrated a high drug loading (81–88%), a narrow size distribution (100–140 nm), and a negatively charged surface. The nanoparticles showed sustained release and higher antitumor activity when compared with free drug and with nontargeted nanoparticles.

#### 12.3.3.4 Hyaluronic Acid

Hyaluronic acid or hyaluronan, a polymer of disaccharides composed of D-glucuronic acid and D-*N*-acetylglucosamine (Fig. 12.4c), is used to target hyaluronan receptors

overexpressed in cancer cells. An *N*-(2-hydroxypropyl)methacrylamide-hyaluronan polymeric DDS was synthesized and used to deliver DOX specifically to cancer cells [59]. Cytotoxicity of DOX delivered by the targeted bioconjugate was higher against human breast cancer, ovarian cancer, and colon cancer cells when compared with the nontargeted conjugate. Both nontargeted and targeted DOX conjugates showed equal minimal toxicity against mouse fibroblasts, which do not overexpress hyaluronic acid receptors.

A novel polyethyleneimine–hyaluronic acid conjugate was used to form complexes with siRNA and deliver the DDS specifically to cancer cells with overexpressed hyaluronan receptors [60]. As with other receptor targeted DDS, these complexes showed a higher efficiency in suppressing a targeted mRNA in cells that overexpress the targeted receptor.

### *12.3.4 Targeting Peptide and Protein Receptors*

#### 12.3.4.1 Somatostatin Receptors

Many protein and peptide receptors are overexpressed in cancer cells and can be potentially used for receptor-mediated targeting of DDSs specific to cancer. Somatostatin is a physiologically important peptide that performs several vital functions in the organism by controlling secretion from the pancreas, pituitary, and the gastrointestinal tract, and acting as a neuromodulator in the brain. Somatostatin receptors belong to the superfamily of mammalian cell surface receptors that couple with trimeric membrane-bound GTP-binding proteins called G proteins. These receptors are characterized by a common seven transmembrane domain structure and a signaling mechanism which involves activation of G proteins leading to either amplification or inhibition of downstream cell functions. Drug targeting to somatostatin receptors on cancer cells leads to inhibition of cell growth and proliferation and to activation of cell death by apoptosis (Fig. 12.5). All five subtypes of somatostatin receptors are expressed in a variety of human tumors, including most tumors of neuroendocrine origin, breast tumors, certain brain tumors, renal cell tumors, lymphomas, and prostate cancer. In addition to small drugs targeting somatostatin receptors and radiolabeled somatostatin analogs used for tumor imaging, ligands to these receptors have been used as targeting moieties to redirect DDS specifically to cancer cells.

Tumor targeted conjugates were prepared by binding somatostatin to dextran (molecular weight 70 kDa) and investigated on cells overexpressing all types of somatostatin receptors [61]. It was found that the developed conjugate showed high affinity binding to all five receptor subtypes. Moreover, somatostatin–dextran conjugates demonstrated a long circulation half-life (~27 h after subcutaneous administration in mice) and exhibited high cytotoxicity against cells expressing somatostatin receptors. These conjugates have been explored in a clinical Phase I–II study in patients with hormone-refractory prostate cancer.

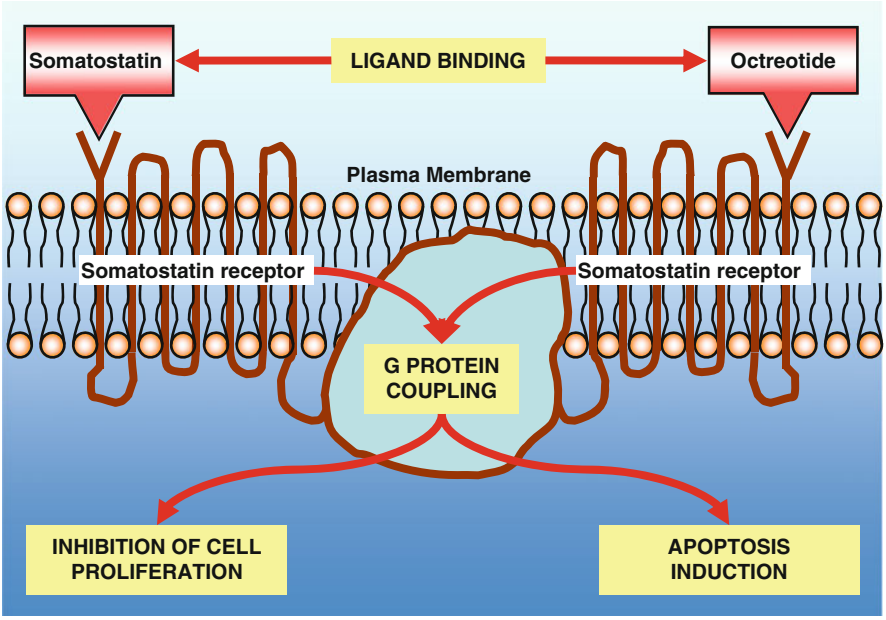


**Fig. 12.5** Cell surface receptors coupling with GTP-binding proteins (G proteins). A simplified scheme of somatostatin receptors is shown. These receptors are characterized by a common seven-transmembrane domain structure and a signaling mechanism which involves activation of G proteins leading in cancer cells to inhibition of cell growth and proliferation, and activation of cell death by apoptosis

Octreotide was investigated as a potential ligand to somatostatin receptors (especially subtype 2) to target PEG-coated liposomes specifically to cancer cells [62]. A spatial arrangement of this DDS was similar to that presented in Fig. 12.2c. These liposomes were used to deliver DOX and were investigated on three types of cancer cells with different expression of type 2 somatostatin receptors. It was clearly shown that intracellular uptake, cytotoxicity, drug distribution in tumor, and pharmacodynamics correlated with expression of the targeted receptors. At the same time, drug pharmacokinetics was independent of that expression. The results obtained showed high potential of octreotide-grafted liposomes for the treatment of somatostatin receptor overexpressing cancers.

#### 12.3.4.2 Growth Factor Receptors

Insulin-like growth factors (IGF) play a central role in cell growth, differentiation, survival, transformation, and metastasis [63, 64]. These growth factors are polypeptides with high sequence similarity to insulin. The biologic effects of IGF are mediated by the IGF receptor (IGF-1 and IGF-2 receptors). IGF-1 is a receptor tyrosine kinase with homology to the insulin receptor, while the IGF-2 receptor lacks tyrosine

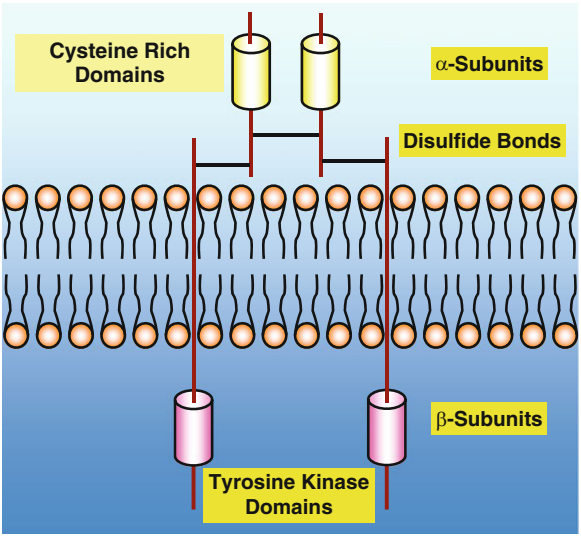


**Fig. 12.6** Simplified organization of insulin-like growth factor-1 (IGF-1) receptors. The receptors are tetrameric glycoproteins composed of two $\alpha$ and two $\beta$ subunits. Extracellular $\alpha$ subunits contain cysteine-rich domains and are linked by disulfide bonds. Transmembrane $\beta$ subunits contain cytoplasmic domain with ATP binding and catalytic sites that generate tyrosine kinase activity. Disulfide bonds also link $\alpha$ and $\beta$ subunits

kinase activity. A simplified structure of the IGF-1 receptor is presented in Fig. 12.6. Activation of the IGF system plays an important role in the progression of multiple cancers, including breast, prostate, lung, colon, and head and neck squamous cell carcinoma.

Despite their importance, IGF receptors only recently have attracted attention as potential targets for the treatment of cancer. To date, around 30 drugs targeting inhibition of IGF receptor signaling are being evaluated as single agents or in combination therapies for the treatment of cancer [63]. In addition to direct inhibition of IGF receptor dependent signaling pathways, IGF receptor binding molecules can potentially be considered as targeting moieties combining tumor-targeting properties with direct therapeutic effects. Potentially, the combination in one DDS of IGF-binding ligand with other anticancer agents can substantially enhance the treatment of IGF receptor expressing cancers by simultaneously targeting cancer cells, blocking IGF signaling, and inducing cell death signals.

Human epidermal growth factor receptors (EGFR) represent another class of tyrosine kinase receptors. EGFR pathways play a critical role in cancer biology and are being used as targets for cancer therapy. In one DDS, EGFR-targeting peptide was grafted onto the surface of type B gelatin-based engineered nanocarrier systems using a hetero-bifunctional poly(ethylene glycol) (PEG) spacer [65]. Plasmid DNA encoding for enhanced green fluorescent protein (GFP) was efficiently encapsulated in this system. The data obtained showed that EGFR targeted DDS have promise as a safe and effective nonviral gene delivery vectors with potential to treat pancreatic cancer.

Novel molecules termed “type II combi-molecules” have been engineered in order to simultaneously block the epidermal growth factor receptor and damage DNA without the need for hydrolytic cleavage [66]. These molecules contained a novel quinazoline-linked chloroethyltriazolinium system. Their ability

to simultaneously target EGFR and induce DNA damage was experimentally confirmed. Chemically synthetic composite polypeptide gene delivery systems, as well as genetically engineered polypeptide containing EGFR ligand complexed with DNA molecules, were developed and tested in EGFR-positive cancer cells both in vitro and in vivo [67]. The results of these investigations confirmed effective intracellular delivery of DNA by EGFR-targeted systems and targeting of the beta-galactosidase gene into EGFR-positive cancer cells both in vitro and in vivo.

Several more complex DDS for delivery of nucleotides and other active components in EGFR-positive cancer cells have also been developed. Recombinant barrel-shaped vault nanoparticles were self-assembled from 96 copies of the major vault protein [68]. The nanocylinders have dimensions 72.5 × 41 nm, with a hollow interior capable of encapsulating several proteins. Several different tags were engineered onto the C-terminus of the major vault protein, including epidermal growth factor containing 55 amino acids. The engineered nanoparticles demonstrated the ability to target EGFR-positive cancer cells.

Another complex DDS was developed based on two components linked by biotin–streptavidin binding [69]. The first component of the system was prepared by conjugating a biotin–PEG–*N*-hydroxylsuccinimide derivative to epidermal growth factor. The second component of nanoparticles was formed by complexing luciferase plasmid DNA with polyethylenimine and further electrostatically coupling the complex with negatively charged streptavidin. Finally, the two components were attached via streptavidin–biotin interaction. Uptake of these complex nanoparticles via receptor-mediated endocytosis was confirmed.

A three-oligopeptide based DDS has been constructed [70]. The system consisted of a ligand oligopeptide for EGFR recognition, a polypeptide for DNA binding, and an endosome-releasing oligopeptide for endosomolysis. The developed nonviral vector was used to transfect wild-type p53 gene into human hepatoma cells with mutated p53. Transfection resulted in growth inhibition of cancer cells.

Vascular endothelial growth factor (VEGF) is a signaling protein involved in both de novo formation and growth of blood vessels (vasculogenesis and angiogenesis, respectively). Many tumors are fast growing and abnormally proliferating neoplasm often overexpresses VEGF receptors. Consequently, these receptors can be used both to target tumors and to suppress their growth by inhibiting angiogenesis. A DDS containing two fragments of human pancreatic RNase I was engineered [71]. The first short N-terminal fragment of RNase I was served as a docking tag and was fused to the N-terminus of human VEGF as a targeting protein. The second longer fragments of RNase I were engineered, expressed, and refolded into active conformations to serve as adapter proteins. Assembled targeted DNA delivery complexes were tested and found to be very effective in receptor-mediated DNA delivery.

PH1 peptide (TMGFTAPRFPHY) was used to target the Tie2 receptor, a receptor tyrosine kinase that plays important roles in vascular angiogenesis, and is highly expressed in many cancer cells [72]. PH1 peptide was bound to a distal end of PEG-coated liposomes that were used to deliver cisplatin. It was found that PH1

peptide targeted liposomes bound tightly to Tie2 positive cancer cells, initiated receptor-mediated endocytosis, and showed significantly higher activity when compared with nontargeted liposomal DDS.

#### 12.3.4.3 Tissue Factor

Tissue factor (TF), a transmembrane receptor for coagulation factor VIIa (FVIIa), is aberrantly expressed in tumor vascular endothelial cells and in cancer cells in many malignant tumors and is not expressed in normal vascular endothelial cells. This makes TF a promising target for cancer therapy. A TF-targeted DDS was constructed to deliver the synthetic curcumin analog EF24 to TF-positive tumors using FVIIa as drug carrier and targeting ligand [73]. The data obtained showed that the resulting conjugate inhibited angiogenesis in experimental tumors, induced apoptosis in tumor cells, and significantly reduced tumor size. Antitumor activity of conjugated EF24 was significantly higher when compared with free unconjugated drug. Consequently, it was concluded that the proposed targeted DDS has the potential to enhance therapeutic efficacy, while reducing adverse side effects on healthy tissues that do not express TF.

#### 12.3.4.4 Integrin Receptors

Integrin receptors are a major family of adhesion receptors that are critically important for adhesive interactions required for the proliferation, survival, and function of all cells. These receptors are overexpressed in certain cancers and therefore can be used as targets for receptor-mediated delivery of therapeutics. Among other ligands for these receptors, peptide ligands containing the arginine–glycine–aspartate (RGD) triad, which displays a strong affinity and selectivity to $\alpha(V)\beta(3)$ integrin, have been developed to target tumor associated cells expressing $\alpha(V)\beta(3)$ receptors [74]. A cyclic RGD peptide-conjugated block copolymer, cyclo[RGDfK(CX-)]-poly(ethylene glycol)-polylysine, was synthesized and used to condense plasmid DNA into polyplex micelles [75]. It was found that these micelles preferentially accumulated in the perinuclear region of integrin receptor positive HeLa cells within 3 h of incubation, and they demonstrated remarkably increased transfection efficiency when compared with nontargeted PEG–polylysine–DNA micelles. Such enhanced transfection efficacy is explained by internalization of the micelles by receptor mediated endocytosis and their transport in membrane limited organelles toward the perinuclear region.

Another integrin receptor ligand, ATN-161 (*N*-acetyl-proline-histidine-serine-cysteine-asparagine-amide, PHSCN), has been used to target DOX containing liposomes specifically to cancer cells [76]. The PHSCN peptide was conjugated to the distal end of PEG polymer coated liposomes. These targeted liposomes actively delivered DOX into tumor neovasculature and tumor cells, demonstrating enhanced cytotoxicity when compared with nontargeted DOX loaded PEG-coated liposomes.

#### 12.3.4.5 Transferrin Receptors

Transferrin and transferrin receptors are responsible for the import of iron into cells. Despite intensive investigations following transferrin's discovery more than half a century ago, precise mechanisms of tranferrin-mediated iron uptake are still unknown. Transferrin has been widely applied as a ligand for active targeting of anticancer agents, proteins, and genes to primary proliferating malignant cells overexpressing transferrin receptors [77]. A transferrin–p53–lipofectamine complex was developed and investigated using experimental tumors [78]. This transferrin receptor targeted DNA complex enhanced p53 gene transfer to hepatic tumors and improved animal survival. In a separate study, PEGylated recombinant human tumor necrosis factor alpha (TNF-α) was bound to transferrin in order to provide targeted killing of cancer cells that overexpress transferrin receptors [79]. This resulted in long circulating conjugate demonstrated by the enhanced antitumor activity of TNF-α.

Several liposomal formulations have been developed utilizing transferrin as a ligand conjugated to the distal end of a PEG polymer coating of liposomes. A study of transferrin-targeted liposomes showed that small (60–80 nm) targeted vesicles were taken up by the liver and brain more efficiently when compared with nontargeted liposomes [80]. DOX [81, 82], cisplatin [83], mercaptoundecahydrododecaborate [84], rhodamines [85], and ASO [86] were used as test payloads or anticancer agents. These studies supported the use of transferrin as a targeting moiety for liposomal DDS with high anticancer efficiency.

#### 12.3.4.6 Vitamin Receptors

Absorption and transport of most vitamins involves specific protein receptors that have an incorporated recognition factor. Similar to other receptors, such proteins initiate endocytosis upon binding a ligand and can be used for drug targeting purposes. Vitamin ligands were used to target DDS specifically to cancer cells. Biotin, a water soluble B-complex vitamin (vitamin B7), is an example of a vitamin used as a cancer targeting moiety. Several DDS that utilize biotin as a targeting moiety have been recently developed and tested. In one system, biotin was conjugated via a cleavable spacer to a second generation taxoid (SB-T-1214) as the cytotoxic agent [87]. The conjugate was examined using three cell lines, L1210FR (biotin receptor overexpressing leukemia cell line), L1210 (leukemia cell line without biotin receptor overexpression), and WI38 (normal human lung fibroblast, biotin receptor negative). As anticipated, the biotin-taxoid system exhibited high specificity only to L1210FR cells. In addition, the tumor targeted system demonstrated higher cytotoxicity in these cells when compared with the biotin-negative cell lines.

A more complex system consisted of functionalized SWNTs linked to biotin and a prodrug (taxoid with a cleavable linker) [88]. Specificity and cytotoxicity of this

DDS were also demonstrated using the same cell lines with different expression of biotin receptors.

Another biotin-targeted DDS was based on poly(L-glutamic acid) dendrimer with a polyhedral oligomeric silsesquioxane nanocubic core as carrier [89]. The dendrimer was conjugated with doxorubicin via pH-sensitive hydrazine bonds and biotin. The conjugates aggregated into nanoparticles with diameters around 50 nm. Experiments showed that DOX release at pH 5.0 was much faster when compared with pH 7.0 due to acid cleavage of the hydrazine bonds.

#### 12.3.4.7 Luteinizing Hormone Releasing Hormone Receptors

Luteinizing hormone releasing hormone (LHRH), also known as gonadotropin releasing hormone and luliberin, is a trophic peptide factor responsible for the release of follicle stimulating hormone and luteinizing hormone from the anterior pituitary gland (Fig. 12.7a). LHRH is synthesized and released from neurons located in the hypothalamus. Targeting of different tumors by LHRH peptide was first proposed and extensively studied in our laboratory [25, 90–96]. We showed that LHRH receptors are overexpressed in ovarian, breast, lung, prostate, cervical, and uterine cancer cells. In contrast, LHRH receptor expression in healthy visceral organs is below the detection limit of PCR. Moreover, expression of LHRH receptors in cancer is significantly higher than in corresponding healthy tissue taken from the same reproductive organ of the same patient. These data form the basis for the use of LHRH peptide to target different cancer cells. For better targeting, the sequence of native LHRH peptide (which is similar in human, mouse, and rat) was modified (Fig. 12.7a) to provide a reactive amino group on the side chain of a lysine residue, which replaced Gly at position 6 to yield the superactive, degradation-resistant LHRH-Lys6-des-Gly10-Pro9-ethylamide luteinizing hormone-releasing hormone analog [97].

All types of DDS presented in Fig. 12.2 were tested for LHRH mediated drug delivery to different cancer cells [25, 90–96]. Targeting of DDS specifically to cancer cells dramatically changed organ distribution of the entire DDS, including the encapsulated drugs. For instance, only around 30% of injected dose of nontargeted liposomal DDS containing paclitaxel reached the tumor and the rest of the drug affected healthy organs (Fig. 12.7b). By contrast, targeted liposomal DDS accumulated predominately in tumor with only minor amounts found in other organs (Fig. 12.7b). Such distribution of tumor targeted drugs created the basis for a high antitumor efficiency of the system and low adverse side effects, which was experimentally confirmed in experiments on nude mice bearing xenografts of human cancer cells.

For instance, paclitaxel delivered by the liposomal DDS targeted to tumor with LHRH peptide led to substantial shrinkage of tumor size in experimental animals, and its antitumor activity was far more pronounced when compared with that of nontargeted liposomal paclitaxel and free drug (Fig. 12.7c). Comparison of different systems revealed an interesting phenomenon. When we used the same cytotoxic

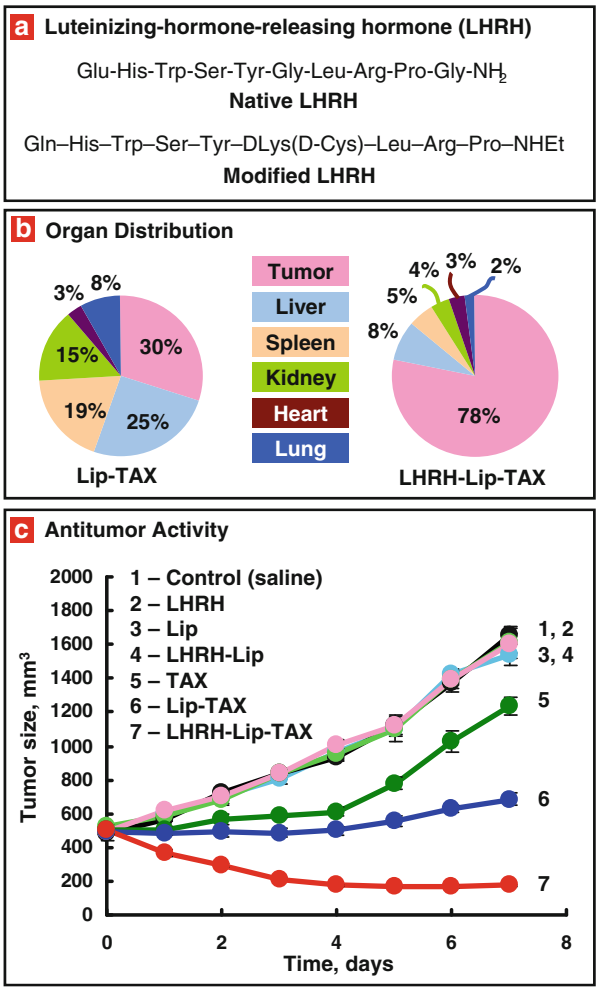


**Fig. 12.7** Targeting of extracellular receptors that are overexpressed in plasma membrane of many types of cancer cells by LHRH peptide increases drug accumulation in the tumor and enhances antitumor activity of liposomal form of paclitaxel (TAX). (**a**) Amino acid composition of native and modified LHRH peptide. (**b**) Organ distribution of paclitaxel delivered by nontargeted (Lip-TAX) and tumor-targeted (LHRH-Lip-TAX) PEGylated liposomes. (**c**) Antitumor activity of different formulations. Mice bearing xenografts of human A549 lung carcinoma were treated with free paclitaxel and different delivery systems with the same dose of TAX (2.5 mg/kg). Tumor volume was measured by a caliper every day for 7 days after the treatment. Means ± SD are shown. Modified from Saad et al. [95]

agent, targeting to tumors by LHRH peptide diminished variations between different DDS in terms of their cytotoxicity and antitumor efficacy. Consequently, internalization and intracellular distribution of DDS, but not size, molecular mass, composition, or architecture of the carrier play a critical role in the anticancer effect of tumor targeted chemotherapy.

This conclusion could have a broad impact on cancer drug delivery. In particular, tumor specific receptor targeting of nanocarriers could provide high antitumor therapeutic activity with low adverse side effects on healthy organs for practically any type of anticancer DDS. At the same time, other parameters of nanocarriers, including size, composition, architecture, etc., can be selected based on other considerations, such as type of therapeutic agent, aqueous solubility, electric charge, chemical structure, etc.

## 12.4 Summary

Targeting of anticancer agents specifically to tumor cells fulfills the following important tasks. First, it facilitates uptake of drugs by cancer cells; therefore, increasing intracellular concentration and enhancing anticancer activity. Second, targeting prevents uptake of antitumor therapeutics by cells in other organs, limiting adverse side effects. Third, drug targeting, receptor mediated endocytosis, and intracellular transport of delivered formulations in membrane limited organelles protect delivered drugs and other active components from drug efflux pumps and detoxification preserving their anticancer activity. Fourth, targeting can efficiently kill both localized primary tumor and spread metastatic cells. The combination of all aforementioned effects enhances the specificity of antitumor therapeutics and increases efficiency and safety of cancer chemotherapy. While this review was focused on cancer targeting, the lessons learned may be applied in other disease systems where cellular sensitivity and specificity of drug action are essential.

## References

1. Ehrlich P (1906) Studies in immunity. Plenium Press, New York
2. Minko T, Dharap SS, Pakunlu RI, Wang Y (2004) Molecular targeting of drug delivery systems to cancer. Curr Drug Targets 5(4):389–406
3. Vyas SP, Singh A, Sihorkar V (2001) Ligand-receptor-mediated drug delivery: an emerging paradigm in cellular drug targeting. Crit Rev Ther Drug Carrier Syst 18(1):1–76
4. Minko T (2004) Drug targeting to the colon with lectins and neoglycoconjugates. Adv Drug Deliv Rev 56(4):491–509
5. De Paoli P (2008) Novel virally targeted therapies of EBV-associated tumors. Curr Cancer Drug Targets 8(7):591–596
6. Kuo WT, Huang HY, Huang YY (2009) Intracellular trafficking, metabolism and toxicity of current gene carriers. Curr Drug Metab 10(8):885–894
7. Roy P, Noad R (2009) Virus-like particles as a vaccine delivery system: myths and facts. Adv Exp Med Biol 655:145–158
8. Pakunlu RI, Cook TJ, Minko T (2003) Simultaneous modulation of multidrug resistance and antiapoptotic cellular defense by MDR1 and BCL-2 targeted antisense oligonucleotides enhances the anticancer efficacy of doxorubicin. Pharm Res 20(3):351–359
9. Pakunlu RI, Wang Y, Tsao W, Pozharov V, Cook TJ, Minko T (2004) Enhancement of the efficacy of chemotherapy for lung cancer by simultaneous suppression of multidrug resistance and antiapoptotic cellular defense: novel multicomponent delivery system. Cancer Res 64 (17):6214–6224
10. Szakacs G, Jakab K, Antal F, Sarkadi B (1998) Diagnostics of multidrug resistance in cancer. Pathol Oncol Res 4(4):251–257
11. Minko T, Kopeckova P, Kopecek J (1999) Comparison of the anticancer effect of free and HPMA copolymer-bound adriamycin in human ovarian carcinoma cells. Pharm Res 16 (7):986–996
12. Harashima H, Shinohara Y, Kiwada H (2001) Intracellular control of gene trafficking using liposomes as drug carriers. Eur J Pharm Sci 13(1):85–89
13. Luzio JP, Parkinson MD, Gray SR, Bright NA (2009) The delivery of endocytosed cargo to lysosomes. Biochem Soc Trans 37(Pt 5):1019–1021

14. Sorkin A, Von Zastrow M (2002) Signal transduction and endocytosis: close encounters of many kinds. Nat Rev Mol Cell Biol 3(8):600–614
15. Torchilin VP (2006) Recent approaches to intracellular delivery of drugs and DNA and organelle targeting. Annu Rev Biomed Eng 8:343–375
16. Torchilin VP, Khaw BA, Weissig V (2002) Intracellular targets for DNA delivery: nuclei and mitochondria. Somat Cell Mol Genet 27(1–6):49–64
17. Beh CW, Seow WY, Wang Y, Zhang Y, Ong ZY, Ee PL, Yang YY (2009) Efficient delivery of Bcl-2-targeted siRNA using cationic polymer nanoparticles: downregulating mRNA expression level and sensitizing cancer cells to anticancer drug. Biomacromolecules 10(1):41–48
18. Cuchelkar V, Kopeckova P, Kopecek J (2008) Synthesis and biological evaluation of disulfide-linked HPMA copolymer-mesochlorin e6 conjugates. Macromol Biosci 8(5):375–383
19. Banerjee SS, Chen DH (2008) Multifunctional pH-sensitive magnetic nanoparticles for simultaneous imaging, sensing and targeted intracellular anticancer drug delivery. Nanotechnology 19(50):505104
20. Kale AA, Torchilin VP (2010) Environment-responsive multifunctional liposomes. Methods Mol Biol 605:213–242
21. Kasuya Y, Lu ZR, Kopeckova P, Minko T, Tabibi SE, Kopecek J (2001) Synthesis and characterization of HPMA copolymer-aminopropylgeldanamycin conjugates. J Control Release 74(1–3):203–211
22. Kasuya Y, Lu ZR, Kopeckova P, Tabibi SE, Kopecek J (2002) Influence of the structure of drug moieties on the in vitro efficacy of HPMA copolymer-geldanamycin derivative conjugates. Pharm Res 19(2):115–123
23. Khandare J, Minko T (2006) Polymer-drug conjugates: progress in polymeric prodrugs. Progr Polym Sci 31:359–397
24. Minko T, Khandare JJ, Jayant S (2007) Polymeric drugs. In: Matyjaszewski K, Gnanou Y, Leibler L (eds) Macromolecular engineering: from precise macromolecular synthesis to macroscopic material properties and application. WILEY-VCH Verlag GmbH & Co, Weinheim, pp 2541–2595
25. Khandare JJ, Chandna P, Wang Y, Pozharov VP, Minko T (2006) Novel polymeric prodrug with multivalent components for cancer therapy. J Pharmacol Exp Ther 317(3):929–937
26. Pack DW, Hoffman AS, Pun S, Stayton PS (2005) Design and development of polymers for gene delivery. Nat Rev Drug Discov 4(7):581–593
27. Kelemen LE (2006) The role of folate receptor alpha in cancer development, progression and treatment: cause, consequence or innocent bystander? Int J Cancer 119(2):243–250
28. Basal E, Eghbali-Fatourechi GZ, Kalli KR, Hartmann LC, Goodman KM, Goode EL, Kamen BA, Low PS, Knutson KL (2009) Functional folate receptor alpha is elevated in the blood of ovarian cancer patients. PLoS One 4(7):e6292
29. Yuan Y, Nymoen DA, Dong HP, Bjorang O, Shih M, Ie PS, Low CG, Low Trope CG, Davidson B (2009) Expression of the folate receptor genes FOLR1 and FOLR3 differentiates ovarian carcinoma from breast carcinoma and malignant mesothelioma in serous effusions. Hum Pathol 40(10):1453–1460
30. Corona G, Giannini F, Fabris M, Toffoli G, Boiocchi M (1998) Role of folate receptor and reduced folate carrier in the transport of 5-methyltetrahydrofolic acid in human ovarian carcinoma cells. Int J Cancer 75(1):125–133
31. Kularatne SA, Low PS (2010) Targeting of nanoparticles: folate receptor. Methods Mol Biol 624:249–265
32. Leamon CP, Low PS (1991) Delivery of macromolecules into living cells: a method that exploits folate receptor endocytosis. Proc Natl Acad Sci USA 88(13):5572–5576
33. Xia W, Low PS (2010) Folate-targeted therapies for cancer. J Med Chem 53(19):6811–6824
34. Atkinson SF, Bettinger T, Seymour LW, Behr JP, Ward CM (2001) Conjugation of folate via gelonin carbohydrate residues retains ribosomal-inactivating properties of the toxin and permits targeting to folate receptor positive cells. J Biol Chem 276(30):27930–27935

35. Yoo HS, Park TG (2004) Folate-receptor-targeted delivery of doxorubicin nano-aggregates stabilized by doxorubicin-PEG-folate conjugate. J Control Release 100(2):247–256
36. Kim YK, Choi JY, Yoo MK, Jiang HL, Arote R, Je YH, Cho MH, Cho CS (2007) Receptor-mediated gene delivery by folate-PEG-baculovirus in vitro. J Biotechnol 131(3):353–361
37. Hwa Kim S, Hoon Jeong J, Chul Cho K, Wan Kim S, Gwan Park T (2005) Target-specific gene silencing by siRNA plasmid DNA complexed with folate-modified poly(ethylenimine). J Control Release 104(1):223–232
38. Zheng Y, Song X, Darby M, Liang Y, He L, Cai Z, Chen Q, Bi Y, Yang X, Xu J, Li Y, Sun Y, Lee RJ, Hou S (2009) Preparation and characterization of folate-poly(ethylene glycol)-grafted-trimethylchitosan for intracellular transport of protein through folate receptor-mediated endocytosis. J Biotechnol 145(1):47–53
39. Zhang C, Gao S, Jiang W, Lin S, Du F, Li Z, Huang W (2010) Targeted minicircle DNA delivery using folate-poly(ethylene glycol)-polyethylenimine as non-viral carrier. Biomaterials 31(23):6075–6086
40. Biswal BK, Debata NB, Verma RS (2009) Development of a targeted siRNA delivery system using FOL-PEG-PEI conjugate. Mol Biol Rep 37(6):2919–2926
41. Wang H, Zhao P, Liang X, Gong X, Song T, Niu R, Chang J (2010) Folate-PEG coated cationic modified chitosan–cholesterol liposomes for tumor-targeted drug delivery. Biomaterials 31(14):4129–4138
42. Yang L, Li J, Zhou W, Yuan X, Li S (2004) Targeted delivery of antisense oligodeoxynucleotides to folate receptor-overexpressing tumor cells. J Control Release 95(2):321–331
43. Zhou W, Yuan X, Wilson A, Yang L, Mokotoff M, Pitt B, Li S (2002) Efficient intracellular delivery of oligonucleotides formulated in folate receptor-targeted lipid vesicles. Bioconjug Chem 13(6):1220–1225
44. Lu T, Sun J, Chen X, Zhang P, Jing X (2009) Folate-conjugated micelles and their folate-receptor-mediated endocytosis. Macromol Biosci 9(11):1059–1068
45. Han X, Liu J, Liu M, Xie C, Zhan C, Gu B, Liu Y, Feng L, Lu W (2009) 9-NC-loaded folate-conjugated polymer micelles as tumor targeted drug delivery system: preparation and evaluation in vitro. Int J Pharm 372(1–2):125–131
46. Fan L, Li F, Zhang H, Wang Y, Cheng C, Li X, Gu CH, Yang Q, Wu H, Zhang S (2010) Co-delivery of PDTC and doxorubicin by multifunctional micellar nanoparticles to achieve active targeted drug delivery and overcome multidrug resistance. Biomaterials 31 (21):5634–5642
47. Kim SH, Jeong JH, Mok H, Lee SH, Kim SW, Park TG (2007) Folate receptor targeted delivery of polyelectrolyte complex micelles prepared from ODN-PEG-folate conjugate and cationic lipids. Biotechnol Prog 23(1):232–237
48. Kang C, Yuan X, Li F, Pu P, Yu S, Shen C, Zhang Z, Zhang Y (2009) Evaluation of folate-PAMAM for the delivery of antisense oligonucleotides to rat C6 glioma cells in vitro and in vivo. J Biomed Mater Res A 93(2):585–594
49. Patri AK, Kukowska-Latallo JF, Baker JR Jr (2005) Targeted drug delivery with dendrimers: comparison of the release kinetics of covalently conjugated drug and non-covalent drug inclusion complex. Adv Drug Deliv Rev 57(15):2203–2214
50. Zhang C, Zhao L, Dong Y, Zhang X, Lin J, Chen Z (2010) Folate-mediated poly(3-hydroxybutyrate-*co*-3-hydroxyoctanoate) nanoparticles for targeting drug delivery. Eur J Pharm Biopharm 76(1):10–16
51. Dhar S, Liu Z, Thomale J, Dai H, Lippard SJ (2008) Targeted single-wall carbon nanotube-mediated Pt(IV) prodrug delivery using folate as a homing device. J Am Chem Soc 130 (34):11467–11476
52. Simonson OE, Svahn MG, Tornquist E, Lundin KE, Smith CI (2005) Bioplex technology: novel synthetic gene delivery pharmaceutical based on peptides anchored to nucleic acids. Curr Pharm Des 11(28):3671–3680

53. Jayant S, Khandare JJ, Wang Y, Singh AP, Vorsa N, Minko T (2007) Targeted sialic acid-doxorubicin prodrugs for intracellular delivery and cancer treatment. Pharm Res 24 (11):2120–2130
54. Oishi M, Nagatsugi F, Sasaki S, Nagasaki Y, Kataoka K (2005) Smart polyion complex micelles for targeted intracellular delivery of PEGylated antisense oligonucleotides containing acid-labile linkages. Chembiochem 6(4):718–725
55. Wakebayashi D, Nishiyama N, Yamasaki Y, Itaka K, Kanayama N, Harada A, Nagasaki Y, Kataoka K (2004) Lactose-conjugated polyion complex micelles incorporating plasmid DNA as a targetable gene vector system: their preparation and gene transfecting efficiency against cultured HepG2 cells. J Control Release 95(3):653–664
56. Cho CS, Cho KY, Park IK, Kim SH, Sasagawa T, Uchiyama M, Akaike T (2001) Receptor-mediated delivery of all *trans*-retinoic acid to hepatocyte using poly(L-lactic acid) nanoparticles coated with galactose-carrying polystyrene. J Control Release 77(1–2):7–15
57. Wang YC, Liu XQ, Sun TM, Xiong MH, Wang J (2008) Functionalized micelles from block copolymer of polyphosphoester and poly(epsilon-caprolactone) for receptor-mediated drug delivery. J Control Release 128(1):32–40
58. Frungillo L, Martins D, Teixeira S, Anazetti MC, Melo Pda S, Duran N (2009) Targeted antitumoral dehydrocrotonin nanoparticles with L-ascorbic acid 6-stearate. J Pharm Sci 98 (12):4796–4807
59. Luo Y, Bernshaw NJ, Lu ZR, Kopecek J, Prestwich GD (2002) Targeted delivery of doxorubicin by HPMA copolymer-hyaluronan bioconjugates. Pharm Res 19(4):396–402
60. Jiang G, Park K, Kim J, Kim KS, Oh EJ, Kang H, Han SE, Oh YK, Park TG, Kwang Hahn S (2008) Hyaluronic acid-polyethyleneimine conjugate for target specific intracellular delivery of siRNA. Biopolymers 89(7):635–642
61. Wulbrand U, Feldman M, Pfestroff A, Fehman HC, Du J, Hiltunen J, Marquez M, Arnold R, Westlin JE, Nilsson S, Holmberg AR (2002) A novel somatostatin conjugate with a high affinity to all five somatostatin receptor subtypes. Cancer 94(4 Suppl):1293–1297
62. Zhang J, Jin W, Wang X, Wang J, Zhang X, Zhang Q (2010) A novel octreotide modified lipid vesicle improved the anticancer efficacy of doxorubicin in somatostatin receptor 2 positive tumor models. Mol Pharm 7(4):1159–1168
63. Rosenzweig SA, Atreya HS (2010) Defining the pathway to insulin-like growth factor system targeting in cancer. Biochem Pharmacol 80(8):1115–1124
64. Laursen LS, Kjaer-Sorensen K, Andersen MH, Oxvig C (2007) Regulation of insulin-like growth factor (IGF) bioactivity by sequential proteolytic cleavage of IGF binding protein-4 and -5. Mol Endocrinol 21(5):1246–1257
65. Magadala P, Amiji M (2008) Epidermal growth factor receptor-targeted gelatin-based engineered nanocarriers for DNA delivery and transfection in human pancreatic cancer cells. AAPS J 10(4):565–576
66. Qiu Q, Domarkas J, Banerjee R, Katsoulas A, McNamee JP, Jean-Claude BJ (2007) Type II combi-molecules: design and binary targeting properties of the novel triazolinium-containing molecules JDD36 and JDE05. Anticancer Drugs 18(2):171–177
67. Dai FH, Chen Y, Ren CC, Li JJ, Yao M, Han JS, Gong Y, Yang SL, Zhu JD, Gu JR (2003) Construction of an EGF receptor-mediated histone H1(0)-based gene delivery system. J Cancer Res Clin Oncol 129(8):456–462
68. Kickhoefer VA, Han M, Raval-Fernandes S, Poderycki MJ, Moniz RJ, Vaccari D, Silvestry M, Stewart PL, Kelly KA, Rome LH (2009) Targeting vault nanoparticles to specific cell surface receptors. ACS Nano 3(1):27–36
69. Lee H, Kim TH, Park TG (2002) A receptor-mediated gene delivery system using streptavidin and biotin-derivatized, pegylated epidermal growth factor. J Control Release 83(1):109–119
70. Lee TK, Han JS, Fan ST, Liang ZD, Tian PK, Gu JR, Ng IO (2001) Gene delivery using a receptor-mediated gene transfer system targeted to hepatocellular carcinoma cells. Int J Cancer 93(3):393–400

71. Backer MV, Gaynutdinov TI, Gorshkova RJ II, Crouch T, Hu R, Aloise M, Arab KP, Backer JM (2003) Humanized docking system for assembly of targeting drug delivery complexes. J Control Release 89(3):499–511
72. Mai J, Song S, Rui M, Liu D, Ding Q, Peng J, Xu Y (2009) A synthetic peptide mediated active targeting of cisplatin liposomes to Tie2 expressing cells. J Control Release 139(3):174–181
73. Shoji M, Sun A, Kisiel W, Lu YJ, Shim H, McCarey BE, Nichols C, Parker ET, Pohl J, Mosley CA, Alizadeh AR, Liotta DC, Snyder JP (2008) Targeting tissue factor-expressing tumor angiogenesis and tumors with EF24 conjugated to factor VIIa. J Drug Target 16(3):185–197
74. Garanger E, Boturyn D, Dumy P (2007) Tumor targeting with RGD peptide ligands-design of new molecular conjugates for imaging and therapy of cancers. Anticancer Agents Med Chem 7 (5):552–558
75. Oba M, Fukushima S, Kanayama N, Aoyagi K, Nishiyama N, Koyama H, Kataoka K (2007) Cyclic RGD peptide-conjugated polyplex micelles as a targetable gene delivery system directed to cells possessing alphavbeta3 and alphavbeta5 integrins. Bioconjug Chem 18 (5):1415–1423
76. Dai W, Yang T, Wang X, Wang J, Zhang X, Zhang Q (2009) PHSCNK-Modified and doxorubicin-loaded liposomes as a dual targeting system to integrin-overexpressing tumor neovasculature and tumor cells. J Drug Target 18(4):254–263
77. Li H, Qian ZM (2002) Transferrin/transferrin receptor-mediated drug delivery. Med Res Rev 22(3):225–250
78. Lu Q, Teng GJ, Zhang Y, Niu HZ, Zhu GY, An YL, Yu H, Li GZ, Qiu DH, Wu CG (2008) Enhancement of p53 gene transfer efficiency in hepatic tumor mediated by transferrin receptor through *trans*-arterial delivery. Cancer Biol Ther 7(2):218–224
79. Jiang YY, Liu C, Hong MH, Zhu SJ, Pei YY (2007) Tumor cell targeting of transferrin-PEG-TNF-alpha conjugate via a receptor-mediated delivery system: design, synthesis, and biological evaluation. Bioconjug Chem 18(1):41–49
80. Hatakeyama H, Akita H, Maruyama K, Suhara T, Harashima H (2004) Factors governing the in vivo tissue uptake of transferrin-coupled polyethylene glycol liposomes in vivo. Int J Pharm 281(1–2):25–33
81. Eavarone DA, Yu X, Bellamkonda RV (2000) Targeted drug delivery to C6 glioma by transferrin-coupled liposomes. J Biomed Mater Res 51(1):10–14
82. Kobayashi T, Ishida T, Okada Y, Ise S, Harashima H, Kiwada H (2007) Effect of transferrin receptor-targeted liposomal doxorubicin in P-glycoprotein-mediated drug resistant tumor cells. Int J Pharm 329(1–2):94–102
83. Iinuma H, Maruyama K, Okinaga K, Sasaki K, Sekine T, Ishida O, Ogiwara N, Johkura K, Yonemura Y (2002) Intracellular targeting therapy of cisplatin-encapsulated transferrin-polyethylene glycol liposome on peritoneal dissemination of gastric cancer. Int J Cancer 99 (1):130–137
84. Maruyama K, Ishida O, Kasaoka S, Takizawa T, Utoguchi N, Shinohara A, Chiba M, Kobayashi H, Eriguchi M, Yanagie H (2004) Intracellular targeting of sodium mercaptoundecahydrododecaborate (BSH) to solid tumors by transferrin-PEG liposomes, for boron neutron-capture therapy (BNCT). J Control Release 98(2):195–207
85. Kakudo T, Chaki S, Futaki S, Nakase I, Akaji K, Kawakami T, Maruyama K, Kamiya H, Harashima H (2004) Transferrin-modified liposomes equipped with a pH-sensitive fusogenic peptide: an artificial viral-like delivery system. Biochemistry 43(19):5618–5628
86. Jhaveri MS, Rait AS, Chung KN, Trepel JB, Chang EH (2004) Antisense oligonucleotides targeted to the human alpha folate receptor inhibit breast cancer cell growth and sensitize the cells to doxorubicin treatment. Mol Cancer Ther 3(12):1505–1512
87. Chen S, Zhao X, Chen J, Kuznetsova L, Wong SS, Ojima I (2010) Mechanism-based tumor-targeting drug delivery system. Validation of efficient vitamin receptor-mediated endocytosis and drug release. Bioconjug Chem 21(5):979–987

88. Chen J, Chen S, Zhao X, Kuznetsova LV, Wong SS, Ojima I (2008) Functionalized single-walled carbon nanotubes as rationally designed vehicles for tumor-targeted drug delivery. J Am Chem Soc 130(49):16778–16785
89. Yuan H, Luo K, Lai Y, Pu Y, He B, Wang G, Wu Y, Gu Z (2010) A novel poly(L-glutamic acid) dendrimer based drug delivery system with both pH-sensitive and targeting functions. Mol Pharm 7(4):953–962
90. Chandna P, Saad M, Wang Y, Ber E, Khandare J, Vetcher AA, Soldatenkov VA, Minko T (2007) Targeted proapoptotic anticancer drug delivery system. Mol Pharm 4(5):668–678
91. Dharap SS, Minko T (2003) Targeted proapoptotic LHRH-BH3 peptide. Pharm Res 20 (6):889–896
92. Dharap SS, Qiu B, Williams GC, Sinko P, Stein S, Minko T (2003) Molecular targeting of drug delivery systems to ovarian cancer by BH3 and LHRH peptides. J Control Release 91 (1–2):61–73
93. Dharap SS, Wang Y, Chandna P, Khandare JJ, Qiu B, Gunaseelan S, Sinko PJ, Stein S, Farmanfarmaian A, Minko T (2005) Tumor-specific targeting of an anticancer drug delivery system by LHRH peptide. Proc Natl Acad Sci USA 102(36):12962–12967
94. Minko T, Patil ML, Zhang M, Khandare JJ, Saad M, Chandna P, Taratula O (2010) LHRH-targeted nanoparticles for cancer therapeutics. Methods Mol Biol 624:281–294
95. Saad M, Garbuzenko OB, Ber E, Chandna P, Khandare JJ, Pozharov VP, Minko T (2008) Receptor targeted polymers, dendrimers, liposomes: which nanocarrier is the most efficient for tumor-specific treatment and imaging? J Control Release 130(2):107–114
96. Taratula O, Garbuzenko OB, Kirkpatrick P, Pandya I, Savla R, Pozharov VP, He H, Minko T (2009) Surface-engineered targeted PPI dendrimer for efficient intracellular and intratumoral siRNA delivery. J Control Release 140(3):284–293
97. Conn PM, Hazum E (1981) Luteinizing hormone release and gonadotropin-releasing hormone (GnRH) receptor internalization: independent actions of GnRH. Endocrinology 109 (6):2040–2045

# Part V
# Applications

# Chapter 13
# Biological Rhythms, Drug Delivery, and Chronotherapeutics

**Michael H. Smolensky, Ronald A. Siegel, Erhard Haus, Ramon Hermida, and Francesco Portaluppi**

**Abstract** Biological processes are highly structured in time as endogenously derived rhythms of short, intermediate, and long periods, with the circadian (24 h) time structure most studied. Staging of key physiological and biochemical circadian rhythms gives rise to 24-h patterns in the exacerbation of chronic medical conditions, including arthritis, asthma, ulcer, and hypertension, plus manifestation of acute severe morbid and mortal events, such as myocardial infarction, stroke,

M.H. Smolensky (✉)
Department Biomedical Engineering, The University of Texas at Austin, 1 University Station, Mail Code CO800, Austin, TX 78712-0238, USA
e-mail: Michael.H.Smolensky@uth.tmc.edu; msmolensky@austin.rr.com

R.A. Siegel
Departments of Pharmaceutics and Biomedical Engineering, University of Minnesota, Minneapolis, MN 55419, USA

Department of Pharmaceutics WDH 9-177, University of Minnesota, 308 Harvard St. S.E., Minneapolis, MN 55455, USA
e-mail: siege017@umn.edu

E. Haus
Department of Laboratory Medicine and Pathology, University of Minnesota, Minneapolis, MN, USA

HealthPartners Medical Group, Regions Hospital, St. Paul, MN, USA
e-mail: Erhard.X.Haus@Healthpartners.com

R. Hermida
Bioengineering & Chronobiology Laboratories, University of Vigo, Campus Universitario, Vigo, Spain
e-mail: Rhermida@uvigo.es

F. Portaluppi
Department of Clinical and Experimental Medicine, Hypertension Center, University Hospital S. Anna, University of Ferrara, Ferrara, Italy
e-mail: prf@unife.it

J. Siepmann et al. (eds.), *Fundamentals and Applications of Controlled Release Drug Delivery*, Advances in Delivery Science and Technology,
DOI 10.1007/978-1-4614-0881-9_13, 

and sudden cardiac death. Body rhythms may also significantly affect patient response to diagnostic tests and pharmacokinetics, pharmacodynamics, and toxicities of diverse classes of medications. This chapter reviews circadian and other period biological rhythm dependencies of the pathophysiology of disease and pharmacology of medications as the basis for chronotherapeutics and development of time-modulated drug-delivery systems.

## 13.1 Introduction

This chapter introduces the concepts of medical chronobiology and chronotherapetics to biomedical engineers and pharmaceutical scientists, particularly those involved in drug-delivery system design. *Chronobiology*, the study of biological rhythms and the mechanisms of biological time keeping, is of fundamental importance to drug-delivery. Herein, we present the perspectives of (1) chronopathology, i.e., rhythms in the manifestation and severity of medical conditions and diseases; (2) chronopharmacology, i.e., biological rhythm dependent differences in the pharmacokinetics (PK) and pharmacodynamics (PD) of medications; (3) time-qualified reference values as they relate to improved clinical laboratory diagnostics and assessment of new drug-delivery pharmaceutical products; (4) chronotherapeutics, i.e., synchronization of therapeutic agents to time patterns in medical conditions and disease pathology; (5) chronotoxicology, i.e., rhythms in tolerance to chemical, physical, and biological interventions; and (6) chronoprevention, i.e., application of biological rhythm-based strategies to minimize, and even avert, risk to health and well being.

The understanding of biological rhythms and biological clocks and applications to medicine and therapeutics are rather recent developments. There are several explanations for this. First, instrumentation and analytical tools, including sophisticated hardware and software to gather and process time series data (data collected over time), to conduct biological rhythm research were not developed until after the middle of the twentieth century. Second, the concept of biological rhythmicity was viewed as being inconsistent with the long-held, primary principle of homeostasis that alleges relative constancy of the *milieu intérieur* (English: internal environment). The concept of homeostasis is based primarily on research conducted by Claude Bernard in France late in the nineteenth century and Walter Cannon in the USA early in the twentieth century. Technology did not exist then to continuously monitor biological parameters, e.g., heart rate, blood pressure, body temperature, and activity level, and at that time methods to determine constituents and their concentrations in biological fluids were slow and bulky, requiring as much as a pint of blood to conduct even a single time-of-day analysis of some variables. Data analysis and mining were difficult and tedious, since computer based methods to detect and quantify time series data for rhythms did not yet exist. Furthermore, most biological and medical research was conducted during the light of the day, at the convenience of diurnally active investigators and staff. Thus, the understanding of animal and human biology in the nineteenth and early twentieth century, and even to a great extent today, is based largely on findings of daytime investigations performed on nocturnally active laboratory mice and rats – a time of day that corresponds to the animals' sleep span – and on diurnally active human beings during their wake span. The results of such single

time-of-day studies are representative only of one particular biological time, which might not be appropriately representative.

Many thousands of articles have been published in highly respected scientific, medical, and pharmacology journals over the past several decades documenting relevant high-frequency or pulsatile oscillations (tenths of seconds to 1–2 h), ultradian (roughly 2–20 h), circadian (~24 h), circaseptan (~7 day), circamensual (~1 month), and circannual (~1 year) rhythms in humans and animals [1, 2]. Nonetheless, the concept of homeostasis continues to be taught as the governing doctrine of the life sciences Thus, it is not surprising that homeostasis continues to be the foundation for conceptualizing most biological, medical, and pharmaceutical research and applications. Perhaps, this explains why highly accomplished scientists assume, a priori, that the time during the day, month, and year when biomedical research is performed and when preclinical and clinical studies of candidate medications or other medical interventions are trialed is of little or no importance. Perhaps this also explains why the vast majority of drug delivery systems are designed for zero-order release, as it is assumed constancy in drug concentration ensures constancy in therapeutic effect and/or drug safety. However, homeostasis and rhythmicity are compatible concepts, as endogenous biological rhythms give rise to high frequency, 24-h, menstrual, and annual oscillations in the set points of homeostatic feedback mechanisms.

## 13.2 Concepts and Terminology of Chronobiology

### *13.2.1 Definition and Characteristics of Biological Rhythms*

#### 13.2.1.1 Biological Rhythm

A biological rhythm is a self-sustaining oscillation of endogenous origin defined by its period, level, amplitude, and phase as illustrated in Fig. 13.1 for the 24-h rhythm in plasma cortisol.

#### 13.2.1.2 Period

Period is the duration of time required to complete a single cycle of a biological rhythm. The spectrum of biological rhythms is broad. Short period rhythms, exemplified by electrical impulses of the central and autonomic nervous systems, cardiac tissue, and intracellular calcium fluxes, exhibit a period of a second or so. Circhoral (~1 h in period) or ultradian (from a few to 20 h in period) rhythms are exemplified by the prominent secretions of the endocrine and neuroendocrine systems. Circadian rhythms, which exhibit a period of ~24 h, have been most explored for their importance to clinical medicine. Infradian rhythms, oscillations of 28 h or longer, include those of roughly a week (circaseptan), month (circamensual), and year (circannual). Individual biological variables and processes are typically organized all across this multifrequency time structure [3].

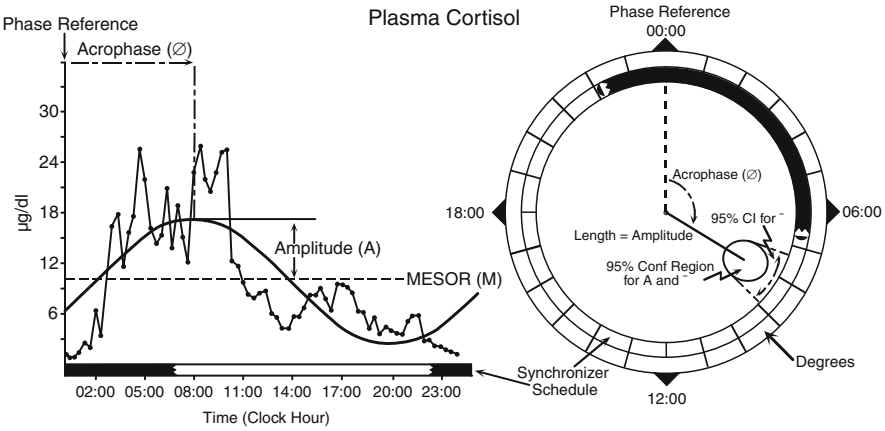


**Fig. 13.1** Plasma cortisol 24-h pattern of one diurnally active (wake span ~06:30 to ~22:30) healthy subject assessed by blood sampling at 20-min intervals during a single 24-h span. *Left*: Time plot (chronogram) of cortisol time series data. Apparent are the prominent, high-frequency pulses commencing during mid-sleep and continuing until ~12:00. Rhythm parameters derived by the Cosinor procedure [84], approximation of the time series data by a 24-h in period cosine curve by the least squares technique, are MESOR, rhythm-adjusted time series mean; amplitude, one-half the peak–trough difference or distance from MESOR to peak (or trough) of the approximating waveform; and acrophase, timing of peak of the rhythm in relation to the chosen phase reference, here local midnight. The less than ideal sinusoidality of the time series data and infrequent sampling are potential pitfalls of the Cosinor method. *Black* and *white portions* of the bottom time axis indicate the subject's usual span of nighttime sleep and daytime activity. *Right*: Polar cosinor plot. The period length (here 24 h) is depicted as a *full circle*, with local midnight (phase reference of acrophase) located at *top* of the *circle*. Rest span is indicated by *darkened band*. Vector extending from the center points to the acrophase (expressed as a negative value [delay] in degrees [$360^{o} = 24$ h; $15^{o} = 1$ h] from local midnight), and its length is proportional to the amplitude of the rhythm. Error ellipse of vector indicates 95% confidence region for amplitude and acrophase [3]

### 13.2.1.3 Level

Level is the baseline, i.e., mean value of the rhythm, around which predictable in time variation is manifested. The level of ultradian rhythms may be modulated in a predictable-in-time manner over the 24 h as a circadian rhythm, which in turn may be modulated in a predictable-in-time manner over the month as a menstrual rhythm, and also over the year as a circannual rhythm.

### 13.2.1.4 Amplitude

Amplitude is a measure of the magnitude of the predictable-in-time variability ascribable specifically to biological rhythmicity of a given period. Many rhythms are of high amplitude, accounting for 50% or more of the total variability observed during the time period. Amplitudes of rhythms may change, e.g., with aging, in disease, and by work pattern (shift work). For example, the circadian rhythm in

antidiuretic hormone (ADH), which regulates urine volume, is of very high amplitude in young adults. Peak ADH concentration occurs during the nighttime to ensure reduced urine formation and volume during sleep, so that urine formation and volume are much greater while awake than asleep. However, the amplitude of the ADH circadian rhythm declines with age. Commencing around the 4th to 5th decade of life, the peak of the 24-h rhythm in urine volume shifts toward the middle of the night, the result being nocturia, with frequent disturbances of nighttime sleep [4, 5]. As a second example, the amplitude of the circadian rhythm in airway caliber of normal lungs is very small, ~5% of the 24-h mean level. However, in persons with mild asthma, amplitude is typically increased to 25%, and in severe asthma it can be as high as 50–60% [6].

#### 13.2.1.5 Phase

Phase refers to the clocking of specific features, such as the peak and trough, of a rhythm relative to a reference point of a given time scale, e.g., for circadian rhythms local midnight, or more appropriately the sleep onset, mid-sleep, or sleep offset time of the 24-h sleep–wake cycle or acrophase (peak time) of another concomitantly studied circadian rhythm. The phasing of the high-amplitude circadian rhythm of serum cortisol concentration relative to local midnight in diurnally active individuals is marked by its prominent peak of ~20 μg/dl around 08:00 and trough of ~0 μg/dl around midnight (Fig. 13.1). Phasing of the same circadian rhythm in persons completely adapted to night-shift work is marked, again relative to local midnight clock time, by its peak ~18:00 and trough ~10:00. If one were to average together the time-of-day data series of cortisol values of both day and night-shift workers, differences in phasing of the cortisol rhythm between the two groups would likely obscure circadian rhythmicity as a group phenomenon. However, if the 24-h time series data were instead referenced to a relevant biological time reference, such as the habitual time of wakening, for each person adapted to his/her daytime or nighttime routine and then averaged, the prominent circadian rhythm would be obvious, with the peak time around usual wake up time and trough around or a few hours after habitual bedtime, no matter the clock time [7–9].

## 13.3 Mechanisms of Biological Time-Keeping

### *13.3.1 Master Biological Clock, the Suprachiasmatic Nuclei*

Circadian rhythms are controlled by an inherited master clock network composed of the paired suprachiasmatic nuclei (SCN) situated in the hypothalamus and pineal gland [10–13]. Rhythmic activities in the SCN of the so-called clock genes, *Per1, Per2, Per3, Bmal, Clock, and Cry*, and their gene products comprise the central time-keeping mechanism. The transcription factors CLOCK and BMAL1 drive the

expression of *Per1, Per2, Cry1, Cry2,* plus a variety of clock controlled genes via E-box sequences in their promoters. PER and CRY proteins negatively feedback on the transcriptional activity of CLOCK:BMAL1, which results in a circadian rhythm in expression of the CLOCK:BMAL1 driven clock and clock controlled genes. The rhythm is stabilized by accessory feedback loops involving the genes *Rev-erbα* and *Rora*. The precision of the period of circadian rhythms is achieved via post-translational modulation of the clock proteins by cyclic environmental time cues, the most important being the 24-h environmental light–dark cycle [14]. The biological time-keeping system also includes the multitude of peripheral circadian clocks located in cells, tissues, and organs, which are regulated by the master SCN clock [11]. The output of the central and peripheral circadian clocks is mediated by various clock-controlled genes, giving rise to the body's circadian time structure (CTS).

The proper phasing of individual circadian rhythms to meet the external cyclic environmental and societal demands and achieve optimal external synchronization of the CTS is conveyed by ambient time cues termed *zeitgebers* (English: time givers and synonymous with the terms of *synchronizers* and *entraining agents*), the light–dark cycle being most powerful under ordinary circumstances [14, 15]. Time cues in the form of ambient light signals sensed by specific non-rod and non-cone cells of the retina are transmitted by the retino-hypothalamic neural projection directly to the SCN and thereafter to the pineal gland by relays involving the paraventricular nucleus and superior cervical ganglion [12]. The major secretory product of the pineal gland is the hormone melatonin. Its synthesis and secretion are highly circadian rhythmic, occurring only during the darkness of night in the diurnally active human species, and for this reason it is termed the hormone of darkness. Melatonin, being water and fat soluble, freely circulates to the cells, tissues, and organs throughout the body, and it also binds to specific melatonin receptor types to induce particular actions [12]. Information of environmental time, specifically, the duration of ambient darkness (time span between sunset and sunrise) daily is conveyed throughout the body by the melatonin onset and offset times. Changes in the duration of time between sunrise and sunset from one day to the next over the course of the year communicate time of year information to the organism via changes in melatonin onset and offset times, i.e., changing duration of melatonin secretion. Exposure to artificial light during the biological nighttime, either in the home, work, or social setting, or to natural environmental light of a new geographic locality following rapid transmeridian displacement by aircraft, alters melatonin synthesis and secretion (Sect. 13.4.2), which by means of feedback to the SCN results over several days in rephrasing of the CTS.

### *13.3.2 Synchronizers of Biological Rhythms*

A *synchronizer* or *zeitgeber* is an environmental time cue that affects the period and/or phase of biological rhythms. The inherited period of circadian clocks, for as yet unknown reasons, is not exactly 24 h; it is a few tenths of an hour longer in most

human beings and slightly shorter in some [15]. The master and subservient peripheral circadian clocks are synchronized in period to 24.00 h and in phase with ambient and social cycles by environmental time cues. For both rodents and human beings, the major *zeitgeber* is the ambient 24-h light–dark cycle [12]. Others include meal schedule, an especially powerful time cue for laboratory animals, and cyclic social phenomena and routines, especially powerful time cues for humans [7, 16]. Features of the natural light–dark cycle vary predictably over the 24 h, month, and year. In human beings, the central circadian clock network relies on the ambient (natural or artificial) daily light–dark cycle to titrate its period to exactly 24 h and to determine phase so as to best meet predictable-in-time environmental demands [17]. The network also registers the duration (sunrise or lights on until sunset or lights off) of the daily environmental photoperiod to adjust the biology seasonally, giving rise to circannual rhythms. The importance of the 28-day lunar cycle on the menstrual cycle in women or on the biology of men is yet to be appropriately explored.

We wish to emphasize that the sleep–wake and environmental light–dark synchronizer cycles are not the source or cause of biological rhythms; rather, they serve only as time cues that synchronize the period and phase of endogenous genetically based circadian clock mechanisms and the oscillations they drive. This distinction is of critical importance in clinical medicine and pharmacology. The phase of circadian rhythms of persons whose time organization is adjusted to a routine of nocturnal activity and work alternating with diurnal sleep will be completely opposite to that of persons whose time organization is adjusted to a routine of diurnal work and activity alternating with nocturnal sleep [8, 9]. This means that clock time, per se, need not be representative of biological time. Review of the methods sections of published human research studies and medication trials reveals that the activity–sleep synchronizer routine is rarely contemplated or stipulated as an inclusion or exclusion criterion for subject selection, except in publications authored by chronobiologists. Similarly, the time of day when investigative procedures are conducted or when a medication is routinely dosed, relative to the sleep in darkness–activity in light synchronizer schedule of subjects, is seldom specified in published research, except in publications authored by chronobiologists. Time of year of investigations is seldom conveyed, and this may be of great importance in certain medication trials, as shown, for example, for human growth hormone and adrenocorticotropic hormone, ACTH [18–20]. Inconsistencies in findings between different human research studies and drug trials can be due to discrepancies in the synchronizer routine of subject samples and/or the chosen timing of procedures, including drug dosing (Sects. 13.5, 13.7, and 13.8).

Timing of the peaks and troughs of circadian rhythms is quite predictable from one day to the next in the majority of people who adhere to a fairly regular activity–sleep routine. However, the phase, and sometimes even exact period, of circadian rhythms in those who are employed in rotating shift work, those who have recently traveled across multiple time zones, or those who have a variable rest–activity routine, are less predictable [8, 9]. This point is of research and clinical importance.

The activity in light and sleep in darkness routine determine when the peak and trough of circadian rhythms will occur with reference to the 24-h time scale, which, in turn, determines when diseases and their symptoms are likely to manifest or exacerbate. It also determines, qualitatively and quantitatively, responses to diagnostic tests (Sect. 13.5) and the efficacy and safety of therapeutic interventions according to their timing (Sects. 13.7 and 13.8).

## 13.4 Biological Time Structure

The biological time structure consists of the spectrum of periodicities and phase relationships within each. Results of numerous biological rhythm studies help define the temporal organization of human beings. The CTS, which is of particular importance to medical and pharmaceutical sciences, is the major focus of this chapter.

### *13.4.1 Circadian Time Structure*

The CTS encompasses the entirety of the body's circadian biological rhythms. One means of illustrating the human CTS is to depict the peak times of selected 24-h rhythms as a clock-like diagram, such as shown in Fig. 13.2, in relation to the synchronizer routine, i.e., sleep in darkness from ~22:30 to ~06:30 and activity during daylight and early night between ~06:30 and ~22:30 [21]. As depicted in the figure, the peak of the circadian rhythms of basal gastric acid secretion, white blood cell count (WBC), calcitonin gene related protein, and atrial natriuretic peptide occurs late at night or early in sleep. The crest of the circadian rhythms in blood lymphocyte and eosinophil number, and plasma concentrations of melatonin, prolactin, growth hormone, thyroid stimulating hormone (TSH), ACTH, follicle stimulating hormone (FSH), and luteinizing hormone (LH) occurs mainly early in sleep. Rhythms of plasma cortisol, renin activity, angiotensin, and aldosterone peak toward the end of the sleep span or commencement of the diurnal activity span, as do those of arterial compliance, vascular resistance, platelet aggregation, and blood viscosity. Hemoglobin and insulin concentrations peak in the afternoon, as do the spirometric measures of airways caliber, $FEV_1$ (forced expiratory volume in one second) and PEF (peak expiratory flow). The circadian rhythms of serum cholesterol and triglycerides and urinary diuresis (young adults) crest early in the evening.

The information conveyed in Fig. 13.2 illustrates the nature of the CTS and its internal and external synchronization. Clearly, the biochemistry and physiology of human beings are not constant. Rather, they vary in a predictable and coordinated manner during the 24 h. It is worth considering that certain high amplitude circadian rhythmic variables, found in health and disease, might be useful

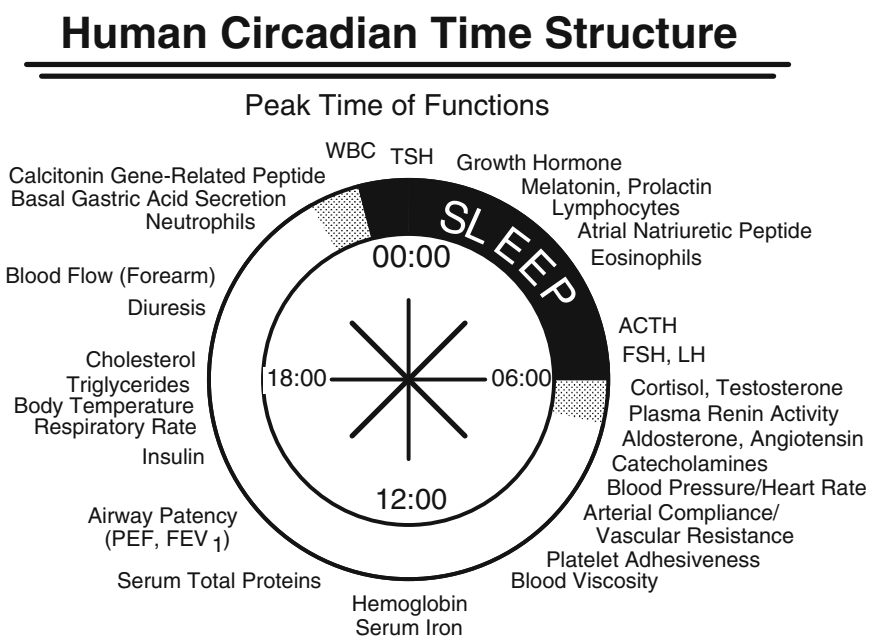


**Fig. 13.2** Clock-like diagram illustrating the circadian rhythmic organization of the acrophases (peak times) of selected biological variables. In diurnally active individuals, thyroid stimulating hormone (TSH), melatonin, prolactin, growth hormone, atrial natriuretic peptide, and lymphocyte and eosinopil numbers peak during first half of sleep (*shaded portion* of the *circular diagram*). Other shown variables peak just before or after the usual time of morning awakening, i.e., follicle stimulating hormone (FSH); luteinizing hormone (LH); adrenocorticotropic hormone (ACTH); cortisol; testosterone; and plasma renin, angiotensin, aldosterone, and catecholamines. In the morning, most persons experience sudden rise in systolic and diastolic blood pressure and heart rate, and arterial compliance and vascular resistance are greatest as are platelet adhesiveness and blood viscosity. Hemoglobin and serum iron levels peak around midday, and serum total proteins, airway patency (spirometric measures of one second forced expiratory volume, i.e., $FEV_1$, and peak expiratory flow, i.e., PEF), plus insulin level peak in the afternoon. Body temperature and respiratory rate circadian rhythms peak in late afternoon or early evening and cholesterol and triglyceride synthesis rhythms peak in early evening. Urine volume is greatest in late afternoon and evening (in young adults), and neutrophil count, basal gastric acid secretion, calcitonin gene-related protein concentration (a vasodilator), and white blood count (WBC) peak late in the evening or around bedtime (reproduced from Smolensky and Peppas [21])

biomarkers to automatically trigger measured medication release from sophisticated biomimetic drug delivery systems.

In individuals who are completely adapted to a schedule of night work, say from 22:00 to 06:00, and daytime sleep, say from 08:00 to 16:00, the clock time entries shown in the diagram would be shifted (delayed) by some 9–10 h; however, the findings of recent studies reveal the majority of night and shift workers do not adapt to such work schedules because of competing social, environmental, and other diurnal zeitgebers [22].

#### 13.4.1.1 Individual differences in CTS

Human beings, because of the genetics of their inherited circadian clock or due to age, sex, lifestyle, or disease, differ in their biological preference for the times of sleep and wakefulness. *Chronotype* refers to the time preference of sleep and activity of individuals and associated minor differences in the exact circadian phasing of their CTS.

#### 13.4.1.2 Circadian Chronotypes

Three different phenotypes of circadian phasing, i.e., chronotypes, can be distinguished using validated questionnaires, such as the Morningness–Eveningness Questionnaire of Horne and Östberg [23]. Morning types, commonly referred to as larks, are most alert and efficient during the morning hours. They express strong preference for early morning waking and early evening bed times, as early as 04:00 and 19:00–21:00, respectively, in extreme morning types. Evening types, commonly referred to owls, are most alert and efficient late in the day and night. They express strong preference for late night bed and late morning or afternoon waking times, as late as 02:00–04:00 and midday or later, respectively, in extreme evening types [24, 25]. The remaining intermediate types constitute the vast majority, perhaps 70–85%, of the population. With reference to the CTS of intermediate types, the clock-time phasing of circadian rhythms, e.g., body temperature, cortisol, and melatonin, of extreme morning types is likely to be advanced on average by ~2 h, while that of extreme evening types is likely to be delayed on average by ~2 h [26–28]. Nonetheless, the CTS of the different chronotypes in most cases shows an internal synchronization, with phasing adjusted to the circadian sleep–wake rhythm, although in extreme owls this may be not the case because of too great a conflict between usual environmental light–dark cycle and societal, school, and work synchronizer schedules versus endogenous biological clock driven preference for very late sleep and activity timings.

### *13.4.2 Phase–Response of Circadian Rhythms*

Pharmacologists, toxicologists, and other biological scientists are well acquainted with the concept of dose–response. An important, yet less known, chronobiologic concept is phase–response. *Phase–response* refers to the difference of effect, advance or delay of individual circadian rhythms or the entire CTS, elicited by environmental time signals, chemicals, or other agents. As previously discussed, phase and period of circadian clocks and rhythms are maintained from day to day by entraining cues provided by the onset and offset times of the natural environmental photoperiod. Figure 13.3 depicts the phase–response curves for both light pulses

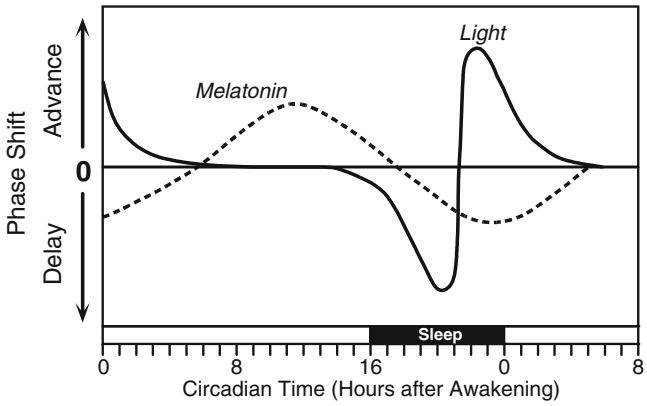


**Fig. 13.3** Phase–response (delay or advance of circadian time structure) curves for light (*solid line*) and melatonin (*dashed line*) in relation to circadian time (expressed relative to the usual time of awakening from nighttime sleep). Exposure of human beings to light of sufficient intensity before customary bedtime and/or during initial hours of sleep results in phase-delay of the circadian rhythm of melatonin and other circadian rhythms the ensuing 24-h, while the same light exposure when timed during the last hours of sleep or initial hours of waking results in phase-advance. The phase–response curve for melatonin is opposite that for light. Ingestion of a physiologic dose (0.25–0.50 mg) of melatonin in the afternoon or early evening results in phase-advance of the melatonin and other circadian rhythms the ensuing 24-h, while ingestion of the same dose of melatonin in the morning results in phase-delay. Indicated at the bottom is circadian time, which represents the expected endogenous phasing of the circadian melatonin rhythm and 24-h time structure of the studied subjects (modified from Burgess et al. [29])

and melatonin administrations when delivered at different circadian times. A single brief exposure of diurnally active human beings to bright artificial light at unusual biological times of the late night or early sleep (dark) span causes phase delay of the CTS by up to 1 h the ensuing 24 h. On the other hand, exposure to the same identical artificial bright light signal very early in the morning, before sunrise and prior to the end of the nocturnal sleep span, causes phase advance of the CTS. In contrast, identical light exposure during the middle of day, when the ambient environment is normally brightly lit, results in no alteration of circadian phase. The phase–response curve for melatonin is opposite the one for light [29–31]. Melatonin administration in the morning is phase delaying, in the early evening phase advancing, and overnight without effect (Fig. 13.3).

Synthesis and secretion of melatonin in the pineal gland are governed by signals from the SCN in the form of sympathetic input, the neurotransmitter being noradrenalin, which acts via pineal gland $ß_1$-receptors and also α-receptors. Acute, mainly single-dose studies show that both $ß_1$-receptor antagonists, especially the (*S*)-enantiomers of atenolol, propranolol, metropolol, and bisoprolol, and α-receptor antagonists, especially when administered in the evening, inhibit melatonin synthesis and secretion, resulting in alteration or abolition of its circadian rhythm [32–35]. The clinical consequences of chronic alteration or inhibition of melatonin rhythmicity can include CTS alteration or desynchronization, biological and

cognitive inefficiency, sleep and mood disorder, and perhaps even certain cancers [36–39]. Thus, it is critical that the administration of $ß_1$- and α-receptor agonists and other classes of medications not disrupt the melatonin circadian rhythm and CTS. The impact of dosing medications at different times of the day or night on the phasing of circadian clocks and rhythms, as an adverse effect of pharmacotherapy, has not been assessed in clinical trials. Nonetheless, a goal of pharmacotherapy ought to be avoidance of phase alterations of the circadian system, the exception being the use of certain chemical (melatonin), physical (artificial bright light), or other therapies to restore abnormal circadian clock function and CTS to normal [40–42].

### *13.4.3 Impact of Transmeridian Travel and Rotating Shift and Permanent Night Work on CTS*

Integrity of the CTS is critical for efficient biological and cognitive functioning and maintenance of health. Millions of people each year are either exposed acutely to transient disruptions of their sleep–wake cycle and CTS by rapid travel across time zones or chronically at regular intervals when working rotating or permanent night shift schedules. In the USA, ~15–20% of the adult labor force is likely to be engaged in some type of shift work at any given time, and in developing countries the proportion is likely to be even greater [43]. Disruption of the CTS due to rapid travel across time zones or rotating work schedule typically results in a set of acute and transient symptoms during the several days of adjustment to the new activity–rest cycle and differently timed environmental synchronizers, including light–dark, social, and meal cycles, among others.

These “jet lag” symptoms, so-called even though they occur in nontravelers as a consequence of rotating between day and night work shifts, include fatigue and sleepiness, difficulty in initiating and maintaining sleep, cognitive and physical deficits, changed mood (melancholy/anxiety), altered appetite, digestive complaints, and disrupted digestive track function [9]. Night and rotating shift workers experience disruption of the CTS and several or all of the same symptoms to some degree with each shift change between day and night work, which occurs at regular, typically weekly or shorter, intervals [8, 9]. Moreover, shifting of the sleep–wake pattern and/or regular exposure to light while at work during the night disrupts the CTS and alters or suppresses the melatonin circadian rhythm [8, 22]. Repetition of these biological insults over one’s shift work career poses health risks, such as sleep/mood disorder, peptic ulcer disease (PUD), hypertension, coronary heart disease, plus elevated risk of breast and colorectal cancer in women and prostate cancer in men [9, 36, 38, 39, 44–48]. Substantiation of these health risks in career shift workers supports the integrity of the CTS as a most important aspect of health, and again indicates that therapeutic interventions by drug delivery systems must avoid disturbance of the circadian time keeping system.

## 13.5 Medical Chronobiology: Application of Biological Rhythms to Clinical Medicine

### *13.5.1 Circadian Rhythms and Clinical Diagnostic Tests*

#### 13.5.1.1 Allergic Rhinitis and Bronchial Asthma

Responses to a variety of common diagnostic tests may be affected by circadian rhythms. The erythema and induration response to intradermally injected allergens, a clinical test for allergies, is two- to threefold greater when performed in the late afternoon and early evening (in diurnally active persons) than morning [49, 50]. Diagnosis of the reversible airway disease asthma, its severity, and its differentiation from fixed airway diseases, namely chronic bronchitis and emphysema, is best accomplished when pulmonary function tests ($FEV_1$ and PEF) are performed as early as feasible after commencement of the diurnal activity span [6, 50]. The airway response to short-acting ß$_2$-agonist bronchodilator aerosol medications, a test to determine the extent to which airway obstruction is reversible, is circadian rhythmic, the response being much stronger in diurnally active individuals when administered in the early morning than afternoon [51]. Thus, early morning so-called reversibility spirometric studies best determine the extent to whether a patient's chronic obstructive pulmonary disease is reversible, as opposed to nonreversible in the case of chronic bronchitis and emphysema, critical information needed for deciding exact pharmacotherapy [50].

#### 13.5.1.2 Systemic Hypertension

The diagnosis of arterial hypertension, a medical condition rather than a disease, which when not properly treated can result in cardiovascular, renal, and other pathologies, is typically based on systolic and diastolic blood pressure (SBP and DBP) measurements made in the doctor's office at a single time of day and interpreted using fixed homeostatic criteria (Table 13.1 [52]). However, as shown by many thousands of around the clock ambulatory blood pressure monitoring (ABPM) studies, SBP and DBP vary considerably during the 24 h and in different individuals as distinctly different circadian patterns (Fig. 13.4). In normotensive persons, BP rises rapidly from reduced sleep-time levels (generally by at least 20 mmHg for SBP and 10–15 mmHg for DBP) with commencement of morning activity. In normotensives, SBP and DBP peak during the day, decline in the evening, and are lowest during sleep. The BP pattern in uncomplicated essential (primary) hypertension in most, although not all, persons is similar to that seen in normotension, although there is abnormal elevation of the 24-h mean, amplitude of variation, and/or reduced sleep-time decline of BP.

**Table 13.1** Categorical classification of adult (>18 years of age) blood pressure (BP) values obtained by conventional clinical cuff and stethoscope measurement

| Blood pressure classification | Systolic blood pressure (mmHg) | | Diastolic blood pressure (mmHg) |
|---|---|---|---|
| Normal | <120 | and | <80 |
| Prehypertension | 120–139 | or | 80–89 |
| Stage 1 hypertension | 140–159 | or | 90–99 |
| Stage 2 hypertension | ≥160 | or | ≥100 |

Conventionally, the same thresholds are used to differentiate arterial normotension from hypertension for women and men and without regard to circadian time. Normative values for systolic (S) and diastolic (D) BP are considered to be less than 120 and 80 mmHg, respectively, and it is assumed that SBP and DBP vary but little over the 24 h. Prehypertension is defined as SBP of 120–139 or/and DBP of 80–89 mmHg; stage 1 hypertension is defined as SBP of 140–159 or/and DBP of 90–99 mmHg; and stage 2 hypertension entails SBP and DBP greater than 160 mmHg or/and 100 mmHg [52]

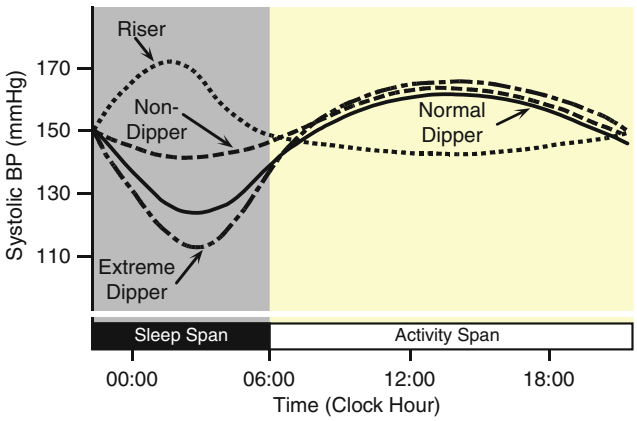


**Fig. 13.4** Types of 24-h blood pressure (BP) rhythms determined by ambulatory blood pressure monitoring (ABPM). Systolic (S) and diastolic (D) BP of most healthy normotensive and essential (primary) hypertensive persons typically are lowest, by 10–20%, during nighttime sleep relative to diurnal activity. In diurnally active persons, ordinarily SBP and DBP begin to rise just before the end of nighttime sleep, showing peak or near peak levels in the morning or early afternoon; they remain elevated until late evening when they begin to decline, reaching lowest levels during sleep. Nondipping and rising SBP and DBP 24-h patterns are becoming more prevalent. Persons who are obese, have metabolic syndrome and/or diabetes, and those who are elderly, have a sleep-disorder, or have hypertension secondary to an existing medical condition are likely to have an attenuated decline of SBP and DBP (i.e., less than expected 10–20% decrease during nighttime sleep relative to daytime activity) or even experience highest SBP and DBP during sleep. Finally, some persons (extreme dippers) exhibit greater than 10–20% decline in the sleep-time SBP and/or DBP. Abnormal, in particular nondipping and riser, SBP and DBP 24-h patterns are risk factors for cardiovascular disease, as discussed in the text, and can only be diagnosed by 24-h ABPM; clinic cuff assessments done during daytime office hours are indicative only of SBP and DBP at that specific time of the day, and even these values may not be properly representative, since many patients are stressed by the clinical setting causing BP to rise above true values (Michael Smolensky, unpublished)

The BP profile of secondary hypertension, i.e., hypertension that is the consequence of another medical condition, such as renal insufficiency, diabetes, sleep apnea, congestive heart failure, and salt sensitivity, however, often is very different. Typically, there is blunting of the nocturnal decline or even increase in BP during sleep relative to daytime activity. Differences in the extent of circadian variation and phase of BP rhythmicity in primary compared to secondary hypertension complicate the differential diagnosis of normotension versus hypertension when based solely on a few daytime measurements made in the clinic, since seldom, if ever, are they representative of the SBP and DBP levels at other times of the day and night. Use of around the clock ABPM is required to make the correct diagnosis – normotension or daytime, night time, or 24-h hypertension or hypotension – and avoid "white coat" effects (nonrepresentative elevated SBP and DBP values due to novelty or anxiety effects of the clinical setting) and masked hypertension (lower than usual SBP and DBP values in the clinic than typical at work and/or home due to stresses external to the doctor's office).

#### 13.5.1.3 Other Routine Clinical Diagnostic Tests

A broad variety of other medical tests can also be affected by body rhythms. Intraocular pressure, measured to make the diagnosis of intraocular hypertension (glaucoma), is circadian rhythmic. In diurnally active persons, intraocular pressure is typically highest nocturnally, between 02:00–04:00, and lowest in the afternoon [53, 54]. The insulin response to the standard oral glucose tolerance tests (GTT) is greater, resulting in lower blood sugar concentrations, when performed in the morning than evening [55, 56]. The findings of certain hematology, coagulation, and hormone studies can vary greatly with the time during the 24 h of blood sampling as discussed in the next section. Although the emphasis of this illustrative discussion has been upon the CTS, day of the menstrual cycle and month of the year may additionally affect the findings of some diagnostic tests.

#### 13.5.1.4 Chronobiologic (Rhythm-Qualified) Chemical Laboratory Reference Values

A clinical measurement for a laboratory sample obtained at one given time of the day, month, or year constitutes only a very limited spot check, since the variable may be rhythmic across several frequencies modulated by environmental factors, which for some variables may explain the great variability encountered in the free-living human population and, in turn, the large range of values considered normal in laboratory medicine diagnostics. In laboratory medicine, biological rhythms represent both a challenge and an opportunity for improved diagnostic accuracy, in addition to better assessment of drug tolerance and therapeutic efficiency. In the case of high amplitude rhythms, time qualified (with regard to biological rhythms) reference ranges are required to make the correct clinical diagnosis. This is because the value obtained at one time of sampling may be above, at, or below a conventional

"reference range" established around a nonperiodic postulated homeostatic "middle value." In addition to improving diagnostic accuracy by establishing time qualified reference values, the parameters of biological rhythms as such may contribute a set of additional reference values describing the human time organization, such as phase and amplitude, so as to allow recognition of temporal changes that may be related to functional disturbances and pathology as well as adverse drug effects.

## Establishment of Chronobiologic Reference Values

A number of biological and environmental factors have to be considered in establishing representative chronobiologic reference values, some of which pertain to the establishment of conventional laboratory medicine values [57, 58]. However, some are especially important in regard to chronobiologic investigations, as detailed elsewhere [59]. Chronobiologic reference values have to be derived from clinically healthy subjects comparable in their population characteristics with the studied subjects or patients, and they have to be obtained under comparable conditions. Time-qualified reference ranges, so-called *chronodesms [*60], can be developed for a single individual by repeated measurements over numerous periods, or they can be determined for groups of comparable subjects by repeated measurement of individuals over a single or limited number of periods (Fig. 13.5).

Choice of peer population will determine the validity of the reference range for a given individual when using a group chronodesm for a given laboratory variable. The number of subjects required for a valid reference population will vary from variable to variable with the prominence and stability of the rhythm, extent of compatibility of the reference group with the subjects to be studied, and degree of desired statistical power for decision making [59, 61, 62]. Depending upon the Gaussian and (very often) non-Gaussian distribution of the data, reference range limits are presented in parametric or nonparametric statistics, e.g., percentiles or confidence and/or tolerance intervals. Time qualified reference ranges in different populations and in different geographic locations and for different frequencies have been presented as chronograms (graphic time plot of data) and/or in their statistically quantified rhythm parameters by numerous investigators [63–76].

## Chronobiologic Reference Values for Accurate Medical Diagnoses

Chronodesms coupled with optimal sampling protocols are indispensable for making the correct diagnosis of medical conditions and disease states. For example, to diagnose adrenal insufficiency, which is characterized by abnormally low plasma cortisol concentration, it is inappropriate to sample blood late at night from habitually day-active subjects. As shown by the chronodesm of Fig. 13.5 for plasma cortisol of healthy subjects, cortisol values are minimally detectable at this time of day. Blood samples that are drawn in the morning, when cortisol is highest, will be of greatest diagnostic utility. Likewise, it would be inappropriate to conduct a diagnostic test for Cushing's syndrome, which is characterized by excessive plasma

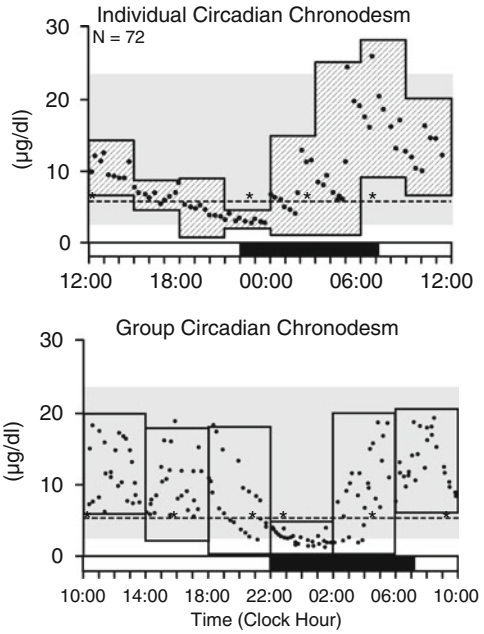


**Fig. 13.5** Circadian chronodesm of plasma cortisol. *Top*: Individual chronodesm in a clinically healthy, diurnally active young adult woman sampled at 20-min intervals over a single 24-h span (72 blood samples in total). Shown is the calculated tolerance interval (determined separately for each 3-h span of the 24 h), indicating the limits within which 90% of measurements is expected to fall with 90% confidence. *Bottom*: Group circadian chronodesm (based on study of a group of diurnally active 15–21-year-old women sampled at 20-min intervals during a single 24-h span). The group circadian chronodesm shows a wider range in the time-qualified tolerance intervals, reflecting individual variation in mesor, amplitude, and/or acrophase of the cortisol circadian rhythm. *Background gray shading* indicates conventionally considered normal range of plasma cortisol values. In both individual and group chronodesms, the same plasma cortisol value, e.g., ~7 µg/dl (represented by *asterisks*), when evaluated without regard to the time of sampling relative to the person's sleep–wake synchronizer routine could be below, within, or above the "usual time-qualified range" of normal. *Black* and *white portions* of bottom time axis indicate usual span of subjects' nighttime sleep and daytime activity from whom the cortisol data were obtained (figure constructed from data of Haus and Touitou [59])

cortisol concentration due to adrenal hyperfunction, by drawing blood samples in the morning when hormone concentration is normally highest. Samples drawn late in the evening will best reveal the correct diagnosis.

## Chronobiologic Reference Values for Assessing Abnormalities of Period, Phase, and Peak Time

Parameters of biological rhythms, in particular, period, phase, and amplitude, constitute additional references of the time of organization of an individual or a group of subjects. The first step in the evaluation of biological rhythms is inspection

of chronograms of the raw data plotted as a function of time. The data of Fig. 13.6 were derived from a group of diurnally active, clinically healthy residents of Minnesota, USA. The temporal variation and waveform can easily be recognized in each of the five different blood cell parameters routinely assessed in patient care. Analysis of variance and *t*-tests indicate only whether time is a statistically significant source of variation. The period of a rhythm can be determined from sufficiently long time series of repeated measurements using periodogram analysis, which can be applied to equal [77–79] or unequal interval [62, 80] data series. Power spectrum analysis can also be used for rhythm detection and validation of period, however, only for equal-interval data series [81, 82].

Curve fitting procedures are typically used in chronobiology to identify the rhythm's period by determining, using least squares techniques, the cosine waveform best approximating the time series data and also to derive its peak time (*acrophase*) and amplitude. "Cosinor" procedures of this nature, introduced and developed by Halberg [83, 84], are suitable for the detection of rhythms in relatively short and noisy time series, even if the data are of unequal interval. However, these methods have limitations [59, 62, 80]. If rhythm parameters like phase and amplitude and their alterations are to be used as quantitative endpoints in single subjects, there may be substantial sampling requirements [59, 61]. The Population Cosinor procedure summarizes rhythm parameters obtained for different individuals belonging to the same population [84, 85] and enables derivation of confidence intervals (95% or other) relating to the entire population. Moreover, rhythm parameters obtained by the Population Cosinor procedure for different groups of individuals, i.e., healthy versus diseased, treated versus nontreated, men versus women, etc., can be compared statistically [86].

Acrophases and amplitudes (with 95% confidence intervals) derived by the Population Cosinor procedure for the blood cell rhythms of Fig. 13.6 are presented in Fig. 13.7. Acrophases of the red blood cell variables occur around midday, while those of the white blood cell variables occur in the early or late evening. Amplitude of the rhythmic variation, i.e., total peak-to-trough difference, derived by the Population Cosinor procedure is rather small. The full extent of the circadian variation only comes to the fore by comparison of the actual values at the peak and trough of the 24-h patterns. When this is done, the range of variation in the raw data (highest value/lowest value $\times$ 100) is much more striking, especially in circulating polymorphonuclear leukocytes and lymphocytes (Table 13.2). Ignoring this clinically and highly significant range of variation can lead to diagnostic and therapeutic mistakes.

Urinary variables are also useful as marker rhythms of the CTS. Urinary sampling is advantageous for variables that show high-amplitude pulsatile or ultradian variation, since they are integrated over the time-interval of sampling. Urinary sampling can be accomplished in babies (by collection vessels fixed to the skin), children, and middle-aged adults by collection of sequential spontaneous voidings. However, it may not be appropriate for elderly subjects who are prone to urinary retention. A weakness of urinary sampling to derive marker rhythms of the CTS is the slight phase difference between the urinary and plasma circadian

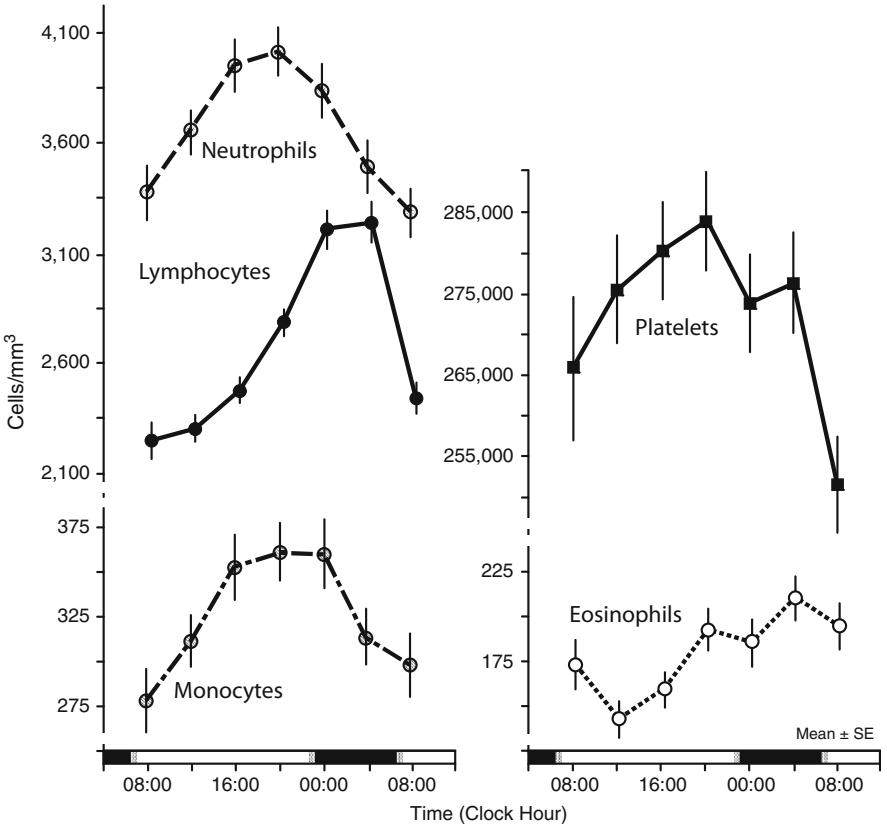


**Fig. 13.6** Circadian rhythm of circulating neutrophils, lymphocytes, monocytes, platelets, and eosinophils in clinically healthy men and women (24 ± 10 years of age). A total of 150 diurnally active, Caucasian subjects (79 men and 71 women) were sampled every 4 h for 24 h, except in the case of platelets, when 55 subjects (30 men and 25 women) were sampled. *Chronograms* (time plots) show average count (±SEM) for each variable, except eosinophils, was lowest at 08:00 and highest at night or during sleep. Peak in eosinophils occurred at 04:00 and trough at 12:00. *Black* and *white portions* of bottom time axis indicate usual nighttime sleep and daytime activity routine of subjects (figure redrafted using data from Haus and Touitou [374])

rhythms of some variables, which in certain cases may be a function of the duration of the intervals between sample collections. A urinary variable which can be used as a reliable phase reference for CTS is the main metabolite of the pineal hormone melatonin, 6-sulfatoxy-melatonin [87–89], which in diurnally active individuals consistently shows highest concentration during the night (Fig. 13.8). The first morning urine contains the major amount of 6-sulfatoxy-melatonin excreted during the 24 h [90, 91]. However, this biomarker can be altered by exposure to artificial (greater than dim level intensity) light at night, even when asleep, thereby limiting its usefulness in lighted environments [92].

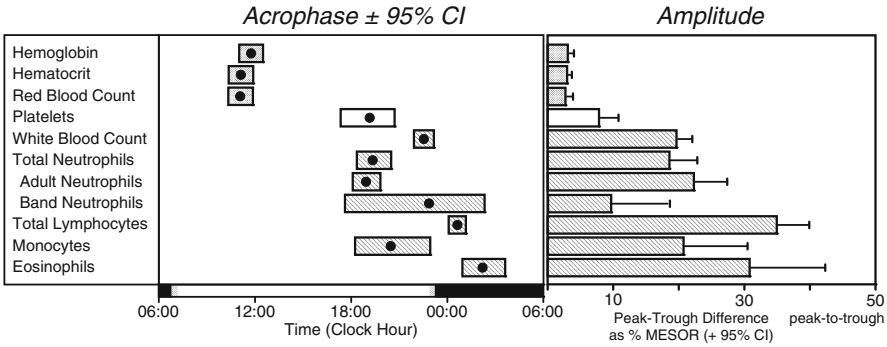


**Fig. 13.7** Circadian acrophase with 95% confidence interval (95% CI) and double amplitude (entire peak-to-trough 24-h variation) expressed as percent of MESOR for hematologic parameters, circulating blood cells, and platelets of the same group of 150 clinically healthy adults as in Fig. 13.6. Mesor, amplitude, and acrophase determined by population mean Cosinor procedure. *Acrophase chart* (*center*) indicates the peak time (with 95% CI) of the group circadian rhythm for each variable and *amplitude chart* (*right*) indicates the extent of group circadian (peak-to-trough) variation relative to the group 24-h mean (MESOR) +95% CI. *Black* and *white portions* of time axis for acrophase at bottom of center plot indicate usual span of nighttime sleep and daytime activity of subjects (figure drawn from data of E. Haus)

**Table 13.2** Extent of circadian variation for peak-to-trough difference in blood cell counts (cells $\times$ $10^3 mm^3$) in terms of the mean $\pm$ SD and absolute range of difference among individuals (left side of table) and also (right side of table) mean $\pm$ SD for percent range of change [(highest count $-$ lowest count)/lowest count] $\times$ 100) and % range of change among individuals for circulating leukocytes (173 healthy diurnally active adults subjects) and platelets (87 healthy diurnally active adult subjects) over a 24-h span

| | Peak–trough difference | | % Range of change | |
|---|---|---|---|---|
| | Mean $\pm$ SD | Range | Mean $\pm$ SD | Range |
| Total White Blood Count | 2,400 $\pm$ 1,000 | 400–6,100 | 41 $\pm$ 18 | 7–133 |
| Total neutrophils | 1,840 $\pm$ 1,028 | 480–7,186 | 66 $\pm$ 42 | 20–346 |
| Adult neutrophils | 1,567 $\pm$ 856 | 330–6,347 | 72 $\pm$ 43 | 18–344 |
| Bands | 563 $\pm$ 350 | 56–1,790 | 152 $\pm$ 114 | 15–780 |
| Lymphocytes | 1,616 $\pm$ 770 | 331–5,556 | 84 $\pm$ 41 | 14–234 |
| Monocytes | 366 $\pm$ 167 | 80–974 | 277 $\pm$ 221 | 30–1,560 |
| Eosinophils | 230 $\pm$ 110 | 40–816 | 292 $\pm$ 190 | 61–1,031 |
| Basophils | 105 $\pm$ 57 | 0–390 | 315 $\pm$ 175 | 27–658 |
| Platelets ($\times 10^3$) | 54 $\pm$ 32 | 12–198 | 23 $\pm$ 15 | 3–83 |

Variation observed between individuals is due to differences in circadian timing rather than amplitude of temporal variation (table constructed from data of Haus and Touitou [374])

The constituents of saliva are also suitable for use as marker rhythms of the CTS, and saliva can even be sampled in babies while asleep. Numerous saliva solutes mirror their plasma concentration, while others are salivary gland secretory products. Steroid hormones can be measured in saliva [72, 93], with the acrophase of salivary cortisol and/or melatonin serving as useful circadian phase markers [94], as shown in Fig. 13.8. There are, however, some peculiarities in the collection and

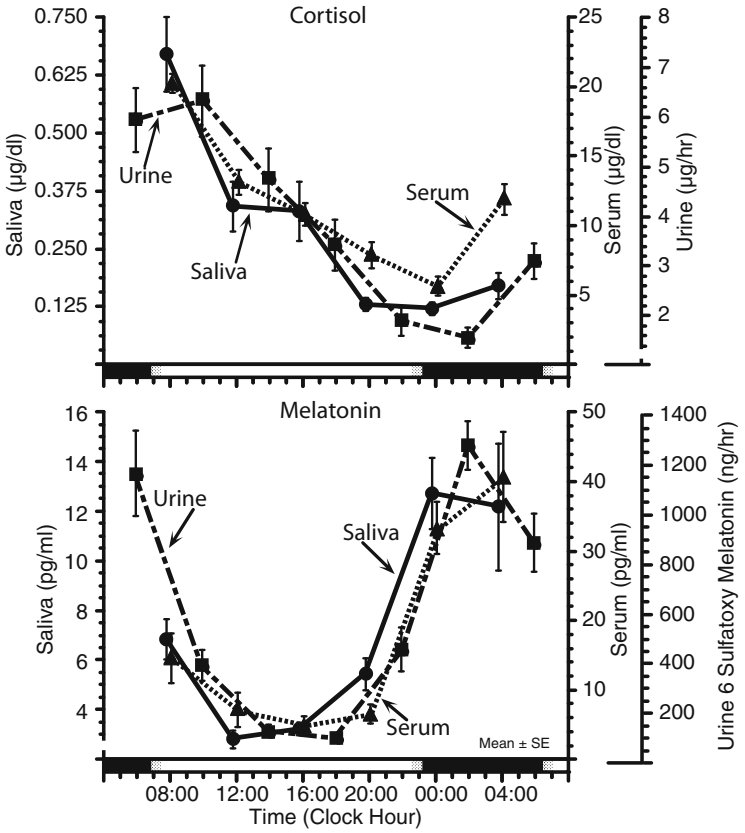


**Fig. 13.8** Circadian variation of salivary and serum melatonin and cortisol and urinary excretion of 6-sulfatoxy melatonin (metabolite of melatonin) and cortisol in 20 diurnally active, healthy adult men (21 ± 2 years of age). Samples were collected every 4 h during a single 24-h span. Circadian patterns of serum, saliva, and urine cortisol concentration and of serum and saliva melatonin and urine 6-sulfatoxy melatonin concentration are remarkably similar, with only slight difference in exact peak and trough times. Peak cortisol concentration in the three biological fluids occurs in morning and peak melatonin and 6-sulfatoxy melatonin concentration occurs during sleep. *Black* and *white portions* of bottom time axis indicate subjects' usual span of nighttime sleep and daytime activity (unpublished data of E. Haus)

use of saliva measures for chronobiologic studies, for example, whether samples are collected by natural flow or stimulation, which have to be understood to obtain meaningful results and avoid pitfalls [59].

In accessible tissues, the study of clock gene expression profiles allows direct access to an individual's circadian phenotype and CTS phasing. Circulating blood mononuclear cells (PBMC) show robust cycling of circadian clock genes [95–99], which are phase-adapted to habitual sleep timing [95, 97], but altered in patients with circadian sleep disorders [98] and cancer [100]. The circadian clock in the PBMC represents a peripheral oscillator usually linked, presumably by humoral

factors, to the central brain (SCN) oscillator, thereby representing an integral marker of the CTS. Alteration of the phase relationship between the central brain clock and PBMC peripheral clock has not been reported in human subjects. Development of a rapid, inexpensive means of determining clock gene expression in PMBC would be useful to identify stages of the circadian clock.

## Chronobiologic Reference Values for Drug-Delivery Systems and Outcomes Assessment of Chronotherapy Trials

Identification of rhythm stage (biologic time) at a given astronomic time, e.g., clock hour, day of week, etc., may be of importance in choosing the time for optimizing desired and/or minimizing adverse drug effects. Marker rhythms are used to denote the stage of a patient's endogenous time organization. Habitual awakening and bed times are the simplest, noninvasive, and least expensive markers of the CTS. Body temperature and activity circadian rhythms, which can be easily measured by noninvasive automatic instrumentation, are other useful markers of the CTS [101, 102].

A variety of circadian marker rhythms are useful to evaluate the outcomes of drug-delivery systems. For example, substitution therapy for adrenal insufficiency conventionally entails oral cortisol administration (25–35 mg/24 h), with or without 9-α-fluorocortisol. Taking the daytime activity–nighttime sleep cycle as the marker rhythm of reference for the CTS leads to the expectation that plasma cortisol be highest in the morning (Fig. 13.5). Cortisol substitution therapy entailing the typical three equal doses per day (at breakfast, lunch, and dinner/bedtime) homeostatic-type schedule greatly alters the CTS from normal relative to pertinent urinary circadian marker rhythms (Fig. 13.9). The acrophases of the circadian rhythm of grip strength and urine concentrations of 17-hydroxycorticosteroids (metabolite of cortisol), 17-ketosteroids (metabolite of sex hormones), potassium, and sodium are abnormally displaced to later phasing by up to 6 h. In contrast, when therapy is applied so most, i.e., 2/3 or 3/4, of the daily dose is ingested in the morning and the rest at bedtime, so as to mimic the normal circadian rhythm of plasma cortisol, the CTS is normalized with reference to the circadian urinary and strength (grip strength) marker rhythms, and patient performance status is best improved [103].

Another example concerns chronic synthetic corticotherapy for inflammatory conditions such as rheumatoid arthritis and bronchial asthma. Determining the best circadian time of methylprednisolone (MP) administration, qualified by minimizing adrenal suppression as an adverse effect, can be judged using time qualified reference values provided by the circadian rhythm of urinary 17-hydroxycorticosteroids. Single 4-h MP infusion at a rate of 660 μg/h between midnight and 04:00, the approximate trough time of the circadian rhythm of cortisol in day-active persons, results in profound adrenal suppression (Fig. 13.10). In comparison, MP infusion in twice the dose, i.e., as an 8-h infusion, between 08:00 and 16:00 causes no adrenal suppression. Finally, 4-h MP infusion commencing either at 04:00

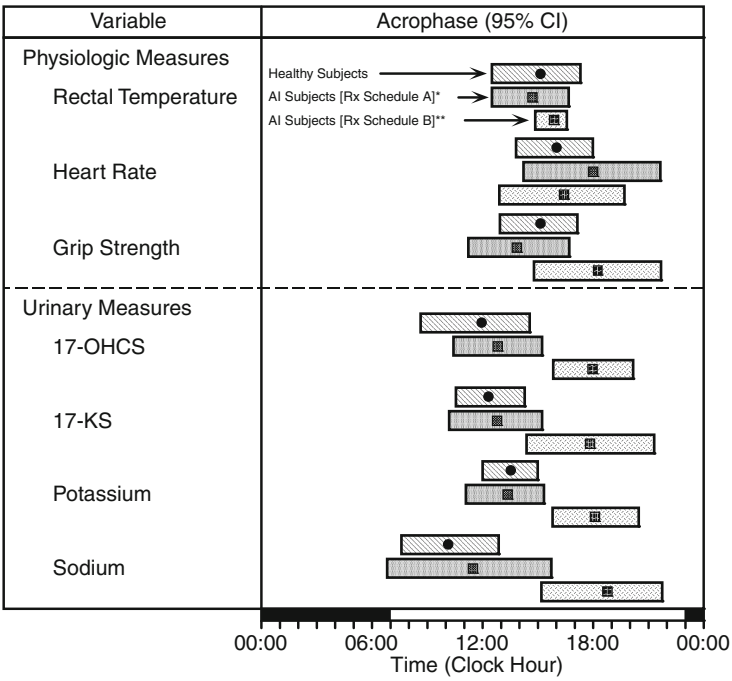


**Fig. 13.9** Circadian acrophase chart with 95% confidence intervals (95% CI) for several physiologic variables in diurnally active (~07:00 to ~23:00) healthy subjects and patients with adrenal insufficiency (AI) treated by different cortisol substitution schedule. Urine and biological measurements were collected at ~4-h intervals during 48-h study spans when following a self-selected diet. Acrophases of circadian rhythms in grip strength and urinary excretion of 17-OHCS (urinary metabolite of cortisol), 17-KS (urinary metabolite of adrenal androgens), $K^+$, and $Na^+$ in patients treated with three equal doses of cortisol (Schedule B, homeostatic substitution schedule: ingestions at roughly equal intervals – 08:00, 13:00, and 20:00) show abnormal phasing, with acrophases lagging by ~6 h behind those of controls and giving rise to a misaligned and biologically inefficient circadian time structure. In contrast, treatment of the same patients with 2/3 or 3/4 (Schedule A, chronotherapy substitution schedule:) of the daily cortisol dose at 07:00 and the remaining fraction at 23:00 preserves the circadian time structure, i.e., circadian acrophases of rhythms in these same variables are comparable to those of healthy subjects. *Black* and *white portions* of bottom time axis indicate usual span of nighttime sleep and daytime activity of the AI patients and healthy controls (drawn using data of Reinberg et al. [103])

or 16:00 results in intermediate level of adrenal suppression [104]. Table 13.3 also shows how the plasma cortisol time qualified reference 08:00 h concentration can be used to assess differences in patient tolerance (absence of plasma cortisol suppression) according to tablet triamcinolone (8 mg/24 h) drug delivery schedule [105]. Accordingly, the first chronotherapy widely applied in clinical medicine, in the 1960s, was the alternate day, morning time schedule of MP tablets [106]. The original clinical trials showed that this MP chronotherapy resulted in significantly better patient tolerance, i.e., reduced adverse effects, and high therapeutic benefit. Recently, a European pharmaceutical company introduced a new chronotherapy,

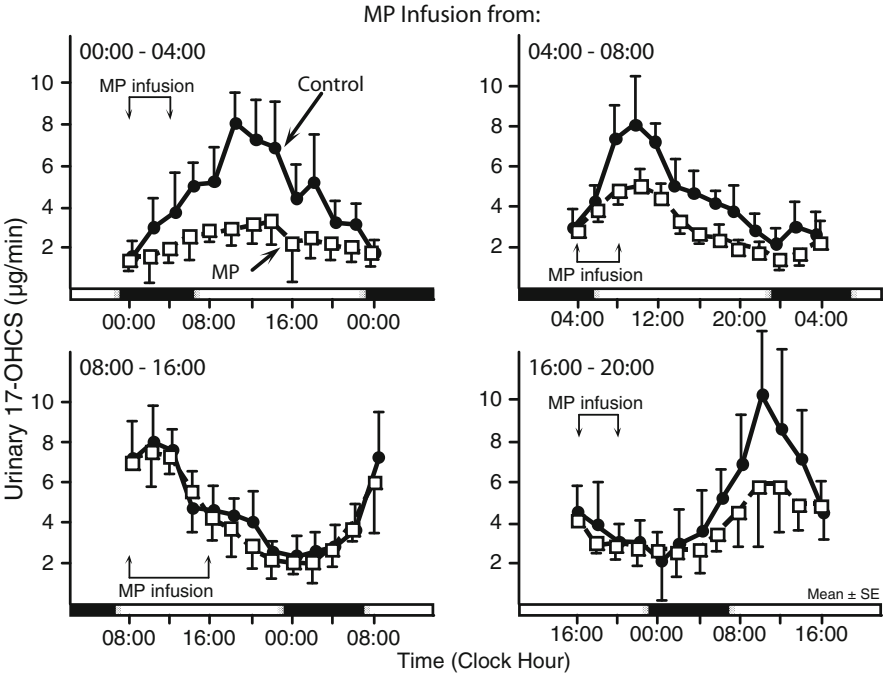


**Fig. 13.10** Circadian rhythm-dependent differences in induction of adverse effect of adrenal suppression, i.e., inhibition of cortisol synthesis and secretion, from methylprednisolone (MP) infused at a rate of 660 µg/h at different circadian times. Urine samples were collected from diurnally active young adult subjects at 2-h intervals and analyzed for concentration of the urinary metabolite of cortisol, 17-OHCS (*solid circles* = control, nontreatment placebo patterns; *open squares* = MP-affected cortisol patterns). Eight-h MP (660 µg/h) infusion during the time of day when endogenous secretion of cortisol is highest, between 08:00 and 16:00 (*lower left panel*) exerts no adrenal suppression; however, MP infusion (660 µg/h) for only 4 h at circadian times when cortisol synthesis and secretion are minimal, between 00:00 and 04:00 (*upper left panel*) or reduced, between 04:00 and 08:00 (upper right panel) or 16:00 and 20:00 (*lower right panel*), induces severe to moderate adrenal suppression, respectively. *Black and white portions* of bottom time axis indicate usual span of subjects' nighttime sleep and daytime activity (figure drawn using data from Angeli [104])

a delayed release synthetic corticosteroid dosage form designed for ingestion at bedtime to achieve highest serum concentration in the morning so as to minimize or avoid completely the adverse effects of this class of medications [107, 108].

Time qualified reference values might also be useful for the development of future biomimetic drug delivery systems. For example, the circadian rhythm of tumor necrosis factor-alpha (TNF-α) seems to be a key biomarker for timing methotrexate (MTX) chronotherapy for rheumatoid arthritis [109]. Cytokines play an important role in the pathogenesis of rheumatoid arthritis and show 24-h rhythms, both in animal models and patients. Studies on animal models, which develop autoimmune disorders that share similarities with human rheumatoid arthritis, found MTX administration exerted best effect when synchronized

**Table 13.3** Triamcinolone (synthetic corticosteroid) schedule of tablet therapy and induction of adverse effect of adrenal suppression: comparison of daily morning versus divided-dose ingestion-time schedules

| Triamcinolone dosing regimen (8 days) | 08:00 baseline* | 08:00 final* |
|---|---|---|
| 8 mg daily at 08:00 | 20.2 ± 1.0 | 19.1 ± 1.6 |
| 8 mg daily – 2 mg/divided (breakfast, lunch, dinner, bedtime) | 21.5 ± 1.4 | 9.0 ± 2.1[§] |

Ingestion by diurnally active adults of the entire 8 mg daily dose of triamcinolone for 8 consecutive days in the morning at 08:00, the expected peak time of the plasma cortisol circadian rhythm, results in no adrenal suppression. In contrast, ingestion by the same subjects on another occasion of the same total 8 mg daily as an equal-dose, equal-interval homeostatic-type regimen, consisting of 2 mg with breakfast, 2 mg with lunch, 2 mg dinner, and 2 mg before bedtime, for the same duration of 8 consecutive days, results in very considerable adrenal suppression as an adverse effect. Dosing of the entire daily dose of synthetic corticotherapies in the morning, at the start of the diurnal activity span, minimizes the risk of adrenal suppression and other potential adverse effects of this medication class (table constructed using data of Grant et al. [105])

*Plasma cortisol (μg/dl), mean ± SE of six men

§$p < 0.05$

with the TNF-α 24-h rhythm [109, 110]. Specifically, in the MRL/lpr mouse animal model, inflammation and TNF-α were best reduced when MTX dosing coincided with the circadian time of TNF-α increase. These findings have been trialed in an initial small pilot study on rheumatoid arthritis patients. Patients were transferred from the standard MTX three times/week treatment schedule, entailing dosing after breakfast and supper on day 1 and after breakfast day 2, to a chronotherapy schedule, entailing the same dose and number of treatments/week but with the MTX administration times changed to bedtime on treatment days so as to coincide with the expected TNF-α rise time. Disease activity scores and health assessment questionnaire ratings were significantly improved by the chronotherapy MTX schedule. Significant symptom relief was observed in 41.2% of patients, and 23.5% of patients achieved clinical remission without significant adverse effects [109, 110]. This example illustrates the value of time qualified reference criteria as circadian rhythm biomarkers of disease activity in animal modeling and patient studies to improve therapeutic outcome and to potentially develop chronotherapeutic drug delivery systems.

### Other Than Circadian Time-Qualified Reference Values

This chapter emphasizes circadian as well as short-period oscillations. In many, but not in all, periodic variables of clinical interest and of potential importance for timed drug delivery, the circadian rhythm is of highest amplitude [59, 68, 111]. However, circadian rhythms are modulated by superimposed rhythms of higher frequencies as well as pulsatile variations which may lead to spurious results and aliasing. Some variables exhibit rhythms of ~7 days (circaseptan) or multiples thereof. An acrophase chart of circaseptan rhythms of some laboratory variables is shown in Fig. 13.11. In the immune system, in particular, a prominent circaseptan periodicity determines in part the host response to introduced antigen,

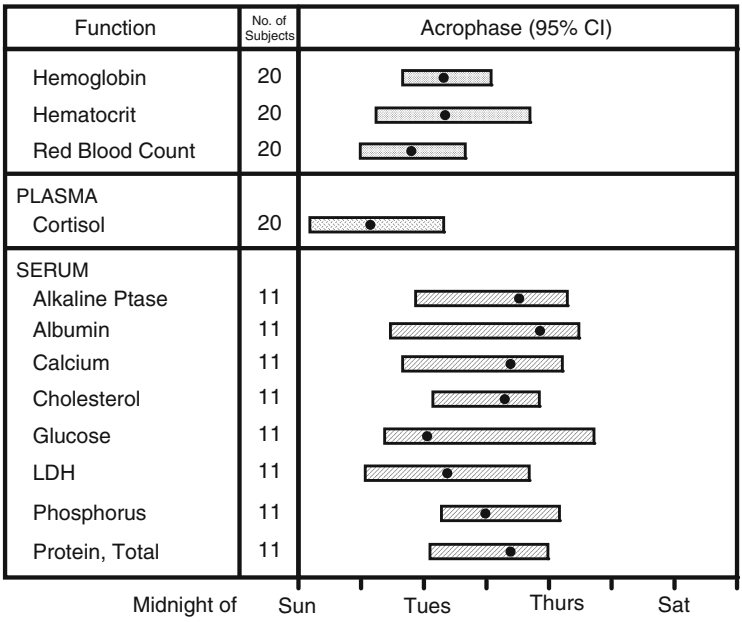


**Fig. 13.11** Circaseptan (~7-day) acrophase chart, with 95% confidence intervals (95% CI), of selected clinical laboratory parameters of blood, plasma, and serum determined in groups ranging in size from 11 to 20 clinically healthy, diurnally active subjects (21–46 years of age) sampled three times/week between 07:30 and 08:00 for several weeks during a 90-day span. Seven-day temporal patterns with acrophases generally on week days are apparent for each variable. Rather large 95% CIs result from relatively infrequent sampling scheme (only three samples/week) and relatively small sample size (figure drawn using data from Haus and Touitou [59])

e.g., in transplantation biology [112, 113]. Circadian/infradian (bioperiodicities >28 h) interactions in the effect of chemical carcinogens also have been identified in animal studies [114, 115]. Circaseptan rhythms in drug effects should be expected in human beings and may be of importance in some settings, but they have yet to be much explored.

## 13.6 Rhythm-Dependent Patterns of Acute and Chronic Medical Events and Conditions

Many biological and chemical processes inherent to disease pathophysiology are rhythmic, giving rise to multifrequency temporal patterns in morbid and mortal events and symptom intensity. In general, circadian patterns in disease have been substantiated by cross sectional, population based epidemiology investigations and by both cross-sectional and longitudinal clinical case series studies.

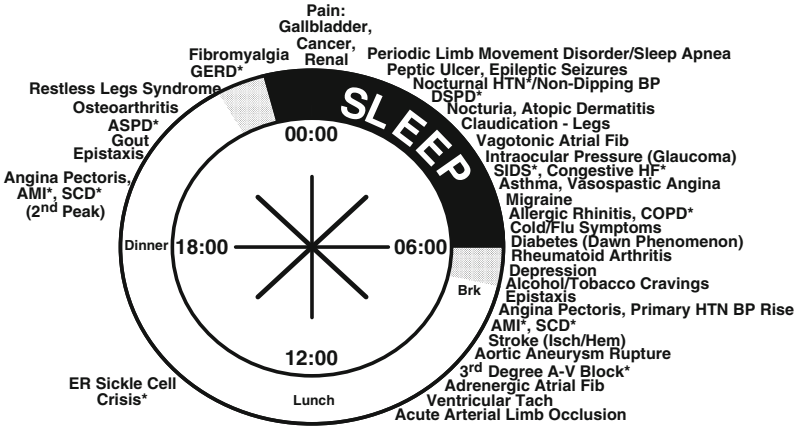


*ER = Emergency Room; ASPD/DSPD = Advanced/Delayed Sleep Phase Disorder; GERD = Gastroesophageal Reflux Disorder; SIDS = Sudden Infant Death Syndrome; HF = Heart Failure; COPD = Chronic Obstructive Pulmonary Disease; AMI = Acute Myocardial Infarct; SCD = Sudden Cardiac Death; A-V = Atrial-Ventricular; HTN = Hypertension

**Fig. 13.12** Approximate time(s) during the 24 h in diurnally active individuals (waking span from ~06:30 to ~22:30 alternating with nighttime sleep from ~22:30 to ~06:30) in the manifestation of the most severe signs and symptoms of various chronic medical conditions, acute severe life-threatening (morbid and mortal) events, and acute infectious and other nonserious medical ailments. Apparent is the large number of medical conditions and events that evidence predictable-in-time (24 h) patterns in symptoms or risk of life-threatening events. Times of greatest risk are approximate, varying to some extent between morning and evening chronotypes, i.e., larks and owls. Some conditions show more than one time of elevated risk, e.g., angina pectoris, acute myocardial infarct (AMI), sudden cardiac death (SCD), epistaxis, and certain epileptic seizure disorders. Such 24-h patterns constitute one important basis for chronotherapeutics. Sleep and activity spans indicated, respectively, as the *darkened* and *white portions* of the *circle* (Smolensky and Haus, unpublished)

### *13.6.1 Circadian Rhythms in the Manifestation and Severity of Disease*

The manifestation and severity of many acute and chronic medical conditions and the occurrence of several life threatening medical events exhibit rather precise timings as depicted in Fig. 13.12. Gout [116, 117], gallbladder [118], renal [119], fibromyalgia [120, 121], and PUD (peptic ulcer disease) attacks [122] are most frequent late at night or initial hours of sleep. Acute pulmonary edema [123], congestive heart failure [124], bronchial asthma and COPD (chronic obstructive pulmonary disease) [125, 126], atopic dermatitis [127], claudication of the legs [128], vagontic atrial fibrillation [129], and nocturia [130] manifest or worsen nocturnally as do sleep apnea [131], restless leg syndrome and periodic limb movement disorders [132], and BP elevation of secondary hypertension [133]. Sudden infant death (SIDS) [134], allergic rhinitis, acute of upper respiratory infectious disease [50, 135, 136], and rheumatoid arthritis [137] are either most intense overnight or in the morning. Migraine headache [138, 139], angina pectoris

[140, 141], ventricular arrhythmia [129], acute myocardial infarction [142], sudden cardiac death [142, 143], ischemic and hemorrhagic stroke [144], fatal pulmonary embolism, and hypertensive crises [145, 146] are most frequent in the morning, as are the symptoms and crises of certain other cardiovascular disease (CVD) conditions, such as adrenergic fibrillation [129], aortic aneurysm rupture, third degree atrial–ventricular heart block, and acute arterial limb occlusion [129]. Depression is most severe in the morning [147, 148], as are alcohol and tobacco cravings [149, 150]. Symptoms of osteoarthritis (OA) worsen during the course of daily activity, typically being most intense in the evening [151, 152]. Perforated and bleeding ulcer is reported to be most common in the afternoon [153, 154], and intraocular pressure of glaucoma rises to peak level during sleep [155, 156]. Some seizure disorders are triggered by specific sleep stages and/or transitions between sleep and wakefulness [157, 158]. Finally, advanced and delayed sleep phase disorders (ASPD and DSPD) manifest in the early evening and middle of the nighttime, respectively [159].

### *13.6.2 Medical Conditions Manifesting as a Disrupted CTS*

It is assumed, even by seasoned chronobiologists, that the CTS is normal and more or less comparable among human beings, excluding differences in phasing seen in the small proportion of extreme morning and evening chronotypes. This assumption is not always valid. Some persons exhibit significant alteration and disruption of the CTS without negative effects, while others are significantly affected, suggesting there may be genetic differences in tolerance to disruption of the CTS, thus the need to develop special therapeutic interventions to reset it to normal.

Certain sleep disorders are directly representative of abnormalities of the circadian time-keeping system [160, 161]. For example, DSPD syndrome is characterized by severe sleep onset insomnia. Typically, sleep is impossible to achieve until 03:00 or later in affected children and adults, and consequently there is great difficulty in awakening the next morning at the normal time. The underlying mechanism of DSPD may be abnormal sensitivity to evening light, causing the clock controlling the sleep–wake cycle to reset to a later time by means of a phase response mechanism [162]. ASPD is characterized by early evening sleep onset, as early as 19:00–20:00 and very early morning awakening. The underlying mechanism of ASPD in some individuals and families involves a genetic difference in the circadian time keeping system [163]. Non-24-h sleep–wake syndrome, a relatively uncommon condition, is characterized by free-running of the activity–rest rhythm from the normal 24-h period. Diagnostic studies show sleep-onset and sleep-offset times from one day to next are progressively delayed in some patients and advanced in others by as much as ~2 h. The period of the inherited biological clock controlling the sleep–wake cycle is abnormal in these individuals, being as long as 26–27 h in some patients and as short as ~23 h in others.

Shift work intolerance is a medical condition that may be manifested in career rotating or permanent night shift workers, typically around the age of 45–50 years. It is characterized by poor quality and inadequate duration of daytime sleep when on the night shift, mild to severe depression and/or irritability, compromised work performance, digestive or PUD, and often hypertension [8, 9]. It appears that the pathology of this condition involves CTS desynchronization, with the period, amplitude, and staging of circadian rhythms altered significantly [164]. Transfer of affected employees from shift to day work will eventually alleviate the disrupted CTS and the associated medical complaints. Currently, no so-called chronobiotics, medications or other interventions capable or resetting and normalizing the CTS are known. Although melatonin and bright-light therapy, depending on their biological timing, are able to shift (delay or advance) or stabilize the CTS in a phase response manner (Fig. 13.3), they are yet to be endorsed by the medical community to treat shift work intolerance.

Blind individuals, who are unable to perceive environmental synchronizing light cues, often show desynchronized CTS, and manifest free running circadian rhythms, chronic sleep problems, and depression. A series of studies have found that physiologic low dose melatonin administered at the right circadian phase can, over time, restore normal CTS to totally blind persons and relieve medical complaints [40, 165]. It is of interest that certain mood disorders, such as seasonal affective mood disorder (SAD), premenstrual dysphoric disorder (PMDD), and even regular endogenous depression, have been associated with abnormalities of the circadian time keeping system [166–169].

## 13.7 Chronopharmacology: Biological Rhythms and Medications

The biological time when medications are administered may affect their pharmacokinetics (PK) and pharmacodynamics (PD), no matter their route of delivery.

### *13.7.1 Chronopharmacology: Definition and Concepts*

*Chronopharmacology* is the study of the manner and extent to which the PK and PD of medications are affected by endogenous biological rhythms, and also how the time of dosing affects biological time keeping and CTS, i.e., period, level, amplitude, and phase [20, 170–174]. The concept of chronopharmacology is in direct conflict with that of homeostasis. The theory of homeostasis promotes as a major goal for drug delivery systems constancy in medication levels, since it is assumed that constancy in drug levels translates to constancy in drug effects and avoidance of adverse effects. The fields of chronopharmacology and chronotherapy

challenge these long held concepts and goals. Indeed, numerous studies clearly indicate the time of ingestion, inhalation, injection, infusion, or cutaneous application of medications, especially with reference to circadian rhythms, can affect PK and PD, and sometimes markedly.

### *13.7.2 Chronokinetics*

*Chronokinetics* refers to dosing-time (i.e., biological rhythm) dependent differences in absorption, distribution, metabolism, and elimination of medications [20, 170, 171]. This is revealed, for example, by administration time differences in PK parameters of various types and classes of therapeutic agents, including time to peak concentration, peak height, elimination rate, volume of distribution, and area under the time–concentration curve [20, 175–178]. These differences result from circadian rhythms in gastrointestinal pH affecting drug dissolution plus circadian rhythms in gastric emptying, motility, and blood flow affecting the rate, and sometimes amount, of drug absorption [179]. Circadian rhythms in hepatic blood flow and enzyme activity affect drug biotransformation and metabolism. Hepatic and kidney rhythms, in bile function and flow and renal glomerular filtration and tubular function, affect drug elimination [175]. Many examples of dosing time differences in the PK of commonly prescribed medications can be found in previous published reviews [176, 178, 180].

### *13.7.3 Chronodynamics*

*Chronodynamics* refers to dosing time (i.e., rhythm dependent) differences in the effects of medications that cannot be attributed to their PK [20, 170]. Such administration time differences result from rhythms in free versus bound drug fraction, number and conformation of drug-specific receptors, second messenger and ion channel dynamics, and rate limiting steps in metabolic pathways [20, 181]. Beneficial and adverse effects of medications may both vary significantly according to their administration time.

Many examples of chronodynamics can be cited. One is the differential effect of constant rate infusion of $H_2$-receptor blocker medication during the 24 h. Gastric acidity exhibits significant circadian rhythmicity, both in healthy subjects and peptic ulcer patients. Under fasting condition, basal (nonfood stimulated) gastric hydrogen ion concentration of diurnally active subjects is higher around and just after bedtime at night than in the morning when awakening (Fig. 13.13a) [122]. Constant rate 24-h infusion of therapeutic doses of the $H_2$ antagonist famotidine exerts differential day–night efficacy, i.e. suppression of gastric acid secretion (Fig. 13.13b) [179]. Drug effect is attenuated in the evening and at night, indicating partial resistance to $H_2$-receptor blockade at this time [182–184].

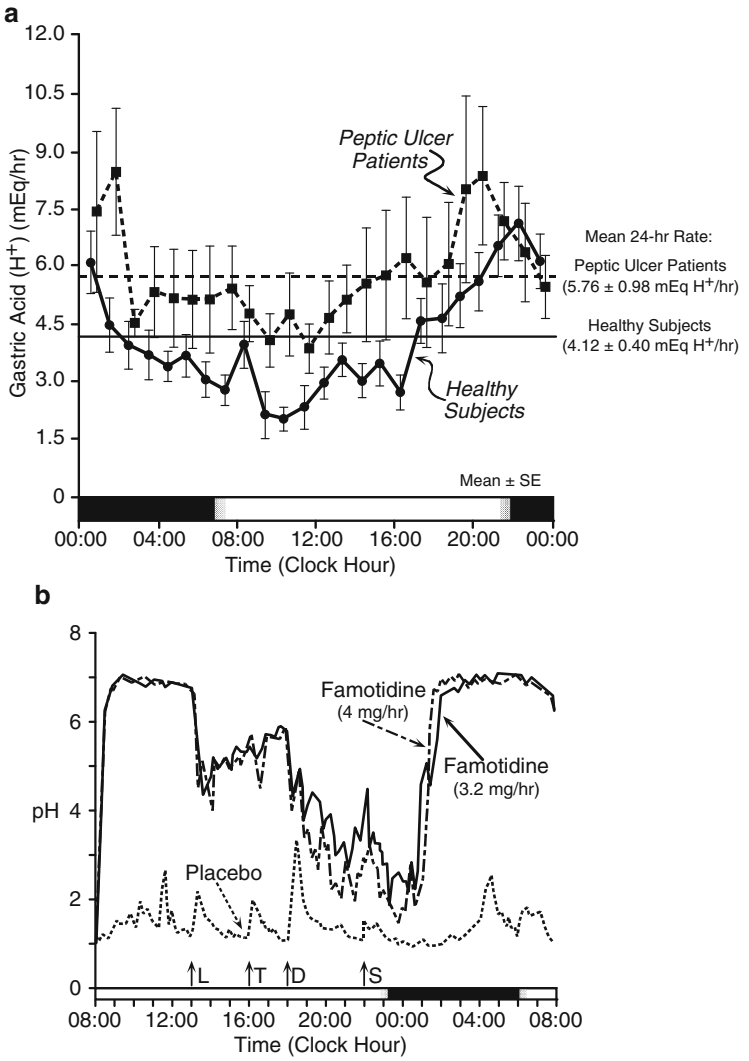


**Fig. 13.13** (**a**) Circadian pattern in basal (fasting) gastric acid secretory rate in 14 active healthy (*closed circles*) and 21 diurnally active, peptic ulcer disease (*closed squares*) subjects. *Dashed horizontal line* represents mean 24-h secretory rate for ulcer group (5.76 ± 0.98 mEq $H^+$/h) and *solid horizontal line* represents mean rate for healthy group (4.12 ± 0.40 mEq $H^+$/h). Note reduced morning and elevated evening gastric acid secretory rate in both groups. *Black* and *white portions* of bottom time axis indicate subjects' usual span of nighttime sleep and daytime activity (figure redrawn using data of Moore and Halberg [122]). (**b**) Median 24-h intragastric pH profiles of 12, ordinarily diurnally active, fed duodenal ulcer patients. *Dashed line* represents control (placebo) 24-h study; *solid line* represents IV continuous infusion of $H_2$-receptor antagonist famotidine at a rate of 3.2 mg/h for 24 h; *dash–dot line* represents IV continuous infusion of famotidine to same subjects at a higher rate of 4.0 mg/h for 24 h. Meals and drink are shown at bottom by *arrows*: L = lunch, T = tea, D = dinner, and S = snack. In spite of constant infusion of the $H_2$-receptor antagonist, intragastric pH exhibits pronounced decline (higher acidity) commencing late afternoon/evening and lasting to the initial hours of usual sleep span, when pH is lowest (placebo curve) and rate of gastric acid secretion is highest (as shown in Fig. 13.13a). *Black* and *white portions* of bottom time axis indicate subjects' usual nighttime sleep and daytime activity spans (figure redrawn using data from Moore and Merki [179])

A second example is the differential anticoagulant effect during the 24 h of constant rate infusion of standard (nonlow-molecular weight) heparin on deep vein thrombosis patients [185, 186]. The effect may be too great overnight, posing risk of hemorrhage, while in the morning it may be subtherapeutic, risking aggravation of the medical condition (Fig. 13.14). These circadian rhythm dependent effects are also found when heparin is administered by other routes [187].

Other examples involve oral dosage forms. For example, clinical trials of nonsteroidal anti-inflammatory drugs (NSAIDs) demonstrate better therapeutic effect on the characteristic morning symptoms of pain, stiffness, and inflammation of rheumatoid arthritis and with less side effects when ingested in the evening or at bedtime than morning [188]. On the other hand, NSAIDs are more effective in reducing the characteristic afternoon and evening peak intensity of OA symptoms when ingested in the morning or around lunch time, although with elevated risk of adverse events compared to evening dosing [188].

Another important set of examples, given the large number of people worldwide diagnosed with hypertension, e.g. an estimated 63 million in the USA and 163 million in China, are the differential ingestion time dependent effects of BP-lowering monotherapies, including angiotension converting enzyme inhibitors (ACEIs), angiotension receptor blockers (ARBs), calcium channel blockers (CCBs), ß-blockers, α-blockers, and diuretics [189]. As shown in Table 13.4, the average enhancement relative to baseline of the bedtime versus upon-awakening regimen of the diuretic torasemide (5 mg/day) amounted to 8.4/6.1 mmHg in the 48-h SBP/DBP means, 8.3/6.2 mmHg in the awake SBP/DBP means, and 8.2/5.5 mmHg in the asleep SBP/DBP means. Further, bedtime compared to conventional upon-awakening scheduling of the ACEIs ramipril (5 mg/day) and spirapril (6 mg/day) resulted in greater reduction of asleep SBP/DBP means relative to baseline of 9.0/7.4 and 7.1/4.0 mmHg, respectively. Finally, in two studies on different cohorts of hypertension patients, bedtime compared to conventional upon-awakening dosing of the ARB valsartan (160 mg/day) better attenuated the asleep SBP/DBP means from baseline by 9.6/5.6 and 8.2/5.8 mmHg, respectively. The differential effect of the timing of BP-lowering medications is not simply dependent on drug half life, as illustrated by findings for the long-half life (24 h) ARB telmisartan (80 mg/day) medication. When taken at bedtime, rather than upon awakening, reduction from baseline of the asleep SBP/DBP means was improved by 5.5/3.3 mmHg. The findings of studies summarized in Table 13.4 are consistent; bedtime as opposed to morning ingestion of different hypertension therapies exerts significantly greater reduction of sleep-time BP and better normalization, restoration, and preservation of the BP circadian pattern.

Normalization of sleep-time BP level seems to be a new and important clinical target for hypertension therapies for at least two reasons. First, recently completed clinical outcome studies indicate the nondipping BP pattern (i.e., absence of 10–20% decline in SBP and DBP during sleep relative to daytime levels) is associated with increased risk of injury to heart, brain, blood vessel, and kidney tissue, plus heightened 5-year risk of CVD mortality as reviewed in Portaluppi and Smolensky [190]. Second, a recently published 5.6-year clinical outcomes trial (Sect. 13.8.2.2) documents that regular ingestion of at least one BP-lowering

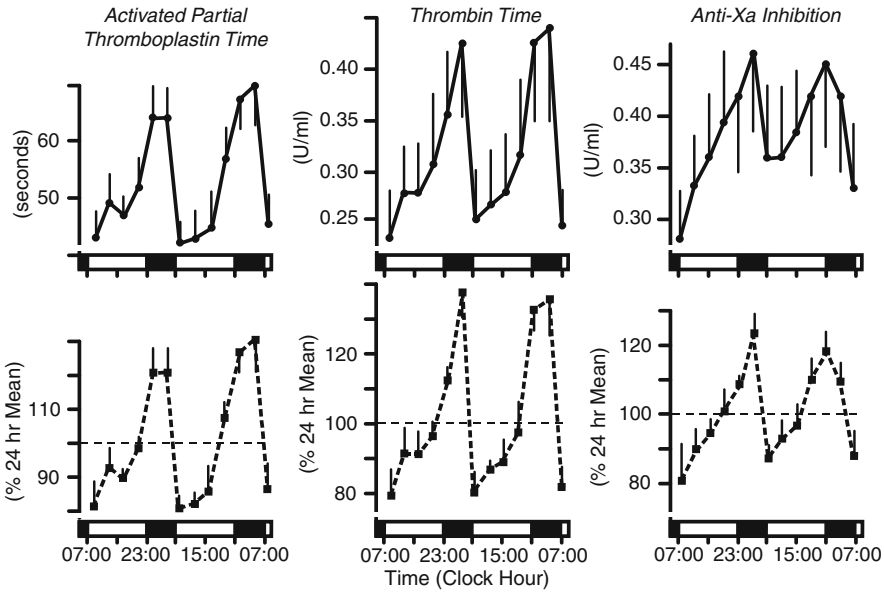


**Fig. 13.14** Circadian variation in three measures of blood coagulation – Activated Partial Thromboplastin Time (aPTT), Thrombin Time (TT), and Factor Anti-Xa inhibition – in six ordinarily diurnally active venous thrombo-embolism patients administered unfractionated heparin by constant-rate continuous intravenous infusion for 48 consecutive hours. Initial daily dose of heparin was adjusted on an individual patient basis to maintain aPPT between 1.5 and 2.5 times the before-treatment 08:00 level. *Top*: Circadian variation in heparin effect on coagulation parameters shown in standard laboratory units. *Bottom*: Circadian variation of the same coagulation parameters after data re-expressed as percent of each subjects' time series mean. Maximal anticoagulation effect was achieved ~04:00 and minimum effect ~08:00. Differences between night and morning values amounted to ~50% for aPTT, 60% for TT, and 40% for Factor Anti-Xa inhibition. In four patients, the nocturnal peak in aPTT exceeded the upper desired limits of anticoagulation and the heparin effect was too great, while during the wake span in some patients heparin produced too weak an anticoagulation effect. Sleep–wake pattern of group is represented at bottom of each figure; *shaded portion* represents nighttime sleep span and white portion represents diurnal wake span (figure drawn using the data of Decousus [185, 186])

medication at bedtime, as opposed to ingestion of all such prescribed medications in the morning upon awakening, results in significantly better protection against heart attack and stroke [191]. Results such as these form the basis for the development of hypertension chronotherapy drug delivery systems.

A growing trend in the treatment of some medical conditions is combination therapy of two or more complementary acting medications. Polytherapies thus far developed and marketed for hypertension entail a morning-time indication with simultaneous release of both medications during the 24-h dosing interval. Rhythm dependencies in the PK and PD of the individual constituents should be suspected and may be especially important in optimizing their synergistic efficacy and safety. One illustrative example is the differential magnitude of therapeutic effect exerted by CCB amlodipine and ARB valsartan when ingested in combination in the

**Table 13.4** Summary of changes from pre-treatment baseline (in mmHg) in the 48-h, awake, and asleep systolic and diastolic BP (SBP and DBP) means by six different classes of hypertension medications when routinely ingested upon awakening versus bedtime by diurnally active adult hypertensive subjects

| Hypertension medication | Dose (mg) | Duration (weeks) | No. of subjects | Effect on 48 h SBP/DBP means | | Effect on awake SBP/DBP means | | Effect on asleep SBP/DBP means | |
|---|---|---|---|---|---|---|---|---|---|
| | | | | Awakening | Bedtime | Awakening | Bedtime | Awakening | Bedtime |
| Doxazosin GITS | 4 | 12 | 39 | −1.8/−3.2 | −6.9/−5.9* | −2.9/−3.7 | −6.0/−5.4 | 0.7/−1.3 | −8.2/−6.5** |
| Doxazosin GITS | 4 | 12 | 52 | −2.2/−1.9 | −5.3/−4.5 | −3.4/−2.9 | −5.9/−4.4 | 0.1/−0.5 | −4.9/−5.3* |
| Nebivolol | 5 | 8 | 173 | −13.0/−11.3 | −12.8/−10.3 | −14.7/−12.4 | −13.4/−10.9 | −7.9/−7.4 | −10.2/−8.1 |
| Torasemide | 5 | 6 | 113 | −6.4/−3.4 | −14.8/−9.5*** | −7.3/−3.7 | −15.6/−9.9*** | −4.3/−2.5 | −12.5/−8.0*** |
| Ramipril | 5 | 6 | 115 | −8.5/−6.2 | −11.2/−9.5** | −10.1/−6.9 | −10.5/−9.0 | −4.5/−4.1 | −13.5/−11.5*** |
| Spirapril | 6 | 12 | 165 | −8.7/−7.0 | −9.8/−6.6 | −9.9/−8.0 | −8.5/−5.7 | −5.7/−4.6 | −12.8/−8.6*** |
| Valsartan | 160 | 12 | 90 | −17.0/−11.2 | −14.6/−11.4 | −17.0/−11.1 | −12.0/−9.8 | −15.9/−10.8 | −17.9/−13.3 |
| Valsartan | 160 | 12 | 100 | −12.3/−6.3 | −15.3/−9.2* | −12.8/−6.6 | −13.0/−8.5 | −10.9/−5.5 | −20.5/−11.1*** |
| Valsartan | 160 | 12 | 200 | −13.0/−8.1 | −15.2/−10.6* | −13.1/−8.3 | −12.6/−9.3 | −12.9/−8.1 | −21.1/−13.9*** |
| Olmesartan | 20 | 12 | 123 | −13.8/−11.2 | −13.9/−10.2 | −14.5/−12.1 | −13.3/−9.6 | −11.2/−8.7 | −15.2/−11.5* |
| Telmisartan | 80 | 12 | 215 | −10.6/−7.9 | −11.7/−8.3 | −11.7/−8.8 | −11.3/−8.2 | −8.3/−6.4 | −13.8/−9.7*** |
| Nifedipine GITS | 30 | 8 | 180 | −9.1/−5.8 | −12.7/−7.6* | −9.9/−6.4 | −12.7/−7.6 | −7.8/−4.7 | −12.6/−7.8** |

Duplicate listing for doxazosin GITS and valsartan represent findings of separate studies on different groups of hypertensive subjects. Reduction of SBP and DBP from baseline, particularly, the sleep-time mean, was greater with the bedtime than morning ingestion schedule, and this dosing-time effect was independent of medication half-life. Mean enhancement of therapeutic effect relative to the pretreatment baseline by bedtime versus upon-awakening scheduling of the diuretic torasemide (5 mg/day) amounted to 8.4/6.1 mmHg in the 48-h SBP/DBP, 8.3/6.2 mmHg in the awake SBP/DBP, and 8.2/5.5 mmHg in the asleep SBP/DBP. Bedtime compared with conventional upon-awakening scheduling of the angiotensin converting enzyme (ACE) inhibitors ramipril (5 mg/day) and spirapril (6 mg/day) more effectively reduced the asleep SBP/DBP means from baseline by 9.0/7.4 and 7.1/4.0 mmHg, respectively. In two studies on different cohorts of mainly nondipper patients, bedtime, compared with conventional upon-awakening, ingestion of the angiotensin receptor antagonist (ARB) valsartan (160 mg/day) better attenuated the asleep SBP/DBP mean from baseline by 9.6/5.6 and 8.2/5.8 mmHg. Finally, the differential asleep BP mean decrease from baseline even with the long half-life ARB telmisartan (80 mg/day) ingested at bedtime compared with upon awakening amounted to 5.5/3.3 mmHg SBP/DBP. Statistical comparison of the extent of reduction in SBP and DBP means from pre-treatment baseline with morning versus bedtime medication ingestion: *$p < 0.05$; **$p < 0.01$; ***$p < 0.001$ (table constructed based on Smolensky et al. [189])

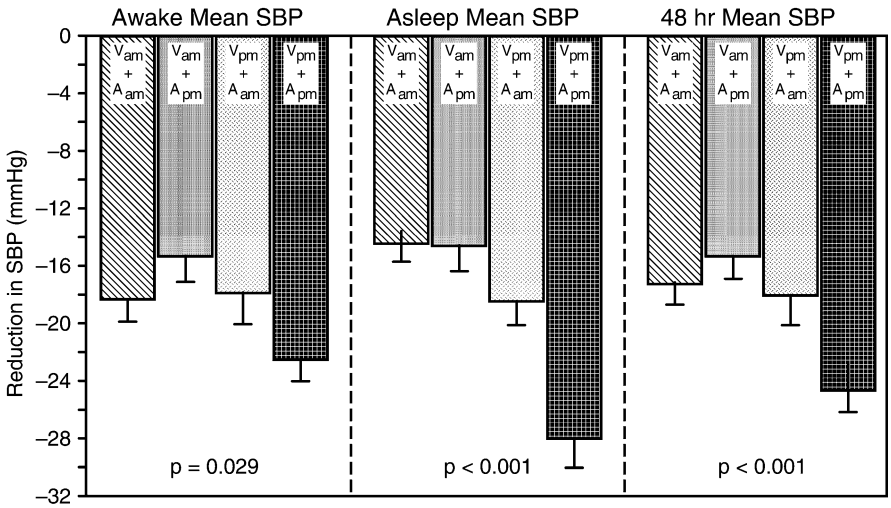


**Fig. 13.15** Changes from before-treatment baseline in awake (active hours), asleep (nighttime sleep span), and 48-h means of systolic blood pressure (SBP) in 203 hypertension persons after 12 weeks of differently scheduled 160 mg valsartan/5 mg amlopidine (angiotensin receptor antagonist/calcium channel blocker) combination therapy: valsartan (V) + amlodipine (A) ingested together on awakening, V ingested on awakening + A ingested at bedtime, V ingested at bedtime + A ingested on awakening, and V + A ingested together at bedtime. Different timings of the V + A combination therapy exerted statistically significant differences in effect on the awake, asleep, and 48-h SBP means. Strongest effect was exerted when V and A were ingested together at bedtime, i.e., the asleep SBP mean (relative to the pre-treatment baseline level) was reduced on average by about twice the amount compared to when V was ingested on awakening and A at bedtime or when V + A were ingested together on awakening. These findings illustrate the potential prominent circadian rhythm-dependent effect of medications used in combination and importance of such phenomena to drug-delivery (figure drawn using data from Hermida et al. [192])

morning versus at bedtime [192]. Hypertension patients were randomized across one of four treatment schedules: (1) ingestion of both medications in the morning upon awakening; (2) ingestion of both medications at bedtime; (3) ingestion of amlodipine upon awakening and valsartan at bedtime; and (4) ingestion of valsartan upon awakening and amlodipine at bedtime. The BP-lowering effect upon the daytime, sleep time, and 48-h SBP and DBP means derived by ABPM was strong no matter the scheduling of the two medications in combination (Fig. 13.15). However, the synergetic effect when both were routinely ingested together at bedtime as compared to upon awakening resulted in a nearly 50% greater mean reduction in daytime BP, more than doubling of the mean reduction in sleep time BP, and more than 50% greater mean reduction in 48-h BP.

While strong BP-lowering effect is a desired clinical outcome, over-correction of BP during nighttime sleep could be problematic for certain patients, since too low nocturnal BP may increase the risk of anterior ischemic optic neuropathy in hypertensive glaucoma patients, and in elderly patients nighttime falls with bone

fracture and even nocturnal stroke. Obviously, the development of combination polytherapies should take into account possible strong circadian rhythm dependencies in synergetic effects of constituent medications, which might enable the use of lower doses, thereby being a potential means of reducing cost of therapy.

#### 13.7.3.1 Administration Time Dependent Differences Between Men and Women in PD of Medications

An increasing number of reports show differences, including treatment-time ones, between men and women in the PD of various classes of medications. Women develop cough related reactions to the ACEI lisinopril three times more often than men [193]. ß-Blockers tend to be less effective in women than men, particularly in stroke prevention, while diuretics may be of more value in older women because of decreased bone loss and reduced risk of hip fracture [194]. Moreover, women tend to show a stronger BP response than men to amlodipine (CCB) [195], candesartan (ARB) [196], and the combination of irbesartan (ARB)/hydrochlorothiazide (diuretic) [197].

Administration-time differences between men and women in therapeutic responses to blood pressure medications also have been detected. The first example involves low-dose (5 mg/day) amlodipine. In this as yet unpublished study lead by one of the authors (R. Hermida), 193 diurnally active hypertensive subjects, 101 men, and 93 women, were randomized to two groups; subjects of one group ingested amlodipine daily upon awakening in the morning, and those of the other group took amlodipine daily at bedtime. Subjects underwent 48-h ABPM before and at the end of treatment. Morning treatment revealed difference between men and women only in the amount of sleep time BP reduction, with the average decrease in sleep time SBP being nearly 50% greater in men than in women (Fig. 13.16). Bedtime treatment, on the other hand, resulted in a much more prominent difference in effect between men and women; average reduction of the wake-time, sleep-time, and 48-h SBP means was ~5 mmHg greater in women than men.

The second example involves the little known effect of low-dose (100 mg/daily) aspirin on SBP and DBP [198]. In a Spanish study, 130 men and 186 women with untreated mild hypertension were randomized to take aspirin either on awakening or at bedtime daily for 3 months. ABPM was performed for 48 h before and after treatment. In men who routinely ingested aspirin upon awakening, the effect relative to baseline on the awake time, sleep time, and 48-h SBP/DBP means was nil; in women aspirin slightly elevated BP levels. In contrast, aspirin ingestion at bedtime significantly reduced all SBP/DBP means, and more so in women than men (Fig. 13.17). Factors influencing the stronger response of BP to low dose aspirin at bedtime included female gender, elevated fasting glucose, and high glomerular filtration rate. This study corroborates significant administration-time-dependent effect of low dose aspirin on ambulatory BP in Spanish subjects with untreated mild hypertension, and further illustrates the significant differences between men

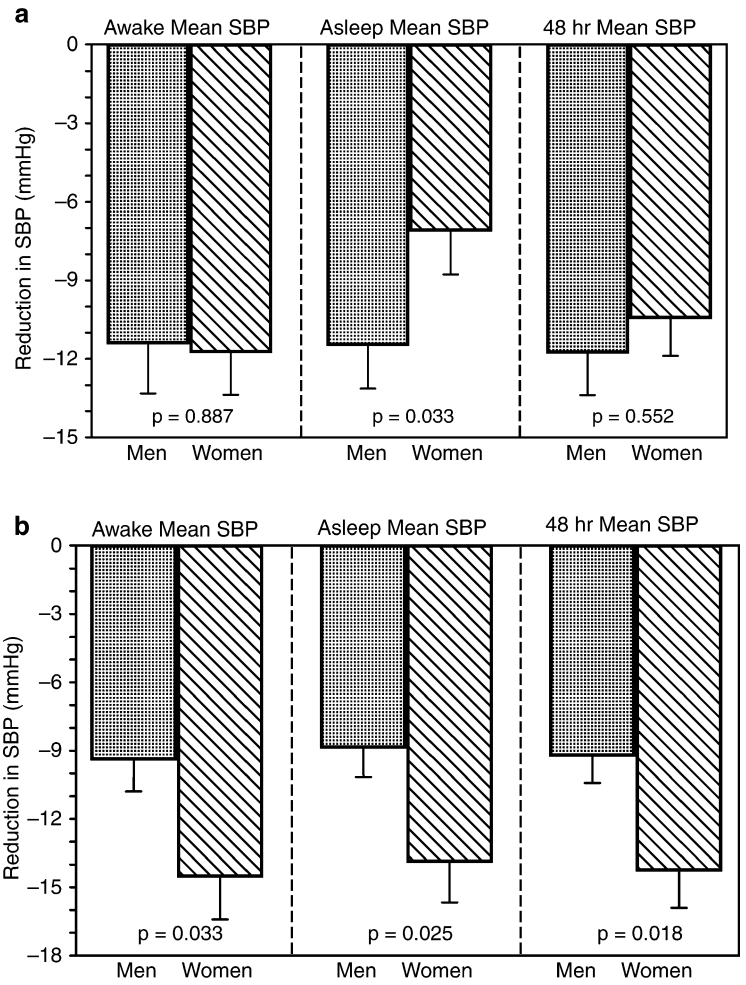


**Fig. 13.16** Sex differences in blood pressure-lowering effects of amlopidine (5 mg) when ingested at different times of the day. Hypertensive subjects, 101 men and 93 women, were randomized to two groups; subjects of one group ingested the medication daily in the morning upon awakening from nighttime sleep, and those of the other group ingested it daily at bedtime. Subjects underwent 48-h ambulatory blood pressure monitoring (ABPM) before and after 12 weeks of treatment. Morning treatment (*Top*, **a**) revealed difference between men and women only in the amount of the sleep-time BP reduction, with average decrease in sleep-time systolic blood pressure (SBP) being ~50% greater in men than women. Bedtime treatment (*Bottom*, **b**) resulted in much greater statistically significant reduction of the wake-time, sleep-time, and 48-h SBP means, on average by ~5 mmHg, in women than men (figure drafted using the data of Hermida et al., unpublished)

and women in the circadian-time-related variation in responses to medications [198]. Additional studies are needed on men and women of other ethnic/racial groups to explore potential sex and racial interactions relative to the circadian dosing time of aspirin and other classes of medications.

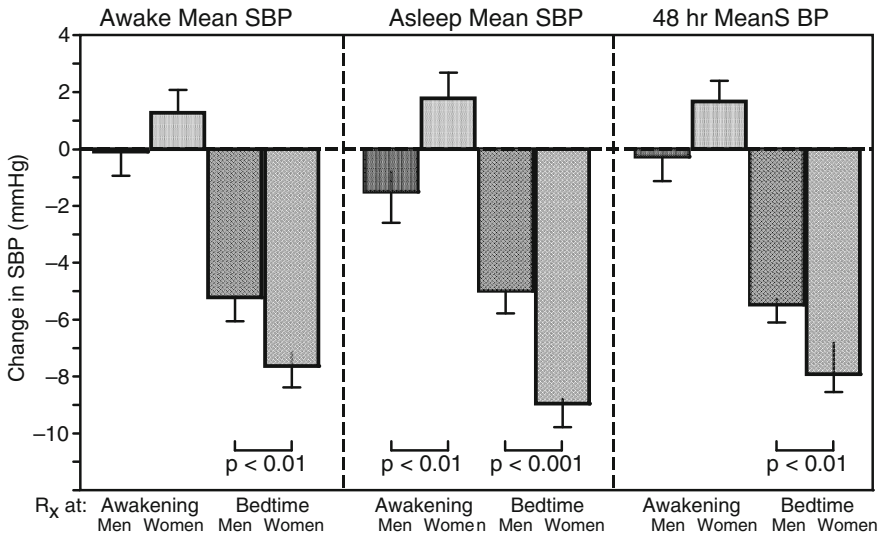


**Fig. 13.17** Differential effect of low-dose (100 mg/daily) aspirin on systolic blood pressure (SBP) reduction when ingested at different times of the day. A group of 316 untreated Spanish (130 men and 186 women) mild hypertension subjects (44.1 ± 13.2 years of age) was randomized to ingest low-dose aspirin either on awakening or at bedtime daily for 3 months. ABPM was performed for 48 h before and after treatment. In both men and women who ingested low-dose aspirin daily upon awakening, SBP wake-time, sleep-time, and 48-h means were unchanged from baseline. In constast, those who ingested low-dose aspirin daily at bedtime, the three SBP means were reduced and significantly more so in women than men (figure redrawn from data published by Ayala and Hermida [198])

The examples presented here call attention to the fact that drug-delivery systems need to be sensitive to potential differences between women and men in the circadian rhythm dependencies of the PD of therapeutic agents. However, not all medications, for example, those used to treat hypertension, are prone to circadian-time/sex interactions, for example, as demonstrated by results of studies with the ARB valsartan [199]. Bedtime dosing of valsartan (160 mg/day) better reduced sleep time SBP and DBP than did morning dosing and without administration time differences between women and men.

### 13.7.3.2 Chronotoxicology: Rhythm Dependencies in Adverse Effects of Medications

*Chronotoxicology*, an aspect of chronodynamics, refers to dosing-time (rhythm-dependent) differences in the susceptibility/resistance to potentially noxious exposures to biological, chemical, or physical agents, including infectious, therapeutic, and radioactive agents [200, 201]. The concept was initially demonstrated 60 years ago through a series of around-the-clock $LD_{50}$ challenge studies of different groups of rodents [202]. Circadian rhythm-dependencies of adverse

effects of medication are rarely explored in preclinical animal investigations and clinical trials. Knowledge of such dependencies comes from studies designed and conducted by chronobiologists. In humans, administration-time differences in the occurrence and severity of adverse effects have been reported, for instance, for synthetic hormone, NSAID, anticoagulant, aminoglycoside antibiotic, and hypertension medications [104, 185, 186, 188, 200, 201, 203].

One example entails the manifestation and severity of adrenocortical suppression, i.e., inhibition of cortisol synthesis and secretion, a potential undesired effect of synthetic anti-inflammatory glucocorticoid medications, such as dexamethasone, prednisolone, methylprednisolone, and triamcinolone. The risk and severity of adrenocortical suppression differ not only with dose, but also with time of ingestion, infusion, or injection of the medications, as demonstrated by a substantial number of animal and clinical studies commencing 50 years ago [50, 104, 105, 204–207]. As discussed in Sect. 5.1.4.4 and shown in Fig. 13.10 and Table 13.3, these medications are best tolerated, i.e., cause least adrenocortical suppression, when the entire dose is administered in the morning at the commencement of daily activity, which corresponds in time to the peak of the cortisol circadian rhythm. They are least tolerated, i.e., cause greatest adrenocortical suppression, when the entire or a significant portion of the daily dose is administered late in the day at supper or bedtime. These chronotoxicological findings have significantly impacted how synthetic corticosteroids are used in clinical practice. Since the 1960s, tablet MP and other such corticotherapies have been recommended as single-daily or alternate-day morning doses to minimize adrenal suppression, especially in patients requiring these potent anti-inflammatory medications chronically [106].

Other clinical examples of chronotoxicity are gastric effects caused by NSAIDs and pedal edema induced by the dihydropyridine CCB nifedipine GITS system. The likelihood of adverse gastric and neurologic effects of the slow release formulation of the NSAID indomethacin is greater when routinely ingested once-daily in the morning as opposed to evening. It is worthy of mention that discontinuance of indomethacin therapy in one large scale study was much more common when patients ingested the medication once-a-day in the morning or midday than at bedtime [188]. Risk of nifedipine-induced pedal edema varies greatly according to treatment time. In one study, the incidence of pedal edema was 13% when the medication was ingested upon-awakening, but only 1% when ingested at bedtime [208].

Medications with high risk of adverse effects and relatively narrow therapeutic range are especially prone to significant dosing time differences in patient tolerance. This is clearly exemplified by the findings of numerous circadian rhythm studies on animal models and patient trials involving cancer therapies [209–213]. Circadian chronotoxicities have been demonstrated for roughly 40 highly prescribed antitumor medications, including arabinosylcytosine, cisplantin, carboplatin, oxaliplatin, cyclophosphamide, docetaxel, doxorubicin, etoposide, 5-fluorouracil, and methotrexate. Moreover, animal studies also show vulnerability to fetal growth defects, malformations, and death due to teratogens, such as cortisone, dexamethasone, hydroxyurea, 5-fluorouracil, cyclophosphamide, cyctosine arabinoside, and ethanol, can sometimes differ greatly with their circadian timing [214].

## 13.8 Chronotherapeutics

Collectively, the examples cited in Sect. 13.7 substantiate the importance of body rhythms in determining the extent of therapeutic effect and safety of medications. They also reveal opportunities for the design of drug delivery systems to improve both desired outcomes and patient tolerance of pharmacotherapies by taking into consideration their specific circadian chonokinetics, chronodynamics, and chronotoxicologies.

### *13.8.1 Definition and Concepts*

*Chronotherapeutics* is the purposeful delivery of medications in time to meet biological-time determinants of disease pathophysiology (*chronopathology*) and chronopharmacology (chronokinetics, chronodynamics, and chronotoxicology) of medications to optimize outcomes and minimize/avoid adverse effects [20, 170]. Chronotherapeutics may involve improved delivery of established therapies or new medicines. In certain instances, chronotherapeutics is achieved by unequal morning and evening dosing schedules of conventional sustained release 12-h tablet and capsule systems, optimal timing of conventional once-a-day delivery systems, or application of special drug-delivery systems to proportion medications over the 24-h cycle in order to meet rhythm determined requirements. Current first generation chronotherapeutic drug delivery systems demand strict adherence by patients to recommended dosing time(s), with reference to the sleep–wake cycle, to achieve desired outcomes. Success of these chronotherapies also requires appropriate understanding by the clinical community of the concepts of chronobiology and chronotherapeutics to ensure their proper application [215].

Revision of dosing schedule, reformulation of the drug-delivery system, and use of programmable infusion pumps to deliver medications at biologically opportune times are some simple chronotherapeutic improvements that may reap enormous benefits. In some instances, chronotherapeutics may entail delivery of medication, especially endocrine and neuroendocrine analogues, in a high frequency mode to mimic the "language" of the endocrine and neuroendocrine systems. Chronotherapeutics may also entail resetting or reorganizing a disordered or desynchronized CTS by a special class of medications termed "chronobiotics," an example of which is melatonin. Judicious choice of ingestion time of a physiologic dose of melatonin by diurnally active persons can result either in a phase advance of the CTS, when dosed in the afternoon or early evening, or phase delay, when dosed in the morning after awakening (Fig. 13.3). When properly timed, melatonin accelerates adjustment (phase shift) of the circadian system of persons rapidly displaced by aircraft across time zones and lessens the duration and severity of jet lag symptoms [92, 216].

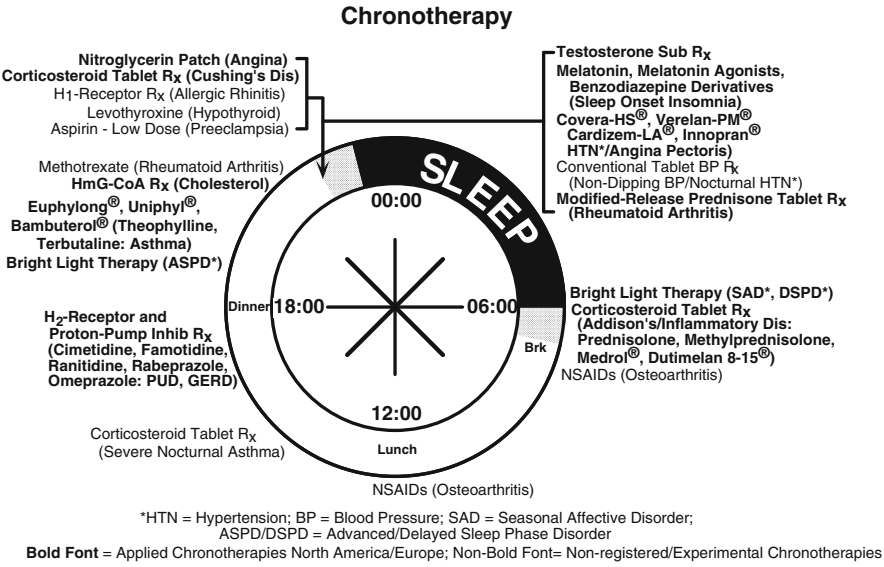


**Fig. 13.18** Registered and experimental chronotherapies. Since the 1960s, various chronotherapies have been introduced into clinical medicine. Some are recommended for administration before dinner, such as the $H_2$-receptor antagonist and proton-pump inhibitor medications for peptic ulcer disease and gastroeosphageal reflux disorder. Statin medications exert best cholesterol-lowering effect when ingested in the evening, and special theophylline and ß$_2$-agonist tablet and capsule formulations for asthma and other chronic obstructive pulmonary diseases are intended for evening ingestion. Evening bright light therapy is recommended to normalize the sleep-wake cycle of advanced sleep phase disorder (ASPD) patients. Other chronotherapies are intended for bedtime use, such as nitroglycerin patch application for angina pectoris, testosterone patch or cream substitution therapies, conventional tablet corticotherapy for Cushing's disease, sleep medications for sleep disorders, controlled onset, extended release calcium channel and ß-blocker hypertension and angina pectoris chronotherapies, and modified-release prednisone chronotherapy. Finally, conventional tablet corticosteroid chronotherapy for inflammatory conditions and as substitution therapy for Addison's disease, and bright light chronotherapy for seasonal affective disorder (SAD) and delayed sleep phase disorder (DSPD) are recommend for morning application. Unregistered or experimental chronotherapies include bedtime tablet $H_1$-receptor antagonists for control of sleep-time and morning peak symptom intensity of allergic rhinitis, levothyroxine for hypothyroidism, low-dose aspirin for prevention of pregnancy-induced hypertension and preeclampsia, and late evening methotrexate therapy for rheumatoid arthritis. Others include bedtime NSAIDS for rheumatoid arthritis and breakfast or lunch NSAIDS for osteoarthritis. Sleep and activity spans are indicated, respectively, as the *darkened* and *white portions* of the circle (Smolensky and Haus, unpublished)

## *13.8.2 Chronotherapeutics: History and Early Applications*

The first widely applied chronotherapy, introduced in the 1960s, entailed alternate-day morning dosing of tablet corticosteroid MP medication [106]. Other chronotherapies have since been widely used in clinical medicine in the USA, Europe, and Asia as summarized in Fig. 13.18. These include special evening

theophylline and ß$_2$-agonist tablet and capsule systems for nocturnal asthma [50, 217, 218], conventional evening $H_2$-receptor antagonists and proton pump therapy for PUD [179, 219], conventional evening tablet statin medications for hyperlipidemia [220], and several delayed onset hypertension formulations [221–225]. In certain centers, based on the results of local clinical trials, some medications, for example, $H_1$-receptor blockers, NIADS, thyroid supplementation, low-dose aspirin, and melatonin, are timed as chronotherapies.

#### 13.8.2.1 Chronotherapy of Nocturnal Asthma

Asthma is a relatively common chronic medical condition affecting in the USA alone, an estimated 6.5 million children and 15.7 million adults. It is characterized by persistent airway inflammation, heightened airway hyperreactivity to antigens and various environmental agents, markedly reduced airway caliber, and often excessive mucus production [50]. Symptoms include dyspnea (difficulty in breathing), wheezy chest, and croupy cough. It is seldom a problem when very mild, but it can significantly affect lifestyle and well being and even be life-threatening when severe.

Asthma is greatly affected by the CTS [50]. Symptoms and attacks of breathing distress occur only at night in most cases. A large multiple center study of more than 3,000 presumably diurnally active asthma patients found crises of breathing distress 70- to 100-fold greater in number between 04:00 and 05:00, during intended nighttime sleep, than between 14:00 and 15:00, middle of daytime activity span (Fig. 13.19) [126]. Turner-Warwick [125], in a 1980s study of a large group of 7,729 noninstitutionalized British patients, reported that 94% experienced disruption of their nighttime sleep by asthma at least once per month, 74% at least once per week, 64% three nights per week, and 39% every night, even though most were medicated with equal interval, equal dose bronchodilator, and anti-inflammatory medications. Perhaps it is because asthma exhibits such an obvious and profound day–night pattern in symptom intensity that it was the first medical condition to be aggressively investigated for circadian rhythm related mechanisms and chronotherapeutic interventions.

The signs and symptoms of asthma are at least partially reversible with bronchodilator and anti-inflammatory medication, plus proper environmental control of exposure to triggering agents. The goals of asthma therapy are (a) prevention of acute and chronic symptoms during night and day, (b) maintenance of normal or near normal pulmonary function (airway caliber), lifestyle, activity, and sleep, and (c) avoidance of medication-induced adverse effects. Specific treatment algorithms have been published by medical societies and governmental agencies [50] to guide patient management and to achieve therapeutic goals, and national and international guidelines exist for grading asthma severity and implementing treatment strategies. Grading of asthma severity is based in part on the frequency of disease-induced awakenings from nighttime sleep and the mean and amplitude of the circadian rhythm in airway caliber, i.e., PEF, self-measured by the patient.

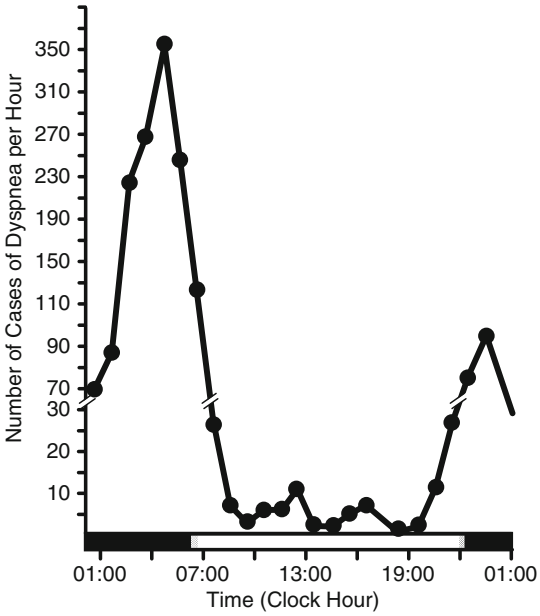


**Fig. 13.19** Day–night difference in asthma (1,632 episodes of dyspnea, i.e., difficult breathing) per hour of the day and night in 3,129 untreated asthma patients, i.e., washed-out of prescribed medications in preparation for trialing of a new asthma therapy. Episodes of dyspnea, signaling asthma, were 70- to 100-fold more common between 04:00 and 05:00, causing disruption of nighttime sleep, than early afternoon between 14:00 and 15:00. This 24-h pattern in asthma risk is the basis for chronotherapy with tablet, capsule, and aerosol bronchodilator and anti-inflammatory medication. *Shaded portion* of bottom time axis represents patients' nighttime sleep span and *white portion* represents diurnal wake span (redrawn after Dethlefsen and Repges [126])

Chronotherapy of nocturnal asthma is based on the day–night pattern in the occurrence and intensity of symptoms, identified underlying rhythm dependencies, and findings that equal interval, equal dose schedules of therapy are not always optimal to avert nighttime episodes of breathing distress. A large variety of medications, such as tablet $\beta_2$-adrenergic agonists, anticholinergics, tablet and capsule theophyllines, and aerosol and tablet anti-inflammatory corticosteroids have been studied for differences in their PK and/or PD as a function of the circadian time of administration [50]. Here, we illustrate the earlier developed theophylline chronotherapies for nocturnal asthma. Chronotherapies of other medications, including aerosol ones, are reviewed in detail elsewhere [50].

During the 1980s, theophylline was a first-line treatment for asthma, and although it is much less prescribed today, it constitutes a useful case study of applied clinical chronotherapeutics. Theophylline chronotherapy entails the purposeful delivery of medication in unequal amounts during the 24 h such that elevated concentration is achieved during nighttime sleep, when the risk of breathing crises is greatest, and reduced concentration occurs during daytime, when risk is lowest. The German pharmaceutical company Byk Gulden was probably the first to embrace the concept of theophylline chronotherapy. It recommended that

Euphyllin® be ingested twice daily in unequal doses, with one third the daily dose in the morning at the commencement of diurnal activity and remaining two thirds in the evening [226]. Similar asymmetric morning–evening dosing schedules have been used with other twice-daily sustained release 12-h theophylline (and also $ß_2$-agonist terbutaline tablet [227]) preparations to better manage nocturnal asthma, and occasionally conventional twice-daily sustained release theophyllines were trialed as evening-only high dose chronotherapies [50]. Although asymmetrical 12-h dosing regimens improved the beneficial effects of some conventionally formulated asthma medications, they posed difficulties for patient adherence and often caused adverse effects, especially when prescribed in high dose to ensure elevated daytime as well as nighttime drug concentrations.

Several once-a-day theophylline chronotherapies, relying on special tablet and capsule (tablet or bead coating) technologies were developed during the 1980s by pharmaceutical companies in Europe and USA. Two popular ones were Euphylong® (Byk Gulden, Germany) and Uniphyl®/Uniphyllin® (Purdue Frederick, USA/Mundipharma, Germany) [217, 218]. Figure 13.20 presents the so-called steady state PK and PD of one theophylline chronotherapy ingested in the evening as recommended, relative to the PK and PD of a popular conventional slow release theophylline medication ingested twice daily at 12-h intervals as recommended [218]. The drug delivery systems and dosing schedules of this conventional medication were intended to achieve the homeostatic goal of constancy in serum theophylline concentration, while the drug delivery system and bedtime dosing schedule of the chronotherapy were intended to achieve unequal levels during the 24 h, with peak drug concentration overnight when asthma risk is greatest.

Results demonstrated that conventionally formulated theophylline preparations do indeed achieve near-constant serum drug concentration, but as shown in Fig. 13.20 they fail to avert significant nocturnal decline of airway caliber. Studies show that the greater the nighttime decline of airway patency, the greater the risk of nocturnal asthma crises [6]. Thus, the extent of nocturnal decline in PEF, a measure of airway patency and ease of breathng, is a key biomarker of the robustness of therapeutic effect of asthma medications. Theophylline chronotherapies of approximately the same dose/24 h, in contrast, achieve considerably higher serum drug concentration during nighttime sleep, while still maintaining daytime therapeutic levels. The high nocturnal serum theophylline concentration achieved by chronotherapy results in substantial moderation of the overnight decline in PEF, leading to better control of symptoms and reduced risk of nighttime asthma, without loss of daytime drug effectiveness.

#### 13.8.2.2 Hypertension Chronotherapy

A second example of clinical chronotherapeutics entails hypertension medications. Toward the end of the twentieth century, special bedtime tablet and capsule BP-lowering medication systems were introduced that proportioned

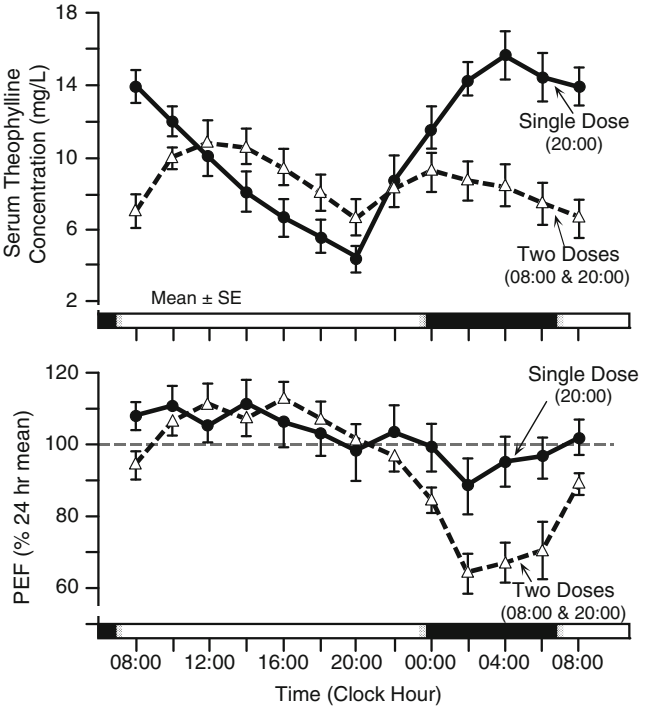


**Fig. 13.20** Pharmacokinetics and pharmacodynamics of comparable doses of conventional sustained-release (SR) twice daily, open triangles and dashed line, and evening chronotherapeutic (Uniphyl®: Purdue Frederick, USA/Uniphyllin®: Mundipharma, Germany), closed circles and solid line, theophylline medications. *Top*: Steady-state serum theophylline concentration for the conventional SR preparation ingested daily at 08:00 and 20:00 and chronotherapeutic preparation ingested daily at 20:00. Theophylline concentration is relatively constant over the 24 h with twice-daily conventional drug dosing; evening theophylline chronotherapy in contrast achieves much higher drug concentration during the sleep span, when asthma risk is greatest. *Bottom*: Effect on airway caliber of the conventional and chronotherapeutic theophylline time-concentration patterns. Conventional equal-interval, equal-dose theophylline regimen fails to avert significant nighttime decline of airway caliber (i.e., PEF or peak expiratory flow, expressed as % of 24-h group mean, designated as 100%), while theophylline chronotherapy does. Greater stability of the 24-h rhythm in airway caliber translates into enhanced protection against breakthrough asthma nocturnally. During the 1980s, when this study was conducted, high theophylline doses were prescribed, as it was believed then high serum concentrations (10–20 mg/ml) were required to achieve sufficient bronchodilation. Today, it is recognized that theophylline exerts anti-inflammatory effect on the airways at considerably lower doses, as now prescribed. *Shaded portion* of bottom time axis represents subjects' nighttime sleep span and *white portion* represents diurnal wake span (figure redrawn after Neukirchen et al [218])

drug concentration in synchrony with a priori assumed day–night patterning in SBP, DBP, and heart rate (HR) of hypertension patients (see Fig. 13.4). In the USA, four delayed onset, controlled release chronotherapeutic systems – Covera HS® (Searle/Pfizer), Verelan PM® (Schwarz), Cardizem LA® (Biovail), and

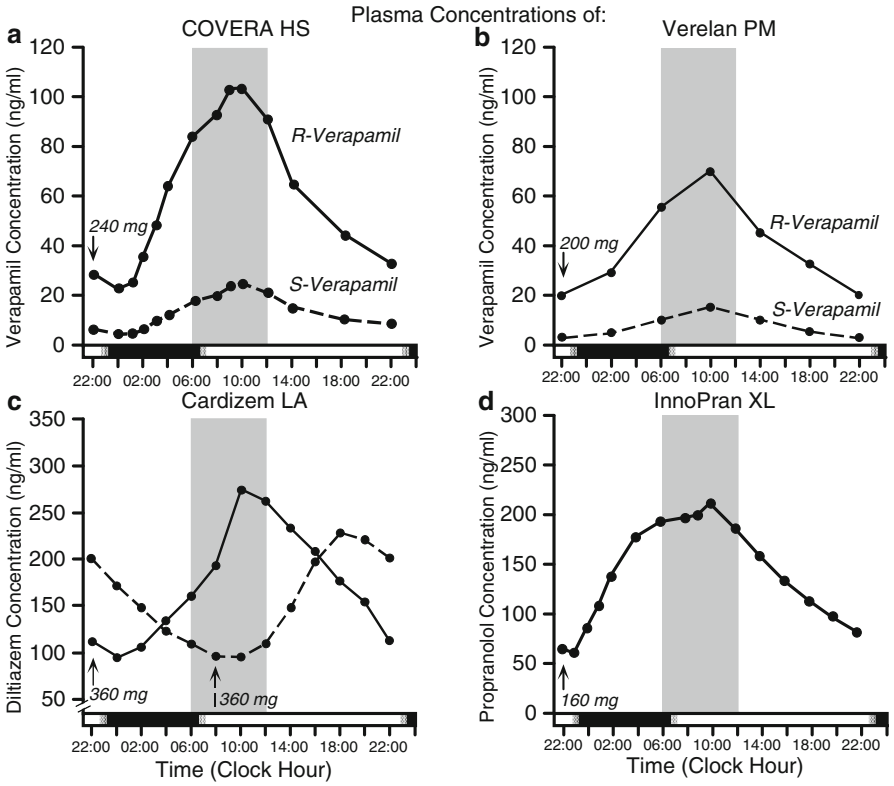


**Fig. 13.21** Steady-state pharmacokinetics of the *R*- and *S*-enantiomers of first generation controlled-onset, extended-release hypertension chronotherapies: (**a**) 240 mg COVERA HS® (calcium channel blocker verapamil; Searle/Pfizer), (**b**) 200 mg Verelan PM® (calcium channel blocker verapamil; Schwarz Pharma), (**c**) 360 mg Cardizem LA® (calcium channel blocker diltiazem; Biovail Pharmaceuticals), and (**d**) 160 mg Innopran XL® (ß-agonist propranolol; Reliant Pharmaceuticals). When these chronotherapies are ingested at bedtime as intended, they produce highest drug concentrations in the morning between 06:00 and 12:00 (*shaded rectangle*), when in dipper hypertension patients systolic and diastolic blood pressure (BP) reaches peak or near-peak level and when angina pectoris, acute myocardial infarct, and sudden cardiac death are of greatest risk, presumably as a consequence of the sudden surge in BP and heart rate at this time of day. In part **c**, the steady-state pharmacokinetics of 360 mg Cardizem LA® is shown when ingested as intended at bedtime, in accordance with the design of the drug-delivery system, and also in the morning upon awakening. Dosing of this hypertension chronotherapy in the morning at the wrong time results in *lowest* concentration of diltiazem in the morning, when BP in essential hypertension patients is likely to be *greatest*, and highest concentrations in the late afternoon and evening, when BP is expected to be declining from daytime elevated levels. *Shaded portion* of bottom time axis represents assumed subjects' nighttime sleep span and *white portion* represents assumed diurnal wake span (figure redrawn from Smolensky et al. [224])

Innopran XL® (Reliant) – were introduced to improve hypertension therapy and reduce morning-time risk of angina pectoris, myocardial infarction, and stroke (Fig. 13.21) [221–225]. Myocardial infarction and stroke are 30–40% higher in incidence during the initial hours of the activity span [142, 144], and it is

hypothesized they are triggered in at-risk patients by the marked morning raise in SBP, DBP, and HR, coincident with peak platelet and blood coagulation level and minimum fibrinolytic activity [228].

The drug delivery system for each of these special products is designed to retard release of medication for ~4 h following bedtime ingestion and to ensure peak or near-peak drug concentrations during morning and daytime activity, in order to maximally control SBP, DBP, and HR, when they are all anticipated to be highest, and to ensure lower, but nonetheless therapeutic, concentrations during the evening and nighttime sleep, when they are anticipated to be lowest. Clinical trials of these special drug delivery medication systems substantiated improved control of morning-time HR and BP compared to conventional medications of the same class and dose. However, complaints of adverse effects, such as daytime fatigue and dizziness, signs suggestive of hypotension, were expressed by some patients. These drug-delivery forms are specifically designed to inhibit discharge of medication for ~4 h following ingestion at bedtime; thus, the entire daily dose is released over 20 rather than 24 h, posing risk of over-correction of BP and daytime hypotension when patients are transferred from the same dose of the same medication formulated for conventional constant-release over the full 24-h dosing interval.

The first intended prospective, large scale assessment of the preventive effects of hypertension chronotherapy was the 5-year international multicenter Controlled Onset Verapamil INvestigation of Cardiovascular Endpoints (CONVINCE) outcomes trial involving 15,000 hypertensive patients with identified CVD risk. This trial was designed to compare the degree of BP control and protection against CVD events afforded by verapamil (Covera HS®) chronotherapy compared to the then considered standard conventional treatment, i.e., β-blocker and diuretic medications [229]. Unfortunately, this community-based outcomes study was terminated prematurely before sufficient number of CVD events had occurred to enable valid assessment of the bedtime chronotherapy [230, 231]. Thus, the merit of delayed-onset, constant release chronotherapeutic systems, relative to conventional therapy, in preventing CVD events as a consequence of improved control of morning-time SBP, DBP, and HR remained unresolved.

In view of the paucity of available data, the prospective MAPEC (Spanish: Monitorización Ambulatoria para Predicción de Eventos Cardiovasculares; English: Ambulatory Blood Pressure Monitoring for Prediction of Cardiovascular Events) study was conducted in Spain by Hermida and collaborators [191, 232]. This recently completed study was specifically designed to test the hypothesis that bedtime chronotherapy with one or more hypertension medications exerts better BP control and better reduces CVD risk than conventional morning dosing of all such medications. All 2,156 hypertensive subjects were evaluated by 48-h ABPM at baseline and thereafter annually, if not more frequently (quarterly) if adjustment of hypertension treatment was required.

At baseline, the two treatment time groups were comparable in their clinic and mean ambulatory SBP and DBP, and prevalence of nondipping 24-h BP pattern. Subjects who ingested the entire daily dose of one or more of their hypertension medications at bedtime, compared to subjects who ingested all their hypertension

medications in the morning, showed at their last available ABPM evaluation significantly lower mean sleep time BP, higher sleep time relative BP decline (an index of normal BP dipping 24-h pattern), reduced prevalence of nondipping BP circadian pattern (34% versus 62%), and higher prevalence of controlled ambulatory BP (62% versus 53%). After a median follow-up of 5.6 years, subjects who consistently ingested at least one prescribed BP-lowering medication at bedtime showed highly statistically significant reduced risk of CVD events, in particular, myocardial infarction and stroke, compared to subjects who ingested all such medications upon awakening (relative risk 0.39 with 95% confidence interval 0.29–0.51). The progressive decrease in the asleep BP and increase in the sleep-time relative BP decline, both indicative of a more normal dipping 24-h pattern, were best achieved when one or more hypertension medications were taken at bedtime, and these two indicators of BP control were the most significant predictors of CVD event-free survival. Results of the prospective MAPEC study thus indicate bedtime chronotherapy with one or more hypertension medications, compared to conventional upon-waking treatment of all medications, more effectively achieves BP control, better decreases the prevalence of BP nondipping, and better normalizes the 24-h BP pattern and, most importantly, significantly reduces CVD morbidity and mortality [191].

#### 13.8.2.3 Nitroglycerin Chronotherapy

Nitroglycerin (glyceryl trinitrate, GTN) is a smooth muscle relaxant that has been used in the treatment of hypertension and, most notably, angina attacks. GTN, upon uptake into cells, is metabolized and converted to nitric oxide, which activates adenylate cyclase and increases cyclic AMP production, which signals smooth muscle relaxation [233–236]. As a small lipophilic molecule, GTN readily permeates epithelial membranes such as those of the skin and cheek. Traditionally, it is prepared in ampule form. During or in anticipation of an angina attack, the ampule is placed in the mouth by the cheek and broken, permitting rapid absorption across the buccal membrane, and providing fast relief. Because of its ease in formulation, permeability properties, and low plasma concentration required for activity (~10 nm), GTN was an early candidate for transdermal patch delivery. It was hoped that GTN patch therapy would exert prophylactic effect and reduce incidence of angina. Several such patches received regulatory approval based on PK studies that demonstrated sustained maintenance of GTN at therapeutic levels. Unfortunately, it was soon observed that biological tolerance to GTN developed after ~12 h. (Interestingly, this tolerance could have been anticipated based on the "Monday rebound" effect reported in munitions workers in the nineteenth century [237, 238].) Numerous hypotheses regarding the mechanism of tolerance have been under investigation for several decades, some attributing it to depletion of cofactors required for GTN metabolism, and others to down-regulation of metabolizing enzymes or adenylate cyclase activation [234, 239–242]. Regardless of mechanism, patches are now prescribed to be

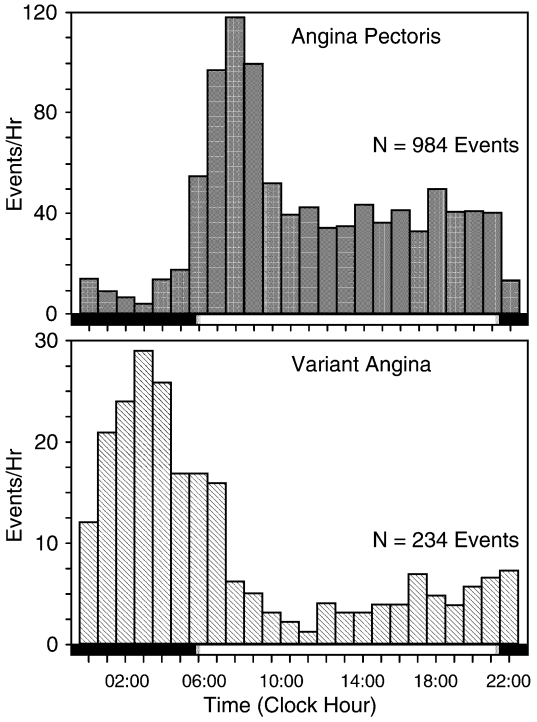


**Fig. 13.22** Twenty-four-hour pattern of exertion-induced angina pectoris (984 ischemic events denoted as ST-segment depression of the electrocardiolographic [ECG] tracings obtained by ambulatory holter monitoring study) recorded in 235 diurnally active, nonmedicated ischemic heart disease patients (*Top*) and also angina pectoris (234 events in total) recorded in a group of diurnally active vasospastic (Prinzmetal, nonexertion variant) patients (*Bottom*). Bouts of conventional angina pectoris are more common during daytime activity, in particular between awakening (~06:00) and noon (12:00). In contrast, bouts of vasospastic angina typically occur during rest, especially during nighttime sleep, between 01:00 and 04:00. Chronotherapy of angina pectoris must take into consideration the circadian pattern in risk during the 24 h and associated temporal requirement for medication. *Shaded portion* of bottom time axis represents presumed nighttime sleep span of subjects and *white portion* represents diurnal wake span (*top graph* created using unpublished data of first author; *bottom graph* created using data of Kimura and Kuroiwa [244, 245])

worn for 12 h, followed by a patch-free period of equal duration during which sensitivity to GTN is regenerated [243]. The notion of tolerance followed by resensitization finds parallel in explanations for pulsatility of neuroendocrine hormones, to be discussed later.

Optimal use of GTN patch therapy has been tied to the circadian rhythm in risk of both exertion- and nonexertion triggered (variant or Prinzmetal) forms of angina (Fig. 13.22), with or without (silent angina pectoris) chest pain. Thus, GTN patch chronotherapy entails evening or bedtime application and midday removal to cover the time span when risk of angina due to physical exertion, coronary vasospasm (variant angina), and cardiac stress induced by hypoxia of sleep apnea is greatest [140, 141, 244, 245].

#### 13.8.2.4 Cancer Chronotherapy

Chronotherapy of cancer medications is based on knowledge that their chronotoxicity varies markedly by cell cycle stage, both in normal and tumor tissue [209–213]. Programmable in time, light weight ambulatory infusion pumps can be used to infuse cancer medications at the desired circadian time when healthy, noncancerous cells are in a nonvulnerable stage. Cancer cells may lose their circadian periodicity and multiply at a faster rate, i.e., with a period <24 h, or at random and, therefore, are likely to be more vulnerable to therapy at a time when noncancerous cells are least susceptible. Results of both laboratory animal and European multicenter patient trials clearly show that proper circadian delivery and timing of cancer medications improve tolerance to therapy, thereby enabling more aggressive treatment [210–212]. However, significant advances in improving long term cancer-free interval and survival, relative to conventional treatment entailing constant infusion of cancer medications during the daytime, have not yet been consistently demonstrated. Nonetheless, clear opportunities exist for the application of advanced drug delivery systems to improve both patient tolerance and outcomes of cancer medications.

### *13.8.3 Noncircadian Chronotherapeutics*

Many endocrine and neuroendocrine secretions exhibit prominent high-frequency and pulsatile variability over time, which may be relevant to the effectiveness of certain neuroendocrine analogues. Indeed, the frequency-modulated or pulsatile mode of drug-delivery systems may be of greater importance than the dose of drug delivered.

#### 13.8.3.1 Gonadotropin Releasing Hormone (GnRH: aka Luteinizing Hormone Releasing Hormone, LHRH) Chronobiology and Chronotherapy

GnRH is a decapeptide, synthesized and secreted by the hypothalamus into the pituitary portal circulation in an intermittent fashion, stimulating pituitary gonadotropes to synthesize and secrete LH and FSH [246, 247]. In a series of exquisite studies on female Rhesus monkeys [248–250], Knobil and coworkers established that the frequency of GnRH delivery determines its biological effect. Lesioning of the hypothalamus abolishes GnRH secretion, and continuous infusion of the decapeptide fails to reinitiate endogenous LH and FSH production. However, frequency modulated GnRH infusion as a single 6-min pulse/h reestablishes normal pituitary function. Of practical interest is that GnRH delivery as five 12-min pulses/h produces an effect similar to constant rate infusion, as it fails to reinitiate endogenous LH and FSH production. An infusion

frequency of two or three pulses of GnRH/h is less efficient or exerts inhibitory effect on FSH and LH, while an infusion frequency to one pulse/3 h changes the LH/FSH ratio.

Pulsatile GnRH secretion is essential for its effect on the pituitary, as confirmed by clinical trials. Pulse pattern and circadian variation of plasma LH in sexually mature women are modulated by the menstrual cycle [251, 252]. During luteal–follicular transition, LH pulse frequency increases markedly, and this accompanies selective FSH rise leading to normal folliculogenesis [253]. Continuous and/or closely repetitive GnRH stimulation leads to blunted gonadotropin response [254, 255] due to pituitary desensitization (analogous to tolerance developed to nitroglycerin, as discussed in Sect. 13.8.2.3, but by a different mechanism) [246]; thus, continuous infusion of constant dose GnRH, or administration of long-acting GnRH analogs, inhibits LH secretion [246, 256]. This knowledge can be used for contraception and to manage hormone-dependent cancers, such as those of the breast and prostate, and sustained-release depot injections of biodegradable microspheres containing GnRH (LHRH) analogs are marketed for this purpose, e.g. Lupron® depot. Pulsatile delivery of GnRH every 60–90 min, on the other hand, is an effective means of obtaining ova for in vitro fertilization [257, 258], and for treating supra-hypophyseal hypogonadotropic hypogonadal anovulation [258–260] and arrested puberty [261–263].

#### 13.8.3.2 Growth Hormone

Growth hormone (GH) is critically important for growth, metabolism, and tissue and organ maintenance. It is used to treat abnormally short stature and dwarfism in children, and increasingly to slow aging of adults. In animal husbandry, GH is commonly used to increase milk yield of dairy cows and enhance muscle mass of pigs and other animals. Prominent pulsatile, ultradian, circadian, and perhaps other periodicities in GH secretion and suspected rhythm dependencies in target tissue responsiveness constitute significant challenges, but also potential opportunities, for drug delivery scientists to achieve or improve desired treatment outcomes and/or avoid negative consequences.

##### Growth Hormone Synthesis and Secretion

GH is synthesized and secreted by somatotrophs of the anterior pituitary and plays a major role in many processes, most notably growth and metabolism. GH is synthesized and secreted in a pulsatile manner, generally with plasma peaks ranging from 5 to 45 ng/mL Greatest GH secretion takes place primarily during sleep in a sex-dependent pattern, with largest and most predictable GH peaks found ~1 h after sleep onset and with ~50% of GH secretion occurring during the third and fourth REM sleep episodes. Between peaks, basal GH levels are low, usually less than 5 ng/mL. Its effects are exerted directly, by binding to its receptors, and indirectly,

by stimulation of mediators, primarily insulin-like growth factor-1 (IGF-1), in liver and other tissues. Growth of organs and tissues is mediated via IGF-1. For example, IGF-1 causes proliferation of chondrocytes (cartilage cells) and thus bone growth, and it induces muscle growth by stimulating differentiation and proliferation of myoblasts. GH participates in blood glucose regulation through its anti-insulin activity, i.e., by suppressing glucose uptake in peripheral tissues and promoting hepatic glucose synthesis. It also promotes protein anabolism and synthesis by enhancing amino acid uptake and slowing protein oxidation, and it stimulates adipocyte fat utilization, inducing triglyceride breakdown and oxidation. Other important actions of GH include bone calcium retention and mineralization, pancreatic islet cell maintenance and function, and immune system maintenance [264–266].

GH is secreted at an elevated rate of ~700 μg/day in young adolescents, but at a lower rate of ~400 μg/day in mature healthy adults. The primary controllers of GH synthesis and secretion are two hypothalamic hormones, growth hormone-releasing hormone (GHRH), which stimulates synthesis and secretion of GH, and somatostatin (SS), which inhibits GH release in response to GHRH and other stimulatory factors (e.g., low blood glucose concentration). The stomach growth hormone secretagogue (GHS) ghrelin binds to receptors on somatotrophs to robustly stimulate GH secretion. GH secretion is regulated by a negative feedback loop involving IGF-1. Elevated blood IGF-1 concentration inhibits GH secretion by suppressing somatotrophs and by stimulating SS release from the hypothalamus. GH also feeds back to inhibit GHRH secretion to exert a direct (autocrine) inhibitory action on its own secretion from somatotrophs.

Regulation of the somatotropic axis, however, is much more complex than overviewed above, since GH synthesis is influenced and moderated by many factors, for example, sex hormones in pubertal boys and girls, androgen secretion (respectively, by the testis and adrenal cortex), and estrogen secretion (respectively, by the adrenal cortex and ovaries). Hypoglycemia, exercise, and deep sleep stimulate GH secretion, while hyperglycemia, free-fatty acids, glucocorticosteroids, and dihydrotestosterone inhibit it. GH secretion levels may also be affected by medications, being stimulated by L-DOPA and clonidine and inhibited by estrogen and testosterone. It may also be modified by estrogen disruptors.

Somatotropic axis regulation is highly organized in time as circadian, ultradian, and pulsatile oscillations [205, 265, 267]. Sex, age, body mass index, and IGF-1, individually and jointly, determine distinct GH dynamics [267]. In the resulting complex pattern of GH secretion, rhythmic and nonrhythmic variations in plasma concentrations determine circadian mean, peak values, and/or trough values, which mediate metabolic effects in target organs [268, 269]. Furthermore, regulation of GH secretion and effects also depends upon interactions with other neuroendocrine and endocrine constituents, including GHS ghrelin [270], sex hormones [271], and other factors [265], many of which are rhythmic. GH effects are also determined by rhythms in target tissues [271, 272], the temporal control of which in the circadian frequency range may be centrally mediated by the hypothalamic body clock (SCN)

plus other periodic phenomena, like the time of food uptake that can synchronize peripheral oscillators, especially in the liver. The complex pattern of GH secretion and plasma concentrations encountered in the periphery consists of regularly recurring rhythmic and pulsatile variations, the amplitude, shape, and spacing of which may be regular or variable [273]. The placement in time of clusters of pulses and variation in their amplitude [274] over the 24 h may represent expression of circadian and/or ultradian oscillations in GH, which may differ between males and females and with age, but are of fundamental importance.

GH secretion is governed by the facilitative and antagonistic effects of GHRH and SS, respectively, and depends upon the relative timing of their releases, with differences in regulation due to sexual dimorphism and age [265, 275, 276]. Sex steroid hormones modulate GH synthesis, release, and actions [266, 277], leading to sex-dependent dimorphism of GH secretion and plasma levels. GHRH and GHS ghrelin amplify GH signals. GHS ghrelin is secreted predominantly, but not exclusively, in the stomach and may amplify, but not set, the timing of this regulatory circle of GHRH/GH pulses [264, 270]. Reciprocal control by GHRH-SS may constitute the oscillator of the somatotropic axis [265] for some, but not all, observed variations. The stimulatory effect of GHRH depends upon age, sex, body composition, and nutritional status and augments the outcome of GHS ghrelin stimulation, which may be altered by underlying diseases [266, 278].

### Sex Differences in GH Secretion and Patterns

Sex hormones determine the pattern of GH secretion and lead to a dimorphic form of plasma GH and, as a consequence, IGF-1 concentrations. Average 24-h GH concentration is higher in women than in men largely due to higher daily trough values between secretory bursts [267]. Irregularity of pulses and narrow sharp elevations ("spikes") are more pronounced in women than in men [267]. Major (eight to tenfold) variation in mean GH pulse size occurs in puberty and during the menstrual cycle caused by a variety of internal and external factors [271]. In men, highest GH pulse, amounting to ~70% of the 24-h secretory output, occurs shortly after sleep onset, coinciding with the first episode of slow-wave sleep (SWS) [279]. In normally cycling women, there is a wider distribution of GH pulses during the 24 h. The sleep onset-associated pulse is also found in most women, but it accounts for a smaller fraction of total 24-h secretory output [280]. During sleep, healthy young men show overnight GH pulses every 35–60 min superimposed on which frequent sampling (30-s intervals) reveals diminutive pulses linked with sleep stage [281]. This association is based on the hypothalamic relationship between GHRH and brain areas involved in sleep regulation [282].

Suppression of endogenous GHRH action by specific antagonists or by immunoneutralization inhibits both sleep and GH secretion [283]. Conversely, substances that promote SWS increase nocturnal GH section [284, 285]. The linkage between the major GH pulse and sleep onset leads to an immediate shift in the circadian rhythm in GH with any alteration of the sleep–wake cycle, e.g., in workers

rotating between day and night shifts and in travelers rapidly displaced across time zones. This linkage also leads to alteration of GH secretions with day-to-day sleep pattern irregularities [279].

### GH Receptors

The presence and action of hormone receptors in peripheral tissues is organotypic, as is their interaction with other hormones. Type of sex steroid and specific target site determine the regulation of GH and IGF-1 receptors at that level [271, 286, 287]. In animal models, GH pulsatility mediates a sexually bimorphic regulation of hepatic and muscle gene expression, somatic growth, and negative feedback upon the hypothalamus [265, 271]. Moreover, the GH pulse pattern determines target tissue responses. For example, exposure of female rats to seven or fewer distinct GH pulses per 24 h induces masculine growth and gene expression patterning in different organs [288]. In contrast, exposure of hypophysectomized male rats to more frequent pulses or continuous infusion of GH evokes feminine growth and gene expression patterning [288, 289]. Furthermore, different target organs appear to have different absolute pulse amplitude dose response dependencies [273]. In subjects with inactivity of human GHRH receptor, i.e., Laron syndrome [290], there is profound reduction in secretory burst mass and disorderliness of GH pulses. Nonetheless, most pulses occur at a normal frequency and in a circadian rhythmic distribution with sex difference in the pattern maintained [271, 291].

### Factors Influencing GH Secretion and Consequences of GH Abnormalities

Aging is associated with reduced mean 24-h GH concentration due to decreased pulse amplitude rather than pulse frequency [292, 293]. Such age associated changes in GH secretion are thought to be due to diminished GHRH responsiveness and increased SS secretion [294].

Abnormalities and lesions of the hypothalamus and pituitary that interfere with GH level and pulse characteristics and/or effects in peripheral target cells result in specific disease states. The consequence of GH deficiency depends upon age of onset. GH deficiency and receptor binding defects during childhood manifest as retarded growth and dwarfism. Excessive GH secretion in young children or adolescents may result in giantism, typically due to somatotroph tumor. In adults, excessive GH secretion is typically due to a benign pituitary tumor and results in acromegaly.

Acromegaly is typically an insidious condition, developing over several years in middle-age adults, causing extremity overgrowth, soft-tissue inflammation, skin thickening and oiliness, jaw and facial abnormalities, hypertension, cardiac hypertrophy, and metabolic derangements, including hyperglycemia and diabetes, among other symptoms and complaints. This disorder is accompanied by alteration of both the amount and pulse pattern of GH secretion. Hormone secretion is irregular in

pattern and timing, with irregularly shaped frequent small peaks superimposed upon high baseline interpulse GH concentrations [295, 296]. High basal values are the likely cause of the characteristic elevation of IGF-1 observed in acromegaly [297]. Difference in GH secretory pattern, rather than in absolute level, determines GH effect, and this explains finding normal overall GH levels but characteristically elevated IGF-1 in a recent study of acromegalic patients [298]. Surgical micro-adenomectomy restores physiologic secretion patterning in most acromegalic patients [299].

Basal GH levels and pulsatile secretory patterns impact body fat metabolism and distribution. Both increased and decreased GH concentrations persisting over a prolonged time span lead to CVD risk. GH deficiency is associated with an increase in CVD risk factors, such as elevated mean total and LDL cholesterol plus C-reactive protein [300, 301], reduced HDL levels, but higher TNF-alpha receptors I and II. GH-deficient patients tend to be overweight or obese and show increased carotid media thickening as evidence of increased vascular complications [301, 302]. GH deficiency is also associated with high incidence of nonalcoholic fatty liver disease [303], which can be reversed by GH administration [304]. C-reactive protein (CRP) and free fatty acids have been found to be significantly elevated in hypopituitary patients with fatty liver [303]. GH replacement therapy improves the lipid profile with the exception of lipoprotein(a) concentrations, which tend to increase after GH therapy [305]. GH replacement therapy in this respect is complementary with HMG-CoA reductase inhibitor (statin) therapy [306].

In obese premenopausal women (BMI >34 kg/m [2]) with abdominal obesity pattern, plasma GH concentration is markedly reduced, due both to diminished basal hormone secretion and disordered pulsatile patterning. This abnormal GH level and secretory pattern persists after substantial weight loss (~40% of visceral fat); thus it is viewed as a cause rather than consequence of the condition, a conclusion supported by the finding that obese women of the same BMI, but with small visceral fat area, show normal GH level and secretory patterning [307]. Increased concentrations of GH in active acromegaly are also associated with increased atherogenic risk factors. For example, increased levels of oxidized low density lipoproteins are probably related to increased levels of pro-oxidants, such as ceruloplasmin, and biomarkers of inflammation, which are linked to increased CVD mortality [308, 309].

### Role of Delivery Pattern on GH Effect

Continuous or pulsatile GH delivery differently affects various parameters of GH action [269, 297, 310, 311]. Continuous, rather than intermittent, GH administration is regarded as the preferential pattern for induction of plasma IGF-1 and muscle IGF-1 mRNA [311], both in pituitary deficient and clinically healthy human subjects. Continuous GH delivery to hypopituitary patients maintains liver-derived IGF-1 and lipoprotein(a) concentrations to a greater degree than repeated injections [297, 312–315]. Conversely, bolus GH injection stimulates visceral lipolysis and

elevates HDL concentrations more effectively than constant infusion [273, 310, 314]. Only pulsatile GH augments rate of lipolysis [311].

In young diabetics, GH pulsing increases insulin requirements more than continuous GH infusion [273], while in healthy young men GH pulses are more effective in promoting SWS [316], indicating organ specificity in effects of GH delivery pattern. Treatment protocols of continuous infusion and of infusions of eight equal boluses every 3 h were most effective in increasing IGF-1 and IGFBP-3 (insulin growth factor-binding protein-3), whereas pulsatile administration had greatest effect on markers of bone formation and resorption [269]. All GH treatments decrease cytochrome P1A2 activity studied by erythromycin breath tests, with greatest effect for pulsatile GH. Pulsatile GH infusion decreases, whereas continuous GH infusion increases, cytochrome P3A4 activity [269]. These cytochromes are mixed function oxidases, which, among others, catalyze many reactions involved in drug metabolism [317, 318].

## Pharmaceutical Uses of GH and GHRH

Treatment of severe childhood growth retardation in the past relied upon GH purified from human cadaver pituitaries. Nowadays, recombinant GH (rhGH) or GHRH may be used. GHRH treatment of children with pituitary insufficiency was most effective when bolus injections were delivered by pump at 3-h intervals [319]. When GH was given by continuous infusion over a 4-week span to adult GH-deficient patients, it was more effective than when given as a once-a-day injection [320]. GHRH is absorbed nasally, but its effectiveness by this route is still not widely confirmed [321]. Of interest for noninvasive timed administration of GH is the nasal delivery of recombinant hGH together with a polymeric absorption enhancer [322]. The current clinical guidelines for evaluation and treatment of childhood [323] and adult GH deficiency by the Endocrine Society [324] do not address optimal time and pattern for GH and GHRH treatment, which may vary in different clinical situations.

The role of GH supplementation in aging remains poorly understood, but some cosmetic symptoms of aging appear to be amenable to therapy. This is an active area of research, and additional information and recommendations concerning risks and benefits, as well as biological timing and patterning during the 24 h, will undoubtedly surface in the near future. Sensitivity to treatment with rhGH is sex-dependent. Women require a substantially higher dose than men to achieve comparable effect on IGF-1 level [325–327] and bone mass [327], and much higher doses are required by women receiving oral estrogen replacement [326]. Older patients show increased susceptibility to GH-related side effects [324] and rhGH dose for GH-deficient patients should be individually titrated according to desired effect, i.e., to maintain serum IGF-1 within the physiologic range and avoid undesirable effects. However, it is not yet resolved how to best deliver rhGH, as a continuous infusion or as intermittent pulses, and if the latter at what frequency, concentration (height/amplitude), and circadian time. Different disorders may require different

temporal patterns of dosing. GH secretion patterns are an independent regulator of GH action in humans [269], which are thus far grossly underexplored and underutilized.

GH is approved and marketed for use in animal husbandry. Administration of bovine somatotropin to lactating cows increases milk yield, and seems to be cost-effective. Administration of porcine GH to growing pigs significantly stimulates muscle growth and reduces fat deposition. However, it is not known whether GH effects in animals can be improved by delivery in a chronotherapeutic mode, which takes into consideration the temporal patterns observed in nature, and if so whether it will be cost-competitive.

Analogs of GHRH and other peptidergic and nonpeptidergic compounds including ghrelin, collectively designated GH secretagogues, have been used as diagnostic tools in GH-deficient states and in relation to aging [328–331]. Treatment with GHRH analogs in single doses in the morning or without regard to circadian phase [329, 332] and the orally active GH secretagogue MK-677, a ghrelin mimetic [328, 331], enhance GH basal interpulse concentrations and GH pulse height in adults and elderly subjects without change in pulse number and pattern. The complex time organization of the somatotropic axis suggests the possibility of drug delivery patterns tailored according to age, sex, and condition to be treated. This is a wide open field which will require further research.

#### 13.8.3.3 Insulin and Glucose Chronobiology and Chronopharmacology

In nondiabetic individuals, insulin is secreted by the pancreas at a low basal rate between meals and rapidly secreted at meal times. The purpose of this switch is to maintain glucose homeostasis in the normoglycemic range of 70–120 mg/dl. The nature of the temporal variation in glucose and insulin concentrations during the 24 h in healthy individuals, based on blood samplings every 5 min during meals and 30 min at other times, is shown in Fig. 13.23 [333]. This figure highlights the substantial rise of the two constituents following each meal of the day and also at the end of the night, the so-called “dawn phenomenon”, as discussed below. The temporal variation, however, is primarily of a high frequency mode. Insulin exerts its control by inducing transport of excess blood glucose into the liver, where it is stored in its polymerized glycogen form, and by mobilizing uptake of glucose into tissues. This automatic control system is disabled in Type I diabetes due to autoimmune destruction of insulin-secreting pancreatic ß cells. For diabetic individuals prescribed insulin, delivery rate should mimic, as closely as possible, that provided by a normally functioning pancreas.

Failure to maintain normoglycemia entails two risks. If insulin is overdosed, then blood sugar levels fall below normal range, exposing the diabetic patient to hypoglycemia. Symptoms of hypoglycemia are typically acute, and may include dizziness, confusion, and sometimes seizures and/or coma. Underinsulination, on the other hand, leads to hyperglycemia. An acute symptom of hyperglycemia is ketoacidosis, which occurs with metabolic shifts due to deficient glucose transport

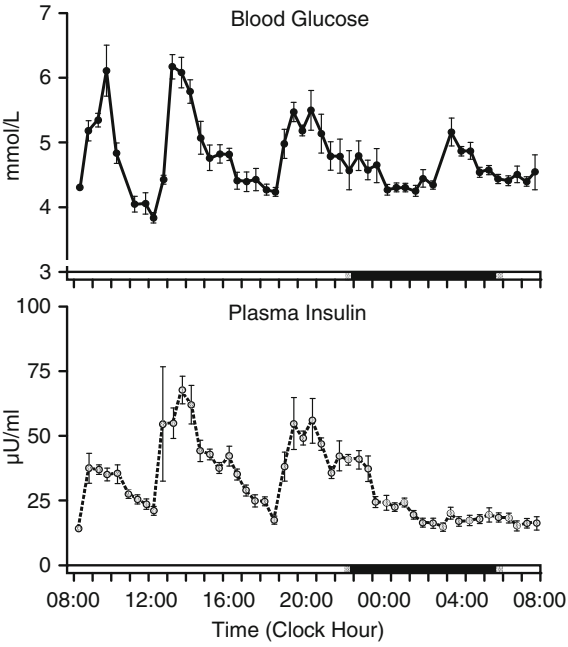


**Fig. 13.23** Average 24-h patterning of blood glucose (*Top*) and plasma insulin (*Bottom*) concentration of five diurnal active, clinically healthy subjects sampled at 5 to 30-min intervals during a single 24-h span. Spikes in glucose and insulin are evident after each meal (breakfast ~08:00, lunch ~12:30, and dinner ~19:00) and in addition ~04:00–05:00, so-called dawn effect. *Shaded portion* of bottom time axis represents subjects' nighttime sleep span and *white portion* represents diurnal wake span (figure redrawn from data published by Mèjean et al. [333])

into metabolizing tissues. Longer term consequences of sustained hyperglycemia include myopathy, retinopathy, nephropathy, and neural and connective tissue degeneration.

Since the isolation of insulin by Banting and Best in the 1920s, extensive effort has been extended to develop and improve insulin-based therapies for Type I diabetes. Slow (insulin glargine, Lantus®) and fast-acting (Lyspro/Humalog®) modified insulins have been developed, respectively, to provide basal levels, especially overnight, and to rapidly respond to postprandial rises in glucose [334]. These insulins can be administered by injection or wearable pump. Glucose monitoring, either discretely by finger sticks or continuously by an in-dwelling glucose sensor, can be utilized to improve timing and dosing decisions. Automatic closed loop systems, in which sensed glucose time series concentration data are used to instruct insulin pumping rates, are the object of continued research [335–339]. Such systems will optimally mimic the proportional, integral, and derivative (PDI) aspects of control by a normally functioning pancreas.

The goal of insulin therapy is to mimic a functioning pancreas and in the words of traditionalists "maintain glucose homeostasis." This result can only be achieved by delivering insulin at a decidedly nonconstant rate and in a chronotherapeutic fashion. Strictly speaking this kind of chronotherapy is not designed primarily around a circadian or ultradian rhythm, however, since demand for insulin at any given time is governed by many factors, the most important ones being the timing, content, and size of meals, counter-regulatory and other hormonal effects, and energy expenditure. There are, however, well established circadian and ultradian

effects of insulin on blood glucose level that are not driven by feeding times [340–345]. For example, both glucose and insulin levels exhibit morning-time peaks (Fig. 13.23). The concurrency of these peaks suggests decreased insulin efficiency in the morning, which has been attributed to the rise of counter-regulatory molecules nocturnally, especially growth hormone. Proper inclusion of this and other circadian and ultradian components of insulin sensitivity into insulin pump algorithms may improve regulation of normal glucose levels and reduce long term morbidities associated with hyperglycemia.

In addition to "slow" wave chronotherapeutic aspects of insulin's regulation of glucose level, attention is required to the fine structure of insulin release from the normally functioning pancreas. Release of insulin from the healthy pancreas occurs in bursts of 10–15-min intervals [346–349]. This rapid, pulsatile behavior appears to be due to entrained intrinsic oscillators of pancreatic ß cells. It has been demonstrated that less overall insulin is required when delivered exogenously with this bursting pattern than when delivered in a continuous manner. Incorporation of such fine structure into pumps, while technically challenging and perhaps engendering added expense, may lead to reduction in side effects that result from prolonged exposure to increased average insulin levels.

Glucose regulation also entails circadian rhythmicity in insulin PK and PD in response to change in blood glucose level and also blood glucose PK and PD in response to change in insulin level. Reduction of blood glucose level by a standardized dosage of insulin (0.05 units/kg body weight) in diurnally active nondiabetic subjects under controlled conditions is ~30% greater when administered at 08:00 than 17:00 (Fig. 13.24) [350]. Moreover, insulin response to 50 g oral glucose loading under controlled and fasting conditions is significantly more rapid and extensive at 09:00 than either 15:00 or 20:00 (Fig. 13.25) [55]. The lower insulin response in the afternoon and evening versus morning needed to regulate blood glucose level when glucose challenged is consistent with the observation that the dose of insulin required by Type I diabetics progressively declines during the course of the day [343, 344, 351, 352].

Differences in the PD of insulin upon blood glucose levels and the latter on the former take place not only during the 24 h but also over the year [205, 353], and perhaps menstrual cycle in young women [354]. The hypoglycemic effects of exercise in Type I diabetics may also differ according to its biological timing in that hypoglycemic risk is reported to be higher for exercise done in the evening than in morning by diurnally active subjects [355].

### Pump-Delivery of Insulin for Diabetes

Recent glucose sensor and pump technologies provide for improvement of treatment of type 1 (DM1) and resistant type 2 (DM2) diabetes. Insulin pump treatment is considered by many as the most physiologic way to imitate the healthy body's insulin profile [356–359]. To approximate circadian and postprandial/ultradian variations in blood glucose and insulin sensitivity, circadian synchronization of

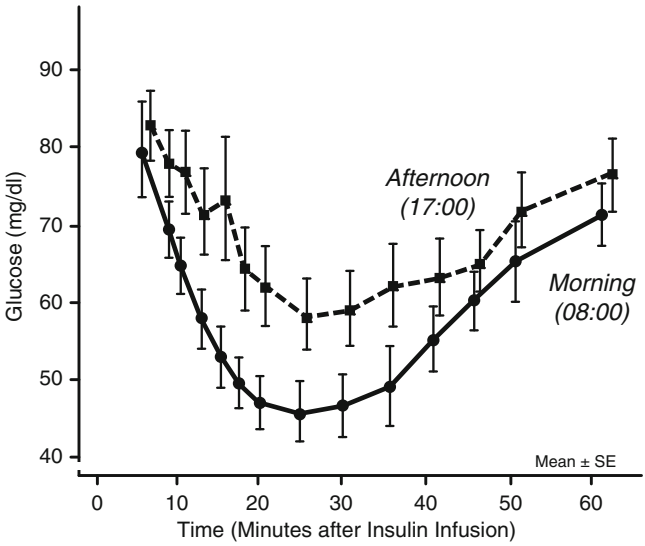


**Fig. 13.24** Mean blood glucose levels in 14 diurnal active, healthy subjects following timed IV insulin infusions (0.05 units/kg body weight). Morning (08:00) and evening (17:00) insulin infusion studies were conducted on different test days. Eight hours prior to each infusion, at 08:00 or 17:00, a 50-g oral glucose meal was given, respectively at 00:00 and 09:00. Subjects fasted until blood glucose was sampled. Effect of morning (08:00, *solid line*) insulin infusion on blood glucose concentration was considerably greater than the afternoon one (17:00, *dashed line*). Findings of this study suggest the pharmacodyamic effect of insulin on blood glucose concentration varies according to circadian time (figure drawn using data of Gibson et al. [350])

the patient has to be considered [205]. Pumps should be programmed and bolus injection timed and quantitated according to need [359, 360]. Use of a bolus calculator may improve glucose control [361]. Hypoglycemic response to insulin is markedly more pronounced in the morning than later in the day [340]. In pump administration studies, greatest insulin requirement was found in the late morning or early afternoon [343, 344]. Since high frequency pulses may provide an advantage in insulin utilization and effect plus avoidance of hypoglycemic episodes, the chronotherapy of insulin-dependent DM requires that the optimal pulse frequency of drug delivery be determined [345, 346]. This combined with an automated reasoning system used to monitor life events with weekly situation assessment can help detect and prevent problems in the use of insulin pumps [362].

Combination of an insulin pump with continuous glucose monitoring can automate the periodic adjustments. Insulin pumps and real time continuous glucose monitoring devices combined can provide a sensor augmented pump (SAP) system and can achieve better control and decrease in insulin requirements as compared to conventional insulin pumps without the sensor. Blood glucose concentration in patients carrying a closed system of sensor and pump spend more time in the target range [363–365]. A FDA approved system providing this combination is presently available (MiniMed Paradigm® REAL-Time, Medtronic). The newest Revel™

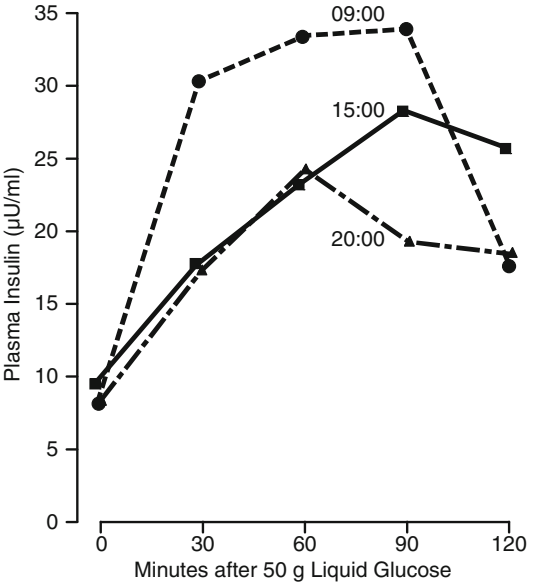


**Fig. 13.25** Mean plasma insulin response of 24 presumably diurnally active healthy subjects following 50 g oral glucose tolerance testing at different circadian times. Three different test times (09:00, 15:00, and 20:00) were explored, each on different days. Insulin response to glucose loading under controlled conditions of this study was greatest and most rapid in morning at 09:00 and slowest and weakest in evening at 20:00. This and other such glucose loading/tolerance studies indicate the pharmacodynamics of the insulin response is circadian, and perhaps other period, rhythmic (figure redrawn using data of Jarrett [55])

model carries, in addition, low and high-glucose alerts that signal up to 30 min before the preset low or high limit of glucose concentration is reached, allowing the pump system to suspend insulin delivery if hypoglycemic threshold is too closely approached or achieved [336, 337]. This feature substantially reduces hypoglycemic episodes. The system also provides time trend graphs of 3, 6, 12, and 24-h, which will enable recognition of circadian and ultradian variations and correction of treatment, if needed [336, 366].

#### 13.8.3.4 High Frequency and Pulsatile Hormone Delivery: Chronotherapeutic Implications

The above examples illustrate the role that can be played by *pulse frequency*, as opposed to *dose*, of drug delivery systems, particularly for hormones. Choice of delivery mode, ultradian pulsatile versus continuous, for GnRH and its analogues is decisive and depends on desired effect, i.e., induction/restoration of reproductive function versus treatment of sex hormone-related cancers. Proper pulsatile and ultradian delivery of insulin, GH, and other neuroendocrine analogues, and perhaps

other medications, may enable better outcomes and reduced doses. However, the clinical and pharmacoeconomic advantages of such chronotherapeutic approaches are yet to be completely assessed. The added compliance burden demanded by precise drug timings and frequency oscillations cannot be ignored, and may slow patient acceptance. Nonetheless, recognition of the critical dependence of high frequency modulation of certain medications, including insulin, to achieve therapeutic outcomes calls for application of new drug-delivery technologies to achieve practical and cost-effective clinical applications.

## 13.9 Chronoprevention: A Complementary Aspect of Chronotherapeutics

*Chronoprevention* is the timing of medications or other interventions according to biological rhythm criteria to avert disease or decline in health status. Chronopreventive strategies take into account the same factors as do chronotherapeutic strategies. However, the goal of chronoprevention is avoidance of disease, pathology, and other deleterious phenomena, while the goal of chronotherapeutics is curative management of existing medical conditions. For example, hypertension is a medical condition, not a disease, but if left untreated or treated inappropriately will result in blood vessel injury, culminating in renal, CVD, and other serious pathologies. Thus, the rationale underlying hypertension chronotherapy is their prevention, which as verifiied by the MAPEC outcomes study (sec. 13.8.2.2) is best achieved by bedtime chronotherapy of one or more hypertension medications (191). Similarly, hyperglycemia, in itself, is not a disease, but its long-term associated morbidities can be reduced or avoided in both type I and type II diabetes by proper management of glycemia, which involves accurate and timely dosing of insulin. Bedtime GTN chronotherapy is also intended to prevent angina attacks that are of greatest risk during nighttime sleep (Prinzmetal or sleep-apnea induced angina) and in the morning (exertion triggered angina) (Fig. 13.22).

The concept of chronoprevention is well illustrated by findings of trials involving low-dose aspirin (ASA) to minimize or avert risk of preeclampsia, a form of toxemia of pregnancy characterized by hypertension, fluid retention, and abnormal albumin level. While initial investigations established the safety of low dose ASA in pregnancy, findings of initial clinical trials were inconsistent in preventing preeclampsia. Review of published studies revealed several potential methodological flaws: trials did not always involve high risk obstetric patients, low dose ASA intervention was not always begun early in pregnancy, and none specified the clock time of dosing.

Hermida et al. [367] wondered whether the disparity in findings between published investigations could be due to differences in when ASA was ingested daily. A prospective double blind, randomized controlled trial of administration time dependent differences in the chronopreventive effect of low dose ASA was initiated to explore this possibility. Diurnally active pregnant women were recruited, 341 in total (181 primipara) who were normotensive but at elevated risk of

developing gestational hypertension and preeclampsia. They were randomized into one of six different groups, each composed of 55–59 participants. Groups were specified by the two treatments, placebo or 100 mg ASA, and three dosing times: upon awakening in the morning, 8 h after awakening (lunch time in Spain), or before sleep at night. SBP and DBP were automatically assessed by ABPM for 48 h, commencing at 12–16 weeks gestation and repeated thereafter at 4-week intervals until term.

The effect of low dose ASA on SBP and DBP was nil when ingested daily upon awakening throughout pregnancy. In contrast, those who ingested ASA in the afternoon exhibited significantly lower 48-h mean SBP and DBP after the first month of treatment, with the difference at term relative to the pretreatment baseline amounting to 4.4 and 3.5 mmHg, respectively. However, the effect of ASA was best, almost twice as strong, when ingested daily at bedtime, with reduced 48-h mean SBP and DBP again apparent after the first month of treatment and with differences at term relative to baseline levels averaging, respectively, 9.7 and 6.5 mmHg.

The preventive effect of ASA against preeclampsia and gestational hypertension in the high-risk pregnant women and their negative consequences on fetal development and well-being also differed dramatically according to treatment time. Average incidence of preeclampsia in the three placebo-treated groups was ~12%. Daily morning low dose ASA was not at all preventive (15% incidence), while afternoon and bedtime ASA was (1% incidence). Gestational hypertension was common, affecting on average ~30% of pregnant women randomized to the three placebo groups. Again, morning ASA dosing offered essentially no protection (25% incidence), whereas afternoon and bedtime dosing did (9 and 7% incidence, respectively). Average incidence of intrauterine growth retardation in the three placebo-treated groups was ~18%. Once again, morning ASA dosing exerted little prevention (16% incidence), while afternoon and, especially, bedtime dosing did (7 and 3% incidence, respectively). Finally, average incidence of preterm birth was ~14% in the three placebo groups. Daily morning low-dose ASA provided no meaningful protection against preterm birth (12% incidence), while afternoon and, in particular, bedtime dosing provided marked and clinically significant protection (3 and 0% incidence, respectively).

## 13.10 Discussion

Living organisms are precisely organized in time as evident by the multifrequency spectrum of biological processes and functions. The range of oscillations is broad, from very short periods and pulses of seconds, minutes, or a few hours to longer periodicities including ultradian (<20 h), circadian (~24 h), and infradian (>28 h) with periods of a week, month, and year. Such temporal variabilities are observed in almost all biological process from the subcellular to organ-system level. A given biological process may simultaneously exhibit many different periodicities, although the prominence, i.e., amplitude, of each may differ. For example, cortisol simultaneously

exhibits very high amplitude pulsatile (minutes to a few hours) oscillations as well as ultradian, circadian, circamensual, and circannual rhythmicities. These diverse rhythmicities, and the unique phase relationships of the multitude of oscillatory variables within each given frequency domain, constitute the biological time structure.

The prominent CTS of human beings gives rise to substantial biological time-dependent differences during the 24 h in one's response to a variety of clinical and laboratory diagnostic tests, risk of severe and life threatening medical events, symptom severity of a great number of common acute and chronic medical conditions, and PK and PD of medications when ingested, injected, infused, inhaled, or applied transcutaneously. Indeed, a medication that proves to be therapeutic and safe when applied at a one biological time may conceivably lack efficacy and/or be poorly tolerated at another. The reverse situation also is plausible; a medication that proves to be subtherapeutic, nontherapeutic, or unsafe at a one biological time may be efficacious and well tolerated at another. This idea was illustrated by several examples in this chapter, among them glucocorticoid, hypertension, NSAID, including low-dose ASA, and cancer medications.

Pharmacotherapy remains essentially guided by the concept of homeostasis. Therefore, it is not surprising that almost all monotherapy and polytherapy drug-delivery systems are designed to achieve, as an *assumed* goal, constancy of medication levels as a presumed means of optimizing and achieving consistency of therapeutic effect. This long-held conceptual dogma of pharmacology and drug delivery is counter to the rhythmic organization of biology that gives rise to predictable-in-time variability in the pathophysiology of medical ailments and conditions, and the PK and PD of therapies. Studies cited in this chapter, particularly with respect to rheumatoid arthritis, nocturnal asthma, and hypertension, demonstrate improvement of therapy and reduction of unwanted side effects achievable by timing medications in synchrony with the patient's CTS. For medications that have a narrow therapeutic range and high risk of adverse effect, such as cancer agents, constant rate delivery may actually potentiate side effects, since they may be delivered in too great a concentration at a wrong biological time.

For certain endocrine and neuroendocrine analogues, desired effectiveness may only be achievable when delivered in a frequency-modulated mode. Indeed, oscillation frequency of drug delivery, rather than dose, can be pivotal in determining therapeutic outcome with some peptide analogues. The pulsatile nature of some peptides may be modulated by circadian and other periodic systems; thus, the expression of pulsatile behavior, itself, maybe restricted to one or only a limited number of phases of circadian, menstrual, and perhaps even annual cycles [205]. This is another very important consideration in the design of drug delivery systems. Thus, it is imperative that the chronobiology of targeted systems be thoroughly known and properly incorporated into the design of drug delivery systems.

Knowledge of (a) CTS and clocks that control it, (b) rhythms in disease pathophysiology and/or associated 24-h patterns in symptom intensity of acute and chronic medical conditions, and (c) chronopharmacology (chronokinetics and chronodynamics) of medications, plus (d) emerging drug delivery technologies will facilitate development of chronotherapeutic dosage forms so as to better attain

desired outcomes while minimizing adverse effects. Some early chronotherapies simply involved unequal morning and evening dosing of conventional, sustained release capsule and tablet (12-h activity) systems or prudent selection of dosing time of conventional once-a-day, ultraslow release therapies. This was illustrated in this chapter by the chronotherapy of rheumatoid arthritis and osteoarthritis with NSAIDs, nocturnal asthma with theophylline, and hypertension with different classes of medications via the MAPEC trial. Such simple chronotherapeutic approaches can greatly improve disease management, for example, allergic rhinitis, asthma, PUD, rheumatoid arthritis/osteoarthritis hypertension, and hypercholesterolemia. Nonetheless, the philosophy and practice of clinical pharmacology continues to be dominated by homeostatic dogma in the design of drug delivery systems and goal to achieve constancy of medication concentrations during the 24 h.

A small number of antihypertensive and coronary heart disease medications that have been termed and marketed as chronotherapies by the pharmaceutical industry have been designed as once-daily, delayed onset drug delivery systems [224]. When ingested at bedtime as recommended, these rather simple systems are able to synchronize the concentration of medication in time during the 24 h to the presumed, but unverified by 24-h ABPM, BP and HR circadian rhythms of hypertensive and coronary heart disease patients. Only around-the-clock ABPM can determine the circadian BP and HR pattern for which the medication is intended. The recently completed MAPEC trial attests to the very significant advantage of the chronotherapeutic as opposed to conventional scheduling of BP lowering medications, not only to better control SBP an DBP and normalize the circadian BP rhythm, but also to (chrono)prevent CVD morbidity and mortality [191]. Development and validation of noninvasive and patient friendly technologies for monitoring direct or surrogate biomarkers of BP temporal variation, and predicting proper medication times, are challenges for future research.

From a chronopharmacologic perspective, combination therapy may pose special problems, since each component medication may exhibit different circadian times of best efficacy and safety. If the patient elects to change the ingestion time from the one recommended, the effect may be different from predicted and desired, as illustrated in this chapter by administration-time difference in synergistic effects on BP by amlodipine–valsartan combination hypertension therapy; when the two medications are ingested together at bedtime, reduction of SBP and DBP is greatly magnified, perhaps enhancing risk of hypotension as an adverse effect in some patients [192].

Chronotherapies thus far developed and used in treatment have required a high degree of participation and attention by the patient. Patients with multiple comorbidities, a common situation of the aged, typically are dependent on several classes of medications. In such cases, the particular dosing-time requirements of chronotherapeutic preparations may be impossible to meet with current, conventional drug delivery systems. Delayed or multiple bolus release, implantable, or transcutaneous pump, patch, spray, dry particle, and hydrogel technologies can be adopted and used in the design of chronotherapeutic oral, buccal, nasal, inhalation, subcutaneous, transdermal, rectal, or vaginal systems [368–370]. More advanced systems based on biomimetic schemes or implantable chips with multiple

addressable depots that can be individually commanded to release their contents in a proper time sequence are also under investigation [371–373]. Fully implantable systems are limited by the volume of required dose and stability of drug at body temperature. On the other hand, route of administration and intrinsic pharmacokinetics may place dynamical constraints on obtainable drug concentration profiles. In this regard, PK parameters, such as time to peak blood concentration following a single dose, and multiple dosing half-life, become important determinants of chrono-efficacy and chronotoxicity.

New and innovative drug delivery systems are needed to ensure future development and application of chronotherapeutic interventions. Optimally, next generation drug delivery systems should be configured so they (a) require minimal volitional adherence or at least minimize patient resistance to compliance, (b) respond to one or more sensitive biomarkers of disease activity that vary predictably in time, and that are also inducible by nonperiodic environmental phenomena that exacerbate disease, to release medication to targeted tissue(s) on an as-needed real-time basis, and (c) are cost-effective. Further, new generation systems should be able to deliver multiple medications, each responsive to unique biomarkers and each capable of meeting circadian and other bioperiodic determinants of efficacy and safety as a comprehensive polychronotherapy of disease states. The complexity of such systems presents quality assurance and regulatory challenges, particularly when combination therapies are contemplated. Overcoming such challenges is expected to lead to significant advances in treatment outcomes and enhanced quality of life.

Additional relevant information regarding chronopharmacology and chronotherapeutics can be found in two theme issues of Advanced Drug Delivery Reviews (vol 59, issues 9-10, 2007; vol 62, issues 9-10, 2010), and in recently published reviews [375–378].

## References

1. Reinberg A, Smolensky MH (1983) Biologic rhythms and medicine. cellular, metabolic, pathophysiologic, and pharmacologic aspects. Springer, Heidelberg
2. Touitou Y, Haus E (eds) (1992) Biologic rhythms in clinical and laboratory medicine. Springer, Heidelberg
3. Haus E, Touitou Y (1992) Principles of clinical chronobiology. In: Touitou Y Haus E (eds) Biological rhythms in clinical and laboratory medicine. New York, Springer, pp 6–34
4. Donahue JL, Lowenthal DT (1997) Nocturnal polyuria in the elderly person. Am J Med Sci 314:232–238
5. Kallas HE, Chintanadilok J, Maruenda J, Donahue JL, Lowenthal DT (1999) A clinical investigation of nocturnal polyuria in patients with nocturia: a diurnal variation in arginine vasopressin secretion and its relevance to mean blood pressure. Drugs Aging 15:429–437
6. Smolensky MH, Halberg F (1977) Circadian rhythm in airway patency and lung volumes. In: McGovern JP, Smolensky MH, Reinberg A, Thomas CC (eds) Chronobiology in allergy and immunology. Springfield, Illinois, pp 117–138
7. Halberg F, Simpson H (1967) Circadian acrophases of human 17-hydroxycorticosteroid excretion referred to midsleep rather than midnight. Hum Biol 39:405–413

8. Reinberg A (1979) Chronobiologic field trials of oil refinery shift workers. Chronobiologia 6 (Suppl 1):1–119
9. Reinberg A, Smolensky MH (1992) Night and shift work and transmeridian and space flights. In: Touitou Y, Haus E (eds) Biologic rhythms in clinical and laboratory medicine. Springer, Heidelberg, pp 242–255
10. Dardente H, Cermakian N (2007) Review: molecular circadian rhythms in central and peripheral clocks in mammals. Chronobiol Int 24:195–214
11. Duguay D, Cermakian N (2009) The crosstalk between physiology and circadian clock proteins. Chronobiol Int 26:1479–1513
12. Hanifin JP, Brainard GC (2007) Photoreception for circadian, neuroendocrine, and neurobehavioral regulation. J Physiol Anthropol 26:87–94
13. Maronde E, Stehle JH (2007) The mammalian pineal gland: known facts, unknown facets. Trends Endocrinol Metab 18:142–149
14. Golombek DA, Rosenstein RE (2010) Physiology of circadian entrainment. Physiol Rev 90:1063–1102
15. Wever RA (1979) The circadian system of man, results of experiments under temporal isolation. Springer, New York
16. Pezuk P, Mohawk JA, Yoshikawa T, Sellix MT, Menaker M (2010) Circadian organization is governed by extra-SCN pacemakers. J Biol Rhythms 25:432–441
17. Khalsa SB, Jewett ME, Cajochen C, Czeisler CA (2003) A phase response curve to single bright light pulses in human subjects. J Physiol 549:945–952
18. Lagoguey M, Reinberg A, Legrand JC (1981) Variations chronobiologiques de la response testiculaire a l'HCG chez l'homme adulte sain. Ann Endocrinol 41:59–60
19. Lagoguey M, Reinberg A (1981) Circadian and circannual changes of pituitary hormones in healthy human males. In: Van Cauter E, Copinschi G (eds) Human pituitary hormones. Martinus Nijhoff Publ, The Hague, pp 261–285
20. Reinberg A (1983) Clinical chronopharmacology: an experimental basis for chronotherapy. In: Reinberg A, Smolensky MH (eds) Biologic rhythms and medicine. cellular, metabolic, pathophysiologic, and pharmacologic aspects. Springer, Heidelberg, pp 243–248
21. Smolensky MH, Peppas N (2007) Chronobiology, drug delivery, and chronotherapeutics. Adv Drug Deliv Rev 59:828–851
22. Folkard S (2008) Do permanent night workers show circadian adjustment? A review based on the endogenous melatonin rhythm. Chronobiol Int 25:215–224
23. Horne JA, Östberg O (1976) A self-assessment questionnaire to determine morningness–eveningness in human circadian rhythms. Int J Chronobiol 4:97–110
24. Duffy JF, Rimmer DW, Czeisler CA (2001) Association of intrinsic circadian period with morningness–eveningness, usual wake time, and circadian phase. Behav Neurosci 115:895–899
25. Roenneberg T, Wirtz-Justice A, Merrow M (2003) Life between the clocks: daily temporal patterns of human chronotypes. J Biol Rhythms 18:80–90
26. Baehr EK, Revelle W, Eastman CI (2000) Individual differences in the phase and amplitude of the human circadian temperature rhythm: with an emphasis on morningness–eveningness. J Sleep Res 9:117–127
27. Bailey SL, Heitkemper MM (2001) Circadian rhythmicity of cortisol and body temperature: morningness–eveningness effects. Chronobiol Int 18:249–261
28. Duffy JF, Dijk DJ, Hall EF, Czeisler CA (1999) Relationship of endogenous circadian melatonin and temperature rhythms to self-reported preference for morning or evening activity in young and older people. J Investig Med 47:141–150
29. Burgess HJ, Sharkey KM, Eastman CI (2002) Bright light, dark and melatonin can promote circadian adaptation in night shift workers. Sleep Med Rev 6:407–420
30. Lewy AJ, Bauer VK, Ahmed S, Thomas KH, Cutler NL, Singer CM, Moffit MT, Sack RL (1998) The human phase response curve (PRC) to melatonin is about 12 hours out of phase with the PRC to light. Chronobiol Int 15:71–83
31. Minors DS, Waterhouse JM, Wirz-Justice A (1991) A human phase-response curve to light. Neurosci Lett 133:36–40

32. Brismar K, Hylander B, Eliasson K, Rössner S, Wetterberg L (1988) Melatonin secretion related to side-effects of beta-blockers from the central nervous system. Acta Med Scand 223:525–530
33. Nathan PJ, Maguire KP, Burrows GD, Norman TR (1997) The effect of atenolol, a beta1-adrenergic antagonist, on nocturnal plasma melatonin secretion: evidence for a dose-response relationship in humans. J Pineal Res 23:131–135
34. Stoschitzky K, Sakotnik A, Lercher P, Zweiker R, Maier R, Liebmann P, Lindner W (1999) Influence of beta-blockers on melatonin release. Eur J Clin Pharmacol 55:111–115
35. Stoschitzky K, Stoschitzky G, Brussee H, Bonelli C, Dobnig H (2006) Comparing beta-blocking effects of bisoprolol, carvedilol and nebivolol. Cardiology 106:199–206
36. Conlon M, Lightfoot N, Kreiger N (2007) Rotating shift work and risk of prostate cancer. Epidemiology 18:182–183
37. Deacon S, English J, Tate J, Arendt J (1998) Atenolol facilitates light-induced phase shifts in humans. Neurosci Lett 242:53–56
38. Schernhammer ES, Laden F, Speizer FE, Willett WC, Hunter DJ, Kawachi I, Colditz GA (2002) Rotating night shifts and risk of breast cancer in women participating in the nurses' health study. J Natl Cancer Inst 93:1563–1568
39. Schernhammer ES, Laden F, Speizer FE, Willett WC, Hunter DJ, Kawachi I, Fuchs CS, Colditz GA (2003) Night-shift work and risk of colorectal cancer in the nurses' health study. J Natl Cancer Inst 95:825–828
40. Lewy A, Emens JS, Lefler BJ, Yuhas K, Jackman AR (2005) Melatonin entrains free-running blind people according to a physiological dose–response curve. Chronobiol Int 22:1093–1106
41. Lewy AJ, Emens J, Jackman A, Yuhas K (2006) Circadian uses of melatonin in humans. Chronobiol Int 23:403–412
42. Hoban TM, Sack RL, Lewy AJ, Miller LS, Singer CM (1989) Entrainment of a free-running human with bright light? Chronobiol Int 6:347–353
43. Costa G, Di Milia L (2008) Aging and shift work. A complex problem to face. Chronobiol Int 25:165–181
44. Haus E, Smolensky MH (2006) Biological clocks and shift work: circadian dysregulation and potential long-term effects. Cancer Causes Control 17:489–500
45. Knutsson A (2003) Health disorders of shift workers. Occup Med 53:103–108
46. Morikawa Y, Nakagawa H, Miura K, Ishizaki M, Tabata M, Nishijo M, Higashiguchi K, Yoshita K, Sagara T, Kido T, Naruse Y, Nogawa K (1999) Relationship between shift work and onset of hypertension in a cohort of manual workers. Scand J Work Environ Health 25:100–104
47. Oishi M, Suwazono Y, Sakata K, Okubo Y, Harada H, Kobayashi E, Uetani M, Nogawa K (2005) A longitudinal study on the relationship between shift work and the progression of hypertension in Japanese male workers. J Hypertens 23:2173–2178
48. WHO-IARC (2010) Painting, firefighting, and shiftwork/IARC working group on the evaluation of carcinogenic risks to humans (2007: Lyon, France). v. 98
49. Lee RE, Smolensky MH, Leach CS, Mc Govern JP (1997) Circadian rhythms in the cutaneous reactivity to histamine and selected antigens, including phase relationship to urinary cortisol excretion. Ann Allergy 38:231–236
50. Smolensky MH, Lemmer B, Reinberg A (2007) The chronobiology and chronotherapy of allergic rhinitis and bronchial asthma. Adv Drug Deliv Rev 59:852–882
51. Gaultier C, Reinberg A, Girard F (1975) Circadian changes in lung resisatnce and dynamic compliance in healthy and asthmatic children. Effects of two bronchodilators. Respir Physiol 31:169–182
52. JNC 7 (2003) The seventh report of the joint national committee on prevention, detection, evaluation, and treatment of high blood pressure, National Heart, Lung, and Blood Institute. JAMA 289:2560-2671
53. Drance SM (1960) The significance of the diurnal tension variations in normal and glaucomatous eyes. Arch Ophthalmol 64:494–501

54. Saccà SC, Rolando M, Marletta A, Macrí A, Cerqueti P, Ciurlo G (1998) Fluctuations of intraocular pressure during the day in open glaucoma, normal-tension glaucoma and normal subjects. Opthalmologica 212:115–119
55. Jarrett RJ (1972) Circadian variations in blood glucose levels, in glucose tolerance and in plasma immunoreactive insulin levels. Acta Diabetol Lat 9:263–275
56. Zimmet PZ, Wall JR, Rome R, Stimmler L, Jarrett RJ (1974) Diurnal variation in glucose tolerance: associated changes in plasma insulin, growth hormone and non-esterified fatty acids. Br Med J 1:485–488
57. Solberg HE (1987) Approved recommendation (1986) on the theory of reference values, Part 1. The concept of reference values. Report of Expert Panel on Theory of Reference Values (EPTRV) of the International Federation of Clinical Chemistry (IFCC). Clin Chim Acta 165:111–118
58. PetitClerc C, Solberg HE (1987) Approved recommendation on the theory of reference values, Part 2. Selection of individuals for the production of reference values. Report of Expert Panel on Theory of Reference Values (EPTRV) of the International Federation of Clinical Chemistry (IFCC). J Clin Chem Clin Biochem 25:639–644
59. Haus E, Touitou Y (1992) Chronobiology in laboratory medicine. In: Touitou Y, Haus E (eds) Biological rhythms in clinical and laboratory medicine. Heidelberg, Springer, pp 673–708
60. Halberg F, Lee JK, Nelson WL (1978) Time-qualified reference intervals – chronodesms. Experientia 34:713–716
61. Haus E (1987) Requirements for chronobiotechnology and chronobiologic engineering in laboratory medicine. In: Scheving LE, Halberg F, Ehret CF (eds) Chronobiotechnology and chronobiological engineering. Appl Sci 120:331–372
62. DePrins J, Hecquet B (1992) Data processing in chronobiological studies. In: Touitou Y Haus E (eds) Biologic rhythms in clinical and laboratory medicine. Springer, Heidelberg, pp 90–113
63. Halberg F, Cornelissen G, Sothern RB, Wallach LA, Halberg E, Ahlgren A, Kuzel M, Radke A, Barbosa J, Goetz F, Buckley J, Mandel J, Schuman L, Haus E, Lakatua D, Sackett L, Berg H, Kawasaki T, Ueno M, Uezono K, Matsouka M, Omae T, Tarquini B, Cagnoni M, Garcia Sainz M, Perez Vega E, Griffiths K, Wilson D, Donati L, Tatti P, Vasta M, Locatelli I, Camagna A, Lauro R, Tritsch G, Wendt HW (1981) International geographic studies of oncological interest on chronobiological variables. In: Kaiser HN (ed) Neoplasms-comparative pathology of growth in animals, plants, and man. Wiley, New York, pp 553–596
64. Halberg F, Lagoguey A, Reinberg A (1983) Human circannual rhythms over a broad spectrum of physiological processes. Int J Chronobiol 8:225–268
65. Haus E, Lakatua DJ, Halberg F, Halberg E, Cornelissen G, Sackett LL, Berg HG, Kawasaki T, Ueno M, Uezono K, Matsouka M, Omae T (1980) Chronobiological studies of plasma prolactin in women and Kyuishu, Japan and Minnesota USA. J Clin Endocrinol Metabol 51:632–640
66. Haus E, Lakatua DJ, Sackett-Lundeen L, Swoyer J (1984) Chronobiology in laboratory medicine. In: Reitveld WT (ed) Clinical aspects of chronobiology. Baarn, Bakker, pp 13–82
67. Haus E, Lakatua DJ, Swoyer J, Sackett-Lundeen L (1983) Chronobiology in hematology and immunology. Am J Anatomy 168:467–517
68. Haus E, Nicolau GY, Lakatua DJ, Sackett-Lundeen L (1988) Reference values for chronopharmacology. Annu Rev Chronopharmacol 4:333–424
69. Kanabrocki EL, Sothern RB, Scheving LE, Vesely DL, Tsai TH, Shelstad J, Cournoyer C, Greco J, Mermall H, Ferlin H, Nemchausky BM, Bushnell DL, Kaplan E, Kahn S, Augustine G, Holmes E, Rumbyrt J, Sturtevant RP, Sturtevant F, Bremer F, Third JLHG, McCormick JB, Mudd CA, Dawson S, Sackett-Lundeen L, Haus E, Halberg F, Pauly JE, Olwin JH (1990) Reference values for circadian rhythms of 98 variables in clinically healthy men in the fifth decade of life. Chronobiol Int 7:445–461
70. Kanabrocki EL, Sothern RB, Scheving LE, Vesely DL, Tsai TH, Shelstad J, Cournoyer C, Greco J, Mermall H, Nemchausky BM, Bushnell DL, Kaplan E, Kahn S, Augustine G, Holmes E, Rumbyrt J, Sturtevant RP, Sturtevant F, Bremer F, Third JLHG, McCormick

JB, Mudd CA, Dawson S, Olwin JH, Sackett-Lundeen L, Haus E, Halberg F, Pauly JE, Hrushesky WJM (1990) Circadian reference data for men in fifth decade of life. In: Hayes, DK, Pauly, JE, Reiter, RE (eds) Chronobiology: its role in clinical medicine, general biology and agriculture. Prog Clin Biol Res, Wiley/Liss, New York, 341A:771–781

71. Touitou Y, Fèvre M, Lagoguey M, Carayon A, Bogdan A, Reinberg A, Beck H, Cesselin F, Touitou C (1981) Age- and mental health-related circadian rhythms of plasma levels of melatonin, prolactin, luteinizing hormone and follicle-stimulating hormone in man. J Endocrinol 91:467–475
72. Touitou Y, Motohashi Y, Pati A, Lévi F, Reinberg A, Ferment O (1986) Comparison of cortical circadian rhythms documented in samples of saliva, capillary (fingertips) and venous blood from healthy subjects. Annu Rev Chronopharmacol 3:297–299
73. Touitou Y, Sulon J, Bogdan A, Touitou C, Reinberg A, Beck H, Sodoyez JC, Demey-Ponsart E, Van Cauwenberge H (1982) Adrenal circadian system in young and elderly human subjects: a comparative study. J Endocrinol 93:201–210
74. Touitou Y, Touitou C, Bogdan A, Reinberg A, Auzeby A, Beck H, Guillet PH (1986) Differences between young and elderly subjects in seasonal and circadian variations of total plasma proteins and blood volume as reflected by hemoglobin, hematocrit and erythrocyte counts. Clin Chem 32:801–804
75. Touitou Y, Touitou C, Bogdan A, Reinberg A, Motohashi Y, Auzeby A, Beck H (1989) Circadian and seasonal variations of electrolytes in aging humans. Clin Chil Acta 180:245–254
76. Reinberg A, Lagoguey M, Cesselin F, Touitou Y, Legrand JC, Delassalle A, Antreassian J, Lagoguey A (1978) Circadian and circannual rhythms in plasma hormones and other variables in five healthy young human males. Acta Endocrinol 88:417–427
77. Hanson EJ (1970) Multiple time series. Wiley, New York
78. MacNeill IB (1974) Tests for periodic components in multiple time series. Biometrika 61:57–70
79. Van Cauter E (1979) Method for characterization of 24-hr temporal variations of blood components. Am J Physiol 237:E255–E264
80. DePrins J, Cornelissen G, Malberg W (1986) Statistical procedures in chronobiology and chronotherapeutics. Annu Rev Chronopharmacol 2:27–141
81. Halberg F, Panofsky H (1961) I. Thermo-variance spectra; method and clinical illustrations. Exp Med Surg 19:284–309
82. Panofsky H, Halberg F (1961) II. Thermo-variance spectra; simplified computational example and other methodology. Exp Med Surg 19:323–338
83. Halberg F, Engeli M, Hamburger C, Hillman D (1965) Spectral resolution of low-frequency, small amplitude rhythms in excreted ketosteroids; probable androgen-induced circaseptan desynchronization. Acta Endocrinol 103(Suppl):5–54
84. Nelson WL, Tong YL, Lee JK, Halberg F (1979) Methods for cosinor rhythmometry. Chronobiologia 6:305–323
85. Halberg F, Tong YL, Johnson EA (1967) Circadian system phase – an aspect of temporal morphology; procedures and illustrative examples. In: von Mayersbach H (ed) The cellular aspects of biorhythms. Heidelberg, Springer, pp 20–48
86. Bingham C, Arbogast B, Cornelissen-Guillaume G, Lee JK, Halberg F (1982) Inferential statistical methods for estimating and comparing cosinor parameters. Chronobiologia 9:397–439
87. Arendt J (1995) Melatonin and the mammalian pineal gland. Chapman Hill, London
88. Mirick DK, Davis S (2008) Melatonin as a biomarker of circadian dysregulation (review). Cancer Epidemiol Biomarkers Prev 17:3306–3313
89. Touitou Y, Motohashi Y, Reinberg A, Touitou C, Bourdeleau P, Bogdan A, Auzéby A (1990) Effect of shift work on the night-time secretory patterns of melatonin, prolactin, cortisol, and testosterone. Eur J Appl Physiol Occup Physiol 60:288–292

90. Schernhammer ES, Hankinson SE (2009) Urinary melatonin levels and postmenopausal breast cancer risk in the Nurses' Health Study cohort. Cancer Epidemiol Biomarkers Prev 18:74–79
91. Schernhammer ES, Rosner B, Willett WC, Laden F, Colditz GA, Hankinson SE (2004) Epidemiology of urinary melatonin in women and its relation to other hormones and night work. Cancer Epidemiol Biomarkers Prev 13:936–943
92. Arendt J (1992) The pineal. In: Touitou Y, Haus E (eds) Biologic rhythms in clinical and laboratory medicine. Springer, Heidelberg, pp 348–362
93. Walker RF, Read GF, Wilson DW, Riad-Fahmy D, Griffiths K (1990) Chronobiology in laboratory medicine: principles and clinical applications illustrated from measurements of neutral steroids in saliva. In: Hayes DK, Pauly JE, Reiter RE (eds) Chronobiology: its role in clinical medicine, general biology and agriculture. Prog Clin Biol Res, Wiley/Liss, New York, 341A:105–117
94. Miles A, Philbrick DRS, Thomas DR, Grey J (1987) Diagnostic and clinical implications of plasma and salivary melatonin assay. Clin Chem 33:1295–1297
95. Archer SN, Viola AU, Kyriakopoulou V, von Schantz M, Dijk DJ (2008) Inter-individual differences in habitual sleep timing and entrained phase of endogenous circadian rhythms of BMAL1, PER2 and PER3 mRNA in human leukocytes. Sleep 31:608–617
96. Boivin DB, James FO, Wu A, Cho-Park PF, Xiong H, Sun ZS (2003) Circadian clock genes oscillate in human peripheral blood mononuclear cells. Blood 102:4143–4145
97. Hida A, Kusanagi H, Satoh K, Kato T, Matsumoto Y, Echizenya M, Shimizu T, Higuchi S, Mishima K (2009) Expression profiles of PERIOD 1, 2 and 3 in peripheral blood mononuclear cells from older subjects. Life Sci 84:33–37
98. Takimoto M, Hamada A, Tomoda A, Ohdo S, Omura T, Sakato H, Kawatani J, Jodoi T, Nakagawa H, Terazono H, Koyanagi S, Higuchi S, Kimura M, Tukikawa H, Irie S, Saito H, Miike T (2005) Daily expression of clock genes in whole blood cells in healthy subjects and a patient with circadian rhythm sleep disorder. Am J Physiol Regul Integr Comp Physiol 289:1273–1279
99. Teboul M, Barrat-Petit MA, Li XM, Claustrat B, Formento JL, Delaunay F, Lévi F, Milano G (2005) Atypical patterns of circadian clock gene expression in human peripheral blood mononuclear cells. J Mol Med 83:693–699
100. Azama T, Yano M, Oishi K, Kadota K, Hyun K, Tokura H, Nishimura S, Matsunaga T, Iwanaga H, Miki H, Okada K, Hiraoka N, Miyata H, Takiguchi S, Fujiwara Y, Yasuda T, Ishida N, Monden M (2007) Altered expression profiles of clock genes hPer1 and hPer2 in peripheral blood mononuclear cells of cancer patients undergoing surgery. Life Sci 80:1100–1108
101. Waterhouse J, Edwards B, Mugarza J, Flemming R, Minors D, Calbraith D, Williams G, Atkinson G, Reilly T (1999) Purification of masked temperature data from humans: some preliminary observations on a comparison of the use of an activity diary, wrist actimetry, and heart rate monitoring. Chronobiol Int 16:461–475
102. Waterhouse J, Weinert D, Minors D, Atkinson G, Reilly T, Folkard S, Owens D, Macdonald I, Sytnik N, Tucker P (1999) The effect of activity on the waking temperature rhythm in humans. Chronobiol Int 16:343–357
103. Reinberg A, Ghata J, Halberg F, Apelbaum M, Gervais P, Boudon P, Abulker C, Dupont J (1974) Treatment schedules modify circadian timing in human adrenocortical insufficiency. In: Scheving LE, Halberg F, Pauly JE (eds) Chronobiology. Igaku Shoin Ltd, Tokyo, pp 168–173
104. Angeli A (1974) Circadian ACTH-adrenal rhythm in man. Chronobiologia 1(Suppl):253–268
105. Grant PH, Forsham PH, DiRaimando VC (1965) Suppression of 17-hydroxycorticosteroids in plasma and urine after single and divided doses of triamcinolone. N Engl J Med 273:1115–1118
106. Harter JG, Reddy WJ, Thorn GW (1963) Studies on an intermittent corticosteroid dosage regimen. N Engl J Med 296:591–595

107. Alten R, Döring G, Cutolo M, Gromnica-Ihle E, Witte S, Straub R, Buttgereit F (2010) Hypothalamus-pituitary-adrenal axis function in patients with rheumatoid arthritis treated with nighttime-release prednisone. J Rheumatol 37:2025–2031
108. Buttgereit F, Döring G, Schaeffler A, Witte S, Sierakowski S, Gromnica-Ihle E, Jeka S, Krueger K, Szechinski J, Alten R (2008) Efficacy of modified-release versus standard prednisone to reduce duration of morning stiffness of the joints in rheumatoid arthritis (CAPRA-1): A double-blind randomised controlled trial. Lancet 371:205–214
109. To H, Irie S, Tomonari M, Watanabe Y, Kitahara T, Sasaki H (2009) Therapeutic index of methotrexate depends on circadian cycling of tumor necrosis factor-α in collagen-induced arthritis rats and mice. J Pharm Pharmacol 61:1333–1338
110. To H, Yoshimatsu H, Tomonari M, Ida H, Tsurumoto T, Tsuji Y, Sonemoto E, Shimasaki N, Koyanagi S, Sasaki H, Ieiri I, Higuchi S, Kawakami A, Ueki Y, Eguchi K (2011) Methotrexate chronotherapy is effective against rheumatoid arthritis. Chronobiol Int 28:267–274
111. Haus E, Cusulos M, Sackett-Lundeen L, Swoyer J (1990) Circadian variations in blood coagulation parameters, alpha-antitrypsin antigen and platelet aggregation and retention in clinically healthy subjects. Chronobiol Int 7:203–216
112. Haus E, Smolensky MH (1999) Biologic rhythms in the immune system. Chronobiol Int 16:581–622
113. Fernandes G (1992) Chronobiology of immune functions: cellular and humoral aspects. In: Touitou Y, Haus E (eds) Biologic rhythms in clinical and laboratory medicine. Heidelberg, Springer, pp 493–503
114. Wrba H, Dutter A, Sánchez de la Peña S, Wu J, Carandente F, Cornélissen G, Halberg F (1990) Secular or circadian effects of placebo and melatonin on murine breast cancer? In: Hayes DK, Pauly JE, Reiter RE (eds) Chronobiology: its role in clinical medicine, general biology, and agriculture. Wiley/Liss, Washington, pp 31–40
115. Wrba H, Halberg F, Dutter A (1986) Melatonin circadian-stage-dependently delays breast tumor development in mice injected daily for several months. Chronobiologia 13:123–128
116. Harris MD, Siegel LB, Alloway JA (1999) Gout and hyperuricemia. Am Fam Physician 59:925–934
117. Sydenham T (1850) The works of Thomas Sydenham. Translated from the Latin by R.G. Lathan
118. Rigas B, Torosis J, McDougall CJ, Vener KJ, Spiro HM (1990) The circadian rhythm of biliary colic. J Clin Gastroenterol 12:409–414
119. Manfredini R, Gallerani K, Cecilia O, Boari B, Fersini C, Portaluppi F (2002) Circadian pattern in occurrence of renal colic in an emergency department; an analaysis of patients notes. BMJ 324:767
120. Bellamy N, Sothern RB, Campbell J (2004) Aspects of diurnal rhythmicity in pain, stiffness, and fatigue in patients with fibromyalgia. J Rheumatol 31:379–389
121. Yunus M, Masi AT, Calabro JJ, Miller KA, Feigenbaum SL (1981) Primary fibromyalgia: clinical study of 50 patients with matched controls. Semin Arthritis Rheum 11:151–171
122. Moore JG, Halberg F (1987) Circadian rhythm of gastric acid secretion in active duodenal ulcer: Chronobiological statistical characteristics and comparison of acid sectretory and plasma gastrin patterns with healthy subjects and post-vagotomy and pyloroplasty patients. Chronobiol Int 4:101–110
123. Cugini P, Di Palma L, Battisti P, Leone G, Materia E, Parenzi A, Romano M, Ferrera U, Moretti M (1990) Ultradian, circadian and infradian periodicity of some cardiovascular emergencies. Am J Cardiol 66:240–243
124. Kroetz C (1940) Ein biologiescher 24-Stunden-Rhythmus des Blutkreislaufs bei Gesundheit und bei Herzschwache zugleich ein Beitrag zur tageszeitlichen Haufung einiger akuter Kreislaufstorungen. Munch Med Wschr 87:314–317
125. Turner-Warwick M (1998) Epidemiology of nocturnal asthma. Am J Med 85:6–8
126. Dethlefsen U, Repges R (1985) Ein neues Therapieprinzip bei nachtlichem Asthma. Med Klin 80:44–47

127. Ebata T, Aizawa H, Kamide R, Niimura M (1999) The characteristics of nocturnal scratching in adults with atopic dermatitis. Br J Dermatol 141:82–86
128. Smolensky MH, Tatar SE, Bergman SA, Losman JG, Barnard CN, Dasco CC, Kraft IA (1976) Circadian rhythmic aspects of human cardiovascular function: A review by chronobiologic statistical methods. Chronobiologia 3:337–371
129. Portaluppi F, Hermida RC (2007) Circadian rhythms in cardiac arrhythmias and opportunities for their chronotherapy. Adv Drug Deliv Rev 59:940–951
130. Tikkinen KA, Johnson TMn, Tammela TL, Sintonen H, Huhtala H, Auvinen A (2010) Nocturia frequency, bother, and quality of life: how much is too often? A population-based study in Finland. Eur Urol 57:488–496
131. Cruz IA, Drummond M, Wimck JC (2011) Obstructive sleep apnea symptoms beyond sleepiness and snoring: effects of nasal APAP therapy. Sleep Breath doi.10.1007/s11325-011-0502-4
132. Natarajan R (2010) Review of periodic limb movement and restless leg syndrome. J Postgrad Med 56:157–162
133. Portaluppi F, Cortelli P, Buonaura GC, Smolensky MH, Fabbain F (2009) Do restless legs syndrome and periodic limb movements of sleep play a role in nocturnal hypertension and increased cardiovascular disease risk in renal patients. Chronobiol Int 26:1206–1221
134. Kelmanson IA (1991) Circadian variation of the frequency of sudden infant death syndrome and of sudden death from life-threatening conditions in infants. Chronobiologia 18:181–186
135. Reinberg AE, Gervais P, Levi F, Smolensky M, Del Cerro L, Ugolini C (1988) Circadian and circannual rhythms of allergic rhinitis: an epidemiologic study involving chronobiologic methods. J Allergy Clin Immunol 81:51–62
136. Smolensky MH, Reinberg A, Labrecque G (1995) Twenty-four hour pattern in symptom intensity of viral and allergic rhinitis: Treatment implications. J Allergy Immunol 95:1084–1096
137. Bellamy N, Sothern RB, Campbell J, Buchanan WW (1991) Circadian rhythm in pain, stiffness, and manual dexterity in rheumatoid arthritis: relation between discomfort and disability. Ann Rhuem Dis 50:243–348
138. Fox AW, Davis RL (1998) Migraine chronobiology. Headache 38:436–441
139. Solomon GD (1992) Circadian rhythms and migraine. Cleveland Clin J Med 59:326–329
140. Mulcahy D, Keegan J, Cunningham D, Quyyumi A, Crean P, Park A, Wright C, Fox K (1998) Circadian variation of total ischemic burden and its alteration with anti-anginal agents. Lancet 2:755–759
141. Rocco MB, Barry J, Campbell S, Nabel E, Cook EF, Goldman L, Selwyn AP (1987) Circadian variation of transient myocardial ischemia in patients with coronary artery disease. Circulation 75:395–400
142. Cohen MC, Rohtla KM, Lavery CE, Muller JE, Mittleman MA (1997) Meta analysis of the morning excess of acute myocardial infarction and sudden cardiac death. Am J Cardiol 79:1512–1516
143. Shaw E, Tofler GH (2009) Circadian rhythm and cardiovascular disease. Curr Atheroscler Rep 11:289–295
144. Elliott WJ (1998) Circadian variation in the timing of stoke onset. A meta-analysis. Stroke 29:992–996
145. Gallerani M, Manfredini R, Fersini C (1993) Chronoepidemiology in human disease. Ann Inst Super Sanita 29:569–579
146. Gallerani M, Manfredini R, Ricci L, Grandi E, Cappato R, Calò G, Pareschi PL, Fersini C (1992) Sudden death from pulmonary thromboembolism: chronobiological aspects. Eur Heart J 6:305–323
147. Rossenwasser AM, Wirz-Justice A (1997) Circadian rhythms and depression: clinical and experimental models. In: Redfern PH, Lemmer B (eds) Physiology and pharmacology of biological rhythms, handbook of experimental pharmacology, vol 125. Springer, Berlin, pp 457–486

148. Wehr TA (1982) Circadian rhythm disturbances in depression and mania. In: Brown FM, Graeber RC (eds) Rhythmic aspects of behavior. Lawrence Erlbaum Ass, New Jersey, pp 399–428
149. Mooney M, Green C, Hatsukami D (2006) Nicotine self-administration: cigarette versus nicotine gum diurnal topography. Hum Psychopharamcol 21:539–548
150. Mützell S (1998) Alcohol consumption, clinical findings and retrospective psycho social data in a random sample of men in suburban Stockholm. Scand J Prim Health Care 6:185–192
151. Bellamy N, Sothern RB, Campbell J (1990) Rhythmic variations in pain perception in osteoarthritis of the knee. J Rheumatol 17:364–372
152. Bellamy N, Sothern RB, Campbell J, Buchanan WW (2002) Rhythmic variations in pain, stiffness, and manual dexterity in osteoarthristis. Ann Rheum Dis 61:1075–1080
153. Manfredini R, Gallerani M, Salmi R, Calò G, Pasin M, Bigoni M, Fersini C (1994) Circadian variation in the time of onset of acute intestinal bleeding. J Emerg Med 12:5–9
154. Svanes C, Sothern RB, Sorbye H (1998) Rhythmic patterns in incidence of peptic ulcer perforation over 5.5 decades in Norway. Chronobiol Int 15:241–264
155. Kim YK, Oh WH, Park KH, Kim JM, Kim DH (2010) Circadian blood pressure and intraocular pressure patterns in normal tension glaucoma patients with undisturbed sleep. Korean J Opththalmol 24:23–28
156. Liu JH, Bouligny RP, Kripke DF, Weinreb RN (2003) Nocturnal elevation of intraocular pressure is detectable in the sitting position. Invest Opththalmol Vis Sci 44(10):4439–4442
157. Baxil CW, Walczak TS (1997) Effects of sleep and sleep stage on epileptic and nonepileptic seizures. Epilepsia 38:56–62
158. Langdon-Down M, Brain WR (1929) Time of day in relation to convulsion in epilepsy. Lancet 1:1029–1032
159. Bjorvatn B, Pallesen S (2009) A practical approach to circadian rhythm sleep disorders. Sleep Med Rev 13:47–60
160. Pandi-Perumal SR, Trakht I, Spence DW, Srinivasan V, Dagan Y, Cardinali DP (2008) The roles of melatonin and light in the pathophysiology and treatment of circadian rhythm sleep disorders. Nat Clin Pract Neurol 4:436–447
161. Lamont EW, James FO, Boivin DB, Cermakian N (2007) From circadian clock genes to pathologies. Sleep Med Rev 8:547–556
162. Aoki H, Ozeki Y, Yamada N (2001) Hypersensitivity of melatonin suppression in response to light in patients with delayed sleep phase syndrome. Chronobiol Int 18:263–271
163. Shanware NP, Hutchinson JA, Kim SH, Zhan L, Bowler MJ, Tibbetts RS (2011) Casein kinease1-dependent phosphorylation of familial advanced sleep phase syndrome-associated residues controls PERIOD 2 stability. J Biochem 286:12766–12774
164. Reinberg A, Ashkanazi I (2008) Internal desynchronization of circadian rhythms and tolerance to shift work. Chronobiol Int 25:625–643
165. Hack LM, Lockley SW, Arendt J, Skene DJ (2003) The effects of low-dose melatonin on the free-running rhythm of blind subjects. J Biol Rhythms 18:420–429
166. Kennaway DJ (2010) Clock genes at the heart of depression. J Pyschopharmacol 24:5–14
167. Kripke D, Drennan MD, Elliott JA (1992) The complex circadian pacemaker in affective disorder. In: Touitou Y Haus E (eds) Biologic rhythms in clinic and laboratory medicine. Springer, Heidelberg, pp 265–276
168. Parry BL, Meliska CJ, Sorenson DL, Martínez LF, López AM, Elliott JA, Hauger RL (2011) Reduced phase-advance of plasma melatonin after bright morning light in the luteal, but not follicular, menstrual cycle phase in premenstrual dysphoric disorder: an extended study. Chronobiol Int 28:415–424
169. Utge SJ, Soronen P, Loukola A, Kronholm E, Ollilia HM, Pirkola S, Porkka-Heiskanen T, Partonen T, Paunio T (2010) Systemic analysis of circadian genes in a population-based sample reveals association of TIMELESS with depression and sleep disturbance. PLos One 5: e9259

170. Reinberg AE (1991) Concepts of circadian chronopharmacology. In: Hrushesky WJM, Langer R, Theeuwes F (eds) Temporal control of drug delivery. Ann N Y Acad Sci 618:102–115
171. Lemmer B (ed) (1989) Chronopharmacology: cellular and biochemical interactions. Marcel Dekker, New York
172. Lemmer B (2005) Chronopharmacology and controlled drug release. Expert Opin Drug Deliv 2:667–681
173. Redfern PH, Lemmer B (eds) (1997) Physiology and pharmacology of biological rhythms. Springer, Heidelberg
174. Bélanger PM (1993) Chronopharmacology in drug research and therapy. Adv Drug Res 24:1–80
175. Bélanger PM, Bruguerolle B, Labrecque G (1997) Rhythms in pharmacokinetics: absorption, distribution, metabolism, and excretion. In: Redfern PH, Lemmer B (eds) Physiology and pharmacology of biological rhythms: handbook of experimental pharmacology, vol 125. Springer, Berlin, pp 177–204
176. Bruguerolle B (1998) Chronopharmacokinetics. Current status. Clin Pharmacokinet 35:83–94
177. Lemmer B (2006) Clinical chronopharmacology of the cardiovascular system: hypertension and coronary heart disease. Clin Ther 157:41–52
178. Lemmer B, Bruguerolle B (1994) Chronopharmacokinetics. Are they clinically relevant? Clin Pharmacokinet 26:419–427
179. Moore J, Merki H (1997) Gastrointestinal tract. In: Redfern PH, Lemmer B (eds) Physiology and pharmacology of biological rhythms, handbook of experimental pharmacology, vol 125. Berlin, Springer, pp 351–373
180. Reinberg AE, Smolensky MH (1982) Circadian changes in drug disposition in man. Clin Pharmacokinet 7:401–420
181. Witte K, Lemmer B (1997) Rhythms in second message mechanism. In: Redfern PH, Lemmer B (eds) Physiology and pharmacology of biological rhythms, handbook of experimental pharmacology, vol 125. Berlin, Springer, pp 135–156
182. Sanders SW, Moore JG, Buchi KN, Bishop AL (1988) Circadian variation in the pharmacodynamic effect of intrvenous ranitidine. Annu Rev Chronopharmacol 5:335–338
183. Sanders SW, Moore JG, Buchi KN, Bishop AL (1989) Pharmacodynamics of intravenous ranitidine after bolus and continuous infusion in patients with healed duodenal ulcer. Clin Pharmacol Ther 46:545–551
184. White C, Smolensky MH, Sanders SW, Buchi KN, Moore JG (1991) Day-night and individual differences in response to constant-rate ranitidine infusion. Chronobiol Int 8:56–66
185. Decousus H (1992) Chronobiology in hemostasis. In: Touitou Y, Haus E (eds) Biologic rhythms in clinical and laboratory medicine. Springer, Heidelberg, pp 554–565
186. Decousus H, Croze M, Lévi F, Perpoint B, Jaubert J, Bonadona JF, Reinberg A, Queneau P (1985) Circadian changes in anticoagulant effect of heparin infused at a constant rate. Br Med J 290:341–344
187. Haus E (2007) Chronobiology of hemostasis and inferences for the chronotherapy of coagulation disorders and thrombosis prevention. Adv Drug Deliv Rev 59:966–984
188. Bruguerolle B, Labrecque G (2007) Rhythm patterns in pain and their chronotherapy. Adv Drug Deliv Rev 59:883–895
189. Smolensky MH, Hermida R, Ayala DE, Portaluppi F (2010) Administration-time-dependent effects of antihypertension medications: basis for the chronotherapy of hypertension (review). Blood Press Monitor 15:173–180
190. Portaluppi F, Smolensky MH (2010) Perspectives on the chronotherapy of hypertension based on the results of the MAPEC study. Chronobiol Int 27:1652–1667
191. Hermida RC, Ayala DE, Mojón A, Fernández JR (2010) Influence of circadian time of hypertension treatment on cardiovascular risk: Results of the MAPEC study. Chronobiol Int 27:1629–1651

192. Hermida RC, Ayala DE, Fontao MJ, Mojón A, Fernández JR (2010) Chronotherapy with valsartan/amlodipine fixed combination: improved blood pressure control of essential hypertension with bedtime dosing. Chronobiol Int 27:1287–1303
193. Os I, Bratland B, Dahlhöf B, Syvertsen JO, Tretli S (1994) Female preponderance for lisinopril cough in hypertension. Am J Hypertens 7:1012–1015
194. Oparil S, Miller AP (2005) Gender and hypertension. J Clin Hypertens 7:305–309
195. Kloner RA, Sowers JR, DiBona GF, Gaffney M, Wein M (1996) Sex- and age-related antihypertensive effects of amlodipine. The Amlodipine Cardiovascular Community Trial Study Group. Am J Cardiol 77:713–722
196. Canzanello VJ, Baranco-Pryor E, Rahbari-Oskoui F, Schwartz GL, Boerwinkle E, Turner ST, Chapman AB (2008) Predictors of blood pressure response to the angiotensin receptor blocker candesartan in essential hypertension. Am J Hypertens 21:61–66
197. Saunders E, Cable G, Neutel J (2008) Predictors of blood pressure response to angiotensin receptor blocker/diuretic combination therapy: a secondary analysis of the irbesartan/hydrochlorothiazide blood pressure reductions in diverse populations (INCLUSIVE) study. J Clin Hypertens 10:27–33
198. Ayala DE, Hermida RC (2010) Sex differences in the administration-time-dependent effects of low-dose aspirin on ambulatory blood pressure in hypertensive subjects. Chronobiol Int 27:354–362
199. Hermida RC, Calvo C, Ayala DE, Domínquez MJ, Covelo M, Fernández JR, Mojón A, López JE (2003) Administration time-dependent effects of valsartan on ambulatory blood pressure of hypertensive subjects. Hypertension 42:283–290
200. Cambar J, L'Azou B, Cal C (1992) Chronotoxicology. In: Touitou Y, Haus E (eds) Biologic rhythms in clinical and laboratory medicine. Springer, Heidelberg, pp 139–150
201. Cambar J, Pons M (1997) New trends in chronotoxicology. In: Redfern PH, Lemmer B (eds) Physiology and pharmacology of biological rhythms, handbook of experimental pharmacology, vol 125. Springer, Berlin, pp 557–588
202. Halberg F (1960) Temporal coordination of physiologic function. Cold Spring Harbor Symp Quant Biol 25:289–310
203. Beauchamp D, Labrecque G (2007) Chronobiology and chronotoxicology of antibiotics and aminoglycosides. Adv Drug Deliv Rev 59:896–903
204. Ceresa F, Angeli A, Buccuzzi G, Molino G (1969) Once-a-day neurally stimulated and basal ACTH secretion phases in man and their response to corticoid inhibition. J Clin Endocrinol 29:1074–1082
205. Haus E (2007) Chronobiology in the endocrine system. Adv Drug Deliv Rev 59:985–1014
206. McHugh RB, Smolensky MH, Halberg F (1975) Biological rhythm experimentation: a longitudinal design and analysis. Chronobiologia 2:1–12
207. Smolensky MH, Reinberg A (1976) The chronotherapy of corticosteroids: a practical application of chronobiological findings to clinical and hospital nursing. J Nursing Clinics 11:609–620
208. Hermida RC, Ayala DC, Mojón A, Fernández JR (2008) Chronotherapy with nifedipin GITS in hypertensive patients: improved efficacy and safety with bedtime dosing. Am J Hypertens 21:948–954
209. Bernard S, Cajavec Bernard B, Lévi F, Herzel H (2010) Tumor growth rate determines the timing of optimal chronomodulated treatment schedules. PLOS Comput Biol 6(3): e1000712
210. Hrushesky WJM, März WJ (1992) Chronochemotherapy of malignant tumors: Temporal aspects of antineoplastic drug toxicity. In: Touitou Y, Haus E (eds) Biologic rhythms in clinical and laboratory medicine. Springer, Heidelberg, pp 611–634
211. Lévi F (1997) Chronopharmacology of anticancer agents. In: Redfern PH, Lemmer B (eds) Physiology and pharmacology of biological rhythms, handbook of experimental pharmacology, vol 125. Springer, Berlin, pp 299–350

212. Lévi F, Focan C, Karaboué A, de la Valette V, Focan-Henrard D, Baron B, Kreutz F, Giacchetti S (2007) Implications of circadian clocks for the rhythmic delivery of cancer medications. Adv Drug Deliv Rev 59:1015–1035
213. Mormont C, Boughattas N, Lévi F (1989) Mechanisms of circadian rhythms in the toxicity and efficacy of anticancer drugs: relevance for the development of new analogues In: Lemmer B (ed) Chronopharmacology: cellular and biochemical interactions. Marcel Dekker Inc, New York, pp 395–437
214. Sauerbier I (1992) Rhythms in drug-induced teratogensis. In: Touitou Y, Haus E (eds) Biologic rhythms in clinical and laboratory medicine. Heidelberg, Springer, pp 151–157
215. Smolensky MH (1998) Knowledge and attitudes of American physicians and public about medical chronobiology and chronotherapeutics. Findings of two 1996 Gallup surveys. Chronobiol Int 15:377–394
216. Arendt J, Aldhous M, Marks V (1986) Alleviation of jet-lag by melatonin: preliminary results of a controlled double-blind trial. Br Med J 292:1170
217. D'Alonzo GE, Smolensky MH, Feldman S, Gianotti LA, Emerson MB, Staudinger H, Steinijans VM (1990) Twenty-four-h lung function in adult patients with asthma: chronoptimized theophylline therapy once-daily dosing in the evening versus conventional twice-daily dosing. Am Rev Respir Dis 142:84–90
218. Neuenkirchen H, Wilkens JH, Oellerich M, Sybrecht GW (1985) Nocturnal asthma: effect of a once per evening dose of sustained-release theophylline. Eur J Respir Dis 66:196–204
219. Merki HS, Witzel L, Hare K, Scheurle E, Bauerfeind P, Blum AL (1987) Single dose treatment with H2-receptor antagonists: Is bedtime too late? Gut 28:451–454
220. Stalenhoff AFH, Mol MJTM, Stuyt PMJ (1989) Efficacy and tolerability of simvastatin. Am J Med 87:39s–43s
221. Sica D, Frishman WH, Manowitz N (2003) Pharmacokinetics of propranolol after single and multiple dosing with sustained released propranolol or propranolol CR (Innopran XL™), a new chronotherapeutic formulation. Heart Dis 5:176–181
222. Sista S, Lai J, Eradiri O, Albert K (2003) Pharmacokinetics of a novel diltiazem HCL extended-release tablet formulation for evening administration. J Clin Pharmacol 43:1149–1157
223. Smith DHG, Neutel JM, Weber MA (2001) A new chronotherapeutic oral drug absorption system for verapamil optimizes blood pressure control in the morning. Am J Hypertens 14:14–19
224. Smolensky MH, Hermida R, Portaluppi F, Haus E, Reinberg A (2005) Chronotherapeutics in the treatment of hypertersion. In: Oparil S, Weber MA (eds) Hypertension: a companion to Brenner and Rector's the kidney, 2nd edn. Philadelphia, Elsevier Saunders, pp 530–542
225. White WB, Anders RJ, MacInyre JM, Black HR, Sica DA (1995) Nocturnal dosing of a novel delivery system of verapamil for systemic hypertension. Am J Cardiol 76:375–380
226. Kunkel G, Steinijans VW, Borner K (1987) Chrono-optimization of the time of evening administration of theophylline with unequally divided twice daily dosing. Chronobiol Int 4:364–368
227. Postma DS, Koëter GH, vd Mark TW, Reig RP, Sluiter HJ (1985) The effects of oral slow-release terbutaline on the circadian variation in spirometry and arterial blood gas levels in patients with chronic air flow obstruction. Chest 87:653–657
228. Portaluppi F, Manfredini R, Fersini C (1999) From a static to a dynamic concept of risk: the circadian epidemiology of cardiovascular risk. Chronobiol Int 16:33–50
229. Black HR, Elliott WJ, Neaton JD, Grandits G, Grambsch P, Grimm RH, Hansson L, Lacoucière Y, Muller J, Sleight P, Weber MA, White WB, Williams G, Wittes J, Zanchetti A, Fakouhi TD (1998) Rationale and design for the Controlled ONset Verapamil INvestigation of Cardiovascular Endpoints (CONVINCE) trial. Control Clin Trials 19:370–390
230. Black HR, Elliott WJ, Grandits G, Grambsch P, Lucente T, White WB, Neaton JD, Grimm RH, Hansson L, Lacourciere Y, Muller J, Sleight P, Weber MA, Williams G, Wittes J, Zanchetti A, Anders RJ, Group CR (2003) Principal results of the Controlled Onset

Verapamil Investigation of Cardiovascular End Points (CONVINCE) trial. JAMA 289:2073–2082
231. Black HR, Elliott WJ, Grandits G, Grambsch P, Lucente T, Neaton JD, Grimm RH, Hansson L, Lacourcière Y, Muller JE, Sleight P, Weber MA, White WB, Williams GH, Wittes J, Zanchett A, Anders RJ, Group CR (2005) Results of the Controlled ONset Verapamil INvestigation of Cardiovascular Endpoints (CONVINCE) trial by geographical region. J Hypertens 23:1099–1106
232. Hermida RC (2007) Ambulatory blood pressure monitoring in the prediction of cardiovascular events of chronotherapy: rationale and design of the MAPEC study. Chronobiol Int 24:749–775
233. Bennett BM, Leitman DC, Schroeder H, Kawamoto JH, Nakatsu K, Murad F (1989) Relationship between biotransformation of glyceryl trinitrate and cyclic GMP accumulation in various cultured cell lines. J Pharmacol Exp Therap 250:316–322
234. Fung H-L, Chung S-J, Bauer JA, Chong S, Kowaluk EA (1992) Biochemical mechanisms of organic nitrate action. Am J Cardiol 70:4B–10B
235. Salvemini D, Pistelli A, Vane J (1993) Conversion of glyceryl trinitrate to nitric oxide in tolerant and non-tolerant smooth muscle cells. Br J Pharmacol 108:162–169
236. Waldman SA, Rapoport RM, Ginsburg R, Murad F (1986) Densitization to nitroglycerin in vascular smooth muscle from rat and human. Biochem Pharmacol 35:3525–3531
237. Enbright GE (1914) The effects of nitroglycerin on those engaged in its manufacture. J Am Med Assoc 62:201–202
238. Stewart D (1888) Remarkable tolerance to nitroglycerin. Philadelphia Polyclinic 6:43
239. Chen Z, Zhang J, Stamler JS (2002) Identification of the enzymatic mechanism of nitroglycerin bioactivation. Proc Natl Acad Sci U S A 99:8306–8311
240. Katz RJ (1990) Mechanism of nitrate tolerance: a review. Cardiovasc Drugs Therapy 4:247–252
241. Hinz B, Schroeder H (1998) Nitrate tolerance is specific for nitric acid esters and its recovery requires intact protein synthesis. Biochem Biophys Res Commun 252:232–235
242. Kenkare S, Benet LZ (1996) Tolerance to nitroglycerin in rabbit aorta. Biochem Pharmacol 51:1357–1361
243. Thadhani U (1992) Role of nitrates in angina pectoris. Am J Cardiol 70:43B–53B
244. Kimura E, Hosoda S, Katoh K, Endo M, Yasue H, Asada S, Kuroiwa A (1978) Panel discussion on the variant form of angina pectoris. Jpn Circ J 42:455–476
245. Kuroiwa A (1978) Symptomology of variant angina. Jpn Circ J 42:459–478
246. Conn PM, Crowley WFJ (1994) Gonadotropin-releasing hormone and its analogs. Annu Rev Med 45:391–405
247. Huirne JA, Lambalk CB (2001) Gonadotropin releasing hormone receptor antagonists. Lancet 358:1793–1803
248. Belchetz PE, Plant TM, Nakai Y, Keogh EJ, Knobil E (1978) Hypophysial response to continuous and intermittent delivery of hypopthalamic gonadotropin releasing hormone. Science 202:632–633
249. Knobil E (1980) The role of signal pattern in the hypothalamic control of gonadotropin secretion. In: Ortavant R, Reinberg A (eds) Rhythmes et reproduction. Paris, Masson, pp 75–80
250. Nakai Y, Plant TM, Hess DL, Keoch EJ, Knobil E (1978) On the sites of negative and positive feedback action of estradiol in the control of gonadotropin secretion in the Rhesus monkey. Endocrinology 102:1008–1014
251. Filicori M, Santoro N, Merriam GR, Crowley WFJ (1986) Characterization of the physiological pattern of episodic gonadotropin secretion throughout the human menstrual cycle. J Clin Endocrinol Metab 62:1136–1144
252. Reame N, Sauder SE, Kelch RP, Marshall JC (1984) Pulsatile gonadotropin secretion during the human menstrual cycle: evidence for altered frequency of gonadotropin-releasing hormone secretion. J Clin Endocrinol Metab 59:328–337

253. Hall JE, Schoenfeld DA, Martin KA, Crowley WFJ (1992) Hypothalamic gonadotropin-releasing hormone secretion and follicle-stimulating hormone dynamics during the luteal-follicular transition. J Clin Endocrinol Metab 74:600–607
254. Knobil E (1980) The neuroendocrine control of the menstrual cycle. Recent Prog Horm Res 36:53–88
255. Crowley WFJ, Vale W, Rivier J, MacArthur JW (1981) LH and RH in hypogonadotropic hypogonadism. In: Zatuchini GI, Schelter JD, Sciarra JJ (eds) LH-RH peptides as female and male contraceptives. Philadelphia, Harper, pp 321–333
256. Santen RJ, Manni A, Harvey H (1986) Gonadotropin releasing hormone (GnRH) analogs for the treatment of breast and prostatic carcinoma. Breast Cancer Res Treat 7:129–145
257. Macklon NS, Stouffer RL, Giudice LC, Fauser BC (2006) The Science behind 25 years of ovarian stimulation for in vitro fertilization. Endocr Rev 27:170–207
258. Gompel A, Poitout P (1997) Inducteurs de l'ovulation. In: Maurais-Jarvis P, Schaison P, Touraine P (eds) Médecine de la reproduction. Paris, Flammarion, pp 604–616
259. Gompel A (2003) Induction de l'ovulation par administration pulsatile de Gn-RH par pompe portable. In: Reinberg AE (ed) Chronobiologie Médicale et Chronothérapeutique. Paris, Flammarion, pp 177–180
260. Leyendecker G, Wildt L, Hansmann M (1980) Pregnancies following chronic intermittent (pulsatile) administration of Gn-Rh by means of a portable pump ("Zyklomat") – a new approach to the treatment of infertility in hypothalamic amenorrhea. J Clin Endocrinol Metab 51:1214–1216
261. Hayes FJ, Seminara SB, Crowley WF Jr (1998) Hypogonadotropic hypogonadism. Endocrinol Metab Clin N Am 27:739–763
262. Santoro N, Filicori M, Crowley WF Jr (1986) Hypogonadotropic disorders in men and women: diagnosis and therapy with pulsatile gonadotropin-releasing hormone. Endocr Rev 7:11–23
263. Spratt DI, Crowley WF Jr, Butler JP, Hoffman AR, Conn PM, Badger TM (1985) Pituitary luteinizing hormone responses to intravenous and subcutaneous administration of gonadotropin-releasing hormone in men. JCE & M 61:890–895
264. Farhy LS, Veldhuis JD (2005) Deterministic construct of amplifying actions of ghrelin on pulsatile growth hormone secretion. Am J Physiol Regul Integr Comp Physiol 288: R1649–R1663
265. Giustina A, Veldhuis JD (1998) Pathophysiology of the neuroregulation of growth hormone secretion in experimental animals and the human. Endocr Rev 19:717–797
266. Veldhuis JD, Bowers CY (2003) Three-peptide control of pulsatile and entropic feedback-sensitive modes of growth hormone secretion: modulation by estrogen and aromatizable androgen (review). J Pediatr Endocrinol Metab 16(Suppl 3):587–605
267. Veldhuis JD, Roelfsema F, Keenan DM, Pincus S (2011) Gender, age, body mass index, and IGF-1 individually and jointly determine distinct GH dynamics: analyses in one hundred healthy adults. J Clin Endocrinol Metab 96:115–121
268. Isgaard J, Carlsson L, Isaksson O, Jansson J (1988) Pulsatile intravenous growth hormone (GH) infusion to hypophysectomized rats increases insulin-like growth factor I messenger ribonucleic acid in skeletal tissues more effectively than continuous GH infusion. Endocrinology 123:2605–2610
269. Jaffe CA, Turgeon DK, Lown K, Demott-Friberg R, Watkins PB (2002) Growth hormone secretion pattern is an independent regulator of growth hormone actions in humans. Am J Physiol Endocrinol Metab 283:E1008–E1015
270. Veldhuis JD, Bowers CY (2010) Integrating GHS into the ghrelin system (Review). Int J Peptides 2010:879503
271. Veldhuis JD, Roemmich JN, Richmond EJ, Bowers CY (2006) Somatotropic and gonadotropic axes linkages in infancy, childhood, and the puberty-adult transition. Endocr Rev 27:101–140
272. Litman T, Halberg F, Ellis S, Bittner JJ (1958) Pituitary growth hormone and mitoses in immature mouse liver. Endocrinology 62:361–364

273. Veldhuis JD, Keenan DM, Pincus SM (2008) Motivations and methods for analyzing pulsatile hormone secretion (review). Endocr Rev 29:823–864
274. Wu FC, Butler GE, Kelnar CJ, Huhtaniemi I, Veldhuis JD (1996) Ontogeny of pulsatile gonadotropin releasing hormone secretion from midchildhood, through puberty, to adulthood in the human male: a study using deconvolution analysis and an ultrasensitive immunofluorometric assay. J Clin Endocrinol Metab 81:1798–1805
275. Farhy LS, Veldhuis JD (2004) Putative GH pulse renewal: periventricular somatostatinergic control of an arcuate-nuclear somatostatin and GH-releasing hormone oscillator. Am J Physiol Regul Integr Comp Physiol 286:R1030–R1042
276. Farhy LS, Straume M, Johnson ML, Kovatchev B, Veldhuis JD (2002) Unequal autonegative feedback by GH models the sexual dimorphism in GH secretory dynamics. Am J Physiol Regul Integr Comp Physiol 282:R753–R764
277. Veldhuis JD, Evans WS, Shah N, Story S, Bray MJ, Anderson SM (1999) Proposed mechanisms of sex-steroid hormone neuromodulation of the human GH-IGP-I axis. In: Veldhuis JD, Giustina A (eds) Sex-steroid interactions with growth hormone. Springer, New York, pp 93–121
278. Arvat E, Ceda GP, Di Vito L, Ramunni J, Gianotti L, Broglio F, Deghenghi R, Ghigo E (1998) Age-related variations in the neuroendocrine control, more than impaired receptor sensitivity, cause the reduction in the GH-releasing activity of GHRPs in human aging. Pituitary 1:51–58
279. Van Cauter E, Plat L, Copinschi G (1998) Interrelations between sleep and the somatotropic axis. Sleep 21:553–566
280. Ho KY, Evans WS, Blizzard RM, Veldhuis JD, Merriam GR, Samojlik E, Furlanetto R, Rogol AD, Kaiser DL, Thorner MO (1987) Effects of sex and age on the 24-h profile of growth hormone secretion in man: importance of endogenous estradiol concentrations. J Clin Endocrinol Metab 64:51–58
281. Holl RW, Hartman ML, Veldhuis JD, Taylor WM, Thorner MO (1991) Thirty-second sampling of plasma growth hormone in man: correlation with sleep stages. J Clin Endocrinol Metab 72:854–861
282. Krueger JM, Obál F Jr (1993) Growth hormone-releasing hormone and interleukin-1 in sleep regulation. FASEB J 7:645–652
283. Ocampo-Lim B, Guo W, DeMott-Friberg R, Barkan AL, Jaffe CA (1996) Nocturnal growth hormone (GH) secretion is eliminated by infusion of GH-releasing hormone antagonist. J Clin Endocrinol Metab 81:4396–4399
284. Gronfier C, Luthringer R, Follenius M, Schaltenbrand N, Macher JP, Muzet A, Brandenberger G (1996) A quantitative evaluation of the relationships between growth hormone secretion and delta wave electroencephalographic activity during normal sleep and after enrichment in delta waves. Sleep 19:817–824
285. Van Cauter E, Plat L, Scharf MB, Leproult R, Cespedes S, L'Hermite-Balériaux M, Copinschi G (1997) Simultaneous stimulation of slow-wave sleep and growth hormone secretion by gamma-hydroxybutyrate in normal young men. J Clin Invest 100:745–753
286. Anderson LA, McTernan PG, Barnett AH, Kumar S (2001) The effects of androgens and estrogens on preadipocyte proliferation in human adipose tissue: influence of gender and site. J Clin Endocrinol Metab 86:5045–5051
287. Leung KC, Johannsson G, Leong GM, Ho KK (2004) Estrogen regulation of growth hormone action. Endocr Rev 25:693–721
288. Davey HW, Wilkins RJ, Waxman DJ (1999) STAT5 signaling in sexually dimorphic gene expression and growth patterns. Am J Hum Genet 65:959–965
289. Rudling M, Norstedt G, Olivecrona H, Reihner E, Gustafsson JA, Angelin B (1992) Importance of growth hormone for the induction of hepatic low density lipoprotein receptors. Proc Natl Acad Sci U S A 89:6983–6987
290. Laron Z (2004) Laron syndrome (primary growth hormone resistance or insensitivity): the personal experience 1958–2003. J Clin Endocrinol Metab 89:1031–1044

291. Roelfsema F, Biermasz NR, Veldman RG, Veldhuis JD, Frölich M, Stokvis-Brantsma WH, Wit JM (2000) Growth hormone (GH) secretion in patients with an inactivating defect of the GH-releasing hormone (GHRH) receptor is pulsatile: evidence for a role for non-GHRH inputs into the generation of GH pulses. J Clin Endocrinol Metab 86:2459–2464
292. van Coevorden A, Mockel J, Laurent E, Kerkhofs M, L'Hermite-Balériaux M, Decoster C, Nève P, Van Cauter E (1991) Neuroendocrine rhythms and sleep in aging men. Am J Physiol 260(4 Pt 1):E651–E661
293. Veldhuis JD, Liem AY, South S, Weltman A, Weltman J, Clemmons DA, Abbott R, Mulligan T, Johnson ML, Pincus S, Straume M, Iranmanesh A (1995) Differential impact of age, sex steroid hormones, and obesity on basal versus pulsatile growth hormone secretion in men as assessed in an ultrasensitive chemiluminescence assay. J Clin Endocrinol Metab 80:3209–3222
294. Martin FC, Yeo AL, Sonksen PH (1997) Growth hormone secretion in the elderly: aging and the somatopause. Baillieres Clin Endocrinol Metab 11:223–250
295. Biermasz NR, Pereira AM, Frölich M, Romijn JA, Veldhuis JD, Roelfsema F (2004) Octreotide represses secretory-burst mass and nonpulsatile secretion but does not restore event frequency or orderly GH secretion in acromegaly. J Clin Endocrinol Metab 286:E25–E30
296. Hartman ML, Pincus SM, Johnson ML, Matthews DH, Faunt LM, Vance ML, Thorner MO, Veldhuis JD (1994) Enhanced basal and disorderly growth hormone secretion distinguish acromegalic from normal pulsatile growth hormone release. J Clin Invest 95:1277–1288
297. Faje AT, Barkan AL (2010) Basal, but not pulsatile, growth hormone secretion determines the ambient circulating levels of insulin-like growth factor-1. J Clin Endocrinol Metab 95:2486–2491
298. Dimaraki EV, Jaffe CA, DeMott-Friberg R, Chandler WF, Barkan AL (2002) Acromegaly with apparently normal GH secretion: implications for diagnosis and follow-up. J Clin Endocrinol Metab 87:3537–3542
299. van den Berg G, Pincus SM, Frölich M, Veldhuis JD, Roelfsema F (1998) Reduced disorderliness of growth hormone release in biochemically inactive acromegaly after pituitary surgery. Eur J Endocrinol 138:164–169
300. Cordido F, Garcia-Buela J, Sangiao-Alvarellos S, Martinez T, Vidal O (2010) The decreased growth hormone response to growth hormone releasing hormone in obesity is associated to cardiometabolic risk factors. Mediators Inflamm 2010:1–8
301. Utz AL, Yamamoto A, Hemphill L, Miller KK (2008) Growth hormone deficiency by growth hormone releasing hormone-arginine testing criteria predicts increased cardiovascular risk markers in normal young overweight and obese women. J Clin Endocrinol Metab 93:2507–2514
302. Sen F, Demirturk M, Abaci N, Golcuk E, Oflaz H, Elitok A, Kutluturk F, Issever H, Unaltuna NE, Ozbey NC (2008) Endothelial nitric oxide synthase intron 4a/b polymorphism and early atherosclerotic changes in hypopituitary GH-deficient adult patients. Eur J Endocrinol 158:615–622
303. Hong JW, Kim JY, Kim YE, Lee EJ (2011) Metabolic parameters and nonalcoholic fatty liver disease in hypopituitary men. Horm Metab Res 43:48–54
304. Barclay JL, Nelson CN, Ishikawa M, Murray LA, Kerr LM, McPhee TR, Powell EE, Waters MJ (2011) GH-dependent STAT5 signaling plays an important role in hepatic lipid metabolism. Endocrinology 152:181–192
305. Christ ER, Cummings MH, Russell-Jones DL (1998) Dyslipidaemia in adult growth hormone (GH) deficiency and the effect of GH replacement therapy: a review. Trends Endocrinol Metab 9:200–206
306. Monson JP, Jönsson P, Koltowska-Häggström M, Kourides I (2007) Growth hormone (GH) replacement decreases serum total and LDL-cholesterol in hypopituitary patients on maintenance HMG CoA reductase inhibitor (statin) therapy. Clin Endocrinol (Oxf) 67:623–628

307. Pijl H, Langendonk JG, Burggraaf J, Frölich M, Cohen AF, Veldhuis JD, Meinders AE (2001) Altered neuroregulation of GH secretion in viscerally obese premenopausal women. J Clin Endocrinol Metab 86:5509–5515
308. Boero L, Cuniberti L, Magnani N, Manavela M, Yapur V, Bustos M, Rosso LG, Meroño T, Marziali L, Viale L, Evelson P, Negri G, Brites F (2010) Increased oxidized low density lipoprotein associated with high ceruloplasmin activity in patients with active acromegaly. Clin Endocrinol (Oxf) 72:654–660
309. Mihailescu DV, Vora A, Mazzone T (2011) Lipid effects of endocrine medications. Curr Atheroscler, Rep, 13
310. Cersosimo E, Danou F, Persson M, Miles JM (1996) Effects of pulsatile delivery of basal growth hormone on lipolysis in humans. Am J Physiol 271:E123–E126
311. Surya S, Horowitz JF, Goldenberg N, Sakharova A, Harber M, Cornford AS, Symons K, Barkan AL (2009) The pattern of growth hormone delivery to peripheral tissues determines insulin-like growth factor-1 and lipolytic responses in obese subjects. J Clin Endocrinol Metab 94:2828–2834
312. Johansson JO, Oscarsson J, Bjarnason R, Bengtsson BA (1996) Two weeks of daily injections and continuous infusion of recombinant human growth hormone (GH) in GH-deficient adults. I. Effects on insulin-like growth factor-I (IGF-I), GH and IGF binding proteins, and glucose homeostasis. Metabolism 45:362–369
313. Jørgensen JO, Møller N, Lauritzen T, Christiansen JS (1990) Pulsatile versus continuous intravenous administration of growth hormone (GH) in GH-deficient patients: effects on circulating insulin-like growth factor-I and metabolic indices. J Clin Endocrinol Metab 70:1616–1623
314. Laursen T, Lemming L, Jorgensen JO, Klausen IC, Christiansen JS (1998) Different effects of continuous and intermittent patterns of growth hormone administration on lipoprotein levels in growth hormone-deficient patients. Horm Res 50:284–291
315. Oscarsson J, Ottosson M, Johansson JO, Wiklund O, Mårin P, Björntorp P, Bengtsson BA (1996) Two weeks of daily injections and continuous infusion of recombinant human growth hormone (GH) in GH-deficient adults. II. Effects on serum lipoproteins and lipoprotein and hepatic lipase activity. Metabolism 45:370–377
316. Marshall L, Mölle M, Böschen G, Steiger A, Fehm HL, Born J (1996) Greater efficacy of episodic than continuous growth hormone-releasing hormone (GHRH) administration in promoting slow-wave sleep (SWS). J Clin Endocrinol Metab 81:1009–1013
317. Johnson TN, Rostami-Hodjegan A, Tucker GT (2006) Prediction of the clearance of eleven drugs and associated variability in neonates, infants and children. Clin Pharmacokinet 45:931–956
318. Nelson DR, Zeldin DC, Hoffman SM, Maltais LJ, Wain HM, Nebert DW (2004) Comparison of cytochrome P450 (CYP) genes from the mouse and human genomes, including nomenclature recommendations for genes, pseudogenes and alternative-splice variants. Pharmacogenetics 14:1–18
319. Thorner MO, Rogol AD, Blizzard RM, Klingensmith GJ, Najjar J, Misra R, Burr I, Chao G, Martha P, Mc Donald J (1988) Acceleration of growth rate in growth hormone-deficient children treated with human growth hormone-releasing hormone. Pediatr Res 24:145–151
320. Laursen T, Jørgensen JO, Jakobsen G, Hansen BL, Christiansen JS (1995) Continuous infusion versus daily injections of growth hormone (GH) for 4 weeks in GH-deficient patients. J Clin Endocrinol Metab 80:2410–2418
321. Hümmelink R, Sippell WG, Benoit KG, Danielson K, Faijerson Y (1993) Intranasal administration of growth hormone-releasing hormone (1–29)-NH2 in children with growth hormone deficiency: effects on growth hormone secretion and growth. Acta Pediatr 388:23–26
322. Steyn D, du Plessis L, Kotzé A (2010) Nasal delivery of recombinant human growth hormone: in vivo evaluation with Pheroid technology and N-trimethyl chitosan chloride. J Pharm Pharm Sci 13:263–273

323. Takeda A, Copper K, Bird A, Baxter L, Frampton GK, Gospodarevskaya E, Welch K, Bryant J (2010) Recombinant human growth hormone for the treatment of growth disorders in children: a systemic review and economic evaluation (Review). Health Technol Assess 14:1–209
324. Endocrine Society (2011) Evaluation and treatment of adult growth hormone deficiency: An endocrine society clinical practice guideline, J. Clin Endocrinol Metabol 96:1587–1609
325. Burman P, Johansson AG, Siegbahn A, Vessby B, Karlsson FA (1997) Growth hormone (GH)-deficient men are more responsive to GH replacement than women. J Clin Endocrinol Metab 82:550–555
326. Cook DM, Ludlam WH, Cook MB (1999) Route of estrogen administration helps to determine growth hormone (GH) replacement dose in GH-deficient adults. J Clin Endocrinol Metab 84:3956–3960
327. Johansson AG, Engström BE, Ljunghall S, Karlsson FA, Burman P (1999) Gender differences in the effects of long term growth hormone (GH) treatment on bone in adults with GH deficiency. J Clin Endocrinol Metab 84:2002–2007
328. Chapman IM, Bach MA, Van Cauter E, Farmer M, Krupa D, Taylor AM, Schilling LM, Cole KY, Skiles EH, Pezzoli SS, Hartman ML, Veldhuis JD, Gormley GJ, Thorner MO (1996) Stimulation of the growth hormone (GH)-insulin-like growth factor I axis by daily oral administration of a GH secretogogue (MK-677) in healthy elderly subjects. J Clin Endocrinol Metab 81:4249–4257
329. Ionescu M, Frohman LA (2006) Pulsatile secretion of growth hormone (GH) persists during continuous stimulation by CJC-1295, a long-acting GH-releasing hormone analog. J Clin Endocroniol Metab 91:4792–4797
330. Micic D, Casabiell X, Gualillo O, Pombo M, Dieguez C, Casanueva FF (1999) Growth hormone secretagogues: the clinical future. Horm Res 51:29–33
331. Nass R, Pezzoli SS, Oliveri MC, Patrie JT, Harrell FEJ, Clasey JL, Heymsfield SB, Bach MA, Vance ML, Thorner MO (2008) Effects of an oral ghrelin mimetic on body composition and clinical outcomes in healthy older adults: a randomized, controlled trial. Ann Intern Med 149:601–611
332. Stanley TL, Chen CY, Branch KL, Makimura H, Grinspoon SK (2011) Effects of a growth hormone-releasing hormone analog on endogenous GH pulsatility and insulin sensitivity in healthy men. J Clin Endocrinol Metab 96:150–158
333. Méjean L, Kolopp M, Drouin P (1992) Chronobiology, nutrition, and diabetes. In: Touitou Y, Haus E (eds) Biologic rhythms in clinical and laboratory medicine. Springer, Heidelberg, pp 375–385
334. Gualandi-Signorini AM, Giorgi G (2001) Insulin formulations – a review. Eur Rev Med Pharmacol Sci 5:73–83
335. Dessau E, Cameron F, Lee HB, Bequette BW, Zisser H, Jovanovic L, Chase HP, Wilson DM, Buckingham BA, Doyle FJ (2010) Real-time hypoglycemia prediction suite using continuous glucose monitoring. Diabetes Care 33:1249–1254
336. Keenan DB, Cartaya R, Mastrototaro JJ (2010) Accuracy of a new real-time continuous glucose monitoring algorithm. J Diabetes Sci Technol 4:111–118
337. Keenan DB, Cartaya R, Mastrototaro JJ (2010) The pathway to the closed-loop artificial pancreas: research and commercial perspectives. Pediatr Endocrinol Rev 7:445–451
338. Lee H, Buckingham BA, Wilson DM, Bequette BW (2009) A closed-loop artificial pancreas using model predictive control and a sliding meal size estimator. J Diabetes Sci Technol 3:1082–1090
339. Parker RS, Doyle FJ, Peppas NA (1999) A model-based algorithm for blood glucose control in type I diabetes. IEEE Trans Biomed Eng 46:148–157
340. Bratusch-Marrain PR, Komjati M, Waldhäusl WK (1986) Efficacy of pulsatile versus continuous insulin administration on hepatic glucose production and glucose utilization in type I diabetic humans. Diabetes 35:922–926

341. Courtney CH, Atkinson AB, Ennis CN, Sheridan B, Bell PM (2003) Comparison of the priming effects of pulsatile and continuous insulin delivery on insulin action in man. Metabolism 52:1050–1055
342. Meier JJ, Veldhuis JD, Butler PC (2005) Pulsatile insulin secretion dictates systemic insulin delivery by regulating hepatic insulin extraction in humans. Diabetes 54:1649–1656
343. Mirouze J, Selam JL, Pham TC (1977) Le pancréas artificial extra-corporel; nouvelle orientation du traitement insulinique. In: XIV Congrès Internat. Thérapeutique, Expansion Scientifique, Montpellier, France, pp 79–91
344. Mirouze J, Selam JL, Pham TC, Orsetti A (1977) Evaluation of exogenous insulin homeostatis by the artificial pancrease in insulin dependent diabetes. Diabetologia 13:273–278
345. Paolisso G, Scheen AJ, Giugliano D, Sgambato S, Albert A, Varricchio M, D'Onofrio F, Lefèbvre PJ (1991) Pulsatile insulin delivery has greater metabolic effects than continuous hormone administration in man; importance of pulse frequency. J Clin Endocrinol Metab 72:607–615
346. Matthews DR, Naylor BA, Jones RG, Ward GM, Turner RC (1983) Pulsatile insulin has greater hypoglycemic effect than continuous delivery. Diabetes 32:617–621
347. Berman N, Chou HF, Berman A, Ipp E (1993) A mathematical model of oscillatory insulin secretion. Am J Physiol 264:R839–R851
348. Jaspan JB, Lever E, Polonsky KS, Van Cauter E (1986) In vivo pulsatility of pancreatic islet peptides. Am J Physiol 251:E215–E226
349. Lefebvre PJ, Paolisso G, Scheen AJ, Henquin JC (1987) Pulsatility of insulin and glucagon release: physiological significance and pharmacological implications. Diabetologia 30:443–452
350. Gibson T, Stimmler L, Jarrett RJ, Rutland P, Shiu M (1975) Diurnal variation in the effects of insulin in blood glucose, plasma non-esterified fatty acids and growth hormone. Diabetologia 11:83–88
351. Debry G, Mejean L, Villaume C, Drouin P, Martin JM, Pointel JP, Gay G (1977) Chronobiologie et nutrition humaine. In: XIV Congrès Internat. Thérapeutique, Expansion Scientifique, Montpellier, France, pp 225–245
352. Mirouze J, Collard F (1973) Continous blood glucose monitoring in brittle diabetes. In: Proceedings 8th Int'l. Congr. Diabetes Fed., pp 532–545
353. Haus E, Nicolau G, Halberg F, Lakatua D, Sackett-Lundeen L (1983) Circannual variations in plasma insulin and C-peptide in clinically healthy subjects. Chronobiologia 10:132
354. Cawood EH, Bancroft J, Steel JM (1993) Perimenstrual symptoms in women with diabetes mellitus and the relationship to diabetic control. Diabet Med 10:444–448
355. Ruegemer JJ, Squires RW, Marsh HM, Haymond MW, Cryer PE, Rizza RA, Miles JM (1990) Differences between pre-breakfast and late afternoon glycemic response to exercise in IDDM patients. Diabetes Care 13:104–110
356. Aye T, Block J, Buckingham B (2010) Toward closing the loop: an update on insulin pumps and continuous glucose monitoring systems. Endocrinol Metab Clin North Am 39:609–624
357. Linkeschova R, Raoul M, Bott U, Berger M, Spraul M (2002) Less severe hypoglycemia, better metabolic control, and improved quality of life in type I diabetes mellitus with continuous subcutaneous insulin infusion (CSII) therapy; an observational study of 100 consecutive patients followed for a mean of 2 years. Diabet Med 19:746–751
358. Olinder AL, Nyhlin KT, Smide B (2011) Clarifying responsibility for self-management of diabetes in adolescents using insulin pumps – a qualitative study. J Adv Nurs 67:1547–1557
359. Revert A, Rossetti P, Calm R, Vehí J, Bondia J (2010) Combining basal-bolus insulin infusion for tight postprandial glucose control: an in silico evaluation in adults, children, and adolescents. J Diabetes Sci Technol 4:1424–1437
360. Walsh J, Roberts R, Bailey T (2010) Guidelines for insulin dosing in continuous subcutaneous insulin infusion using new formulas from a retrospective study of individuals with optimal glucose levels. J Diabetes Sci Technol 4:1174–1181

361. Cukierman-Yaffe T, Konvalina N, Cohen O (2011) Key elements for successful intensive insulin pump therapy in individuals with type 1 diabetes. Diabetes Res Clin Pract 92:69–73
362. Schwartz FL, Vernier SJ, Shubrook JH, Marling CR (2010) Evaluating the automated blood glucose pattern detection and case-retrieval modules of the 4 Diabetes Support System. J Diabetes Sci Technol 4:1563–1569
363. Dudde R, Vering T, Piechotta G, Hintsche R (2006) Computer-aided continuous drug infusion: setup and test of a mobile closed-loop system for the continuous automated infusion of insulin. IEEE Trans Inf Technol Biomed 10:395–402
364. Scaramuzza AE, Iafusco D, Rabbone I, Bonfanti R, Lombardo F, Schiaffini R, Buono P, Toni S, Cherubini V, Zuccoti GV, Diabetes Study Group of the Italian Society of S. Paediatric Endocrinology and Diabetology T (2011) Use of integrated real-time continuous glucose monitoring/insulin pump system in children and adolescents with type 1 diabetes: a 3-year follow-up study. Diabetes Technol Ther 13:99–103
365. Welsh JB, Kannard B, Nogueira K, Kaufman FR, Shah R (2010) Insights from a large observational database of continuous glucose monitoring adoption, insulin pump usage and glycemic control: the CareLinkTM database. Pediatr Endocrinol Rev 7:413–416
366. Mastrototaro J, Shin J, Marcus A, Sulur G (2008) The accuracy and efficacy of real-time continuous glucose monitoring sensor in patients with type 1 diabetes. Diabetes Technol Ther 10:385–390
367. Hermida RC, Ayala DE, Iglesias M (2003) Administration time-dependent influence of aspirin on blood pressure in pregnant women. Hypertension 41:651–656
368. Peppas N, Leobandung W (2004) Stimuli-sensitive hydrogels: ideal carriers for chronobiology and chronotherapy. J Biomater Sci Polym Ed 15:124–144
369. Rathbone MJ, Hadgraft J, Roberts MS (eds) (2003) Modified-release drug delivery technology. Marcel Dekker, New York
370. Youan B-BC (ed) (2009) Chronopharmaceutics. Wiley, Hoboken
371. Moschou EA, Peteu SF, Bachas LG, Madou MJ, Daunert S (2004) Artificial muscle material with fast electroactuation under neutral pH conditions. Chem Mater 16:2499–2502
372. Prescott JH, Lipka S, Baldwin S, Sheppard NFJ, Maloney JM, Coppeta J, Yomtov B, Staples MA, Satini JTJ (2006) Chronic, programmed polypeptide delivery from an implanted, multireservoir microchip device. Nat Biotechnol 24:437–438
373. Santini JT, Cima MJ, Langer R (1999) A controlled release microchip. Nat Biotechnol 397:335–338
374. Haus E, Touitou Y (1992) Chronobiology in circulating blood cells and platelets. In: Touitou Y, Haus E (eds) Chronobiology in laboratory medicine. Heidelberg, Springer, pp 504–526
375. Ohdo S, Koyanagi S, Matsunaga N, Hamdan A (2011) Molecular basis of chronopharmaceutics. J Pharm Sci 100:3560–3576
376. Mandal AS, Biswas N, Karim KM, Guha A, Chatterjee S, Behera M, Kuotsu K (2010) Drug delivery systems based on chronobiology–a review. J Control Release 147:314–325
377. Khan Z, Pillay V, Choonara YE, du Toit L (2010) Drug delivery technologies for therapeutic applications. Pharmaceut Develop Technol 14:602–612
378. Sewlall S, Pillay V, Danckwerts MP, Choonara YE, Ndesendo VM, du Toit LC (2010) A timely review of state-of-the-art chronopharmaceuticals synchronized with biological rhythms. Curr Drug Deliv 7:370–388

# Chapter 14
# Site Specific Controlled Release for Cardiovascular Disease: Translational Directions

**Ilia Fishbein, Michael Chorny, Ivan S. Alferiev, and Robert J. Levy**

**Abstract** Cardiovascular diseases remain the leading cause of mortality worldwide. Despite tremendous progress in prophylaxis, diagnostics, and pharmacology of cardiovascular disorders, a number of disease states cannot be successfully treated even with the most sophisticated therapeutics. A significant part of the problem is a lack of adequate systems for the focal delivery of therapeutic agents to disease sites in the heart and blood vessels. Over the last 30 years, basic and translational research on the interface of pharmacology, pharmaceutics, physiology, biomaterials, and nanotechnology have made possible the emergence of clinical grade site specific controlled release devices, which have become standards of care in cardiovascular medicine. There are multiple advantages of controlled release systems for localized site specific treatments, including increased efficacy, reduced side effects, and favorable tissue scaffolding properties.

## 14.1 Introduction

Over the past two decades, remarkable progress has been made in both the surgical and medical therapy of cardiovascular disease, leading to significantly improved outcomes. Despite this, cardiovascular disease remains the leading cause of death in developed countries. The use of controlled release drug delivery systems for treating cardiovascular disease is a relatively new area that has made a major impact, and the initial success of controlled release systems for cardiovascular disease indicates that there is a wide range of opportunities for research and development along these lines. Because cardiovascular disease in general is localized to either specific sites in the myocardium or foci of arterial disease, controlled release systems

I. Fishbein • M. Chorny • I.S. Alferiev • R.J. Levy (✉)
Abramson Research Center, The Children's Hospital of Philadelphia, 3615 Civic Center Blvd, Suite 702, Philadelphia, PA 19104, USA
e-mail: levyr@email.chop.edu

J. Siepmann et al. (eds.), *Fundamentals and Applications of Controlled Release Drug Delivery*, Advances in Delivery Science and Technology,
DOI 10.1007/978-1-4614-0881-9_14, © Controlled Release Society 2012

have involved implants in general either at sites of disease or in locations where the pathophysiology can be locally inhibited. This chapter focuses on the rationale for the use of controlled release drug delivery systems for cardiovascular disease, summarize progress, assess unmet needs, and then describe some of the emerging strategies for advanced controlled release systems.

## 14.2 The Pathophysiology of Cardiovascular Disease: Diagnostic Techniques Offer the Possibility for Guiding Therapeutic Implants

Diseases of the circulatory system involve either disorders affecting the heart, primarily, or blood vessels, or both. The most common cardiac disorder is ischemic heart disease due to atherosclerosis of the coronary arteries. Coronary artery atherosclerosis leads to obstruction of blood flow to the myocardium, resulting in heart failure and eventually death. Primary cardiac disease can be due to either cardiomyopathies – disorders of the heart muscle or congenital malformations, which are major birth defects resulting in anatomically defective cardiac chamber formation that can be associated with severe pathophysiologic abnormalities. This chapter does not discuss venous disorders, which are common and most often involve thromboembolic disease of the lower extremities. Venous thromboembolic disease is currently treated with anticoagulant therapy and with device interventions to prevent embolization. At present, there are no controlled release strategies for venous diseases. However, the opportunity that this represents should not be overlooked.

A common feature to all of these cardiovascular disorders is that various imaging modalities permit rapid diagnosis and sophisticated localization of disease foci. These diagnostic techniques historically began with cardiac catheterization and fluoroscopic angiography of the diseased heart and blood vessels. The field has progressed to high resolution noninvasive techniques such as cardiac ultrasound, vascular ultrasound, and magnetic resonance imaging. Emerging imaging techniques that will likely be a part of future cardiovascular diagnostic studies include positron imaging tomography (PET scanning) and optical imaging. Imaging modalities, in general, are used to guide placement of controlled release implants at key sites for treating or preventing disease progression.

## 14.3 Cardiac Controlled Release Systems

Implanting or delivering a sustained release preparation to the myocardium represents a major challenge, for a number of reasons. The rapid mechanical action of the beating heart makes stable implantation difficult. In addition, different

regions of the heart have characteristic susceptibilities. Thus, regions such as conducting tissue or blood vessels could be locally damaged by site-specific implants, and this could make controlled release system implantation potentially risky. In addition the myocardium is highly vascularized and thus released agents are rapidly cleared, compromising attainment of adequate therapeutic levels of many agents of interest. There have been a number of experimental configurations of controlled release systems ranging from epicardial polymers to hydrogels injected into the myocardium. However, these approaches have not in general led to preclinical studies or novel medical device implants. Nevertheless, the steroid eluting endocardial cardiac pacing lead has been highly successful and is discussed in detail.

### *14.3.1 The Steroid Eluting Cardiac Pacing Lead: The Only Routinely Used Myocardial Controlled Release System*

Over the past 40 years, implantable pacemakers have revolutionized the treatment of cardiac rhythm disorders. These devices consist of electronic generators that administer continuously paced electrical impulses through an electrode placed permanently in the myocardium. These paced impulses, which are electronically generated and monitored by sophisticated implantable pacemakers, maintain heartbeat for hundreds of thousands of patients whose cardiac rhythm systems have failed.

One of the problems that was noted early on in this field was the tendency for the electrical pacing capture threshold to rise due to fibrous tissue formation at the site of pacer electrode implantation. This problem was solved through investigations of a controlled release implant at the myocardial contact point of the metal tips of the pacing electrodes that would provide antiscarring therapy at the site of electrode contact, as illustrated in Fig. 14.1. Dexamethasone, a potent anti-inflammatory steroid was the drug chosen for elution from this silicone-based controlled release system. A series of successful animal studies led to eventual clinical approval and routine use of steroid eluting cardiac pacing electrodes [1]. This approach has justifiably become the standard of care.

### *14.3.2 Unmet Needs in the Field of Myocardial Drug Delivery*

Although the steroid eluting pacer electrode tip is a major innovation and an important clinical device, this design concept unfortunately does not address many potentially important controlled release applications that could be applied to

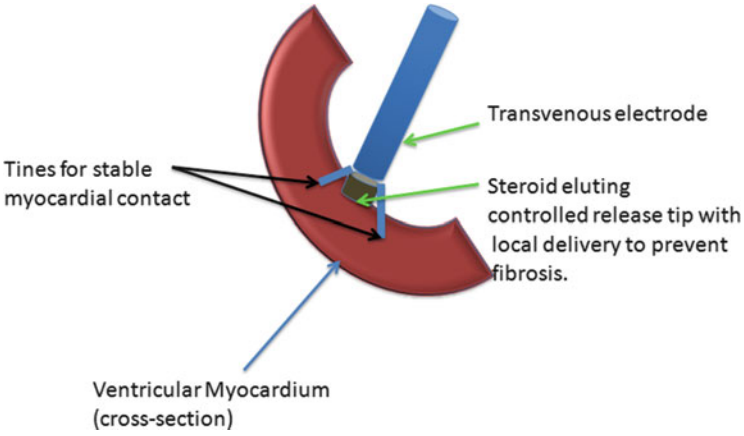


**Fig. 14.1** Steroid eluting pacemaker electrode in contact with the myocardium to prevent fibrosis at pacer lead contact

myocardial disease. For example, at present there is no satisfactory therapy for heart failure. Heart failure may be defined as inadequate cardiac function due to either coronary artery disease or a primary myocardial disorder that leads to insufficient cardiac output and a terminally debilitated state of the affected patient. There has been little progress in this field for the past two decades. Local delivery of agents that could improve myocardial function to ameliorate heart failure is a hypothetical concept that would require both drug discovery and the development of a feasible delivery system to administer such an agent. Similarly, novel drug therapies for cardiac arrhythmias have made relatively little progress over the past 20 years. Cardiac arrhythmias are abnormalities of heart beat that can lead to loss of consciousness, heart failure, and sudden death. While controlled release epicardial implants for treating arrhythmias have been studied experimentally, none of these systems have progressed to even a preclinical stage of development.

## 14.4 Controlled-Release Systems for Arterial Disease

Atherosclerosis is a chronic disease of the arterial system that is the pathophysiologic basis for heart attack and stroke. Atherosclerosis is caused in part by increased levels of cholesterol-containing lipoproteins, and the interaction of other risk factors including hypertension and cigarette smoking. Care of patients with atherosclerotic vascular disease has been greatly improved by introduction of a class of cholesterol lowering medications, known as the statins, which inhibit cholesterol production.

Coronary artery disease has also been successfully treated in many cases by coronary artery bypass graft surgery. In the 1980s, stent angioplasty emerged as a

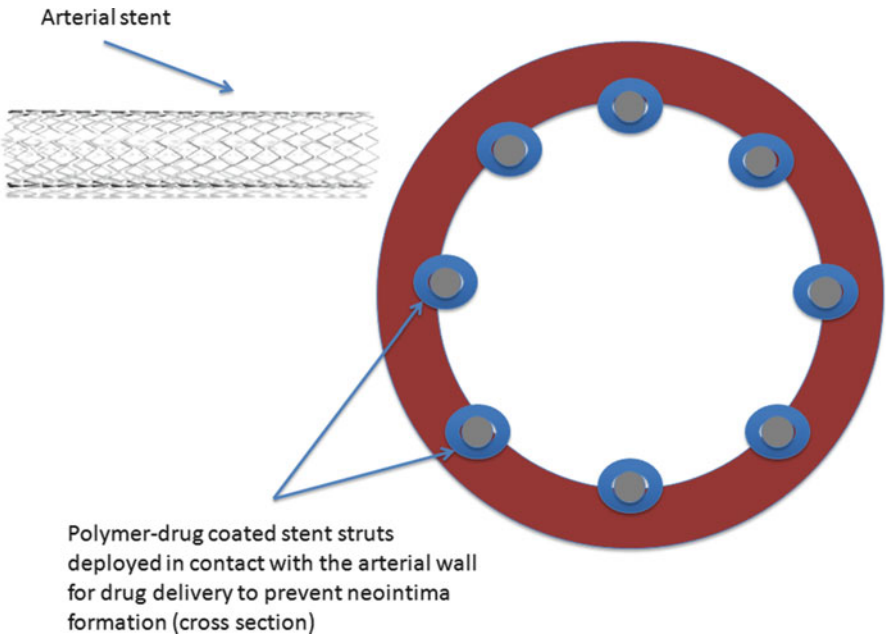


**Fig. 14.2** Schematic of drug-eluting stent delivery to the arterial wall

novel and potentially very important interventional approach for treating coronary disease, and arterial occlusive disease in general. A stent (Fig. 14.2) may be defined as an expandable framework that can be delivered to the site of an arterial obstruction by a catheter and is then deployed either by inflation of an inner coaxial balloon catheter, or by self-expansion of struts consisting of shape memory alloys such as nitinol (nickel–titanium). However, while the use of stents led to acute improvement in most patients, 30–50% of these individuals developed reobstruction of the stented arterial region, a disease process known as in-stent restenosis (ISR), in less than 1 year [2]. To address this problem, controlled release drug eluting stents (DES) were developed [2, 3]. Over the past decade, the DES has become one of the most widely used controlled release treatments, and thus, it is a major focus of this chapter.

## 14.5 Drug Eluting Stents: Challenges and Solutions (Table 14.1 and Fig. 14.2)

Placing a polymeric drug delivery system on the struts of a balloon deployable or self-expanding stent is a very logical but challenging approach to local delivery of agents that can prevent disease processes leading to ISR. ISR has been extensively

**Table 14.1** Drug eluting metallic stents with nondegradable polymers as coatings in clinical use

| Device (Manufacturer) | Drug | Polymer coating | Polymer structure | Release (28 days) |
|---|---|---|---|---|
| Taxus® (Boston Scientific) | Paclitaxel | Poly(styrene-*b*-isobutylene-*b*-styrene) (SIBS) | Fig. 14.4a | <10% |
| Cypher® (Cordis, Johnson and Johnson) | Sirolimus | Polyethylene-*co*-vinyl acetate and Poly-*n*-butyl methacrylate | Fig. 14.4b, c | 80% |
| Endeavor® (Medtronic) | Zotarolimus | Phosphorylcholine-based polymer system | Fig. 14.4d | 95% |
| Xience® (Abbott) | Everolimus | Poly(vinylidene fluoride-*co*-hexafluoropropylene) and Poly-*n*-butyl methacrylate | Fig. 14.4e | 80% |

studied clinically, and well validated experimental models have been developed for investigating novel therapies. The challenges and constraints involved in delivering a sustained release preparation are as follows: (1) the surface capacity of the typical coronary sized stent is small, typically less than 1 $cm^2$; (2) the stent coating with contained drug cannot interfere with the mechanical expansion of the stent, thus limiting the amount and types of polymers that might be used; (3) the biocompatibility and inflammatory characteristics of the polymer coating for controlled release are of importance in view of the potential for a host response to the deployed stent; (4) because of these factors, the amount of drug that can be contained on a stent is small, without an obvious possibility for redosing; and (5) owing to the latter factor, drugs of choice must be highly potent and thus may have broad cytotoxic effects.

DES development for the treatment of coronary disease has successfully addressed many of these issues [4, 5], but with some notable limitations (Table 14.1). At present, there are only two types of pharmaceutical agents, taxanes such as paclitaxel (Fig. 14.3a), and sirolimus (Fig. 14.3b) or its related analogs used in DES devices. These agents have been shown to be clinically effective in DES for preventing coronary ISR. Paclitaxel is a well established anticancer agent and the most widely used agent of the taxanes, a class of agents that inhibits cell proliferation by disrupting microtubule formation [5]. Sirolimus and its analogs, such as zotarolimus and everolimus, inhibit cell proliferation through cell cycle disruption via inhibition of mTOR, a receptor known as the mammalian target of rapamycin [5]. Both paclitaxel and sirolimus in DES inhibit regeneration of the endothelium. Thus, patients with DES are at risk for thromboembolic complications and, therefore, are maintained on long term antiplatelet therapy, using daily oral administration of agents such as clopidogrel and similar pharmaceuticals. Nevertheless, for coronary disease the incidence of ISR has fallen to 5% or fewer after 1 year [5]. However, this statistic still accounts for 200,000 or more patients in the USA alone with ISR. Because of this and other limitations of DES therapy to be discussed below, there are great opportunities for continuing research and improvements.

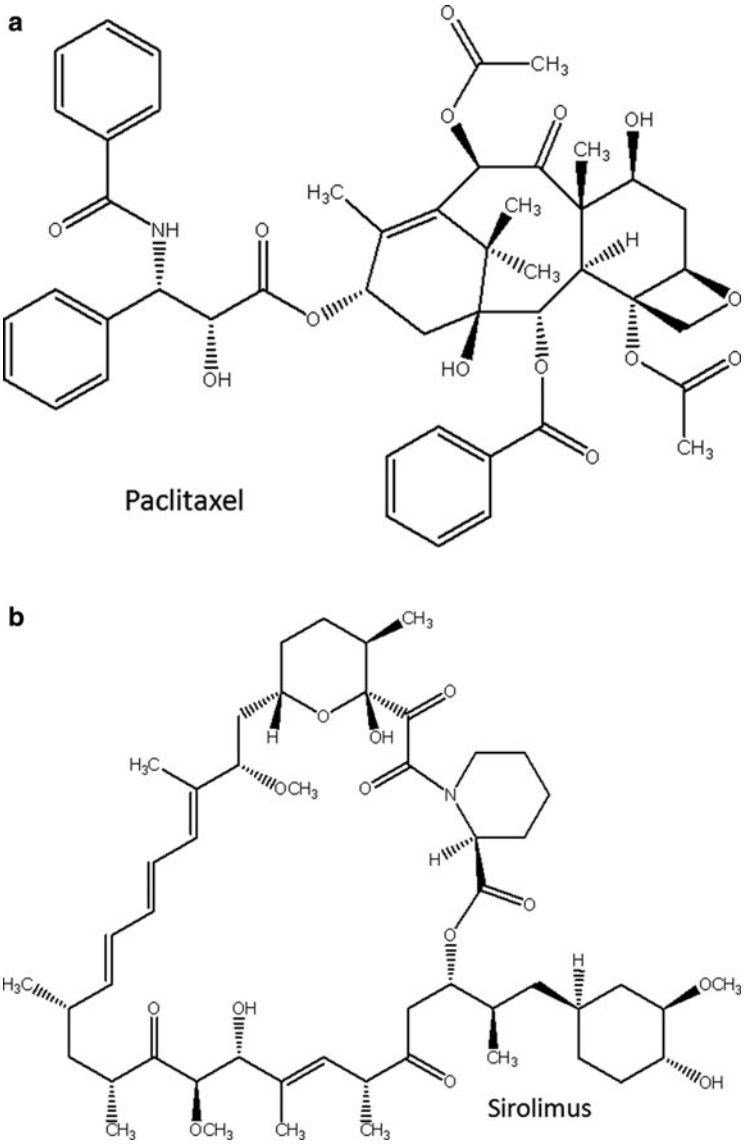


**Fig. 14.3** Chemical structures of paclitaxel (**a**) and sirolimus (**b**)

### *14.5.1 Basics of Drug Release from DES*

Minimal requirements for DES as an implantable drug delivery system consist of the ability to provide effective but safe local drug concentration, i.e., fit the therapeutic window of concentrations, sufficient release duration (still disputable [6], but obviously no less than 1 month), and spatial uniformity, i.e., avoidance of significant

variation in the amount of drug released from the different parts of the device. Additionally, mechanical reliability, biocompatibility, and deliverability should not be compromised compared to bare metal stents (BMS). Unfortunately, no currently approved DES device fully possesses all of these properties.

To affect vascular pathology, a drug molecule first must be released from the bulk of the DES-associated drug depot to the DES–artery boundary, where it partitions into the arterial wall. The processes driving a drug release from the polymer matrix of DES are distinct from the forces governing biodistribution of released drug in the stented artery. However, these two phases are intrinsically linked [7].

#### 14.5.1.1 DES Coatings

The central technological feature of DES is the association of a drug of interest with the stent material in a form that allows protracted leaching of the drug molecules into the vascular environment. In most cases, drug is deposited in conjunction with a polymeric or nonpolymeric matrix that constitutes the stent coating either in the dissolved form or as discrete drug nanoparticles [8]. Some recent technologies utilize direct drug deposition on struts by exposing the stent to a saturated solution of the drug in organic solvent with subsequent rapid solvent evaporation. However, unless the stent surface is porous, this type of coating requires an additional protective layer of biocompatible polymer to retard loss of drug [4].

Two main release mechanisms exploited in currently available and experimental DES are diffusion through the matrix and matrix disintegration [9, 10]. The latter can take the form of dissolution for water soluble matrices, or chemical degradation, usually due to hydrolysis for water insoluble biodegradable polymers. As it bears to diffusion driven mechanisms, the release rate of a drug is determined by (1) matrix thickness, (2) the partition coefficient of drug molecules between the matrix and external environment, collectively represented by cellular and extracellular components of the arterial wall and blood, (3) matrix porosity and tortuosity, (4) surface area, (5) the drug loading in the matrix, i.e., drug concentration, and (6) the time elapsed since commencement of release (secondary to the changes in drug concentration). Drug release rates of stent coatings diminish after the early burst phase due to depletion of drug in the outermost layers of matrix, resulting in an increased distance through which molecules must diffuse to be released. This explains the non-first order release kinetics observed in monolithic diffusion controlled DES coatings, exemplified by the Taxus® stent (Boston Scientific, Natick, MA). The Taxus® system uses a 316L stainless steel Express 2 stent (132 μm struts), coated with a 16 μm single layer of Translute SIBS [poly(styrene-*b*-isobutylene-*b*-styrene); Fig. 14.4a] triblock polymer containing paclitaxel, which elutes over about 90 days. Coatings with significantly different release properties can be formulated by varying the ratio between the amount of paclitaxel and polymer, while keeping the total amount of the drug constant.

The problem of release attenuation over time is addressed with the Cypher® stent (Cordis, J&J, Bridgewater, NJ), which is a rapamycin containing DES system.

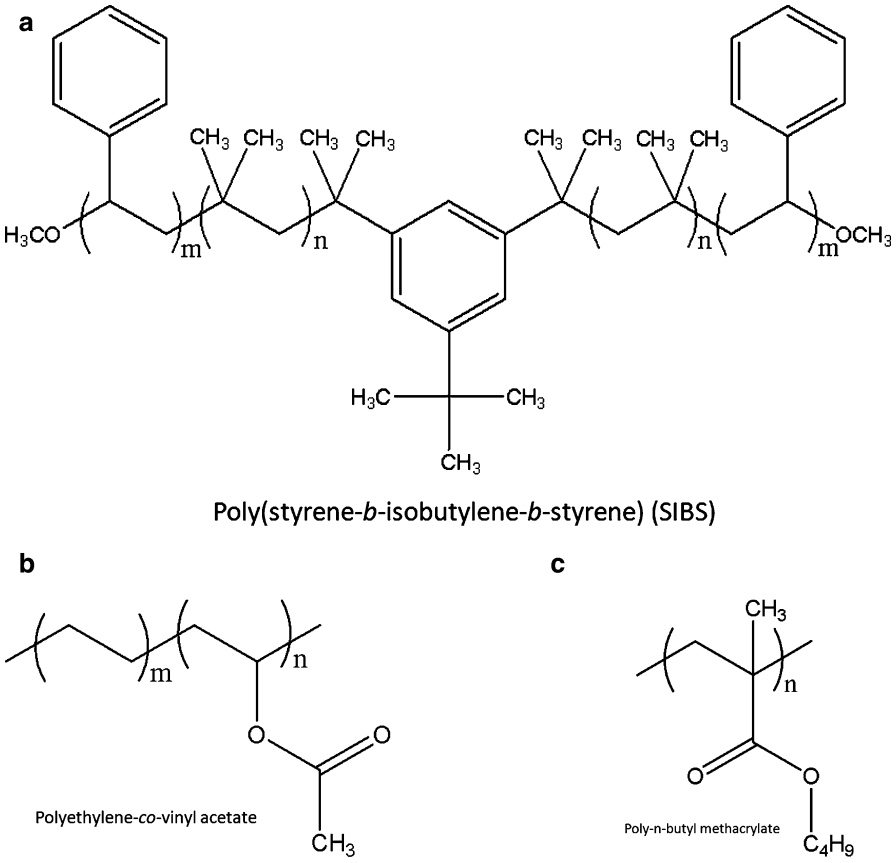


**Fig. 14.4** Chemical structures of polymers used in nondegradable stent coatings

Cypher® consists of a 316L stainless steel BXVelocity stent platform (140 μm struts), with a 12.6 μm, 3-layer coating comprised of a 2 μm chemical vapor deposited Parylene C [poly(*p*-xylylene)] base coat, a 10 μm main coat of poly (ethylene-*co*-vinyl acetate) (PEVA; Fig. 14.4b), poly(*n*-butyl methacrylate) (PBMA; Fig. 14.4c) and sirolimus, and a 0.6 μm top coat of PBMA. Sirolimus elutes from this stent over about 30 days. The top coat of pure PBMA is a rate limiting membrane that significantly controls the overall release rate. Thus, Cypher® approximately embodies a reservoir based, diffusion controlled release system. With the exception of the burst release period in the first 3–4 days, release fits zero order kinetics until the depot is nearly exhausted.

DES with biodegradable coatings exhibit a continuous layer (4–15 μm) of PLA (Fig. 14.5a), PLGA (Fig. 14.5b), or PLA-*co*-PCL (Fig. 14.5c) over the struts with the drug dispersed in a biodegradable polymeric matrix. Some systems (e.g., INFINNIUM®, Sahajanand Medical, India) are equipped with an additional topcoat layer of polyvinyl pyrrolidone (PVP; Fig. 14.5d) for the modulation of

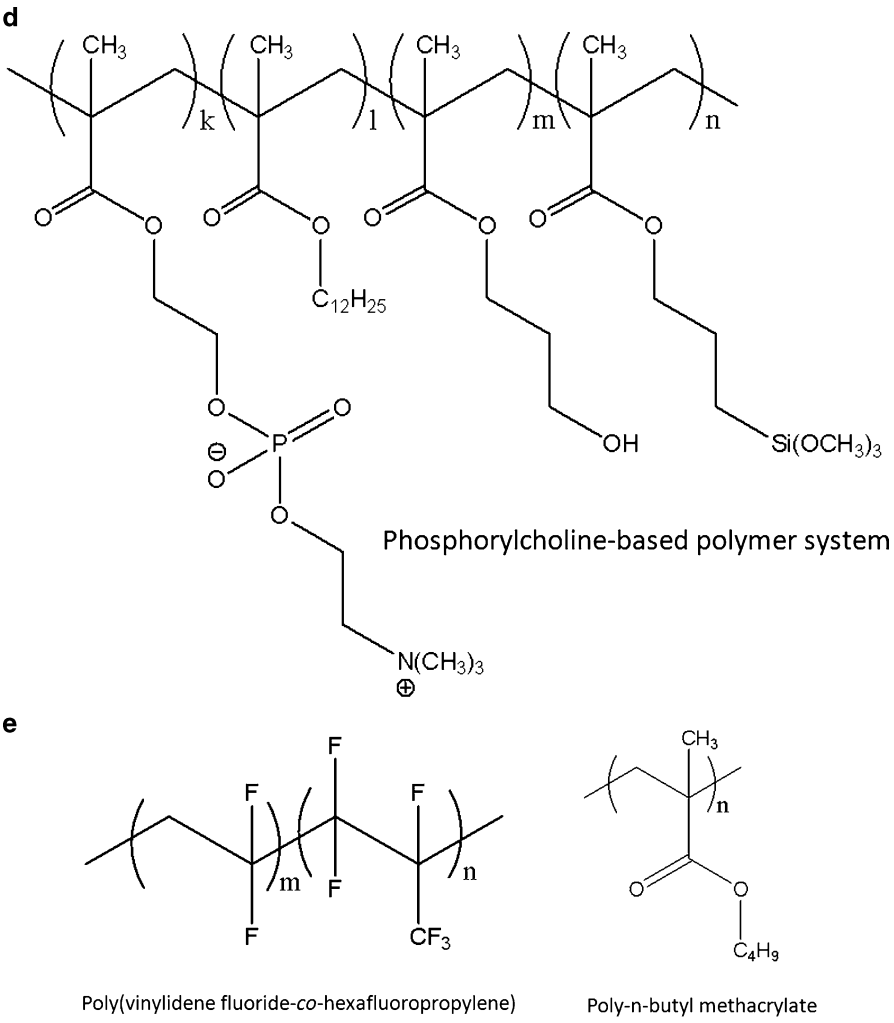


**Fig. 14.4** (continued)

release rate, while others (e.g., EXCEL, JW Medical Systems, China) do not have any additional rate-limiting features. Importantly, the main mechanism of release in this group of stent devices is still diffusion of the drug through the biodegradable matrix with matrix decomposition (complete by 6–9 months) being a secondary mechanism of the drug release. Depending on the respective rates of polymer hydrolysis and the diffusion of the water inside the matrix, degradation of the polymeric matrix can occur as surface erosion or bulk erosion. This has implications for the release profile (usually, a zero order kinetics for the surface erosion and a second order kinetics for the bulk degradation). However, this may not be relevant if diffusion based release occurs more rapidly than degradation.

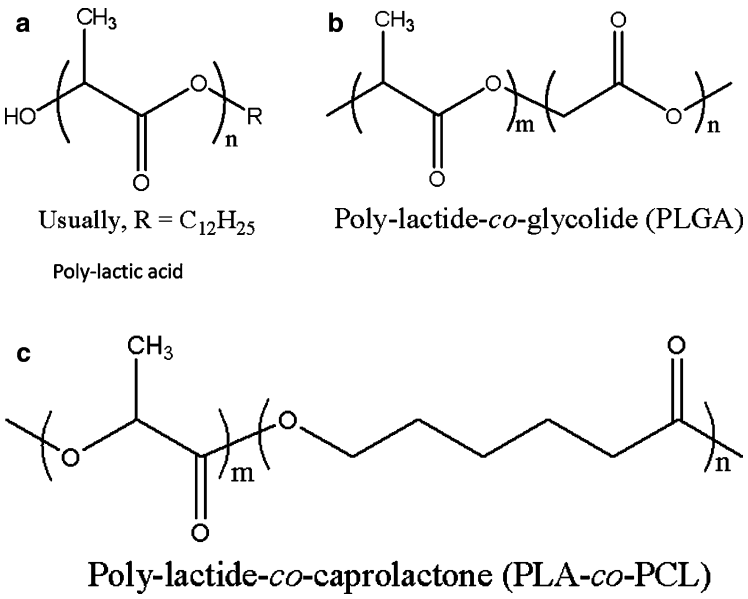


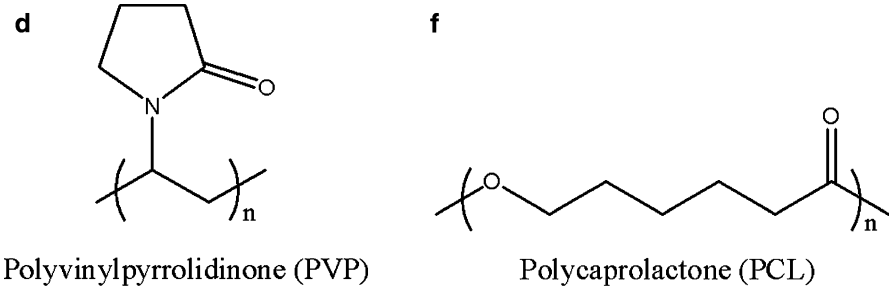


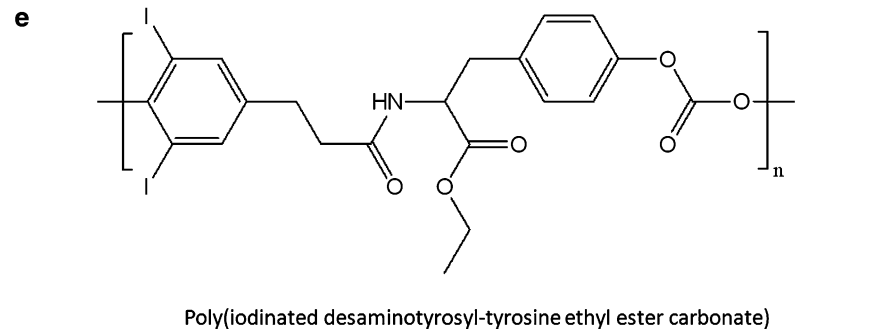


**Fig. 14.5** Chemical structures of polymers used in biodegradable stent coatings

#### 14.5.1.2 Arterial Biodistribution of DES-Delivered Pharmacological Agents

Local arterial pharmacokinetics of drugs delivered by DES is determined by the processes of diffusion and convection [10]. Diffusion reflects the gradient-driven spreading of a pharmacological agent by random motion, while convection describes mass transfer of drug molecules due to the hydraulic pressures and fluid transport across the vessel wall. These two mechanisms explain the dynamics of mass transfer through the vessel wall of any given pharmacologic agent, but do not predict the actual concentrations of the antirestenotic drugs in the different compartments of a stented arterial segment. Arterial drug levels are primarily determined by the amount of the drug released from the stent (which in turn is dependent on the drug loading and the release profile of the DES device) and the physicochemical properties of the pharmacological agent [7, 10]. These properties, such as hydrophobicity vs. hydrophilicity, polarity, molecular mass, govern a series of partitioning events of drug molecules between intra- and extracellular components of the arterial wall and blood, which eventually determine the drug concentrations in various vessel compartments and thus dictate both the therapeutic effectiveness and toxic side effects of DES.

#### 14.5.1.3 Mathematical Modeling of Arterial Drug Pharmacokinetics

Mathematical modeling of complex interactions between DES-delivered drugs and the dynamic environment of the vessel wall has been applied in an attempt to predict the therapeutic and toxic endpoints of various DES systems [11, 12]. In some cases [7, 13, 14], in silico calculations have been correlated with ex vivo and in vivo data allowing partial conclusions regarding the accuracy and predictive values of different mathematical models. Over the last several years, computational approaches based on one-, two- and three dimensional geometrical domains accounting for the effects of polymer coating, stent geometry, drug binding to the cellular and extracellular arterial targets, blood flow, arterial matrix porosity and tortuosity, and presence of atherosclerotic plaque and thrombus have been suggested and developed, resulting in a number of important insights as described below [11, 15].

Effects of Polymer Coating

Several models predict [7, 10] that the amount of the drug incorporated into the DES coating and the kinetics of its release are the main factors determining arterial drug levels. Balakrishnan et al. [7] modeled vastly different diffusion rates of the

drug from the polymer coating, with diffusion coefficients ranging from $10^5$ to $10^{-5}$ $\mu m^2/s$, and showed that extreme cases of the release kinetics are inefficient in terms of transferring drug to the arterial wall. Ultrafast release, approximating a bolus injection, results in high drug levels at the stent–artery boundary, which are not translated into significant arterial drug loading, since the capacity of the vessel wall to absorb the drug is overwhelmed, and the drug is lost into the circulation. On the contrary, extremely slow diffusion through the polymer (less than $10^{-5}$ $\mu m^2/s$) avoids loss of pharmaceutical agent, but peak drug levels at the stent–artery interface at steady state are too low to provide tissue concentrations required for pharmacological activity.

### Effects of Drug's Physicochemical Properties

By changing the relative contribution of diffusion- and convection related mechanisms on a drug's mass transfer, the physicochemical properties of the pharmacological agent, e.g., hydrophobicity vs. hydrophilicity, size and charge, affect the pattern of drug distribution in the artery. Simulations by Hwang et al. [16, 17] predict that spatial variation of drug concentration across the arterial tunica media, given comparable effects of diffusion and convection on drug transport, is lower for hydrophilic drugs such as heparin than for hydrophobic compounds such as paclitaxel, although the latter exhibit much higher overall arterial drug levels. Moreover, hydrophilic drugs are more readily washed out by blood, leading to a decrease in concentrations of stent-delivered hydrophilic compounds at locales close the arterial lumen [16, 17].

### Effects of Stent Design and Deployment Technique

Simulations consistently show highest transient drug concentrations in arterial tissue immediately surrounding drug-bearing struts, and the lowest concentrations at midpoints between adjacent struts [14]. However, specific strut geometry, the number of struts, the distance between them, and depth of tissue penetration (determined mainly by deployment pressure) determine the actual spatial pattern of drug concentration. An interesting consequence of underembedment of the strut in the tissue is formation of shielded low flow "pockets" on both sides of the strut, creating a stagnant pool of released drug, allowing reuptake of the antirestenotic agent from the circulation into arterial tissue [14].

### Effects of Atherosclerotic Plaque and Mural Thrombosis

Experiments and mathematical models that deal with normal healthy vasculature assume uniformity of the arterial substrate within a given compartment. However,

atherosclerotic changes in the arteries treated with DES result in marked dissimilarities in drug pharmacokinetics between different locales. These differences derive from the changing ratio of focally applied diffusion and convection forces and from point-to-point variations in partitioning of therapeutic agents into pathological vascular substrates.

Since some degree of peristrut thrombosis is invariably present following stent deployment in both experimental animals and humans, Hwang's [18] and Balakrishnan's [13] studies modeled the effect of attending thrombosis on arterial drug uptake following DES implantation. The authors demonstrated that variability in extent and location of thrombus does not affect drug release from the coating, but may significantly alter the process of drug uptake and retention by the stented artery. Computer simulations carried out by Balakrishnan and coauthors [13] show that the focal thrombi that do not spread beyond individual struts increase cumulative drug exposure and respective arterial peak drug levels by 80% due to increasing residence time and surface contact of drug with the arterial wall. Moreover, a diffuse intrastrut thrombus may increase drug uptake by 250% since the diffuse thrombus effectively hinders washout of the absorbed drug into luminal blood. Importantly, when these in silico data were correlated with the pharmacokinetic and histological experimental findings in the pig coronary model, a fair correlation between variability in extent of thrombosis and the variability in sirolimus arterial content was found 3–14 days after the deployment of sirolimus-eluting Cypher® stents [13].

Recently the same research group from MIT [19] has published an experimental study in which they used both human autopsy atherosclerotic aortic samples and balloon injured atherosclerotic rabbit arteries to determine effects of lipid rich atherosclerotic plaque on tissue accumulation of three different lipophilic drugs used in DES devices: paclitaxel, sirolimus, and everolimus. Surprisingly, drug levels found in human and rabbit arterial tissue inversely correlated with lipid content of the samples, defying the predominant theory that lipophilic drugs are partitioned to the higher extent into the lipid-laden portions of the atherosclerotic arteries. Using a fluorescently labeled paclitaxel analog, Tzafriri et al. [19] demonstrated that drug accumulation occurs focally at sites of increased expression of intracellular tubulin, the molecular target of paclitaxel. Similarly, sirolimus and everolimus accumulation in the cryosectioned rabbit tissue correlated with abundance of the intracellular sirolimus target, FKBP-12. Both tubulin and FKBP-12 were upregulated by arterial injury and were reduced in the lipid-laden portions of the arteries [19]. Although DES were not employed in the study, these important data indicate that the difference in local arterial pharmacokinetics following DES-mediated delivery to healthy versus atherosclerotic arteries may be related to dissimilar drug partitioning due to the differential expression of intracellular proteins with specific affinities to the drug molecules.

**Table 14.2** Drug eluting stents fabricated without nondegradable polymers as coatings presently in coronary clinical trials

| Device (Manufacturer) | Drug | Drug delivery mechanism | Polymer structure/ characteristics | Release Kinetics |
|---|---|---|---|---|
| AmazoniaPAX (Minvasys) | Paclitaxel | Microdrop spray crystallization on stent wires | None | 98% over 30 days |
| Yukon (Translumina) | Sirolimus | Crystals imbedded on microporous surface | None | 67% over 7 days |
| XTENT (XTENT) | Biolimus | Polylactic acid coating on metallic stent | Polylactic acid (Fig. 14.5a) | 45% over 30 days |
| Infinnium (Sahajanand) | Paclitaxel | Polylactic acid coating on metallic stent | Polylactic acid (Fig. 14.5a) | 50% over 9 days |
| IDEAL stent (Bioabsorbable Therapeutics) | Sirolimus | Entirely biodegradable stent | Salicylic acid-derived poly (anhydride-esters) (Fig. 14.5e) | Complete stent degradation in 12 months |
| BVS (Bioabsorbable Vascular Solutions) | Sirolimus | Entirely biodegradable stent | Polylactic acid (Fig. 14.5a) | Complete stent degradation in 24 months |

### *14.5.2 Translational Systems: Novel DES in Clinical Trials (Table 14.2)*

The sirolimus eluting Cypher® stent (FDA approved in 2003) and paclitaxel eluting Taxus® stent (FDA approved in 2004) have changed the face of interventional cardiology and markedly improved outcomes of patients [5]. However, safety concerns focused on increased rate of late stent thrombosis (LST), as well as the nonoptimal ISR control in some patient populations have fueled continuous efforts to improve the existing DES platform [2, 4, 5]. This multiyear task culminated in the recent addition of two new products, the everolimus eluting Xience V® stent (Abbott Vascular, Santa Clara, CA) and the zotarolimus eluting Endeavor® stent (Medtronic, Minneapolis, MN). Both devices, collectively known as the second-generation DES, received FDA approval in 2008. Compared to the first generation Cypher® and Taxus® stents, these DES feature improved stent architecture (thinner wires made of cobalt–chromium alloy as opposed to 316L stainless steel of the first-generation products), a much thinner polymer layer (also nondegradable but with improved biocompatibility, see Fig. 14.4d, e) and novel, more selective, sirolimus analogs as pharmacological agents. Although 2–3 year follow ups with both Xience V® and Endeavor® platforms show

ISR and LST statistics superior to those of the first generation stents [5], the quest for new ideas to improve DES technology is ongoing [4, 20]. New concepts that will most likely be incorporated into design of future "third-generation" DES devices are discussed in this section.

#### 14.5.2.1 Stent Material

Several studies have demonstrated that strut thickness is an independent risk factor for ISR [21] by showing a reduced ISR rate associated with the use of stents featuring a 50 μm struts compared to stents with 140 μm struts. Therefore, there is a clear rationale for using the thinnest possible struts in stent design. However, reduction of stent wire diameter must not compromise the radial strength of the deployed stent needed to scaffold the diseased artery. Additionally, the strut material needs to be thick enough to be radio-opaque to allow radiographic imaging. Presently, a platinum–chromium alloy employed in several platforms (e.g., Promus Element™ by Boston Scientific) seems to be the leading material under investigation. Use of other alloys might be justified if dictated by stent design or delivery concept, such as shape memory nitinol alloy for self-deployed stents or magnetizable 304-grade stainless steel for magnetically guided nanoparticle loading onto the stent [22], as discussed below.

#### 14.5.2.2 Fenestrated Struts

The NEVO™ stent (Cordis) is a special open cell cobalt–chromium platform featuring oval-shaped drug reservoirs configured inside the struts, excluding the hinge regions. The reservoirs are filled with sirolimus (Fig. 14.3b) admixed with PLGA (Fig. 14.5b). The total dose of sirolimus and its release kinetics approximate those of Cypher®; however, the polymer, being biodegradable, completely erodes in 90 days, leaving behind a BMS. Additionally, the polymer laden surface area of NEVO™ is less than 25% that of Cypher®, so diminished adverse effects due to the polymer-induced inflammation are anticipated. As of this writing, clinical data on NEVO™ are limited to the 6-month results of the NEVO RES-I trial, which showed superiority of NEVO™ compared to Taxus® in late lumen loss, the angiographic endpoint of ISR [23].

#### 14.5.2.3 Unidirectional Release

Attempts to decrease the drug and polymer burden by currently designed stents eliminate the polymer and drug deposits that are laid on the inside aspect of the stent meshwork, since with typical deployment techniques this part of the stent (lumen facing, or luminal) never comes into contact with the vessel wall, and the loaded

drug is leached into circulation. Instead the drug (with or without polymer coating) is deposited on the external, abluminal aspect of the stent. This design feature has been realized in the Nobori® stent (Terumo, Leuven, Belgium), Biomatrix® stent (Biosensors, Morges, Switzerland), which both contain Biolimus A9 in a biodegradable PLA coating, and the coatless paclitaxel eluting Amazonia Pax® stent (Minvasys, Genevilliers, France).

An interesting extension of the partial stent coating concept was recently reported [24] describing an anti-CD34 antibody bearing (Genous R™ stent) design with an abluminal biodegradable sirolimus containing coating. The idea behind this combination of treatment mechanisms in one device is to counteract sirolimus-induced inhibition of reendothelialization using the prohealing properties of stent-immobilized anti-CD34 antibody.

#### 14.5.2.4 Biodegradable Stents

Biodegradable stents have been investigated for almost two decades, and have now become a clinical reality [4]. BMS were found to be superior to plain balloon angioplasty as they scaffold the artery postintervention, preventing elastic recoil and negative remodeling, which both contribute to lumen loss and restenosis. However, the third component of restenosis, neointimal hyperplasia, is actually augmented compared to balloon angioplasty, partially due to the permanent presence of the implant. Although metallic stents thus far have been well tolerated over time, there have been concerns about long term effects and even chronic inflammation due to the interaction of arterial wall pulsation with a rigid stent structure. Therefore, the concept of a biodegradable stent that remains at the deployment site long enough to prevent recoil and pathological remodeling, delivers drug that prevents injury-related SMC proliferation, and disappears when its task has been completed, is appealing. Although the first prototype of a completely biodegradable stent implant (Igaki-Tamai® stent) was engineered more than 10 years ago and was successfully used in patients in small clinical trial [25], the field did not progress until recently. The main reasons for lack of progress were unsolved issues regarding sufficient mechanical rigidity of nonmetallic stents, and concerns related to the local toxicity of the polymer degradation products.

At present there are a number of biodegradable DES advancing from preclinical studies to clinical trials (Table 14.2). The everolimus-eluting bioresorbable vascular scaffold (Abbott Vascular, Santa Clara, CA) is made of poly-L,L-lactide (PLLA) top-coated with a thin layer of poly-D,L-lactide (PDLA) admixed with everolimus (8.2 μg/mm stent length). Everolimus elution from this stent is complete after 3 months. The device is totally resorbed in 24 months, as assessed by intravascular ultrasound imaging. Recent clinical trial results (ABSORB study) indicate the safety and noninferiority of biodegradable polymer stents composed of polylactic acid compared to BMS [4]. As of this writing, Abbott's bioresorbable vascular scaffold commercialized under the name Absorb™ has been approved for clinical use in European Union.

Another prospective candidate is the sirolimus-loaded REVA stent (REVA Medical, San Diego, CA). The stent material is a poly(iodinated desaminotyrosyl-tyrosine ethyl ester) carbonate (Fig. 14.5e). The polymer degrades completely within 3 years of implantation into nontoxic excretable molecules. This DES system allows 95% of its sirolimus dose to be released over 3 months.

### *14.5.3 Addressing the Inflammatory Potential of Polymer Coatings Used in DES*

Despite the success of DES, the inflammatory response to polymer coatings over time remains an important issue [4]. This has been born out in animal studies from the beginning of research in the field, and is also evident in clinical pathology results documenting a continued inflammatory response to DES in human explants years after implantation. Although stent manufacturers have claimed to have developed inflammation resistant polymers, there is little scientific evidence to support this claim. The most likely reason for the success of coronary DES has to do with the potency of the drugs themselves in suppressing the inflammatory response during the period of active drug release, which is actually only a few weeks to months. After this time, arterial patency is probably maintained by the scaffolding effect of the overexpanded stent, which maintains optimal blood flow despite the development of a neointima.

While these circumstances have proved satisfactory for the majority of patients with coronary disease, neither BMS nor DES result in satisfactory outcomes when used for peripheral arterial disease (PAD), an occlusive arterial disease affecting most commonly the femoral artery and its branches in the lower extremities (see below). Thus, translational research efforts at this time are exploring novel polymer coatings for stents and biodegradable stents with DES capability as options for improving the biocompatibility and reducing the inflammatory response to DES coatings.

### *14.5.4 Drug Eluting Stents: Unmet Needs*

While stent angioplasty has led to a paradigm shift with improved outcomes for coronary disease, there is room for improvement. As mentioned above, the restenosis incidence of roughly 5% after 1 year accounts for more than 200,000 affected patients in the USA alone. In addition, neither BMS nor DES, despite widespread aggressive use, offer much in the way of improved clinical outcomes for PAD. PAD affects more than 27 million individuals in North American and Europe and accounts for an annual economic health care burden of more than $100 billion in the USA alone. In addition, DES as currently designed have limited pharmacologic

potential since they contain only a single drug, one dose, no refill capability, and they cannot be removed from vascular sites except through biodegradation. Furthermore, stents have been investigated for use as cell therapy platforms in a limited number of experimental studies, and while this approach represents a promising idea for regenerating the endothelium postangioplasty, none of the concepts studied thus far have advanced to preclinical investigations. These unmet needs are the focus of ongoing experimental activity.

## 14.6 Controlled Release Delivery Systems and Platforms for the Molecular and Cell Therapy of In-Stent Restenosis

The importance of the delivery system concept has mostly been overlooked in prior gene and cell therapy trials. However, proper delivery is crucial to the effectiveness of complex therapeutics. Since gene transduction in blood vessels requires prolonged contact of a vector with the tissue substrate, a successful gene delivery platform should be noninvasively guided to the delivery site, and should be able to concentrate and immobilize the vector at the tissue interface. Similarly, prolonged contact of delivered cells with the extracellular matrix increases the chances of proper cell anchoring via integrin-mediated mechanisms.

The main purpose of a gene or cell delivery system is to deploy and lodge the formulation close to or directly at the intended site of action. Minimizing contact between the vectors and bodily fluids prior to deployment at the intended location is of paramount importance, since it decreases dilution of the vectors and cells, and protects their surfaces from nonspecific interactions that are detrimental to vector activity and cell viability. A valid delivery system must also grant physical persistence of the vectors at the site of delivery in the transduction-competent state, thereby increasing the chances of delivering transgene to the cells. Moreover, delivery systems can be designed to incorporate elements facilitating gene transfer to the target cell population by local modification of the extracellular matrix or by rendering cells more susceptible to transduction by foreign DNA [26]. Finally, the gene delivery system can be coformulated with conventional pharmaceuticals with the aim of fine-tuning the therapeutic activity of the transgene. Thus, the localized nature of cardiovascular pathology and direct accessibility via endovascular catheters enables implementation of a wide array of platforms for targeted delivery of cardiovascular therapeutics.

### *14.6.1 Molecular Therapies for Restenosis Prevention*

The introduction of DES in clinical practice has led to a significant reduction of the incidence of ISR in patients [27]. However, it has become apparent that the reduction of ISR is associated with an increased rate of late thrombosis in

DES-treated lesions [3]. Aborted healing response, delayed reendothelialization, unresolved inflammation, and stent malapposition have been suggested as the major culprits of this life threatening complication [28].

Conceptually, all DES have an important design flaw, since their use is based on the premise that a single dose device will provide life long protection of the treated artery against ISR. In fact, all clinically used DES devices have a finite amount of drug incorporated in the polymer coating on the stent struts. Therefore, the drug depot is inevitably depleted to the extent that the release rate of antirestenotic drug becomes inadequate to sufficiently suppress SMC proliferation and migration. When that happens, the disease can progress unopposed by pharmacotherapy. Increasing the thickness of the polymer layer to introduce higher drug loads is unrealistic, since polymer coatings on the stent–vessel interface are consistently shown to promote inflammation [29]. Therefore, stent based therapeutics with the capacity of permanent modification of vascular substrate are a conceptually appealing alternative to DES technology. These novel stent-based therapeutic modalities make use of gene and cell therapy approaches or the combination of both.

#### 14.6.1.1 Gene Therapy

In broad terms, gene therapy is a modulation of abnormal physiological functions at either the cellular or organism level achieved by the introduction of exogenous genetic material. Depending on the vector used for gene delivery and the nature of the transgene, gene transfer to cardiovascular tissue can be associated with either transient or permanent modification of tissue substrate. The possibility to effect proliferation and migration of various cell populations, extracellular matrix deposition, and thrombogenicity of the vessel wall, i.e., the processes pivotal to both atherosclerosis and restenosis, has prompted numerous vascular gene delivery experiments pursuing both knock-in and knockdown genetic approaches [30].

Nonviral gene delivery vectors, i.e., formulations of plasmid DNA stabilized with cationic molecules (peptides, polymers or lipids), are the safest choice for therapeutic gene transfer in the vasculature [30, 31]. However, transgene expression following nonviral gene transfer to injured arteries is typically suboptimal in both magnitude and duration [30].

All of the major categories of viral vectors including retroviral, lentiviral, adenoviral, Adeno-associated virus vector [30, 32, 33], as well as more "exotic" viral constructs based on the Semliki Forest virus [34] and hemagglutinating virus of Japan [35] have been investigated for vascular gene delivery. Such vectors differ significantly in onset, extent, and duration of therapeutic transgene expression and severity of local and systemic inflammatory/immune reactions they elicit.

Currently, nonviral vectors, the third-generation adenovirus vectors, devoid of the viral genes triggering immune response (helper-dependent or "gutless" vectors) and the Adeno-associated virus vectors, appear to have the highest potential as platforms for the development of clinical grade vascular gene therapies for ISR prevention and treatment.

Catheter based delivery of viral and nonviral gene vectors to stented arterial segments is now a well established experimental modality that has shown therapeutic effectiveness in rodent, pig, and primate models of vasculoproliferative disease, including restenosis [36]. Recently, several Phase I human trials have demonstrated the feasibility and safety of gene transfer for prevention of restenosis arena [37, 38].

#### 14.6.1.2 Cell Therapy

Loss of the protective endothelial layer due to stenting injury is an important precipitating factor of ISR [39]. Moreover, delayed regrowth of endothelium related to DES usage underlies LST, a rare (<1.5%) but serious complication associated with 30% mortality [3]. Therefore, promoting early reendothelialization is a rational and realistic approach for the prevention of ISR and LST.

Endothelial cell therapy has been realized by several different approaches. Initially, attempts were made to immobilize autologous [40] or xenogeneic [41] endothelial cells on the stent surface prior to stent deployment. This was achieved by culturing cells in a bioincubator in the presence of the stent. Although a significant fraction of the cells was lost during the high pressure stent deployment, the remaining surviving cells located mostly on the lateral aspect of the struts were able to proliferate and speed up reendothelialization of stented arteries [40, 41].

Later developments in the field employed "dwelling" delivery of concentrated suspensions of endothelial cells [42, 43] and endothelial progenitor cells (EPC) [44–47] in the lumen of the injured segment of artery immediately after endothelial denudation. Although no active cell capturing strategy was employed in these studies, incorporation of delivered cells in lieu of missing endothelium in rodent [46] and rabbit [43–45, 47] models has been demonstrated by several groups. Moreover, restoration of normal vascular responses to vasoconstrictors and vasodilators [44, 47], and in some cases attenuation of neointimal formation [45, 46, 48] achieved with these therapies, are indicative of functional competence of the delivered cells.

The latest development in the field of cell therapy to mitigate restenosis is an EPC capture stent. This product (Genous Bioengineered R™ stent; OrbusNeich, FL, USA) is a dual helix R-stent platform, onto which an anti-CD34 antibody is incorporated. Following stent deployment, CD34-positive cells from circulation, a significant fraction of which are EPC, are captured and tethered to the stent as they pass across the stented segment. Extremely rapid (1 h) reendothelialization of the stent and lack of mural thrombus with the R-stent were demonstrated in the pig coronary model [49]. However, clinical utility of this stent is yet to be demonstrated [50]. One potential problem with this capture strategy is recruitment of SMC precursors in addition to EPC, since this cell type co-expresses CD34 on the cell membrane. Unlike EPC, SMC precursors are proatherogenic and are known to promote neointimal formation after vascular injury [51].

#### 14.6.1.3 Combinatory Approach

As discussed above, rapid reendothelialization of injured arteries has been shown to protect the stented arterial segment against restenosis. However, as demonstrated in several studies, the delivered endothelial cells and EPC do not survive in the endothelial location beyond 4 weeks after delivery. To reconcile these findings with the lasting antirestenotic effects of delivered cells, sustained antirestenotic activity was attributed to the ability of delivered EPC to secrete factors that induce repopulation of injured arteries by normal healthy endothelium on the edges of the injured arterial segments. In order to enhance the ability of delivered cells to recruit adjacent noninjured endothelium and to promote survival of the delivered EPC, several groups have pursued the idea of ex vivo EPC transduction with the genes exhibiting antiapoptotic and antirestenotic activities prior to delivering the cells to the denuded arteries in vivo [52, 53]. In general, a more profound inhibition of neointimal formation was observed in the groups of animals treated with transduced cells compared to nontransduced control EPC [52, 53].

#### 14.6.1.4 Other Molecular Therapies

A delicate balance between proliferation and apoptosis of cell populations in normal and injured vasculature, controlled ingress of blood borne cell types into vessel wall, and the dynamics of extracellular matrix synthesis and breakdown is achieved by elaborate interplay of multiple growth factors, cytokines, and chemokines [54–56]. These protein molecules exert their specific effects by activating cognate receptors on the cell surface. An additional layer of complexity is superimposed onto this intricate network by the context specific nature of cell signaling. Thus, the ultimate physiologic outcome of a specific protein–receptor pair interaction is dependent on the status of other signaling pathways. Along these lines, the complex and sometimes redundant molecular pathophysiology of restenosis provides multiple therapeutic "vantage points" for pharmacological modulation of neointimal hyperplasia [55, 57]. Indeed, both low molecular weight inhibitors of several growth factors promoting SMC proliferation and migration [57–61], and neutralizing antibodies against growth factors [62–64] and cytokines [65, 66] were shown to have marked antirestenotic activity in various animal models of restenosis, including ISR [58, 63].

Importantly, modulation of signaling cascades in stented arteries during the first several hours after the stenting procedure cannot be achieved by gene therapy approaches, since even fast acting gene delivery systems require a gap of at least 6 h between cell transduction and the onset of production of a therapeutic product. Therefore, the optimal pharmaceutical strategy to address pathological processes activated in the vascular wall immediately upon iatrogenic trauma may require a combination of a growth factors or inhibitors to instantly modify signaling processes in the stented artery, and a matching gene therapy allowing for sustained

pathway modulation. The same logic is relevant in the case of some protein inhibitors of the coagulation cascade [67] and of key enzymes of the antioxidant defense system [68], since both intramural thrombosis and reactive oxygen species-mediated potentiation of mechanical injury are early and potentially preventable elements of restenosis pathology.

### *14.6.2 Gene Delivery Stents*

Immobilization of gene vectors on stents may represent an alternative to DES, since (1) gene therapy can attain a longer lasting therapeutic modification of the vascular substrate, addressing both primary atherosclerotic process and restenosis as a response to iatrogenic vascular trauma; (2) gene interventions allow more choices than conventional low molecular weight drugs for selective inhibition of SMC proliferation and migration while maintaining and even enhancing endothelial regrowth; and (3) expression levels of a transgene and modulation of its biological activity can both be controlled with low molecular weight compounds, providing an additional level of pharmacologic regulation.

From the pharmacokinetic standpoint, stents represent an advantageous platform for local vascular gene therapy due to several circumstances common to DES and gene eluting stents: (1) higher arterial concentration of gene vectors can be achieved with stent-immobilized in comparison to nonimmobilized vectors following administration of smaller input dose; (2) vector immobilization on the stent minimizes distal spread of gene therapeutics, limiting inadvertent inoculation of nontarget tissues; (3) since cell activation and proliferation in the setting of ISR are almost exclusively observed in the vicinity of stent struts, tethering of gene vectors to stent wires places the genes close to the anticipated action site.

Previous experimental work from our group [26, 69, 70], as well as from others [31, 71–73] has established feasibility and therapeutic efficacy of gene vector immobilization on the surface of stents for prevention of ISR. However, methods previously used for tethering gene therapeutics to stent struts do not allow for strict control of release rate of the vectors. Numerous reports [74, 75] have documented that suppressed neointimal growth can recur if the inhibiting modality is withdrawn early, thus advocating for sustained release of gene vector over a 2–4 week vulnerability period. However, in the majority of published studies employing passive immobilization of gene vector in a stent coating, up to 90% of vector payload is typically released within 12–24 h [73, 76]. Furthermore, bulk immobilization of viral and nonviral vectors in polymer coatings engineered on the surface of stents is associated with a polymer-triggered inflammatory reaction [29].

Our prior research [77] investigated a concept of surface tethering of adenoviral (Ad) vectors to BMS using surface modification of steel with polyallylamine bisphosphonate (PAB; Fig. 14.6a), which is capable of forming strong coordination bonds with Fe, Ni, and Cr atoms on the steel surface. Primary amine groups of PAB were further utilized to derivatize the stent surface with Ad-binding affinity

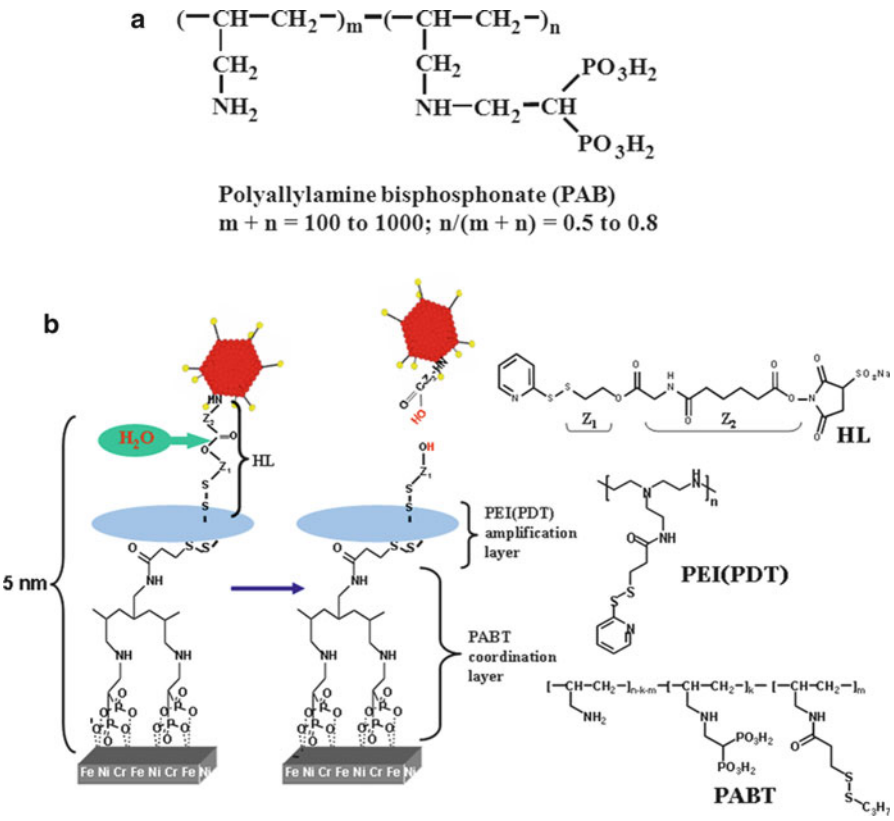


**Fig. 14.6** (**a**) Chemical structure of polyallylamine bisphosphonate (PAB). (**b**) Replication defective adenoviruses (Ad) were modified by reacting lysine residues of capsid proteins with a bifunctional amine/thiol reactive hydrolyzable crosslinker (HL) possessing a hydrolyzable ester bond separating fragments Z1 and Z2. Stainless steel meshes or stents were consecutively exposed to a solution of polyallylamine bisphosphonate comprising latent thiol groups (PABT) and a reducing agent, TCEP, to activate thiol groups on the surface. To expand the amount of available thiol functions, a subsequent treatment with polyethyleneamine modified with pyridyldithio groups, PEI(PDT), and dithiothrietol was used. Finally, HL-modified Ad vectors reacted with thiolated metal surfaces, leading to covalent tethering of Ad. Subsequent release of covalently immobilized Ad is dependent on hydrolysis of the ester bond in the HL backbone. Reproduced from [78]

molecules, enabling high affinity binding of Ad vectors to stents. Two virus binding moieties investigated in these studies were the high affinity monoclonal antibody (clone E 980407) to the knob protein of serotype 5 human adenovirus, and the D1 domain of Coxsackie-Adenovirus Receptor, an Ad-binding domain of the naturally occurring Ad receptor on the surface of epithelial and mesenchymal cells.

Using affinity immobilization of Ad vectors to model meshes and stents we demonstrated site specific transgene expression in SMC in vitro and in the rat carotid model of stent angioplasty, respectively. The intensity of transgene expression

measured with two reporter systems (GFP and luciferase) was approximately tenfold higher for D1-tethering compared with antiknob antibody tethering, which correlated well with reported higher affinity of the antibody–Ad interaction (kD = $10^{-9}$ M) compared to the D1–virus interaction (kD = $10^{-8}$ M). Moreover, D1-mediated tethering of adenoviruses encoding inducible form of nitric oxide synthase (Ad-iNOS) on stents significantly decreased neointimal formation compared to BMS 2 weeks after deployment in rats [77]. It is noteworthy that the total thickness of the PAB molecular monolayer did not exceed 5 nm and was shown not to aggravate stent-triggered inflammation in comparison with BMS.

The main disadvantages of the protein affinity-binding immobilization technology are difficulties in scaling up the process and poor control over vector release kinetics. Although we demonstrated the presence of vector at the interface between the struts and arterial wall 24 h postdeployment and reporter (GFP) activity in all three arterial layers 7 days poststenting, the duration of vector binding to the stent in vivo may be far from optimal. It is problematic to prolong vector linkage to struts with the affinity binding technique, since the vector association with stents is determined by the D1/knob or anti-knob antibody/knob affinity, local pH, and protein content of blood and tissue fluid, i.e., by factors that cannot be changed deliberately. Furthermore, protein affinity binding technology cannot be immediately adapted to other viral and especially nonviral vectors, since it implies availability of a vector binding molecule with Kd in the range $10^{-8}$–$10^{-9}$ M. Moreover, vector binding strategies based on protein affinity interactions are difficult to adapt to manufacturing scale primarily because of protein stability and species specificity.

Driven by the limitations of affinity immobilization, we have recently developed a new methodology for the reversible binding of recombinant replication-defective adenoviruses to metal surfaces [78] (Fig. 14.6b). This method is based on hydrolyzable crosslinker (HC) molecules that directly append vectors to poly (allylamine bisphosphonate) activated steel. Subsequent release of the vectors is governed by the kinetics of crosslinker hydrolysis and can be modulated by using crosslinkers with varying hydrolysis rates. A new conjugation strategy necessitated a change of PAB chemical design with the introduction of latent thiol groups in the side chains of polymer molecule. This novel compound, PABT (T indicating a thiol-reactive group), was successfully synthesized and characterized [78].

The covalent linkage between virus and HC is achieved due to the interaction of the *N*-hydroxysuccinimidyl group at one end of linear HC molecule with lysine amines of viral capsid. The pyridyldithio (PDT) group at the opposite end of HC is then utilized to link the virus/multi-HC conjugate to thiols introduced onto the surface of steel after deprotection of latent thiol groups of PABT. This linking strategy by itself was sufficient to achieve significant binding of Ad particles to the surface of model steel samples. However, we chose to expand the amount of available thiol group on the metal surface introducing an additional amplification step, exposing the thiol-activated metal samples to aqueous solution of pyridyldithio-engrafted polyethyleneimine, PEI(PDT) followed by reduction of

PDT back to thiols with dithiothreitol. We demonstrated that the "amplification" protocol resulted in 4.5 fold higher Ad immobilization, compared with the basic "no amplification" protocol [78].

Release rate of Ad from the model steel surface was studied by fluorescence microscopy using fluorophore-labeled virus particles immobilized via crosslinker tethering. After a burst release of 30% viral load in the first 5 days, the release curve approximated a zero order fit resulting in 80% Ad released over the 30 day course of the experiment. Importantly, moderate modification of Ad capsid with HC (up to $1{:}2 \times 10^4$ reagents molar ratio) had no adverse effects on Ad infectivity towards SMC. Transduction experiments with covalent attachment of Ad vectors through the cleavable linker demonstrated robust site specific reporter expression in vitro and in vivo. Moreover, a significant antirestenotic effect of Ad-iNOS immobilized on the stent surface via HC tethering in comparison with BMS was demonstrated in the rat carotid models [78].

### *14.6.3 Nanoparticle Based Controlled Drug Release Strategies for Cardiovascular Disease*

A major paradigm shift in the treatment of cardiovascular disease is expected to emerge from the development of new concepts in drug, gene and cell therapies. These experimental therapies combining biomedical nanotechnology and pharmaceutics have the potential to radically change the way these diseases are treated today by creating novel, safe and effective approaches based on the use of particles smaller than 1 μm (namely, nanoparticles) that have unique properties as controlled delivery vehicles [79]. As drug delivery carriers, nanoparticles (NP) can offer several important advantages: (1) therapeutic agents associated with NP can potentially be concentrated at the disease site, preventing their distribution to healthy tissues (targeting); (2) the incorporated drug can be released at a rate that is adjusted to the pathological course of a disease (controlled release); and (3) after releasing the drug the particles will be gradually broken down into nontoxic small molecules that can be excreted (i.e. biodegradability).

While biomedical nanotechnology has shown promise to redefine the modern concepts of disease therapy, there are a number of significant challenges that need to be addressed before research discoveries can be translated into clinic. The most obvious ones are related to safety. Our knowledge of how NP, whether derived and modified from natural sources, or artificial, interact with the human body, and how their parameters should be tuned to achieve optimal biocompatibility is still lacking. Thus, in addition to basic safety prerequisites applying to all injectable drug formulations, such as the submicron size range that is essential to prevent blockage of small blood vessels in the body, a set of specific requirements accounting for the unique nature of pharmaceutical nanocarriers is currently being defined through extensive preclinical research. Identification of

the potential causes of toxicity associated with nanoparticulate formulations is critical for developing fully biocompatible and nontoxic NP as drug/gene delivery vehicles.

The desire to develop drugs with minimal adverse effects and high efficacy has led scientists to seek a "magic bullet," a highly selective pharmacotherapy that acts directly on its target while minimally affecting healthy tissues. This "ideal drug" concept was originally proposed and developed by Paul Ehrlich, a recipient of the Nobel Prize for Physiology or Medicine in 1908 [80]. Considerable efforts are now being invested in developing new and safer drug molecules. However, the therapeutic window, defined as the dose range where a pharmacological effect can be achieved without significant adverse reactions, remains extremely narrow or even nonexistent for a large number of clinically used and experimental agents due to their limited specificity and the resultant off-target effects on healthy cells and tissues. Poor selectivity of drug effect can potentially be addressed using drug targeting strategies. However, despite the long history of drug targeting research, only recently have the first targeted therapeutics been introduced into clinical use. Standards of pharmacological selectivity adopted by the drug development industry are constantly increasing, which is the main driving force behind an intensive ongoing search for novel targeting principles as the basis for original, clinically useful methods.

Targeted delivery of drugs formulated in biodegradable NP has the potential to make therapeutically adequate local drug concentrations achievable at significantly reduced doses, thus preventing systemic exposure to toxic drug levels and improving safety of treatment. An important factor determining the success of a treatment strategy is the ability to provide sustained presence of therapeutic agent at the site of disease at a therapeutically adequate amount. As an example, drug release from DES may occur too rapidly in noncoronary vasculature, which may be the main cause of the suboptimal performance of DES in peripheral artery disease [81]. Thus, there is an unmet need for drug delivery systems whose drug release rate can be adjusted for a specific therapeutic application. In this respect the use of NP formulations with controlled release properties and capacity for targeting may offer important advantages.

#### 14.6.3.1 Nanoparticulate Delivery Systems for Restenosis Treatment

Nanoparticulate systems possess a unique combination of pharmaceutical and logistic characteristics making them a promising platform for local delivery of conventional drugs and molecular therapeutics in the context of restenosis. Incorporation of active pharmacological moieties into a NP carrier serves several purposes: (1) it increases local drug concentration in the tissues, into which NP are partitioned, thus allowing reduced total administered dose and achieving better control of drug-related adverse effects; (2) due to sustained release characteristics, incorporation into NP extends the presence of drug in the tissue and prolongs their pharmacological activity; (3) administration of extremely hydrophobic molecules

that cannot be given as free drug because of the low solubility in plasma is possible in the NP form; (4) protection of nonreleased drug from enzymatic and nonenzymatic disintegration is achieved; (5) NP incorporation facilitates the passive and active targeting to specific tissues; and (6) inclusion into NP accelerates uptake of pharmaceuticals into cells.

## Types of NP Systems Used for the Prevention of Restenosis

A broad definition of NP includes all varieties of monolith- and reservoir-type submicron carriers, including polymer-based and nonpolymeric (e.g., liposomes) systems. In the context of the present review, nonmodified viruses are not considered NP.

Several types of polymers have been studied in conjunction with NP-based drug and gene delivery for prevention and treatment of restenosis. Owing to their biodegradability, polylactide (PLA) [82, 83] and polylactide-*co*-glycolide (PLGA) [84, 85], including polyvinyl alcohol-grafted PLGA [86] and polyethylene glycol-grafted PLGA [87], have been investigated more systematically than other polymers. These versatile polyesters lend themselves to several NP formulation techniques such as emulsification–evaporation, solvent displacement, salting out, and emulsification–diffusion [83], allowing high yield incorporation of hydrophobic drugs. Moreover, formulation variables can be adjusted to impart partial control over NP size and drug release rate [83].

Release of the drug loaded in NP is governed predominantly by diffusion rather than breakdown of the polymer, since the degradation of PLA and PLGA is typically insignificant in the time frame over which drug release takes place. Release rate of a drug depends primarily on the partition coefficient of the drug between the leaching media and polymeric matrix and on NP size, smaller size being associated with faster release. For the majority of reported PLA- and PLGA-based NP formulations nearly complete drug release is observed over a 0.5–2 day period if sink conditions are properly modeled.

PEG-modified poly-(epsilon-caprolactone)- [88] and albumin [89] based matrix type NP (both loaded with paclitaxel) have also been investigated as antirestenotic treatments. In these cases PEG surface modification was used to confer delayed processing by the reticulo-endothelial system. Recently, NP consisting of three dimensional crosslinked polymeric networks obtained by free radical polymerization of poly(*N*-isopropylacrylamide), PEG-maleic anhydride, and vinyl pyrrolidone have been used to locally deliver rapamycin to balloon-injured rat arteries [90].

Several groups have pursued development of liposome based nonpolymeric NP carriers for local vascular application in restenosis prevention studies, e.g. lipid/PEG-stabilized perfluorocarbon emulsions with rapamycin incorporated into a surfactant layer [91] and HSPC/cholesterol vesicles loaded with prednisone [92]. It is currently not clear whether lipid based NP systems provide any advantages compared to polymer-based entities for local treatment of restenosis.

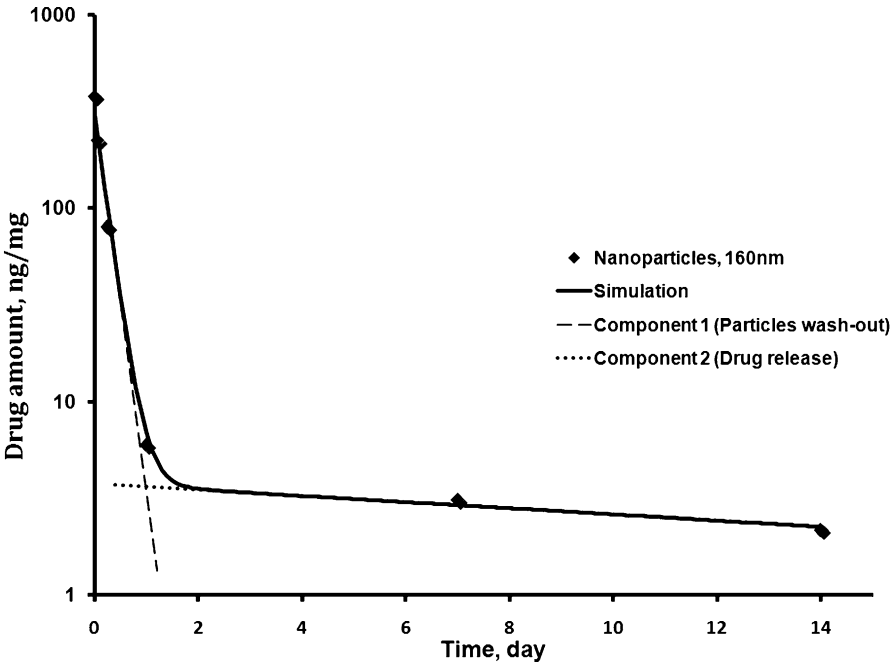


**Fig. 14.7** Focal arterial levels (logarithmic scale) of a tyrphostin drug, AG-1295 delivered from PLA nanoparticles (160 nm, 530 μg/ml, 1.5% w/w drug in polymer) as function of time after delivery (*solid line*). Also shown is a biexponential fit reflecting the decrease of arterial drug concentration over time as a sum of two first order kinetic processes with fast (*dashed line*) and slow (*dotted line*) kinetics. Reproduced from [93]

### Elimination Kinetics of Drugs Delivered with NP Systems

Tissue damage associated with balloon angioplasty and stenting creates multiple tears and crevices in arterial media [93, 94]. Upon local delivery of NP to stented arteries, these spaces become accumulation hubs for NP, which can reside for prolonged periods of time shielded from the shear forces of flowing blood. Less protected NP, dwelling in more accessible sites, are rapidly lost during the first minutes of recirculation [93]. Therefore, two separate processes are responsible for the decrease of drug concentration in the arterial wall after local vascular delivery, namely loss of the particles into circulation and release of drug from those NP that remain associated with the artery (Fig. 14.7). After being released from the polymer matrix, some drugs degrade rapidly and thus cannot be detected by standard analytic methods such as HPLC. The processes of NP elimination and drug release from the carrier may have dissimilar kinetics and thus in some instances can be differentiated by careful analysis of the drug elimination curve [93]. After completion of the particle washout phase, drug elimination from the arteries approximates the kinetics of drug release from NP, provided $t_{1/2}$ of the released drug is short relative to the time required for its release [93].

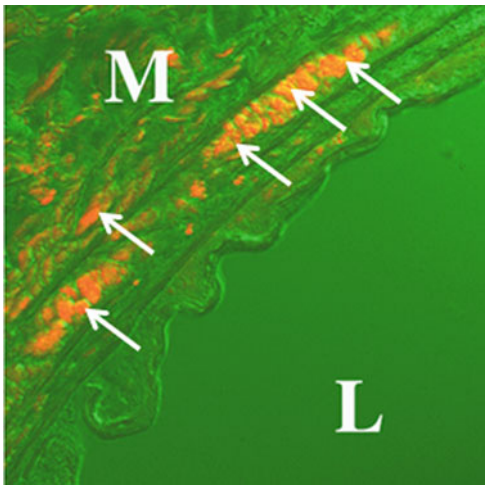


**Fig. 14.8** Nanoparticle penetration of the arterial wall as shown by a fluorescence photomicrograph of rat carotid artery locally treated by Nile Red-loaded fluorescent nanoparticles (500 μg/ml, 1.5% w/w drug in polymer, 160 nm). Arteries were harvested 6 h following 15 min intralumenal delivery. Discrete granular fluorescent foci of particle aggregates (*arrows*) are clearly distinguished in the medial layer. L and M denote lumen and media, respectively. Original magnification is 200×. Adapted from [93]

## NP for Targeted Delivery to Blood Vessels

Effective targeting of NP formulation to stented vascular tissue is of great importance, as it allows for achieving therapeutic efficacy with lower drug doses, which in its turn can reduce off target side effects. Four distinct targeting paradigms amenable to vascular tissue targeting of NP systems have been described in the literature. The first mechanism exploits localized structural alterations in arterial tissue introduced by vascular intervention per se. Limited injury of arterial wall can facilitate localized vascular uptake of NP formulation upon both systemic and local administration. Focal delivery of fluorescently labeled NP to balloon injured, but not normal healthy arteries has consistently been shown to result in NP accumulation in medial and adventitial compartments (Fig. 14.8). According to Uwatoku et al. [95], local vascular trauma induces a temporary state of enhanced permeability and retention (EPR) effect, which facilitates ingress of NP into deeper layers of the vessel wall. In accordance with their hypothesis, these authors have shown marked antirestenotic effects of intravenously injected doxorubicin incorporated into a polymer micelle carrier system, but not of an equivalent dose of free doxorubicin in the single and the double injury rat carotid model [95].

The second and the third targeting schemes capitalize on the enhancement of affinity between NP surface and vascular substrate. The difference between them is in the degree of specificity of these NP-anchoring interactions. Many studies have investigated nonspecific targeting of NP to the arterial wall after balloon or stent

injury by exploiting electrostatic interaction between positively charged NP and negatively charged extracellular matrix exposed due to the vascular trauma. This is the second targeting approach. For example, 7–10 fold higher arterial drug levels were observed in balloon-injured dog and porcine arteries using PLGA particles modified with the cationic compound didodecyldimethylammonium bromide, compared with nonmodified NP [96]. Additionally, use of polymeric surfactants with tissue adhesive properties, e.g., carbopol [97] was demonstrated to increase NP residence in vascular tissue due to the physical entanglement of tissue glycoproteins with NP polymer chains, forming multiple hydrogen bonds and anchoring the NP in situ.

The third approach involves more specific targeting. For example, NP surface has been decorated with RGD peptide motifs for integrin tethering, or short peptide sequences identified by phage biopanning against ECM [98] or balloon injured arteries [99]. Other studies have investigated arterial targeting properties of the sequences derived from apoB100 apolipoprotein [100] that previously have been shown to mediate affinity of low-density lipoproteins to vascular tissue [101]. Furthermore, covalent derivatization of the surface of liposomes with antibodies to tissue factor was demonstrated to increase liposome association with injured porcine carotid arteries [102].

Finally, physical force-driven concentration of NP or cells in the region of interest, exemplified by magnetic targeting approaches, represents the fourth vascular targeting paradigm, which will be dealt in detail in Sect. 14.6.4.

### Routes of Administration

Typically, NP-based antirestenotic therapies are administered as local or regional instillations of NP suspension into the stented or otherwise injured arterial segments. This approach requires catheterization of a culprit artery, rendering the concept less attractive (albeit not prohibitive) to clinically oriented researchers. An important alternative to the local NP delivery paradigm is the use of systemically administered nanoformulations of clodronate and related bisphosphonates, either as liposomes [103] or solid polymeric NP [104]. As with any sterically unprotected nanoparticulate matter in the 200–400 nm size range, these particles are rapidly cleared from the circulation by the reticuloendothelial system, mainly through phagocytosis by specialized macrophages in spleen (red pulp sinusoidal cells) and liver (Kupffer cells) causing apoptotic death of these cells. Monocytes in the blood are also effectively depleted by this treatment [104]. Since postinjury infiltration of vascular tissue by monocyte derived macrophages is one of the central themes in the multifaceted pathogenesis of restenosis [105], depletion of macrophages significantly decreases the severity of arterial narrowing after balloon injury and stenting in rodents and rabbits [103]. Interestingly, local arterial delivery of the same liposomal formulation that ameliorates restenosis upon systemic administration demonstrates only marginal antirestenotic effectiveness [103].

It is of importance that the pharmacologically distinct antirestenotic activity of bisphosphonate containing liposomes [102], which act through systemic

macrophage depletion, in comparison with the NP formulations of locally active cytotoxic drugs (e.g., paclitaxel), would appear, at least in experimental settings, to eliminate the requirements for significantly protracted release of antirestenotic agents. Indeed, after uptake by monocytes/macrophages, which takes place within minutes of systemic injection, fast release of the incorporated clodronate may be even advantageous. This circumstance provides a valid example of a principle that NP system design should be governed by the anticipated pharmacological activity of the nanoparticulate drug.

Additionally, systemic administration of NP formulations with local pharmacological activity is also feasible for long circulating NP that exhibit exceptionally effective targeting properties for injured arterial tissue, as exemplified by a recent publication describing preferential accumulation of "nanoburrs" in angioplastied rat arteries [98]. In addition to the PEG surface shell bestowing long circulating properties, these nanodevices are modified by some PEG molecules conjugated with a targeting peptide sequence, KLWVLPK. This peptide sequence was identified by phage display against collagen IV, the main constituent of arterial basement membrane.

#### 14.6.3.2 NP-Based Systems for Gene Delivery

Since cationic polymers and cationic lipids condense DNA molecules into distinct particles satisfying the size requirements of nanosystems, lipoplexes, polyplexes, and more complex tricomponent systems such as lipopolyplexes fall into the category of nonviral gene delivery NP vectors. Lipoplex [106] and polyplex [107] type nonviral gene delivery systems were among the earliest gene delivery vehicles examined for vascular gene therapy. Owing to their proven safety record, they remain actively investigated in both experimental [108] and clinical settings [38].

Monolithic PLGA NP have also been demonstrated to be suitable for incorporation of DNA molecules for gene therapy application [109]. The main problems with inclusion of DNA into solid polymeric NP are the hydrophilic properties of DNA molecules, necessitating the development of special techniques such as the double emulsion method for adequate incorporation into NP, and the use of organic solvents and vigorous mixing of organic and aqueous phases that can permanently denature DNA in the process of NP formation. However, these obstacles have been partially resolved as evidenced by the plethora of studies reporting effective gene transfer in vitro and in vivo [110, 111] with PLGA-based NP systems. Another approach was applied by Chorny et al. for magnetically enhanced DNA delivery capitalizing on DNA complexation with PLA-based magnetic NP modified in situ by polyethyleneimine surface deposition using an oleate ion pairing strategy [112].

The effectiveness of viral vector mediated gene transfer can also be improved by NP complexation. One recent example [113] is surface derivatization of PLA-based NP with CAR-D1, a recombinant protein that is the adenovirus binding domain of the Coxsackie-Adenovirus receptor, using photochemical anchoring of thiol-reactive polymer into the PLA matrix with subsequent covalent attachment of an end-thiolated

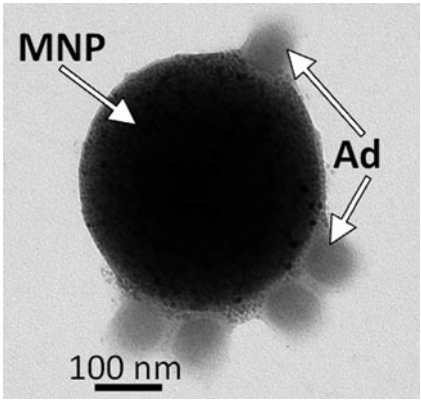


**Fig. 14.9** Transmission electron micrograph of a magnetic nanoparticle–adenovirus affinity complex. Reproduced from [22]

form of CAR-D1. This platform has enabled high-affinity binding of adenoviral vectors to the surface of activated NP, resulting in the formation of characteristic rosettes as evidenced by transmission electron microscopy studies (Fig. 14.9).

Vector uptake inhibition experiments employing an excess of free knob protein to compete with the Ad binding to CAR-D1 receptors on the cell surface have demonstrated that Ad–NP complexes utilize a distinct mechanism of cell entry that does not involve engagement of CAR receptors. This finding correlates with significantly increased transduction of cell types exhibiting low level CAR expression by Ad/NP complexes in comparison with unmodified Ad vectors. This affinity complexation approach was further shown to be effective for creating Ad complexes with magnetically responsive NP [114], enabling magnetically guided gene delivery, as discussed below.

### *14.6.4 Magnetic Stent Targeting with Nanoparticles as an Example of an Advanced Controlled-Release Strategy*

Magnetically targeted delivery offers several important advantages in the context of antirestenotic therapy. The underlying mechanism of magnetic targeting makes it an active targeting strategy [115], as it enables externally controlled guidance of a therapeutic agent to the site of disease in contrast to targeting approaches that do not actively influence the local or systemic distribution of a drug carrier, but rather attempt to control its therapeutic or adverse effects by either improving its binding and retention at the site of disease, or by engineering such agents to exhibit pharmacological activity only in their target organs and not elsewhere.

The idea of using magnetic force for targeted therapy is not new and is seemingly straightforward. In its simplest form, which can be termed as a "one source" approach: (1) a drug or gene vector is bound to a magnetically responsive nanoparticle (MNP); (2) a suspension of such MNP is injected in the bloodstream; and (3) a strong magnet is used to concentrate the drug-loaded MNP at the site of disease.

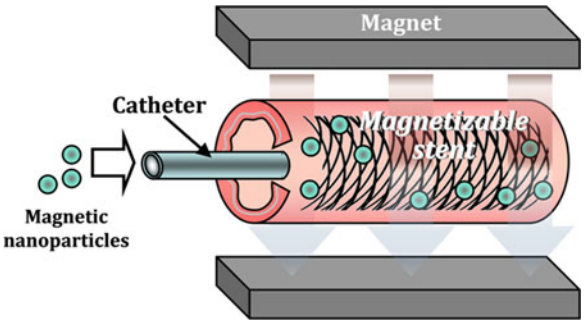


**Fig. 14.10** Targeted local delivery of MNP to a magnetizable stainless steel stent in the presence of a uniform field generated by paired electromagnets. The field induces high gradients on the stent and magnetizes drug-loaded MNP, thus creating a magnetic force driving MNPs to the stent struts and adjacent arterial tissue. Reproduced from [22]

Importantly, both strong magnetic fields and MNP in the form of nanocrystalline iron oxides have a long history of clinical use in magnetic resonance imaging, and their safety and biocompatibility are well established [116].

Why has magnetic targeting remained unrealized despite the intensive efforts by many research groups worldwide? The answer is in the limitations of the currently used magnetic guidance systems and the challenge in developing MNP that are both biocompatible and adequate for magnetically controlled delivery. Straightforward magnetic guidance by an externally applied strong magnet is not suitable for concentrating magnetic carrier nanoparticles deep inside the body, since the physics of magnetic interactions precludes focusing the magnetic force at a distance from the magnet [117]. This is the main reason why this approach, which has been shown to be successful in small animal models (typically mice), where the penetration depth of an externally applied magnetic field is of the same order as the animal body dimensions, is difficult to translate into clinical settings. Implantation of a permanent magnetic device for the purpose of attracting MNP to the target site, while feasible, may not be useful in practice, since its presence poses a safety concern, and therefore, its surgical removal is required. Thus, potentially viable applications of this strategy in humans are limited to sites localized close to the body surface [118]; however, it is not readily applicable for targeting nonsuperficially localized blood vessels.

A conceptually different principle of magnetic targeting ("two source" strategy) was first described theoretically and then realized experimentally in several studies [22, 119, 120] discussed below in more detail. This novel approach is unique in taking advantage of a vessel stent made of a magnetically susceptible material, such as 304 grade stainless steel, as a platform for site-specific delivery of MNP, as shown in Fig. 14.10. As opposed to the traditional "one source" approach (externally applied strong magnet), this "two source" strategy makes use of a powerful and deep penetrating uniform magnetic field created by the first field source, such as a clinically used MRI scanner or catheter guidance magnetic navigation system, as a switch controlling the magnetic interaction between the stent and MNP.

Because of its uniformity, this magnetic field alone is not sufficient for exerting a magnetic force on MNP. However, when the field is applied, the stent deployed in a target blood vessel becomes magnetized (acting as a "second source"), breaking the uniformity of the magnetic field in its vicinity. This locally generated field nonuniformity, usually referred to as a field gradient, is essential for generating the magnetic force, and results in an attraction of MNP strongly magnetized by the first magnetic field source to the stent and surrounding tissue [22].

Importantly, such a stent can potentially be safely used in human subjects, as it is not a permanent magnet. The lack of adverse phenomena upon exposure to a static uniform field has been demonstrated with analogous stents in human patients [121]. This novel "two source" magnetic targeting approach based on uniform field-induced magnetization is, thus, best implemented therapeutically in combination with stent angioplasty and is directly applicable in the context of ISR treatment.

#### 14.6.4.1 Magnetic Nanoparticles as Targeted Drug/Gene Carriers: Formulation and Properties

In order to be efficient, the magnetic targeting strategy should employ MNP properly designed for magnetically guided delivery of their cargo. MNP used for magnetic resonance imaging, while safe, are too small to be sufficiently responsive to the magnetic force. Therefore, MNP intended for magnetically targeted delivery should be redesigned to provide stronger magnetic responsiveness. Their design should address several basic requirements. First, MNP should not be permanently magnetic or retain magnetization after exposure to a magnetic field [122] to avoid their irreversible association into aggregates that can form emboli. In other words, they should be highly magnetizable in the absence of magnetic remanence (i.e. superparamagnetic). Second, the composition of the particles should allow for their complete elimination from the body when their "task" is completed. Third, such particles should bind their cargo efficiently, yet reversibly, allowing for its release at the target site. Fourth, the size of MNP should be readily controlled within a suitable range to provide optimal efficiency and avoid toxicity.

MNP formulation by polymer precipitation methods [123] using biodegradable polyesters, such as PLA (Fig. 14.5a), PLGA (Fig. 14.5b), or polycaprolactone (PCL; Fig. 14.5f), is a suitable approach where the biodegradable polymer "glues" together a large numbers of nanocrystallites of iron oxide, a magnetic material with proven safety that is clinically used as a contrast agent [116]. Thus, incorporation of multiple small-sized nanocrystals whose individual magnetic responsiveness is too low to allow guidance by the magnetic force results in a strongly magnetizable particle with size compatible with injection into the bloodstream. Importantly, due to their composite design, the property of superparamagnetism is retained in particles with a size sufficiently large for exhibiting magnetic responsiveness adequate for targeted delivery applications.

To form MNP using the polymer precipitation approach, nanocrystalline iron oxide is first suspended in an organic solvent or a mixture of solvents with the help of a suitable surface active agent, typically oleic acid. Solvents are chosen based on

their ability to provide a good medium for dispersion of iron oxide, and the capacity to dissolve the particle forming polymer and a drug compound [22]. The organic phase containing the particle forming components is then emulsified in an aqueous phase, and a suspension of solid MNP is obtained upon solvent removal. Importantly, use of a mixture of water miscible and immiscible solvents, such as tetrahydrofuran and chloroform, incorporated in the organic phase at predetermined ratios, enables size control of the resultant MNP, an essential determinant of their safety and utility for magnetic stent targeting. Control is achieved by varying the amount of chemical energy released upon the redistribution of the water miscible solvent into the external medium promoting the generation of smaller sized MNP [124]. Practically, it was shown that increasing tetrahydrofuran volume fraction in the organic phase from 0 to 75% can reduce the MNP size about twofold (185 $\pm$ 3 nm vs. 375 $\pm$ 10 nm) [112]. Thus, MNP can be formed using polymer precipitation methodology, with a controllable size and a composite structure well suited for magnetic targeting, and their properties can be optimized by adjusting relevant formulation variables.

#### 14.6.4.2 Paclitaxel Loaded Magnetic Nanoparticles as a Model of Formulation for Stent-Targeted Delivery of a Small Molecule Therapeutic Agent

Rationale

In a recent study, polymer precipitation methodology has been applied to formulate MNP loaded with paclitaxel (PTX) as a model small molecule pharmaceutical with established antirestenotic efficacy [22].

From the pharmaceutical viewpoint, formulation of PTX in controlled delivery systems poses several considerable challenges. It is sparingly soluble in water (~1 mg/L [125]), yet it rapidly undergoes degradation and inactivation when exposed to an aqueous environment. Its mode of action is highly nonspecific, as it affects division and function of cells in healthy tissues. These issues can be addressed by the use of MNP due to their high loading capacity for PTX, ability to protect it from degradation and resultant loss of functionality, and ability to achieve a local therapeutic effect with a minimal systemic exposure via magnetically driven stent-targeted delivery. This strategy can be seen as a potential adjunct or alternative approach to drug delivery using polymer coated drug eluting stents.

In Vitro Characterization

PTX-loaded MNP were first characterized in vitro with respect to their size and morphology, magnetic properties, drug loading and release kinetics [22]. Electron microscopic analysis showed that MNP were near-spherical in shape with a large amount of small sized iron oxide crystallites embedded in the polymeric matrix (Fig. 14.11a). Their size, measured by Photon Correlation Spectroscopy, was

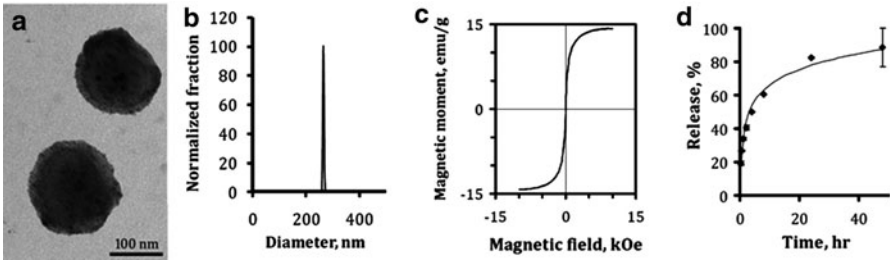


**Fig. 14.11** Physical characterization of MNP. MNP morphology and structure were examined by transmission electron microscopy (**a**). MNP size distribution was measured by Photon Correlation Spectroscopy (**b**). Magnetometer results demonstrate no remanent magnetization, a finding that is consistent with superparamagnetic behavior of MNP (**c**). PTX release kinetics was determined under sink conditions using a modified external sink method (**d**). Released drug was assayed spectrophotometrically ($\lambda = 230$ nm) in periodically replaced acceptor medium (1:1 mixture of *n*-heptane and 1-octanol) immiscible with an MNP aqueous suspension. Reproduced from [22]

shown to be uniform with an average diameter of 263 nm, in good correlation with the results of electron microscopy (Fig. 14.11b). As expected based on their previously discussed composite design, MNP exhibited a strong magnetic responsiveness with absence of retained magnetization (Fig. 14.11c).

Release of PTX from MNP measured under sink conditions [126] was biphasic with a rapid initial phase (60% of the drug released after 8 h) followed by a more sustained release over 40 h (Fig. 14.11d). The kinetics on this time scale are in accordance with diffusion driven release of a small molecule compound incorporated in a solid, monolithic submicron particle [127].

The therapeutically relevant effect of PTX-impregnated MNP was next examined in cultured rat aortic smooth muscle cells with or without exposure to a high-gradient magnetic field, in comparison to free drug and blank MNP prepared without PTX. Near-complete cell growth inhibition was observed over a wide dose range of PTX-loaded MNP applied in the presence of a high gradient field, in contrast to a significantly weaker effect of the free drug or PTX-loaded MNP without field exposure. No antiproliferative effect was observed with the blank MNP control treatment.

To investigate the underlying mechanism of the magnetically enhanced growth inhibitory effect of MNP-associated PTX, MNP were prepared with the inclusion of a green fluorescent-labeled polylactide and a red fluorescent PTX derivative admixed to PTX prior to the emulsification step. Cells were treated with this dual-labeled MNP formulation with or without magnetic exposure and later examined by fluorescence microscopy. Under magnetic conditions, cell uptake of both MNP and their cargo was significantly enhanced, suggesting that the increase in the intracellular levels of PTX delivered by magnetically guided MNP was responsible for its more efficient antiproliferative effect on smooth muscle cells in culture.

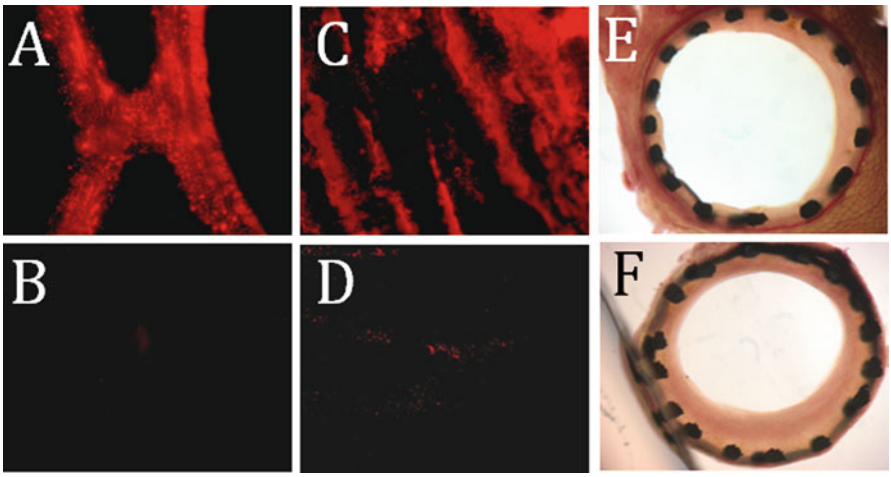


**Fig. 14.12** In vivo targeting of MNP to stented arteries in the rat carotid stenting model using the two-source magnetic targeting strategy. Fluorescent-labeled MNP were delivered to arterial segments with or without the presence of a uniform field (1,200 G) after the deployment of 304-grade stainless steel stents. Stents and arteries harvested from animals treated under magnetic vs. nonmagnetic conditions (**a** vs. **b** and **c** vs. **d**, respectively) were examined by fluorescence microscopy 2 h postdelivery. The antirestenotic effect of PTX loaded MNP magnetically targeted to stented carotid arteries determined 14 days post surgery in comparison with "no treatment" control animals (**e** vs. **f**). Reproduced from [22]

### In Vivo Distribution and Antirestenotic Efficiency

Fluorescently labeled MNP were used in a comparative study of particle distribution and elimination after uniform field controlled targeting to stented rat carotid arteries [22]. Stented animals treated with MNP without exposure to the uniform field were included as controls. Localization of MNP to stented arterial segments was observed by fluorescence microscopy (Fig. 14.12a–d) and determined by measuring fluorescent labeled PLA extracted from harvested tissue samples. Localization was increased fourfold by uniform field induced magnetization in comparison to nonmagnetic conditions, and local levels of MNP remained 5.5–9.5 fold higher over 5 days in the stented arteries of magnetically treated animals vs. controls. A reduction in the respective amounts of MNP associated with the stented region was observed over time in the both animal groups. However, the increased local levels of MNP maintained in the magnetically treated animals vs. controls translated into a significantly stronger antirestenotic effect of MNP-bound PTX (Fig. 14.12c vs. Fig. 14.12d). Notably, the total dose of PTX that effectively reduced ISR when applied as part of the magnetically targeted delivery approach was considerably lower than the reported systemic toxicity threshold [128].

#### 14.6.4.3 MNP for Magnetically Targeted Adenoviral Gene Delivery

Adenovirus is one of the most widely investigated vectors for gene therapeutic applications including cardiovascular therapy due to its efficient nuclear entry, high transgene capacity, ability to deliver genes in both quiescent and dividing cells, and lack of integration into the host cell genome [129]. The rationale for using targeted delivery strategies to improve the performance of Ad in cardiovascular disease therapy is provided by the relatively low permissivity of vascular cells toward Ad and the resultant high and potentially toxic doses of the vector required for exerting a local therapeutic effect.

In one study, the polymer precipitation approach was modified to enable formulation of superparamagnetic MNP further used for preparing stable, magnetically responsive affinity complexes with Ad [114] (Fig. 14.9). Importantly, this approach, in which the gene vector is complexed to the surface of preformed MNP, preserves the integrity and functionality of the vector and allows for using the same MNP formulation for making magnetically responsive complexes with different Ad. Association between MNP with Ad was mediated by an adaptor molecule, a D1 domain of the Coxsackie adenovirus receptor (CAR), covalently attached to the MNP surface (see above). The high binding affinity of the vector and D1-coated MNP was essential for magnetically enhanced cell interaction and a shift observed in the Ad uptake mechanism to a pathway whose efficiency far exceeded that used by Ad alone. As a result of the switch to the different processing mechanism, levels of adenoviral gene transfer in cultured vascular cells were greatly increased. The key role of the magnetically responsive complexes in increasing the transgene expression in comparison to free vector was further confirmed by statistical data analysis [114].

#### 14.6.4.4 Magnetically Guided Delivery of Therapeutic Proteins Formulated in Nonpolymeric MNP

Targeted delivery of biologically active proteins holds great promise in cardiovascular disease therapy. In the context of restenosis treatment, antioxidant enzymes such as catalase and superoxide dismutase are of interest, considering the major contribution of reactive oxygen species to the pathophysiology of the disease [130]. A considerable challenge that has to be addressed to make antioxidant enzyme therapy clinically viable is related to the physical and functional instability of these redox modulating proteins in a biological environment. Enzyme encapsulation in biodegradable nanoparticles has been explored as a means for protecting the proteins from inactivation [131]. However, the harsh conditions employed in creating nanoparticles may be a concern [132]. Formulation methodology and carrier design should be modified to enable protein encapsulation under mild conditions with a minimal loss of protein functionality. Importantly, the encapsulated protein should be protected from proteolysis, yet it should remain accessible to its substrate.

Formulation of antioxidant enzymes in MNP has been accomplished using a novel method, controlled aggregation/precipitation precipitation, in which nonpolymeric particles are formed by inducing precipitation of an oleate stabilized aqueous suspension of nanocrystalline oxide with calcium chloride in the presence of the cargo protein and a surface-active agent, Pluronic F-127 [132]. Notably, while the particle matrix-forming compound, calcium oleate, is lipophilic, it is obtained in situ by combining water soluble oleate and calcium salts without using organic solvents that could potentially affect the activity of the cargo molecule.

The protective effect of catalase encapsulation in these nonpolymeric MNP was shown in vitro in comparison to free protein by measuring catalytic activity after exposure to proteolytic enzymes. MNP-encapsulated catalase retained its ability to decompose hydrogen peroxide to a significant extent, while free enzyme was rapidly inactivated by proteolysis. Catalase-loaded MNP applied to endothelial cells in the presence of a high gradient magnetic field efficiently prevented reactive oxygen species-mediated cell death, while only minimal protective effect was observed under nonmagnetic conditions or with blank MNP. This magnetically enhanced protective effect was consistent with increased cell uptake of MNP-associated catalase applied to cells with magnetic exposure.

#### 14.6.4.5 Magnetically Guided Cell Delivery for Restenosis Therapy

The importance of restoring the protective endothelial cell layer in preventing injury triggered vessel renarrowing and thrombosis has provided the rationale for exploring the utility of magnetic guidance for targeting endothelial cells to stented arteries. MNP used for magnetic cell loading should be strongly magnetizable and biodegradable, and their internalization by endothelial cells should be achieved reasonably rapidly without adversely affecting cell viability. Importantly, such MNP can also be formulated with gene delivery vectors as described above and potentially be used to concomitantly deliver a therapeutically relevant gene to enhance the effect of the cell therapy. Cell culture experiments carried out with model MNP prepared using the polymer precipitation strategy have demonstrated efficient, magnetically controllable MNP uptake, imparting a strong magnetic responsiveness to endothelial cells [119]. Further in vitro proof of concept experiments modeling uniform field mediated magnetic cell targeting to stents under flow conditions have shown rapid capture and retention of viable endothelial cells on the struts of a magnetizable stainless steel stent. In vivo feasibility was shown in the rat carotid stenting model providing evidence of efficient cell localization to the injured vessel achievable by using the two-source magnetic targeting approach as opposed to nonmagnetic conditions. This was the first study integrating the uniform field-controlled magnetic delivery strategy in a targeted cell therapy of vascular disease, and its antirestenotic potential needs to be further explored in combination with MNP-mediated gene transfer. If proven effective, the combined magnetically guided gene/cell therapy can provide a novel and safe means of preventing ISR in human patients.

## 14.7 Conclusions

Controlled release systems for local delivery to treat cardiovascular disease have been shown to be highly effective in two important clinically used device configurations, the steroid eluting pacemaker electrode for preventing fibrosis at the endomyocardial contact, and the DES, locally releasing antiproliferative agents to prevent arterial reobstruction poststent deployment. Progress in this field will be strongly driven by investigations into novel therapeutic payloads, biodegradable polymers, and biomedical nanotechnology.

**Acknowledgments** The authors thank Susan Kerns, the Children's Hospital of Philadelphia, for her assistance in reviewing the manuscript and preparing materials for submission. The research at the Children's Hospital of Philadelphia reported in this chapter was supported in part by a grant from the National Institutes of Health (HL72108), Scientist Development Grants from the American Heart Association, a QED-Grant from the University Science Center of Philadelphia, and The William J. Rashkind Endowment of The Children's Hospital of Philadelphia.

## References

1. Ellenbogen KA, Wood MA, Gilligan DM, Zmijewski M, Mans D (1999) Steroid eluting high impedance pacing leads decrease short and long-term current drain: results from a multicenter clinical trial. CapSure Z investigators. Pacing Clin Electrophysiol 22:39–48
2. Daemen J, Serruys PW (2007) Drug-eluting stent update 2007: part I. A survey of current and future generation drug-eluting stents: meaningful advances or more of the same? Circulation 116:316–328
3. Daemen J, Wenaweser P, Tsuchida K, Abrecht L, Vaina S, Morger C, Kukreja N, Juni P, Sianos G, Hellige G, van Domburg RT, Hess OM, Boersma E, Meier B, Windecker S, Serruys PW (2007) Early and late coronary stent thrombosis of sirolimus-eluting and paclitaxel-eluting stents in routine clinical practice: data from a large two-institutional cohort study. Lancet 369:667–678
4. Garg S, Serruys PW (2010) Coronary stents: looking forward. J Am Coll Cardiol 56:S43–S78
5. Garg S, Serruys PW (2010) Coronary stents: current status. J Am Coll Cardiol 56:S1–S42
6. Sousa JE, Serruys PW, Costa MA (2003) New frontiers in cardiology: drug-eluting stents: Part I. Circulation 107:2274–2279
7. Balakrishnan B, Dooley JF, Kopia G, Edelman ER (2007) Intravascular drug release kinetics dictate arterial drug deposition, retention, and distribution. J Control Release 123:100–108
8. Ranade SV, Miller KM, Richard RE, Chan AK, Allen MJ, Helmus MN (2004) Physical characterization of controlled release of paclitaxel from the TAXUS Express2 drug-eluting stent. J Biomed Mater Res A 71:625–634
9. Acharya G, Park K (2006) Mechanisms of controlled drug release from drug-eluting stents. Adv Drug Deliv Rev 58:387–401
10. Yang C, Burt HM (2006) Drug-eluting stents: factors governing local pharmacokinetics. Adv Drug Deliv Rev 58:402–411
11. McGinty S, McKee S, Wadsworth RM, McCormick C (2011) Modelling drug-eluting stents. Math Med Biol 28(1):1–29
12. Pontrelli G, de Monte P (2009) Modeling of mass dynamics in arterial drug-eluting stents. J Porous Media 12:19–28

13. Balakrishnan B, Dooley J, Kopia G, Edelman ER, Dooley JF, Tzafriri AR, Seifert P, Groothuis A, Rogers C (2008) Thrombus causes fluctuations in arterial drug delivery from intravascular stents. J Control Release 131:173–180
14. Balakrishnan B, Tzafriri AR, Seifert P, Groothuis A, Rogers C, Edelman ER (2005) Strut position, blood flow, and drug deposition: implications for single and overlapping drug-eluting stents. Circulation 111:2958–2965
15. O'Connell BM, McGloughlin TM, Walsh MT (2010) Factors that affect mass transport from drug eluting stents into the artery wall. Biomed Eng Online 9:15
16. Hwang CW, Wu D, Edelman ER (2003) Impact of transport and drug properties on the local pharmacology of drug-eluting stents. Int J Cardiovasc Intervent 5(1):7–12
17. Hwang CW, Wu D, Edelman ER (2001) Physiological transport forces govern drug distribution for stent-based delivery. Circulation 104(5):600–605
18. Hwang CW, Levin AD, Jonas M, Li PH, Edelman ER (2005) Thrombosis modulates arterial drug distribution for drug-eluting stents. Circulation 111:1619–1626
19. Tzafriri AR, Vukmirovic N, Kolachalama VB, Astafieva I, Edelman ER (2010) Lesion complexity determines arterial drug distribution after local drug delivery. J Control Release 142:332–338
20. Wessely R (2010) New drug-eluting stent concepts. Nat Rev Cardiol 7:194–203
21. Pache J, Kastrati A, Mehilli J, Schuhlen H, Dotzer F, Hausleiter J, Fleckenstein M, Neumann FJ, Sattelberger U, Schmitt C, Muller M, Dirschinger J, Schomig A (2003) Intracoronary stenting and angiographic results: strut thickness effect on restenosis outcome (ISAR-STEREO-2) trial. J Am Coll Cardiol 41:1283–1288
22. Chorny M, Fishbein I, Yellen BB, Alferiev IS, Bakay M, Ganta S, Adamo R, Amiji M, Friedman G, Levy RJ (2010) Targeting stents with local delivery of paclitaxel-loaded magnetic nanoparticles using uniform fields. Proc Natl Acad Sci USA 107:8346–8351
23. Ormiston JA, Abizaid A, Spertus J, Fajadet J, Mauri L, Schofer J, Verheye S, Dens J, Thuesen L, Dubois C, Hoffmann R, Wijns W, Fitzgerald PJ, Popma JJ, Macours N, Cebrian A, Stoll HP, Rogers C, Spaulding C (2010) Six-month results of the NEVO RES-ELUTION I (NEVO RES-I) Trial: a randomized, multicenter comparison of the NEVO Sirolimus-eluting coronary stent with the TAXUS Liberte Paclitaxel-eluting stent in de novo native coronary artery lesions. Circ Cardiovasc Interv 3:556–564
24. Granada JF, Inami S, Aboodi MS, Tellez A, Milewski K, Wallace-Bradley D, Parker S, Rowland S, Nakazawa G, Vorpahl M, Kolodgie FD, Kaluza GL, Leon MB, Virmani R (2010) Development of a novel prohealing stent designed to deliver sirolimus from a biodegradable abluminal matrix. Circ Cardiovasc Interv 3:257–266
25. Tamai H, Igaki K, Kyo E, Kosuga K, Kawashima A, Matsui S, Komori H, Tsuji T, Motohara S, Uehata H (2000) Initial and 6-month results of biodegradable poly-l-lactic acid coronary stents in humans. Circulation 102:399–404
26. Perlstein I, Connolly JM, Cui X, Song C, Li Q, Jones PL, Lu Z, DeFelice S, Klugherz B, Wilensky R, Levy RJ (2003) DNA delivery from an intravascular stent with a denatured collagen-polylactic-polyglycolic acid-controlled release coating: mechanisms of enhanced transfection. Gene Ther 10:1420–1428
27. Williams DO, Abbott JD, Kip KE (2006) Outcomes of 6906 patients undergoing percutaneous coronary intervention in the era of drug-eluting stents: report of the DEScover Registry. Circulation 114:2154–2162
28. Virmani R, Farb A, Guagliumi G, Kolodgie FD (2004) Drug-eluting stents: caution and concerns for long-term outcome. Coron Artery Dis 15:313–318
29. van der Giessen WJ, Lincoff AM, Schwartz RS, van Beusekom HM, Serruys PW, Holmes DR Jr, Ellis SG, Topol EJ (1996) Marked inflammatory sequelae to implantation of biodegradable and nonbiodegradable polymers in porcine coronary arteries. Circulation 94:1690–1697
30. Appleby CE, Kingston PA (2004) Gene therapy for restenosis–what now, what next? Curr Gene Ther 4:153–182

31. Walter DH, Cejna M, Diaz-Sandoval L, Willis S, Kirkwood L, Stratford PW, Tietz AB, Kirchmair R, Silver M, Curry C, Wecker A, Yoon YS, Heidenreich R, Hanley A, Kearney M, Tio FO, Kuenzler P, Isner JM, Losordo DW (2004) Local gene transfer of phVEGF-2 plasmid by gene-eluting stents. An alternative strategy for inhibition of restenosis. Circulation 110:36–45
32. Gaffney MM, Hynes SO, Barry F, O'Brien T (2007) Cardiovascular gene therapy: current status and therapeutic potential. Br J Pharmacol 152:175–188
33. Rissanen TT, Yla-Herttuala S (2007) Current status of cardiovascular gene therapy. Mol Ther 15:1233–1247
34. Roks AJ, Henning RH, Buikema H, Pinto YM, Kraak MJ, Tio RA, de Zeeuw D, Haisma HJ, Wilschut J, van Gilst WH (2002) Recombinant Semliki Forest virus as a vector system for fast and selective in vivo gene delivery into balloon-injured rat aorta. Gene Ther 9:95–101
35. Kotani H, Nakajima T, Lai S, Morishita R, Kaneda Y (2004) The HVJ-envelope as an innovative vector system for cardiovascular disease. Curr Gene Ther 4:183–194
36. Sharif F, Daly K, Crowley J, O'Brien T (2004) Current status of catheter- and stent-based gene therapy. Cardiovasc Res 64:208–216
37. Laitinen M, Hartikainen J, Hiltunen MO, Eranen J, Kiviniemi M, Narvanen O, Makinen K, Manninen H, Syvanne M, Martin JF, Laakso M, Yla-Herttuala S (2000) Catheter-mediated vascular endothelial growth factor gene transfer to human coronary arteries after angioplasty. Hum Gene Ther 11:263–270
38. von der Leyen HE, Muegge A, Hanefeld C, Hamm CW, Rau M, Rupprecht HJ, Zeiher AM, Fichtlscherer S (2010) A prospective, single-blind, multicenter, dose escalation study of intracoronary iNOS lipoplex (CAR-MP583) gene therapy for the prevention of restenosis in patients with de novo or restenotic coronary artery lesion (REGENT I Extension). Hum Gene Ther 18:18
39. Versari D, Lerman LO, Lerman A (2007) The importance of reendothelialization after arterial injury. Curr Pharm Des 13:1811–1824
40. Flugelman MY, Virmani R, Leon MB, Bowman RL, Dichek DA (1992) Genetically engineered endothelial cells remain adherent and viable after stent deployment and exposure to flow in vitro. Circ Res 70:348–354
41. Scott NA, Candal FJ, Robinson KA, Ades EW (1995) Seeding of intracoronary stents with immortalized human microvascular endothelial cells. Am Heart J 129:860–866
42. Berinyi LK, Conte MS, Mulligan RC (1992) Repopulation of injured arteries with genetically modified endothelial cells. J Vasc Surg 15:932–934
43. Thompson MM, Budd JS, Eady SL, Hartley G, Early M, James RF, Bell PR (1994) Platelet deposition after angioplasty is abolished by restoration of the endothelial cell monolayer. J Vasc Surg 19:478–486
44. Gulati R, Jevremovic D, Peterson TE, Witt TA, Kleppe LS, Mueske CS, Lerman A, Vile RG, Simari RD (2003) Autologous culture-modified mononuclear cells confer vascular protection after arterial injury. Circulation 108:1520–1526
45. Gulati R, Jevremovic D, Witt TA, Kleppe LS, Vile RG, Lerman A, Simari RD (2004) Modulation of the vascular response to injury by autologous blood-derived outgrowth endothelial cells. Am J Physiol Heart Circ Physiol 287:H512–H517
46. Werner N, Junk S, Laufs U, Link A, Walenta K, Bohm M, Nickenig G (2003) Intravenous transfusion of endothelial progenitor cells reduces neointima formation after vascular injury. Circ Res 93:e17–e24
47. He T, Smith LA, Harrington S, Nath KA, Caplice NM, Katusic ZS (2004) Transplantation of circulating endothelial progenitor cells restores endothelial function of denuded rabbit carotid arteries. Stroke 35:2378–2384
48. Gulati R, Simari RD (2004) Autologous cell-based therapies for vascular disease. Trends Cardiovasc Med 14:262–267
49. Kipshidze N, Dangas G, Tsapenko M, Moses J, Leon MB, Kutryk M, Serruys P (2004) Role of the endothelium in modulating neointimal formation: vasculoprotective approaches to attenuate restenosis after percutaneous coronary interventions. J Am Coll Cardiol 44:733–739

50. Aoki J, Serruys PW, van Beusekom H, Ong AT, McFadden EP, Sianos G, van der Giessen WJ, Regar E, de Feyter PJ, Davis HR, Rowland S, Kutryk MJ (2005) Endothelial progenitor cell capture by stents coated with antibody against CD34: the HEALING-FIM (Healthy Endothelial Accelerated Lining Inhibits Neointimal Growth-First In Man) Registry. J Am Coll Cardiol 45:1574–1579
51. Schober A, Hoffmann R, Opree N, Knarren S, Iofina E, Hutschenreuter G, Hanrath P, Weber C (2005) Peripheral CD34+ cells and the risk of in-stent restenosis in patients with coronary heart disease. Am J Cardiol 96:1116–1122
52. Griese DP, Ehsan A, Melo LG, Kong D, Zhang L, Mann MJ, Pratt RE, Mulligan RC, Dzau VJ (2003) Isolation and transplantation of autologous circulating endothelial cells into denuded vessels and prosthetic grafts: implications for cell-based vascular therapy. Circulation 108:2710–2715
53. Kong D, Melo LG, Mangi AA, Zhang L, Lopez-Ilasaca M, Perrella MA, Liew CC, Pratt RE, Dzau VJ (2004) Enhanced inhibition of neointimal hyperplasia by genetically engineered endothelial progenitor cells. Circulation 109:1769–1775
54. Andres V (2004) Control of vascular cell proliferation and migration by cyclin-dependent kinase signalling: new perspectives and therapeutic potential. Cardiovasc Res 63:11–21
55. Charron T, Nili N, Strauss BH (2006) The cell cycle: A critical therapeutic target to prevent vascular proliferative disease. Can J Cardiol 22(Suppl B):41B–55B
56. Schober A (2008) Chemokines in vascular dysfunction and remodeling. Arterioscler Thromb Vasc Biol 28:1950–1959
57. Levitzki A (2005) PDGF receptor kinase inhibitors for the treatment of restenosis. Cardiovasc Res 65:581–586
58. Banai S, Gertz SD, Gavish L, Chorny M, Perez LS, Lazarovichi G, Ianculuvich M, Hoffmann M, Orlowski M, Golomb G, Levitzki A (2004) Tyrphostin AGL-2043 eluting stent reduces neointima formation in porcine coronary arteries. Cardiovasc Res 64:165–171
59. Banai S, Wolf Y, Golomb G, Pearle A, Waltenberger J, Fishbein I, Schneider A, Gazit A, Perez L, Huber R, Lazarovichi G, Rabinovich L, Levitzki A, Gertz SD (1998) PDGF-receptor tyrosine kinase blocker AG1295 selectively attenuates smooth muscle cell growth in vitro and reduces neointimal formation after balloon angioplasty in swine. Circulation 97:1960–1969
60. Fishbein I, Waltenberger J, Banai S, Rabinovich L, Chorny M, Levitzki A, Gazit A, Huber R, Mayr U, Gertz SD, Golomb G (2000) Local delivery of platelet-derived growth factor receptor-specific tyrphostin inhibits neointimal formation in rats. Arterioscler Thromb Vasc Biol 20:667–676
61. Golomb G, Fishbein I, Banai S, Mishaly D, Moscovitz D, Gertz SD, Gazit A, Poradosu E, Levitzki A (1996) Controlled delivery of a tyrphostin inhibits intimal hyperplasia in a rat carotid artery injury model. Atherosclerosis 125:171–182
62. Giese NA, Marijianowski MM, McCook O, Hancock A, Ramakrishnan V, Fretto LJ, Chen C, Kelly AB, Koziol JA, Wilcox JN, Hanson SR (1999) The role of alpha and beta platelet-derived growth factor receptor in the vascular response to injury in nonhuman primates. Arterioscler Thromb Vasc Biol 19:900–909
63. Stefanadis C, Toutouzas K, Stefanadi E, Lazaris A, Patsouris E, Kipshidze N (2007) Inhibition of plaque neovascularization and intimal hyperplasia by specific targeting vascular endothelial growth factor with bevacizumab-eluting stent: an experimental study. Atherosclerosis 195:269–276
64. Wolf YG, Rasmussen LM, Ruoslahti E (1994) Antibodies against transforming growth factor-beta 1 suppress intimal hyperplasia in a rat model. J Clin Invest 93:1172–1178
65. Schober A, Knarren S, Lietz M, Lin EA, Weber C (2003) Crucial role of stromal cell-derived factor-1alpha in neointima formation after vascular injury in apolipoprotein E-deficient mice. Circulation 108:2491–2497
66. Wang CH, Anderson N, Li SH, Szmitko PE, Cherng WJ, Fedak PW, Fazel S, Li RK, Yau TM, Weisel RD, Stanford WL, Verma S (2006) Stem cell factor deficiency is vasculoprotective: unraveling a new therapeutic potential of imatinib mesylate. Circ Res 99:617–625

67. Yin X, Yutani C, Ikeda Y, Enjyoji K, Ishibashi-Ueda H, Yasuda S, Tsukamoto Y, Nonogi H, Kaneda Y, Kato H (2002) Tissue factor pathway inhibitor gene delivery using HVJ-AVE liposomes markedly reduces restenosis in atherosclerotic arteries. Cardiovasc Res 56:454–463
68. Levonen AL, Vahakangas E, Koponen JK, Yla-Herttuala S (2008) Antioxidant gene therapy for cardiovascular disease: current status and future perspectives. Circulation 117:2142–2150
69. Klugherz BD, Jones PL, Cui X, Chen W, Meneveau NF, DeFelice S, Connolly J, Wilensky RL, Levy RJ (2000) Gene delivery from a DNA controlled-release stent in porcine coronary arteries. Nat Biotechnol 18:1181–1184
70. Klugherz BD, Song C, DeFelice S, Cui X, Lu Z, Connolly J, Hinson JT, Wilensky RL, Levy RJ (2002) Gene delivery to pig coronary arteries from stents carrying antibody-tethered adenovirus. Hum Gene Ther 13:443–454
71. Johnson TW, Wu YX, Herdeg C, Baumbach A, Newby AC, Karsch KR, Oberhoff M, Johnson T, Karsch KK (2005) Stent-based delivery of tissue inhibitor of metalloproteinase-3 adenovirus inhibits neointimal formation in porcine coronary arteries. Arterioscler Thromb Vasc Biol 25:754–759
72. Sharif F, Hynes SO, McMahon J, Cooney R, Conroy S, Dockery P, Duffy G, Daly K, Crowley J, Bartlett JS, O'Brien T (2006) Gene-eluting stents: comparison of adenoviral and adeno-associated viral gene delivery to the blood vessel wall in vivo. Hum Gene Ther 17:741–750
73. Takahashi A, Palmer-Opolski M, Smith RC, Walsh K (2003) Transgene delivery of plasmid DNA to smooth muscle cells and macrophages from a biostable polymer-coated stent. Gene Ther 10:1471–1478
74. Carter AJ, Aggarwal M, Kopia GA, Tio F, Tsao PS, Kolata R, Yeung AC, Llanos G, Dooley J, Falotico R (2004) Long-term effects of polymer-based, slow-release, sirolimus-eluting stents in a porcine coronary model. Cardiovasc Res 63:617–624
75. Sirois MG, Simons M, Kuter DJ, Rosenberg RD, Edelman ER (1997) Rat arterial wall retains myointimal hyperplastic potential long after arterial injury. Circulation 96:1291–1298
76. Ohtani K, Egashira K, Nakano K, Zhao G, Funakoshi K, Ihara Y, Kimura S, Tominaga R, Morishita R, Sunagawa K (2006) Stent-based local delivery of nuclear factor-kappaB decoy attenuates in-stent restenosis in hypercholesterolemic rabbits. Circulation 114:2773–2779
77. Fishbein I, Alferiev IS, Nyanguile O, Gaster R, Vohs JM, Wong GS, Felderman H, Chen IW, Choi H, Wilensky RL, Levy RJ (2006) Bisphosphonate-mediated gene vector delivery from the metal surfaces of stents. Proc Natl Acad Sci USA 103:159–164
78. Fishbein I, Alferiev I, Bakay M, Stachelek SJ, Sobolewski P, Lai M, Choi H, Chen IW, Levy RJ (2008) Local delivery of gene vectors from bare-metal stents by use of a biodegradable synthetic complex inhibits in-stent restenosis in rat carotid arteries. Circulation 117:2096–2103
79. Godin B, Sakamoto JH, Serda RE, Grattoni A, Bouamrani A, Ferrari M (2010) Emerging applications of nanomedicine for the diagnosis and treatment of cardiovascular diseases. Trends Pharmacol Sci 31:199–205
80. Strebhardt K, Ullrich A (2008) Paul Ehrlich's magic bullet concept: 100 years of progress. Nat Rev Cancer 8:473–480
81. Umashankar PR, Hari PR, Sreenivasan K (2009) Effect of blood flow on drug release from DES: an experimental study. Int J Cardiol 131:415–417
82. Chorny M, Fishbein I, Danenberg HD, Golomb G (2002) Lipophilic drug loaded nanospheres prepared by nanoprecipitation: effect of formulation variables on size, drug recovery and release kinetics. J Control Release 83:389–400
83. Chorny M, Fishbein I, Golomb G (2000) Drug delivery systems for the treatment of restenosis. Crit Rev Ther Drug Carrier Syst 17:249–284
84. Feng SS, Zeng W, Teng Lim Y, Zhao L, Yin Win K, Oakley R, Hin Teoh S, Hang Lee RC, Pan S (2007) Vitamin E TPGS-emulsified poly(lactic-co-glycolic acid) nanoparticles for cardiovascular restenosis treatment. Nanomedicine (Lond) 2:333–344

85. Klugherz BD, Meneveau N, Chen W, Wade-Whittaker F, Papandreou G, Levy R, Wilensky RL (1999) Sustained intramural retention and regional redistribution following local vascular delivery of polylactic-coglycolic acid and liposomal nanoparticulate formulations containing probucol. J Cardiovasc Pharmacol Ther 4:167–174
86. Westedt U, Kalinowski M, Wittmar M, Merdan T, Unger F, Fuchs J, Schaller S, Bakowsky U, Kissel T (2007) Poly(vinyl alcohol)-graft-poly(lactide-co-glycolide) nanoparticles for local delivery of paclitaxel for restenosis treatment. J Control Release 119:41–51
87. Zweers ML, Engbers GH, Grijpma DW, Feijen J (2006) Release of anti-restenosis drugs from poly(ethylene oxide)-poly(DL-lactic-co-glycolic acid) nanoparticles. J Control Release 114:317–324
88. Deshpande D, Devalapally H, Amiji M (2008) Enhancement in anti-proliferative effects of paclitaxel in aortic smooth muscle cells upon co-administration with ceramide using biodegradable polymeric nanoparticles. Pharm Res 25:1936–1947
89. Kolodgie FD, John M, Khurana C, Farb A, Wilson PS, Acampado E, Desai N, Soon-Shiong P, Virmani R (2002) Sustained reduction of in-stent neointimal growth with the use of a novel systemic nanoparticle paclitaxel. Circulation 106:1195–1198
90. Reddy MK, Vasir JK, Sahoo SK, Jain TK, Yallapu MM, Labhasetwar V (2008) Inhibition of apoptosis through localized delivery of rapamycin-loaded nanoparticles prevented neointimal hyperplasia and reendothelialized injured artery. Circ Cardiovasc Interv 1:209–216
91. Cyrus T, Zhang H, Allen JS, Williams TA, Hu G, Caruthers SD, Wickline SA, Lanza GM (2008) Intramural delivery of rapamycin with alphavbeta3-targeted paramagnetic nanoparticles inhibits stenosis after balloon injury. Arterioscler Thromb Vasc Biol 28:820–826
92. Joner M, Morimoto K, Kasukawa H, Steigerwald K, Merl S, Nakazawa G, John MC, Finn AV, Acampado E, Kolodgie FD, Gold HK, Virmani R (2008) Site-specific targeting of nanoparticle prednisolone reduces in-stent restenosis in a rabbit model of established atheroma. Arterioscler Thromb Vasc Biol 28:1960–1966
93. Fishbein I, Chorny M, Banai S, Levitzki A, Danenberg HD, Gao J, Chen X, Moerman E, Gati I, Goldwasser V, Golomb G (2001) Formulation and delivery mode affect disposition and activity of tyrphostin-loaded nanoparticles in the rat carotid model. Arterioscler Thromb Vasc Biol 21:1434–1439
94. Westedt U, Barbu-Tudoran L, Schaper AK, Kalinowski M, Alfke H, Kissel T (2002) Deposition of nanoparticles in the arterial vessel by porous balloon catheters: localization by confocal laser scanning microscopy and transmission electron microscopy. AAPS PharmSci 4:E41
95. Uwatoku T, Shimokawa H, Abe K, Matsumoto Y, Hattori T, Oi K, Matsuda T, Kataoka K, Takeshita A (2003) Application of nanoparticle technology for the prevention of restenosis after balloon injury in rats. Circ Res 92:e62–e69
96. Labhasetwar V, Song C, Humphrey W, Shebuski R, Levy RJ (1998) Arterial uptake of biodegradable nanoparticles: effect of surface modifications. J Pharm Sci 87:1229–1234
97. Zou W, Cao G, Xi Y, Zhang N (2009) New approach for local delivery of rapamycin by bioadhesive PLGA-carbopol nanoparticles. Drug Deliv 16:15–23
98. Chan JM, Zhang L, Tong R, Ghosh D, Gao W, Liao G, Yuet KP, Gray D, Rhee JW, Cheng J, Golomb G, Libby P, Langer R, Farokhzad OC (2010) Spatiotemporal controlled delivery of nanoparticles to injured vasculature. Proc Natl Acad Sci USA 107:2213–2218
99. Michon IN, Hauer AD, von der Thusen JH, Molenaar TJ, van Berkel TJ, Biessen EA, Kuiper J (2002) Targeting of peptides to restenotic vascular smooth muscle cells using phage display in vitro and in vivo. Biochim Biophys Acta 1591:87–97
100. Nah JW, Yu L, Han S, Ahn CH, Kim SW (2002) Artery wall binding peptide-poly(ethylene glycol)-grafted-poly(L-lysine)-based gene delivery to artery wall cells. J Control Release 78:273–284
101. Olsson U, Camejo G, Hurt-Camejo E, Elfsber K, Wiklund O, Bondjers G (1997) Possible functional interactions of apolipoprotein B-100 segment that associate with cell proteoglycans and the apoB/E receptor. Arterioscler Thromb Vasc Biol 17:149–155

102. Hamilton AJ, Huang SL, Warnick D, Rabbat M, Kane B, Nagaraj A, Klegerman M, McPherson DD (2004) Intravascular ultrasound molecular imaging of atheroma components in vivo. J Am Coll Cardiol 43:453–460
103. Danenberg HD, Fishbein I, Gao J, Monkkonen J, Reich R, Gati I, Moerman E, Golomb G, Cohen-Sela E, Rosenzweig O, Epstein H (2002) Macrophage depletion by clodronate-containing liposomes reduces neointimal formation after balloon injury in rats and rabbits. Circulation 106:599–605
104. Cohen-Sela E, Rosenzweig O, Gao J, Epstein H, Gati I, Reich R, Danenberg HD, Golomb G (2006) Alendronate-loaded nanoparticles deplete monocytes and attenuate restenosis. J Control Release 113:23–30
105. Welt FG, Rogers C (2002) Inflammation and restenosis in the stent era. Arterioscler Thromb Vasc Biol 22:1769–1776
106. Takeshita S, Gal D, Leclerc G, Pickering JG, Riessen R, Weir L, Isner JM (1994) Increased gene expression after liposome-mediated arterial gene transfer associated with intimal smooth muscle cell proliferation. In vitro and in vivo findings in a rabbit model of vascular injury. J Clin Invest 93:652–661
107. Riessen R, Rahimizadeh H, Blessing E, Takeshita S, Barry JJ, Isner JM (1993) Arterial gene transfer using pure DNA applied directly to a hydrogel-coated angioplasty balloon. Hum Gene Ther 4:749–758
108. Muhs A, Heublein B, Schletter J, Herrmann A, Rudiger M, Sturm M, Grust A, Malms J, Schrader J, Von Der Leyen HE (2003) Preclinical evaluation of inducible nitric oxide synthase lipoplex gene therapy for inhibition of stent-induced vascular neointimal lesion formation. Hum Gene Ther 14:375–383
109. Abbas AO, Donovan MD, Salem AK (2008) Formulating poly(lactide-co-glycolide) particles for plasmid DNA delivery. J Pharm Sci 97:2448–2461
110. Yang J, Zeng Y, Li Y, Song C, Zhu W, Guan H, Li X (2008) Intravascular site-specific delivery of a therapeutic antisense for the inhibition of restenosis. Eur J Pharm Sci 35:427–434
111. Cohen H, Levy RJ, Gao J, Fishbein I, Kousaev V, Sosnowski S, Slomkowski S, Golomb G (2000) Sustained delivery and expression of DNA encapsulated in polymeric nanoparticles. Gene Ther 7:1896–1905
112. Chorny M, Polyak B, Alferiev IS, Walsh K, Friedman G, Levy RJ (2007) Magnetically driven plasmid DNA delivery with biodegradable polymeric nanoparticles. FASEB J 21:2510–2519
113. Chorny M, Fishbein I, Alferiev IS, Nyanguile O, Gaster R, Levy RJ (2006) Adenoviral gene vector tethering to nanoparticle surfaces results in receptor-independent cell entry and increased transgene expression. Mol Ther 14:382–391
114. Chorny M, Fishbein I, Alferiev I, Levy RJ (2009) Magnetically responsive biodegradable nanoparticles enhance adenoviral gene transfer in cultured smooth muscle and endothelial cells. Mol Pharm 6:1380–1387
115. Alexiou C, Jurgons R, Schmid RJ, Bergemann C, Henke J, Erhardt W, Huenges E, Parak F (2003) Magnetic drug targeting–biodistribution of the magnetic carrier and the chemotherapeutic agent mitoxantrone after locoregional cancer treatment. J Drug Target 11:139–149
116. Weissleder R, Stark DD, Engelstad BL, Bacon BR, Compton CC, White DL, Jacobs P, Lewis J (1989) Superparamagnetic iron oxide: pharmacokinetics and toxicity. Am J Roentgenol 152:167–173
117. Grief AD, Richardson G (2005) Mathematical modelling of magnetically targeted drug delivery. J Magn Magn Mater 293:455–463
118. Dobson J (2006) Magnetic nanoparticles for drug delivery. Drug Dev Res 67:55–60
119. Polyak B, Fishbein I, Chorny M, Alferiev I, Williams D, Yellen B, Friedman G, Levy RJ (2008) High field gradient targeting of magnetic nanoparticle-loaded endothelial cells to the surfaces of steel stents. Proc Natl Acad Sci USA 105:698–703
120. Yellen BB, Forbes ZG, Halverson DS, Fridman G, Barbee KA, Chorny M, Levy R, Friedman G (2005) Targeted drug delivery to magnetic implants for therapeutic applications. J Magn Magn Mater 293:647–654

121. Hiramoto JS, Reilly LM, Schneider DB, Skorobogaty H, Rapp J, Chuter TA (2007) The effect of magnetic resonance imaging on stainless-steel Z-stent-based abdominal aortic prosthesis. J Vasc Surg 45:472–474
122. Gupta AK, Gupta M (2005) Synthesis and surface engineering of iron oxide nanoparticles for biomedical applications. Biomaterials 26:3995–4021
123. Allémann E, Gurny R, Leroux JC (1998) Biodegradable nanoparticles of poly(lactic acid) and poly(lactic-co-glycolic acid) for parenteral administration. In: Lieberman HA, Rieger MM, Banker GS (eds) Pharmaceutical dosage forms: disperse systems. Marcel Dekker, New York, pp 163–193
124. Quintanar-Guerrero D, Allemann E, Fessi H, Doelker E (1998) Preparation techniques and mechanisms of formation of biodegradable nanoparticles from preformed polymers. Drug Dev Ind Pharm 24:1113–1128
125. Liggins RT, Hunter WL, Burt HM (1997) Solid-state characterization of paclitaxel. J Pharm Sci 86:1458–1463
126. Chorny M, Fishbein I, Danenberg HD, Golomb G (2002) Study of the drug release mechanism from tyrphostin AG-1295-loaded nanospheres by in situ and external sink methods. J Control Release 83:401–414
127. Washington C (1990) Drug release from microdisperse systems: a critical review. Int J Pharm 58:1–12
128. Vassileva V, Grant J, De Souza R, Allen C, Piquette-Miller M (2007) Novel biocompatible intraperitoneal drug delivery system increases tolerability and therapeutic efficacy of paclitaxel in a human ovarian cancer xenograft model. Cancer Chemother Pharmacol 60:907–914
129. Williams PD, Ranjzad P, Kakar SJ, Kingston PA (2010) Development of viral vectors for use in cardiovascular gene therapy. Viruses 2:334–371
130. Misra P, Reddy PC, Shukla D, Caldito GC, Yerra L, Aw TY (2008) In-stent stenosis: potential role of increased oxidative stress and glutathione-linked detoxification mechanisms. Angiology 59:469–474
131. Simone E, Dziubla T, Shuvaev V, Muzykantov VR (2010) Synthesis and characterization of polymer nanocarriers for the targeted delivery of therapeutic enzymes. Methods Mol Biol 610:145–164
132. Chorny M, Hood E, Levy RJ, Muzykantov VR (2010) Endothelial delivery of antioxidant enzymes loaded into non-polymeric magnetic nanoparticles. J Control Release 146:144–151

# Chapter 15
# Drug Delivery Systems to Fight Cancer

**Vivekanand Bhardwaj and M.N.V. Ravi Kumar**

**Abstract** The delivery system is as important as the active substance, and it becomes all the more important when it comes to cancer chemotherapy. An ideal systemic delivery vehicle is expected to minimize systemic burden while concentrating in the tumor; however, this is far from reality. On the contrary, implantable delivery systems can deliver drug regionally, avoiding nontarget tissue distribution and minimizing the dose, but such treatments are restricted to certain anatomic sites. This chapter provides a state of the art review of current developments in this area.

## 15.1 Introduction

The application of drug delivery systems for treatment of cancers is aimed at targeting the cancer cells, thereby minimizing the systemic burden and toxicity in nontarget organs. With rising costs involved with drug discovery, novel delivery approaches offer attractive strategies not only to make the existing drugs act better, but also to enhance their commercial value. Advances in this area have been aided by the development of functional material and better understanding of the physiology of cancers. Various approaches have been tried, and many are in clinical trials, mostly due to a relenting protocol for anticancer drugs.

The preclinical success of a lot of drug candidates is not matched in the human body due to the factors affecting absorption, distribution, metabolism, and excretion; on the contrary, the reliability of animal models cannot be ignored. The use of drug delivery systems addresses one or more of the following questions related to the drug [1]:

V. Bhardwaj • M.N.V.R. Kumar (✉)
Strathclyde Institute of Pharmacy and Biomedical Science
University of Strathclyde, Glasgow, UK
e-mail: mnvrkumar@strath.ac.uk

J. Siepmann et al. (eds.), *Fundamentals and Applications of Controlled Release Drug Delivery*, Advances in Delivery Science and Technology,
DOI 10.1007/978-1-4614-0881-9_15, © Controlled Release Society 2012

1. Physicochemical or physiological instability
2. Poor aqueous solubility or permeability
3. Insufficient drug concentration in target tissue
4. High volume of distribution
5. Nontarget organ toxicity
6. Rapid clearance from the body

Diverse formulation strategies can be employed to tackle these challenges, depending on the design of the delivery system, chemical properties of the carrier, and altered conditions in cancerous tissue. Simple strategies such as derivatization and prodrugs have been used cleverly to reduce toxicity (e.g. epirubicin), alter pharmacokinetic profile (e.g. by PEGylation), and prevent degradation before reaching target organs. The physiology of solid tumors is different from the normal tissues in four major ways: angiogenesis, leaky vasculature, poor lymphatic drainage, and microenvironment in the interior regions. All these have been explored for targeting anticancer drugs to the tumors [2].

The larger size of pores in the tumor vasculature and reduced lymphatic drainage allows polymers, large compounds, and particulate carriers to accumulate, thereby providing an opportunity to concentrate the drug in the target locales. Maeda and coworkers have reviewed the role of the enhanced permeation and retention (EPR) effect in tumors [3, 4]. Drug delivery systems for the therapeutic use of cytotoxic chemotherapies are an essential aspect of successful treatment and remain under active evaluation [5]. The following sections discuss the development and application of drug delivery systems in treatment of cancers.

## 15.2 Submicron Carriers

The advent of new functional materials and the patentability of new technologies are fuelling research in drug delivery. Advances in techniques for formulation design, characterization, and tracking have resulted in a new class of products that have taken drug delivery beyond just control of absorption. One stark feature of such products is their size being less than a micrometer. Drug delivery systems based on submicron particulates have attracted most attention in cancer treatment in recent years due to their ability to incorporate and deliver different kinds of molecules, relatively simple manufacture, and a wide range of carrier materials to choose from. They can protect a drug in the core, can increase concentration of the drug in tumor, and can be modified to achieve favorable pharmacokinetics to allow their use in chemotherapy [6].

Mechanistic studies are explaining how the formulations transport and deliver their payload. These can be classified on the basis of the nature of material or specific arrangements thereof used for introducing functionality into the carrier. Examples include size modified drugs, biodegradable and nonbiodegradable polymers, lipids, and proteins. They can take specific shapes such as nanoparticles, micelles, and vesicles. The drug may be covalently bound, entrapped in the core, or

physically adsorbed on the surface of a particle. Additional properties may be imparted to modulate hydrophilicity (e.g. PEG), receptor interaction (vitamins and proteins), or identification (e.g. antibodies).

### *15.2.1 Nanoparticulates*

Advances in protein engineering and materials science have contributed to novel nanoscale targeting approaches. Some therapeutic nanocarriers have been approved for clinical use. However, to date, there are only a few clinically approved nanocarriers that incorporate molecules to selectively bind and target cancer cells. Some of the nanotechnology based approved formulations have been discussed in recent reviews [7, 8]. Select clinical studies have been reviewed that are likely to affect clinical investigations and their implications for advancing treatment of patients with cancer [9, 10].

Achieving drug delivery by the aid of nanotechnology is not new [11, 12], but the last few years have seen an overwhelming research thrust in this area [13–16]. Small particles have been shown to be taken up through and across biomembranes by unique mechanisms, though the debate is still on, to be more precise on the underlying principles, which can address one or more of the bioavailability problems [17, 18]. The particles are believed to be delivered to the circulatory system through the lymphatics, with absorption more pronounced and rapid for smaller particles.

The performance of nanotechnology-based drug delivery systems is influenced mostly by size [19, 20] and surface properties (charge and hydrophilicity), shape and flexibility [21]. Nanoparticles have been designed to improve the biodistribution of cancer drugs, by fine-tuning their size and surface characteristics to increase their circulation time in the bloodstream, and thereby the chance of better accumulation in the tumors [10].

### *15.2.2 Liposomes*

Liposomes or vesicles are microscopic phospholipid structures with a bilayered membrane arrangement. Their development, and recent advances in clinical applications or investigations have been extensively reviewed [22] (see also Chaps. 11 and 12).

Liposomal formulations, though covered under the definition of nanoparticulate formulations, have certain properties and have been successful to a degree that warrants them to be studied as an independent class. Drummond and coworkers [23] have extensively reviewed the use of liposomes in the treatment of solid tumors. These systems offer advantages such as that they can change the pharmacologic and pharmacodynamic properties of an active drug in preclinical screens to meet the therapeutic need. For example, unstable or insoluble agents can be formulated in a manner to allow effective exposure in the tumor [24].

## 15.3 Delivery Enabled Products

### *15.3.1 Micronized Drug Crystals*

According to the Noyes–Whitney equation, the rate of dissolution of a compound is directly proportional to the surface area presented to the dissolution media. Thus, increasing surface area by reducing particle size is expected to increase the bioavailability of water insoluble drugs. These drugs can be suspended in a micronized form in a liquid vehicle and either injected or administered orally. The particles slowly dissolve in the body providing sustained drug levels.

Panzem® is an orally active compound that has antiproliferative, antiangiogenic, and anti-inflammatory properties, and the company's focus has been on cancer and rheumatoid arthritis. In contrast to conventional chemotherapeutics, Panzem® targets rapidly growing cells with relative high specificity and while sparing the nondividing cells. It also acts as a potent inhibitor of angiogenesis by restricting the development of the blood vessels that transport life sustaining nutrients to tumors. Panzem® NCD (Nano-Crystal Dispersion) is a nanocrystalline formulation of 2-methoxyestradiol (2-ME2) based on Elan Drug Technology's nanocrystal platform. It involves reducing the size of crystals of water-insoluble drugs to less than 2 μm by various means such as wet milling, homogenization, supercritical fluids, or precipitation. The nanocrystalline drug is then stabilized in an aqueous medium by surface adsorption of biologically safe excipients. The liquid suspension of Panzem® NCD was found to have superior bioavailability to that of Panzem® capsules in a phase I trial. Entremed Inc. recently completed phase II clinical trials for this product alone or in combination for various kinds of cancer (http://clinicaltrials.gov). 2-ME2 was designated as orphan drug by FDA in 2001.

Developed and tested as ABI-007, Abraxane® is composed of 20–400 nm (US patent 6096331) albumin-bound paclitaxel (Fig. 15.1). It is prepared using high pressure homogenization of paclitaxel in presence of human serum albumin and helps in increasing the maximum tolerable dose (MTD) to 300 mg/m$^2$ from 200 to 250 mg/m$^2$ for conventional Taxol [25]. Micronization of paclitaxel can be carried out using sonication, nanoprecipitation, spray drying, and ball milling

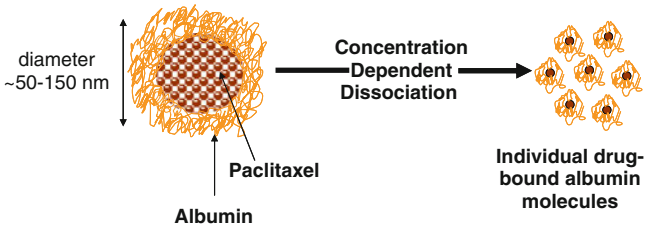


**Fig. 15.1** Concept of nanoparticle albumin-bound (nab) paclitaxel, where albumin functions as a surface active polymer providing charge and steric stabilization to paclitaxel nanoparticles to prevent aggregation. Stabilization is by weak interactive forces, thereby both substances freely dissociate after reconstitution as shown and the drug is in amorphous state

(US patents 5439686, 5498421). It is the first product in the market based on Abraxis Bioscience's nanoparticles-albumin bound (nab™) technology. The nab™ technology is a subset of a broader Protosphere™ platform based on using proteins to make nanoparticles for delivery of water insoluble drugs. The reasons behind the choice of carrier material are based on three pathways in which tumor cells feed their high growth rate. First, albumin is the most abundant protein in the body and is used by body to transport nutrients, which are utilized at a higher than normal rate by the rapidly multiplying cancer cells. Second, tumors employ the gp60 pathway by which nutrients are preferentially transported across the endothelial barrier when attached to albumin [26, 27]. Third, tumors secrete a specialized protein called Secreted Protein Acidic and Rich in Cysteine (SPARC) into their interstitium that specifically binds albumin-bound nutrients and concentrates them within the tumor's interstitium. In clinical trials, it has shown greater efficacy and reduced toxicity compared to standard paclitaxel [28]. Other advantages over Taxol are that less saline is required for infusion of this formulation, premedication for prevention of immune reactions is not required, and there is no danger of leaching of harmful chemicals from the plastic infusion sets.

### *15.3.2 Polymer Based Systems*

Easy manipulation of physicochemical properties by altering chemical groups and size has allowed polymers to develop as the most potent carriers. Additionally, drugs or other functional chemicals can be tagged, labeled, and linked to attain a desired role in therapeutics [29]. Biodegradable and biocompatible polymers can be fabricated into various dosage forms of desired shape and size.

#### 15.3.2.1 Implants

Polymeric drug delivery systems are often either surgically placed or injected in the body as implants. The objective is either to provide a regional or sustained delivery of the drug. Regional delivery serves to reduce the body burden of the drug and limits nontarget organ toxicity. It helps in targeting the drug and reducing the dose. The majority of the formulations target to maintain castration equivalent hormone levels in prostate cancer patients. The incorporated luteinizing hormone releasing hormone (LHRH) agonists are used for palliative treatment. Since these drugs are very potent and the therapy is long lasting, it is impractical to devise daily dose formulations. Implants that provide a sustained extended release have been devised based on both biodegradable and nonbiodegradable polymers. Many formulations are based on microspheres that provide bulk as well as surface erosion from the matrices. Approved implants for delivery of anticancer drugs are summarized in Table 15.1.

**Table 15.1** List of polymeric implants of anticancer drugs

| Drug | Product | Developer | Polymer | Shape and size | Indication | Release duration |
|---|---|---|---|---|---|---|
| Abarelix | Plenaxis | Praecis Pharmaceuticals Inc., Speciality European Pharma | Carboxymethylcellulose | Powder for injection | Prostate cancer | 4 weeks |
| Buserelin | Profact depot | Sanofi Aventis | PLGA | Rod-shaped implant | Prostate cancer | Over 2–3 months |
| Carmustine | Gliadel | MGI Pharma | Polifeprosan 20 or poly (carboxyphenoxypropane/ sebacic acid) anhydride | Wafer | Glioma multiformis | 2–3 weeks |
| Goserelin acetate | Zoladex for depot | Zeneca Pharmaceuticals | PLGA | 1.5 mm diameter cylindrical rod | Prostate cancer | 1 or 3 month |
| Histrelin acetate | Vantas, Supprelin LA | Valera | 2-hydroxyethyl methacrylate, 2-hydroxypropyl methacrylate, trimethylolpropane trimethacrylate | Nonbiodegradable, 3 cm × 3.5 mm cylindrically shaped hydrogel reservoir | Prostate cancer | 12 months |
| Leuprolide | Eligard | Sanofi/Tolmar Inc. | PLGA, *N*-methyl-2-pyrrolidone | Liquid for depot injection | Prostate cancer | 1,3,4,6 months |
| Leuprolide acetate | Lupron depot | TAP pharmaceuticals | PLA or PLGA | Microspheres | Prostate cancer | 1, 3 and 4 months |
| Leuprolide acetate | Viadur | Alza; discontinued due to commercial reasons | Polyurethane rate-controlling membrane, elastomeric piston, and a polyethylene diffusion moderator | 4 × 45 mm implant | Prostate cancer | 12 months |
| Leuprorelin acetate | Leuplin, Enantone | Takeda | PLGA | Microspheres | Prostate cancer, premenopausal breast cancer | |

| | | | | | | |
|---|---|---|---|---|---|---|
| Leuprorelin acetate | Trenantone | Takeda | PLA | Microspheres | Prostate cancer, premenopausal breast cancer | |
| Triptorelin | Decapeptyl | Ferring | PLGA | Microspheres | Prostate cancer | |
| Triptorelin | Decapeptyl SR or Gonapeptyl depot | Ipsen | PLGA | Microspheres | Prostate cancer | From 4 weeks to 3 months. |
| Triptorelin | Trelstar Depot | Pfizer | PLGA | | Prostate cancer | 1 month |

**Table 15.2** Comparison of different strengths of Eligard depot injection

| Dosage | 7.5 mg | 22.5 mg | 30 mg | 45 mg |
|---|---|---|---|---|
| Release duration (months) | 1 | 3 | 4 | 6 |
| Composition | Copolymer containing carboxyl endgroups | Copolymer with hexanediol | Copolymer with hexanediol | Copolymer with hexanediol |
| Lactide:glycolide ratio | 50:50 | 75:25 | 75:25 | 85:15 |
| NMP to polymer ratio | 1.94 | 1.22 | 1.22 | 1.00 |

Eligard® is administered subcutaneously, where it forms a solid drug depot. It uses Atrigel®, which is a platform delivery system consisting of a biodegradable poly(DL-lactide-*co*-glycolide) polymer formulation dissolved in *N*-methyl-2-pyrrolidone (NMP). After injection, the biocompatible solvent diffuses away leaving behind the solid depot. It is available in different strengths that last from 1 to 6 months (Table 15.2). The release rates are controlled by the copolymer composition of the PLGA. As the glycolide content decreases, the release rate is diminished due to the higher hydrophobicity of the lactide moiety, which slows down degradation of the polymer. Similarly, decreasing the ratio of NMP to polymer also delays the release of the drug.

Viadur® was a sustained release delivery system for leuprolide acetate based on Alza's Duros® platform. The system consists of an osmotic tablet placed inside a 4 mm by 45 mm titanium alloy reservoir that consists of a polyurethane rate-controlling membrane, an elastomeric piston, and a polyethylene diffusion moderator. The osmotic tablets are composed of sodium chloride, sodium carboxymethyl cellulose, and povidone. Wetting of the tablet exerts osmotic pressure that forces the drug out of the device through the membrane at a predetermined controlled rate. This system reduced testosterone to castrate levels for 12 months. The marketing of this formulation was stopped in 2008 due to commercial reason.

Gliadel® wafer is a flat disk approximately 1.45 cm in diameter and 1 mm thick made of polifeprosan 20, a copolymer of carboxypropane and sebacic acid containing carmustine that is implanted in the brain following surgery. The usual number of implants is up to eight (61.6 mg of carmustine), and the implant is given only once; however, the number of disks varies depending on tumor size. These implants release the entrapped carmustine in a sustained fashion over 2–3 weeks and the implants will slowly dissolve away, not requiring surgical removal after the release. This intervention formulation is effective in prolonging survival following surgeries [30].

Lupron® depot yields a sustained release of the hormone analog leuprolide for up to 4 months and provides palliative care in prostate cancer. Lupron® depot is a sterile formulation of lyophilized microspheres made of polylactic acid containing leuprolide acetate. It is available in a prefilled dual chamber syringe; the front

chamber contains leuprolide acetate, polylactic acid, and D-mannitol and the second chamber contains diluent, carboxymethylcellulose sodium, D-mannitol, polysorbate 80, water for injection, and glacial acetic acid for pH control.

Zoladex® for depot injection is an implantable 1.5 mm diameter cylindrical rod that is injected subcutaneously with a 14 gauge needle for palliative treatment of prostate cancer. Triptorelin is an LHRH agonist used in the treatment of prostate cancer. It is available as either Decapeptyl® SR or Gonapeptyl® depot and provides drug release from 4 weeks to 3 months. The PLGA based, rod shaped implantable formulation of buserelin that is an analog of LHRH provides sustained release over 2–3 months.

#### 15.3.2.2 Micelles

Micelles are spherical structures formed due to the assembly of bipolar molecules. They attain thermodynamic stability by minimizing surface energy. Since physiological fluids are aqueous, micelles for drug delivery are almost invariably considered in aqueous media wherein hydrophobic groups of the amphiphilic molecules arrange themselves to have a hydrophobic core and hydrophilic exterior. The hydrophobic core allows entrapment of poorly water soluble drugs, giving a system in which the drug is considered to have been solubilized. Besides all the advantages provided as a virtue of their submicron size, the primary objective of micelles is drug solubilization and thus can aid in oral delivery of drugs [31]. Micelles for drug delivery have been extensively reviewed [32–35].

Tween 80 (polyoxyethylene sorbitan mono oleate) is used for solubilizing etoposide (*Etopophos*®, *Toposar*®, *VePesid*®) along with polyethylene glycol (PEG) 300. It is also used in the marketed formulation of docetaxel (Taxotere®), and the investigational RPR 109881A. Cremophor® EL (polyethoxylated castor oil) is used in DHA–paclitaxel and BMS-184476. The latter is an analog of paclitaxel with better solubility, uses 80% less cremophor® EL, and requires no premedication. An interesting feature of these solubilizers such as Tween® 80, cremophor® EL, and TPGS is that they have been shown to inhibit the P-glycoprotein (Pgp) efflux pump.

Paclitaxel is a high molecular weight plant product that is practically insoluble in water. To solve the problem of its solubility, Bristol Myers Squibb developed Taxol®, which is a micellar formulation of paclitaxel prepared by dissolving it in 50:50 mixture of cremophor EL and ethanol. It is diluted in intravenous fluids to be administered as either 3 or 24 h infusions. It was the first commercial formulation of paclitaxel, allowing the use of this potent natural compound for cancer treatment. The excipient cremophor EL has since been implicated in toxicities, especially hypersensitivity reactions requiring premedication, triggering research to come up with formulations free of this solubilizer [36]. Genexol-PM® is a micellar formulation of paclitaxel developed by Samyang Genex Corp (South Korea) using methoxy-poly(ethylene glycol)-poly(lactide) [mPEG-PLA]. These micelles,

consisting of a hydrophobic core and a hydrophilic surface, entrap paclitaxel in the center and are dispersed in an aqueous environment. The micelles are self-forming, acquiring size ranges of 5–200 nm and are thermodynamically stable due to a low critical micellar concentration.

Nanoxel® is another paclitaxel formulation in which the drug is delivered as micelles using a polymeric carrier. It is approved in India for marketing by Dabur and is in phase I clinical trials in the USA in a study sponsored by Fresenius Kabi Oncology Ltd. The material used is a pH sensitive copolymer of *N*-isopropyl acrylamide (NIPAM) and vinylpyrrolidone (VP) monomers. Smooth spherical particles of 80–100 nm show up to threefold higher uptake in target cancer cells as compared to cremophor paclitaxel [37].

DACH-platin is an active metabolite of Oxaliplatin, with stronger anticancer activity. It has been incorporated in PEG-polyglutamate micelles. These micelles are derived from a platform called Medicelle™ from Nanocarrier (Japan) comprising of a hydrophilic polymer exterior and inner polyamino acid based hydrophobic core. The platform has been licensed for DACH-platin by Debiopharm and is in Phase I clinical trials. Micelles of 20–100 nm are readily formed in water from the diblock copolymers developed from the hydrophilic component PEG and a hydrophobic polyamino acid. NC-6004 Nanoplatin™ is a related formulation in early phase II trials, in which cisplatin makes a coordination complex with polyamino acids in the core of the micelles. The coordination complexes provide sustained release. The aim of this formulation is to reduce the nephrotoxicity and neurotoxicity of the parent drug.

NK-105, a paclitaxel micelle formulation of Nippon Kayaku, is in late Phase II clinical trials using the Medicelle™ platform. However, it uses polyaspartate as the polyamino acid. The drug is physically entrapped and the formulation helps in increasing the mean residence time of the paclitaxel. SN-38 (7-ethyl-10-hydroxy-camptothecin) has been bound to the carboxylic acid on a polyglutamate chain of block copolymer through the ester bond. This product called NK-012 is based on Medicelle™ platform product and is in phase I clinical trial [34]. The chemistry of the polymers plays an important role in the clinical outcome of these delivery systems, and excellent reviews are available in literature [38].

In addition to increasing solubility of drugs and imparting targeted delivery, micelles are being explored to incorporate additional functionality. For example, SP1049C is a micellar formulation of doxorubicin with Pluronic® F-127 in which an additional Pluronic® L-61 has been added to disrupt the P-glycoprotein efflux pump [39, 40]. Recently concluded phase II trials have demonstrated superior antitumor activity compared to doxorubicin in esophageal adenocarcinoma [41].

The advantages of polymeric micelle drug carrier systems [38] are

- Low toxicity
- High water solubility
- High structural stability
- Small diameter with narrow distribution (10–100 nm)
- Functionality of the two phases (interior and exterior) can be separately controlled

One of the drawbacks of the polymeric micelle systems is the immature technology for drug applications. Incorporation efficiencies are dependent on drug incorporation methods and no universal method is applicable to all polymers. Therefore, researchers have to optimize drug loading for each drug through trial and error. The other problem lies with the difficulty of synthesis of these block copolymers, which are not easy to control or scale up for industrial applications [38]. The long term stability of the product as such cannot be overlooked.

#### 15.3.2.3 Drug Conjugates

Drug conjugates can be considered as macromolecular prodrugs, as they are cleaved inside the body to release the active parent molecule. They are composed of three essential components; an anticancer drug, a polymer, and a biodegradable linker. Drugs have been covalently linked to polymers to modulate their pharmacokinetic profiles. The flexibility of chemical alteration in polymers can be exploited to impart other desirable properties such as biocompatibility, hydrophilicity for avoiding scavenging by the reticuloendothelial system (RES), controlled resistance to chemical or enzymatic degradation, proportion of drug loading, targeting to specific locations, and size of the carrier itself. When the drug is hydrophobic, these conjugates often assume a unilamellar micelle conformation of average size 5–20 nm [42]. Hydroxypropylmethacrylamide (HPMA) copolymers were the first category of polymers to be explored in this direction. The development and use of polymer-drug conjugates have been extensively reviewed [43–45] (see also Chap. 12). The important factors governing the use of polymers for drug conjugation are molecular weight and type of linker. It was established in a study performed on rats with HPMA copolymers that for nonbiodegradable polymers, the molecular weight should be less than 40,000 g/mol to prevent accumulation in the body [46].

Following the success of SMANCS, there are several polymer–drug conjugates in various stages of clinical trials now. ProLindac (AP5346, Access Pharmaceuticals) is a prodrug of 1,2-diaminocyclohexane (DACH) platinum bound to HPMA. It is a water soluble biodegradable formulation. DACH is itself a metabolite of oxaliplatin, which causes neurotoxicity due to an oxalate group. Because of the size, the conjugate is passively accumulated in tumors by the EPR effect. Phase II clinical trials have been completed.

Opaxio™ is a product of Cell Therapeutics in Phase III clinical trials comprising of a conjugate of paclitaxel with a biodegradable polymer, poly-L-glutamic acid. Also known as Xyotax, CT-2103, Paclitaxel poliglumex, and PPX, the conjugate is water soluble and thus provides a formulation free of cremophor EL. Phase I studies show pharmacokinetics to be comparable to unconjugated drug [47]. Early phase III trials revealed similar activity to existing therapies. However, the formulation exhibited significant activity in non-small cell lung cancer in female patients below 55 years of age. The pooled data from the STELLAR 3 and 4 trials hinted toward a hormone dependence of the clinical performance of the formulation. The clinical trials of Opaxio have been comprehensively reviewed [45]. The conjugate

is taken inside cells by endocytosis and cleaved by lysosomal enzymes, chiefly cathepsin B, the activity of which is dependent on estradiol concentration. The activity of the formulation is, thus, expected to be higher in premenopausal female patients.

IT-101 (Cerulean Pharma) is a conjugate of camptothecin and a linear, cyclodextrin based polymer presently undergoing phase I trials for advanced solid tumors. The delivery platform known as Cyclosert™ was licensed from Calando Pharmaceuticals and consists of β-cyclodextrin, which can form inclusion complexes with the drug [48]. The conjugated polymer assembles into nanoparticles of average size 30–40 nm. Various other products based on conjugates have entered in clinical trials and reached different degrees of success, including FCE 28068 (doxorubicin), FCE 28069 (doxorubicin with active targeting moiety galactosamine), PNU 166945 (paclitaxel), PNU 166148 (camptothecin), CT-2106, and DE-310 [45].

#### 15.3.2.4 PEGylated

PEGylation or conjugation with polyethylene glycol imparts hydrophilicity to a molecule. The RES identifies molecules primarily by their hydrophobicity and thus PEGylation provides a means to reduce chances of rejection of a drug delivery system or drug in the body. By increasing the molecular weight, EPR benefits for passive tumor targeting can be achieved. Additionally, the stability of the complex is increased against chemical and enzymatic degradation. The effect of PEG on the performance of pharmaceuticals has been reviewed [49].

SN-38 (EZN-2208) has been linked with PEG by Enzon pharmaceuticals to enhance its solubility and increase the circulation time in the body. PEG-SN-38 is in phase II trials for metastatic breast cancer and metastatic colorectal cancer. Similarly, irinotecan has been PEGylated (NKTR-102) and the product is undergoing Phase II trials for advanced ovarian and breast cancer and Phase III trials for colorectal cancer.

#### 15.3.2.5 Environmentally Sensitive

OncoGel™ is a controlled release depot formulation of paclitaxel in ReGel delivery system. ReGel® is a triblock copolymer comprised of poly(D,L lactide-*co*-glycolide) (PLGA) and polyethylene glycol (PEG) with the basic structure of PLGA–PEG–PLGA. It is a thermosensitive polymer system that exists as a solution at low temperatures, but converts to a gel at body temperature. Additionally, it can solubilize water-insoluble drugs. After gel formation, the system makes a depot at the site of injection from which the drug will then slowly leach out providing sustained delivery. The paclitaxel containing product is presently undergoing phase II clinical trials.

## 15.3.3 Lipidic Systems

### 15.3.3.1 Vesicular

Lipidic material can make multilayered sheets collapsed into a spherical architecture to yield vesicles and called liposomes (when composed of lipids), niosomes (when made of nonionic surfactants), or sphingosomes (when one of the components is sphingosine). The sheets are mostly bilayered with hydrophobic groups inside and hydrophilic surfaces outside. Thus the exterior surface as well as the interior core of the vesicles are hydrophilic. It is for this reason that they act as carriers for water soluble drugs. However, even water insoluble drugs can be encapsulated within the layers (coat). Lipidic systems in various stages of clinical development are summarized in Table 15.3 (see also Chap. 11).

Myocet® is a marketed liposomal product of doxorubicin made by Enzon Pharmaceuticals. The most significant benefit of liposomal doxorubicin is reduced cardiotoxicity of the parent drug. Moreover, it does not exhibit the incidence of hand–foot syndrome, which is often encountered with a PEGylated liposomal product. DaunoXome® is an approved lipidic vesicular formulation (Gilead Sciences Inc) that contains an aqueous solution of daunorubicin citrate in the core. The lipid bilayer is composed of distearoylphosphatidylcholine and cholesterol. The mean diameter of the liposomes is about 25–45 nm, and they contain about 5.3% of the drug w/w of total lipid. DaunoXome® is indicated as a first line cytotoxic therapy for advanced HIV-associated Kaposi's sarcoma.

NeoPharm uses proprietary lipids to prepare its liposomal products under the Neolipid® technology platform. LE-SN38 incorporates SN-38 in nanosized liposomes (<200 nm) with high drug entrapment efficiency (>95%) [50]. The product is presently undergoing phase II trials. Other products based on this platform include LE-DT® for docetaxel (Phase I in the USA) and LEP-ETU® for Paclitaxel (Phase II in India). Lipusu® (Shandong Luye Pharmaceutical Co.) is a liposomal formulation of paclitaxel indicated for chemotherapy of oophoron and metastatic carcinoma of ovary and may have combined use with cisplatin. Lipusu is indicated with for the treatment of breast cancer after administering adriamycin for standard chemotherapy or relapse. It is also indicated for chemotherapy of non-small cell lung carcinoma (NSCLC) with combination of cisplatin, as this carcinoma cannot be treated by surgery or radiotherapy. Marqibo® is a sphingosine cholesterol encapsulation product (sphingosome) of vincristine sulfate. Though its trials were discontinued in patients with multiply relapsed or refractory aggressive non-Hodgkin's lymphoma after phase II results, Marqibo is in phase II trials for relapsed acute lymphoblastic leukemia (rALLy) and metastatic malignant uveal melanoma. Maximum tolerated dose was approximately twice that of free vincristine [51].

Medigene is exploring its lipofectin-based product Endotag™-1 for pancreatic cancer in phase II cancer trials. It is a liposomal product that used cationic lipids (US patents 7112338, 7238369) consisting of *N*-[1-(2,3-Dioleoyloxy)propyl]-*N*,*N*,

**Table 15.3** Clinical status of lipid-based anticancer drug delivery systems

| Drug | Product | Company | Clinical status | Indication |
|---|---|---|---|---|
| Annamycin | Liposomal annamycin | Callisto Pharmaceuticals | Phase I/II | Refractory or relapsed acute lymphocytic leukemia |
| Cisplatin | Lipoplatin™ | Regulon, Inc | Phase II/III | Advanced breast cancer, NSCLC, squamous cell carcinoma of the head and neck |
| Cytarabine (ara-C) | DepoCyte | Mudipharma International Limited | Phase I<br>Approved | Solid tumors<br>Lymphomatous meningitis |
| Daunorubicin | DaunoXome | Diatos SA, in-licensed from Gilead Sciences, Inc | Withdrawn from the USA, relaunched in Europe | Kaposi's sarcoma, acute leukemia |
| Docetaxel | LE-DT | NeoPharm | Completed Phase I | Metastatic solid tumors |
| Doxorubicin | Myocet | Enzon Pharmaceuticals | Approved | Metastatic breast cancer in combination with another chemotherapy drug, cyclophosphamide |
| Irinotecan | PEP02 | HERMES Biosciences, Inc./Merrimack Pharmaceuticals | Phase I/Phase II | Colorectal/metastatic pancreatic cancer and gastric gastroesophageal junction |
| Irinotecan | CPT-II | University of California | Phase I | Recurrent high-grade gliomas |
| Lipotecan | Lipotecan | Taiwan Liposome Company | Phase I | Advanced solid tumors |
| Paclitaxel | Endotag | Medigene AG | Phase II | Pancreatic, breast cancer |
| Pacilitaxel | Liposomal Paclitaxel | Nanjing Sike Pharmaceutical Co., Ltd | Phase I | Solid tumors in Chinese patients |
| Paclitaxel | LEP-ETU | NeoPharm | Phase II in India | Metastatic breast cancer |
| Paclitaxel | LIPUSU | Luye Pharma | Approved | Oophoron and metastatic carcinoma of ovary, Non-small-cell lung carcinoma (NSCLC), Kaposi's sarcoma |

(continued)

**Table 15.3** (continued)

| Drug | Product | Company | Clinical status | Indication |
|---|---|---|---|---|
| SN-38 | LE-SN38 | NeoPharm | Phase II | Metastatic colorectal cancer treatment |
| Topotecan | Brakiva™ | Hana Biosciences | Enrolling patient for Phase I | Small-cell lung cancer, solid tumors and ovarian cancer |
| Vinorelbine | Alocrest™ | Hana Biosciences | Phase I | Advanced solid tumors, non-Hodgkin's lymphoma or Hodgkin's disease |
| Vinorelbine | VNB | Taiwan Liposome Company | Phase II | Colon cancer |

*N*-trimethylammonium methylsulfate (DOTAP) and derivatives of phosphatidylcholine and phosphatidylethanolamine. Paclitaxel is dissolved in the lipid bilayer from where it slowly leaches after the formulation binds to dividing endothelial cells. Owing to the differential rates of growth in normal tissue and tumors, the binding is significantly higher for vessels supplying the tumors [52]. Recent phase II data in triple receptor negative breast cancer shows that combination therapy of Endotag™-1 with paclitaxel resulted in a higher progression-free survival of 59% compared to 48% for paclitaxel alone.

#### 15.3.3.2 PEGylated

Doxil® (or Caelyx®) is a marketed liposomal formulation of doxorubicin for Ovarian Cancer, AIDS-Related Kaposi's Sarcoma and Multiple Myeloma. The liposomes are coated with PEG to evade RES scavenging. This increases their circulation time in the body and alters the toxicity profile of doxorubicin. Like other submicron delivery systems, selective accumulation is postulated due to the EPR effect. The liposomes are composed of *N*-(carbonyl-methoxypolyethylene glycol 2000)-1,2-distearoyl-sn-glycero-3-phosphoethanolamine sodium salt (MPEG-DSPE), fully hydrogenated soy phosphatidylcholine (HSPC), and cholesterol. The most significant aspect is the reduction of cardiotoxicity of the drug. Since the cumulative maximum tolerated dose of Doxil® can be significantly higher than that of free doxorubicin [53], a study of the potential of this formulation to reduce cumulative toxicity in patients is advocated [54]. However, the PEG component results in accumulation of the drug in skin and causes hand–foot syndrome in about half of the patients and may thus be inferior to non-PEGylated liposomal doxorubicin in this aspect.

#### 15.3.3.3 Drug Conjugates

Lipids are important components of cell membrane and biomolecules and are in high demand in rapidly multiplying cancerous cells. Therefore, combining lipids with anticancer drugs makes the latter accumulate in cancers. Additionally, this can address issues such as low water solubility and rapid metabolism of the drug in the body. Moreover, since lipids are absorbed through chylomicrons in the intestine, there is a possibility to develop oral dosage forms for the drugs that are presently only administered parenterally [55].

Taxoprexin® is a lipid conjugate of docosahexaenoic acid (DHA) with paclitaxel. The covalently bonded conjugate itself is nontoxic and was developed on the hypothesis of greater uptake due to high demand of DHA in cancer cells. DHA is an omega-3 fatty acid, is a component of the cell membrane and is used as a nutritional supplement. The prodrug provided a marked decrease in volume of distribution and clearance and a seven fold increase in plasma half life in phase I trial [56]. Phase II trials have shown only moderate activity in oesophagogastric cancer [57].

Ara-C is itself a prodrug that requires conversion to a triphosphate form for its activity. It is a nucleoside analog with appreciable activity against hematological tumors but limited activity in solid tumors. It is rapidly cleared from the body following iv administration. To increase residence in the body, a derivative containing elaidic acid chain has been prepared that showed activity against solid tumors also. This product, CP-4055 (Elacyt™, Clavis Pharma) exhibited significantly better activity and better tolerance than cytarabine in Phase II trials in acute myeloid leukemia [58]. While the cellular uptake of parent drug is dependent on a nucleoside transporter hENT1 (human equilibrative nucleoside transporter 1) in the cell membrane, the prodrug is internalized via an independent mechanism based on lipid transport. Clavis Pharma is also using this Lipid Vector Technology for gemcitabine (CP-4126) [59], which is in phase II clinical trials for pancreatic cancer. Owing to the possibility of oral absorption of the formulation, it is also being tested as a tablet formulation in a phase I study.

### *15.3.4 Protein- and Peptide Based Systems*

DTS-201 (CPI-0004Na) is a peptidic prodrug of doxorubicin based on VectorCell™ technology of Diatos (now Cellectis). It has exhibited an improved therapeutic index of the drug in experimental models [60]. Chemically, it is *N*-succinyl-β-alanyl-L-leucyl-L-alanyl-L-leucyl-doxorubicin and is stable and cell-impermeable. The prodrug is cleaved by tumor specific endopeptidases that are released extracellularly in the tumor environment to *N*-L-alanyl-L-leucyl-doxorubicin and *N*-L-leucyl-doxorubicin. These fragments are cell permeable and are further converted to free doxorubicin inside the cell. Thus, the normal body burden is decreased, and the drug is selectively accumulated in tumors [61, 62]. Phase I trials have been completed for this product.

**Table 15.4** Folate receptor-based products in clinical development

| Product | Drug | Clinical status | Indication |
|---|---|---|---|
| EC145 | Folate-conjugated Vinca alkaloids, binds to folate vitamin receptor (FR) | Phase II | Advanced NSCLC, ovarian cancer and endometrial cancer |
| EC20 | Folate targeted imaging agent, diagnostic agent | Phase I, II | Diagnostic for metastatic tumors overexpressing folate receptor |
| EC17 | Folate–Hapten Conjugate | Phase II terminated | Renal cell carcinoma |
| EC0225 | Folic acid–desacetylvinblastine hydrazide conjugate | Phase I | Refractory or metastatic tumors |
| EC0489 | Folate-receptor targeted chemotherapy | Phase I | Refractory or metastatic tumors in patients who have exhausted standard therapeutic options |

## *15.3.5 Active Targeting Conjugates*

Antineoplastic drugs should ideally selectively kill cancer cells. One possible approach is to deliver the drug as a prodrug to the site of action and activate it in situ (tumor-activated prodrugs; TAP). The activator strategy can be based on tumor physiology (such as selective enzyme expression, hypoxia, and low extracellular pH), or tumor specific delivery techniques (such as antibody directed enzyme prodrug therapy or ADEPT) [63]. These approaches constitute the active targeting techniques employing various categories of guides.

### 15.3.5.1 Tumor Specific Antigens and Receptors

Vitamins such as B12, E, and folic acid are being explored for targeting. Folic acid is an important nutrient for cells for synthesis of purine and pyrimidine in cells, and rapidly multiplying cancerous cells overexpress the folate receptor on the cell membrane. A molecule linked with folate will, thus, have a high probability to interact with the cell membrane and be internalized by endocytosis. Normal cells take up folic acid by a reduced affinity folate uptake mechanism that does not allow these tagged drugs to pass through them, thereby reducing toxicity. The backbone of these delivery systems is the linker that cleaves inside the cell. A few folate receptor based drug delivery systems being developed by Endocyte are in clinical trials (Table 15.4).

Transferrin is one other such ligand that imparts active targeting and has been attached to nanoparticles for delivery of oxaliplatin (MBP-426, Mebiopharm Inc.). Transferrin is a plasma glycoprotein for transport of iron in the body, and its receptors are overexpressed in cancer cells. This product is in Phase I (for solid tumors) and Phase IIa (for gastric or gastroesophageal junction cancer) trials. Calando

pharmaceuticals is developing a cyclodextrin formulation for delivery of siRNA for cancer therapy using RNAi/Oligonucleotide Nanoparticle Delivery (RONDEL) platform. This product called CALAA-01 is presently in phase I clinical trials. The system not only protects the siRNA from enzymatic degradation but also provides active targeting using transferrin [64, 65]. Being negatively charged, siRNA binds to the positively charged cyclodextrin backbone. Additionally, PEG is covalently bound to the cyclodextrin via the hydrophobic molecule adamantine. These opposing polarities force the system into self assembled particles about 70 nm in diameter, with a hydrophobic core and hydrophilic coating of PEG, which provides prolonged circulation [64].

#### 15.3.5.2 Cytokine Aided

PE-38 is a bacterial agent from Pseudomonas and is cytotoxic. To provide tumor cell specificity, it has been linked to an immune regulatory cytokine IL13. The rationale is that malignant glioma cells overexpresss IL13 receptors. IL13–PE38 (NeoPharm/Nippon Kayaku) is used as an adjunct to therapy to prevent relapse by administering directly to the tumor through catheters inserted in the brain [66]. This recombinant protein based product is presently undergoing phase I and II clinical trials.

#### 15.3.5.3 Antibody Based Immunoconjugates

This technology relies on the linking of purified monoclonal antibody (mAb) fragments that are linked by enzyme cleavable bonds to cytotoxic drugs. The complexes bind specifically to the antigens present on cancer cells, and are internalized. The lysosomes then break the conjugate to release the drug within the cell. Thus, cancer cells are targeted with high specificity. The first clinically approved mAb–drug conjugate, gemtuzumab ozogamicin, contains an acid labile hydrazone linker and a sterically hindered disulfide. The key is to find a linker to bond the mAb to the drug that should be stable till it reaches the target site within the cancer cells [67–69].

In addition to anticancer drugs, radionuclides have been attached with the humanized murine mAb's. The use of radionuclides such as $^{99m}$Tc- and $^{111}$In has been primarily focused on imaging of tumors, especially after the advent of positron emission tomography (PET). This field has indirectly contributed to drug delivery by imaging the receptors and other targets to which the drugs or the delivery systems thereof are directed [70]. One advantage of using antibodies for targeted therapy is that they have inherently long plasma half life. However, it can be a disadvantage with radioconjugates [71].

Owing to the amalgamation of molecular biology with drugs and chemical linking techniques, immunoconjugates are the most advanced form of drug delivery systems. From chemosensitization to radiotherapy and molecular signal inhibition,

this class of drugs has given a new dimension to antineoplastic chemotherapy [72]. A major limitation of gemtuzumab ozogamicin is resistance to the drug if the tumors overexpress Pgp. One of the most interesting but unrealized concept of this approach is the possibility to reverse drug resistance mediated by efflux transporters such as Pgp [71]. In addition to the chemical linkers, efforts are being made to identify and use enzymatic targets for release of drug within the cell especially those in lysosomes such as Cathepsin B [73]. These peptide based linkers are much more stable than chemical linkers based on moieties such as hydrazones and allow significant dose reduction and highly specific cancer cell cytotoxicity. For the synthetic auristatin derivative monomethyl auristatin E, target cytotoxicity has been achieved at a dose 60 times less than the maximum tolerated dose [69]. Three conjugates are already approved and various others are in different stages of clinical trials. Table 15.5 lists the products based on antibody–drug conjugates (ADCs).

## 15.4 Conclusion

Among the different classes of drugs, the relative importance of delivering the anticancer drugs specifically to the target cells or tissues is the greatest due to their cytotoxic effect. However, drug delivery techniques have facilitated the clinical debut and efficacy of many molecules in a variety of ways ranging from increasing their solubility to making them orally bioavailable. Owing to the large expenses involved in drug development, especially during clinical trials, profitability is largely dependent on patent protection. Though cremophor® EL often invites a lot of criticism for its toxicity in the standard paclitaxel formulation, Taxol®, one has to appreciate that this molecule enabled the marketing of an almost abandoned drug. With a wider variety of available excipients and technology platforms, the drugs of today stand a far better chance of being available to the cancer patient. Many kinds of inorganic, natural, and synthetic organic materials are being explored to design delivery systems that would allow even poorly water soluble or chemically or enzymatically unstable drugs to be able to selectively reach cancer cells. Promising technologies such as dendrimers should soon enter clinical trials.

Advances in technologies and new functional materials have allowed developers to harness the increased understanding of molecular pharmaceutics and modes of drug delivery. Specifically, forays in the areas of polymer chemistry and molecular biology techniques aided by improved screening of both toxicity and efficacy of novel biomaterials have made mankind stand inches from the magic bullet against cancer. Polymeric and immunoconjugates of drugs are the most rapidly advancing categories of products in the developmental arsenal. The uniqueness of submicron delivery systems in exploiting the EPR effect has provided pivotal leverage to targeting techniques. Newer techniques are combining different technologies to incorporate as many desirable features as possible in a single

**Table 15.5** Antibody–drug conjugates in clinical development

| Agent | Clinical status | Drug | Developer | Target | Indication |
|---|---|---|---|---|---|
| AVE9633 | Phase I | Maytansine | Immunogen | CD33 | Acute myelogenous leukemia |
| Bexxar or tositumomab | Approved | I-131 | GSK | CD-20 | Non-Hodgkin's lymphoma |
| Brentuximab vedotin or SGN-35 | Phase I, II, III | Monomethyl auristatin E | Seattle Genetics | CD30 | Relapsed/refractory Hodgkin lymphoma<br>Systemic anaplastic large cell lymphoma (ALCL)<br>Retreatment of Hodgkin lymphoma, systemic ALCL<br>Frontline Hodgkin lymphoma |
| CDX-011 | Phase II | Auristatin | Celldex | Glycoprotein NMB or osteoactivin | Locally advanced or metastatic breast cancer and stage III or IV melanoma |
| HuC242-DM4 | Phase I | Maytansine | Immunogen | CanAg | Colorectal cancer |
| IMGN901 | Phase II | Maytansinoid, DM1 | Immunogen | CD56 | Small cell lung cancer, MCC, ovarian cancer and other CD56+ solid tumors |
| Inotuzumab Ozogamicin | Phase III | Calicheamicin | Pfizer | CD22 | Non-Hodgkin's lymphoma |
| Mylotarg or Gemtuzumab Ozogamicin | Approved | Calicheamicin | Pfizer | CD33 | Acute myelogenous leukemia |
| SGN-15 | Phase II completed | Doxorubicin | Seattle Genetics | Lewis-y | Refractory prostate cancer |
| SGN-75 | Phase I | Monomethyl auristatin F | Seattle Genetics | CD-70 | Renal cell carcinoma, non-Hodgkin's lymphoma |
| Trastuzumab-MCC-DM1 or T-DM1 | Phase II | Maytansine | Genentech/Roche | Her2/neu | Breast cancer |
| Zevalin or Ibritumomab Tiuxetan | Approved | Y-90, In-111 | Spectrum Pharmaceuticals | CD-20 | Follicular non-Hodgkin's lymphoma |

delivery system. While scientists venture to discover activity of molecules specific to cancers, drug delivery strives to artificially induce that capability for the existing drugs.

## References


1. Allen TM, Cullis PR (2004) Drug delivery systems: entering the mainstream. Science 303:1818–1822
2. Brown JM, Giaccia AJ (1998) The unique physiology of solid tumors: opportunities (and problems) for cancer therapy. Cancer Res 58:1408–1416
3. Iyer AK et al (2006) Exploiting the enhanced permeability and retention effect for tumor targeting. Drug Discov Today 11:812–818
4. Maeda H, Bharate GY, Daruwalla J (2009) Polymeric drugs for efficient tumor-targeted drug delivery based on EPR-effect. Eur J Pharm Biopharm 71:409–419
5. Hennenfent KL, Govindan R (2006) Novel formulations of taxanes: a review. Old wine in a new bottle? Ann Oncol 17:735–749
6. Malam Y, Loizidou M, Seifalian AM (2009) Liposomes and nanoparticles: nanosized vehicles for drug delivery in cancer. Trends Pharmacol Sci 30:592–599
7. Peer D et al (2007) Nanocarriers as an emerging platform for cancer therapy. Nat Nano 2:751–760
8. Lammers T, Hennink WE, Storm G (2008) Tumour-targeted nanomedicines: principles and practice. Br J Cancer 99:392–397
9. Davis ME, Chen Z, Shin DM (2008) Nanoparticle therapeutics: an emerging treatment modality for cancer. Nat Rev Drug Discov 7:771–782
10. Cho K et al (2008) Therapeutic nanoparticles for drug delivery in cancer. Clin Cancer Res 14:1310–1316
11. Kante B et al (1980) Tissue distribution of [3H]actinomycin D adsorbed on polybutylcyanoacrylate nanoparticles. Int J Pharm 7:45–53
12. Couvreur P, Tulkens P, Roland M (1977) Nanocapsules: a new type of lysosomotropic carrier. FEBS Lett 84:323–326
13. Moghimi SM, Kissel T (2006) Particulate nanomedicines. Adv Drug Deliv Rev 58:1451–1455
14. Hanes J (2006) New polymeric nanomedicines for targeted and controlled drug delivery. Nanomedicine 2:273
15. Alonso MJ (2004) Nanomedicines for overcoming biological barriers. Biomed Pharmacother 58:168–172
16. Duncan R (2005) Nanomedicine gets clinical. Mater Today 8:16–17
17. Florence AT (1997) The oral absorption of micro- and nanoparticulates: neither exceptional nor unusual. Pharm Res 14:259–266
18. Sakuma S, Hayashi M, Akashi M (2001) Design of nanoparticles composed of graft copolymers for oral peptide delivery. Adv Drug Deliv Rev 47:21–37
19. Mathiowitz E et al (1997) Biologically erodable microspheres as potential oral drug delivery systems. Nature 386:410–414
20. Desai N et al (2004) Increased transport of nanoparticle albumin-bound paclitaxel (ABI-007) by endothelial gp60-mediated caveolar transcytosis: a pathway inhibited by Taxol. Eur J Cancer Suppl 2:182–183
21. Ruenraroengsak P, Cook JM, Florence AT (2010) Nanosystem drug targeting: facing up to complex realities. J Control Release 141:265–276
22. Torchilin VP (2005) Recent advances with liposomes as pharmaceutical carriers. Nat Rev Drug Discov 4:145–160

23. Drummond DC et al (1999) Optimizing liposomes for delivery of chemotherapeutic agents to solid tumors. Pharmacol Rev 51:691–744
24. Shapira I et al (2009) Evolving lipid-based delivery systems in the management of neoplastic disease. Oncol Rev 3:113–124
25. Ibrahim NK et al (2002) Phase I and pharmacokinetic study of ABI-007, a cremophor-free, protein-stabilized, nanoparticle formulation of paclitaxel. Clin Cancer Res 8:1038–1044
26. Schnitzer JE (1992) gp60 is an albumin-binding glycoprotein expressed by continuous endothelium involved in albumin transcytosis. Am J Physiol Heart Circ Physiol 262: H246–H254
27. Desai N et al (2006) Increased antitumor activity, intratumor paclitaxel concentrations, and endothelial cell transport of cremophor-free, albumin-bound paclitaxel, ABI-007, compared with cremophor-based paclitaxel. Clin Cancer Res 12:1317–1324
28. Gradishar WJ et al (2005) Phase III trial of nanoparticle albumin-bound paclitaxel compared with polyethylated castor oil-based paclitaxel in women with breast cancer. J Clin Oncol 23:7794–7803
29. Vicent MJ, Duncan R (2006) Polymer conjugates: nanosized medicines for treating cancer. Trends Biotechnol 24:39–47
30. Brem H et al (1995) Placebo-controlled trial of safety and efficacy of intraoperative controlled delivery by biodegradable polymers of chemotherapy for recurrent gliomas. Lancet 345:1008–1012
31. Qiu L et al (2007) Polymeric micelles as nanocarriers for drug delivery. Expert Opin Ther Pat 17:819–830
32. Matsumura Y, Kataoka K (2009) Preclinical and clinical studies of anticancer agent-incorporating polymer micelles. Cancer Sci 100:572–579
33. Matsumura Y (2008) Poly (amino acid) micelle nanocarriers in preclinical and clinical studies. Adv Drug Deliv Rev 60:899–914
34. Matsumura Y (2008) Polymeric micellar delivery systems in oncology. Jpn J Clin Oncol 38:793–802
35. Torchilin V (2007) Micellar nanocarriers: pharmaceutical perspectives. Pharm Res 24:1–16
36. Gelderblom H et al (2001) Cremophor EL: the drawbacks and advantages of vehicle selection for drug formulation. Eur J Cancer 37:1590–1598
37. Singh AT et al (2008) A novel nanopolymer based tumor targeted delivery system for paclitaxel. ASCO Meet Abstr 26:11095
38. Yokoyama M (2010) Polymeric micelles as a new drug carrier system and their required considerations for clinical trials. Expert Opin Drug Deliv 7:145–158
39. Batrakova EV et al (2001) Mechanism of sensitization of MDR cancer cells by Pluronic block copolymers: selective energy depletion. Br J Cancer 85:1987–1997
40. Venne A et al (1996) Hypersensitizing effect of Pluronic L61 on cytotoxic activity, transport, and subcellular distribution of doxorubicin in multiple drug-resistant cells. Cancer Res 56:3626–3629
41. Valle J et al (2011) A phase 2 study of SP1049C, doxorubicin in P-glycoprotein-targeting 665 pluronics, in patients with advanced adenocarcinoma of the esophagus and gastroesophageal junction. Invest New Drugs 29:1029–1037.
42. Paul A, Vicent MJ, Duncan R (2007) Using small-angle neutron scattering to study the solution conformation of N-(2-Hydroxypropyl)methacrylamide copolymer doxorubicin conjugates. Biomacromolecules 8:1573–1579
43. Duncan R (2009) Development of HPMA copolymer-anticancer conjugates: clinical experience and lessons learnt. Adv Drug Deliv Rev 61:1131–1148
44. Duncan R et al (2001) Polymer-drug conjugates, PDEPT and PELT: basic principles for design and transfer from the laboratory to clinic. J Control Release 74:135–146
45. Li C, Wallace S (2008) Polymer-drug conjugates: recent development in clinical oncology. Adv Drug Deliv Rev 60:886–898

46. Seymour LW et al (1987) Effect of molecular weight (Mw) of N-(2-hydroxypropyl) methacrylamide copolymers on body distribution and rate of excretion after subcutaneous, intraperitoneal, and intravenous administration to rats. J Biomed Mater Res 21:1341–1358
47. Mita M et al (2009) Phase I study of paclitaxel poliglumex administered weekly for patients with advanced solid malignancies. Cancer Chemother Pharmacol 64:287–295
48. Schluep T et al (2009) Pharmacokinetics and tumor dynamics of the nanoparticle IT-101 from PET imaging and tumor histological measurements. Proc Natl Acad Sci USA 106:11394–11399
49. Harris JM, Chess RB (2003) Effect of pegylation on pharmaceuticals. Nat Rev Drug Discov 2:214–221
50. Zhang JA et al (2004) Development and characterization of a novel liposome-based formulation of SN-38. Int J Pharm 270:93–107
51. Rodriguez MA et al (2009) Vincristine sulfate liposomes injection (Marqibo) in heavily pretreated patients with refractory aggressive non-Hodgkin lymphoma. Cancer 115:3475–3482
52. Martin EE et al (2010) Vascular targeting by EndoTAG™-1 enhances therapeutic efficacy of conventional chemotherapy in lung and pancreatic cancer. Int J Cancer 126:1235–1245
53. Gabizon AA (2001) Pegylated liposomal doxorubicin: metamorphosis of an old drug into a new form of chemotherapy. Cancer Invest 19:424–436
54. Leonard RCF et al (2009) Improving the therapeutic index of anthracycline chemotherapy: focus on liposomal doxorubicin (Myocet(TM)). Breast 18:218–224
55. Reddy LH, Couvreur P (2010) Lipid-based anticancer prodrugs. In: Macromolecular anticancer therapeutics. Springer, New York, pp 291–328
56. Henningsson A et al (2001) Mechanism-based pharmacokinetic model for paclitaxel. J Clin Oncol 19:4065–4073
57. Jones R et al (2008) A phase II open-label study of DHA-paclitaxel (Taxoprexin) by 2-h intravenous infusion in previously untreated patients with locally advanced or metastatic gastric or oesophageal adenocarcinoma. Cancer Chemother Pharmacol 61:435–441
58. O'Brien S et al (2009) A phase II multicentre study with elacytarabine as second salvage therapy in patients with AML. ASH Annu Meet Abstr 114:1042
59. Nilsson B et al (2009) First-in-human study of a novel nucleoside analogue, CP-4126, in patients with advanced solid tumors. ASCO Meet Abstr 27:2577
60. Ravel D et al (2008) Preclinical toxicity, toxicokinetics, and antitumoral efficacy studies of DTS-201, a tumor-selective peptidic prodrug of doxorubicin. Clin Cancer Res 14:1258–1265
61. Dubois V et al (2002) CPI-0004Na, a new extracellularly tumor-activated prodrug of doxorubicin: in vivo toxicity, activity, and tissue distribution confirm tumor cell selectivity. Cancer Res 62:2327–2331
62. Trouet A et al (2001) Extracellularly tumor-activated prodrugs for the selective chemotherapy of cancer: application to doxorubicin and preliminary in vitro and in vivo studies. Cancer Res 61:2843–2846
63. Denny WA (2001) Prodrug strategies in cancer therapy. Eur J Med Chem 36:577–595
64. Davis ME (2009) The first targeted delivery of siRNA in humans via a self-assembling, cyclodextrin polymer-based nanoparticle: from concept to clinic. Mol Pharm 6:659–668
65. Bartlett DW et al (2007) Impact of tumor-specific targeting on the biodistribution and efficacy of siRNA nanoparticles measured by multimodality in vivo imaging. Proc Natl Acad Sci 104:15549–15554
66. Kawakami K et al (2006) Intratumoral therapy with IL13-PE38 results in effective CTL-mediated suppression of IL-13Rα2-expressing contralateral tumors. Clin Cancer Res 12:4678–4686
67. Ezogelin O et al (2008) Combination of the anti-CD30-auristatin-E antibody-drug conjugate (SGN-35) with chemotherapy improves antitumour activity in Hodgkin lymphoma. Br J Haematol 142:69–73
68. Senter PD (2009) Potent antibody drug conjugates for cancer therapy. Curr Opin Chem Biol 13:235–244

69. Wu AM, Senter PD (2005) Arming antibodies: prospects and challenges for immunoconjugates. Nat Biotechnol 23:1137–1146
70. Weber WA et al (2008) Technology insight: novel imaging of molecular targets is an emerging area crucial to the development of targeted drugs. Nat Clin Pract Oncol 5:44–54
71. Sharkey RM, Goldenberg DM (2006) Targeted therapy of cancer: new prospects for antibodies and immunoconjugates. CA Cancer J Clin 56:226–243
72. DeNardo SJ (2005) Concluding remarks: tenth conference on cancer therapy with antibodies and immunoconjugates. Clin Cancer Res 11:7201s–7202s
73. Dubowchik GM, Walker MA (1999) Receptor-mediated and enzyme-dependent targeting of cytotoxic anticancer drugs. Pharmacol Ther 83:67–123

# Chapter 16
# Fundamentals of Vaccine Delivery in Infectious Diseases

**Sevda Şenel**

**Abstract** Infectious diseases continue to be the major causes of illness, disability, and death. Moreover, in recent years, new infectious agents and diseases are being identified, and some diseases that were previously considered under control have reemerged. Furthermore, antimicrobial resistance has grown rapidly in a variety of hospital as well as community acquired infections. Thus, humanity still faces big challenges in the prevention and control of infectious diseases. Vaccination, generally considered to be the most effective method of preventing infectious diseases, works by presenting a foreign antigen to the immune system to evoke an immune response. The administered antigen can either be a live, but weakened, form of a pathogen (bacteria or virus), a killed or inactivated form of the pathogen, or a purified material such as a protein. However, no vaccine is completely safe; therefore, vaccine safety research and monitoring are necessary to minimize vaccine related harms. From the formulation point of view, the goal continues to be to improve the quality and global availability of vaccine delivery systems. This chapter provides an introduction to vaccine formulation, describes the delivery routes that are utilized, and discusses the factors that affect the safety and stability of a vaccine formulation.

## 16.1 Introduction

Despite the outstanding successes in control of diseases provided by improved sanitation, immunization, and antimicrobial therapy, infectious diseases continue to be a common and significant medical problem. Infectious diseases take many

S. Şenel (✉)
Department of Pharmaceutical Technology, Hacettepe University, 06100 Ankara, Turkey
e-mail: ssenel@hacettepe.edu.tr

J. Siepmann et al. (eds.), *Fundamentals and Applications of Controlled Release Drug Delivery*, Advances in Delivery Science and Technology,
DOI 10.1007/978-1-4614-0881-9_16, 

manifestations. The most common disease of mankind, the common cold is an infectious disease, just as the fearsome modern disease acquired immune deficiency syndrome (AIDS) is. Some chronic neurological diseases that were previously thought to be degenerative have now been proven to be infectious as well.

Infectious diseases are caused by infective agents, pathogens (such as bacteria, viruses, and fungi) or parasites. Some infectious diseases can be passed from person to person. Some, however, are transmitted via animals. Others are acquired by ingesting contaminated food or water or other exposures in the environment. These microbes, especially viruses, are unstable and evolve rapidly.

During the past 30 years, more than 30 new organisms have been identified worldwide [1]. The emergence of the new or newly recognized pathogens, such as the viruses causing novel viral hepatitis, severe acute respiratory syndrome (SARS), Ebola, and highly pathogenic modified strains of influenza virus, has altered the entire insight of public health. There is also increasing awareness of the potential for novel or established infections of animals to cross the species barrier and affect man, such as the avian flu and swine flu. Many old infectious diseases, such as tuberculosis, have become renascent due to relaxation of control measures as a result of satisfaction, increasing resistance to antimicrobial agents, and social factors that include increased travel, social displacement and poverty [2]. Some long established infections have expanded to previously unaffected regions, for example, West Nile virus in North America. The threat of bioterrorism has raised the spectra of new outbreaks of highly infectious and deadly diseases, such as smallpox, anthrax, prion diseases such as variant Creutzfeldt–Jakob disease (vCJD) and plague. There is now some evidence that global climate change might be contributing to the spread of infectious disease [3]. Unless controlled effectively, emerging infectious diseases will take a heavy toll of human life regardless of age, gender, lifestyle, ethnic background, and socioeconomic status.

Infectious diseases may not only cause suffering and death but also impose an enormous financial burden on society hence efforts continue for prevention, care, and treatment of the infectious diseases. Both the conventional and the novel formulation technologies for various drugs, which are described in elsewhere in this book, are also applicable for delivery of the chemotherapeutic agents used to treat infectious diseases via the oral, parenteral, transdermal, and transmucosal routes. However, the focus of this chapter is on vaccines that are used for the prevention and/or therapy of infectious diseases, and that require quite different formulation approaches when compared to those used to deliver conventional drugs.

## 16.2 Vaccines

Vaccines for the prevention of infectious diseases have made a major contribution to the improvement in the health of people world-wide during the past century. Vaccines work by presenting an antigen to the immune system to evoke an immune

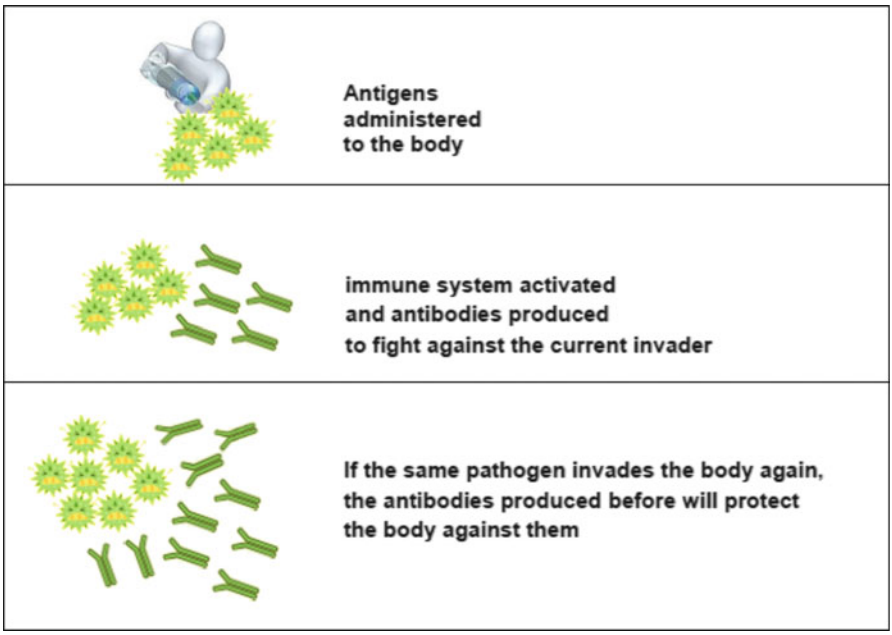


**Fig. 16.1** How does a vaccine work?

response that improves the body resistance to the effects of an infectious pathogen or a disease process [4]. Receiving a vaccination (antigen) activates the immune system's "memory" allowing the body to react quickly by releasing antibodies to future exposures and thereby destroying the pathogen before it can cause illness (Fig. 16.1). Antibodies, which are also known as immunoglobulins (Ig), are gamma globulin proteins found in blood and are used by the immune system to identify and neutralize bacteria and viruses.

Most of the vaccines used today involve killed or attenuated microorganisms (bacteria, viruses, fungi, etc.) or chemically detoxified toxins (toxoids) from bacteria. However, despite the efficacy of killed and attenuated vaccines, there is concern over their safety. Killed bacterial or viral vaccines often have residual toxicity following inactivation and might contain toxic components, such as lipopolysaccharide [5]. To overcome this problem, although often less immunogenic, subunit vaccines composed of purified antigenic components of the microorganism have been developed. Extensive research has been carried out to also identify the antigens expressed on microorganisms that evoke a protective immune response. Recombinant vaccines have been developed, in which genes for desired antigens are inserted into a vector, usually a virus, which has a very low virulence. The vector expressing the antigen may be used as the vaccine, or the antigen may be purified and injected as a subunit vaccine [6]. Among the subunit recombinant vaccines currently available on the market are the Hepatitis

B Virus (HBV) Vaccine (Engerix-B®, GSK; Recombivax Hb®, Merck and Co. Inc) and Human Papilloma Virus (HPV) (Cervarix®, GSK; Gardasil®, Merck and Co. Inc) based on the ability of the viral L1 capsid protein to form virus-like particles (VLP), which are self assembling particles composed of one or more viral proteins.

DNA vaccines based on the injection of plasmid DNA encoding the protective antigenic protein have also been investigated [7–9]. The USDA (US Department of Agriculture) recently granted full licensure for a therapeutic DNA vaccine to help extend survival time of dogs with oral melanoma. The first and only USDA approved vaccine, Oncept™, developed by Merial in partnership with the Memorial Sloan-Kettering Cancer Center and the Animal Medical Center of New York, uses a DNA plasmid containing a gene for the human version of tyrosinase, a protein present on melanoma cancer cells in humans and dogs [10]. For the subunit and DNA vaccines to reach their full potential, it is important to get them to the right place, at the right time, in the right condition [11]. Therefore, delivery systems for vaccines need to be advanced and innovative as well. A successful vaccine formulation must be effective; in other words, it should be capable of inducing appropriate immune response; it should be safe to administer and should be stable, reproducible, and easily affordable.

## *16.2.1 Formulation of Vaccines*

Traditional live vaccines based on attenuated pathogens typically do not require the addition of any other agents into the formulation but are generally dispersed in buffer solution, whereas vaccines based on inactivated viruses or bacteria may require adjuvants to enhance their immunogenicity. While subunit vaccines, such as purified protective proteins or carbohydrates, provide a much cleaner, safer, and more immunologically defined alternative to live or killed whole cell vaccines, these vaccines are not sufficiently immunogenic on their own; thus, the use of an adjuvant is required to enhance their ability to evoke effective immune responses [12–14].

### 16.2.1.1 Adjuvants

Adjuvants are defined as molecules, compounds, or macromolecular complexes that boost the potency and longevity of specific immune response to antigens, causing only minimal toxicity or long lasting immune effects on their own [15]. Adjuvants act by a diverse series of pathways that may involve changing the properties of the antigen, providing a slow release antigen depot, targeting innate immune pathways to selectively activate specific pathways of immunity [16–20].

In regard to their mechanism of action, the adjuvants can be classified into two groups as follows [15, 21]:

1. Immunostimulants: these act directly on the immune system to increase the response to antigens that stimulate immune responses. Examples include TLR (Toll-like receptor) ligands, MPL®, cytokines (GM-CSF, IL-2, IFN-γ, and Flt-3), saponins, and bacterial exotoxins (*CT* cholera toxin, *LT* heat labile enterotoxin of *Escherichia coli*).
2. Vehicles (delivery systems): these present vaccine antigens to the immune system in an optimal manner, including controlled release and depot delivery systems, to increase the specific immune response to the antigen, and can also serve to deliver the immunostimulants. Examples include the following: mineral salts (aluminum) [22]; emulsions (montanide®) [23], MF59™ [24, 25]; virosomes [26, 27]; liposomes; biodegradable polymeric microparticles; and immune stimulating complexes – ISCOMs.

Currently, there are very few adjuvants and delivery systems licensed for human use. These include Alum, MF59™ (an oil-in-water emulsion containing nonionic surfactants and squalene incorporated in influenza vaccines, Fluad® and Focetria®, Novartis), AS03 (10% oil-in-water emulsion containing squalene incorporated in pandemic H1N1 influenza vaccine, Pandemrix®, GSK), MPL® (monophosphoryl lipid A), AS04 [Alum + MPL®, incorporated in Human papilloma virus vaccine, Cervarix®, and hepatitis B virus (HBV) vaccine, Fendrix®, GSK], virus-like particles (VLP) (self-assembling particles composed of one or more viral proteins); immunopotentiating reconstituted influenza virosomes (IRIV) (Epaxal®, hepatitis A virus particles adsorbed on the surface of the IRIV, and Inflexal® V, influenza, Berna, a Crucell Company), and cholera toxin. Safety of adjuvants still remains an important issue, as many of the adjuvants are reported to show some undesired effects [28, 29].

#### 16.2.1.2 Preservatives

Preservatives such as phenol, benzethonium chloride, and 2-phenoxyethanol are also added into formulations to prevent bacterial and fungal growth in some vaccines during storage, and particularly during the use of opened multidose vials. Thiomersal (also known as thimerosal; mercurothiolate and sodium 2-ethylmercuriothio-benzoate), which is approximately 50% mercury by weight, is one of the most commonly used preservatives in vaccine formulations. It has also been used during vaccine production both to inactivate certain organisms and toxins and to maintain a sterile production line. Recently, there have been some concerns about the safety of this compound due to its mercury content. Such safety concerns have led to initiatives in some countries to eliminate, reduce, or replace thiomersal in vaccines, both in single dose and multidose presentations. However, the WHO Global Advisory Committee on Vaccine Safety [30] continues to recommend the use of vaccines containing thiomersal for global immunization programmes because the benefits of using such products far outweigh any theoretical risk of toxicity.

#### 16.2.1.3 Stabilizers and Solubilizers

Stabilizers and solubilizers such as polyoxyethylene sorbitan monooleate (Tween® 80), t-octylphenoxypolyethoxyethanol (octoxynol 9, Triton® X-100) are added into vaccine formulations to improve formulation characteristics such as dispersibility. Sugars such as sucrose and lactose, amino acids such as glycine or the monosodium salt of glutamic acid, and proteins such as human serum albumin or gelatin are also added as stabilizers. They are sometimes added to help protect the vaccine from the effects of adverse conditions such as are encountered in the freeze drying process, for those vaccines that are freeze dried.

Most vaccine preparations have to be stored within a specific temperature range to maintain potency. The "cold chain" system (often 2 to 8°C) is a means for storing and transporting vaccines in a potent state from the manufacturer to the person being immunized (Fig. 16.2). This approach is very important since all vaccines lose potency over time if exposed to heat and/or when frozen [31]. However, for innovative technology based vaccines, the cold chain system may be very costly due to the requirements for significantly more space in transportation and storage. Therefore, development of thermostable vaccine formulations becomes an important consideration.

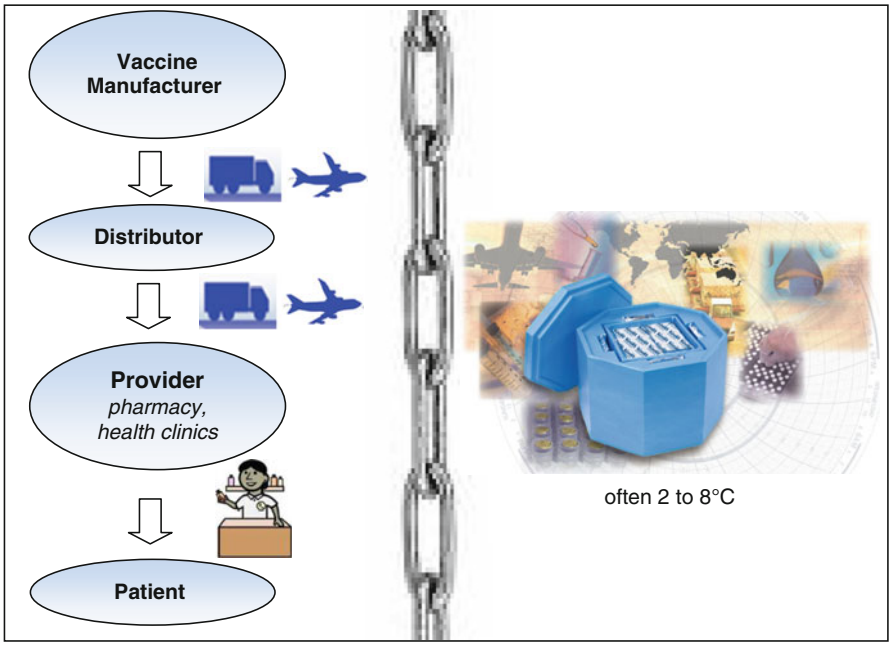


**Fig. 16.2** Schematic presentation of cold chain for vaccines

### *16.2.2 Vaccine Delivery Routes*

The vast majority of vaccines are delivered intramuscularly (im) or subcutaneously (sc) using a needle and syringe. Traditionally, the intradermal (id) route for delivery has been used as the route of choice for only a very limited number of vaccines, such as Bacille Calmette Guérin (BCG) for tuberculosis (TB), and in some countries, for postexposure rabies vaccination. However, over the past few years, the use of the intradermal administration as an alternative delivery route for several other vaccines including hepatitis B (HBV), measles, and influenza has attracted attention due to the possible advantages it offers compared to the intramuscular and subcutaneous routes. These advantages include reduced dose (therefore reduced cost and improved access to vaccines with limited supply), improved safety, and improved logistics [32].

However, there are concerns over inadequate safe injection practices such as reuse of equipment, unsafe collection, and unsafe disposal (resulting in risk of infections and disease transmission, e.g., HIV via contaminated syringes) as well as the availability of trained personnel to administer injections safely. These problems are more critical during mass campaigns when millions of doses of vaccine are administered. Furthermore, patient compliance is restricted with injection. All of these concerns lead to the search for alternate, noninvasive means of vaccine delivery that do not require a needle and syringe. These studies have been accelerated by recent concerns regarding pandemic disease, bioterrorism, and disease eradication campaigns. Noninvasive vaccine delivery would allow large mass vaccinations to be possible by increasing the ease and speed of delivery, and by providing improved efficacy, safety and compliance, decreasing costs, and reducing pain associated with vaccinations. Methods currently in use and under development are focused on needle free injection devices, transcutaneous immunization, and mucosal immunization.

#### 16.2.2.1 Transcutaneous Immunization

Transcutaneuos immunization (TCI) is a novel vaccination route involving the topical application of vaccine antigens onto the skin surface [33]. It has been shown that skin has an effective immune system, and its physical barrier is not as impermeable as previously thought; hence, it became an attractive route for noninvasive delivery of vaccines. Studies in several animal species and clinical trials in humans have established the proof of principle [34].

#### 16.2.2.2 Mucosal Immunization

Mucosal immunization has focused on oral, nasal, and aerosol vaccines. Vaccines that induce protective mucosal immunity are attractive since most infectious agents come into contact with the host at mucosal surfaces. Mucosal delivery of vaccines

allows concerted action against diseases caused by pathogens that either invade through, or cause disease at, mucosal surfaces [35]. The general approach is to combine systemic response and local mucosal immune response to induce specific protection in distant mucosal sites [36, 37].

### *16.2.3 Vaccine Delivery Systems*

In response to fears of injection (needle and syringe) mentioned above, alternative delivery technologies have been developed and some of them have already become available on the market. The World Health Organization (WHO) has undertaken a prioritization exercise to determine which delivery technologies (such as jet injector, nasal, aerosol, transcutaneous, ballistic) will be the most feasible and have the greatest impact for existing and future vaccines that will set the global vaccine delivery agenda for the forthcoming years [38]. New immunization supportive technologies anticipated by 2015 are jet injectors, vaccine patches, vaccine nasal sprays, vaccine aerosols, and thermostable vaccines [38].

#### 16.2.3.1 Needle Free Injection

Jet injectors are needle free devices that deliver vaccine through a nozzle orifice via a high pressure, high speed narrow stream that penetrates the skin [39]. They generate improved or equivalent immune responses compared to needle and syringe. A vaccine can be delivered to intradermal, subcutaneous, or intramuscular tissue depending on the mechanical properties of the fluid stream [40]. Multidose jet injectors were used widely in the 1960s–1980s, with billions of immunizations given with these devices. However, concerns about the transmission of blood borne diseases via these devices led to their withdrawal. New generation multidose jet injectors with disposable caps on the nozzle have been developed in an attempt to overcome this risk; however, they were not found to be adequately safe [46]. The older injectors that used the same nozzle on consecutive patients have been superseded by a new generation of disposable cartridge jet injectors (DCJIs), which are currently being used in the USA for needle free immunization in adults and pediatric populations with several vaccines (Fig. 16.3). The devices currently in

**Fig. 16.3** Disposable-cartridge jet injectors (DCJIs) for intradermal (skin) injection for flu vaccination (CDC Web site – Needle Free injection technology)

use are relatively expensive and not suited for use in developing countries; hence, the development of smaller, lighter, and cheaper designs, which could be applicable for both routine and campaign immunization, is required.

#### 16.2.3.2 Vaccine Patches

Travelers' Diarrhea (TD) Vaccine Patch (Intercell) has been reported to have entered clinical Phase III development [41]. The TD vaccine system consists of a self-adhesive patch containing the vaccine antigen and a single use device used to prepare the skin at the site of patch administration (the Skin Preparation System), which partially disrupts the stratum corneum of the skin. The dry patch contains the antigen in a stabilizing excipient formulation and delivers the antigen to the skin. Activated Langerhans cells take up the antigen and deliver it to the draining lymph nodes. If approved, it will be the first vaccine delivered with a patch and to prevent TD, which is caused by enterotoxigenic *E. coli*. (Note added in proof: Development of this product was halted following failure in Phase III.)

Similarly, a patch containing a trivalent inactivated influenza vaccine (TIV) has been developed in a dried, stabilized formulation for transcutaneous delivery [42]. The dry TIV patch has been described as a major advance for needle free influenza vaccination due to its effectiveness in vaccine delivery and its superior thermostable characteristics.

#### 16.2.3.3 Vaccine Nasal Sprays

The nasal route offer several benefits to the administration of vaccines, such as its highly vascular mucous membranes, low enzymatic degradation compared to oral vaccines, and greater acceptability to patients. Nasal vaccines, however, have to overcome several limitations, including mucociliary clearance and inefficient uptake of soluble antigens. Therefore, nasal vaccines require potent adjuvants and delivery systems to enhance their immunogenicity and to protect their antigens. Among the various bioadhesive polymers studied for nasal vaccine delivery, chitosan has been shown to exhibit advantages as a vaccine carrier due to its immune stimulating activity and bioadhesive properties that enhance cellular uptake, permeation and antigen protection, as well as being well tolerated by humans [21, 43, 44].

FluMist® (MedImmune, LLC, the USA) is the first FDA approved needle free influenza vaccine made from a weakened live virus (Live, attenuated influenza vaccine – LAIV). It is given as a gentle mist, with a quick spray in each nostril. FluMist® is engineered to not cause disease, and replicates efficiently only in the cooler temperatures of the nasopharynx, but not in the warmer temperatures of the lower respiratory tract. Influenza A (H1N1) 2009 Monovalent Vaccine, Live (MedImmune, LLC, the USA) is the second nasal vaccine that has been approved recently by the FDA for pandemic influenza. Neither of these vaccine formulations contain any adjuvants.

#### 16.2.3.4 Vaccine Aerosols

The Measles Aerosol Project was established in 2002 by WHO, in collaboration with the US Centers for Disease Control and Prevention and the American Red Cross, with the purpose of conducting the necessary studies to achieve the licensure of a product (device and vaccine) administered through this route [45]. It has long been recognized that new delivery systems may facilitate measles immunization efforts, especially mass campaigns, and that such approaches may facilitate the long-term sustainability of measles mortality reduction and measles elimination goals. Studies are to be undertaken for at least three devices for aerosol administration of reconstituted vaccine and, if feasible in the time frame, a dry powder device.

#### 16.2.3.5 Particulate Delivery Systems

Vaccine delivery systems are generally particulate systems, e.g., emulsions, polymeric micro/nanoparticles [47–53], ISCOMs [54, 55], and liposomes [56, 57]. They mainly function to target associated antigens into antigen presenting cells (APC), including macrophages and dendritic cells, which facilitate the immune response by holding antigens on its surface and presenting them to lymphocytes. Significantly enhanced immune responses have been reported with encapsulation or adsorption of antigens onto particles. Polyanhydrides, polyorthoesters, hyaluronic acid, and poly(lactic-*co*-glycolic acid) (PLGA) are the most commonly investigated polymers for the preparation of particulate systems [58–60]. Preparation methods employed to obtain such systems have been reported to be an important parameter for the stability of the antigen. In many cases, an organic solvent and high temperatures are needed for preparation of the particles, which may result in degradation and denaturation of the antigen during processing or after loading [61, 62]. The use of alginates [63, 64] and chitosan offers advantages over other polymers by avoiding use of organic solvents and requiring mild conditions for preparation [43, 52, 65–67].

Particulate systems with a particle size smaller than 10 μm were reported to significantly improve the immune response [61]. However, a variety of systems within a wide range of particle size (between 5 nm and 10 μm) have been investigated for antigen delivery [51, 68, 69]. These investigations showed that there was no clear confirmation that decreasing the particle size of the delivery system improved the immune response. Also there is still an inconsistency in the literature about the differential uptake of nanoparticles by antigen presenting cells (APCs), which changes according to the particle and antigen properties as well as the application route. Currently, there are no vaccine products available on the market based on polymeric particulate systems.

#### 16.2.3.6 Oral Mucosal Vaccines

Oral immunization with vaccines against intestinal infectious diseases has been extensively explored for several decades. Despite the immunologic and economic rationale behind oral immunization, only a few mucosal vaccines are available for the prevention of mucosal infections due to the limited absorption from the intestinal tract and sensitivity to degradation. "Oral" polio vaccine (OPV) contains live but weakened poliovirus and is the WHO-recommended vaccine for polio eradication. However, because of the risk of a rare, but serious, condition called vaccine-associated paralytic poliomyelitis, the use of the oral polio vaccine in the USA was discontinued in 2000.

Currently, two oral vaccines have approval from the FDA. These are Typhoid Vaccine Live Oral Ty21a (Vivotif®, enteric coated tablet, Berna, Ltd), and Rotavirus Vaccine, Live, Oral (Rotateq®, ready-to-use liquid doses, MSD; Rotarix®, a lyophilized vaccine that is reconstituted with a liquid diluent in a prefilled oral applicator, GSK) [70].

#### 16.2.3.7 Edible Plant Derived Vaccines

Recently, new live-attenuated bacterial and viral or edible plant derived vaccines have been introduced for oral vaccination [39, 71]. Plants are used as recombinant biofactories to express a number of vaccines [72]. Plant derived vaccine antigens have been found to be safe and induce a sufficiently high immune response in humans. Hence transgenic plants, including edible plant parts, have been suggested as excellent alternatives for the production of vaccines and economic scaleup through cultivation [73]. Such edible encapsulation protects the antigen through the mucosal and gut systems to allow its uptake. Furthermore, oral plant based vaccines are reported to be stable during storage at ambient temperatures, thereby eliminating the need for a cold chain. In addition, they do not require syringes, needles, or trained personnel for administration [74]. These features also favor use of these vaccines for large scale immunization programmes, particularly in developing countries where resources to provide a cold chain and the equipment and personnel needed for injections are limited. Initially the transgenic fruit or vegetable expressing an antigen from a virus or bacteria as the edible vaccine was intended to be eaten raw without any processing to evoke the protective immune response against a particular disease. However, recently the approach to "edible vaccines" has been replaced by "plant-derived vaccine antigens." This approach results in the antigen in a pure form and at standardized concentrations [73]. In general plants with high food value are being chosen as expression systems such as apple, banana, tomato, and guava (fruits), peanut, corn, soybean, and chickpea (seeds), cabbage, lettuce, potato, and spinach (vegetables) [73]. Recently, a rice based mucosal vaccine expressing CT-B (MucoRice CT-B) has been reported as a new possible form of oral cholera vaccine [75]. Transgenic rice has been

shown to be stable in the harsh environment of the gastrointestinal tract, also eliminating the need for syringe/needle administration as well as the cold chain storage process, and providing physicochemical stability. However, it has been pointed out that a highly sophisticated and a closed soil-less farming facility with artificial sunlight would be required for technical advancement of the rice based transgenic vaccine system.

## 16.3 Therapeutic Vaccines

Vaccines are by definition prophylactic, but in recent years therapeutic vaccines have been developed for chronic viral infections such as those caused by hepatitis B virus, human papilloma virus (HPV), herpes simplex virus, and HIV [76]. Therapeutic vaccines are intended to treat persistent, recurrent, or chronic infections, where drug intervention is either ineffective or suboptimal, and where intracellular pathogens have established mechanisms to escape from the immune system [77]. Unlike the traditional vaccines, which are administered to healthy individuals to prevent infection, therapeutic vaccines are designed to stimulate immune defences in patient populations after they have been infected/colonized with a pathogen, or even after they developed a disease. Therapeutic vaccination is proposed as an satisfactory replacement for, or as an adjunct to, existing therapies [78].

## 16.4 Concluding Remarks

There are always risks and benefits associated with the use of vaccines. The side effects of vaccines are often reported; however, considering the fact that a person is at risk from most infections, and that more and more reports are confirming the safety of vaccines, immunization should be considered the first line of defense against infectious diseases. In response to challenges in global immunization, WHO and UNICEF have developed the Global Immunization Vision and Strategy (GIVS), which covers the period 2006–2015 [79]. This strategy aims to assist countries to immunize more people, from infants to seniors, with a greater range of vaccines, and introduce a range of newly available vaccines and technologies to fulfill their main mission of "a world in which all people at risk are protected against vaccine-preventable diseases."

As a formulator, we also have a mission in the immunization of people, i.e., "to develop safe and more potent vaccine delivery systems, which are stable at all temperatures, self-administrable, with suitable packaging for storage and transportation, and which are affordable."

## References


1. WHO-combating emerging infectious diseases in the South-East Asia region. Accessed 7 Nov 2009
2. Girard MP, Fruth U, Kieny MP (2005) A review of vaccine research and development: tuberculosis. Vaccine 23:5725–5731
3. Snell NJ (2003) Examining unmet needs in infectious disease. Drug Discov Today 8:22–30
4. Ogra PL, Faden H, Welliver RC (2001) Vaccination strategies for mucosal immune responses. Clin Microbiol Rev 14:430–445
5. Ryan EJ, Daly LM, Mills KH (2001) Immunomodulators and delivery systems for vaccination by mucosal routes. Trends Biotechnol 19:293–304
6. Soler E, Houdebine LM (2007) Preparation of recombinant vaccines. Biotechnol Annu Rev 13:65–94
7. Brennan FR, Dougan G (2005) Non-clinical safety evaluation of novel vaccines and adjuvants: new products, new strategies. Vaccine 23:3210–3222
8. Garmory HS, Perkins SD, Phillpotts RJ, Titball RW (2005) DNA vaccines for biodefence. Adv Drug Deliv Rev 57:1343–1361
9. Greenland JR, Letvin NL (2007) Chemical adjuvants for plasmid DNA vaccines. Vaccine 25:3731–3741
10. ONCEPT consumer release. http://us.merial.com/merial_corporate/news/press_releases/02-16-2010_ONCEPT_consumer_release.asp. Accessed 1 Apr 2010
11. Eriksson K, Holmgren J (2002) Recent advances in mucosal vaccines and adjuvants. Curr Opin Immunol 14:666–672
12. Griffin JF (2002) A strategic approach to vaccine development: animal models, monitoring vaccine efficacy, formulation and delivery. Adv Drug Deliv Rev 54:851–861
13. Mills KH (2009) Designer adjuvants for enhancing the efficacy of infectious disease and cancer vaccines based on suppression of regulatory T cell induction. Immunol Lett 122:108–111
14. Perrie Y, Mohammed AR, Kirby DJ, McNeil SE, Bramwell VW (2008) Vaccine adjuvant systems: enhancing the efficacy of sub-unit protein antigens. Int J Pharm 364:272–280
15. Reed SG, Bertholet S, Coler RN, Friede M (2009) New horizons in adjuvants for vaccine development. Trends Immunol 30:23–32
16. Cox E, Verdonck F, Vanrompay D, Goddeeris B (2006) Adjuvants modulating mucosal immune responses or directing systemic responses towards the mucosa. Vet Res 37:511–539
17. Liang MT, Davies NM, Blanchfield JT, Toth I (2006) Particulate systems as adjuvants and carriers for peptide and protein antigens. Curr Drug Deliv 3:379–388
18. Petrovsky, N. 2006. Novel human polysaccharide adjuvants with dual Th1 and Th2 potentiating activity. Vaccine 24 Suppl 2: S2-26–29
19. Trujillo-Vargas CM, Mayer KD, Bickert T, Palmetshofer A, Grunewald S, Ramirez-Pineda JR, Polte T, Hansen G, Wohlleben G, Erb KJ (2005) Vaccinations with T-helper type 1 directing adjuvants have different suppressive effects on the development of allergen-induced T-helper type 2 responses. Clin Exp Allergy 35:1003–1013
20. Wilson-Welder JH, Torres MP, Kipper MJ, Mallapragada SK, Wannemuehler MJ, Narasimhan B (2009) Vaccine adjuvants: current challenges and future approaches. J Pharm Sci 98:1278–1316
21. Arca HC, Gunbeyaz M, Şenel S (2009) Chitosan-based systems for the delivery of vaccine antigens. Expert Rev Vaccines 8:937–953
22. Lin X, Hudock H, Arumugham R, Loun B (2008) Identification of particulates in vaccine formulations containing aluminum phosphate. Vaccine 26:6814–6817
23. Miles AP, McClellan HA, Rausch KM, Zhu D, Whitmore MD, Singh S, Martin LB, Wu Y, Giersing BK, Stowers AW, Long CA, Saul A (2005) Montanide ISA 720 vaccines: quality control of emulsions, stability of formulated antigens, and comparative immunogenicity of vaccine formulations. Vaccine 23:2530–2539

24. de Bruijn I, Meyer I, Gerez L, Nauta J, Giezeman K, Palache B (2007) Antibody induction by virosomal, MF59-adjuvanted, or conventional influenza vaccines in the elderly. Vaccine 26:119–127
25. Schultze V, D'Agosto V, Wack A, Novicki D, Zorn J, Hennig R (2008) Safety of MF59 adjuvant. Vaccine 26:3209–3222
26. Cavanagh DR, Remarque EJ, Sauerwein RW, Hermsen CC, Luty AJ (2008) Influenza virosomes: a flu jab for malaria? Trends Parasitol 24:382–385
27. Li Q, Gao JQ, Qiu LY, Cui FD, Jin Y (2007) Enhanced immune responses induced by vaccine using Sendai virosomes as carrier. Int J Pharm 329:117–121
28. Mutsch M, Zhou W, Rhodes P, Bopp M, Chen RT, Linder T, Spyr C, Steffen R (2004) Use of the inactivated intranasal influenza vaccine and the risk of Bell's palsy in Switzerland. N Engl J Med 350:896–903
29. O'Hagan DT, MacKichan ML, Singh M (2001) Recent developments in adjuvants for vaccines against infectious diseases. Biomol Eng 18:69–85
30. WHO-Global Advisory Committee on Vaccine Safety. http://www.who.int/vaccine_safety/en/. Accessed 23 Nov 2009
31. WHO-safe vaccine handling, cold chain and immunizations. http://www.who.int/vaccines-documents/docsPDF/WWW9825.pdf. Accessed 23 November 2009
32. WHO-intradermal delivery of vaccines. http://www.who.int/immunization_delivery/systems_policy/Intradermal-delivery-vaccines_report_2009-Sept.pdf. Accessed 23 Nov 2009
33. Skountzou I, Kang SM (2009) Transcutaneous immunization with influenza vaccines. Curr Top Microbiol Immunol 333:347–368
34. Partidos CD, Beignon AS, Mawas F, Belliard G, Briand JP, Muller S (2003) Immunity under the skin: potential application for topical delivery of vaccines. Vaccine 21:776–780
35. Del Giudice G, Pizza M, Rappuoli R (1999) Mucosal delivery of vaccines. Methods 19:148–155
36. Holmgren J, Czerkinsky C (2005) Mucosal immunity and vaccines. Nat Med 11:S45–53
37. Neutra MR, Kozlowski PA (2006) Mucosal vaccines: the promise and the challenge. Nat Rev Immunol 6:148–158
38. WHO-immunization service delivery and accelerated disease control, new vaccines and technologies. http://www.who.int/immunization_delivery/new_vaccines/technologies/en/index.html. Accessed 23 Nov 2009
39. Giudice EL, Campbell JD (2006) Needle-free vaccine delivery. Adv Drug Deliv Rev 58:68–89
40. Jackson LA, Austin G, Chen RT, Stout R, DeStefano F, Gorse GJ, Newman FK, Yu O, Weniger BG (2001) Safety and immunogenicity of varying dosages of trivalent inactivated influenza vaccine administered by needle-free jet injectors. Vaccine 19:4703–4709
41. Intercell smart vaccines. http://www.intercell.com/main/forbeginners/news/not-in-menu/news-full/back_to/travelers-diarrhea-vaccine-patch/article/intercell-starts-european-pivotal-phase-iii-clinical-trial-for-the-patch-based-travelers-diarrhea-v/. Accessed 23 Nov 2009
42. Frolov VG, Seid RC Jr, Odutayo O, Al-Khalili M, Yu J, Frolova OY, Vu H, Butler BA, Look JL, Ellingsworth LR, Glenn GM (2008) Transcutaneous delivery and thermostability of a dry trivalent inactivated influenza vaccine patch. Influenza Other Respi Viruses 2:53–60
43. Illum L, Jabbal-Gill I, Hinchcliffe M, Fisher AN, Davis SS (2001) Chitosan as a novel nasal delivery system for vaccines. Adv Drug Deliv Rev 51:81–96
44. Klas SD, Petrie CR, Warwood SJ, Williams MS, Olds CL, Stenz JP, Cheff AM, Hinchcliffe M, Richardson C, Wimer S (2008) A single immunization with a dry powder anthrax vaccine protects rabbits against lethal aerosol challenge. Vaccine 26:5494–5502
45. WHO-Immunization Service Delivery and Accelerated Disease Control, New Vaccines and Technologies, Measles Aerosol Project. http://www.who.int/immunization_delivery/new_vaccines/technologies_aerosol/en/index.html. Accessed 23 Nov 2009
46. WHO-immunization service delivery and accelerated disease control. Disposable cartridge jet injectors. http://www.who.int/immunization_delivery/new_vaccines/technologies_disposable/en/index.html. Accessed 23 Nov 2009

47. Borges O, Borchard G, Verhoef JC, de Sousa A, Junginger HE (2005) Preparation of coated nanoparticles for a new mucosal vaccine delivery system. Int J Pharm 299:155–166
48. Estevan M, Gamazo C, Grillo MJ, Del Barrio GG, Blasco JM, Irache JM (2006) Experiments on a sub-unit vaccine encapsulated in microparticles and its efficacy against Brucella melitensis in mice. Vaccine 24:4179–4187
49. He X, Jiang L, Wang F, Xiao Z, Li J, Liu LS, Li D, Ren D, Jin X, Li K, He Y, Shi K, Guo Y, Zhang Y, Sun S (2005) Augmented humoral and cellular immune responses to hepatitis B DNA vaccine adsorbed onto cationic microparticles. J Control Release 107:357–372
50. O'Hagan DT, Singh M, Ulmer JB (2006) Microparticle-based technologies for vaccines. Methods 40:10–19
51. Peek LJ, Middaugh CR, Berkland C (2008) Nanotechnology in vaccine delivery. Adv Drug Deliv Rev 60:915–928
52. Sayın B, Şenel S (2008) Chitosan and its derivatives for mucosal immunization. In: Jayakumar R, Prabaharan M (eds) Current research and development on chitin in biomaterial science. Research Signpost, Kerala, India, pp 145–165
53. Zhao A, Rodgers VG (2006) Using TEM to couple transient protein distribution and release for PLGA microparticles for potential use as vaccine delivery vehicles. J Control Release 113:15–22
54. Pearse MJ, Drane D (2005) ISCOMATRIX adjuvant for antigen delivery. Adv Drug Deliv Rev 57:465–474
55. Wee JL, Scheerlinck JP, Snibson KJ, Edwards S, Pearse M, Quinn C, Sutton P (2008) Pulmonary delivery of ISCOMATRIX influenza vaccine induces both systemic and mucosal immunity with antigen dose sparing. Mucosal Immunol 1:489–496
56. Jaafari MR, Badiee A, Khamesipour A, Samiei A, Soroush D, Kheiri MT, Barkhordari F, McMaster WR, Mahboudi F (2007) The role of CpG ODN in enhancement of immune response and protection in BALB/c mice immunized with recombinant major surface glycoprotein of Leishmania (rgp63) encapsulated in cationic liposome. Vaccine 25:6107–6117
57. Yan W, Huang L (2009) The effects of salt on the physicochemical properties and immunogenicity of protein based vaccine formulated in cationic liposome. Int J Pharm 368:56–62
58. Alpar HO, Somavarapu S, Atuah KN, Bramwell VW (2005) Biodegradable mucoadhesive particulates for nasal and pulmonary antigen and DNA delivery. Adv Drug Deliv Rev 57:411–430
59. Florindo HF, Pandit S, Goncalves LMD, Alpar HO, Almeida AJ (2008) Streptococcus equi antigens adsorbed onto surface modified poly-epsilon-caprolactone microspheres induce humoral and cellular specific immune responses. Vaccine 26:4168–4177
60. Kipper MJ, Wilson JH, Wannemuehler MJ, Narasimhan B (2006) Single dose vaccine based on biodegradable polyanhydride microspheres can modulate immune response mechanism. J Biomed Mater Res A 76:798–810
61. O'Hagan DT, Singh M (2003) Microparticles as vaccine adjuvants and delivery systems. Expert Rev Vaccines 2:269–283
62. Singh M, Fang JH, Kazzaz J, Ugozzoli M, Chesko J, Malyala P, Dhaliwal R, Wei R, Hora M, O'Hagan D (2006) A modified process for preparing cationic polylactide-co-glycolide microparticles with adsorbed DNA. Int J Pharm 327:1–5
63. Mutwiri G, Bowersock T, Kidane A, Sanchez M, Gerdts V, Babiuk LA, Griebel P (2002) Induction of mucosal immune responses following enteric immunization with antigen delivered in alginate microspheres. Vet Immunol Immunopathol 87:269–276
64. Wee S, Gombotz WR (1998) Protein release from alginate matrices. Adv Drug Deliv Rev 31:267–285
65. Borges O, Tavares J, de Sousa A, Borchard G, Junginger HE, Cordeiro-da-Silva A (2007) Evaluation of the immune response following a short oral vaccination schedule with hepatitis B antigen encapsulated into alginate-coated chitosan nanoparticles. Eur J Pharm Sci 32:278–290

66. Sayın B, Somavarapu S, Li XW, Sesardic D, Şenel S, Alpar OH (2009) TMC-MCC (N-trimethyl chitosan-mono-N-carboxymethyl chitosan) nanocomplexes for mucosal delivery of vaccines. Eur J Pharm Sci 38:362–369
67. Sayın B, Somavarapu S, Li XW, Thanou M, Sesardic D, Alpar HO, Şenel S (2008) Mono-N-carboxymethyl chitosan (MCC) and N-trimethyl chitosan (TMC) nanoparticles for non-invasive vaccine delivery. Int J Pharm 363:139–148
68. Allaker RP, Ren G (2008) Potential impact of nanotechnology on the control of infectious diseases. Trans R Soc Trop Med Hyg 102:1–2
69. McGeary RP, Olive C, Toth I (2003) Lipid and carbohydrate based adjuvant/carriers in immunology. J Pept Sci 9:405–418
70. FDA-list of approved products. http://www.fda.gov/BiologicsBloodVaccines/Vaccines/ApprovedProducts/ucm093833.htm. Accessed 23 Nov 2009
71. Mestecky J, Nguyen H, Czerkinsky C, Kiyono H (2008) Oral immunization: an update. Curr Opin Gastroenterol 24:713–719
72. Green BA, Baker SM (2002) Recent advances and novel strategies in vaccine development. Curr Opin Microbiol 5:483–488
73. Tiwari S, Verma PC, Singh PK, Tuli R (2009) Plants as bioreactors for the production of vaccine antigens. Biotechnol Adv 27:449–467
74. Streatfield SJ, Howard JA (2003) Plant-based vaccines. Int J Parasitol 33:479–493
75. Takahashi I, Nochi T, Yuki Y, Kiyono H (2009) New horizon of mucosal immunity and vaccines. Curr Opin Immunol 21:352–358
76. Sela M, Arnon R, Schechter B (2002) Therapeutic vaccines: realities of today and hopes for the future. Drug Discov Today 7:664–673
77. Moingeon P, Almond J, de Wilde M (2003) Therapeutic vaccines against infectious diseases. Curr Opin Microbiol 6:462–471
78. Vandepapeliere P (2002) Therapeutic vaccination against chronic viral infections. Lancet Infect Dis 2:353–367
79. Global immunization vision and strategy. http://www.who.int/immunization/givs/en/index.html. Accessed 1 Apr 2010

# Chapter 17
# Tissue Engineering in Drug Delivery

**Charles T. Drinnan, Laura R. Geuss, Ge Zhang, and Laura J. Suggs**

**Abstract** Over the last 20 years, the fields of tissue engineering and regenerative medicine have emerged with the goals of restoring, maintaining, or improving tissue function. This is currently addressed with the creation of biologically active biomaterials or scaffolds seeded with either progenitor or differentiated cells that substitute for tissue or organs. Paracrine factors or other drugs are incorporated into these scaffolds to promote tissue regeneration and function. Precise control of both timing and presentation of these drugs is necessary for sufficient efficacy. This chapter provides an overview of the common biomaterials and drugs encountered in bone, cartilage, neural, and cardiovascular tissue engineering, as well as current strategies and future directions for drug delivery in tissue engineering.

## 17.1 Tissue Engineering

Tissue engineering and regenerative medicine are multidisciplinary fields that incorporate aspects of engineering, medicine, and the life sciences. The primary goal of tissue engineering is the creation of biologically active substitutes of tissues or organs to restore, maintain, or improve tissue function. Further, tissue engineered constructs have diagnostic applications for testing drug efficacy, toxicity, metabolism, and pathogenicity. The current paradigm of tissue engineering involves seeding

C.T. Drinnan • L.J. Suggs (✉)
Department of Biomedical Engineering, University of Texas at Austin,
1 University Station, Mail Code C0800, Austin, TX 78712, USA
e-mail: laura.suggs@mail.utexas.edu

L.R. Geuss
Department of Cellular and Molecular Biology, University of Texas at Austin, Austin, TX, USA

G. Zhang
Department of Biomedical Engineering, University of Akron, Akron, OH, USA

J. Siepmann et al. (eds.), *Fundamentals and Applications of Controlled Release Drug Delivery*, Advances in Delivery Science and Technology,
DOI 10.1007/978-1-4614-0881-9_17, 

progenitor or differentiated cells onto a substrate that mimics the extracellular matrix (ECM) with or without the presence of paracrine factors or drugs to promote a specific tissue function. This paradigm is derived from the observation that cells interact with the ECM and require a matrix upon which to adhere, proliferate, and express function. Thus, knowledge of biomaterials, cell biology, and drug delivery is required to form a functional tissue engineered construct.

### *17.1.1 Stem or Progenitor Cells*

While fully functional or differentiated cells can be used in tissue engineered constructs, they are limited with respect to cell number and proliferative capacity. The discovery of stem cells that have high proliferative capacity and differentiation potential can address these concerns, and the capability to expand stem cells ex vivo and form functional tissues is advantageous. Stem cells are defined as cells that can renew themselves and differentiate into cells with specialized functions. Stem cells are categorized by their potency, i.e. their differentiation potential to form other cell types. Totipotent cells can form both embryonic and extraembryonic cells and thus are capable of forming a complete, viable organism. Pluripotent stem cells are capable of forming all embryonic cell lineages and thus can form any cell in a postnatal or adult organism. Multipotent cells are capable of differentiating into multiple cell lineages, but the differentiation potential is limited compared to pluripotent cells. Unipotent cells or progenitor cells are limited to one cell lineage. Stem cells can be further divided into embryonic and adult stem cells that are appropriate for differing applications.

#### 17.1.1.1 Embryonic Stem Cells

Embryonic stem (ES) cells are pluripotent cells derived from the inner cell mass of a blastocyst and are capable of differentiating into cells of all three germ layers. ES cells have nearly unlimited proliferative capacity if maintained in the correct culture conditions. Until recently for human ES cell lines, a feeder layer of mouse embryonic fibroblasts and the presence of basic fibroblast growth factor (bFGF) were required, increasing the operating and labor costs of maintaining ES cells. Recent work by Amit et al. has described feeder free culture with serum and growth factor supplementation [1]. Most current strategies utilizing ES cells are designed as allografts or xenografts, which are inherently immunogenic. However, tactics such as immune matching or genetic manipulation can potentially address these concerns.

Since ES cells are pluripotent, they can differentiate into all adult cell types. Uncontrolled differentiation of ES cells can lead to the formation of teratomas, a tumor containing multiple cell types, following implantation. Further, as little as one single undifferentiated ES cell can lead to a teratoma, since ES cells have nearly unlimited proliferative capacity. Complete differentiation of ES cells prior to implantation is, therefore, essential. Differentiation of stem cells is achieved via

numerous signals including mechanical and chemical. Chemical cues such as growth factors must be presented correctly both temporally and spatially to ensure proper differentiation. Thus, controlled delivery of chemical signals is advantageous to ensure a viable tissue engineered construct utilizing ES cells.

#### 17.1.1.2 Adult Stem Cells

Adult stem cells are nonembryonic stem cells derived from a postnatal organism. Adult stem cells are heterogeneous in both source and potency but can typically be obtained from the patient, leading to autografts, thereby reducing the potential for rejection. Adult stem cells are classified as unipotent, multipotent, or pluripotent. While the differentiation potential of unipotent stem cells is limited to one cell lineage, numerous strategies using unipotent cells including neural and hematopoietic stem cells are in development (see [2] for more information). Examples of multipotent adult stem cells include mesenchymal (MSCs) and adipose-derived stem cells (ASCs), while pluripotent adult stem cells have been derived from postnatal cells using genetic manipulation. These cells are termed induced pluripotent stem (iPS) cells.

##### Mesenchymal and Adipose-Derived Stem Cells

MSCs and ASCs are multipotent stem cells with the capacity to differentiate into many cell lineages including neural, osteogenic, chondrogenic, and vascular cell lineages [3, 4]. MSCs have been isolated from numerous non-marrow stromal tissues including muscle and dental pulp. They are frequently isolated from the bone marrow, in particular from the iliac crest. The heterogeneous cell population, which is derived as a result of adherence to tissue culture plastic, may be more appropriately termed "bone marrow stromal cells" (BMSCs) or "multipotent stromal cells." ASCs are located within adipose tissue and are generally isolated during liposuction procedures. ASCs are similar to MSCs in proliferative capacity and differentiation potential, but the large amount of aspirate following liposuction procedures leads to greater numbers of available cells. Compared to ES cells, MSCs and ASCs have limited proliferative capacity and potency, but their ease of isolation and their potential use as autografts can make them advantageous. Further, MSCs can avoid allogenic recognition by forming an immunosuppresive environment, although this capability can vary depending on the donor [5]. Additionally, MSCs and ASCs lack the potential to form teratomas due to their limited potency. Nevertheless, their differentiation beyond mesenchymal tissues is difficult to promote.

##### Induced Pluripotent Stem Cells

IPS cells are a recently characterized cell population that combines many of the advantages of ES and multipotent adult stem cells. They are genetically modified

adult fibroblasts or other somatic cells that function similarly to ES cells because they have nearly unlimited proliferative capacity and are pluripotent [6]. Thus, they can differentiate into all embryonic cell types, be easily expanded in vitro, be obtained from autogenic sources, and are readily available. Teratoma formation can still occur, and thus tight differentiation control is required. Further, for patients with genetic disorders, autografts of iPS cells will maintain the genetic anomalies.

### *17.1.2 Biomaterials for Tissue Engineering*

Cell function is promoted and maintained through a variety of signals including spatial, mechanical, electrical, and chemical cues. Regardless of function, all cells require a substrate upon which to attach, proliferate, and provide structural support. For hard tissues such as bone, biomaterials such as hydroxyapatite or tricalcium-phosphate are used, since they match the mechanical properties of the native tissue. Hydrogels are routinely employed for tissue engineered constructs due to their high hydration levels and viscoelastic properties similar to native soft tissue. Most materials utilized for tissue engineering are biodegradable, allow for cell binding, and biocompatible. This allows cells or the host to remodel the biomaterials for the particular application. Eventually, most tissue engineering strategies aim to integrate the tissue engineered construct into the native tissue to complement or replace the damaged tissue.

Categories of biomaterials used in tissue engineering include natural, synthetic, and inorganic materials (Table 17.1). Natural materials are derived from proteins or polysaccharides and are generally biocompatible, biodegradable and allow for cell binding. The mechanical strength of natural materials is typically lower than synthetic or inorganic materials, but this range can vary depending on formulation. Synthetic materials allow for greater control of material properties such as mechanical strength, swelling ratios, degradation rates, etc., but require the inclusion of cell attachment domains. Further, biocompatibility is of greater concern compared to natural biomaterials. Hybrid materials incorporate aspects of both synthetic and natural materials. Generally, hybrid materials provide greater control of material properties while incorporating domains for cell binding, biodegradation, and/or biocompatibility. Inorganic materials are typically employed for bone applications, since they provide high mechanical strength.

### *17.1.3 Drug Delivery in Tissue Engineering*

As mentioned previously, cell function and stem cell differentiation are controlled from a variety of cues including spatial, mechanical, electrical, and chemical. Spatial cues include density of cell attachment domains, which dictate cell–matrix

**Table 17.1** Common biomaterials for tissue engineering

| | Material | Application | Advantages | Disadvantages |
|---|---|---|---|---|
| Natural polymers | Agarose | Cartilage, nerve | Biocompatible<br>Biodegradable | Mechanical properties |
| | Alginate | Cartilage | Biocompatible<br>Biodegradable | Degradation rate, Poor cell adhesion |
| | Chitosan | Bone, cartilage, skin | Biocompatible<br>Mechanical properties | Poor solubility |
| | Collagen | Bone, cartilage, nerve, soft tissue | Biocompatible<br>Biodegradable | Mechanical properties |
| | Fibrin | Cardiovascular, cartilage, nerve | Biocompatible<br>Biodegradable | Mechanical properties |
| | Gelatin | Cardiovascular, soft tissue | Biocompatible<br>Biodegradable | Mechanical properties |
| | Hyaluronic acid (HA) | Cartilage, nerve, skin | Biodegradable<br>Biocompatible | Stability in vivo |
| | Silk | Bone, cartilage, cardiovascular, soft tissue | Biodegradable<br>Mechanical properties | Pretreatment required |
| Synthetic polymers | PGA, PLA, PLGA | Bone, cartilage, cardiovascular, nerve, musculoskeletal | Biocompatible<br>Biodegradable tailored degradation | Acidic by-products |
| | PCL | Bone, skin | Biodegradable | Acidic by-products |
| | PEG or PEO | Bone, nerve, cardiovascular | Biocompatible<br>Low immunogenicity | Mechanical properties |
| | PET | Cardiovascular | Mechanical properties | Inflammation, limited durability |
| | OPF | Cartilage | Biocompatible | |
| Inorganic polymers | TCP | Bone | Mechanical properties<br>Biodegradable | |
| | Hydroxyapatite (HA) | Bone | Mechanical properties | Not biodegradable, Fragility, Contour limitations |

*PGA* poly(glycolic acid), *PLA* poly(lactic acid), *PLGA* poly(lactide-*co*-glycolide), *PCL* poly(ε-caprolactone), *PEG* poly(ethylene glycol), *PEO* poly(ethylene oxide), *PET* poly(ethylene terephthalate), *OPF* oligo(poly(ethylene glycol) fumarate), *TCP* tricalciumphosphate

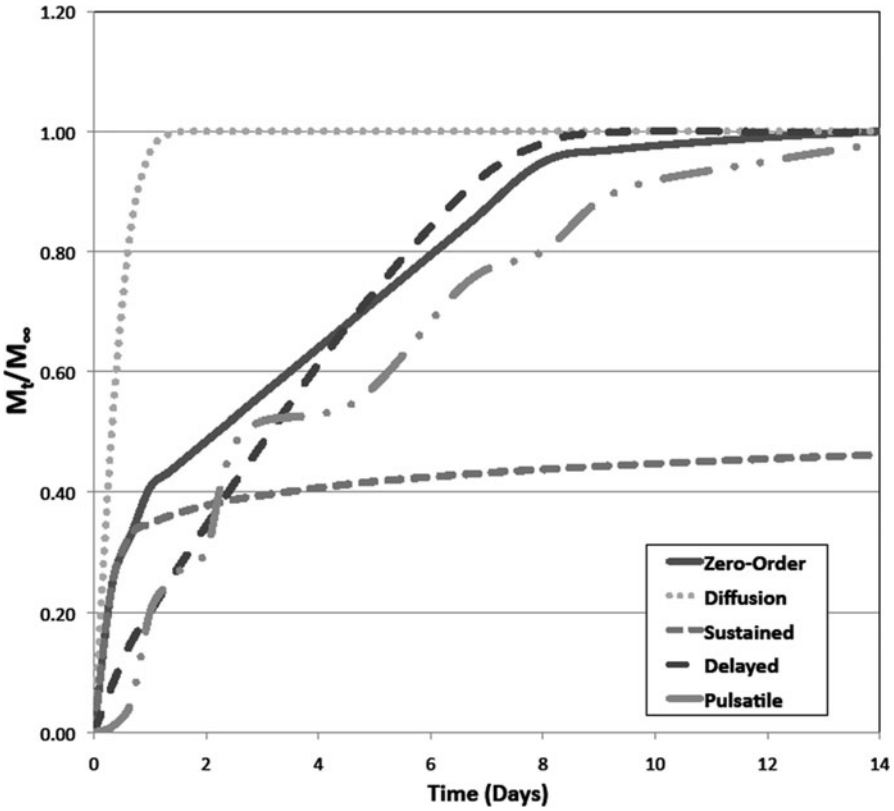


**Fig. 17.1** Graph depicting generalized release curves for different release profiles utilized in tissue engineering. Both zero order and sustained release profiles incorporate a burst release occurring over 1 day. The delayed release profile limits the burst effect

interactions and subsequent cell density. The role of mechanical properties in stem cell differentiation has been examined more thoroughly in recent years with the discovery that stem cell fate can be guided by varying the mechanical stiffness of substrates [7]. In vitro, paracrine or growth factors can be added exogenously to cell media to promote differentiated function. However, this is nonoptimal for in vivo systems and in physiological systems, since the interactions of drugs with the native ECM may alter drug presentation, release, and activity. Additionally, many systems may require multiple drugs to induce cell proliferation, differentiation, and stabilization of tissue engineered constructs. Control of drug uniformity, release, timing, and stability is desirable to ensure differentiation and desired cell function. Thus, a system that combines drug delivery schemes with biomaterial design could improve the efficacy of tissue engineered systems.

Drug delivery systems can be designed with various release profiles to match the desired timing. Common release profiles for tissue engineering include zero order, delayed, sustained, and diffusional (Fig. 17.1). An initial burst is typically present

in both the sustained and zero order release profiles, while a delayed profile has limited burst effect. Multimodal release of multiple drugs can be accomplished by designing systems with multiple release profiles, allowing for tight, temporal control of drug presentation. Release profiles are primarily controlled by the drug loading mechanism. Drugs loaded via physical incorporation or electrostatic interactions typically follow a diffusional release profile, where the apparent diffusion constant depends on the association and dissociation constants between the biomaterial and the drug. Covalent conjugation can lead to multiple release profiles dependent on the biodegradability of the linker. Biodegradable linkers are typically associated with zero order or delayed release profiles, while nondegradable linkers are more common with sustained release profiles. Burst effects can be minimized by removing or limiting unassociated drug.

Growth factors and cytokines are the primary drugs utilized in tissue engineering, and this chapter focuses on their delivery. While controlled delivery of growth factors to cells has been shown to be beneficial in regeneration, the extent of cell activity is limited by availability and short bioactivity half lives (typically on the order of hours). Gene delivery provides an alternative means to induce cells to overexpress their own proteins for tissue renewal [8, 9]. The DNA corresponding to the growth factors of interest can be transformed into the cell genome by either viral [10, 11] or nonviral means [12].

The use of viral vectors for gene transfer is an effective and efficient approach, infecting both dividing and nondividing cells, but immunogenicity is associated with the technique [12]. Viral transfer is often performed with adenoviral vectors, which has a high level of protein expression and can be used to introduce inserts of up to 8 kb [13]. These viruses can be used for the transformation of nondividing cells as well as dividing cells. Simply, the genes coding for the growth factor of interest are transformed into a plasmid, incorporated into adenoviral DNA by homologous recombination, after which the adenoviruses are incorporated into a scaffold where they can target the cells of interest. Additionally, cell markers such as green fluorescent protein (GFP) can be delivered, which when transcribed by the host cell replication machinery will fluoresce green. Immunogenicity can be circumvented by nonviral gene transfer techniques. Nonviral techniques use electroporation, direct injection, or lipid mediated transfection to introduce the genes corresponding to growth factors directly into the cells [12]. At a certain frequency, which varies depending on the cell type [14], a vector containing the growth factor DNA gets incorporated into the target cell genome. Both viral and nonviral vectors can be incorporated into a scaffold, allowing for either sustained or timed plasmid presentation.

## 17.2 Cartilage and Bone

### *17.2.1 Introduction*

As with numerous tissues, the efficiency of self-repair for bone and cartilage is dependent on the type and extent of injury sustained. The potential for repair is limited by the cell's inherent repair potential and an injury microenvironment that

prevents regeneration. The osteoblasts of bone [15] and the chondrocytes of cartilage [16] generally secrete limited amounts of ECM proteins and only remodel their environment to maintain general stability. As a result, the cells alone are not enough to fill the void that is left by the trauma of injury.

Generally, grafts must not only mimic the structural and mechanical requirements of the tissue they are replacing, but they should also promote cell attachment, migration, proliferation, and differentiation [17, 18]. This guidance can be accomplished by a combination of mechanical cues provided by the material as well as chemical cues. The latter are of particular interest because cytokines and growth factors play a significant role in tissue regeneration. The precise combinations and concentrations of these biochemical cues that produce structurally viable autologous tissue are under current investigation [17]. This section focuses on drug delivery strategies for bone and cartilage regeneration.

## *17.2.2 Biological Properties of Bone and Cartilage*

### 17.2.2.1 Bone

Bone provides many important biological functions not only for structural support but also for tendon, ligament, and muscle attachment [19]. Bone is made up of primarily an inorganic calcium phosphate matrix with embedded macromolecular fibers. ECM proteins deposited by osteoblasts, one of the primary cell types of bone, in combination with glycosaminoglycans such as hyaluronic acid (HA) and chondroitin sulfate collectively contribute to bone's strength and integrity [20, 21]. These osteoblasts, along with osteocytes (mature osteoblasts), osteoclasts (matrix degrading cells), and progenitor cells, become embedded among the fibrous tissues containing collagen types X and I, which make up the bulk of ECM proteins and provide the mechanical integrity required for proper function following mineralization [21]. Bone is a dynamic tissue and is constantly being remodeled by the coordination of both matrix synthesis and degradation. Bone morphogenic proteins (BMPs) and other signals are critical for coordinating these processes. This coordination is performed by numerous signals, the most important of which include BMPs. The combination of these events promotes bone regeneration following injury.

The ability to regenerate bone postinjury depends on the size of the defect. If the defect is small enough, osteoblasts can secrete enough ECM to regenerate any bony tissue that had been damaged [15, 22]. Typically, the cytokines that trigger wound healing responses are sufficient to regenerate the bony tissue of small defects [23, 24]. However, as defects become larger, the likelihood that osteoblasts will be able to synthesize enough collagen to fill in the void left by injury diminishes. For these reasons, injuries following trauma or disease require surgical intervention.

#### 17.2.2.2 Cartilage

Cartilage plays an important role in vivo by providing a frictionless, smooth surface to mediate load transfer for the subchondral bone [25]. The primary cells of cartilage, chondrocytes, are responsible for maintaining the ECM, which consists of collagen type II, glycosaminoglycans (GAGs), and proteoglycans (PG). The actual cell concentration within the mature tissue is low; 2% of the total volume of cartilage is composed of cells [26]. The low concentration of cells, as well as their low mitotic activity, limits the extent of cartilage tissue regeneration following injury. In addition to injury, osteoarthritis is one disease that can lead to cartilage loss [27, 28].

Tissue engineering strategies for repair have mostly focused on articular cartilage. Articular cartilage, which lubricates the tibia and femur in the knee joint, is particularly susceptible to tears. Since the most effective treatment methods to replace cartilage use autologous grafts [29], cartilage plugs from a non-load bearing region are removed and transferred to the injured area [30]. However, autologous grafts often exhibit donor site morbidity that can interfere with overall patient recovery. Another common repair strategy includes microfracture, where small fractures are created in the injured cartilage to expose the vasculature underneath the subchondral bone [25]. The presence of blood within the area of injury provides the source of cells and cytokines required to facilitate repair.

For both bone and cartilage, current methods of surgical intervention are very expensive. In 2005, it was reported that at least $3.6 billion was spent on bone repair alone [31]. Further, over 46 million people in the USA suffer from osteoarthritis, and this number is projected to increase in the future [32]. Consequently, tissue engineering has a potential niche in the discovery of new and improved ways to treat bone and cartilage injuries. The ability to generate a construct ex vivo that could fully regenerate damaged bone and cartilage is becoming a larger focus of the biotechnology industry around the world.

### *17.2.3 Biomaterials for Bone and Cartilage Tissue Engineering*

#### 17.2.3.1 Bone

Natural Polymers

Natural polymers, such as collagen and HA, are often used in tissue engineering strategies for their optimal properties. Both collagen type I [33, 34] and HA [35, 36] have been utilized in sponge form as a scaffold to support tissue remodeling in vivo. However, a disadvantage of fabricating sponges of collagen or HA alone is that these constructs have poor mechanical strength. To address this, hydroxyapatite [34] or poly(glycolic acid) (PGA) crystals [37] can be incorporated into scaffolds to

increase their strength. Cells seeded on these composite materials have higher DNA content, ECM deposition, and gene expression profiles, which have all been implicated in bone maturation.

Synthetic Polymers

One of the main advantages of using synthetic biomaterials in tissue engineering is that the mechanical and resorption properties can be altered more easily than natural polymers. Altering the concentration of poly(lactic acid) (PLA) or PGA in poly(lactide-*co*-glycolide) (PLGA) can alter its rate of resorption in vivo while providing improved strength over natural polymers [38]. However, despite the improved mechanical properties and strength compared to natural polymers, their integrity is still inadequate for full bone recovery. Another disadvantage of PLGA is the potentially acidic by-products that are released during resorption [19].

Alloplastics are synthetic polymers derived from poly(methylmethacrylate) (PMMA) with higher mechanical stability compared to other synthetic polymers [39]. Hard Tissue Replacement (HTR®) is a type of alloplastic that has been developed specifically for bone reconstruction. This FDA approved device has spherical pores that promote bone formation and can also be loaded with proteins to further cell proliferation and bone regeneration [39].

Calcium phosphate cements (CPCs) are also frequently used in bone tissue engineering because of their mechanical integrity and natural porosity [40–42]. Calcium phosphates occur naturally in vivo and are relatively easy to synthesize in a laboratory [38]. They are also versatile and harden in vivo to form hydroxyapatite [38, 41]. Ultimately, protein modification can improve the load bearing potential, biocompatibility, and mechanical integrity of these biomaterials [41, 42].

#### 17.2.3.2 Cartilage

Natural Polymers

A popular biomaterial for cartilage tissue engineering is collagen, and both collagen types I and II have been investigated for cartilage regeneration [43]. While collagen type II is predominant in cartilage [15], collagen type I scaffolds (as well as hybrid scaffolds) are often chosen for tissue engineering applications because of their greater availability [27, 44, 45]. As cells attach and proliferate on these porous scaffolds, the type I collagen will eventually be replaced by the type II collagen secreted by chondrocytes. As for bone regeneration, there are some concerns about the mechanical stability of 3D collagen scaffolds without further modification by other proteins.

Fibrin gels are particularly useful in tissue engineering because of their biocompatibility and controllable resorption rates. Fibrin gels are formed by thrombin-mediated crosslinking of fibrinogen, which forms a network into which cells and

other proteins can be embedded [27, 46]. Fibrin is typically prepared in hydrogel form so that cells are completely encapsulated by the matrix. These gels support chondrocyte outgrowth and ECM deposition and have been shown to promote cartilage regeneration [47]. Fibrin gel mechanical properties, resorption rates in vitro and in vivo, and contraction can be modified by crosslinking other polymers such as poly(ethylene glycol) (PEG) [47, 48].

Silk is another natural polymer with potential in cartilage tissue engineering. Silk fibroin is generated by insects and spiders and has historically been used for surgical sutures [38]. This polymer also benefits from its mechanical robustness and degradability both in vitro and in vivo. However, silk fibroin alone is not biocompatible and needs to be washed and undergo protein modification prior to its use. Modification by RGD (Arginine–Glycine–Aspartic Acid) [49–51], or plasma treatment [52], has been used to improve biocompatibility and cell attachment. Studies have demonstrated that cells cultured on porous silk scaffolds had increased GAG and collagen type II production compared to controls [50, 51].

Alginate and agarose are other materials that can promote cartilage regeneration. Cells can be encapsulated in alginate, which is a biomaterial derived from algae that mimics ECM, ultimately supporting cell function [53, 54]. Encapsulation of chondrocytes or chondrocyte precursors provides the cells with a suitable ECM while minimizing potential mass transfer limitations [54].

Agarose has also been used in hydrogel form to entrap cells and promote chondrogenesis of precursor cells [55, 56]. These agarose hydrogels can be combined with a more structurally sound scaffold to further enhance the potential of regenerating a cartilage-like product in vitro and in vivo.

### Synthetic Polymers

Synthetic polymers used as scaffolds in cartilage tissue engineering can withstand significant amounts of stress present in load bearing areas of articular cartilage. Often, natural polymers are most effective for cell encapsulation. However, an additional material is required to provide the mechanical integrity to support knee function. Synthetic materials are also much more reproducible compared to natural polymers, offering more controlled properties including degradation rate and microstructure [15].

Porous, sponge-like scaffolds are the most effective options for development of functional cartilage tissue. The porosity allows for cell migration and uniform cell distribution within the graft. The design also provides a template for cartilage formation, while maintaining mechanical integrity. PLGA has been demonstrated to be more labile than PLA or PGA alone [29]. Many studies have focused on the combination of polymers such as PLGA or PLLA with hydrogels containing the cells [57–59]. These hybrid scaffolds significantly improve collagen deposition, protein production, and gene expression compared to controls.

While the ability to tailor properties of PLGA is advantageous, some reports have suggested that there are still mechanical limitations in the development of a

porous scaffold [60]. Poly(ε-caprolactone) (PCL) is another popular synthetic, degradable polymer that overcomes these issues [43, 61]. This material satisfies many requirements necessary for a graft: it is malleable, facilitates chondrogenesis, and has a high initial stiffness while still being resorbable over time [61]. Like PLGA, this material might be best utilized in combination with an ECM based hydrogel that promotes cell proliferation and differentiation, with minimal mass transfer limitations.

### *17.2.4 Drug Delivery Strategies*

Mechanical stimulation of cells by the presence of a scaffold is not enough to effectively drive bone or cartilage regeneration. In vivo, cells are exposed to multiple protein signals that direct cell fate. These signals induce a cascade of signaling events, which ultimately lead to transcription of genes and synthesis of specific cytokines or proteins. These cytokines are particularly important during development and wound healing events. They can increase the activity of an already differentiated cell (such as increasing ECM production), or they can guide the differentiation of a progenitor cell or stem cell. The use of growth factors in combination with biomaterials can lead to the development of a more functional tissue.

However, one particular issue that still demands attention is control of cell response. Simple injection or soluble delivery of a growth factor can affect the fate of the target cells, as well as the cells around them. This could lead to undesirable side effects. Drug delivery strategies attempt to address this problem by providing controlled release of a growth factor to a defined area [17]. This can be accomplished by simple adsorption of proteins to the scaffold, or by encapsulation so that cells are continuously being exposed to specific concentrations of growth factors. This section describes some of the strategies, growth factors, and material combinations that are potentially effective for bone and cartilage tissue engineering.

#### 17.2.4.1 Drug Delivery in Bone Tissue Engineering

BMP-2 and BMP-7

BMPs occur in many different isotypes and have important roles in the development of bone as well as cartilage. BMP-2 and BMP-7 specifically have been shown to have the potential to induce osteogenic differentiation of stem cells. Some studies have suggested that BMP-2 may be specifically osteogenic, while BMP-7 induces a chondrogenic phenotype in stem cells under appropriate conditions [62, 63].

Effective delivery of BMPs to a site of injury requires a material that is osteoconductive, osteoinductive, and osteogenic [64]. Materials that have been

tested for BMP-2 and BMP-7 delivery include chitosan microspheres [63, 65], gelatin [66], collagen [65, 67], PLGA [68], and inorganic materials such as hydroxyapatite [69] and CPC [67]. For most of these applications, the polymers are formed into sponges individually or in composite form, and a hydrogel is prepared as a carrier for BMP. Composite materials are beneficial in that they allow a more sustained growth factor release [65]. Studies have demonstrated that controlled delivery of BMPs by these systems could enhance osteogenesis in vivo [65] and in vitro [69].

### IGF-1

Insulin-like growth factor-1 (IGF-1) is a regulator of bone formation and is involved in cell differentiation into osteoblasts [24]. Jayasuriya's group [24] examined the release kinetics of IGF-1 from a bone-like mineral layer (BLM), which was coated on a PLGA scaffold. The group found there was a burst release of IGF-1 over the first 3 days, followed by a sustained release over the remaining 30 days. Over the duration of the release, IGF-1 remained active and the bone marrow stem cells (BMSC) exposed to the IGF-1 became osteogenic.

### VEGF

Vascular endothelial growth factor (VEGF) is a cytokine that is important in the development of vasculature and wound healing. Since revascularization is an important part of wound healing, controlled delivery of VEGF to a bone defect might accelerate reformation. Composite alginate–chitosan microspheres have been created by emulsification and gelation methods [70], and loaded with various concentrations of VEGF. Results demonstrated that a burst release of 13% occurred within the first 24 h, followed by a zero-order release over 5 weeks. The growth factor remained localized within the site of delivery, and VEGF remained bioactive over this time period.

### PDGF-BB

Another neovascularization-promoting growth factor, the BB isoform of platelet-derived growth factor (PDGF-BB), showed similar results when embedded in a natural polymer called carrageenan [71]. Following an initial burst release around 3 days, PDGF-BB was released with a zero order profile. These studies indicate that the delivery of a combination of proangiogenic and osteogenic growth factors by controlled release holds promise in bone regeneration.

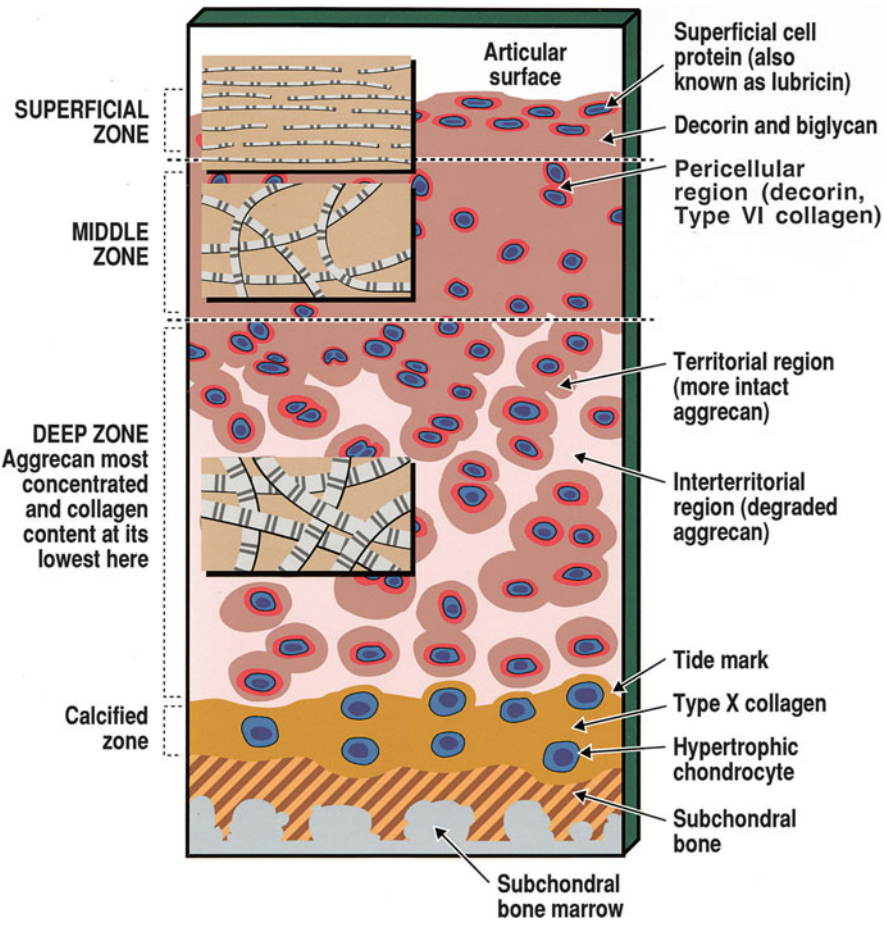


**Fig. 17.2** Schematic representing the structure of human articular cartilage from an adult including zones, regions, and special features of molecular contents. *Insets* demonstrate relative diameters and organizations of collagen marcrofibrils in different zones. Reprinted with permission from Poole et al. [72]

#### 17.2.4.2 Drug Delivery in Cartilage Tissue Engineering

Cartilage repair is challenging because of its zonal composition. Cartilage is composed of multiple zones (Fig. 17.2), each with different structural properties. Repair of larger defects in the articular cartilage would need to address the biological properties of each zone to achieve full functional recovery [27]. For this reason, controlled release of growth factors to the area of injury could achieve higher levels of repair.

### TGF-β1 and TGF-β3

Transforming growth factor-β1 (TGF-β1) has been well established to be a growth factor necessary for progenitor cell differentiation into cartilage tissue. Supplementation of this growth factor in MSC culture medium increases collagen type II synthesis and ECM production by chondrocytes [27]. Consequently, TGF-β1 has been used for controlled release applications in cartilage regeneration. Materials that have been tested include PLGA–PEG composites [73], PCL [74], gelatin [75], chitosan [76, 77], and polyesters [78].

A typical controlled release construct used in cartilage tissue engineering is a combination of TGF-β1 containing microspheres with a sponge-like scaffold developed by drying the gel under a vacuum. The scaffold can be used not only as a structural support but also to physically entrap TGF-β1 within the pores [78]. Subsequently, TGF-β1 is only released as the scaffold itself resorbs. Thus, release rate is sustained and dependent on scaffold resorption. In studies that used this controlled release method, chondrogenesis was significantly improved as made evident by increased collagen type II levels and decreased DNA synthesis [74, 78].

Alternatively, TGF-β1 has been encapsulated in microspheres and has been incorporated into a sponge-like scaffold. The rate of release varies depending on the materials used to create the composite scaffolds. In PLGA/PEG constructs, a burst release of TGF-β1 was observed as high as 70% in 1 day [73], while there was only 45% release of TGF-β1 from chitosan–collagen–GAG composite scaffolds in the first 7 days [76]. Overall, the release of TGF-β1 has been shown to enhance chondrogenesis.

While TGF-β3 is another potent prochondrogenic growth factor, limited research has been performed to characterize its potential compared to TGF-β1. TGF-β3 is commonly used as a supplement for differentiation of stem cells into chondrocytes during pellet culture [26, 79]. Studies have shown that TGF-β3 stimulates GAG and ECM synthesis when supplemented temporally for up to 3 weeks when released from gelatin microspheres [26]. After 3 weeks, the stimulatory effect of this growth factor appears to diminish [80].

### IGF-1 and TGF-β1 Codelivery

TGF-β1 alone may be insufficient to guide differentiation toward chondrogenic phenotypes. It was hypothesized that both IGF-1 and TGFβ1 would be required to definitively guide stem cell differentiation. In this study, soluble TGF-β1 was provided to the culture medium of stem cells seeded into an IGF-1 loaded silk scaffold [51]. Researchers observed that scaffolds further supplemented with TGF-β1 did not significantly increase collagen production or gene expression of chondrogenic markers compared to IGF-1 alone [51].

FGF

Fibroblast growth factor-2 (FGF-2) has also demonstrated the potential to promote chondrogenesis in vitro [81]. FGF-2 release for articular cartilage regeneration has not been investigated; however, studies have observed benefits to tracheal cartilage regeneration [82]. When physically entrapped in a gelatin sponge, the sustained release of FGF-2 would significantly increase tracheal cartilage over time. Further studies would need to be carried out to demonstrate that these results translate into articular cartilage repair.

## *17.2.5 Future Directions*

### 17.2.5.1 Dual Growth Factor Delivery

In vivo, growth factors can work in concert, stimulating biological processes that are required for uniform tissue development. As described above, most groups have been studying the most effective ways to deliver single growth factors, either with microparticles or localized delivery by adsorption into a porous scaffold. The next generation of controlled release technology is the delivery of multiple growth factors or combinations of signals to an injured area.

Current research for bone tissue engineering is focused on the potential of IGF-1 and BMP delivery to cells. Research suggests that delivery of growth factors would have an additive effect on bone regeneration [83]. In a periodontal bone regeneration study, both IGF-1 and BMP-2 were individually encapsulated into microspheres and these microspheres were loaded into porous gelatin scaffolds for delivery to defects [83]. Results suggest that repair could be improved by the controlled release of both growth factors versus delivery of the proteins individually.

As mentioned previously, MSC differentiation has been guided by loading a growth factor into a scaffold (IGF-1) while simultaneously providing a soluble growth factor (TGF-β1). These experiments were taken an extra step forward by developing a controlled release system for both growth factors together [75, 84]. The combined delivery of IGF-1 and TGF-β1 lead to increased GAG and collagen type II synthesis by chondrocytes compared to each growth factor individually [85]. Consequently, the development of more sophisticated release systems may increase the functional outcome of tissue engineered products.

## 17.3 Neural Tissue Engineering

### *17.3.1 Introduction*

#### 17.3.1.1 Physiology of the Nervous System

The nervous system is derived from the dorsal portion of the embryonic ectoderm and classified into the central nervous system (CNS) and the peripheral nervous system (PNS). The CNS includes the brain and spinal cord, while the PNS connects the CNS to other parts of the body. Neural tissue is made up of neurons and associate glial cells. Neurons are the basic structural and functional elements of the nervous system. Neurons consists of a cell body, branch-like extensions off the cell body called dendrites, and at least one longer extension off the cell body called an axon. The dendrites conduct signals from their tips toward the neuron cell body. The axon carries messages away from the cell body toward the terminal end of the axon, where it communicates with other cells. Glial cells are support cells and they maintain the extracellular environment to best suit and nourish neighboring neurons. The CNS and PNS have two distinct types of glial cells. In the PNS, the glial cells are Schwann cells, which produce myelin to facilitate more effective transportation of neurotransmitters. In the CNS, the glial cells are oligodendrocytes and astrocytes, which both play key roles in CNS support and metabolism. However, unlike Schwann cells, oligodendrocytes and astrocytes inhibit axon regeneration. Therefore, the CNS has limited ability to regenerate, in contrast to the PNS.

### *17.3.2 Nerve Injury and Regeneration*

Nerves are bundles of axons from different neurons that carry signals in the same direction. Nerves can be damaged either through trauma or disease. The most dramatic and serious nerve damage occurs to the spinal cord. Damage to the lower spinal column may lead to paralysis of the lower extremities, and damage to the upper spinal column may lead to paralysis of all four extremities. The incidence of spinal cord injury in the USA is 11,000 per year, and the prevalence is 250,000–400,000 [86]. The cost to support a patient with a spinal cord injury through his or her lifetime is estimated to lie between $400,000 and $2.1 million, depending on the severity of injury [87]. The injured spinal cord produces a complex inhibitory environment that suppresses nerve regeneration. After injury, a fluid filled cavity forms at the site of injury and becomes surrounded by a dense glial scar. Glial scarring and inhibitory molecules prevent neurons from infiltrating the injury site, resulting in a loss of axonal connection and motor function.

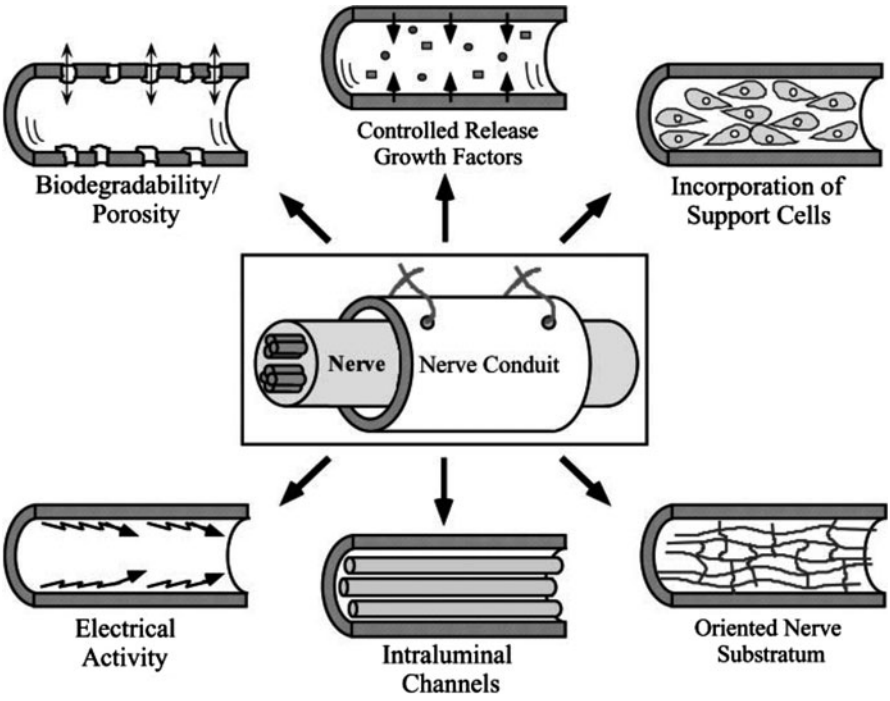


**Fig. 17.3** Schematic presenting the properties of an ideal nerve guidance channel. *Clockwise from top left*: Biodegradable; able to release growth factors; incorporation of supporting cells; oriented matrix to promote cell migration; intraluminal channels that mimic nerve fasicles; and electrical activity. Reprinted with permission from Hudson et al. [92]

### *17.3.3 Biomaterials for Neural Tissue Engineering*

The clinical approach to nerve repair has been to suture together the fascicles of nerves from either side of an injury to bridge the gap [88]. Suturing fascicles together provides a connective tissue conduit for the outgrowth of new axons and helps guide them to their original targets. Currently, this strategy is most successful with PNS nerves. However, even in the best clinical results, only a fraction of the axons in an injured nerve reintegrate to their target. In the CNS, axonal injury carries much poorer prognosis and there have been no substantial clinical successes in regenerating axons in the CNS after traumatic injury. Further, for larger gaps, autologous grafts are inserted between the nerves with limited recovery. The emerging field of neural tissue engineering has provided alternative strategies for restoring nerve function after injury [89–91]. Researchers have designed implantable scaffolds to bridge nerve tissue, creating physical and chemical guides to stimulate axonal regeneration. Compared with autologous grafts, where appropriate donor material may be difficult to obtain, these artificial scaffolds offer a number of important advantages. They can be constructed with desired mechanical and chemical properties to control drug delivery (Fig. 17.3).

#### 17.3.3.1 Natural Materials

Agarose, collagen, fibrin, and hyaluronic acid (HA) are selected examples of natural materials that have been highly investigated in neural tissue engineering. Agarose hydrogels can be used to stimulate and maintain three dimensional neurite extension from primary sensory ganglia in vitro. Previous work has identified the optimal concentration (1 w/v%) of agarose for neural tissue applications [93, 94]. Collagen is the major protein component of the ECM and has been extensively characterized as a potential scaffold for neural tissue engineering [95, 96]. The softness and large compliance of the fibrin gel appear to be essential for its efficiency as a matrix for cells, such as neurons, that normally reside in very soft tissues such as brain [97–99]. HA is a high molecular weight GAG found naturally in the brain ECM, which make it an attractive choice for neural tissue engineering [100].

#### 17.3.3.2 Synthetic Materials

Synthetic materials have also been widely used for neural tissue engineering. Synthetic materials can be tailored to produce a wide range of mechanical properties and degradation rates. They also have known compositions and can be designed to minimize the immune response. Currently, poly(ethylene oxide) (PEO or PEG), poly(ethylene-*co*-vinyl acetate) (EVAc), poly(glycolic acid) (PGA), poly (lactic acid) (PLA), and polypyrroles (Ppys) are commonly used [101–104].

### *17.3.4 Drug Delivery in Neural Tissue Engineering*

Numerous drug delivery strategies have been explored in an attempt to enhance nerve regeneration. A large portion of research has focused on exogenously administering therapeutic drugs, which include neurotrophins, anti-inflammation drugs, and other growth factors (Table 17.2).

Many methods have been developed in the production of sustained drug release systems from scaffolds for neural tissue engineering. One of the most common methods is to utilize the physical properties of the scaffold materials to regulate the amount of drug delivery. Therapeutic drugs are incorporated into scaffolds during fabrication by mixing with the scaffold precursors. In such systems, drug release is regulated by the diffusion constant. The pore size, crosslink density, and the degradation rate of the scaffold affect the release kinetics. For treatment of peripheral nerve injury, these drug delivery scaffolds are usually fabricated into nerve guidance conduits (NGCs) (Fig. 17.3). A variety of growth factors including nerve growth factor (NGF), neurotrophin-3 (NT-3), brain-derived growth factor (BDGF), and glial cell-derived neurotrophic factor (GDNF) have been tested for release from the NGCs [105, 106]. Drug delivery from these NGCs was

**Table 17.2** Therapeutic drugs for neural tissue engineering

| Type | Drug | Function |
|---|---|---|
| Neurotrophins | NGF | Enhance survival of neurons |
| | NT-3 | Neurogenesis |
| | NT-4/5 | Maintenance of nervous system |
| | BDNF | Direct neural development |
| Other growth factors | GDNF | Neuroprotective |
| | | Trophic factor for dopaminergic neurons |
| | CNTF | Enhance motor neuron survival and outgrowth |
| | TGF-β1 | Reduce astrocyte proliferation |
| | bFGF | Induce angiogenesis |
| | | Promote cell proliferation |
| Anti-inflammation drugs | Dexamethasone | Reduce inflammation and immune response |
| | α-MSH | Inhibit production of inflammatory cytokines |

*NGF* nerve growth factor, *NT-3* neurotrophin-3, *NT-4/5* neurotrophin-4/5, *BDNF* brain derived neurotropic factor, *GDNF* glial derived neurotrophic factor, *CNTF* ciliary neurotrophic factor, *TGF-β1* transforming growth factor-β1, *bFGF* basic fibroblast growth factor, *α-MSH* α-melanocyte stimulating hormone

characterized by an initial burst followed by sustained release for up to 30 days. Collagen scaffolds were tested to deliver NT-3 to the site of spinal cord injury in animal models and showed improved functional recovery compared to the animals that only received the collagen scaffold without growth factor [107]. Bellamkonda's group has demonstrated that BDGF released from agarose scaffolds can improve axon infiltration into the scaffold and decrease the immune response caused by spinal cord injury [108].

Affinity based drug delivery scaffolds have also been developed for neural tissue engineering. Many drugs will bind noncovalently to heparin, which can be incorporated into a scaffold and released with a sustained profile as the drug disassociates from the heparin molecule. Recently, heparin binding systems have been used in conjunction with fibrin scaffolds to treat nervous system injury. This system consists of four components: a scaffold (e.g. fibrin), a bidomain peptide, heparin, and a growth factor. The peptide consists of a factor XIIIa substrate, which allows the covalent incorporation into fibrin scaffolds, and a heparin binding domain derived from antithrombin III. This peptide binds to heparin, sequestering it inside of the scaffold. The heparin, in turn, can bind the desired growth factor. It has been reported that fibrin scaffolds containing a heparin binding system and NT-3 promoted neuronal fiber sprouting when compared to animals treated with fibrin without the delivery system [109].

Another approach that has been used for drug delivery involves the covalent conjugation of drugs into scaffolds. One way of covalently tethering proteins to the scaffold is using photochemistry. Researchers have bound NGF to polydimethysiloxane using this method [110]. Many types of amine and carboxyl attachment chemistries have been developed to immobilize drugs to scaffolds. An important consideration of this approach is to ensure that the covalent binding process does not affect the bioactivity of the drugs.

### 17.3.5 Conclusions and Future Directions

Neural tissue engineering provides a potential treatment for nervous system injuries. Many different scaffold materials, drugs, and methods of controlled release have been developed. Recent studies indicate that the locations where the neural precursor cells reside (known as NSC niche) regulate stem cell behavior and tightly control their potential to proliferate, differentiate, and survive as newly formed neurons. The cues encountered within these sites consist a broad range of signaling mechanisms. A number of signaling pathways, such as Wnt and sonic hedgehog homolog (Shh), are conserved and function prominently in both the developing nervous system and the germinal zones of the adult brain, supporting the neurogenic niche.

In addition, the vasculature has been identified within the adult NSC niche as a prominent feature, which suggests that it plays an important role in niche regulation and maintenance. The vascular derived molecules shown to locally regulate the adult NSC niche include leukemia inhibitory factor (LIF), BDGF, VEGF, PDGF-BB, pigment epithelium-derived factor (PEDF), and laminins. Endothelial cells have also been reported to exert their influence over NSCs to regulate fate specification by either secreted factors and cytokines or direct contact.

In the future, a solid understanding of the cellular mechanisms underlying neuronal regeneration, and the important role of the vasculature, will enable the development of more appropriate scaffolds for neural tissue engineering. Multiple growth factors may be required to cause a synergistic effect on neuronal regeneration.

## 17.4 Cardiovascular Tissue Engineering

### 17.4.1 Introduction

The cardiovascular system includes the heart and associated arteriole and venous circulation. The contractile myocardium is composed of a dense, layered tissue containing cardiomyocytes, cardiac fibroblasts, and associated vasculature. Repair in the cardiac environment is limited due to the low regenerative capacity of cardiomyocytes. Blood vessels provide oxygenated blood to the heart in addition to the rest of the body tissues. Muscular vessels comprise varying thicknesses of three important structural layers: the intima is the innermost layer of the endothelium that mediates the interaction with blood, the media is the middle layer containing contractile smooth muscle cell, and the outer adventitia is primarily composed of fibroblasts in a connective matrix.

Cardiovascular disease (CVD) involves the heart or blood vessels and is the leading cause of death in the developed world. Uncontrolled CVD leads to myocardial infarction (MI) and stroke with resulting tissue ischemia and loss of

function. The most common surgical treatment for MI remains autologous cardiac bypass grafting using saphenous veins or mammary arteries. Unfortunately, many patients with CVD do not have a viable source for grafting due to vessel damage. Further, synthetic grafts are not suitable for small diameter vessel reconstruction due to the high incidence of thrombosis in these conduits. Current strategies for cardiovascular tissue engineering include the development of tissue engineered vascular grafts for blood vessel replacement, targeted drug delivery of angiogenic factors toward ischemic tissue, and delivery of fully differentiated or progenitor cells to replace or repair vascular structures.

## *17.4.2 Challenges and Strategies for Cardiovascular Tissue Engineering*

### 17.4.2.1 Tissue-Engineered Vascular Grafts

Tissue engineering strategies have been applied to the creation of vascular grafts. The current paradigm employs seeding cells onto an engineered scaffold and culturing the construct in the presence of soluble paracrine factors with or without mechanical conditioning. Critical to the replacement of the coronary artery is the replacement of the medial layer of contractile smooth muscle as well as the nonthrombogenic lumenal layer. Medial equivalents aim to recapitulate the medial layer of the arterial wall thus providing mechanical strength sufficient for bypass grafting. Typically, cells are seeded onto a construct with or without exogenous or loaded growth factors and cultured in vitro over weeks to months. Medial equivalents can be cultured under pulsatile flow to mimic the natural loading of blood vessels, improving mechanical strength and aligning cells in the direction of flow [111]. Nevertheless, medial equivalents are limited by cell number and the long incubation time required in vitro.

Endothelium presents a nonthrombogenic surface, and providing an endothelial layer to the lumen of vascular grafts could improve patency of both synthetic and tissue engineered grafts. Clinical trials with Dacron grafts seeded with endothelial cells have described a 90.5% patency rate after 1 year following implantation [112]. Nevertheless, this method is limited by the number and proliferation capacity of endothelial cells (ECs). The use of endothelial progenitor cells (EPCs) or other stem cells may alleviate this issue, but requires a system to promote differentiation. Drugs to promote host endothelial migration and proliferation have been released from vascular implants but are limited by the number and proliferative capacity of available host endothelial cells. Pioneering work by Weinberg and Bell reported a vascular graft composed of layers of smooth muscle cells (SMCs) in a collagen gel and a Dacron mesh containing fibroblasts, followed by EC seeding [113]. While a graft could be formed, it had insufficient mechanical strength for vessel replacement. High strength, completely biological, blood vessel substitutes have been described. ECs and SMCs isolated from human umbilical veins and fibroblasts isolated from human dermis have been cultured over extended periods with measured burst strengths of 2,000 mmHg [114].

#### 17.4.2.2 Revascularization

Revascularization of ischemic tissue has the potential to enhance healing if new vessel growth can be maintained. Therapeutic angiogenesis aims to revascularize ischemic tissue by controlling drug or growth factor delivery. There have been a number of clinical and preclinical trials utilizing growth factor delivery systems to individually enhance neovascularization in distinct applications [115–117]. However, they have been suboptimal in the clinical setting due, in part, to a lack of vessel stabilization. Specifically, delivered growth factors induce the formation of new vessels. However, without the necessary vessel stabilization cues, the newly formed vasculature regresses. In addition, growth factors have reduced stability in aqueous solutions, leading to limited functionality [118]. Controlled growth factor delivery would maintain bioactivity, allow for control of the release rate, and improve revascularization of the ischemic site. More biologically relevant strategies make use of multiple growth factors and combinations of cells and/or growth factors.

Cell based approaches to neovascularization in vivo have relied on the manipulation of fully differentiated cells, but sourcing and expanding differentiated cells for therapeutic use is problematic and has driven research into stem and progenitor cells. Vascular progenitor cells including EPCs have been isolated from peripheral blood and bone marrow [119]. EPCs have been shown to differentiate toward ECs in culture both with and without VEGF [119, 120]. Populations of smooth muscle progenitor cells (SPCs) have also been isolated from peripheral blood. SPCs grown in culture in the presence of PDGF-BB were positive for SMC markers, but also presented bone marrow angioblastic markers [121]. SMC phenotype has also been induced from bone marrow derived MSCs as a result of TGF-β1 exposure [122]. Drugs and cytokines associated with angiogenesis have demonstrated similar functionality in vascular development, and thus similar strategies are employed. Differentiation of stem and progenitor cells to ECs and SMCs has not only been demonstrated in culture in response to cytokines but also to varying extents in vivo. Furthermore, several progenitor cell types have been shown to improve perfusion and recovery in ischemic muscle models.

### *17.4.3 Biomaterials for Cardiovascular Tissue Engineering*

#### 17.4.3.1 Natural Scaffolds

The most commonly investigated natural materials in vascular tissue engineering include fibrin, collagen, gelatin, and alginate. Fibrin is the main constituent of blood clots and is formed by thrombin mediated and covalent crosslinking of fibrinogen monomers [46]. Fibrin contains cell attachment domains and is biodegradable by specific proteases including plasmin and matrix metalloproteinases. Concentrations of

fibrin(ogen) in the range of 1–10 mg/ml are suitable for vascular tissue engineering, but will degrade within 2 weeks in vivo. For vascular grafts constructed in vitro, SMCs or SPCs will compact the gel in the presence of ε-aminocaproic acid to enhance longevity and strength [123]. Further, the fibrin matrix can be replaced or supplemented with other ECM molecules such as collagen or laminin [124]. Additional methods include the incorporation of covalent crosslinks via a homobifunctional amine-reactive PEG molecule [48] or factor XIIIa. These modified gels have maintained angiogenic and vasculogenic properties both in vitro and in vivo [48].

A common method to release GFs from fibrin gels is entrapping the GF during the gelation process. The reaction conditions are gentle and can take advantage of fibrin and GF physical affinity [125–127], but release typically follows a profile indicating diffusion control. Some GFs such as bFGF and TGF-β1 have relatively high affinity for the fibrin matrix, and the release is sustained and correlated to gel degradation. Nevertheless, loading efficiency with this strategy is limited by GF–fibrin affinity and stability of the GF [128–131]. Other proteins or domains with physical affinity for GFs can be incorporated into fibrin gels to promote GF retention and release via matrix remodeling. Further, many GFs bind to heparin, which can be incorporated into fibrin gels via a heparin binding peptide. The GF release rate is controlled by varying the concentrations of heparin, GFs, and the heparin binding peptide [132, 133].

Collagen and its derivative gelatin are commonly used for tissue engineered vascular grafts because fibrils will align when processed under a mechanical constraint [134]. Conditioning of the collagen grafts with cyclic loading improves mechanical function and facilitates SMC viability [134]. However, ECM deposition and proliferation is still limited [123]. EPCs have been injected within a collagen gel in an in vivo, ischemic murine hindlimb model. EPC retention and host revascularization was improved compared to cells or gels alone [135].

#### 17.4.3.2 Synthetic Scaffolds

Synthetic scaffolds are advantageous for tissue engineered constructs due to increased control of material properties, but the implant can thrombose or encapsulate limiting biocompatibility. Synthetic grafts are widely used for bypass grafting due to their high biocompatibility and strength; however, they can cause thrombosis with negative downstream consequences. This is particularly apparent as the inner diameter approaches 6 mm or less. Thus, tight control must be implemented to ensure nonthrombogenic surfaces and high biocompatibility.

Synthetic degradable polymers are popular for the formation of tissue engineered vascular grafts because the material will ultimately be remodeled. PLGA, PLA, or PGA are widely investigated because the degradation end products are nontoxic. In a seminal work, Niklason et al. seeded SMC onto a modified PGA surface shaped into a tubular construct and cultured the cells under pulsatile flow for 8 weeks. Following the 8 week in vitro culture, ECs were seeded onto the

luminal surface to create a fully functional vascular graft. These grafts were implanted into an in vivo miniature pig model and demonstrated high patency compared to grafts cultured in nonpulsatile conditions [111]. Niklason's group has continued with these constructs by utilizing MSCs in lieu of differentiated SMCs. Differentiation of MSCs toward SMCs was signaled with the exogenous addition of TGF-β1 and PDGF-BB [136].

PEG hydrogels are widely used for tissue engineered vascular grafts because they are biocompatible and have controllable mechanical properties. Many PEG hydrogels are diacrylate derivatives of PEG that in the presence of UV and a photoinitiator will form a hydrogel. Thus, they have the potential to be formed in situ at the site of ischemia. Cell adhesion peptides can be incorporated within the hydrogels by conjugating an RGDS peptide to the matrix with a heterobifunctional acryloyl–PEG–NHS [137]. However, SMCs cultured in these scaffolds demonstrate decreased proliferation and matrix production [138]. Tethering GFs such as TGF-β1 using the same acryloyl–PEG–NHS chemistry increases matrix production and elastic modulus. It is hypothesized that local presentation of the GF maintains bioactivity and promotes localized effects [139]. This same chemistry could incorporate other GFs to promote EC proliferation or activity [140]. Further, the cell adhesive domain RGDS can be patterned within gels to promote EC tubulogenesis [141].

Therapeutic revascularization does not lend itself toward treatment using monolithic synthetic materials. While ischemic tissue experiences a reduction in cell number and function, there is no loss of volume, thereby limiting the use of prefabricated scaffolds. Microspheres are widely investigated since they are typically biodegradable and allow for host infiltration. VEGF has been incorporated into PLGA and PEG microspheres and maintained bioactivity when exposed to ECs in vitro [142]. Further, VEGF and PDGF-BB have been incorporated into a PLGA scaffold and microspheres, respectively, and released with varying profiles to promote activity and proliferation of ECs and SMCs. When implanted in an in vivo model, increased capillary and SMC density was demonstrated [143].

### *17.4.4 Delivery of Angiogenic Factors*

As stated above, numerous factors have been discovered that demonstrate high potential for angiogenesis and vasculogenesis (Table 17.3). Many of these factors are pleiotropic and demonstrate numerous functionalities within angiogenesis. Nevertheless, clinical trials with direct injection showed limited efficacy due to low protein stability, nonlocalized delivery, and insufficient stability of formed capillaries [144]. Delivery from a graft or scaffold should stabilize bioactivity, provide a site for revascularization, and could provide stabilization signals for newly formed vessels.

**Table 17.3** Angiogenic and vasculogenic growth factors

| Growth factor/drug | Function |
|---|---|
| VEGF | EC migration, proliferation, and vessel formation |
| | Migration and differentiation of EPCs |
| bFGF | Angiogenesis induced from ECs |
| | Smooth muscle cell proliferation |
| | Differentiation of stem cells toward ECs and SMCs |
| PDGF-BB | Recruits SMCs and pericytes to stabilize de novo vessels |
| | SMC differentiation |
| Angiopoietins (Ang-1 and Ang-2) | Promotes survival and migration of ECs |
| | Regulates mural differentiation and migration |
| | Stabilizes de novo vessels |
| TGF-β1 | Migration, stabilization, differentiation, and ECM synthesis of ECs and SMCs |
| HGF | Indirect factor that promotes upregulation of VEGF |
| SDF-1α | Migration of EPCs and stem cells to ischemic site |

#### 17.4.4.1 VEGF

VEGF is a highly investigated angiogenic GF and acts specifically on ECs to induce migration, proliferation, and formation of blood vessels. At sites of ischemia, it promotes migration of EPCs to signal revascularization, as well as EPC differentiation. VEGF has been incorporated into fibrin [132, 133, 145], collagen [146], gelatin [147], PLGA [143], and PEG [140, 141] scaffolds. Further, VEGF has been encapsulated into PEG/PLGA [142] and alginate [148] microspheres. VEGF bioactivity is maintained in vitro [132, 133, 140–142, 145, 146, 148] and has demonstrated increased capillary density and revascularization in vivo [143].

#### 17.4.4.2 bFGF

Another important GF for angiogenesis is basic FGF (bFGF or FGF-2), which recruits supporting pericytes and SMCs to EC sites and stimulates EC and SMC proliferation and migration [149]. Further, bFGF and VEGF can activate each other to promote an angiogenic phenotype of ECs in vitro and neovascularization in vivo [150, 151]. BFGF contains a heparin binding domain and has been incorporated into heparin loaded fibrin gels for sustained release [132]. BFGF loaded gelatin scaffolds [152] and alginate microspheres [153] have demonstrated improved revascularization when implanted in vivo.

#### 17.4.4.3 TGF-β1

TGF-β1, when exposed to a coculture of ES cells and ECs, has stabilized capillary-like structures formed in vitro within Matrigel [154]. TGF-β1 is a pleiotropic growth

factor that has an indirect effect on the angiogenesis cascade by upregulating production of VEGF and bFGF from SMCs [155]. Additionally, it has been hypothesized that TGF-β1 may recruit inflammatory cells that release VEGF, bFGF, and PDGF-BB and thus further influence angiogenesis [156, 157]. Evidence has indicated that TGF-β1 may induce SMC phenotype from a population of MSCs [122, 158, 159]. TGF-β1 can be encapsulated into fibrin gels and associated with the matrix via physical affinity. Release rate is sustained and correlated to degradation rate, allowing control by altering the degradation rate [130, 131]. TGF-β1 has been incorporated into diacrylate-PEG gels via acrylate–PEG–NHS chemistry and exposed to encapsulated SMCs. SMCs demonstrated increase proliferation and activity due to the local presentation of TGF-β1 [139].

#### 17.4.4.4 Other Growth Factors

Numerous other GFs and proteins have demonstrated angiogenic properties including angiopoietins, PDGF-BB, NGF, IGF-1, Shh, hepatocyte growth factor (HGF), and stromal derived growth factor-1α (SDF-1α). SDF-1α has been incorporated into fibrin gels PEGylated with a homobifunctional amine reactive PEG derivative. The homobifunctional PEG provides additional crosslinks increasing the longevity while providing domains for GF conjugation. SDF-1α had a zero order release over 6 days and recruited a greater number of stem cells to an acute MI site compared to controls [160]. HGF has been incorporated in a similar manner and implanted with MSCs into an acute MI model. MSC retention was greater compared to MSC injection alone, and improvement in heart function was demonstrated compared to controls (Fig. 17.4) [161].

### *17.4.5 Future Directions and Challenges*

Much of the therapeutic vasculogenesis or angiogenesis field has focused on the delivery of single GFs to promote revascularization. Unfortunately, capillaries regress without additional GFs or stabilization signals reducing the efficacy of therapeutic angiogenesis schemes. Further, many tissue engineered constructs for vascular grafting would benefit from SMC infiltration and matrix deposition, which could stabilize the system. Multiple GFs could promote both EC and SMC infiltration, proliferation, differentiation, and function for revascularization. Dual GF systems have been formulated to sequentially release two GFs [131, 143] to match the timing cascade described in embryonic vasculogenesis [162, 163]. Nevertheless, research is still required to develop multiple GF release platforms to screen different GFs for their use in vasculogenesis.

As tissue engineered constructs become larger, diffusion limits the volumetric size of three dimensional scaffolds due to reduced nutrient and waste exchange. Currently, the limit for scaffold thickness is on the order of 100 μm and a

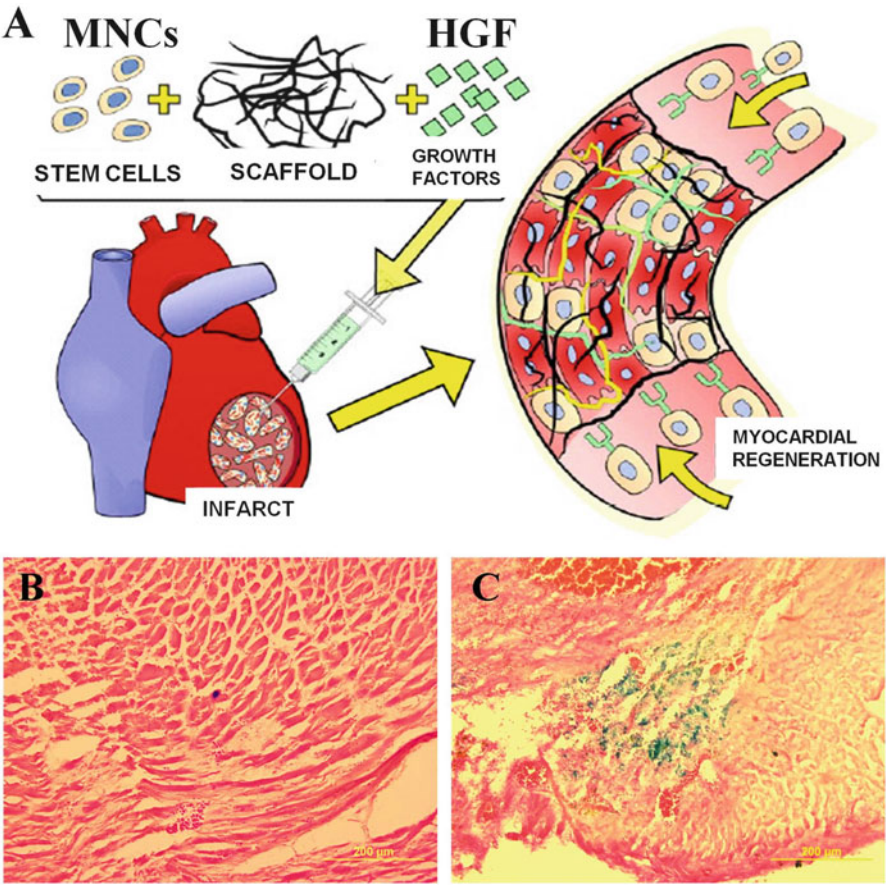


**Fig. 17.4** (**a**) Schematic demonstrating a combination strategy for the delivery of HGF and bone marrow mononuclear cells (BMNCs) using a PEGylated fibrin gel. Combination strategy was evaluated in a murine infarct model and compared against direct BMNC injection. The nuclei of transplanted BMNCs were stained blue by X-gal and the slides were counterstained by eosin (*red*). By direct injection only a few cells were detected at the periscar region. (**b**) When delivered by injectable biomatrix the transplanted BMNCs formed clusters at the periscar (**c**) area. Cell retention rate was significantly increased when delivered by combination strategy compared with control. Reprinted with permission from Zhang et al. [161]

vascularized construct would be required for patency of larger tissues. GFs could be incorporated into scaffolds to either promote vascular cell differentiation or infiltration. Additionally, physical parameters could effect vascularization of the construct. Poly(ester ether) copolymers were constructed with varying pore sizes and examined for vascularization. Pore sizes above 250 μm promoted vascular ingrowth and function when evaluated in a dorsal skin fold mouse model [164]. However, the relative dependencies of GFs and physical parameters on vasculogenesis are still unknown.

## References


1. Amit M, Shariki C, Margulets V, Itskovitz-Eldor J (2004) Feeder layer- and serum-free culture of human embryonic stem cells. Biol Reprod 70(3):837–845
2. Barrilleaux B, Phinney DG, Prockop DJ, O'Connor KC (2006) Review: Ex vivo engineering of living tissues with adult stem cells. Tissue Eng 12(11):3007–3019
3. Pittenger MF, Mackay AM, Beck SC, Jaiswal RK, Douglas R, Mosca JD, Moorman MA, Simonetti DW, Craig S, Marshak DR (1999) Multilineage potential of adult human mesenchymal stem cells. Science 284(5411):143–147
4. Zuk PA, Zhu M, Ashjian P, De Ugarte DA, Huang JI, Mizuno H, Alfonso ZC, Fraser JK, Benhaim P, Hedrick MH (2002) Human adipose tissue is a source of multipotent stem cells. Mol Biol Cell 13(12):4279–4295
5. Ryan JM, Barry FP, Murphy JM, Mahon BP (2005) Mesenchymal stem cells avoid allogeneic rejection. J Inflamm (Lond) 2(8):8
6. Park IH, Zhao R, West JA, Yabuuchi A, Huo H, Ince TA, Lerou PH, Lensch MW, Daley GQ (2008) Reprogramming of human somatic cells to pluripotency with defined factors. Nature 451(7175):141–146
7. Engler AJ, Sen S, Sweeney HL, Discher DE (2006) Matrix elasticity directs stem cell lineage specification. Cell 126(4):677–689
8. Yoo JJ, Atala A (1997) A novel gene delivery system using urothelial tissue engineered neo-organs. J Urol 158(3 Pt 2):1066–1070
9. Saraf A, Mikos AG (2006) Gene delivery strategies for cartilage tissue engineering. Adv Drug Deliv Rev 58(4):592–603
10. Li Z, Sharma RV, Duan D, Davisson RL (2003) Adenovirus-mediated gene transfer to adult mouse cardiomyocytes is selectively influenced by culture medium. J Gene Med 5 (9):765–772
11. Meinel L, Hofmann S, Betz O, Fajardo R, Merkle HP, Langer R, Evans CH, Vunjak-Novakovic G, Kaplan DL (2006) Osteogenesis by human mesenchymal stem cells cultured on silk biomaterials: comparison of adenovirus mediated gene transfer and protein delivery of BMP-2. Biomaterials 27(28):4993–5002
12. Capito RM, Spector M (2007) Collagen scaffolds for nonviral IGF-1 gene delivery in articular cartilage tissue engineering. Gene Ther 14(9):721–732
13. Glick BR, Pasternak JJ (1998) Molecular biotechnology: principles and applications of recombinant DNA. ASM, Washington, DC
14. Gresch O, Engel FB, Nesic D, Tran TT, England HM, Hickman ES, Korner I, Gan L, Chen S, Castro-Obregon S, Hammermann R, Wolf J, Muller-Hartmann H, Nix M, Siebenkotten G, Kraus G, Lun K (2004) New non-viral method for gene transfer into primary cells. Methods 33(2):151–163
15. van Blitterswijk C (2008) Tissue engineering. Academic, London
16. Tran-Khanh N, Hoemann CD, McKee MD, Henderson JE, Buschmann MD (2005) Aged bovine chondrocytes display a diminished capacity to produce a collagen-rich, mechanically functional cartilage extracellular matrix. J Orthop Res 23(6):1354–1362
17. Biondi M, Ungaro F, Quaglia F, Netti PA (2008) Controlled drug delivery in tissue engineering. Adv Drug Deliv Rev 60(2):229–242
18. Allori AC, Sailon AM, Warren SM (2008) Biological basis of bone formation, remodeling, and repair-part II: extracellular matrix. Tissue Eng B Rev 14(3):275–283
19. Marquis ME, Lord E, Bergeron E, Drevelle O, Park H, Cabana F, Senta H, Faucheux N (2009) Bone cells-biomaterials interactions. Front Biosci 14:1023–1067
20. Heino TJ, Hentunen TA, Vaananen HK (2004) Conditioned medium from osteocytes stimulates the proliferation of bone marrow mesenchymal stem cells and their differentiation into osteoblasts. Exp Cell Res 294(2):458–468
21. Cartmell S (2009) Controlled release scaffolds for bone tissue engineering. J Pharm Sci 98 (2):430–441

22. Shi X, Wang Y, Varshney RR, Ren L, Gong Y, Wang DA (2010) Microsphere-based drug releasing scaffolds for inducing osteogenesis of human mesenchymal stem cells in vitro. Eur J Pharm Sci 39(1–3):59–67
23. Khan Y, Yaszemski MJ, Mikos AG, Laurencin CT (2008) Tissue engineering of bone: material and matrix considerations. J Bone Joint Surg Am 90(Suppl 1):36–42
24. Jayasuriya AC, Shah C (2008) Controlled release of insulin-like growth factor-1 and bone marrow stromal cell function of bone-like mineral layer-coated poly(lactic-co-glycolic acid) scaffolds. J Tissue Eng Regen Med 2(1):43–49
25. Woodfield TB, Bezemer JM, Pieper JS, van Blitterswijk CA, Riesle J (2002) Scaffolds for tissue engineering of cartilage. Crit Rev Eukaryot Gene Expr 12(3):209–236
26. Fan H, Zhang C, Li J, Bi L, Qin L, Wu H, Hu Y (2008) Gelatin microspheres containing TGF-beta3 enhance the chondrogenesis of mesenchymal stem cells in modified pellet culture. Biomacromolecules 9(3):927–934
27. Klein TJ, Rizzi SC, Reichert JC, Georgi N, Malda J, Schuurman W, Crawford RW, Hutmacher DW (2009) Strategies for zonal cartilage repair using hydrogels. Macromol Biosci 9(11):1049–1058
28. Sohier J, Moroni L, van Blitterswijk C, de Groot K, Bezemer JM (2008) Critical factors in the design of growth factor releasing scaffolds for cartilage tissue engineering. Expert Opin Drug Deliv 5(5):543–566
29. Kerker JT, Leo AJ, Sgaglione NA (2008) Cartilage repair: synthetics and scaffolds: basic science, surgical techniques, and clinical outcomes. Sports Med Arthrosc 16(4):208–216
30. Temenoff JS, Mikos AG (2000) Review: Tissue engineering for regeneration of articular cartilage. Biomaterials 21(5):431–440
31. Slater BJ, Kwan MD, Gupta DM, Panetta NJ, Longaker MT (2008) Mesenchymal cells for skeletal tissue engineering. Expert Opin Biol Ther 8(7):885–893
32. AAOS (2008) In: Katz SI (ed) Burden of musculoskeletal diseases in the United States: Prevalence, Societal and Economic Cost. AAOS, Washington, DC
33. Mourino V, Boccaccini AR (2010) Bone tissue engineering therapeutics: controlled drug delivery in three-dimensional scaffolds. J R Soc Interface 7:209
34. Yoshida T, Kikuchi M, Koyama Y, Takakuda K (2010) Osteogenic activity of MG63 cells on bone-like hydroxyapatite/collagen nanocomposite sponges. J Mater Sci Mater Med 21 (4):1263–72
35. Sahoo S, Chung C, Khetan S, Burdick JA (2008) Hydrolytically degradable hyaluronic acid hydrogels with controlled temporal structures. Biomacromolecules 9(4):1088–1092
36. Tortelli F, Cancedda R (2009) Three-dimensional cultures of osteogenic and chondrogenic cells: a tissue engineering approach to mimic bone and cartilage in vitro. Eur Cell Mater 17:1–14
37. Hosseinkhani H, Inatsugu Y, Hiraoka Y, Inoue S, Tabata Y (2005) Perfusion culture enhances osteogenic differentiation of rat mesenchymal stem cells in collagen sponge reinforced with poly(glycolic Acid) fiber. Tissue Eng 11(9–10):1476–1488
38. Ratner BD (2004) Biomaterials science: an introduction to materials in medicine. Elsevier Academic, Amsterdam
39. Diniz Oliveira HF, Weiner AA, Majumder A, Shastri VP (2008) Non-covalent surface engineering of an alloplastic polymeric bone graft material for controlled protein release. J Control Release 126(3):237–245
40. Espanol M, Perez RA, Montufar EB, Marichal C, Sacco A, Ginebra MP (2009) Intrinsic porosity of calcium phosphate cements and its significance for drug delivery and tissue engineering applications. Acta Biomater 5(7):2752–2762
41. Weir MD, Xu HH (2008) High-strength, in situ-setting calcium phosphate composite with protein release. J Biomed Mater Res A 85(2):388–396
42. Wu C, Zreiqat H (2009) Porous bioactive diopside (CaMgSi(2)O(6)) ceramic microspheres for drug delivery. Acta Biomater 6(3):820–9
43. Stoddart MJ, Grad S, Eglin D, Alini M (2009) Cells and biomaterials in cartilage tissue engineering. Regen Med 4(1):81–98

44. Glowacki J, Mizuno S (2008) Collagen scaffolds for tissue engineering. Biopolymers 89 (5):338–344
45. Zheng L, Fan HS, Sun J, Chen XN, Wang G, Zhang L, Fan YJ, Zhang XD (2010) Chondrogenic differentiation of mesenchymal stem cells induced by collagen-based hydrogel: an in vivo study. J Biomed Mater Res A 93(2):783–92
46. Mosesson MW (2005) Fibrinogen and fibrin structure and functions. J Thromb Haemost 3 (8):1894–1904
47. Sage A, Chang AA, Schumacher BL, Sah RL, Watson D (2009) Cartilage outgrowth in fibrin scaffolds. Am J Rhinol Allergy 23(5):486–491
48. Zhang G, Wang X, Wang Z, Zhang J, Suggs L (2006) A PEGylated fibrin patch for mesenchymal stem cell delivery. Tissue Eng 12(1):9–19
49. Altman GH, Diaz F, Jakuba C, Calabro T, Horan RL, Chen J, Lu H, Richmond J, Kaplan DL (2003) Silk-based biomaterials. Biomaterials 24(3):401–416
50. Meinel L, Hofmann S, Karageorgiou V, Zichner L, Langer R, Kaplan D, Vunjak-Novakovic G (2004) Engineering cartilage-like tissue using human mesenchymal stem cells and silk protein scaffolds. Biotechnol Bioeng 88(3):379–391
51. Uebersax L, Merkle HP, Meinel L (2008) Insulin-like growth factor I releasing silk fibroin scaffolds induce chondrogenic differentiation of human mesenchymal stem cells. J Control Release 127(1):12–21
52. Motta A, Maniglio D, Migliaresi C, Kim HJ, Wan X, Hu X, Kaplan DL (2009) Silk fibroin processing and thrombogenic responses. J Biomater Sci Polym Ed 20(13):1875–1897
53. Ghidoni I, Chlapanidas T, Bucco M, Crovato F, Marazzi M, Vigo D, Torre ML, Faustini M (2008) Alginate cell encapsulation: new advances in reproduction and cartilage regenerative medicine. Cytotechnology 58(1):49–56
54. Kock LM, Schulz RM, van Donkelaar CC, Thummler CB, Bader A, Ito K (2009) RGD-dependent integrins are mechanotransducers in dynamically compressed tissue-engineered cartilage constructs. J Biomech 42(13):2177–2182
55. Gong Y, He L, Li J, Zhou Q, Ma Z, Gao C, Shen J (2007) Hydrogel-filled polylactide porous scaffolds for cartilage tissue engineering. J Biomed Mater Res B Appl Biomater 82 (1):192–204
56. Awad HA, Wickham MQ, Leddy HA, Gimble JM, Guilak F (2004) Chondrogenic differentiation of adipose-derived adult stem cells in agarose, alginate, and gelatin scaffolds. Biomaterials 25(16):3211–3222
57. Dai W, Kawazoe N, Lin X, Dong J, Chen G (2010) The influence of structural design of PLGA/collagen hybrid scaffolds in cartilage tissue engineering. Biomaterials 31(8):2141–52
58. Kawazoe N, Inoue C, Tateishi T, Chen G (2010) A cell leakproof PLGA-collagen hybrid scaffold for cartilage tissue engineering. Biotechnol Prog 26(3):819–26
59. Prabaharan M, Rodriguez-Perez MA, de Saja JA, Mano JF (2007) Preparation and characterization of poly(L-lactic acid)-chitosan hybrid scaffolds with drug release capability. J Biomed Mater Res B Appl Biomater 81(2):427–434
60. Klompmaker J, Jansen HW, Veth RP, de Groot JH, Nijenhuis AJ, Pennings AJ (1991) Porous polymer implant for repair of meniscal lesions: a preliminary study in dogs. Biomaterials 12 (9):810–816
61. Cao T, Ho KH, Teoh SH (2003) Scaffold design and in vitro study of osteochondral coculture in a three-dimensional porous polycaprolactone scaffold fabricated by fused deposition modeling. Tissue Eng 9(Suppl 1):S103–112
62. Knippenberg M, Helder MN, Zandieh Doulabi B, Wuisman PI, Klein-Nulend J (2006) Osteogenesis versus chondrogenesis by BMP-2 and BMP-7 in adipose stem cells. Biochem Biophys Res Commun 342(3):902–908
63. Niu X, Feng Q, Wang M, Guo X, Zheng Q (2009) Preparation and characterization of chitosan microspheres for controlled release of synthetic oligopeptide derived from BMP-2. J Microencapsul 26(4):297–305

64. Haidar ZS, Hamdy RC, Tabrizian M (2009) Delivery of recombinant bone morphogenetic proteins for bone regeneration and repair. Part B: Delivery systems for BMPs in orthopaedic and craniofacial tissue engineering. Biotechnol Lett 31(12):1825–1835
65. Engstrand T, Veltheim R, Arnander C, Docherty-Skogh AC, Westermark A, Ohlsson C, Adolfsson L, Larm O (2008) A novel biodegradable delivery system for bone morphogenetic protein-2. Plast Reconstr Surg 121(6):1920–1928
66. Yamamoto M, Takahashi Y, Tabata Y (2003) Controlled release by biodegradable hydrogels enhances the ectopic bone formation of bone morphogenetic protein. Biomaterials 24 (24):4375–4383
67. Barnes B, Boden SD, Louis-Ugbo J, Tomak PR, Park JS, Park MS, Minamide A (2005) Lower dose of rhBMP-2 achieves spine fusion when combined with an osteoconductive bulking agent in non-human primates. Spine 30(10):1127–1133
68. Woo BH, Jiang G, Jo YW, DeLuca PP (2001) Preparation and characterization of a composite PLGA and poly(acryloyl hydroxyethyl starch) microsphere system for protein delivery. Pharm Res 18(11):1600–1606
69. Kim HD, Valentini RF (2002) Retention and activity of BMP-2 in hyaluronic acid-based scaffolds in vitro. J Biomed Mater Res 59(3):573–584
70. De la Riva B, Nowak C, Sanchez E, Hernandez A, Schulz-Siegmund M, Pec MK, Delgado A, Evora C (2009) VEGF-controlled release within a bone defect from alginate/chitosan/PLA-H scaffolds. Eur J Pharm Biopharm 73(1):50–58
71. Santo VE, Frias AM, Carida M, Cancedda R, Gomes ME, Mano JF, Reis RL (2009) Carrageenan-based hydrogels for the controlled delivery of PDGF-BB in bone tissue engineering applications. Biomacromolecules 10(6):1392–1401
72. Poole AR, Kojima T, Yasuda T, Mwale F, Kobayashi M, Laverty S (2001) Composition and structure of articular cartilage – a template for tissue repair. Clin Orthop Rel Res 391: S26–S33
73. DeFail AJ, Chu CR, Izzo N, Marra KG (2006) Controlled release of bioactive TGF-beta 1 from microspheres embedded within biodegradable hydrogels. Biomaterials 27(8):1579–1585
74. Jung Y, Chung YI, Kim SH, Tae G, Kim YH, Rhie JW (2009) In situ chondrogenic differentiation of human adipose tissue-derived stem cells in a TGF-beta1 loaded fibrin-poly(lactide-caprolactone) nanoparticulate complex. Biomaterials 30(27):4657–4664
75. Holland TA, Tabata Y, Mikos AG (2005) Dual growth factor delivery from degradable oligo (poly(ethylene glycol) fumarate) hydrogel scaffolds for cartilage tissue engineering. J Control Release 101(1–3):111–125
76. Lee JE, Kim KE, Kwon IC, Ahn HJ, Lee SH, Cho H, Kim HJ, Seong SC, Lee MC (2004) Effects of the controlled-released TGF-beta 1 from chitosan microspheres on chondrocytes cultured in a collagen/chitosan/glycosaminoglycan scaffold. Biomaterials 25(18):4163–4173
77. Lee JE, Kim SE, Kwon IC, Ahn HJ, Cho H, Lee SH, Kim HJ, Seong SC, Lee MC (2004) Effects of a chitosan scaffold containing TGF-beta1 encapsulated chitosan microspheres on in vitro chondrocyte culture. Artif Organs 28(9):829–839
78. Sohier J, Hamann D, Koenders M, Cucchiarini M, Madry H, van Blitterswijk C, de Groot K, Bezemer JM (2007) Tailored release of TGF-beta1 from porous scaffolds for cartilage tissue engineering. Int J Pharm 332(1–2):80–89
79. Fan H, Hu Y, Li X, Wu H, Lv R, Bai J, Wang J, Qin L (2006) Ectopic cartilage formation induced by mesenchymal stem cells on porous gelatin-chondroitin-hyaluronate scaffold containing microspheres loaded with TGF-beta1. Int J Artif Organs 29(6):602–611
80. Huang AH, Stein A, Tuan RS, Mauck RL (2009) Transient exposure to transforming growth factor beta 3 improves the mechanical properties of mesenchymal stem cell-laden cartilage constructs in a density-dependent manner. Tissue Eng A 15(11):3461–3472
81. Solchaga LA, Penick K, Goldberg VM, Caplan AI, Welter JF (2010) Fibroblast growth factor-2 enhances proliferation and delays loss of chondrogenic potential in human adult bone marrow-derived mesenchymal stem cells. Tissue Eng A 16(3):1009–19

82. Igai H, Yamamoto Y, Chang SS, Yamamoto M, Tabata Y, Yokomise H (2007) Tracheal cartilage regeneration by slow release of basic fibroblast growth factor from a gelatin sponge. J Thorac Cardiovasc Surg 134(1):170–175
83. Chen FM, Chen R, Wang XJ, Sun HH, Wu ZF (2009) In vitro cellular responses to scaffolds containing two microencapulated growth factors. Biomaterials 30(28):5215–5224
84. Park H, Temenoff JS, Tabata Y, Caplan AI, Raphael RM, Jansen JA, Mikos AG (2009) Effect of dual growth factor delivery on chondrogenic differentiation of rabbit marrow mesenchymal stem cells encapsulated in injectable hydrogel composites. J Biomed Mater Res A 88 (4):889–897
85. Elisseeff J, McIntosh W, Fu K, Blunk BT, Langer R (2001) Controlled-release of IGF-I and TGF-beta1 in a photopolymerizing hydrogel for cartilage tissue engineering. J Orthop Res 19 (6):1098–1104
86. Taylor CA, Braza D, Rice JB, Dillingham T (2008) The incidence of peripheral nerve injury in extremity trauma. Am J Phys Med Rehabil 87(5):381–385
87. Chen L, Gu YD, Xu L (2004) Clinical application of axonal repair technique for treatment of peripheral nerve injury. Chin J Traumatol 7(3):153–155
88. Flores AJ, Lavernia CJ, Owens PW (2000) Anatomy and physiology of peripheral nerve injury and repair. Am J Orthop (Belle Mead NJ) 29(3):167–173
89. Wu D, Zhao D (1997) Tissue engineering study on repairment of injured nerve gap in rat. Sheng Wu Yi Xue Gong Cheng Xue Za Zhi 14(2):108–110
90. Ichihara S, Inada Y, Nakamura T (2008) Artificial nerve tubes and their application for repair of peripheral nerve injury: an update of current concepts. Injury 39(Suppl 4):29–39
91. Yuan JD, Nie WB, Fu Q, Lian XF, Hou TS, Tan ZQ (2009) Novel three-dimensional nerve tissue engineering scaffolds and its biocompatibility with Schwann cells. Chin J Traumatol 12(3):133–137
92. Hudson TW, Evans GRD, Schmidt CE (1999) Engineering strategies for peripheral nerve repair. Clin Plast Surg 26(4):617
93. Martin BC, Minner EJ, Wiseman SL, Klank RL, Gilbert RJ (2008) Agarose and methylcellulose hydrogel blends for nerve regeneration applications. J Neural Eng 5(2):221–231
94. Labrador RO, Buti M, Navarro X (1995) Peripheral nerve repair: role of agarose matrix density on functional recovery. Neuroreport 6(15):2022–2026
95. Koopmans G, Hasse B, Sinis N (2009) Chapter 19: The role of collagen in peripheral nerve repair. Int Rev Neurobiol 87:363–379
96. Kemp SW, Syed S, Walsh W, Zochodne DW, Midha R (2009) Collagen nerve conduits promote enhanced axonal regeneration, schwann cell association, and neovascularization compared to silicone conduits. Tissue Eng A 15(8):1975–1988
97. Kalbermatten DF, Pettersson J, Kingham PJ, Pierer G, Wiberg M, Terenghi G (2009) New fibrin conduit for peripheral nerve repair. J Reconstr Microsurg 25(1):27–33
98. Choi BH, Han SG, Kim SH, Zhu SJ, Huh JY, Jung JH, Lee SH, Kim BY (2005) Autologous fibrin glue in peripheral nerve regeneration in vivo. Microsurgery 25(6):495–499
99. Martins RS, Siqueira MG, Da Silva CF, Plese JP (2005) Overall assessment of regeneration in peripheral nerve lesion repair using fibrin glue, suture, or a combination of the 2 techniques in a rat model. Which is the ideal choice? Surg Neurol 64(Suppl 1):10–16; discussion S11:16
100. Jansen K, van der Werff JF, van Wachem PB, Nicolai JP, de Leij LF, van Luyn MJ (2004) A hyaluronan-based nerve guide: in vitro cytotoxicity, subcutaneous tissue reactions, and degradation in the rat. Biomaterials 25(3):483–489
101. Colen KL, Choi M, Chiu DT (2009) Nerve grafts and conduits. Plast Reconstr Surg 124(6 Suppl):e386–394
102. Guo SZ, Ren XJ, Wu B, Jiang T (2010) Preparation of the acellular scaffold of the spinal cord and the study of biocompatibility. Spinal Cord 48(7):576–81
103. Subramanian A, Krishnan UM, Sethuraman S (2009) Development of biomaterial scaffold for nerve tissue engineering: biomaterial mediated neural regeneration. J Biomed Sci 16:108

104. Madigan NN, McMahon S, O'Brien T, Yaszemski MJ, Windebank AJ (2009) Current tissue engineering and novel therapeutic approaches to axonal regeneration following spinal cord injury using polymer scaffolds. Respir Physiol Neurobiol 169(2):183–199
105. Pfister LA, Papaloizos M, Merkle HP, Gander B (2007) Nerve conduits and growth factor delivery in peripheral nerve repair. J Peripher Nerv Syst 12(2):65–82
106. Yang Y, De Laporte L, Rives CB, Jang JH, Lin WC, Shull KR, Shea LD (2005) Neurotrophin releasing single and multiple lumen nerve conduits. J Control Release 104(3):433–446
107. Houweling DA, Lankhorst AJ, Gispen WH, Bar PR, Joosten EA (1998) Collagen containing neurotrophin-3 (NT-3) attracts regrowing injured corticospinal axons in the adult rat spinal cord and promotes partial functional recovery. Exp Neurol 153(1):49–59
108. Yu X, Bellamkonda RV (2003) Tissue-engineered scaffolds are effective alternatives to autografts for bridging peripheral nerve gaps. Tissue Eng 9(3):421–430
109. Taylor SJ, Sakiyama-Elbert SE (2006) Effect of controlled delivery of neurotrophin-3 from fibrin on spinal cord injury in a long term model. J Control Release 116(2):204–210
110. Kapur TA, Shoichet MS (2003) Chemically-bound nerve growth factor for neural tissue engineering applications. J Biomater Sci Polym Ed 14(4):383–394
111. Niklason LE, Gao J, Abbott WM, Hirschi KK, Houser S, Marini R, Langer R (1999) Functional arteries grown in vitro. Science 284(5413):489–493
112. Laube HR, Duwe J, Rutsch W, Konertz W (2000) Clinical experience with autologous endothelial cell-seeded polytetrafluoroethylene coronary artery bypass grafts. J Thorac Cardiovasc Surg 120(1):134–141
113. Weinberg CB, Bell E (1986) A blood vessel model constructed from collagen and cultured vascular cells. Science 231(4736):397–400
114. L'Heureux N, Paquet S, Labbe R, Germain L, Auger FA (1998) A completely biological tissue-engineered human blood vessel. FASEB J 12(1):47–56
115. Ennett AB, Mooney DJ (2002) Tissue engineering strategies for in vivo neovascularisation. Expert Opin Biol Ther 2(8):805–818
116. Mandinov L, Mandinova A, Kyurkchiev S, Kyurkchiev D, Kehayov I, Kolev V, Soldi R, Bagala C, de Muinck ED, Lindner V, Post MJ, Simons M, Bellum S, Prudovsky I, Maciag T (2003) Copper chelation represses the vascular response to injury. Proc Natl Acad Sci USA 100(11):6700–6705
117. Post MJ, Simons M (2003) The rational phase of therapeutic angiogenesis. Minerva Cardioangiol 51(5):421–432
118. Wakefield LM, Winokur TS, Hollands RS, Christopherson K, Levinson AD, Sporn MB (1990) Recombinant latent transforming growth factor-beta-1 has a longer plasma half-life in rats than active transforming growth factor-beta-1, and a different tissue distribution. J Clin Invest 86(6):1976–1984
119. Boyer M, Townsend LE, Vogel LM, Falk J, Reitz-Vick D, Trevor KT, Villalba M, Bendick PJ, Glover JL (2000) Isolation of endothelial cells and their progenitor cells from human peripheral blood. J Vasc Surg 31(1 Pt 1):181–189
120. Gehling UM, Ergun S, Schumacher U, Wagener C, Pantel K, Otte M, Schuch G, Schafhausen P, Mende T, Kilic N, Kluge K, Schafer B, Hossfeld DK, Fiedler W (2000) In vitro differentiation of endothelial cells from AC133-positive progenitor cells. Blood 95(10):3106–3112
121. Simper D, Stalboerger PG, Panetta CJ, Wang S, Caplice NM (2002) Smooth muscle progenitor cells in human blood. Circulation 106(10):1199–1204
122. Seruya M, Shah A, Pedrotty D, du Laney T, Melgiri R, McKee JA, Young HE, Niklason LE (2004) Clonal population of adult stem cells: life span and differentiation potential. Cell Transplant 13(2):93–101
123. Grassl ED, Oegema TR, Tranquillo RT (2002) Fibrin as an alternative biopolymer to type-I collagen for the fabrication of a media equivalent. J Biomed Mater Res 60(4):607–612
124. Isenberg BC, Willilams C, Tranquillo RT (2006) Endothelialization and flow conditioning of fibrin-based media-equivalents. Ann Biomed Eng V34(6):971–985

125. Sahni A, Francis CW (2000) Vascular endothelial growth factor binds to fibrinogen and fibrin and stimulates endothelial cell proliferation. Blood 96(12):3772–3778
126. Sahni A, Odrljin T, Francis CW (1998) Binding of basic fibroblast growth factor to fibrinogen and fibrin. J Biol Chem 273(13):7554–7559
127. Grainger DJ, Wakefield L, Bethell HW, Farndale RW, Metcalfe JC (1995) Release and activation of platelet latent TGF-Beta in blood-clots during dissolution with plasmin. Nat Med 1(9):932–937
128. Ishii I, Mizuta H, Sei A, Hirose J, Kudo S, Hiraki Y (2007) Healing of full-thickness defects of the articular cartilage in rabbits using fibroblast growth factor-2 and a fibrin sealant. J Bone Joint Surg Br 89(5):693–700
129. Giannoni P, Hunziker EB (2003) Release kinetics of transforming growth factor-beta1 from fibrin clots. Biotechnol Bioeng 83(1):121–123
130. Catelas I, Dwyer JF, Helgerson S (2008) Controlled release of bioactive transforming growth factor beta-1 from fibrin gels in vitro. Tissue Eng C Methods 14(2):119–128
131. Drinnan CT, Zhang G, Alexander MA, Pulido AS, Suggs LJ (2010) Multimodal release of transforming growth factor-beta1 and the BB isoform of platelet derived growth factor from PEGylated fibrin gels. J Control Release 147(2):180–6
132. Sakiyama-Elbert SE, Hubbell JA (2000) Development of fibrin derivatives for controlled release of heparin-binding growth factors. J Control Release 65(3):389–402
133. Zisch AH, Schenk U, Schense JC, Sakiyama-Elbert SE, Hubbell JA (2001) Covalently conjugated VEGF-fibrin matrices for endothelialization. J Control Release 72(1–3):101–113
134. Seliktar D, Black RA, Vito RP, Nerem RM (2000) Dynamic mechanical conditioning of collagen-gel blood vessel constructs induces remodeling in vitro. Ann Biomed Eng 28 (4):351–362
135. Suuronen EJ, Veinot JP, Wong S, Kapila V, Price J, Griffith M, Mesana TG, Ruel M (2006) Tissue-engineered injectable collagen-based matrices for improved cell delivery and vascularization of ischemic tissue using CD133+ progenitors expanded from the peripheral blood. Circulation 114:138–144
136. Gong ZD, Niklason LE (2008) Small-diameter human vessel wall engineered from bone marrow-derived mesenchymal stem cells (hMSCs). FASEB J 22(6):1635–1648
137. Mann BK, Gobin AS, Tsai AT, Schmedlen RH, West JL (2001) Smooth muscle cell growth in photopolymerized hydrogels with cell adhesive and proteolytically degradable domains: synthetic ECM analogs for tissue engineering. Biomaterials 22(22):3045–3051
138. Mann BK, West JL (2002) Cell adhesion peptides alter smooth muscle cell adhesion, proliferation, migration, and matrix protein synthesis on modified surfaces and in polymer scaffolds. J Biomed Mater Res 60(1):86–93
139. Mann BK, Schmedlen RH, West JL (2001) Tethered-TGF-beta increases extracellular matrix production of vascular smooth muscle cells. Biomaterials 22(5):439–444
140. Leslie-Barbick JE, Moon JJ, West JL (2009) Covalently-immobilized vascular endothelial growth factor promotes endothelial cell tubulogenesis in poly(ethylene glycol) diacrylate hydrogels. J Biomater Sci Polym Ed 20(12):1763–1779
141. Moon JJ, Hahn MS, Kim I, Nsiah BA, West JL (2009) Micropatterning of poly(ethylene glycol) diacrylate hydrogels with biomolecules to regulate and guide endothelial morphogenesis. Tissue Eng A 15(3):579–585
142. King TW, Patrick CW (2000) Development and in vitro characterization of vascular endothelial growth factor (VEGF)-loaded poly(DL-lactic-co-glycolic acid)/poly(ethylene glycol) microspheres using a solid encapsulation/single emulsion/solvent extraction technique. J Biomed Mater Res 51(3):383–390
143. Richardson TP, Peters MC, Ennett AB, Mooney DJ (2001) Polymeric system for dual growth factor delivery. Nat Biotechnol 19(11):1029–1034
144. Henry TD, Annex BH, McKendall GR, Azrin MA, Lopez JJ, Giordano FJ, Shah PK, Willerson JT, Benza RL, Berman DS, Gibson CM, Bajamonde A, Rundle AC, Fine J,

McCluskey ER (2003) The VIVA trial: vascular endothelial growth factor in ischemia for vascular angiogenesis. Circulation 107(10):1359–1365
145. Wong C, Inman E, Spaethe R, Helgerson S (2003) Fibrin-based biomaterials to deliver human growth factors. Thromb Haemost 89(3):573–582
146. Koch S, Yao C, Grieb G, Prevel P, Noah EM, Steffens GCM (2006) Enhancing angiogenesis in collagen matrices by covalent incorporation of VEGF. J Mater Sci Mater Med 17 (8):735–741
147. Ravin AG, Olbrich KC, Levin LS, Usala AL, Klitzman B (2001) Long- and short-term effects of biological hydrogels on capsule microvascular density around implants in rats. J Biomed Mater Res 58(3):313–318
148. Keshaw H, Forbes A, Day RM (2005) Release of angiogenic growth factors from cells encapsulated in alginate beads with bioactive glass. Biomaterials 26(19):4171–4179
149. Nugent MA, Iozzo RV (2000) Fibroblast growth factor-2. Int J Biochem Cell Biol 32 (2):115–120
150. Presta M, Dell'Era P, Mitola S, Moroni E, Ronca R, Rusnati M (2005) Fibroblast growth factor/fibroblast growth factor receptor system in angiogenesis. Cytokine Growth Factor Rev 16(2):159–178
151. Wiedlocha A, Sorensen V (2004) Signaling, internalization, and intracellular activity of fibroblast growth factor, signalling from internalized growth factor receptors, vol 286. Springer, Berlin, pp 45–79
152. Thompson JA, Anderson KD, Dipietro JM, Zwiebel JA, Zametta M, Anderson WF, Maciag T (1988) Site-directed neovessel formation in vivo. Science 241(4871):1349–1352
153. Perets A, Baruch Y, Weisbuch F, Shoshany G, Neufeld G, Cohen S (2003) Enhancing the vascularization of three-dimensional porous alginate scaffolds by incorporating controlled release basic fibroblast growth factor microspheres. J Biomed Mater Res A 65A(4):489–497
154. Darland DC, D'Amore PA (2001) TGF beta is required for the formation of capillary-like structures in three-dimensional cocultures of 10T1/2 and endothelial cells. Angiogenesis 4 (1):11–20
155. Isner JM, Takayuki A (1998) Therapeutic angiogenesis. Front Biosci 3:e49–69
156. Ahrendt G, Chickering DE, Ranieri JP (1998) Angiogenic growth factors: a review for tissue engineering. Tissue Eng 4(2):117–130
157. Li J, Zhang YP, Kirsner RS (2003) Angiogenesis in wound repair: angiogenic growth factors and the extracellular matrix. Microsc Res Tech 60(1):107–114
158. Wang D, Park JS, Chu JS, Krakowski A, Luo K, Chen DJ, Li S (2004) Proteomic profiling of bone marrow mesenchymal stem cells upon transforming growth factor beta1 stimulation. J Biol Chem 279(42):43725–43734
159. Ross JJ, Hong Z, Willenbring B, Zeng L, Isenberg B, Lee EH, Reyes M, Keirstead SA, Weir EK, Tranquillo RT, Verfaillie CM (2006) Cytokine-induced differentiation of multipotent adult progenitor cells into functional smooth muscle cells. J Clin Invest 116(12):3139–49
160. Zhang G, Nakamura Y, Wang X, Hu Q, Suggs LJ, Zhang J (2007) Controlled release of stromal cell derived Factor-1 alpha in situ increases C-kit+ cell homing to the infarcted heart. Tissue Eng 13(8):2063–2071
161. Zhang G, Hu Q, Braunlin EA, Suggs LJ, Zhang J (2008) Enhancing efficacy of stem cell transplantation to the heart with a PEGylated fibrin biomatrix. Tissue Eng A 14(6):1025–1036
162. Hirschi KK, Rohovsky SA, Beck LH, Smith SR, D'Amore PA (1999) Endothelial cells modulate the proliferation of mural cell precursors via platelet-derived growth factor-BB and heterotypic cell contact. Circ Res 84(3):298–305
163. Hirschi KK, Rohovsky SA, D'Amore PA (1998) PDGF, TGF-B, and heterotpic cell-cell interactions mediate endothelial cell-induced recruitment of 10T1/2 cells and their differentiation to smooth muscle fate. J Cell Biol 141(3):805–814
164. Druecke D, Langer S, Lamme E, Pieper J, Ugarkovic M, Steinau HU, Homann HH (2004) Neovascularization of poly(ether ester) block-copolymer scaffolds in vivo: long-term investigations using intravital fluorescent microscopy. J Biomed Mater Res A 68A(1):10–18

# Part VI
# Future Outlook

# Chapter 18
# The Shaping of Controlled Release Drug Product Development by Emerging Trends in the Commercial, Regulatory, and Political Macroenvironment

**Stephen Perrett and Michael J. Rathbone**

**Abstract** Many factors affect the successful commercialization of a modified release dosage form. This chapter provides a brief opinion on the future market challenges for this type of formulation within the broader, economic, regulatory, legal, and drug delivery technology arena. In particular, the macroenvironment and the market factors that influence the development process, and those that ultimately reward the investment of time, effort, and money, are considered. The risks of drug development are increasing as a result of changes taking place concerning intellectual property, regulatory and safety standards, payer pricing demands and reimbursement. The degree of advance that is demanded of new drug based therapies over the standard of care, from both a medical and an economic perspective, has inevitably increased.

## 18.1 Introduction

It has been said that the only guide that we have to the future is the past, and starting with this in mind it is worth considering the recent past relating to the macro factors that are in play in pharma today, namely intellectual property, pricing, safety, and commercial and regulatory risks. This chapter reviews the recent past and provides opinion on the influence this past will have on future prospects for modified release dosage forms.

S. Perrett (✉)
Portfolio Development, Eurand, Yardley, PA, USA
e-mail: s.perrett@eurand.com

M.J. Rathbone
School of Pharmacy, Griffith University, Southport, QLD, Australia
e-mail: m.rathbone@griffith.edu.au

J. Siepmann et al. (eds.), *Fundamentals and Applications of Controlled Release Drug Delivery*, Advances in Delivery Science and Technology,
DOI 10.1007/978-1-4614-0881-9_18, 

## 18.2 Recent Macro Factors Affecting Pharma

### *18.2.1 Intellectual Property*

Intellectual property has become more difficult to obtain. Prior art is increasing at an exponential rate not only due to the passage of time, but more significantly there has been an explosion of patent filings from China, India, and other countries as they continue their rapid economic growth. There have also been developments in patent law, such as the US Supreme Court's ruling on *KSR vs Teleflex*, which has lowered the bar for rejections based on obviousness. This has made patents, formulation patents in particular, harder to obtain, and the modified release dosage form is perhaps one of the oldest and most worked on formulations available. Currently, the Supreme Court is considering *Microsoft vs i4i* regarding Microsoft's seeking to reduce the standard for establishing patent invalidity.

If we look back, other relevant trends have emerged. From 1989 to 1996, 46% of all patents challenged in litigation were invalidated [1]. From 1992 to 2000, generics prevailed 73% of the time, whereas from 2000 to 2009 generics prevailed in 48% of cases that went to trial [1]. The final caveat is crucial to understanding how things are evolving, however, since payments to generic challengers in return for not launching their product were held lawful following *Schering–Plough vs Upsher-Smith* in 2006. There has been about a sevenfold increase in settlements since that time, with over 50 such settlements reached in 2009 [2].

### *18.2.2 Pricing*

Favorable pricing for reformulations is difficult to obtain without a significant pharmacoeconomic argument, and improved convenience and/or compliance of reformulations alone does not drive reimbursement. In the USA, this means that high priced reformulated products without significant medical or economic improvement are placed on tier 3. This limits the market opportunity for switches to once a day or easier to take forms, such as the modified release or orally disintegrating tablet forms. That being said, this is not to say that the economics cannot work with the right pricing and couponing strategy. For example, the muscle relaxant cyclobenzaprine is a three times a day tablet, and is the 30th most prescribed drug in the USA, with 21 million prescriptions in 2009 or 1 billion doses dispensed annually. The average price per dose is $0.22, translating to $217 million in generic sales. Compare this to once a day Amrix®, priced at $11 and in tier 3, despite the fact that a modest 475,000 prescriptions were written in 2010, representing a 1.5% market share by volume, with resultant sales of $150 million. Amrix® has the added differentiation that in clinical studies less somnolence was seen with the modified (extended) release dosage form. The take home message

from this critique is that despite the fact that once a day dosing and reduced side effects are clearly preferable, 98.5% of payers are not prepared to pay brand pricing for it.

It is worth considering several other examples of dose frequency reduction to highlight the take home message. Lialda® is a tablet designed to target the colon and to slowly release drug throughout the entire colon and was, in 2007, the first once a day mesalamine formulation for the treatment of ulcerative colitis. This product was launched into a market with two other mesalamine formulations already present – Asacol® and Pentasa®, which are dosed three or four times a day. In this case, the once a day dosing of Lialda® resulted in very rapid market acceptance to the point, where sales are now $326 million 4 years after launch, and it is now the second best selling mesalamine brand out of four.

That once a day dosing offered by modified release forms is such a clear advantage is underscored by the fact that Asacol®, the market leader, is working very hard to obtain a label with reduced dosing frequency. The reason that Lialda® was so successful is that there were no generic mesalamines and, although things may now be changing, there has been no bioequivalence-based ANDA route to approval. This meant that Lialda® could adopt brand pricing on launch, like its peers. As it did not have an economic downside, the benefits of the formulation could be fully appreciated. Again, the take home message is that improved convenience is something that consumers like very much, but not at a significantly increased cost.

A further example is offered by Concerta® (methylphenidate) for the treatment of attention deficit hyperactivity disorder, which was formulated using the Oros® modified release technology. This product was launched into a generic market with reduced dose frequency being its primary differentiating feature. This product adopted brand pricing but was very successful because, in this case, the elimination of mid-day dosing brought more than convenience. Methylphenidate is a controlled substance which is prescribed to children, and mid day dosing meant a visit to the school nurse, which was both very inconvenient and stigmatizing. Again, the take home message is that payers are prepared to pay brand pricing in a generic market, if the benefits offered by reformulation are large enough.

A final example of how pricing can affect commercial success is Makena®, an injectable form of hydroxyprogesterone caproate. Makena® has orphan designation and is a recently approved form of a drug product that was previously made by compounding pharmacies, and its development as an approved product was supported by the March of Dimes and many OBGYNs, anticipating that it would increase the quality and availability of the product. When a price of $1,500 per injection (as opposed to the prior cost of $10–20 from a compounding pharmacy) was announced, the shock wave traveled all the way to the government and the FDA responded by announcing that it does not intend to take enforcement action against pharmacies that compound hydroxyprogesterone caproate, provided appropriate standards are observed. This is an apparent contradiction to initiative to remove approved products from the market and to the exclusivity offered to orphan products, and illustrates the level of concern that pricing can raise.

### 18.2.3 Safety and Efficacy

Nowadays, safety is more heavily scrutinized than ever before, and the efficacy standard is often against "standard of care," which may or may not reflect approved dosing, or even indications, for the therapies that are used. Further, drugs that may be otherwise safe and efficacious are not looked on favorably if they do not offer some advantage over existing therapies. In addition, postmarketing commitments, such as risk evaluation mitigating strategies (REMSs), are increasing, as are approval times, and prescription drug user fee act (PDUFA) dates are extended with increasing frequency. All of this is reflected in a steady decline in new molecular entity (NME) new drug applications (NDAs), with only 25 in 2009 despite a $35 billion investment, which is three times that invested in 1999, when 35 NME NDAs were filed [3].

In November 2010, Darvocet® was withdrawn as propoxyphene was determined to be unsafe due to potential heart rhythm abnormalities. In October 2010, Qnexa® was delayed due to evaluation of the drug's potential for causing birth defects and heart problems. Avandia® was withdrawn in Europe and prescribing is considerably restricted in the USA. Vioxx® was withdrawn from the market and NSAIDS now carry boxed warnings. Nicox and Pozen have seen their products fail to gain approval as a result of increased safety awareness and stricter application of risk/benefit by the FDA, despite nitro-naproxen being a modification of an existing drug and metoclopramide and sumatriptan being a simple combination of two marketed drugs.

The take home message is that safety is at the top of the mind of consumers of medicines and at the FDA.

### 18.2.4 Formulation Exclusivity

Generic companies have also developed sophisticated formulation capabilities which more often than not include the ability to work around patents, meaning technical barriers apply less and less and generic entry is consequently rapid.

Thus, a successful demonstration of clinical efficacy or a successful reformulation does not necessarily mean that the product has commercial value. In short, competition is significant.

### 18.2.5 Commercial and Regulatory Risks

Commercial and regulatory risks increasingly outweigh scientific risks for developers of drug products. This is clearly seen in several recent examples, where even success in phase 3 does not always mean that a product will be launched. For example, dutogliptin from Phenomix was returned by its partner,

Forest, citing business reasons after successful phase 3 results were announced. Similarly, despite FDA approval of Gralise®, Depomed's partner Abbott returned the product to Depomed, who has now launched it themselves. Whether this decision was driven by the perceived growth potential of the product or the strategic direction of Abbott has been speculated upon: however, either case serves to illustrate unpredictability.

Undifferentiated NCEs also face a much tougher environment than they once did. As an example, Onglyza® appears to be struggling owing to a lack of differentiation and a launch later than its direct competitor Januvia®, despite being second to the market in type 2 diabetes.

In all the examples above, the differentiation over the standard of care is arguably very small. The bottom line is that payers pay only for meaningful and relevant differentiation.

## 18.3 Opportunities

### *18.3.1 The Opportunity Landscape*

So far in this chapter, we have spoken only of the problems. However, there are also opportunities for those who understand that:

- They must respond to what payers want.
- New therapies need to be better than old ones.
- Significant price increases must mean significant medical benefits.
- Risk concerns tend to outweigh those of benefit.

These factors are likely to push drug delivery down the path now, somewhat reluctantly, being followed by big pharma and pioneered by biotech – that of personalized medicine. For drug delivery, this means technologies adapted to specific patient subsets and specific molecules. Life cycle management through drug delivery is likely to become less relevant; incremental changes to existing drugs are not highly valued by payers. This is a new challenge for the industry as these have become low cost and low risk strategies. Meaningful differentiation may be easier to achieve through safety rather than efficacy or convenience benefits, going forward.

### *18.3.2 Modified Release Drug Delivery Opportunities*

There is a lot more that can be done with drug delivery if the problems are properly framed. Anyone looking at individual pharmacokinetic data for the first time from an orally dosed drug is generally surprised by the very large differences in drug absorption from patient to patient and from day to day. Orally dosed drugs are also delivered to just about every part of the body – in effect, mostly where they are not wanted. This means that large amounts of drug needs to be formulated, or highly

potent drugs are needed as they undergo substantial dilution in the body. As side effects of oral delivery, gut bacterial ecosystems are destroyed, gastrointestinal (GI) tracts become ulcerated, and patients experience constipation, diarrhea, etc. An orally dosed drug also goes straight to the liver, where most of it may be destroyed before it has a chance to act. The reason the oral route is used is that it is so very convenient, and eating and drinking come naturally, but in reality it is not a good way to deliver a drug unless formulation technology can intervene to overcome these limitations.

Better designed and more targeted therapy is with us, and more is on the way in the form of the biologics, but these are by necessity injections as they do not survive the gastrointestinal tract whose function is, after all, to digest proteins. That people do not like injections is a significant challenge. Bridging the gap between oral dosing convenience and biologic specificity would have a high value, such as an injection that is as convenient as a tablet or a tablet that delivers drug only to the site of action. Transdermal technologies are becoming increasingly sophisticated and are undoubtedly making progress in this area, but the skin is a tough barrier to breach without injury or reaction. Inhaled delivery of insulin was achieved by Exubera®, but this was a long and expensive road to no financial return, and an early example of not enough benefit for the price. Safety also remains a significant barrier for this delivery route. Despite these issues, we now know that pulmonary delivery of insulin is possible, and if insulin were being developed as an NCE today, the inhaled route may well have been preferred over injection.

## 18.4 Conclusions

The landscape is challenging for new modified release dosage forms. Intellectual property has become more difficult to obtain since prior art is increasing at an exponential rate and there has been an explosion of patent filings from rapid economic growth countries. Patent law is not static, and changes that are occurring are making intellectual property harder to obtain and defend.

Safety and efficacy are heavily scrutinized. Payers appear to be prepared to pay brand pricing for a new formulation in the generics market, but only if the benefits offered by the technology are large enough. Formulation itself does not bring regulatory exclusivity for drug delivery based life cycle management strategies, and often extensive and costly clinical efficacy studies are required to gain just 3 years of regulatory exclusivity. Generic companies are then very adept at bringing their formulations to the market as soon as this exclusivity expires. Commercial and regulatory risks are tending to outweigh scientific risks to the extent that undifferentiated NMEs also face a much tougher competitive environment.

The current landscape does, however, offer opportunities for those who respond to what payers want and who understand that new therapies need to offer a real advance to be valued medically and commercially. Improvements in safety are tending to be valued over those of efficacy. The problems, and hence needs, are

relatively clear, but the solutions are less so. It is unlikely that platform technologies will provide the benefits sought – if there were a broad panacea, it is likely that it would have already emerged.

The advances needed are likely to come from specific technologies designed for specific products. If the best technology for the patient group becomes a part of product development, then it becomes an integral part of the product and its safety, efficacy, and ease of use profile. The combined package is much more likely to satisfy the innovative requirements of the patent office and to move an NME over the added benefit bar, which all stakeholders are continuing to raise.

## References

1. Higgins MJ, Graham SJH (2009) Balancing innovation and access: patent challenges yip the scales. Science 326:370–371
2. Federal Trade Commission (2011) Agreements filed with the Federal Trade Commission under the Medicare Prescription Drug Improvement and Modernization Act of 2003. Overview of agreements filed in FY 2010
3. Salzman E (2010) Defined health, proof of relevance, the new standard for partnering (Definedhealth.com)

# Index




J. Siepmann et al. (eds.), *Fundamentals and Applications of Controlled Release Drug Delivery*, Advances in Delivery Science and Technology,
DOI 10.1007/978-1-4614-0881-9, © Controlled Release Society 2012